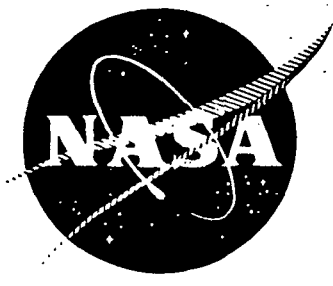


NASA CR-135444  
R78AEG510



# ENERGY EFFICIENT ENGINE

## Preliminary Design and Integration Studies

### FINAL REPORT

*by*

**ADVANCED ENGINEERING AND TECHNOLOGY PROGRAMS DEPARTMENT**

**GENERAL  ELECTRIC**

(NASA-CR-135444) ENERGY EFFICIENT ENGINE:  
PRELIMINARY DESIGN AND INTEGRATION STUDIES  
Final Report, Jan. 1977 - Apr. 1978 (General  
Electric Co.) 417 p HC A18/ME A01 CSCI 21E

N78-31108

Unclas  
G3/D7 30236

**SEPTEMBER 1978**



*Prepared For*

**NATIONAL AERONAUTICS and SPACE ADMINISTRATION**

Lewis Research Center  
21000 Brookpark Road  
Cleveland, Ohio 44135

NAS3-20627

1. Report No. NASA CR-135444		2. Government Accession No.		3. Recipient's Catalog No.	
4. Title and Subtitle Energy Efficient Engine - Preliminary Design and Integration Study - Final Report				5. Report Date September, 1978	
				6. Performing Organization Code	
7. Author(s) R.P. Johnston, R. Hirschcron, C.C. Koch, R.E. Neitzel, P.W. Vinson				8. Performing Organization Report No. R78AEG510	
9. Performing Organization Name and Address General Electric Company Aircraft Engine Group Cincinnati, Ohio 45215				10. Work Unit No. 716-01-02	
				11. Contract or Grant No. NAS3-20627	
				13. Type of Report and Period Covered Final; Jan. 1977-April 1978	
12 Sponsoring Agency Name and Address National Aeronautics and Space Administration Lewis Research Center 21000 Brookpark Road, Cleveland, Ohio 44135				14. Sponsoring Agency Code	
15 Supplementary Notes Project Manager: Neal T. Saunders, NASA-Lewis Research Center, Cleveland, Ohio 44135 Project Engineer: Gerald A. Kraft, NASA-Lewis Research Center, Cleveland, Ohio 44135					
16 Abstract  Parametric design and mission evaluations of advanced turbofan configurations were conducted for future transport aircraft application. Economics, environmental suitability and fuel efficiency were investigated and compared with goals set by NASA. Of the candidate engines which included mixed- and separate-flow, direct-drive and geared configurations, an advanced mixed-flow direct-drive configuration was selected for further design and evaluation. All goals were judged to have been met except the acoustic goal. Also conducted was a performance risk analysis and a preliminary aerodynamic design of the 10-stage 23:1 pressure ratio compressor used in the study engines.					
17. Key Words (Suggested by Author(s)) Energy Efficient Engine Integrated Composite Nacelle advanced clearance control mixed exhaust			18. Distribution Statement  Unclassified - Unlimited		
19. Security Classif. (of this report) Unclassified		20. Security Classif (of this page) Unclassified		21. No. of Pages	22. Price*

For sale by the National Technical Information Service, Springfield, Virginia 22161

PRECEDING PAGE BLANK NOT FILMED

TABLE OF CONTENTS

<u>SECTION</u>		<u>PAGE NO.</u>
I	Summary . . . . .	1
II	Introduction . . . . .	5
III	Task I - Engine Cycle Definition . . . . .	11
IV	Task II - Engine Airframe Integration . . . . .	51
V	Task III - Initial Preliminary Design . . . . .	147
VI	Task IV - Risk/Cost/Benefits Sensitivity Evaluation .	309
VII	Task V - Aerodynamic Design of Core Compressor . . .	327
VIII	Conclusions . . . . .	345
APPENDIX A	Task II Subcontractor Studies . . . . .	349
APPENDIX B	Task III Subcontractor Studies . . . . .	379
APPENDIX C	Nomenclature/Symbols . . . . .	407
	References . . . . .	411

SECTION I

SUMMARY

The purpose of this study was to provide additional substantiation and refinement of promising advanced fuel efficient turbofan engine cycles and conceptual designs identified in earlier NASA sponsored studies. Four engine types were examined and evaluated. Recommendations were made for more detailed study of selected engine types and cycles judged to be most capable of meeting NASA engine performance study goals. Engine technology levels capable of being demonstrated in the mid-1980's were assumed.

The NASA goals for this study were for a:

- 12% reduction in installed sfc
- 5% reduction in installed DOC

relative to a current CF6-50C reference engine installed on an advanced subsonic turbofan transport that could be introduced in service after 1990.

Other environmental goals were:

- Emissions-EPA standards for newly certificated engines after January 1, 1981.
- Engine noise - 10 EPNdB below FAR 36 (1969) requirements.

An additional NASA goal was to have engine growth potential without compromise of the above goals.

Further substantiation of the performance and the achievement of the above goals was obtained by more in-depth engine design and performance analysis coupled with aircraft/engine integration evaluations provided by selected airframe companies under subcontract to General Electric.

The study also provided insight into the effect of component and engine performance shortfalls on the expected benefits from an advanced turbofan. A final task of the study provided more detailed preliminary aerodynamic design data on the high pressure compressor for the advanced turbofan core engine.

The work of the study was broken into five technical tasks. Following is a brief summary of the major results for each task.

Task I - Engine Cycle Definition

Four engine types were examined including mixed and separate flow versions of direct-drive and geared-fan engines. All were studied and installed on an advanced transport aircraft to develop some preliminary estimates of performance and economic benefits. The conclusions reached include the following:



## Task I Result Comparison

	Exhaust System		Drive System	
	Mixed-Flow (Base)	Separate Flow	Direct-Drive (Base)	Geared-Drive
● Fuel Burned	--	3-6% Penalty	--	3-4% Benefit
● DOC	--	2.5-3.5% Penalty	--	0.5% Benefit
● Emissions	--	No Difference	--	10-20% Benefit
● Noise	--	0-3 EPNdB Penalty	--	2-4 EPNdB Benefits
● Growth Potential	--	No Difference	--	Better
● Deterioration	--	No Difference	--	No Difference

From the above, the mixed-flow exhaust system with both the direct-drive and geared-fan engines were carried into Task II for further study.

### Task II - Engine Airframe Integration

The benefits of both the advanced geared and direct-drive engines, as compared to a properly scaled CF6-50C, were estimated in this technical task. Additional design and performance refinements were accomplished as well as aircraft/engine integration studies by three airframe company sub-contractors.

For all engines sized at the maximum climb thrust level at 10668m (35,000 ft) altitude and 0.8M, the following benefits were estimated based on a General Electric study aircraft. Benefits were calculated based on maximum cruise  $\Delta sfc$  only, as integrated mission benefits were not yet available.

	<u>Scaled CF6-50C</u>	<u>Task II Direct-Drive</u>	<u>Task II Geared-Drive</u>
● Installed $\Delta sfc$ - %	Base	-12.1	-14.6
● Installed $\Delta DOC$ - %	Base	- 8.2	- 6.9
● Installed $\Delta W_f$ - %	Base	-17.8	-18.7

The above values were for an average 1296Km (700 N. mile) domestic mission at 55% load factor and using 92.46  $\$/m^3$  (35¢/gallon) fuel. Initial engine and maintenance costs were not evaluated for the advanced engine as part of the DOC benefit due to the preliminary state of such estimates.

The noise goals of FAR 36 (1969) - 10 EPNdB were met or approached at all conditions as indicated below for the domestic airplane:

	<u>Direct-Drive Engine</u>	<u>Geared-Drive Engine</u>
Takeoff	- 9.3 EPNdB	- 9.5 EPNdB
Sideline	-15.5 EPNdB	-15.4 EPNdB
Approach	- 8.1 EPNdB	-10.4 EPNdB

The noise levels presented above and later throughout this report, are based on an assumed broadband total inflight spectrum requiring no significant tone correction. They also have no engineering margin included. In practice, a 3 to 5 EPNdB margin would be required to ensure certification compliance.

The 1981 EPA emission goals were met by the geared engine. The direct-drive engine slightly exceeded the NO<sub>x</sub> limit of 3.0 with a 3.1 NO<sub>x</sub> emission estimate.

The direct-drive engine was recommended for further study in Task III, but further cycle and configuration work was performed to increase the sfc advantage over the reference CF6-50C. In addition, a more detailed study of a geared fan main transmission gear was undertaken in Task III to help verify Task II geared fan study results.

### Task III - Initial Preliminary Design

Modifications were made to the Task II direct-drive engine to improve its projected sfc margin over the CF6-50C from the original 12.1% to 14.4% at the maximum cruise power comparison point. Overall engine pressure ratio and rating temperatures were not altered, but fan pressure ratio, staging and LPT configurations were changed. In addition, a fuel/air heat exchanger (regenerator) and a higher-temperature-capability vane alloy was used to achieve the improved sfc performance.

The major changes are as follows for the design size core:

	<u>Task II</u> →	<u>Task III</u>
● Fan p/p (Maximum Climb)	1.71	→ 1.65
● Fan Diameter - m (In.)	2.02(79.7)	→ 2.11(83.0)
● Fan Tip Speed (Maximum Climb)-m/sec (ft/sec)	457(1500)	→ 411(1350)
● β (Maximum Climb)	6.2	→ 6.8
● Supercharging Provision	Fan Hub	→ Fan Hub + Quarter Stage
● HPT to LPT Coupling	Close Coupled	→ Small Transition Duct
● LPT Pitch Line		→ Increased
● Fuel Heater Regenerator	None	→ Added
● 2nd Stage HPT Vane Material	Rene' 125	→ Rene' 150

Benefits relative to a CF6-50C powered advanced General Electric study aircraft for an average 1296 Km (700 N. mile) domestic mission were estimated to be:

	<u>Scaled</u> <u>CF6-50C</u>	<u>Task III</u> <u>Direct-Drive</u>	<u>Task II</u> <u>Geared-Drive with</u> <u>Task III Mod.*</u>
● Installed Max. Cr. Δsfc - %	Base	-14.4	-15.1
● Installed ΔDOC - %	Base	-11.1	- 9.0
● Installed ΔW <sub>f</sub> (mission) - %	Base	-18.0	-16.1

\*Fuel heater and Rene' 150 vane material on Stage 2 of HPT

For the ΔDOC calculation, the effects of estimated initial engine price and mature engine maintenance costs were included.

A preliminary design of an advanced main transmission gear for the geared turbofan of Task II was carried out during Task III. As a result of the more detailed design definition, the system benefits of the Task II geared turbofan were slightly reduced. The  $\Delta$ DOC increased 0.15% over the Task II value and mission fuel usage increased 0.07% (increases reflect only the effect of the gear design changes). It was concluded that the Task III gearbox study did not uncover any potential for further improvements in the advanced geared turbofan system performance. Therefore, the Task III direct-drive, mixed-exhaust engine was the engine recommended for future NASA-sponsored technology development efforts.

#### Task IV - Risk/Cost/Benefits/Sensitivity Evaluation

In this part of the study, the magnitude of engine performance response to shortfalls in individual component performance levels was evaluated through engine performance derivatives. Another aspect of Task IV was the systematic evaluation, through statistical methods, of the probability of the recommended engine meeting full flight propulsion system goals and the reduced goals set for a demonstrator Integrated Core/Low Spool test vehicle in a projected technology development program. Using individual component performance/probability estimates generated through a modified "Delphi" method, the probability of meeting a demonstrator target of 12.4% sfc reduction was estimated to be about 95% and of meeting the full projected 14.4% sfc reduction goal was only about 20%. A hypothetical program benefit in terms of future cash savings was also developed for an assumed domestic and intercontinental fleet. Operating savings in excess of ten billion dollars were accumulated over the assumed fleet life of approximately twenty years.

#### Task V - Aerodynamic Design of Core Compressor

This task entailed a more detailed aerodynamic study and design of the advanced 23:1 ten-stage compressor proposed for this advanced engine. Staging information, blade and vane count, estimated performance maps, and some estimates of off-design performance were made. A comparison of typical parameters with the CF6-50C is indicated below.

	<u>CF6-50C</u>	<u>E<sup>3</sup></u>
Number of Stages	14	10
Total Pressure Ratio	13	23
Number of Rotor Blades and Stator Vanes	1713	1602

## SECTION II

### INTRODUCTION

Since 1973, NASA has sponsored advanced studies with the specific purpose of defining more fuel efficient subsonic transport aircraft and engines. For the engine studies, these have taken the form of investigating advanced cycles and configurations (References 1 and 2) and advanced material technologies for use in these future engines (References 3, 4, and 5).

The purpose of this study was primarily to select, define, and evaluate more fully advanced energy efficient engines ( $E^3$ ) from four promising engine types. This engine(s) would be suitable for use on advanced technology transport aircraft after 1990. Other purposes of the study were to determine the effect on engine benefit caused by shortfalls in performance and to provide additional design information about the high pressure compressor used in the engine.

Performance goals established by NASA for the study engines were:

- 12% installed sfc reduction
- 5% installed DOC reduction

relative to the reference CF6-50C engine installed on an advanced aircraft.

Environmental goals established were:

- Emissions - meet EPA standards for post 1981 certificated engines
- Noise - at least 10 EPNdB below FAR 36 (1969) requirements

An additional goal was potential engine thrust growth without compromise of the above goals.

- Task I - Engine Cycle Definition

Four engines were evaluated in this portion of the study. A mixed- and separate-flow exhaust version of both a direct-drive and geared-fan engine were the configurations investigated. Properly scaled CF6-50C engines were used as a basis for comparison. From this task came a recommendation of two engines for further study in the subsequent tasks.

- Task II - Engine/Airframe Integration

Using the two recommended engines from Task I, a benefit analysis was performed by General Electric and by the three airframe subcontractors, Boeing, McDonnell/Douglas, and the Lockheed California Company. Variations of the two selected engine cycles were also studied. From this Task, one advanced engine configuration and cycle was recommended for further work.

- Task III - Initial Preliminary Design

The original task was altered in order to do more engine cycle and configuration optimization and to perform a preliminary design of a main gearbox system for a geared engine. A more refined preliminary design was then performed on the newly optimized direct-drive mixed-flow advanced engine. In addition, the Task II benefit analyses were updated by General Electric and the airframe subcontractors. Maintenance and initial engine cost effects were also incorporated into the General Electric benefit analysis to obtain a more complete comparison with the reference CF6-50C engine.

- Task IV - Risk/Cost/Benefits/Sensitivity Evaluation

In this task, the effect on the engine system due to small changes in projected component performance was evaluated and treated statistically to obtain the probability of obtaining various levels of total engine performance during an anticipated technology development and demonstration program. Benefits of the advanced engine in terms of a hypothetical airline fleet were also evaluated.

- Task V - Aerodynamic Design of Core Compressor

A more detailed aerodynamic design of the selected core compressor was accomplished during this task. More blading design information and staging data were developed along with anticipated off-design performance.

TABLE OF CONTENTS

	<u>PAGE NO.</u>
SECTION III . . . . .	11
TASK I - ENGINE CYCLE DEFINITION . . . . .	11
A. Introduction/Approach . . . . .	11
1. Advanced Engines Selected for Study . . . . .	11
2. Approach . . . . .	11
B. Significant Results . . . . .	22
1. sfc Reductions . . . . .	22
2. Weight and Geometry Comparison . . . . .	22
3. Advanced Engine Growth . . . . .	27
4. Emissions . . . . .	27
5. Noise Evaluation . . . . .	27
6. Mission Evaluation . . . . .	37
C. Conclusions/Recommendations . . . . .	37

LIST OF FIGURES  
SECTION III  
TASK I - ENGINE CYCLE DEFINITION

<u>FIGURE NO.</u>	<u>TITLE</u>	<u>PAGE NO.</u>
1	The General Electric CF6-50 Engine Cross Section	15
2	Advanced Candidate Engine: 1.71 P/P Direct-Drive Fan/Mixed-Flow Exhaust	16
3	Advanced Candidate Engine: 1.71 P/P Direct-Drive Fan/Separate-Flow Exhaust	17
4	Advanced Candidate Engine: 1.55 P/P Geared-Fan/Mixed-Flow Exhaust	18
5	Advanced Candidate Engine: 1.55 P/P Geared-Fan/Separate-Flow Exhaust	19
6	Effects of Exhaust Velocity Ratio Variations for Advanced Engines with Separate-Flow Exhaust/Direct-Drive Fan	20
7	Effects of Exhaust Velocity Ratio Variations for Advanced Engines with Separate-Flow Exhaust/Geared-Fan	21
8	Low Emission Combustor Fuel Staging	30
9	Advanced Engine Installation, Low Noise Features	32
10	Takeoff, Estimated Noise Levels - Domestic Aircraft	33
11	Sideline, Estimated Noise - Domestic Aircraft	34
12	Approach, Estimated Noise Levels - Domestic Aircraft	35
13	NPRM 75-37C Proposed Monitoring Point Locations	36
14	Growth at Takeoff, Estimated Noise Levels - Domestic Aircraft	38
15	Mission Evaluation - Sensitivity to Price and Maintenance Costs, Advanced Technology Direct-Drive Mixed-Flow Engine vs Current Technology CF6-50C Engine (Scaled), 200 PAX Advanced Tech A/C, 55% Load Factor	42
16	Mission Evaluation Summary, Comparisons with Direct-Drive Mixed Turbofan	43

LIST OF TABLES  
SECTION III  
TASK I - ENGINE CYCLE DEFINITION

<u>TABLE NO.</u>	<u>TITLE</u>	<u>PAGE NO.</u>
1	Baseline Engine: Cycle and Aerodynamic Design	12
2	Baseline Engine Advanced Design Features	13
3	Description of Engines Studied in Task I	14
4	Sources of sfc Improvement for Advanced Direct-Drive Mixed-Flow Engine	23
5	sfc Comparison of Advanced Technology Engines	24
6	Engine Weight and Dimension Results	25
7	Advanced Engine Performance Deterioration Estimates	26
8	Typical Engine Growth Pattern	28
9	Typical Engine Growth Configurations	29
10	Emissions Estimates	31
11	Summary of Candidate Engine Characteristics	39
12	GE Study Aircraft Description	40
13	Mission Trade Factors	41



SECTION III

TASK I - ENGINE CYCLE DEFINITION

A. Introduction/Approach

Prior NASA studies reported in References 1, 2, and 6 and other inhouse studies provided the background for selection of the E<sup>3</sup> Task I engines. These studies resulted in the selection of a baseline direct-drive fan, unboosted core, mixed flow engine described in Table 1.

Advanced design features incorporated in the baseline engine are summarized in Table 2. These selected advanced design features had been identified in prior studies as having significant payoff in fuel consumption reduction and are considered to be consistent with service introduction during the early 1990's. This baseline engine was exercised in the Task I evaluation to determine fuel savings and economic potential relative to the most modern in-service GE engine - the CF6-50C.

1. Advanced Engines Selected for Study

Additional advanced technology engines defined for the Task I study were:

- A separate-flow direct-drive fan
- A mixed-flow geared fan
- A separate-flow geared fan

Principal features of the selected advanced technology engine cycles are summarized in Table 3 and compared to the CF6-50C Reference engine. All of the advanced engines were initially sized with a 54.43 kg/sec (120 lb/sec) airflow core and were subsequently scaled as required to meet specific mission requirements. The core design for all four of the advanced engines was the same except for size.

The CF6-50C cross section is shown in Figure 1, and typical advanced engine installation layouts for the four advanced engines are illustrated in Figures 2 through 5.

Both of the geared study engines employed an advanced star-epicyclic 2.5:1 single reduction gearset to match the fan and low pressure turbine to their respective optimum design tip speeds.

The advanced separate-flow engine cycles were adjusted for optimum core energy extraction as shown in Figures 6 and 7. An exhaust velocity ratio of 1.4 at maximum climb was chosen for both engines with separate-flow cycles to provide minimum mission fuel consumption (based on  $W_f$  values).

2. Approach

In this portion of the study, four engine configurations were evaluated which included direct- and geared-fan drive for separate- and mixed-flow

TABLE 1BASELINE ENGINE: CYCLE AND AERODYNAMIC DESIGN

<u>CYCLE</u>	- .8 M <sub>n</sub> , 10,668 m (35K ft.) Max. Climb Des. Pt. β = 6.2 Fan P/P = 1.71 Cycle P/P = 38 T <sub>41</sub> = 1360°C (2480°F) Takeoff	<u>HIGH PRESSURE COMPRESSOR</u>	- No. Stages - 10 - P/P = 23 - U <sub>T</sub> /√θ = 455.1 m/s (1495 fps) - r/r = .50
<u>FAN</u>	- U <sub>T</sub> /√θ = 457.2 m/sec (1500 fps) - r/r = 0.36 - Hub P/P = 1.67	<u>HIGH PRESSURE TURBINE</u>	- No. Stages = 2 - $\bar{\psi}_p = 0.7$
<u>BOOSTERS</u>	- None (One in Growth)	<u>LOW PRESSURE TURBINE</u>	- No. Stages = 4 - $\bar{\psi}_p = 1.5$
		<u>EXHAUST</u>	- Mixed - 24 Lobe Short Mixer - Fan Reverser Only

TABLE 2

TASK I BASELINE ENGINE: ADVANCED DESIGN FEATURES

- FAN
  - Mid-Span Shrouded Ti Blades
  - Composite Outer Vane-Frame Integrated with Nacelle
  - High Hub Boost (1.67 P/P)
  
- HIGH PRESSURE COMPRESSOR
  - High P/P on One Rotor
  - 23:1 P/P in 10 Stages\*
  - Casing Cooled and Insulated for Clearance Control
  - Low Aspect Ratio Rugged Blades
  
- COMBUSTOR - Double Annular for Emissions
  
- HIGH PRESSURE TURBINE
  - Advanced Nickel-Based Directionally Solidified Castings Blades & Vanes
  - Blades with Inserts and Curved Dovetails
  - Expander Cooling Supply - Stage 1
  - Bore-Entry Cooling - Stage 2
  - Active Clearance Control
  - Ceramic Shrouds
  
- LOW PRESSURE TURBINE
  - 4-Stage Uncooled Advanced Nickel-Based Directionally Solidified Castings - Rotor 1 and Stator 1
  - High Aerodynamic Loading
  
- CONTROL
  - FADEC (Full Authority Digital Engine Control) - Including Power Management & Condition Monitoring Features
  
- INSTALLATION
  - Thin Inlet,  $D_{HL}/D_{MAX} = 0.88$
  - Composite Nacelle
  - Pylon-Mounted Accessories
  - Dual-Blocker Cascade Reverser
  - Mixed Exhaust - Aerodynamic Spoiling of Core Thrust in Reverse Mode
  - Bulk-Absorber Acoustic Treatment

\*Modification of compressor described in reference 6. Aspect ratio has been reduced.

TABLE 3

## DESCRIPTION OF ENGINES STUDIED IN TASK I

	Reference Engine (CF6-50C)	Advanced Engines - Design Size Twin Spool Turbofans 54.43 kg/sec (120 lb/sec) Core Size			
		Direct	Direct	Geared	Geared
Fan Drive	Direct	Direct	Geared	Geared	Geared
Exhaust Configuration	Separate	Mixed	Separate	Mixed	Separate
SLS T/O $F_n$ , kn(lb)	223.5(50250)	154.8(34800)	157.0(35300)	177.0(39800)	176.1(39600)
Fan Diameter, m(in)	2.195(86.4)	2.004(78.9)	2.123(83.6)	2.334(91.9)	2.446(96.3)
Fan P/P	1.75	1.71	1.71	1.55	1.55
Bypass Ratio, MxC1/MxCr	4.2/4.3	6.1/6.3	7.0/7.1	8.4/8.6	9.4/9.6
Overall Pressure Ratio, MxC1/MxCr	32/30	38/36	→		
Takeoff Pressure Ratio	30	30	→		
Turbine Temperature, °C/(°F) (T/O, Std + 27°F Day) (T/O, Std + 15°C Day)	1316(2400)	1360(2480)	→		
No. Stages Fan/LPC/HPC/HPT/LPT	1/3/14/2/4	1/0/10/2/4	1/0/10/2/5	1/1/10/2/3	1/1/10/2/3
Reverse $F_n$ @ 100 Kts/SLS % $F_n$	60-80 <sup>(2)</sup>	43-50 <sup>(1)</sup>	40-47 <sup>(1)</sup>	48-55 <sup>(1)</sup>	45-52 <sup>(1)</sup>

(1) Minimum estimate to maximum estimate, cascade fan reverser (no tailoring)

(2) With cascade fan and turbine reverser (no tailoring)

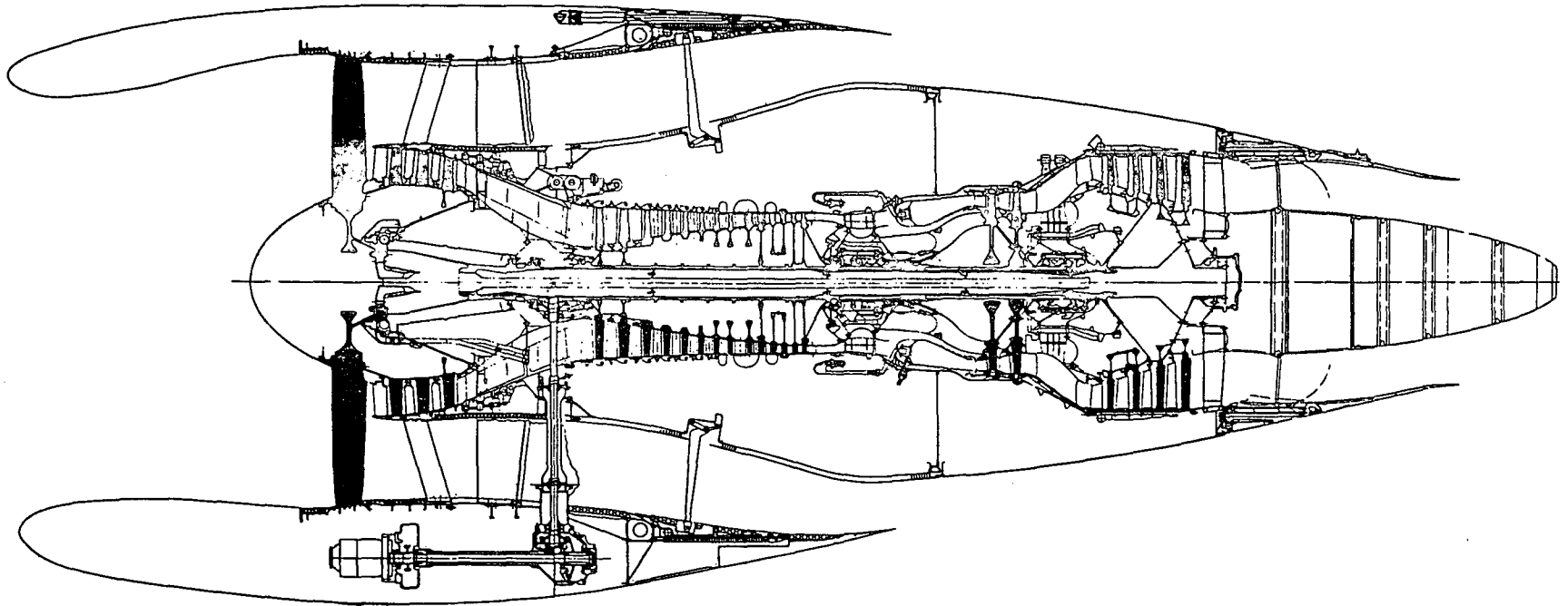


Figure 1. The General Electric CF6-50 Engine Cross Section.

MX CR OVERALL P/P 36  
MX CR BYPASS RATIO 6.3  
TAKEOFF  $T_{41}$  1360°C (2480°F)

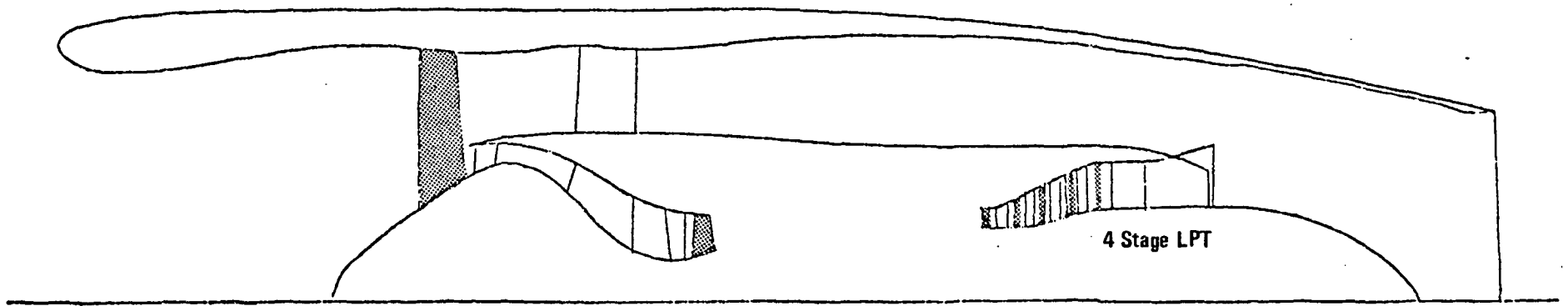


Figure 2. Advanced Candidate Engine: 1.71 P/P Direct-Drive Fan/Mixed-Flow Exhaust

MX CR OVERALL P/P 36  
MX CR BYPASS RATIO 7.1  
TAKEOFF  $T_{41}$  1360°C (2480°F)

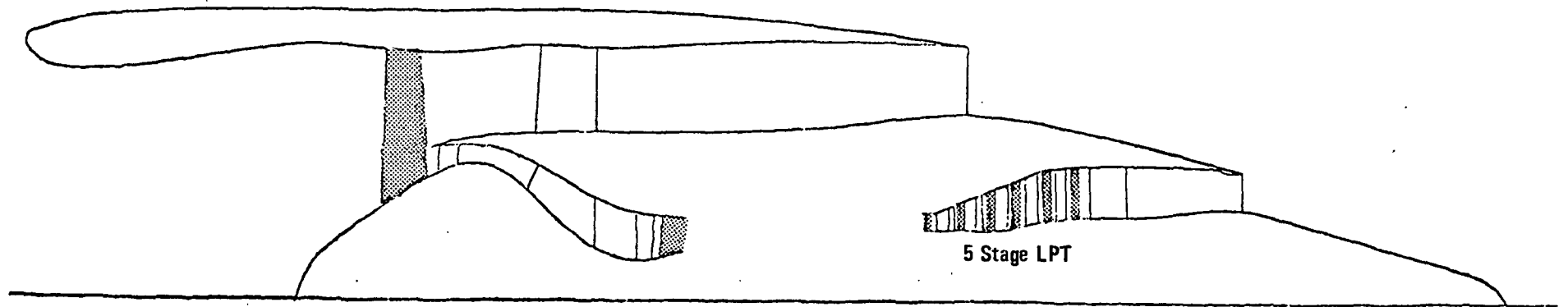


Figure 3. Advanced Candidate Engine: 1.71 P/P Direct-Drive Fan/Separate-Flow Exhaust

<b>MX CR OVERALL P/P</b>	<b>36</b>
<b>MX CR BYPASS RATIO</b>	<b>8.6</b>
<b>TAKEOFF <math>T_{41}</math></b>	<b>1360<sup>0</sup>C (2480<sup>0</sup>F)</b>

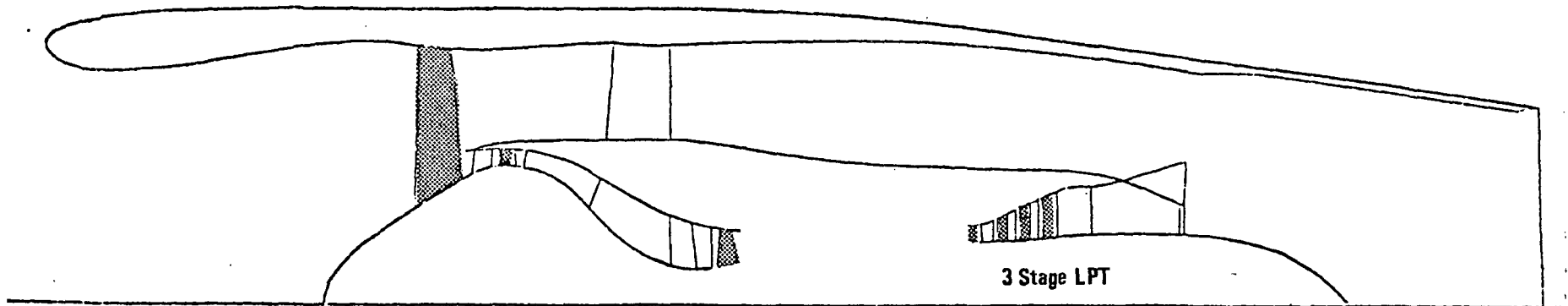


Figure 4. Advanced Candidate Engine: 1.55 P/P Geared Fan/Mixed-Flow Exhaust



MX CR OVERALL P/P 36  
MX CR BYPASS RATIO 9.6  
TAKEOFF  $T_{41}$  1360°C (2480°F)

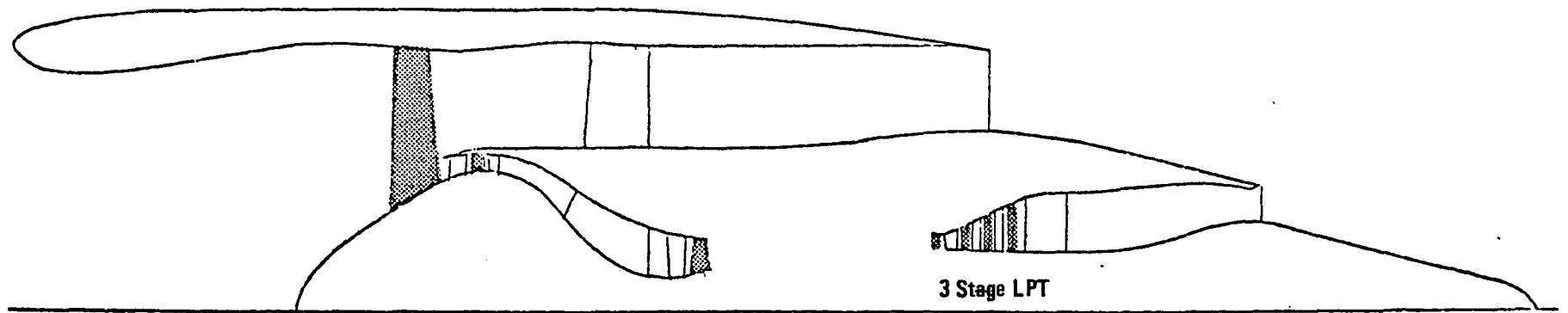


Figure 5. Advanced Candidate Engine: 1.55 P/P Geared Fan/Separate-Flow Exhaust

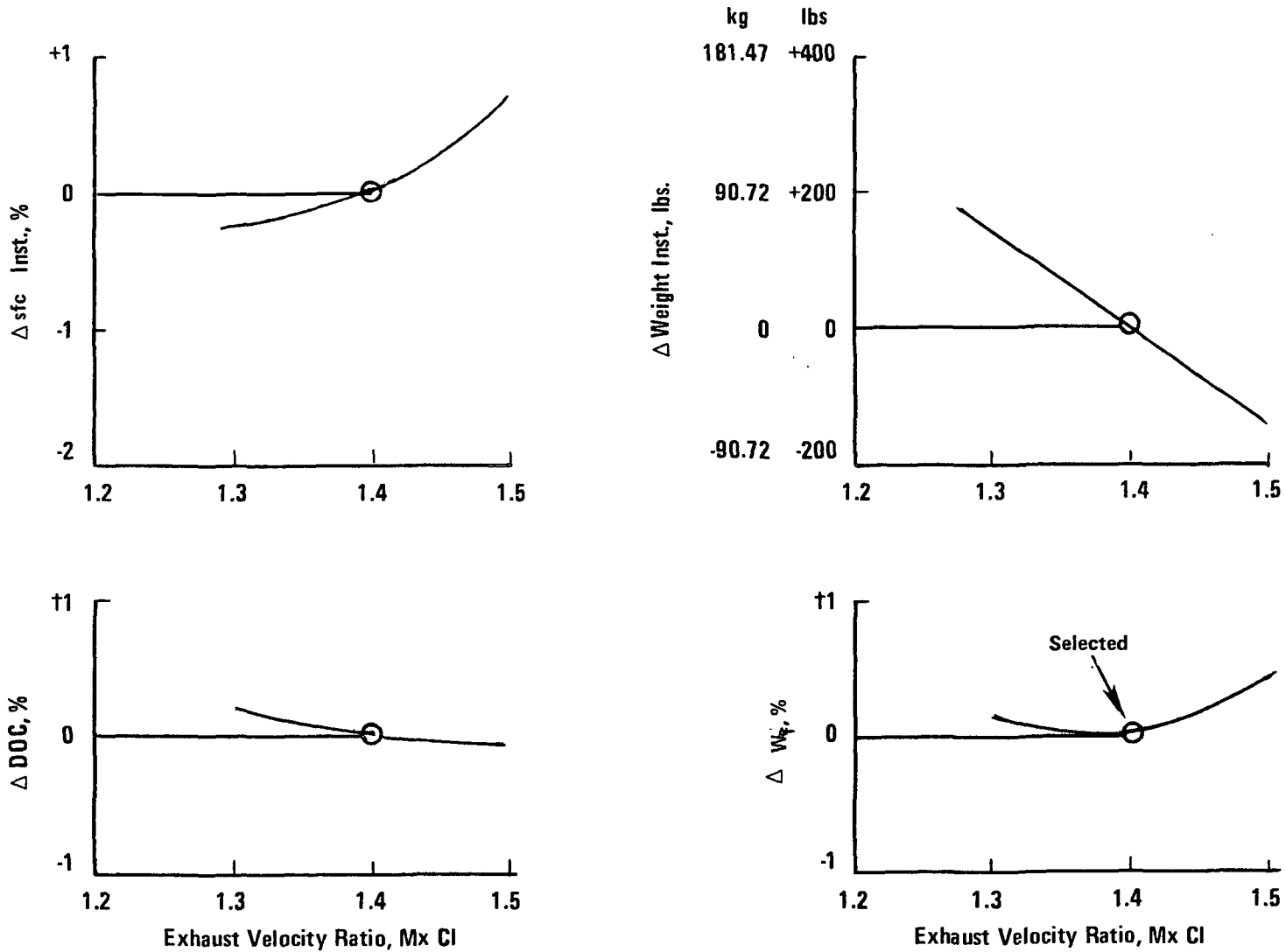


Figure 6. Effects of Exhaust Velocity Ratio Variations for Advanced Engines with Separate-Flow Exhaust/Direct-Drive Fan

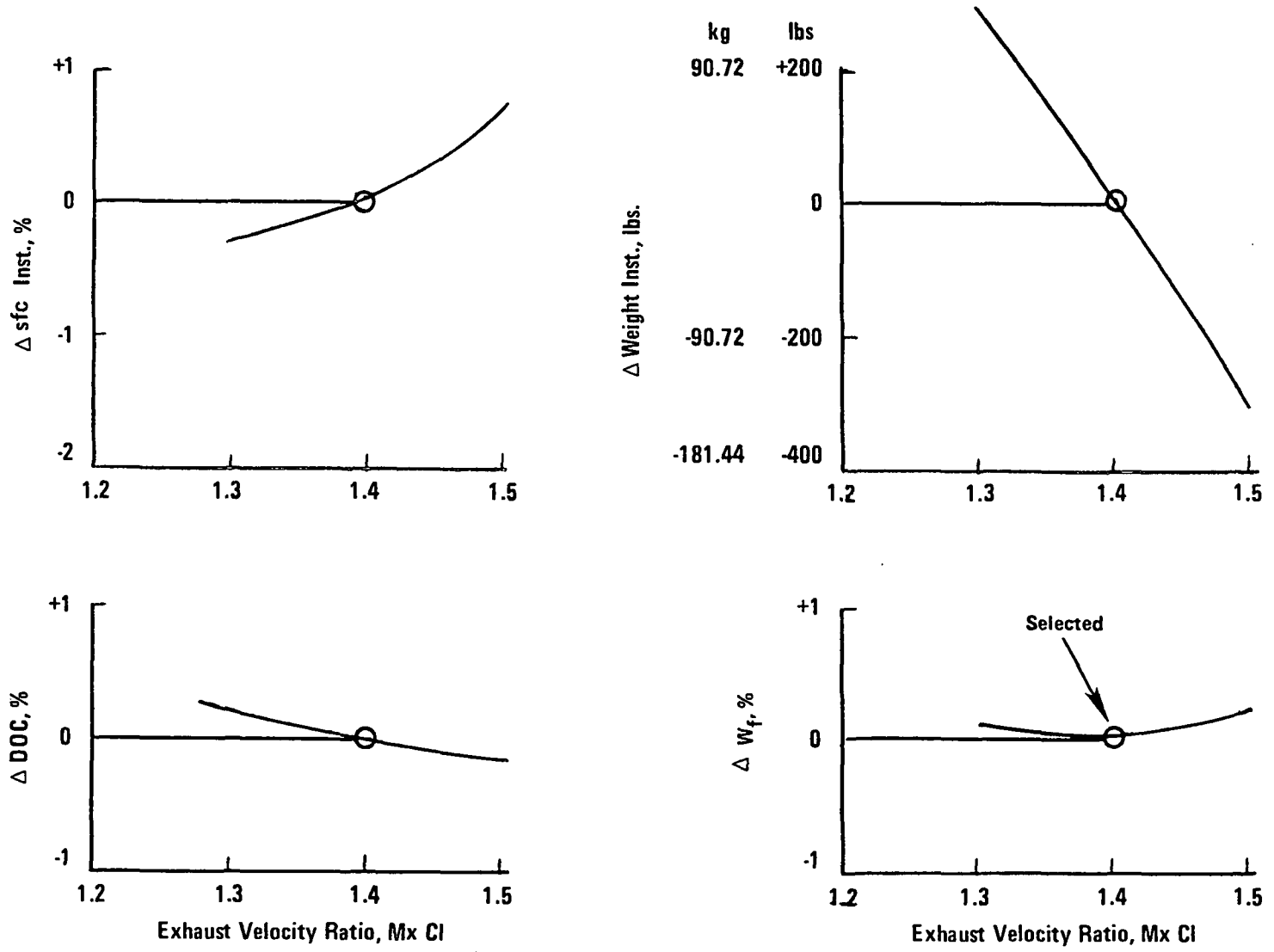


Figure 7. Effects of Exhaust Velocity Ratio Variations for Advanced Engines with Separate-Flow Exhaust/Geared-Fan

exhausts. For all engines, the core engine configuration, flow, inlet conditions, and firing temperature were kept constant by suitable low pressure components.

A preliminary design was made of each of the engines assuming technology level consistent with the time period of eventual engine certification. Estimates of weight, cost, maintenance, and performance were developed. In addition, for the separate flow engines, increased low pressure turbine work extraction was assumed to more nearly optimize the separate-flow exhaust performance for best fuel efficiency.

Each engine was then scaled to the proper thrust to produce equivalent net installed thrust for a study subsonic transport aircraft developed in an earlier study (Reference 1). Economic and performance differences between each engine were then calculated based on the trade factors associated with the modeled study aircraft. From these calculations came comparative rankings. Besides the economic and performance comparison, environmental (noise and emission) assessments were made for each engine along with estimates of any differences in deterioration or the capability of the various study engines to be modified for a 20% increase in thrust for growth.

## B. Significant Results

### 1. sfc Reductions

As shown in Table 4, the advanced direct-drive mixed-flow engine was estimated to have about a 12% installed sfc improvement relative to the CF6-50C. An estimated 5% of this improvement is related to core components and cycle effects. LP spool components and propulsive efficiency effects are estimated to contribute 2% of the improvement, and the mixed-flow exhaust system is estimated to contribute 4%. The remaining 1/2 to 1% improvement is attributable to the advanced nacelle design.

Table 5 illustrates the estimated installed sfc potential of the advanced separate flow and geared engines relative to the baseline direct-drive advanced engine. The separate-flow engine installed sfc is estimated to be 2.2% poorer than the baseline mixed-flow engine with the separate-flow exhaust and installation disadvantages outweighing the improved LP spool component and cycle advantages. The advanced geared-fan mixed-flow engine shows a 5.6% bare engine sfc advantage while installation effects are 1.1% poorer than the baseline configuration for a net installed sfc advantage of 4.5%.

### 2. Weight and Geometry Comparison

A size and weight comparison of the four candidate advanced engines is shown in Table 6.

Each of the advanced engines was assessed for performance deterioration as shown in Table 7. Work currently in progress in other parallel NASA programs is pointed towards identifying specific component deterioration rates and to identify design features to reduce deterioration. Pending results of that investigation, the advanced engines were assessed for equal component changes as indicated in Table 7 with the result that none of the engines had a distinct advantage or disadvantage relative to deterioration.

TABLE 4

SOURCES OF SFC IMPROVEMENT FOR ADVANCED DIRECT-DRIVE MIXED-FLOW ENGINE

	<u>Improvement in Installed sfc vs. CF6-50C</u>
<u>Core Related</u>	
Incl. Cycle P/P and $T_{41}$ @ Cruise, Component Design & Performance, High Temperature Technology	5%
<u>LP Spool Related</u>	
Incl. Propulsive Efficiency (FN/WA) Component Design and Performance	2%
<u>Mixed Exhaust</u> (At Constant FN/WA)	4%
<u>Advanced Nacelle</u> (At Constant FN/WA)	<u>1/2 - 1%</u> ~ 12%

TABLE 5

SFC COMPARISON OF ADVANCED TECHNOLOGY ENGINES

	Separate Flow Relative to Mixed Exhaust <u>(Direct-Drive)</u>	Geared Relative to Direct-Drive <u>(Mixed-Flow)</u>
<u>Core Related @</u>		
Constant Cycle P/P, $T_{41}$ and High Temp. Technology	0	0
<u>LP Spool Related</u>		
Incl. Propulsive Efficiency ( $F_n$ /WA) Component Performance	-1.4%	-5.6%
<u>Mixed Exhaust</u> (At Constant $F_n$ /WA)	+2.8%	0
<u>Installation</u> (At Constant $F_n$ /WA)	<u>+ .8%</u>	<u>+1.1%</u>
Total	+2.2%	-4.5%

TABLE 6

ENGINE WEIGHT AND DIMENSION RESULTS

INSTALLED MAX. CLIMB  $F_{NI} = 37.943K N$  (8350 LBS) [ $.8 M_n$ , 10,866 m (35K Ft.) ALT., STD. + 10°C(18°F)]

Engine Fan Drive Exhaust Configuration	Task I - Advanced Engines		Geared	
	Direct Mixed	→ Separate	→ Mixed	→ Separate
Engine Fan Diameter, m (in)	2.004 (78.9)	2.146 m (84.5)	2.268 (89.3)	2.416 (95.1)
Engine Length, m (in)	2.776 (109.3)	3.108 (122.2)	2.963 (112.7)	3.010 (118.5)
Nacelle Max. Dia., m (in)	2.304 (90.7)	2.466 (97.1)	2.581 (101.6)	2.748 (108.2)
Nacelle O'All Length, m (in)	5.537 (218)	6.147 (242)	6.299 (248)	6.731 (265)
Engine Weight, kg (lbs)	2708 (5970)	3075 (6780)	3157 (6960)	3533 (7790)
Nacelle Weight, kg (lbs)	939 (2070)	966 (2130)	1170 (2580)	1184 (2610)
Total Install., Weight, kg (lbs)	3647 (8040)	4041 (8910)	4327 (9540)	4717 (10400)

TABLE 7

ADVANCED ENGINE PERFORMANCE DETERIORATION ESTIMATES

At 3000 Hrs. Service

Engine	Direct Mixed	$\xrightarrow{\hspace{1.5cm}}$ Separate	Geared Mixed	$\xrightarrow{\hspace{1.5cm}}$ Separate
$\Delta$ % sfc @ Max Cruise <sup>(1)</sup>	1.2	1.3	1.2	1.3
$\Delta$ EGT @ TO, °C (°F) <sup>(1)</sup>	16 (+29)	16 (+29)	16 (+29)	16 (+29)

<sup>(1)</sup> Based on Assumed Component Deterioration Changes @ 3000 Hrs. Service

$\Delta \eta_C$	- .15%
$\Delta \eta_F$	- .31%
$\Delta \eta_{T\ HP}$	- .8%
$\Delta \eta_{T\ LP}$	- .47%
$\Delta$ Leakage	+ .1%

$\eta_C$     Compressor Efficiency  
 $\eta_F$     Fan Efficiency  
 $\eta_{T\ HP}$     HP Turbine Efficiency  
 $\eta_{T\ LP}$     LP Turbine Efficiency



### 3. Advanced Engine Growth

A typical direct drive mixed flow engine growth pattern to provide 40% balanced thrust growth relative to the initial service rating is shown in Tables 8 and 9. The initial thrust increase of 15% is achieved by a simple throttle push to achieve design level ratings. The "ultimate" growth, Step B, to 40% thrust increase is achieved by redesigning the fan for higher pressure ratio, further over-speeding of the fan and core, and the addition of a booster stage.

An alternate step B growth which employs a larger diameter fan is also shown. Selection of constant diameter vs larger fan diameter growth is expected to be influenced by aircraft requirements. Similar growth patterns are applicable to the other Task I advanced engines.

### 4. Emissions

All of the advanced engines employ a double dome low emissions combustor as shown in Figure 8. Only the primary stage is fueled at low power settings to reduce HC and CO emissions while both domes are fueled at high power settings to obtain low NOx emissions.

Advanced engine emissions estimates are summarized in Table 10. These estimates indicate that the proposed goals on CO and HC will be met while the NOx standard is met only by the geared engines (by virtue of having a smaller core).

### 5. Noise Evaluation

Advanced nacelle design features used to achieve lower noise are shown in Figure 9. Both the inlet and the fan exhaust duct are treated with an advanced bulk absorber to suppress fan noise. The low pressure turbine employs high blade numbers in the last two stages. This was done to raise the source frequency of the turbine noise to a very high level in order to reduce PNL weighting of the turbine spectrum. These features were selected based on prior studies which showed the fan to predominate at takeoff and low pressure turbine noise to predominate at approach.

Since size selection will influence both engine noise and the regulation levels, evaluation of the various advanced engines was performed on a selected advanced domestic aircraft described later under the heading Mission Evaluation.

Overall system noise levels at takeoff, sideline and approach for the advanced engines are shown in Figures 10 through 12 and compared to applicable regulations. The appropriate monitoring positions associated with NPRM 75-37C are shown in Figure 13. As noted previously the geared fan mixed flow engine alone meets the FAR 36-10 noise level on takeoff without cutback while all of the advanced engines are significantly below the sideline regulation level. At approach only the direct drive separate flow engine noise is above the FAR 36-10 level.

TABLE 8

TYPICAL ENGINE GROWTH PATTERN

## CONSTANT FAN DIAMETER

	Constant Fan Diameter $\longrightarrow$				
	Initial Rating	Design	Initial Growth "A"	Ultimate Growth "B"	Ultimate Growth Larger Fan Dia.
$\Delta \% F_n$ Takeoff + Max Climb	Base	+15	+25	+40	+45
$\Delta T_{41}$ Takeoff, °C (°F)	-78 (-140)	Base	0	89 (+160)	67 (+120)
$\Delta P_3, \Delta T_3$ Takeoff $N/m^2/^\circ C$ (lbs/in <sup>2</sup> /°F)	-75842/-28 (-11/-50)	Base	110316/36 (+16/+65)	199948/64 (+29/+115)	199948/64 (+29/+115)
$\Delta \% sfc$ Max Cruise Bare	- .1	Base	+1.2	+3.3	-1.0
$\Delta$ Fan RPM, %	-4.1	Base	+2.2	+3.3	0
$\Delta$ Core RPM, %	-2.2	Base	+2.5	+4.7	+3.6

TABLE 9

TYPICAL ENGINE GROWTH CONFIGURATIONS

	← Constant Fan Dia. →				Alternate Growth
	Initial Rating	Design	Initial Growth "A"	Ultimate Growth "B"	Ultimate Growth "B"
Fan Diameter	← Base →				Increase
No. Booster Stages	0	0	1	1	1
No. Compressor Stages	10	→			10
No. of HPT Stages	2	→			2
No. of LPT Stages	4	→			4
LPT Flow Function	Nom	Nom	+5%	+5%	+5%

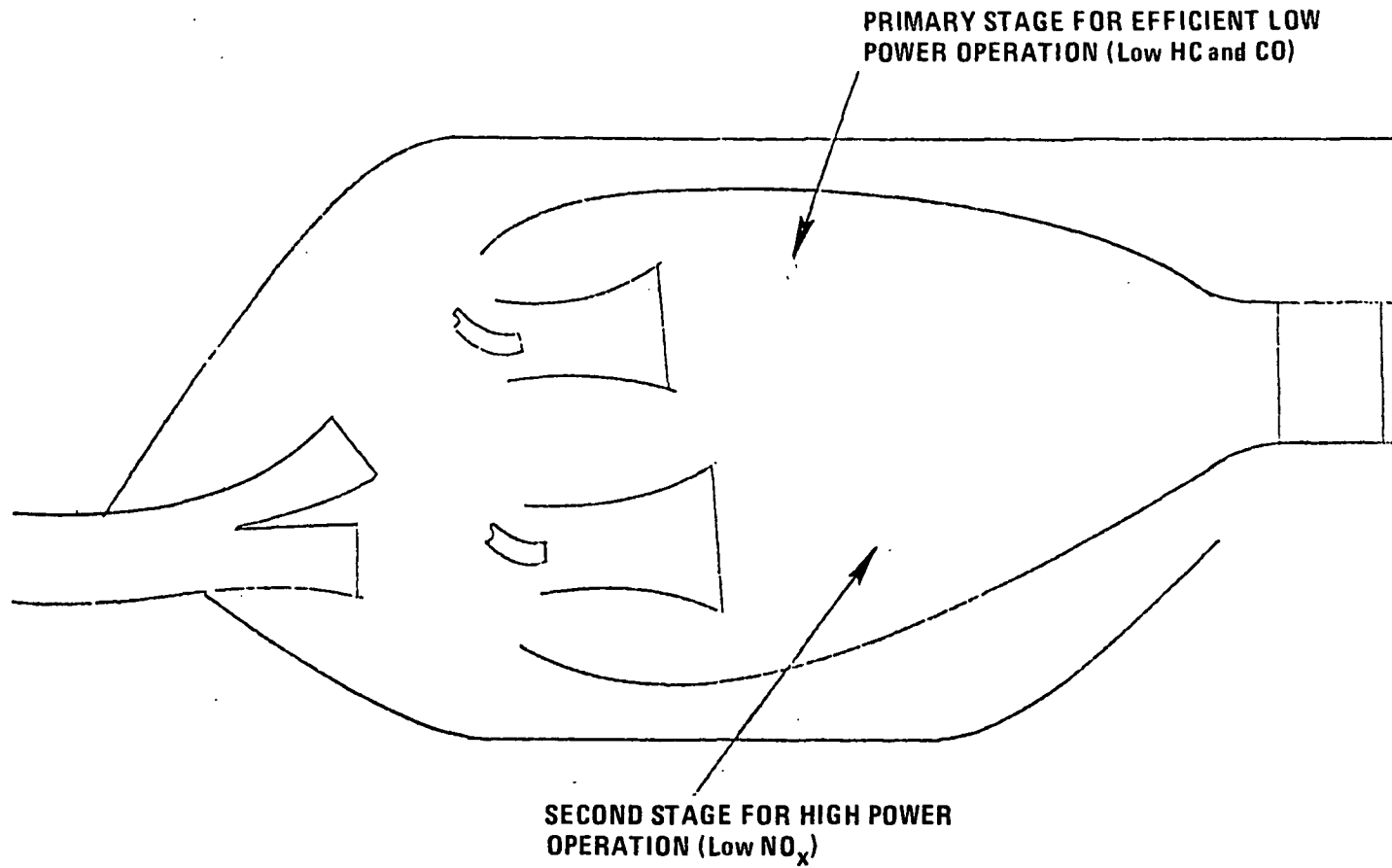


Figure 8. Low Emission Combustor Fuel Staging

TABLE 10

EMISSIONS ESTIMATES

Max. Climb  $F_{NI} = 37943 \text{ N (8530 Lbs)}$   
Advanced Engines

Fan Drive Exhaust Config.	Direct $\xrightarrow{\hspace{2cm}}$		Geared $\xrightarrow{\hspace{2cm}}$		<u>Study Goals</u>
	Mixed	Separate	Mixed	Separate	
SLS T/O $F_n$ , N (lbs)	154798 (34800)	160581 (36100)	167253 (37600)	171701 (38600)	
	EPA Parameter (No Margin)				
CO*	2.4	2.4	2.2	2.2	3.0
HC*	.25	.25	.24	.24	.4
NO <sub>x</sub>	3.5	3.6	3.0	3.0	3.0

\* = Idle Thrust at 3...2% of T/O Thrust

**.58 L/D TREATED INLET -  
ADVANCED BULK ABSORBER**

**TREATED VANE/FRAME  
2.0 CHORD SPACING**

**MIXED FLOW EXHAUST**

**HIGH BLADE  
NUMBER TURBINE**

**SEPARATE FLOW EXHAUST**

**FULLY TREATED FAN EXHAUST DUCT -  
ADVANCED BULK ABSORBER**

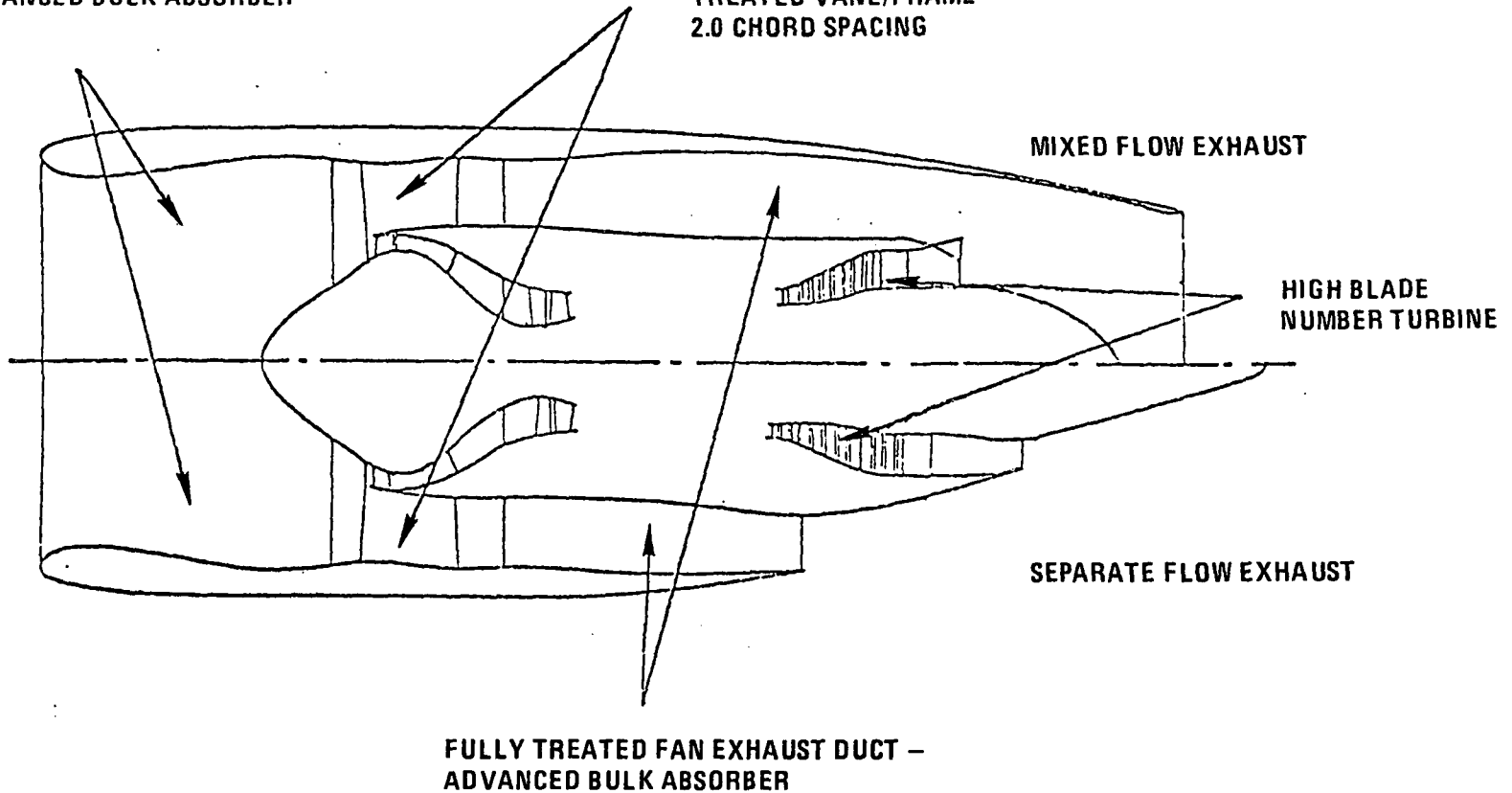


Figure 9. Advanced Engine Installation, Low Noise Features.

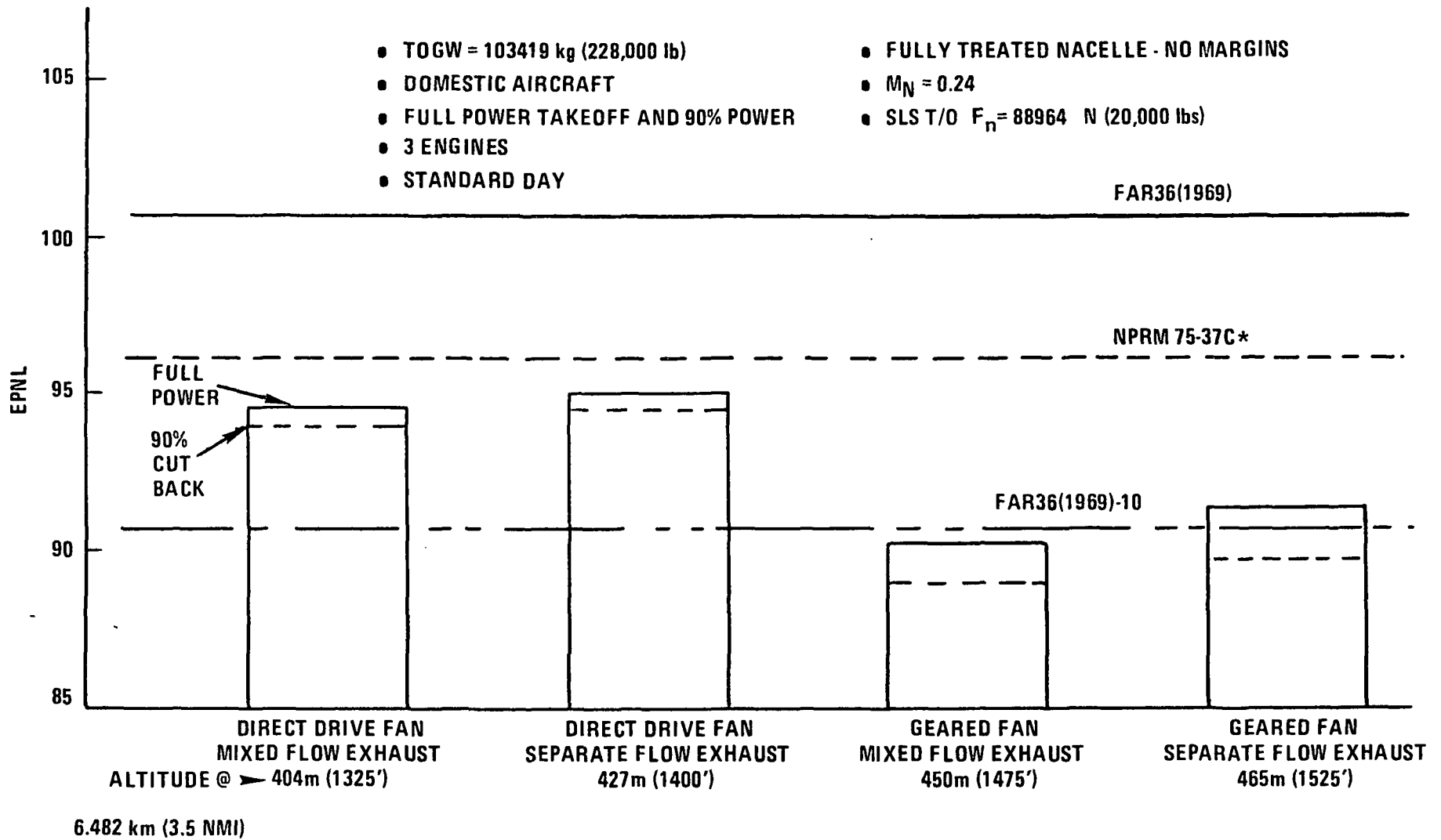


Figure 10. Takeoff, Estimated Noise Levels - Domestic Aircraft

\*Similar to FAR 36 (1977).

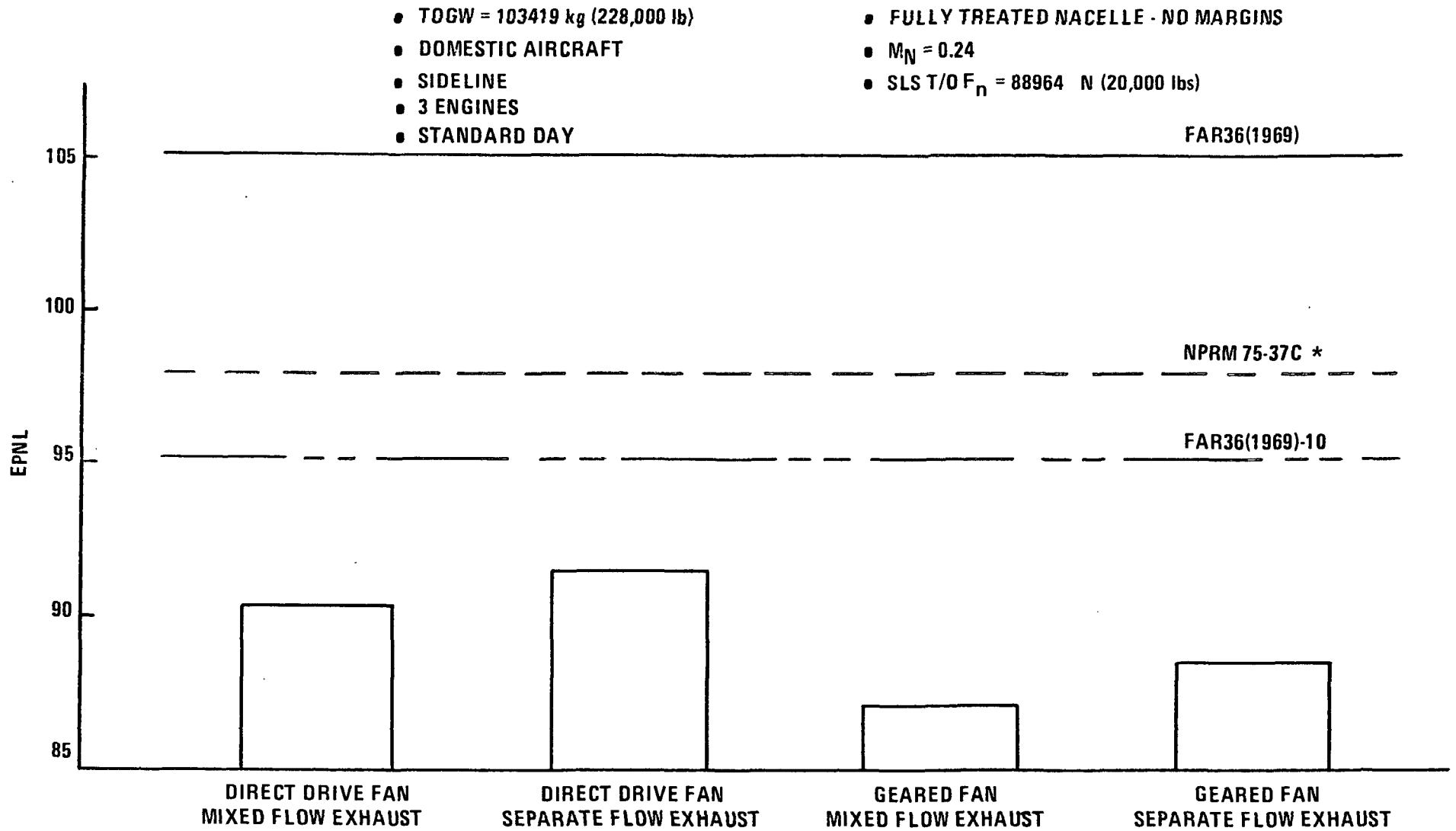


Figure 11. Sideline, Estimated Noise - Domestic Aircraft

\*Similar to FAR 36 (1977)



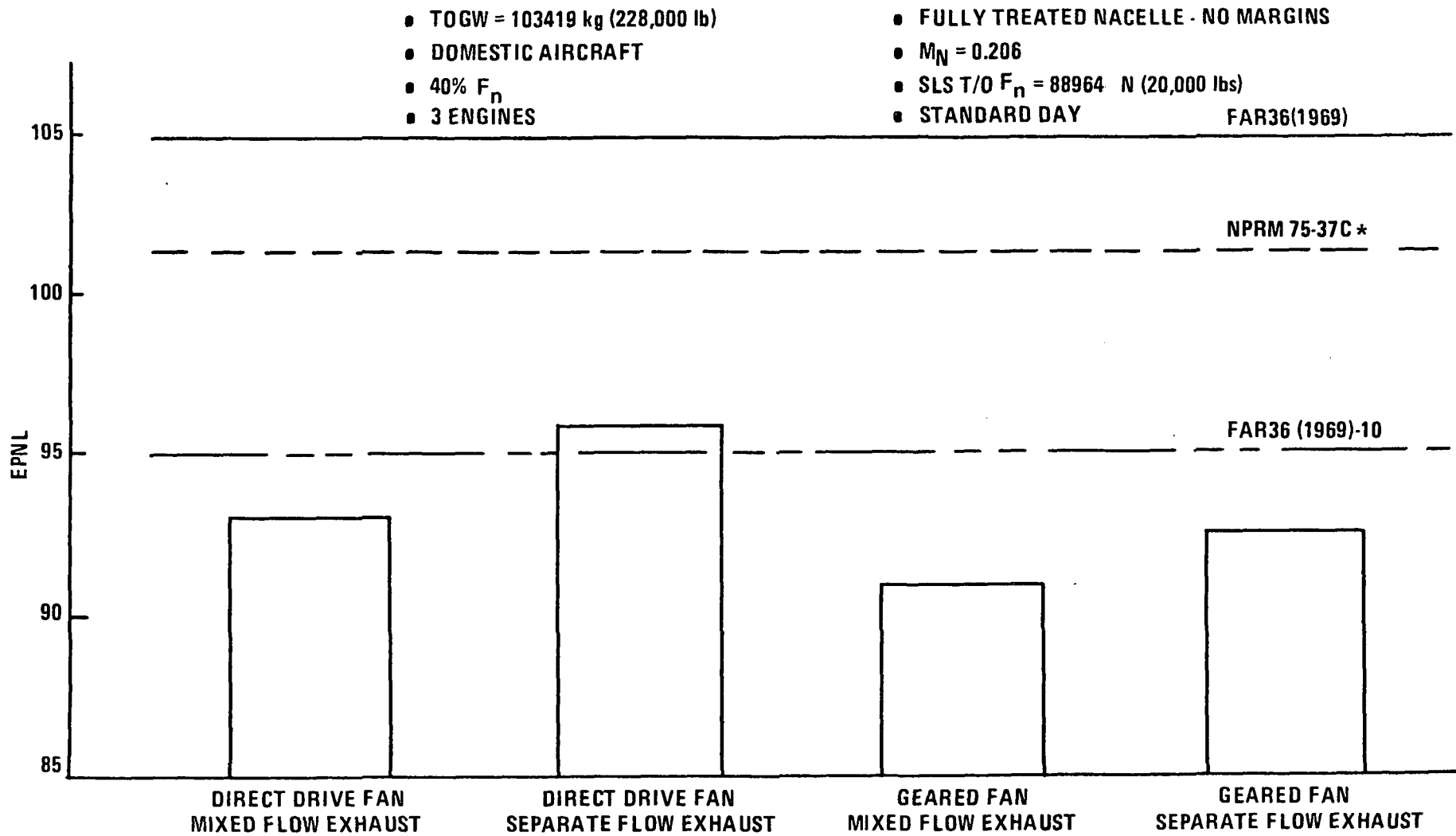


Figure 12. Approach, Estimated Noise Levels - Domestic Aircraft

\*Similar to FAR 36 (1977)

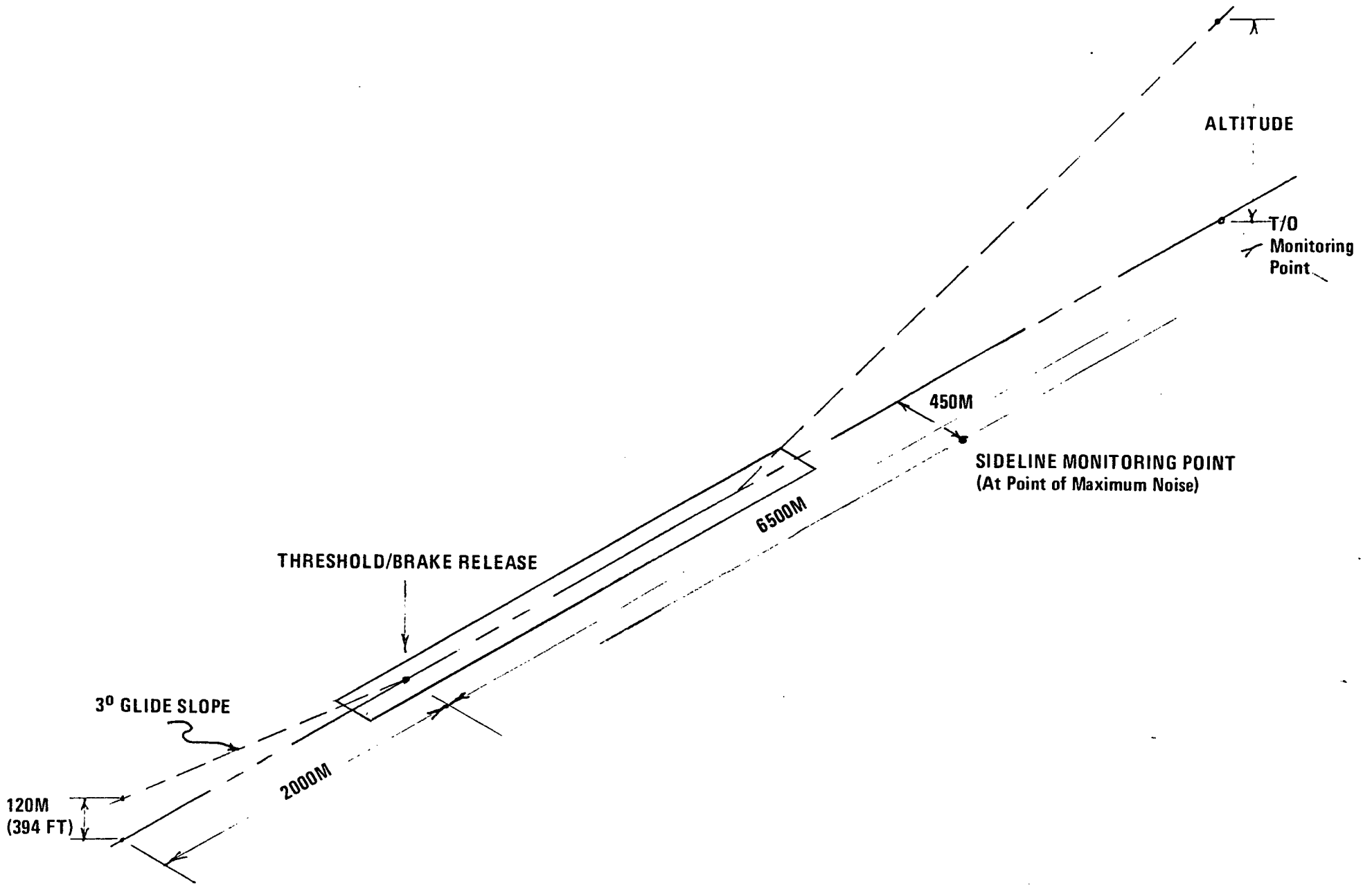


Figure 13 NPRM 75-37C Proposed Monitoring Point Locations

Growth takeoff noise levels are illustrated in Figure 14. Note that only the geared-fan mixed-flow engine falls below the FAR 36-10 level and cutback is required to achieve that. Gearbox noise was not included in this evaluation or any of the geared engine work in this report. The gear noise was assumed to be much lower than other sources of noise and, therefore, not a problem.

In all of the cases discussed above (and throughout this report), noise levels are presented without an engineering margin. In practice, a 3 to 5 PNdB margin would be required to ensure noise certification compliance. The noise estimation procedure used in these studies has been developed by General Electric for preliminary design efforts in which specific component and suppression spectra are not defined. Component and suppression estimates are made on the basis of PNL. The PNdB levels are summed logarithmically to obtain a total system PNL which is then corrected to EPNL using an empirical relationship. For the PNL to EPNL correction, the total inflight spectrum is assumed to be primarily broadband in nature and requires no significant tone correction.

## 6. Mission Evaluation

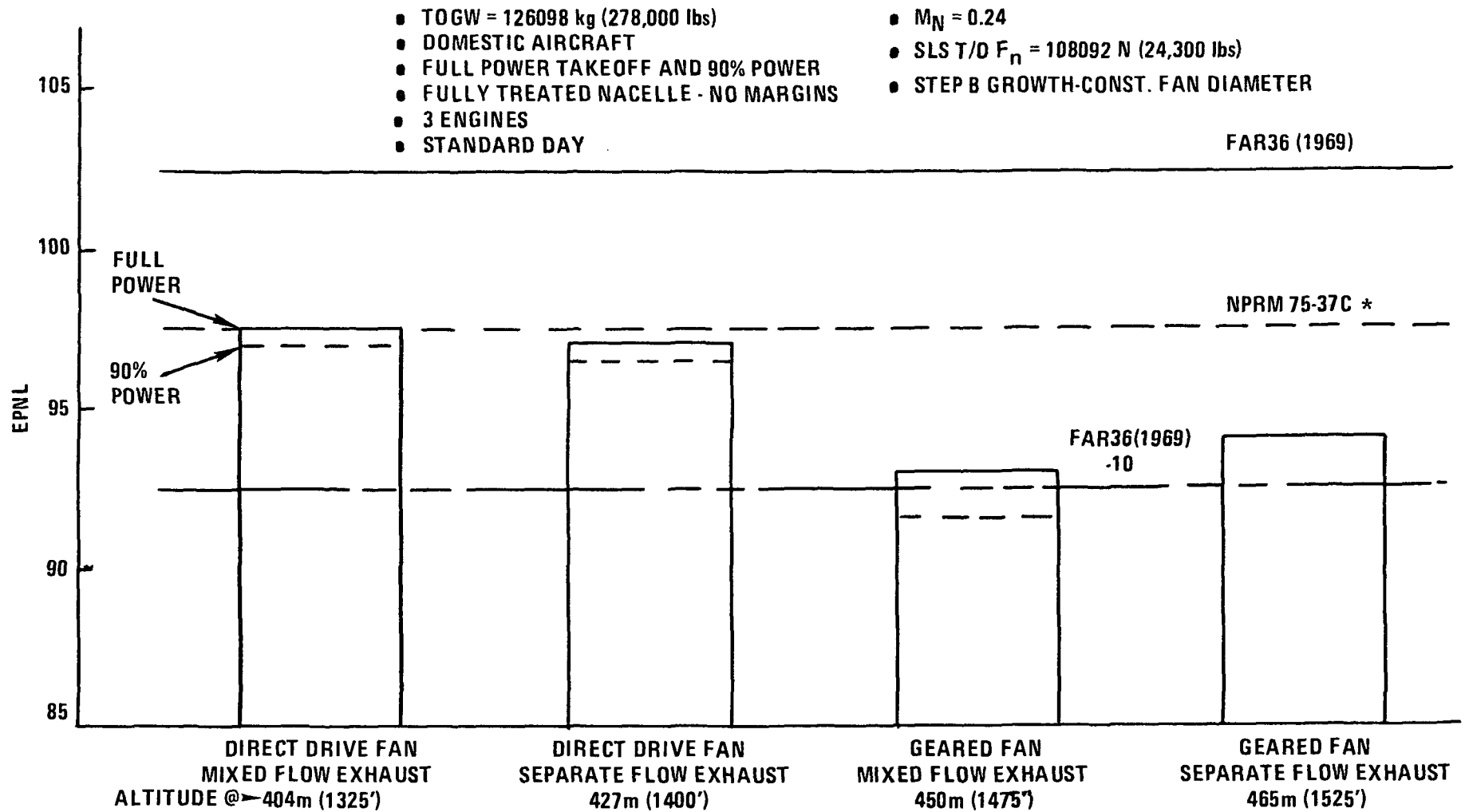
Table 11 summarizes the relative characteristics of the four candidate advanced engines utilized in the mission evaluation.

Advanced technology aircraft defined in Reference 1 were used in the mission evaluation for Task I. Table 12 summarizes principal design features for the two aircraft; domestic and intercontinental. Average mission trade factors for the two aircraft are shown in Table 13. These trade factors are identical to those used in Reference 1 with adjustments in economic factors to 1977.

Because of many indeterminate factors, including inflation and competitive pressures, influence engine pricing, no attempt was made to define advanced engine price relative to current engines at this time. Instead, the evaluation results are shown in Figure 15 as a function of maintenance cost and price differentials to the reference CF6-50C engine. While the DOC reduction goal of 5% is obviously achievable in the intercontinental aircraft, it is apparent that the advanced engine price and maintenance cannot greatly exceed the CF6-50C values in the domestic aircraft if the 5% goal is to be met. Mission benefit evaluation, including estimated price and maintenance  $\Delta$ 's for a comparative mission of the advanced engines, is shown in Figure 16. It is estimated that the geared-fan mixed-flow engine has a fuel use advantage of 3 to 4% over the baseline direct-drive mixed-flow engine. However, the economics are within 1/2 percent of the baseline engine with the geared engine being poorer in the domestic aircraft and slightly superior in the intercontinental aircraft.

### C. Conclusions/Recommendations

Based upon Task I results, both the direct-drive and geared-fan versions of the mixed-flow engines were selected for refinement in the Task II engine-airframe integration study. Although the geared-fan mixed-flow engine shows potential for greater fuel saving, the economics and customer acceptability of such an engine require further study.



6.482 km (3.5 NMI)

Figure 14. Growth at Takeoff, Estimated Noise Levels - Domestic Aircraft

\*Similar to FAR 36 (1977)

TABLE 11

SUMMARY OF CANDIDATE ENGINE CHARACTERISTICS

Installed Max. Climb  $F_{NI} = 37943 \text{ N (8530 lbs)}$  [ $.8 M_n$ , 10668 m (35K), Std. + 10°C(18°F)]

Design Level	Direct Drive Fan		Geared Fan	
	Mixed Flow Exhaust	Separate Flow Exhaust	Mixed Flow Exhaust	Separate Flow Exhaust
$\Delta F_n$ SLS T/O	Base * ↓	+4%	+8%	+11%
$\Delta$ sfc Installed 35K, $M_n .8$ Max CR		+2.2%	-5%	-1%
$\Delta$ Weight Installed		+11%	+19%	+29%
$\Delta$ Price Installed		+5%	+10%	+13%
$\Delta$ Maintenance Cost		+9%	+6%	+7%
Noise				
Takeoff } Domestic		+ .6 $\Delta$ EPNL	-4.2 $\Delta$ EPNL	-3 $\Delta$ EPNL
Approach } A/C		+3 $\Delta$ EPNL	-2.1 $\Delta$ EPNL	-.5 $\Delta$ EPNL
Emissions Takeoff $\Delta$ HC/CO/ $NO_x$		0/0/+ .1	-.2/0/-.5	-.2/0/-.5

\*Base levels in above table are:

$F_D$	154798 N (34800 lbs)
sfc	0.0611 Kg/N-hr (0.599 lb/lb-hr)
Weight	3647 Kg (8040 lbs)
Price	
Maintenance	
Noise Takeoff	94.6 dB EPNL
Approach	93.1 dB EPNL
Emissions HC	2.4 Kg/1000 Kg-hr
CO	0.25 Kg/1000 Kg-hr
$NO_x$	3.5 Kg/1000 Kg-hr

TABLE 12

GE STUDY AIRCRAFT DESCRIPTION

	<u>Transcon Trijet</u>	<u>Intercon Quadjet</u>
● Technology Level	Advanced* $\xrightarrow{\hspace{10em}}$	
● Design Range	5556 km (3000 N. Mi)	10,186 km (5500 N. Mi)
● Cruise Altitude	10,668 m (35,000 ft.)	10,668 m (35,000 ft.)
● Cruise Mach Number	.80	.80
● TOGW	101,151 kg (223,000 lbs.)	145,109 kg (320,000 lbs.)
● Number of Passengers	200	200
● Design Payload	18,597 kg (41,000 lbs.)	19,502 kg (43,000 lbs.)
● SLS T/O $F_n$ /Engine	88,964 N (20,000 lbs.)	93,413 N (21,000 lbs.)
● Wing Aspect Ratio	12	12
● Cruise L/D Avg.	17	18

\* Based on Boeing Terminal Area Compatible Aircraft Study, NASCR-132068.

TABLE 13

MISSION TRADE FACTORS

	Transcon Trijet				Intercon Quadjet			
Average Mission Range (N. Miles)	1296 Km (700 N. Mi.)				3704 Km (2000 N. Mi.)			
Load Factor (%)	55				55			
Fuel Costs \$/m <sup>3</sup> (¢/Gal)	92.46 (35¢)				118.88 (45¢)			
	<u>Δ'S - %</u>				<u>Δ'S - %</u>			
	DOC	ROI	TOGW	W <sub>f</sub>	DOC	ROI	TOGW	W <sub>f</sub>
1% sfc	.42	-.12	.47	1.09	.71	-.25	.87	1.44
45 Kg (100 lb) Engine/Nacelle Wt.	.17	-.06	.32	.26	.22	-.09	.39	.31
\$1/FLT. Hr - Maint. Cost	.17	-.03	-	-	.19	-.04	-	-
\$1000 Engine/Nacelle Initial Price	.006	-.004	-	-	.005	-.003	-	-

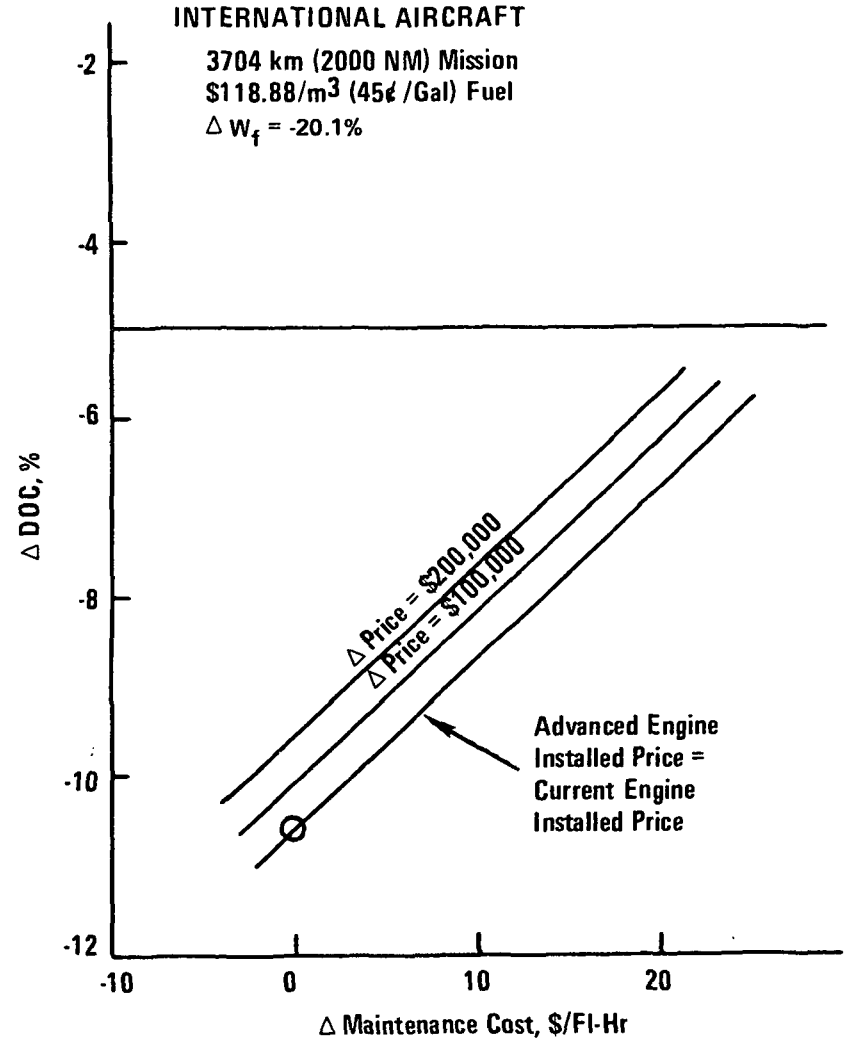
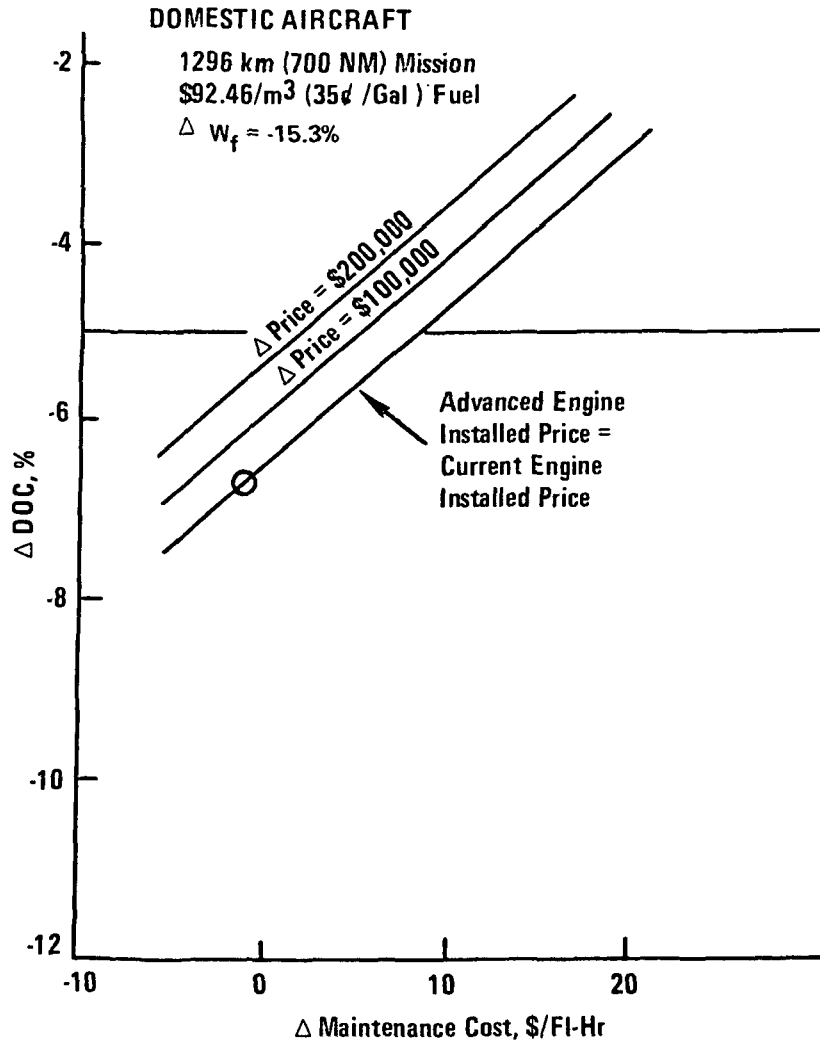
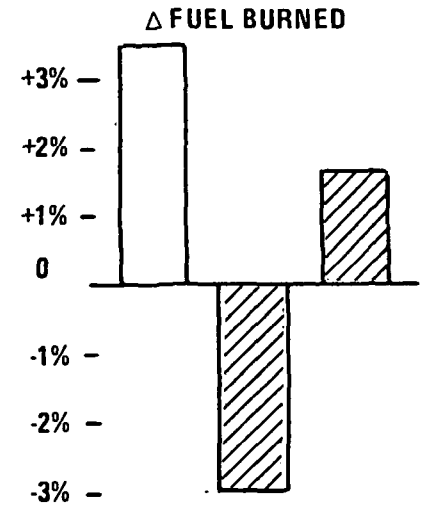
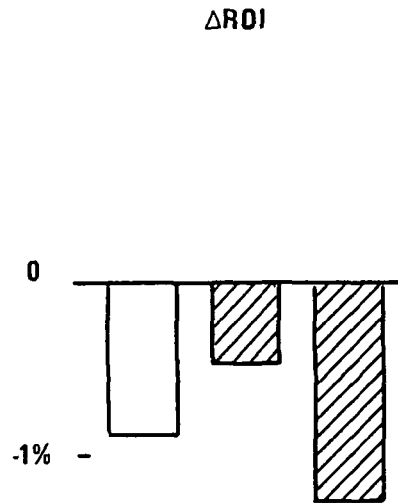
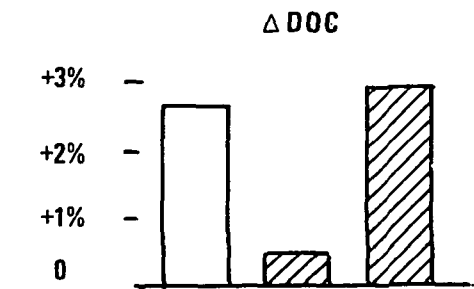


Figure 15. Mission Evaluation - Sensitivity to Price and Maintenance Costs, Advanced Technology Direct-Drive Mixed-Flow Engine vs Current Technology CF6-50C Engine (Scaled), 200 PAX Advanced Tech A/C, 55% Load Factor



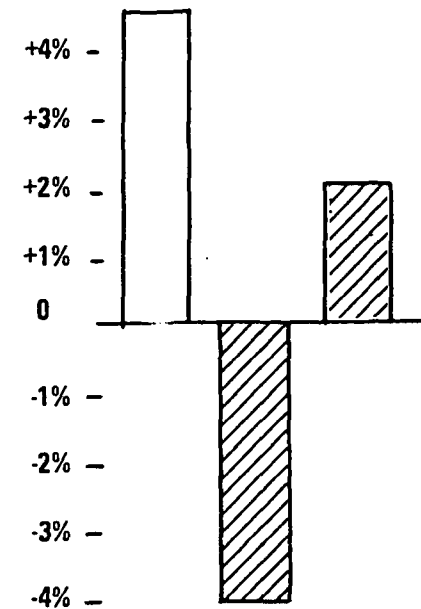
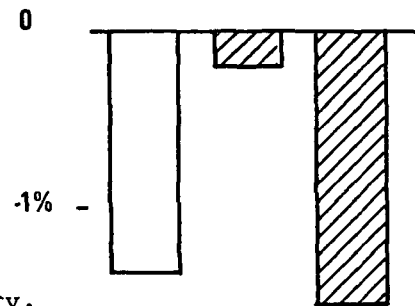
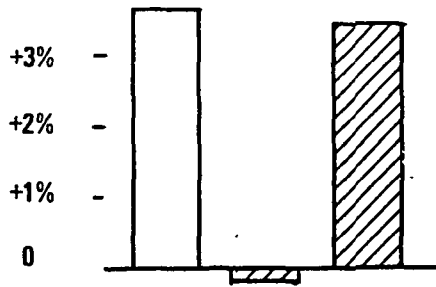


DOMESTIC

DIRECT GEARED GEARED  
SEPARATE MIXED SEPARATE

DIRECT GEARED GEARED  
SEPARATE MIXED SEPARATE

DIRECT GEARED GEARED  
SEPARATE MIXED SEPARATE



INTERCON

Figure 16. Mission Evaluation Summary, Comparisons with Direct-Drive Mixed Turbofan.

TABLE OF CONTENTS

	<u>PAGE NO.</u>
SECTION IV . . . . .	51
TASK II - ENGINE AIRFRAME INTEGRATION . . . . .	51
A. Introduction/Approach . . . . .	51
B. Significant Results . . . . .	51
1. Advanced Technology Direct-Drive Turbofan . . . . .	51
a. Engine and Installation Design Features . . . . .	51
b. Performance . . . . .	55
c. Fan Tip Speed and LPT Staging Study . . . . .	55
d. Turbine Inlet Temperature Study . . . . .	62
e. Weight Comparison . . . . .	62
f. Growth . . . . .	70
g. Exhaust Emission Estimates . . . . .	70
h. Noise Estimates . . . . .	70
i. Mission Evaluation . . . . .	74
2. Advanced Technology Geared Drive Turbofan . . . . .	82
a. Engine and Installation Design Features . . . . .	82
b. Performance . . . . .	82
c. Weight Comparison . . . . .	82
d. Engine Cost Factors . . . . .	90
e. Growth . . . . .	90
f. Exhaust Emission Estimate . . . . .	90
g. Noise Estimates . . . . .	90
h. Mission Evaluation . . . . .	90
i. Overall Comparison of Direct-Drive and Geared Engine . . . . .	98
3. Alternate Engine Configuration/Cycles for Reduced Noise . . . . .	98
a. Lower Fan Pressure Ratio . . . . .	98
b. Increased Duct Length and Blade and Vane Solidity . . . . .	106
c. FAR36 (1969) -10 to -15 EPndB Suppression Study . . . . .	106
1. Penalties . . . . .	106
2. Cycle and Performance Evaluation . . . . .	113
3. Installation Evaluation . . . . .	117
4. Acoustic Evaluation . . . . .	118
C. Summary of Aircraft Subcontractor Studies . . . . .	124
D. Conclusions/Recommendations . . . . .	137

LIST OF FIGURES  
SECTION IV  
TASK II - ENGINE-AIRFRAME INTEGRATION

<u>FIGURE NO.</u>	<u>TITLE</u>	<u>PAGE NO.</u>
17	Advanced-Technology Baseline Engine: Direct-Drive Fan and Mixed-Flow Exhaust	52
18	Advanced-Technology Baseline Engine Installation	53
19	Fan Tip Speed and LPT Stage Selection, Domestic A/C	61
20	Direct-Drive - Mixed-Flow - Advanced Technology $\Delta\%$ sfc Installed vs $T_{41}$ Level	63
21	Direct-Drive - Mixed-Flow - Advanced Technology $\Delta\%$ Weights vs $T_{41}$ Level	64
22	Direct-Drive - Mixed-Flow - Advanced Technology $\Delta\%$ Costs vs $T_{41}$ Level	65
23	Direct-Drive - Mixed-Flow - Advanced Technology $\Delta\%$ DOC and $\Delta\%$ ROI vs $T_{41}$ Level	66
24	Direct-Drive - Mixed-Flow - Advanced Technology $\Delta\%$ TOGW and $\Delta\%$ $W_f$ vs $T_{41}$ Level	67
25	Weight Summary, Advanced Technology Direct-Drive	68
26	Advanced Engine Installation, Low Noise Features Mixed-Flow Exhaust	73
27	Aircraft Economics - Advanced Technology Direct-Drive Mixed-Flow Engine vs Current Technology CF6-50C Engine (Scaled)	81
28	Geared Turbofan Design	83
29	Geared Fan Dimensional Comparison with Direct-Drive Engine, Cruise Sized, $F_{NI} = 37050$ N (8330 lb) @ $M_{xCl}$	84
30	Geared Engine Weight Comparison with Direct-Drive Engine	89
31	Geared Engine Price Comparison with Direct-Drive Engine	91
32	Geared Engine Maintenance Cost Comparison with Direct-Drive Engine	92
33	Geared Fan Evaluation Sensitivity to Fuel Price, Relative to Direct-Drive Engine	99
34	Sensitivity to Gearset Price and Maintenance Cost, Domestic A/C, Average Mission	100
35	Low Fan Pressure Ratio Comparison with Baseline	102
36	Economic Penalties of Additional Noise Suppression Full Power Takeoff	109
37	Economic Penalties of Additional Noise Suppression 36% Approach Power	110
38	Max Cruise $\Delta W_f$ and $\Delta DOC$ vs Takeoff Noise	114
39	Highly Suppressed Engine, Nacelle Drag, $M .8/35K$	120
40	$E^3$ Exhaust System Schematic	121
41	Cycle Effect on Takeoff Noise	125
42	Cycle Effect on Approach Noise with Aircraft Noise Included	126
43	Cycle Effect on Approach Noise without Aircraft Noise	127

LIST OF FIGURES  
SECTION IV - CONTINUED

<u>FIGURE NO.</u>	<u>TITLE</u>	<u>PAGE NO.</u>
44	Aircraft Gross Weights, Advanced Direct-Drive Engine	130
45	Engine Thrust Sizes, Advanced Direct-Drive Engine	131
46	Estimated Economic Improvements of Advanced Direct-Drive Engine vs Reference Engine (Scaled CF6-50C)	133
47	Noise Summary - Direct-Drive Advanced Engine Including A/C Noise, No Margins	135

LIST OF TABLES  
SECTION IV  
TASK II - ENGINE AIRFRAME INTEGRATION

<u>TABLE NO.</u>	<u>TITLE</u>	<u>PAGE NO.</u>
14	Engine Dimensions and Staging	54
15	Advanced Technology Engine Direct-Drive Mixed Advanced Design Features	56
16	Advanced Technology Engine Installation Design Features	57
17	Overall Performance Parameters	58
18	Overall Performance Summary	59
19	Advanced Technology Engine, Direct-Drive, Nacelle Drag (W/O Pylon) 0.8/10668 m (35K ft) Max. Cruise	60
20	Propulsion System Weights	69
21	Advanced Direct-Drive Mixed-Flow Engine Growth Pattern	71
22	Advanced Direct-Drive Mixed-Flow Engine	72
23	Estimated Engine Noise, Advanced Technology Direct-Drive Mixed-Flow Engine	75
24	Advanced Technology Direct-Drive Engine Growth	76
25	Economic Evaluation of Advanced Direct-Drive Engine vs Current Engine (CF6-50C) in General Electric Domestic Trijet	77
26	DOC Percentage Breakdown Based on GE Studies for Domestic Trijet	78
27	Economic Evaluation of Advanced Direct-Drive Engine vs Current Engine (CF6-50C) in General Electric International Trijet	79
28	DOC Percentage Breakdown Based on GE Studies for International Trijet	80
29	Task II Geared-Fan vs Direct-Drive Engine Components	85
30	Gear Technology Comparison	86
31	Task II Geared Fan vs Direct-Drive Performance Comparison-Mixed-Flow	87
32	Source of Geared Fan sfc Reduction Relative to Task I Direct-Drive/Mixed-Flow Engine	88
33	Geared Fan Growth Pattern - Constant Fan Diameter	93
34	Geared Fan Emissions Summary	94
35	Geared Fan Noise Estimates Including A/C Noise - No Margin	95
36	Geared Fan Mission Evaluation, Domestic Aircraft	96
37	Geared Fan Mission Evaluation, Intercontinental Aircraft	97
38	Summary of Comparison Between Advanced Geared and Direct-Drive Engine and CF6-50C Installed on Domestic Transport	101
39	Lower Pressure Ratio vs Direct-Drive Engine Components	103
40	Lower Fan Pressure Ratio Performance vs Baseline Direct-Drive Engine	104
41	Lower Fan Pressure Ratio Evaluation, Domestic Aircraft	105

LIST OF TABLES  
SECTION IV - CONTINUED

<u>TABLE NO.</u>	<u>TITLE</u>	<u>PAGE NO.</u>
42	Lower Fan Pressure Ratio Direct-Drive Engine Noise Estimates, General Electric Study Aircraft	107
43	Lower Fan Pressure Ratio Noise Suppression Study Summary	108
44	Suppressed Engine Dimensions	111
45	Suppressed Engine Performance	112
46	$\Delta$ DOC Breakdown for Suppressed Engines	115
47	Cycle and Low Spool Component Performance Summary	116
48	Parametric Engine Noise Evaluation Nacelle Geometries	119
49	Exhaust System Internal Pressure Loss Summary	122
50	Scaled Thrust and Noise Checkpoint Altitude	123
51	Aircraft Designs Based on Advanced Direct-Drive Engines	128
52	Mission Performance, Advanced Direct-Drive vs Scaled CF6-50C	132
53	Noise Summary, Direct-Drive Mixed - Baseline Suppression, A/C Noise Included	134
54	Engine Thrust Matching - Advanced Direct-Drive Engine	136

SECTION IV

TASK II - ENGINE-AIRFRAME INTEGRATION

A. Introduction/Approach

In Task II, engine-aircraft integration studies were conducted, taking into account results of studies by Boeing, Douglas, and Lockheed under subcontract to General Electric. Domestic and intercontinental missions with corresponding advanced aircraft configurations were selected using General Electric and subcontractor study results. Advanced technology engines were compared with a scaled current technology reference engine in these missions. The CF6-50C, which is General Electric's most modern engine in commercial transport service, was used as the reference engine.

Advanced engines, selected with agreement by NASA, were the mixed-flow direct-drive and mixed-flow geared-fan engines. These engines were refined beyond Task I levels. Alternate cycle and acoustic performance variations were studied to define economics and fuel consumption sensitivities of selected noise-related parameters. In all cases, noise levels are presented without an engineering margin. In practice, a 3 to 5 PNdB margin would be required to ensure noise certification compliance.

Cycle selections were based on prior contract studies and were chosen to balance fuel usage, DOC, growth capability, and noise. The engine and installation technology was also based on previous contract and in-house studies. Core size of the advanced engines was designed at 54.4 kg/sec (120 pps) and scaled as required for mission evaluation. Direct-drive and geared engines had an identical core design except for scale size. Fan and low pressure turbine technology was also kept consistent to the extent possible on these engines.

B. Significant Results

1. Advanced Technology Direct-Drive Turbofan

a. Engine and Installation Design Features

The direct-drive mixed-exhaust baseline advanced engine evolved directly from the Task I study counterpart engine. The engine cross-section is shown in Figure 17 and the corresponding installation section is in Figure 18. These views may be compared with Figure 1 of the Task I section of this report which shows the installed CF6-50 reference current technology engine. Dimensions and staging of these engines are summarized in Table 14. The primary change in Task II was the use of a more lightly-loaded five-stage low pressure turbine instead of a four-stage turbine. Study indicated that an improvement of about 1% in sfc and fuel usage was obtainable without a DOC penalty by making this LPT change. Mechanical studies indicated the five-stage close-coupled turbine would have satisfactory rotor dynamics with the desired two-frame support system.

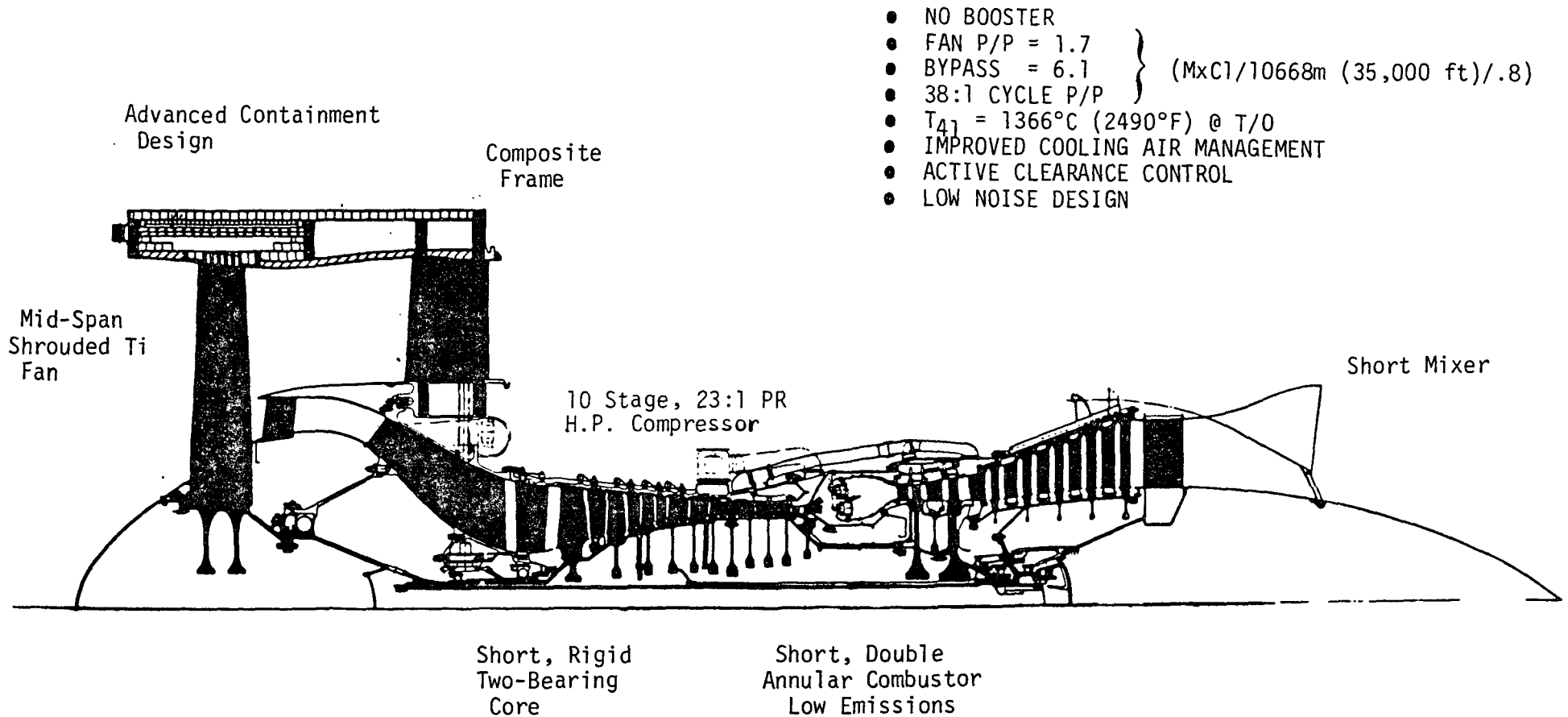


Figure 17. Advanced-Technology Baseline Engine: Direct-Drive Fan and Mixed-Flow Exhaust



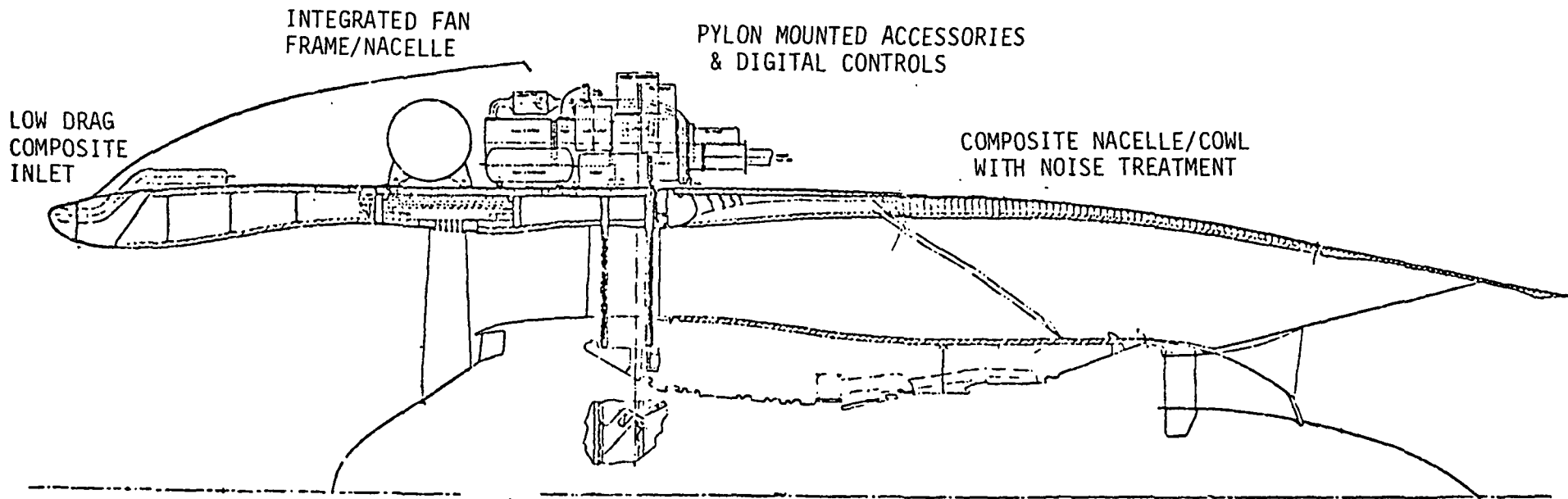


Figure 18. Advanced-Technology Baseline Engine Installation

TABLE 14

ENGINE DIMENSIONS AND STAGING

Equivalent Max. Cl. FN @ 35 10668 m (35K ft) .8 M<sub>n</sub> Std. + 10°C (18°F) Day

	<u>Current Engine (CF6-50 Scaled)**</u>	<u>Baseline Engine Direct-Drive Mixed-Flow</u>
Fan Diameter, meters (inches)	1.948 (76.7)	2.024 (79.7)
Engine Length*, meters (inches)	3.962 (156)	3.048 (120)
No. Stages:		
Fan/LPC/HPC/HPT/LPT	1/3/14/2/4	1/0/10/2/5
Total	24	18
No. of Frames/Bearings	4/8	2/5

\*Flange to Flange

\*\*CF6-50 Scaled to Same MxCl Thrust Level as Baseline Engine

Other design and materials changes were made in the engine, particularly in the hot section, to improve the balance between performance, cost, and maintenance features, and to incorporate results of concurrent materials benefit studies. Design features are shown in Table 15 with asterisks at the items changed in Task II. Active clearance control was added to the aft-casing of the compressor.

High pressure turbine blade dovetails were changed from curved to straight for cost reduction. HPT vanes went from integrally cast sectors to brazed vanes in separate bands to improve structural support and maintainability.

Stage 1 HPT rotor cooling was changed from expander type to side-plate compressor type for mechanical simplification and improved coolant air pressure delivery. Stage 2 HPT rotor cooling was changed from bore-entry to side-plate type for similar reasons.

In the low-pressure turbine, addition of a fifth stage was the major change, but cooling was added to the stage 1 vanes, stator casing cooling was added, and some materials were also changed.

Installation design for the advanced engines includes several advancements over current technology as shown on Table 16. Accessories are arranged to fit within the pylon.

#### b. Performance

The cycle at the primary operating conditions is compared with the reference CF6-50C in Table 17. The advanced engine operates at the same takeoff overall pressure ratio as does the CF6-50C. At maximum climb and cruise, however, it operates at substantially higher pressure and turbine inlet temperatures. This reduces the takeoff thrust relative to cruise thrust, but provides better sfc at the cruise condition. Table 18 shows that uninstalled cruise sfc is 11.1% better than the current engine, and that installed cruise sfc including isolated nacelle drag is 12.1% better.

Nacelle drag is less on the advanced engine because the mixed flow exhaust eliminates scrubbing drag at the aft core cowl and this is a stronger factor than the increase in the pressure and friction drag on the fan cowl aft exterior. Table 19 shows a breakdown of these nacelle drag components.

#### c. Fan Tip Speed and LPT Staging Study

Sensitivity of economics and fuel usage to fan tip speed and LPT staging was evaluated in Task II as shown on Figure 19. At each speed studied the engine was resized to account for changes in fan efficiency, bypass ratio, fan turbine loading and efficiency, and installation characteristics. Weights, costs, maintenance cost and FOD resistance were estimated.

TABLE 15

ADVANCED DESIGN FEATURES OF BASELINE ENGINE: DIRECT-DRIVE FAN, MIXED-FLOW EXHAUST

- FAN
  - Mid-Span Shrouded Ti Blades
  - Composite Outer Vane Frame Integrated with Nacelle
  - High Hub Boost
- COMPRESSOR
  - High P/P on One Rotor
  - 23:1 P/P in 10 Stages
  - Active Clearance Control on Aft Casing\*
  - Low Aspect Ratio Rugged Blades
- COMBUSTOR
  - Double Annular for Emissions
- HIGH PRESSURE TURBINE
  - Adv. Ni-Base DS Cast Blades
  - Straight Dovetails on Blades\*
  - MA754/Rene' 125 Vanes\*
  - Side Plate Compressor Cooling - Stage 1\*
  - Side Plate Compressor Cooling - Stage 2\*
  - Active Clearance Control
  - Ceramic Shrouds
  - Long Life Design\*
  - Cooling System Design Not\* Sized for Growth Engine
- LOW PRESSURE TURBINE
  - 5 Stage, Lower Aero Loading\*
  - Stage 1 Vane Cooled Cast
  - Stage 2 Blade Uncooled NI76XB
- MIXER
  - Short Mixing Length
  - Reverse Thrust Spoiler
- CONTROL
  - FADEC - Including Power Management & Condition Monitoring Features

\*Change from Task I

TABLE 16

ADVANCED TECHNOLOGY ENGINE INSTALLATION DESIGN FEATURES

(Refer to Figure 17)

- Thin Inlet,  $D_{HL} / D_{MAX} = 0.88$
- Composite Nacelle
- Pylon Mounted Accessories
- Dual Blocker Cascade Reverser
- Mixed Exhaust - Aerodynamic Spoiling of Core Thrust in Reverse Mode
- Bulk Absorber Acoustic Treatment

TABLE 17

OVERALL PERFORMANCE PARAMETERS

RATING	Current (CF6-50C Scaled)			Task II Baseline Engine (Direct-Drive/Mixed-Flow)		
	T/O	MxC1	MxCr	T/O	MxC1	MxCr
ALTITUDE/ $M_n$	0/0	10668 m (35K ft)/.8 →		0/0	10668 m (35K ft)/.8 →	
Overall Press. Ratio	30	32	30	30	38	36
Turbine Rotor Inlet Temp. °C (°F)	1316 (2400)	1177 (2150)	1160 (2120)	1366 (2490)	1310 (2390)	1268 (2315)
Std + Δ T Day - °C/(°F)	+15 (+27)	+10 (+18)	+10 (+18)	+15 (+27)	+10 (+18)	+10 (+18)
Fan Pressure Ratio	1.71	1.76	1.75	1.53	1.71	1.67
Core Exhaust Velocity, m/sec (ft/sec)	472 (1550)	500 (1640)	497 (1630)	300 (985)	357 (1170)	353 (1158)
Fan Exhaust Velocity, m/sec (ft/sec)	317 (1040)	323 (1060)	320 (1050)			
$F_n$ Max. Climb/ $F_n$ SL .25M	.28			.33		

TABLE 18

OVERALL PERFORMANCE SUMMARY

	<u>Current Engine (CF6-50C Scaled)</u>	<u>Task II Baseline Engine (Direct-Drive/Mixed-Flow)</u>
Exhaust Configuration	Separate	Mixed
Fan Diameter, m (inches)	1.948 (76.7)	2.024 (79.7)
SLS T/O $F_n$ , N (lbs)	176060 (39580)	152350 (34250)
T/O $T_{41}$ °C (°F) Std + 15°C (27°F) Day	1316 (2400)	1366 (2490)
0.8/10668 m (35K ft) Max Climb $F_n$ , N (lbs)	39230 (8820)	38830 (8730)
Drag, N (lbs)	2170 (488)	1780 (400)
Net $F_{NI}$ (Max. Climb - Drag), N (lbs)	37050 (8330)	37050 (8330)
Max. Cruise $F_n$ , 0.8/10668 m (35K ft) N (lbs)	36340 (8170)	36120 (8120)
Bypass Ratio Mx Cl/Mx Cr	4.2/4.3	6.1/6.2
Drag/ $F_n$ Max. Cruise, %	6.0	4.9
Max. Cruise sfc Δ%	Base	-11.1
Max. Cruise sfc Installed Δ%	Base	-12.1

TABLE 19

ADVANCED TECHNOLOGY ENGINE  
 DIRECT-DRIVE  
 NACELLE DRAG (W/O PYLON)  
0.8/10668 m (35 K ft) MAX. CRUISE

	<u>Current</u> <u>CF6-50C Scaled</u>	<u>Task II</u> <u>Baseline Engine</u>
Fan $D_T$ , m (inches)	1.948 (76.7)	2.024 (79.7)
$W\sqrt{\theta/\delta}$ , kg/sec (lb/sec)	544 (1200)	581 (1281)
$F_{NI}$ Max. Climb, N (lb)	37050 (8330)	37050 (8330)
$F_{NI}$ Max. Cruise, N (lb)	34160 (7680)	34340 (7720)
$F_n$ Uninstalled, N (lb)	36340 (8170)	36120 (8120)
$D_{MAX}$ , m (in)	2.479 (97.6)	2.304 (90.7)
L O'ALL, m (in)	6.655 (262)	5.656 (333.7)
$D/F_n$ Pressure, %	1.4	1.8
$D/F_n$ Friction, %	2.3	3.1
$D/F_n$ Scrubbing, %	2.3	-
$D/F_n$ Total, %	6.0	4.9



225 PAX, 1296 km (700 NM) MISSION, 55% LOAD FACTOR  
 \$92.46/m<sup>3</sup> (35¢/Gal) FUEL COST  
 10668m (35k ft)/.80/Std + 10°C (18°F) MAX CRUISE

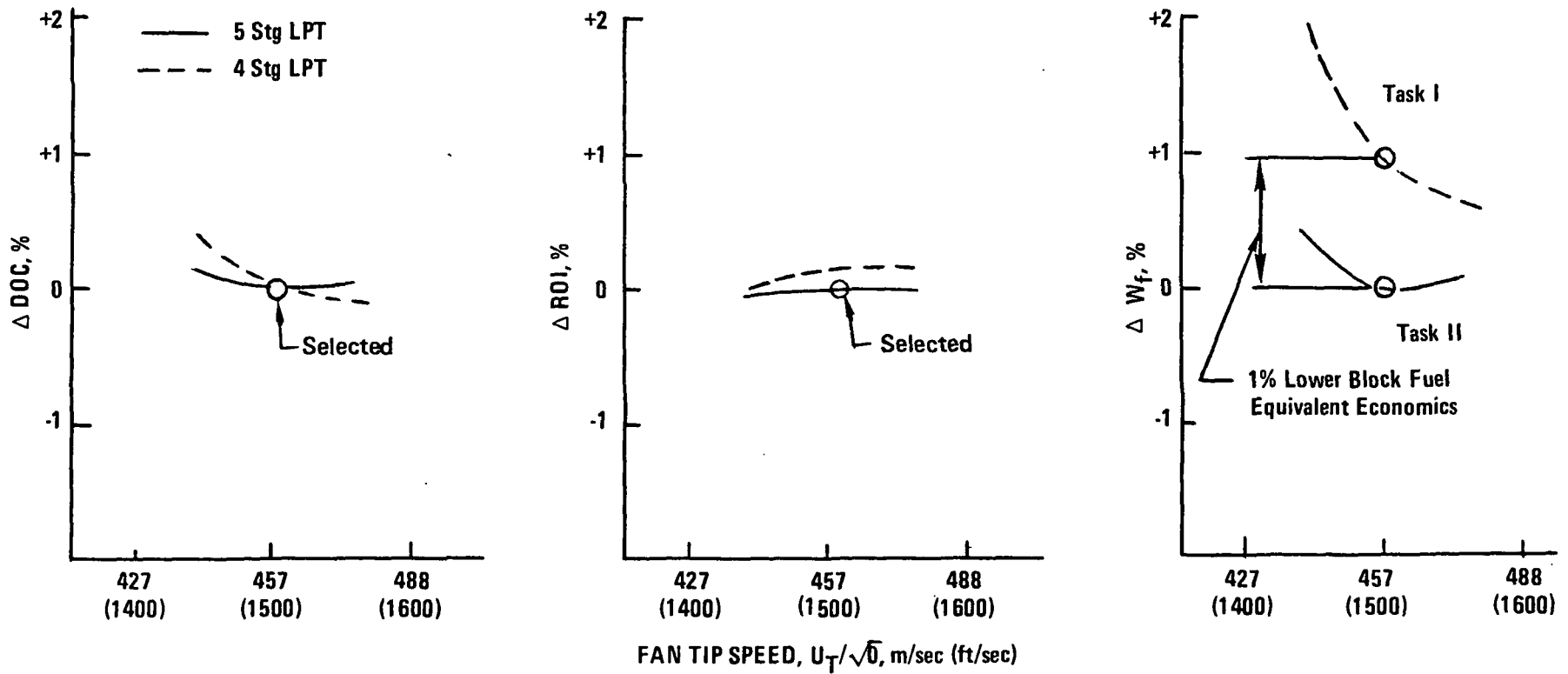


Figure 19. Fan Tip Speed and LPT Stage Selection, Domestic A/C.

For fan blade mechanical integrity, foreign object strike resistance and noise, it was desirable to choose the lowest fan tip speed possible without economic penalties. Figure 19 shows that DOC and ROI are less sensitive to lower tip speed with a five stage LP turbine than with the four stage. The deciding factor, however, was fuel usage. The Task I to Task II change from a 463 m/Sec (1520 fps) fan/4 stage LPT to a 457 m/Sec (1500 fps) fan/5 stage LPT provided 1% lower fuel usage with only slight effect on DOC and ROI.

#### d. Turbine Inlet Temperature Study

Turbine inlet temperature level was also studied in depth in Task II. As cycle temperature is elevated thermal efficiency rises, but this gain tends to be offset by the cost of higher temperature materials, maintenance cost and increased cooling flow. This study was initiated using advanced turbine materials shown to be cost effective in in-house or MATE studies. Turbine rotor inlet temperature,  $T_{4.1}$  (or  $T_{41}$ ) was varied from 1316°C (2400°F) to 1432°C (2700°F); and the engine was resized for each case to account for cooling design and flow changes required to hold constant hot part life. Maximum climb installed thrust was held constant throughout. The result was a lowest SFC near the Task II selected baseline of 1366°C (2490°F), as shown in Figure 20.

Core engine weight at elevated  $T_{4.1}$  drops relative to the fan and installation giving an overall weight reduction as shown in Figure 21.

Engine costs reflect the core size reduction and follow a trend similar to weights, as shown in Figure 22.

For the General Electric domestic aircraft, the effects of sfc, weight, cost and performance give economic factor results as shown in Figure 23. The return-on-investment and direct operating cost curves show a level-off with no significant payoff for  $T_{4.1}$  levels above approximately 1427°C (2600°F). The 1427°C (2600°F) level is therefore planned for growth. Note that higher cost fuel degrades the advantage of higher operating temperature because SFC is poorer and more fuel is being burned.

Fuel usage is minimum near the selected 1366°C (2490°F) temperature as shown in Figure 24.

The trends of economics, fuel usage and takeoff gross weight versus cycle temperature are similar for the Intercontinental Trijet as in the above discussion of the Domestic Trijet.

#### e. Weight Comparison

An 11% lighter installed weight was calculated for the advanced direct drive engine compared to the CF6-50C scaled to the same maximum climb installed thrust. The bar graphs in Figure 25 and weights in Table 20 show that lighter advanced engine nacelle components based upon extensive use of composites account for this weight reduction. Use of composites lightens the fan duct and fan reverser.

Engine weights are nearly equivalent, though the distribution of weight is different. The advanced engine has less core weight, but greater LPT weight. Controls and accessories are expected to be lighter than the CF6-50C.

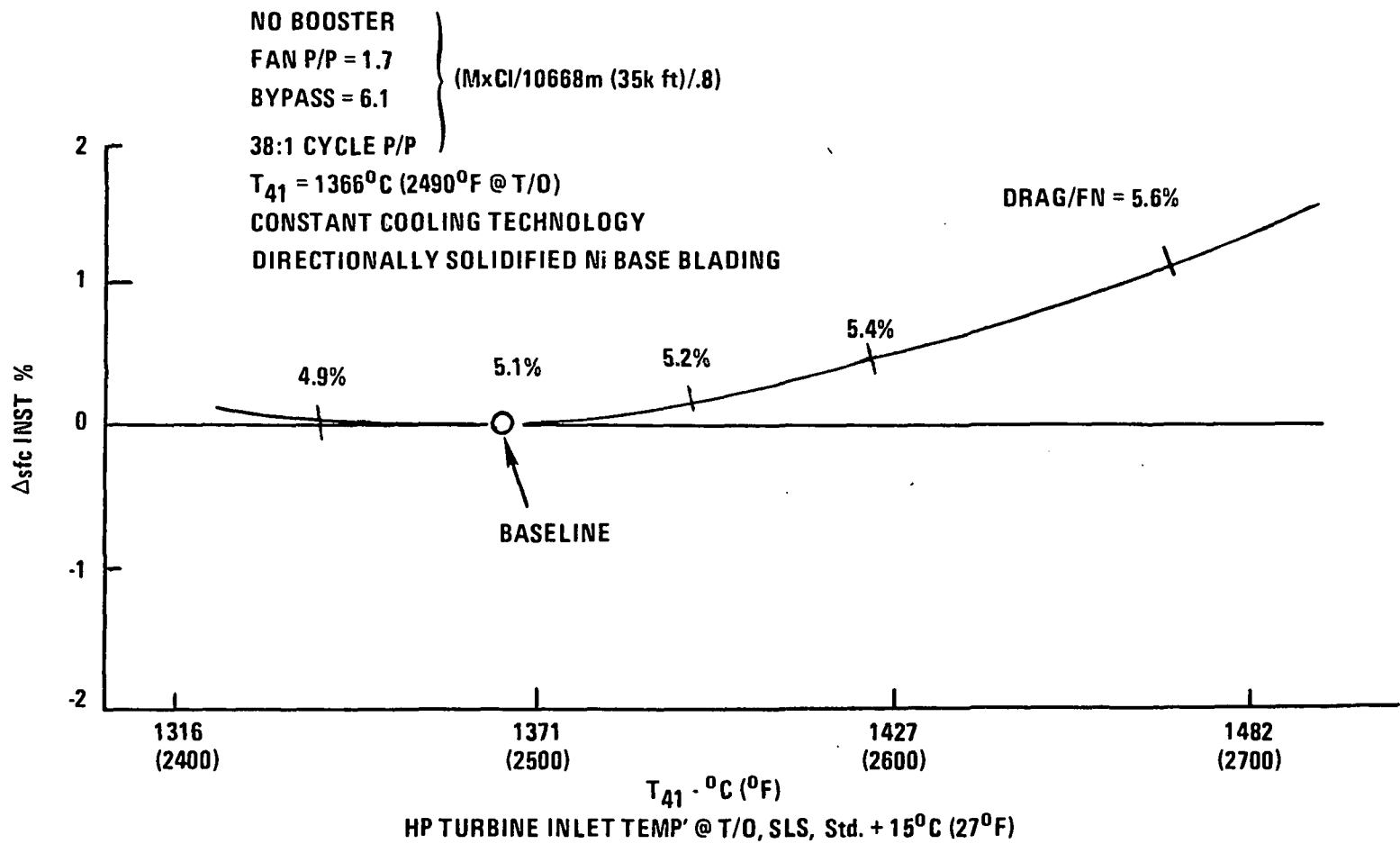


Figure 20. Direct-Drive - Mixed-Flow - Advanced Technology,  
 $\Delta \%$  sfc Installed vs.  $T_{41}$  Level

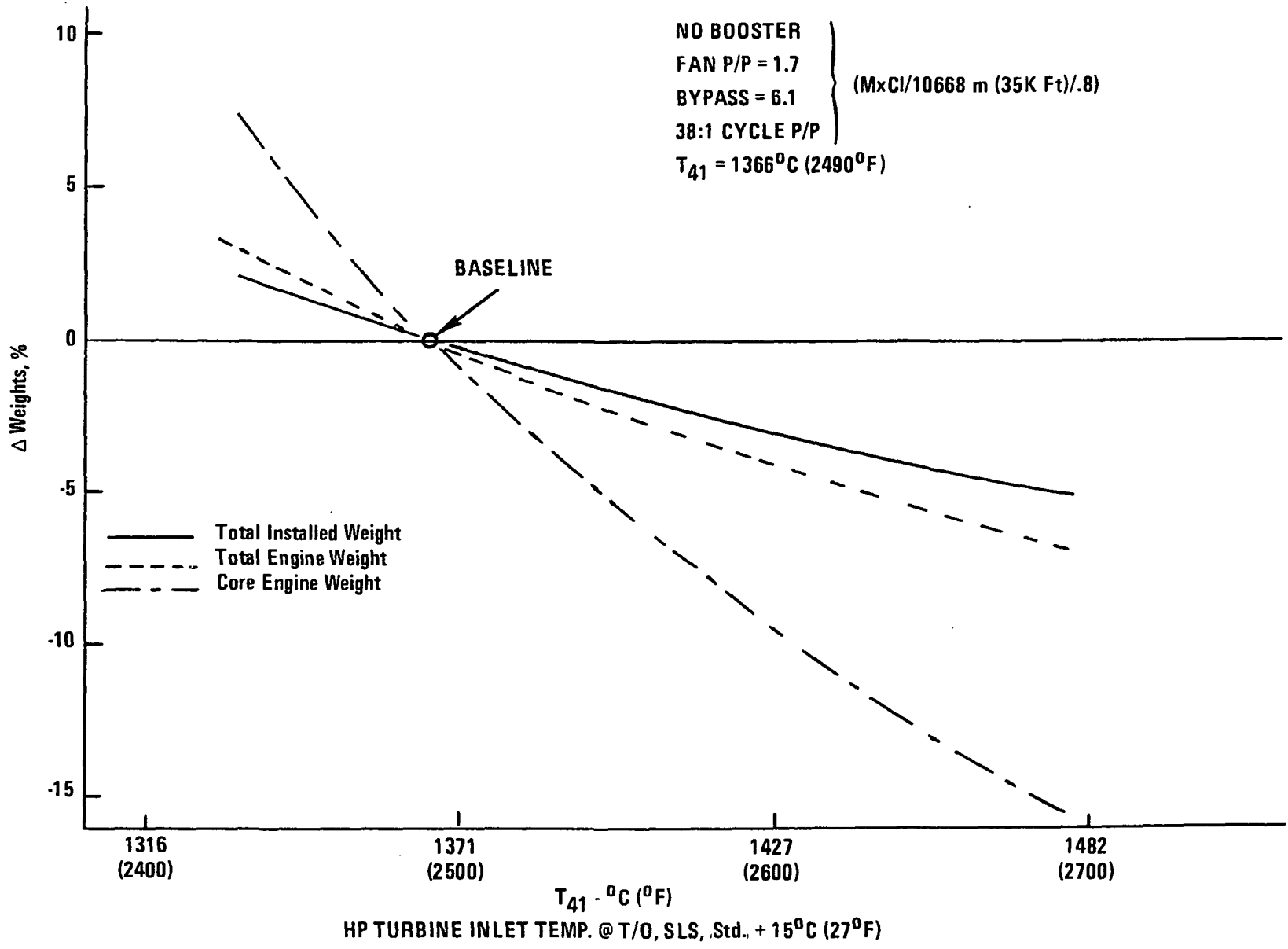


Figure 21. Direct-Drive - Mixed-Flow - Advanced Technology,  
 Δ% Weights vs T<sub>41</sub> Level

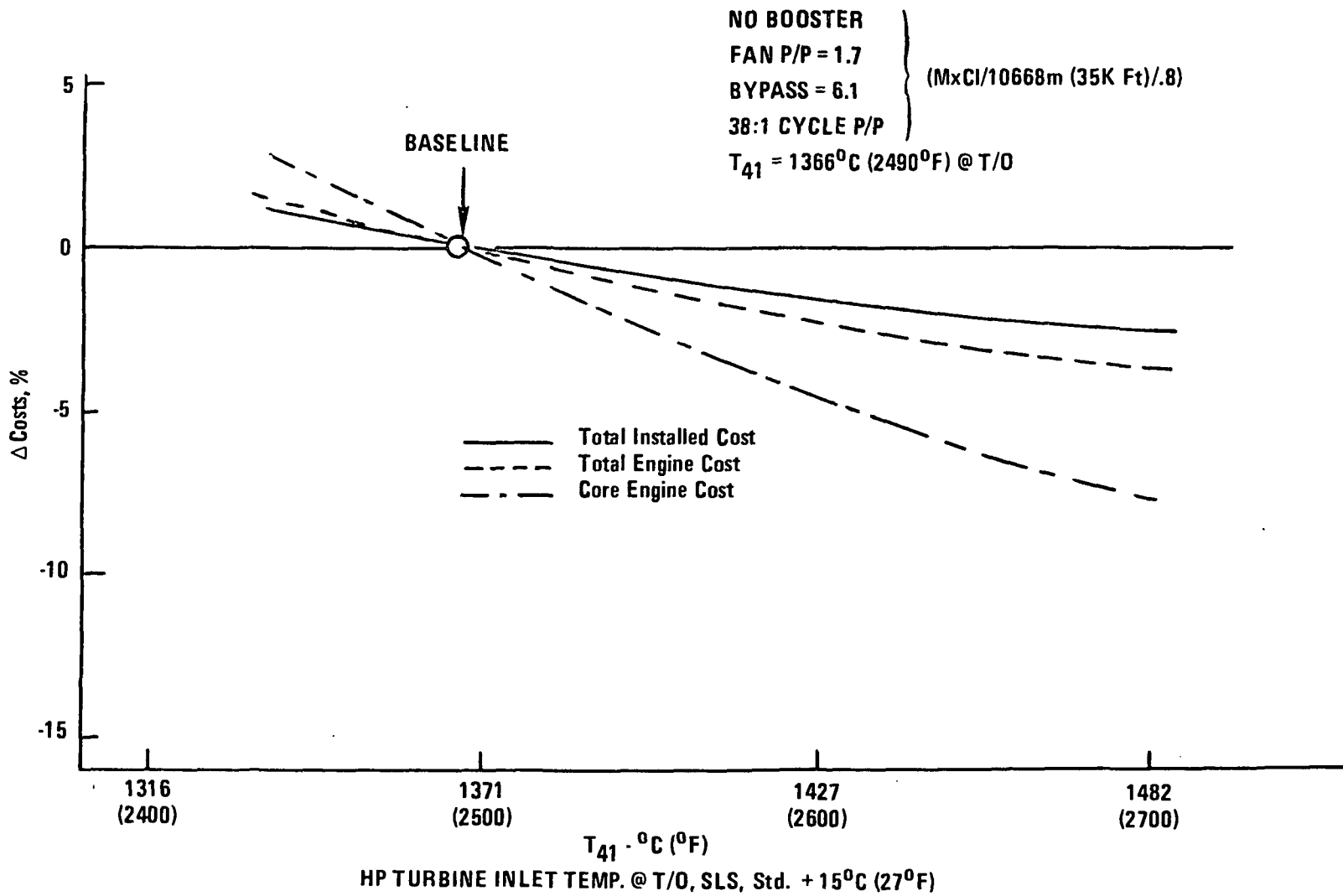


Figure 22. Direct-Drive - Mixed-Flow - Advanced Technology,  
 $\Delta\%$  Costs vs.  $T_{41}$  Level

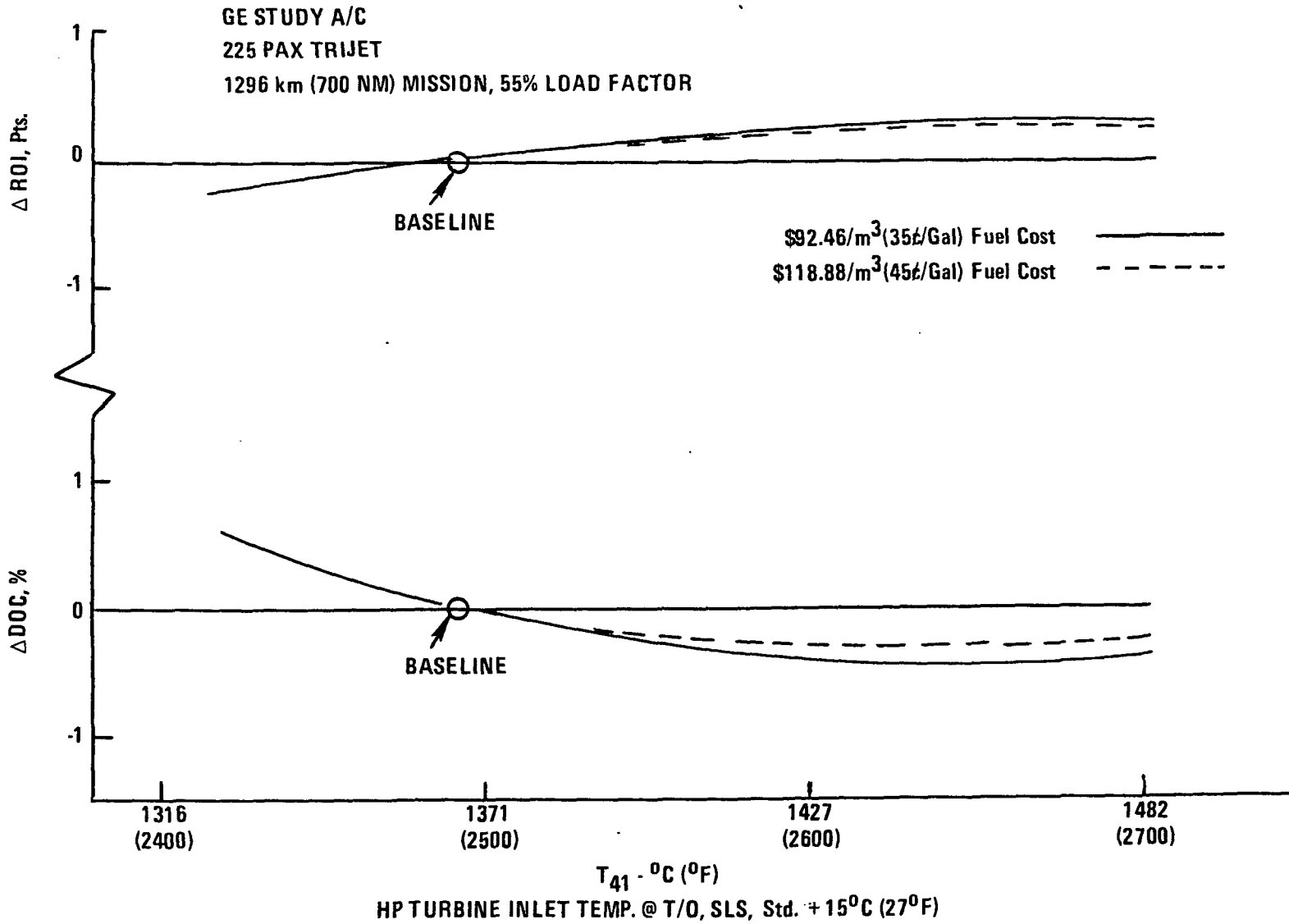


Figure 23. Direct-Drive - Mixed-Flow - Advanced Technology,  $\Delta$ % DOC and  $\Delta$ % ROI vs  $T_{41}$  Level.

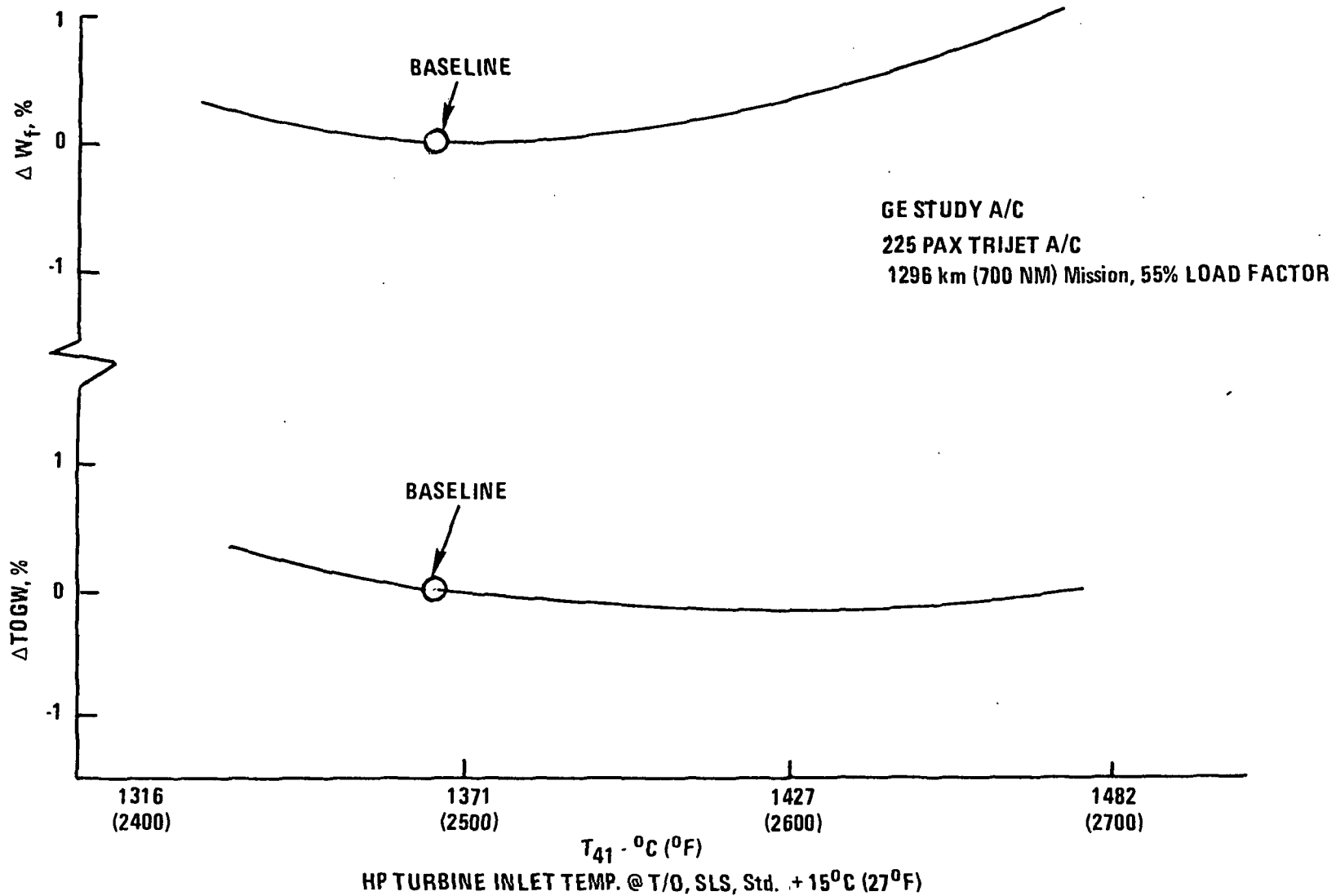


Figure 24. Direct-Drive - Mixed-Flow - Advanced Technology,  
 $\Delta\%$  TOGW and  $\Delta\%$   $W_f$  vs.  $T_{41}$  Level

$F_{NI} = 37050 \text{ N (8330 lbs) } .8/10668 \text{ m (35 K Ft.) MAX CLIMB}$

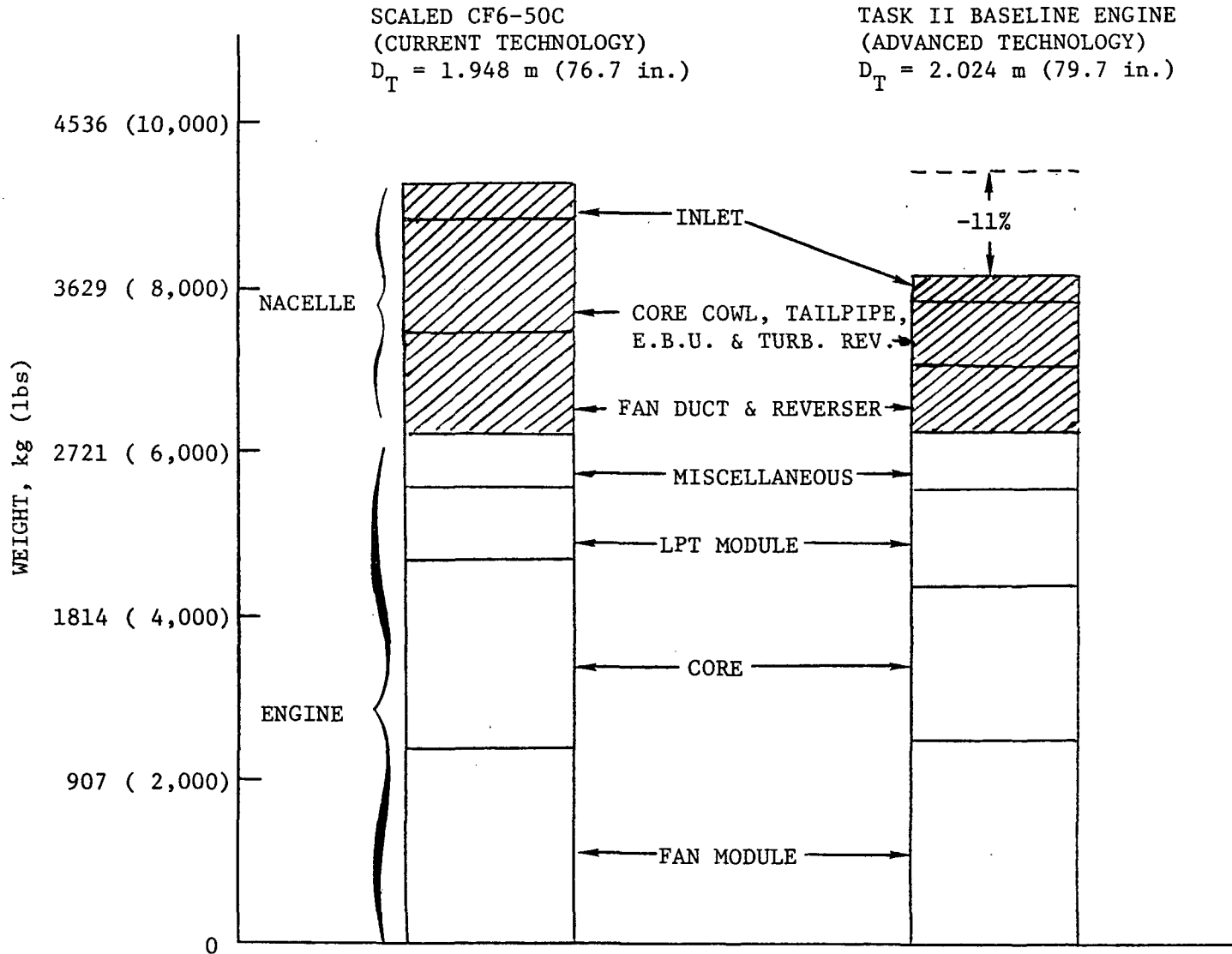


Figure 25. Weight Summary, Advanced Technology Direct-Drive



TABLE 20

PROPULSION SYSTEM WEIGHTS

$$F_{NI} = 37050 \text{ N (8330 lbs) } .8 \text{ M}_n / 10668 \text{ m (35K Ft) MxC1}$$

	<u>CF6-50C</u> (Current Technology)		<u>Task II</u> <u>Baseline Engine</u> (Advanced Technology)	
	Kg	(lbs)	Kg	(lbs)
Inlet	215	( 475)	160	( 352)
Core Cowl, Tailpipe, E.B.U. & Turb. Rev.	601	(1325)	349	( 770)
Fan Duct & Reverser	558	(1230)	379	( 836)
Miscellaneous	298	( 658)	307	( 677)
LPT Module	376	( 829)	540	(1190)
Core	1027	(2265)	871	(1920)
Fan Module	<u>1083</u>	<u>(2388)</u>	<u>1095</u>	<u>(2413)</u>
Total	4158	(9170)	3701	(8158)

#### f. Growth

A growth plan for the engine was formulated as shown in Table 21. The 'Initial Rating' is set at -10% thrust/-56°C (-100°F)  $T_{4.1}$  relative to the 'Design' baseline performance. A simple throttle push accomplishes the increase from initial to design performance level. The use of an initial rating would allow accumulation of experience and design refinement at conservative power output levels.

Step 1 in growth is accomplished by adding a fan shaft booster stage and upspeeding the rotors. No cooling system changes are required.

Growth step 2 is based on operation at higher cycle temperatures made possible by incorporation of a fan redesigned for higher pressure ratio, and by more effective hot part cooling components. Nominally 20% more thrust is provided relative to design size.

An alternate 'growth step 2' was examined to show the effect of increasing fan size with the same core as step 2. Table 21 shows that alternate growth step 2 has 0.6% better SFC than the design cycle, with 23% more thrust. Note that the parameters in Table 21 are for bare engines and that mission analyses of installed growth engines were not conducted. The alternate growth step 2 would have price and drag penalties which would at least partially offset its apparent gains.

#### g. Exhaust Emission Estimates

Emissions of carbon monoxide (CO), hydrocarbon (HC) and nitrous oxides (NOx) were estimated with the advanced technology combustion features with no margins included. Calculations were based on EPA criteria as they existed in early 1977. Results are shown in Table 22 for the baseline, maximum and alternate maximum growth steps. Also shown are effects of scaling the design level thrust from 97,860 to 222,410 N (22,000 to 50,000 pounds).

EPA limits and the methods of calculation of the parameters are changing and are not yet finalized. The emissions data in this report should be used for relative comparisons only.

#### h. Noise Estimates

An estimate of noise was made for the GE domestic and international aircraft using a noise model based on an analysis of current technology engine noise constituents. Noise suppression features and technology expected to be available in the 1980's were employed on the baseline engine as shown on Figure 26.

The noise estimation procedure used in these studies has been developed by General Electric for preliminary design efforts in which specific component and suppression spectra are not defined. Component and suppression estimates are made on the basis of PNL. The PNdB levels are summed logarithmically to obtain a total system PNL which is then corrected to EPNL using an empirical relationship. For the PNL to EPNL correction, the total inflight spectrum is assumed to be primarily broadband in nature and requires no significant tone correction.

TABLE 21

ADVANCED DIRECT-DRIVE MIXED-FLOW  
ENGINE GROWTH PATTERN

	Initial Rating	Design	Step 1 Growth	Step 2 Growth	Step 2 Growth Alternate
$\Delta$ Fan Diameter, m (in)	Base	—————→			.16 (+6.3)
Fan Pressure Ratio (MxC1)	1.62	1.71	1.75	1.84	1.73
$\Delta$ Booster Stages	0	0	+1	+1	+1
Turbine Cooling System	Base	—————→		Reconfigured	Reconfigured
$\Delta$ % $F_n$ Max Climb, Uninstalled	-10	Base	+8.7	+20	+23
$\Delta$ sfc Max Cruise, Uninstalled	-.1	Base	+ .7	+2.6	-.6
$\Delta T_{41}$ , °C (°F) T/O	-56 (-100)	Base	+8 (+15)	+61 (+110)	+61 (+110)
$\Delta P_3$ N/m <sup>2</sup> (psia)/ $T_3$ °C (°F), T/O	-48260/-19 (-7/-35)	Base	+489530/+37 (+71/+67)	+813580/+61 (+118/+110)	+861845/+64 (+125/+116)
$\Delta$ Fan RPM, %	-2.9	Base	+3.1	+4.1	0
$\Delta$ Core RPM, %	-1.6	Base	+2.5	+3.9	+4.1

TABLE 22

ADVANCED DIRECT-DRIVE MIXED-FLOW ENGINEEmissions Estimation - No Margin

	Base Design	+20% MxC1Fn Growth Const. Dia. Fan	+23% MxC1Fn Growth 2.19 m (86.3 in) Dia. Fan
SLS T/O F <sub>n</sub> , N (lbs)	152350 (34250)	177040 (39800)	190160 (42750)

EPA Parameter (No Margin) kg (lbs)/1000 kg-hr (lbs-hr)

CO	1.7	1.2	1.1
HC	.1	.04	.02
NO <sub>x</sub>	3.1	4.7	4.6

Scale Effect From 97860 (22,000) To 222410 (50,000) - Design Level

	97860 (22,000)	152350 (34,250)	222410 (50,000)
CO	1.7	1.7	1.7
HC	.1	.1	.1
NO <sub>x</sub>	2.9	3.1	3.3

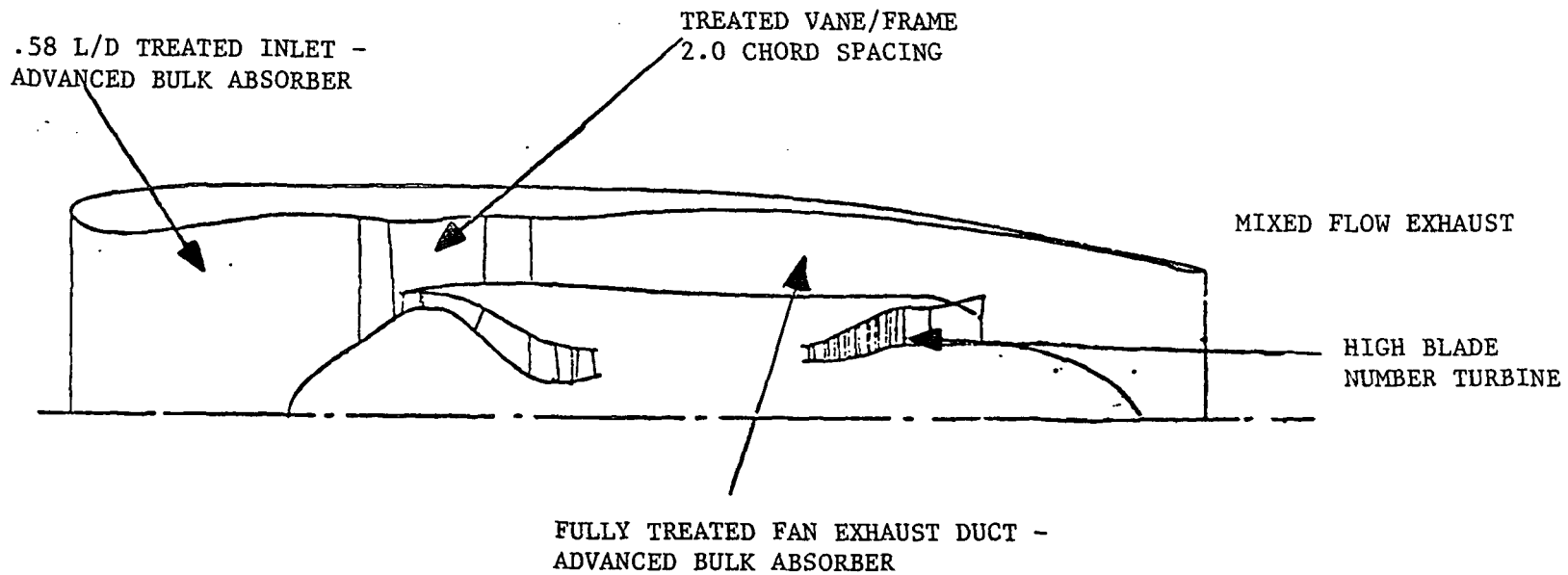


Figure 26. Advanced Engine Installation, Low Noise Features,  
Mixed-Flow Exhaust

A summary of the takeoff (with and without cutback), sideline and approach noise levels for both the baseline domestic and international aircraft is given on Table 23. As can be seen on this chart, both aircraft nearly meet the FAR36 (1969) -10 goal established for the E<sup>3</sup> program but without the margin that would be needed. Also shown are comparisons with more recently proposed requirements (NPRM 75-37C). Note that the approach noise estimate includes an estimate of aircraft-only noise.

Additional work was done to examine the noise level change which would result if the engine were required to deliver a greater thrust level for growth. Two growth cycles were reviewed: 1) a constant fan diameter with a higher speed and 2) a larger fan diameter at the same speed. The results are shown on Table 24 and indicate that the larger fan will deliver the increased thrust with less increase in noise. However, both growth engines would satisfy the new proposed requirements at the higher thrust levels; although the smaller fan version is marginal unless cutback is employed.

#### 1. Mission Evaluation

Baseline advanced engine mission economics were studied by General Electric using domestic and international trijet aircraft. Economics were first analyzed for a scaled CF6-50C engine in these aircraft, then repeated with the advanced engine. Two levels of fuel cost were examined for each mission, as listed on Tables 25 and 27.

Results for the domestic mission show a significant margin of improvement in DOC relative to E<sup>3</sup> program goals. Table 25 shows the contributions of sfc and installed weight to total economic factor gains. The advanced engine has 0.1% sfc margin and 3.2 to 4.9% DOC margin over E<sup>3</sup> improvement goals. Refer to Table 26 for a typical breakdown of DOC for a domestic trijet.

International trijet aircraft would have considerably greater advanced engine improvements over the current reference, as shown in Table 27. A typical breakdown of DOC is presented in Table 28 for an international trijet.

In both missions DOC will, of course, improve more sharply if fuel costs are higher than the studied levels.

Since engine and nacelle price and maintenance are difficult to establish on a preliminary design basis, the above data assumed advanced engine price and maintenance to be equivalent to current engine levels. The effect of price increments on DOC for each mission was then separately examined over a range of maintenance cost differentials to the current engine. Figure 27 shows that the domestic aircraft is more sensitive to price, but will still meet the E<sup>3</sup> DOC goal if engine price is up to \$400,000 more and if maintenance is simultaneously about \$7.50 per engine flight hour more.

The international aircraft is much less sensitive to price and/or maintenance cost increases and would better the E<sup>3</sup> goal even with much more severe (unlikely) price and maintenance cost increments over the current engine levels.

TABLE 23

ESTIMATED ENGINE NOISE ADVANCED TECHNOLOGY  
DIRECT-DRIVE MIXED-FLOW ENGINE

- Nominal Suppressed Noise Levels - No Margin
- Airframe Noise Included

	Domestic (General Electric)				International (General Electric)			
A/C Takeoff Gross Weight	126,550 kg (279,000 lb)				200,940 kg (443,000 lb)			
No. of Engines	3				3			
SLS/Thrust/Engine	112,540 N (25,300 lb)				165,030 N (37,100 lb)			
	AC Noise EPNdB	Total Noise EPNdB	$\Delta$ Relative To FAR36 (1969)	$\Delta$ Relative To NPRM 75-37C	AC Noise EPNdB	Total Noise EPNdB	$\Delta$ Relative To FAR36 (1969)	$\Delta$ Relative To NPRM 75-37C
Takeoff		93.1	- 9.3	-4.5		96.5	- 9.1	-3.6
Takeoff Power Cutback <sup>(1)</sup>		91.5	-10.9	-7.0		95.8	- 9.8	-4.3
Sideline		90.0	-16	-9.3		91.5	-16	-8.8
Approach $F_n$ <sup>(2)</sup>	92.8	97.4	- 8.8	-5.4	94.9	99.3	- 8.2	-5.0

Takeoff Alt. 482 m (1580 ft) for Domestic and 375 m (1230 ft) for International Aircraft

(1) Cutback  $F_n$  71% for Domestic, 75% for International.

(2) Power Setting at Approach 36% of TO  $F_n$  for Both Aircraft (Includes Aircraft Noise).

TABLE 24

ADVANCED TECHNOLOGY DIRECT-DRIVE ENGINE GROWTH

- Supressed Noise Levels - No Margin
- Growth Aircraft T/W Constant, TOGW 155,450 kg (342,700 lb)

Domestic Aircraft

	<u>Engine Noise EPNdB</u>	<u>Δ Relative To FAR36 (1969)</u>	<u>Δ Relative To NPRM 75-37C *</u>
Growth, 22% $F_n$			
<u>Constant Fan Diameter</u>			
Takeoff, 100% T/O $F_n$	98.2	- 5.7	- .6
Takeoff, Cutback 76% T/O $F_n$	94.8	- 9.9	-4.8
Growth, +23% $F_n$			
<u>Larger Fan Diameter</u>			
Takeoff, 100% T/O $F_n$	95.6	- 8.3	-3.2
Takeoff, Cutback 69% T/O $F_n$	93.0	-10.9	-5.8

\*Similar to FAR 36 (1977)



TABLE 25

ECONOMIC EVALUATION\*OF ADVANCED DIRECT-DRIVE ENGINE  
 VS. CURRENT ENGINE (CF6-50C) IN GENERAL ELECTRIC DOMESTIC TRIJET

700 NM, 55% LF

Parameter	$\Delta W_f$ %	$\Delta sfc$ %	$\$92.46/m^3$ (35¢/Gal.) Fuel		$\$118.88/m^3$ (45¢/Gal.) Fuel	
			$\Delta$ DOC	$\Delta$ ROI	$\Delta$ DOC	$\Delta$ ROI
$\Delta$ sfc Installed,	-15.9	-12.1	-6.4	+2.1	-7.1	+2.2
$\Delta$ Weight, Inst., -426 kg (-940 lbs)	- 1.9		-1.8	+ .8	-1.8	+ .8
Total	-17.8		-8.2%	+2.9%	-9.9%	+3.8%
E <sup>3</sup> Goals		<span style="border: 1px solid black; padding: 2px;">12.0</span>	<span style="border: 1px solid black; padding: 2px;">-5.0</span>		<span style="border: 1px solid black; padding: 2px;">-5.0</span>	

\*No price or maintenance effects included and based on max. cruise savings only.

TABLE 26

DOMESTIC TRIJET

DOC PERCENTAGE BREAKDOWN BASED ON G E STUDIES

1977\$

% BREAKDOWN

	<u>E<sup>3</sup> ENGINE</u>	<u>CF6-50C</u>
	<u>%</u>	<u>%</u>
DEPRECIATION	29.7	28.9
FUEL* AND OIL	25.0	27.9
CREW	21.0	19.7
INSURANCE	2.2	2.2
A/F MAINT MAT'L	3.7	3.6
A/F MAINT LABOR	3.2	3.1
ENGINE MAINT MAT'L	3.6	3.4
ENGINE MAINT LABOR	1.5	1.5
REVERSER MAINT MAT'L	.2	.2
REVERSER MAINT LABOR	.2	.1
LABOR BURDEN	9.7	9.4
TOTAL	100.0	100.0
INTEREST-AVERAGE	11.9	11.5

\*Fuel cost \$92.46/m<sup>3</sup> (35¢/Gal.)

TABLE 27

ECONOMIC EVALUATION\*OF ADVANCED DIRECT-DRIVE ENGINE  
VS. CURRENT ENGINE (CF6-50C) IN GENERAL ELECTRIC INTERNATIONAL TRIJET

2000 NM, 55% LF

Parameter	$\Delta W_f$ %	$\Delta$ sfc %	$\$118.88/m^3$ (45¢/Gal.)		$\$145.29/m^3$ (55¢/Gal.)	
			Fuel		Fuel	
			$\Delta$ DOC	$\Delta$ ROI	$\Delta$ DOC	$\Delta$ ROI
$\Delta$ sfc Installed	-20.4	-12.1	-11.3	+4.4	-11.9	+4.6
$\Delta$ Weight, Inst., -426 kg (-940 lbs)	- 2.3		- 1.9	+ .9	- 1.9	+ .9
Total	-22.7		-13.2	+5.3	-13.8	+5.5
$E^3$ Goals		12.0	- 5.0		- 5.0	

\*No price or maintenance effects included and based on max. cruise savings only.

TABLE 28

INTERNATIONAL TRIJET

DOC PERCENTAGE BREAKDOWN BASED ON G E STUDIES

1977\$

% BREAKDOWN

	<u>E<sup>3</sup> ENGINE</u>	<u>CF6-50C</u>
	<u>%</u>	<u>%</u>
DEPRECIATION	25.5	24.8
FUEL* AND OIL	32.8	36.6
CREW	20.2	18.2
INSURANCE	1.9	1.9
A/F MAINT MAT'L	2.9	2.8
A/F MAINT LABOR	2.5	2.4
ENGINE MAINT MAT'L	3.8	3.5
ENGINE MAINT LABOR	1.6	1.5
REVERSER MAINT MAT'L	.2	.2
REVERSER MAINT LABOR	.1	.1
LABOR BURDEN	8.5	8.0
TOTAL	100.0	100.0
INTEREST-AVERAGE	10.2	9.9

\*Fuel Cost \$118.88/m<sup>3</sup> (45¢/Gal.)

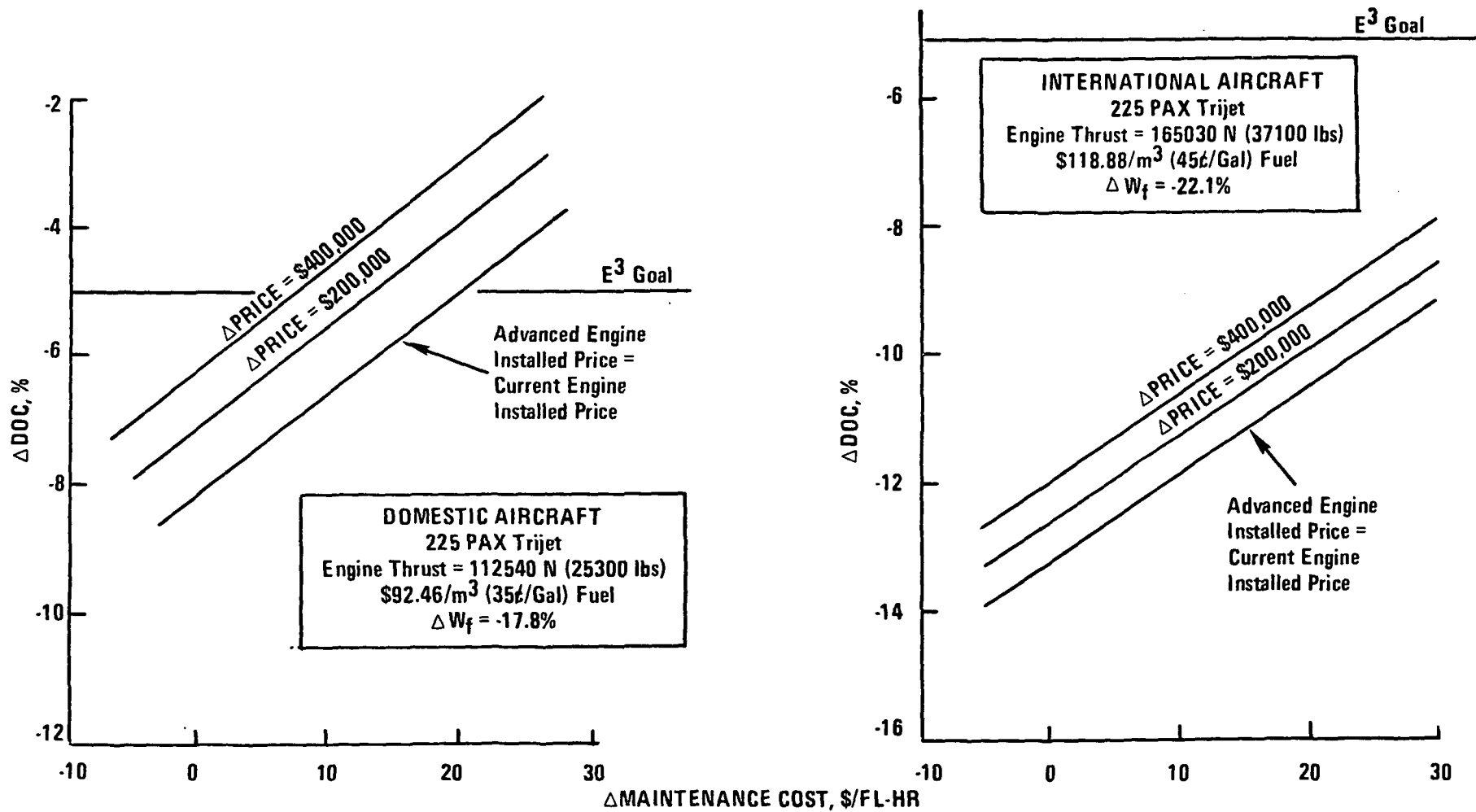


Figure 27. Aircraft Economics - Advanced Technology Direct-Drive Mixed-Flow Engine vs. Current Technology CF6-50C Engine (Scaled).

## 2. Advanced Technology Geared Drive Turbofan

### a. Engine and Installation Design Features

Design of the Task I gear driven fan engine (Figure 28) was modified in Task II in parallel with that of the direct-drive advanced engine. All core engine design and related improvements were applied simultaneously to the geared engine, keeping the core common except for size.

Compared to the direct-drive fan engine for comparable thrust, the geared engine has a larger fan, a booster stage, a smaller core, and a 3 stage LP turbine instead of five. Figure 29 shows a back-to-back comparison of dimensions of the geared and direct-drive engines at equivalent installed cruise thrust. The geared engine is 4.5% longer and 11.5% larger in diameter.

Characteristics of the two engines are compared further in Table 29. The geared fan runs at lower tip speed and lower pressure ratio. Core inlet pressure is regained by use of a fan shaft booster stage.

The Task II engine gearset was relocated to a position aft of the fan instead of the original forward mounted location. This reduced structural support weight and engine length but makes the gearset less accessible for maintenance.

Success of the geared engine would depend upon development of new light weight, efficient, and durable gearing. Star epicyclic single stage gearing similar to QCSEE technology (Reference 8), but more advanced, was chosen for this program. As shown in Table 30, the E<sup>3</sup> design uses materials capable of operating at significantly higher temperature than used in the QCSEE program. This permits use of much less cooling oil flow which, in turn, results in lower losses, a lighter gearset and smaller cooling components.

### b. Performance

The geared engine cycle provides a 2.9% installed SFC advantage over the direct drive at 10668 m (35K Ft) 0.80 Mach Max. Cruise, as shown in Table 31. It accomplishes this with 25% more fan flow and 35% higher bypass ratio. Propulsive efficiency and LP component efficiency advantages overcome the 1% penalty due to higher nacelle drag.

Compared to the Task I engines, the geared fan SFC advantage decreased as the engines were refined as shown on Table 32. The primary factor causing the decreased geared fan advantage was the gain in direct drive engine LP turbine efficiency with a fifth stage added.

### c. Weight Comparison

Installed weight of the geared fan engine is 18% greater than the direct drive engine scaled to the same cruise thrust. This weight differential exists despite smaller core size because of the larger fan and nacelle, and the gearset with cooling system. Component weight breakdown is compared graphically with the direct drive in Figure 30.

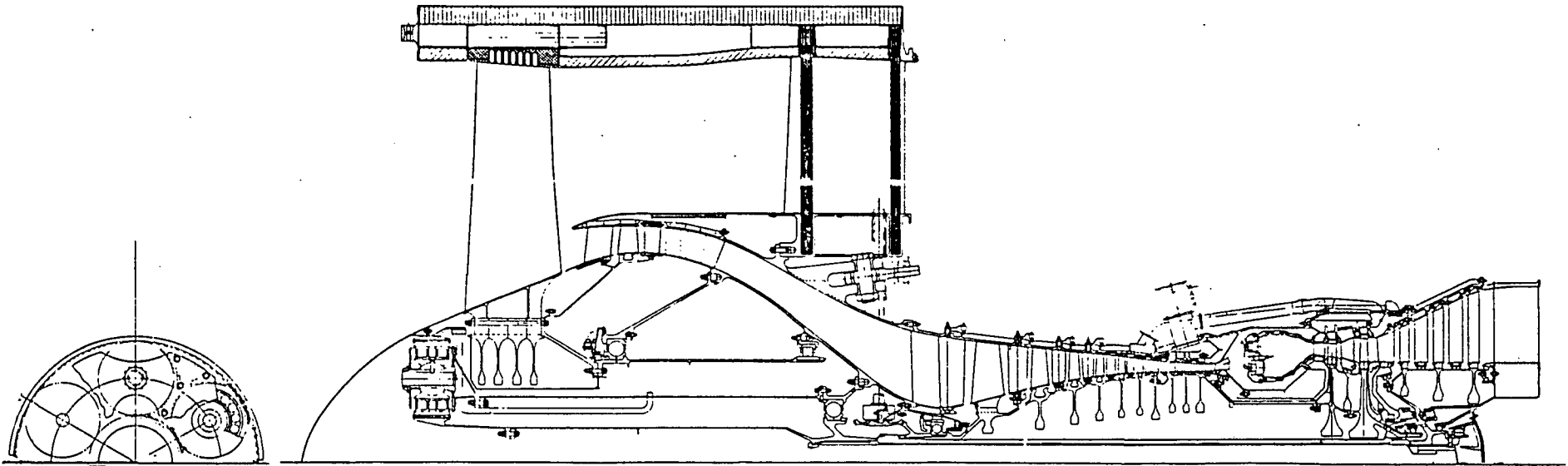


Figure 28. Task I Geared Turbofan Design

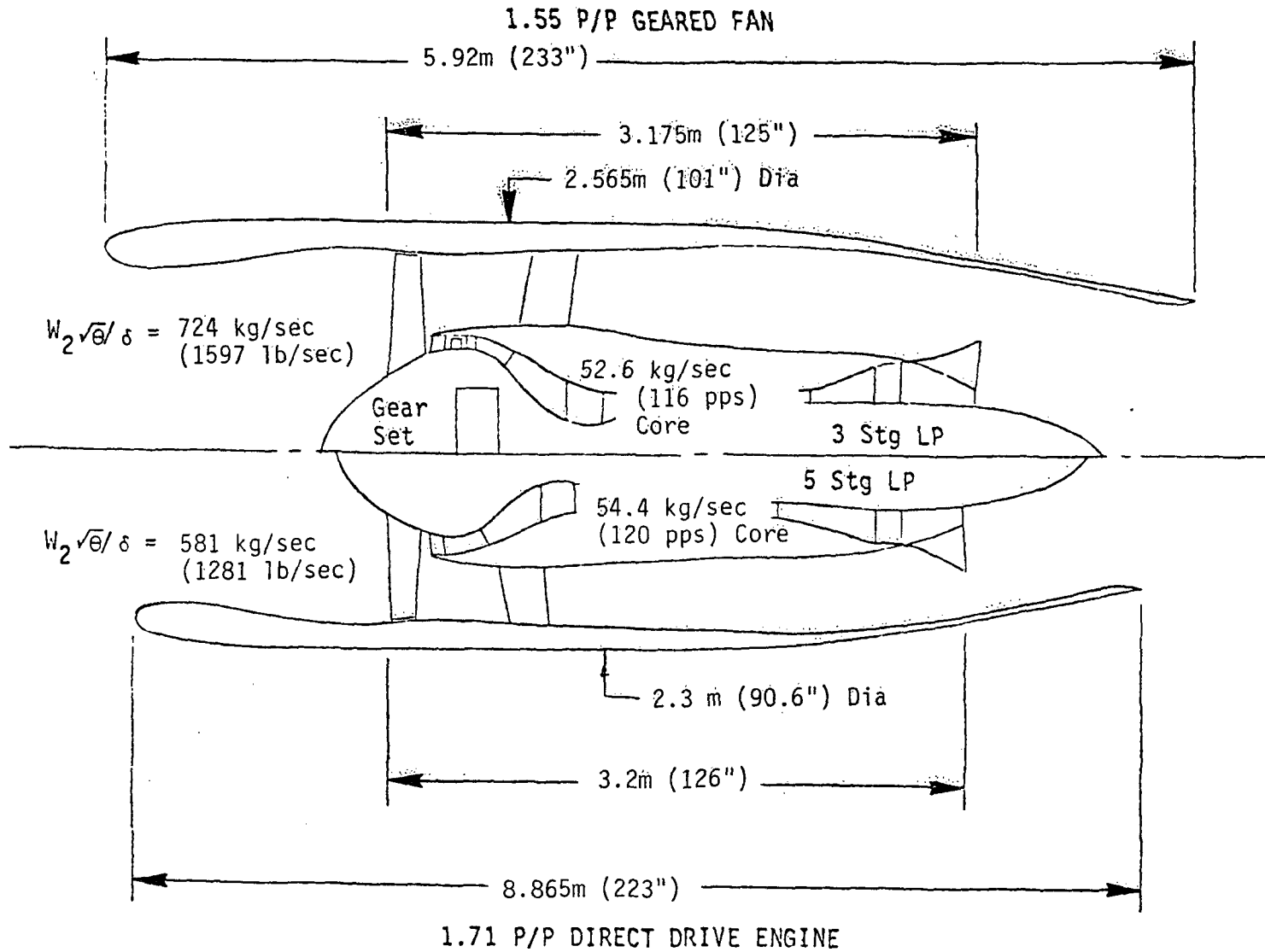


Figure 29. Geared Fan Dimensional Comparison with Direct-Drive Engine, Cruise Sized,  
 $F_{NI} = 37050 \text{ N (8330 lb)}$  @  $M_{xCl}$



TABLE 29

TASK II GEARED-FAN VS. DIRECT-DRIVE ENGINE COMPONENTS

		<u>DIRECT DRIVE</u>	<u>GEARED FAN</u>
Fan	Pressure Ratio	1.71	1.55
	Tip Speed, $U_T/\sqrt{\theta}$ M/Sec (Ft/Sec)	457 (1500)	396 (1300)
Boosters	No. Stages	0	1
	Boost Pressure Ratio (Incl. Fan Hub)	1.67	1.67
LP Turbine	No. Stages	5	3
	Pitch Loading	1.25	.7
Gearing	Type	-	Single Reduction Epicyclic
	Reduction	-	2.5:1

TABLE 30

GEAR TECHNOLOGY COMPARISON

	<u>QCSEE Level (Scaled to E<sup>3</sup>)</u>	<u>E<sup>3</sup> Level (Design Size)</u>
Watt (Horsepower)	24,012,000 (32,200)	24,012,000 (32,200)
Estimated Weight, kg (lbs.)	278 (612)	209 (460)
Gear Material	Hardened 9310	Nitralloy Class
Max. Gear Metal Temperature, °C (°F)	163 (325)	260+ (500+)
Bearing Material	M50, 9310	Ausforged M50
Max. Bearing Metal Temperature °C (°F)	163 (325)	260+ (500+)
Max. Oil Temperature, °C (°F)	127 (260)	218 (425)
Oil Flow Required, m <sup>3</sup> /Min (GPM)	.227 (60)	.076 (20)
Estimated System B <sub>10</sub> Life, Hrs.	1575	36,000
Pitch Velocity, m/Min (FPM)	5837 (19,150)	6675 (21,900)

TABLE 31

TASK II GEARED FAN VS. DIRECT-DRIVE PERFORMANCE COMPARISON-MIXED FLOW

CRUISE SIZED -  $F_{N1} = 37050$  N (8330 LBS) @ 10668m (35K FT)/.80 MAX. CLIMB/STD. + 10°C (+ 18°F) DAY

	<u>Direct Drive</u>	<u>Geared Fan</u>	<u>Δ's</u>
Fan Tip Diameter, m (in.)	2.024 (79.7)	2.261 (89.0)	+12%
<u>10668 m (35K Ft)/.80 Mach</u>			
$F_n - N$ (Lbs), Std. + 10°C (Std. + 18°F)	38830 (8730)	39230 (8820)	
$W_2/\theta/\delta$ kg/sec (lb/sec) Std. + 10°C (Std. + 18°F)	581 (1281)	724 (1597)	+25%
$T_{41}$ °C (°F), Std. + 10°C (Std. + 18°F)	1310 (2390)	1310 (2390)	-
Cycle Pressure Ratio	38	38	
Core Corrected Flow, kg/sec (lb/sec) Std. + 10°C (Std. + 18°F)	54.4 (120)	52.6 (116)	-3%
$F_n - N$ (Lbs) Std. + 10°C (Std. + 18°F)	36120 (8120)	36430 (8190)	
Bypass Ratio, Std. Day	6.2	8.4	+35%
sfc Bare Engine, Std. Day, kg/N-hr (lb/lb-hr)	.0566 (.555)	.0544 (.533)	-3.9%
Drag/ $F_n$	.050	.060	+1%
sfc Installed Std. Day, kg/N-hr (lb/lb-hr)	.0596 (.584)	.0578 (.567)	<span style="border: 1px solid black; padding: 2px;">-2.9%</span>
<u>Sea Level</u>			
$F_n - N$ (lbs), Flat to +15°C (+27°F)	152570 (34300)	164580 (37000)	
$T_{41}$ °C (°F), Std. + 15°C (Std + 27°F)	1366 (2490)	1366 (2490)	

TABLE 32

SOURCE OF GEARED FAN SFC REDUCTION RELATIVE TO TASK I DIRECT-DRIVE/MIXED-FLOW ENGINE\*

	$\Delta$ sfc %		
	<u>Task I</u>	<u>Task II</u>	<u>Reason for Change</u>
<u>Cycle Effects</u>			
Bypass Ratio	-2.9	-2.9	
<u>Component Effects</u>			
Fan Tip	-.9	-.9	
Fan Hub (+ Booster)	-1.0	-.5	Refined Estimate of Booster Performance
LP Turbine	-1.5	-.4	5 Stg. Direct Drive LPT
Gearing	+.7	+.9	Refined Gear Loss
Duct Losses	0	-.1	Loss Refinement
Nacelle Drag	<u>+1.0</u>	<u>+1.0</u>	
Total $\Delta$ SFC	-4.6%	-2.9%	

\*Refer to Tables 1 and 2.

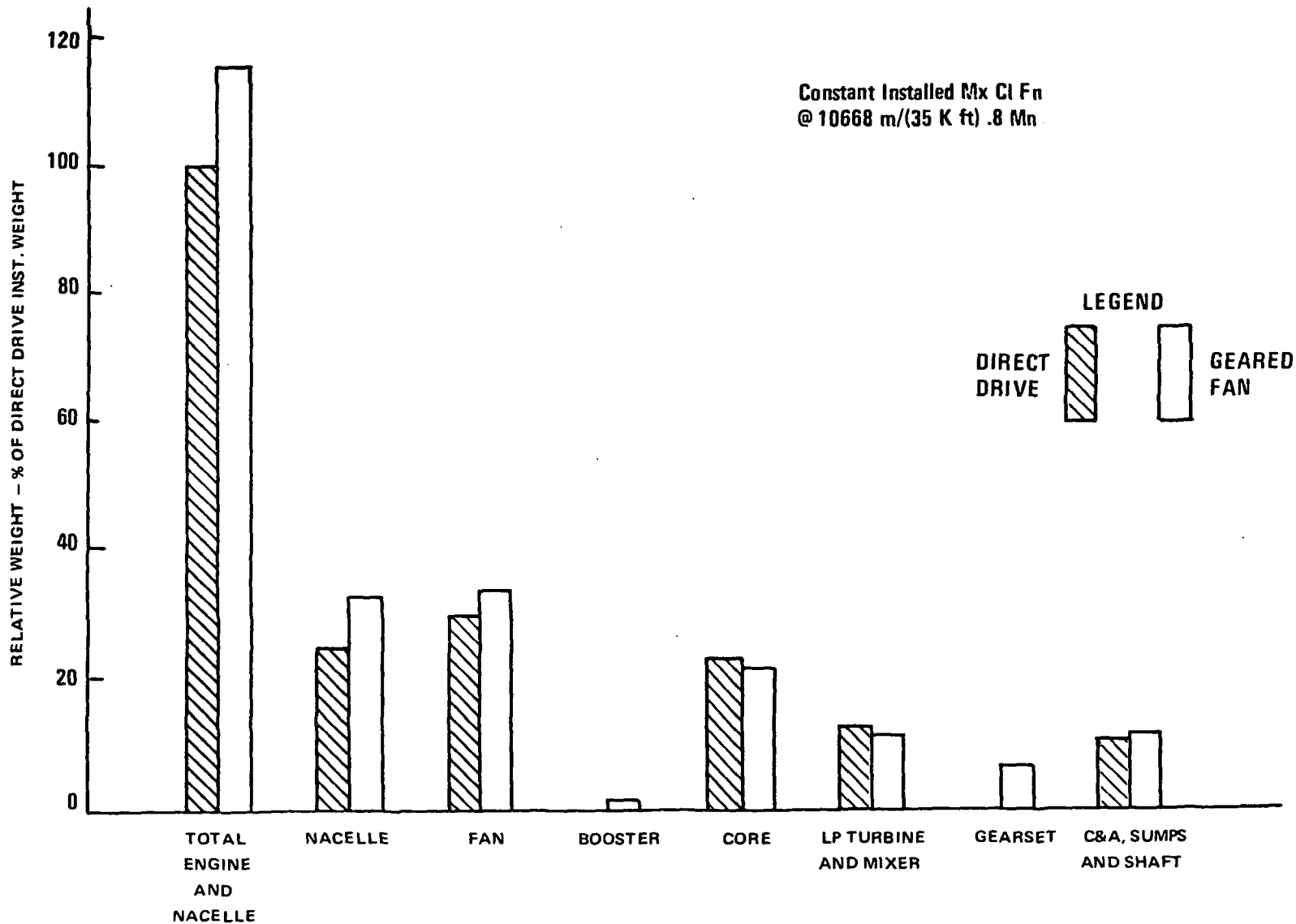


Figure 30. Geared Engine Weight Comparison with Direct-Drive Engine.

#### d. Engine Cost Factors

Estimated price of the geared fan engine relative to direct drive parallels weight, but differences are less pronounced. As shown in Figure 31, the geared engine is estimated to be about 6% higher in price than the direct drive total installation.

There is no significant difference between estimated maintenance costs for geared versus direct-drive fan engines. As shown in Figure 32, lower geared engine maintenance costs in the smaller core and fan turbine offset the maintenance cost of the added booster and gearset and the larger, slower fan. It has been assumed in this evaluation that the gearset would be designed and developed to have low maintenance costs.

#### e. Growth

The geared fan engine growth plan parallels the direct drive steps with some differences. Table 33 shows that the initial rating is a simple -10% derate of the design level.

Growth step 1 uses an added booster stage, increased LPT flow function, and upspeedings to add 9% thrust.

The second growth step to 22% higher thrust than design level is accomplished by fan blading redesign and further upspeeding of both rotors. Fan redesign is required for the pressure ratio and flow rate.

#### f. Exhaust Emission Estimate

The geared fan engine has a double annular combustion system for low exhaust emissions like the advanced direct drive engine. Additionally the higher static thrust obtained with a given core size makes the emissions parameter results lower for the geared engine, using early 1977 EPA formulae. Table 34 shows these results for the design level and growth step 2. Although the design size engine is estimated to meet all of the study goals, the growth version would exceed the  $\text{NO}_x$  goal.

#### g. Noise Estimates

Aircraft noise levels for GE domestic and international aircraft using geared fan engines were estimated as shown in Table 35 for takeoff, sideline and approach. Noise very nearly meets the FAR36 (1969) -10 goal with the design geared engine in both aircraft. Noise margins relative to MPRM75-37C are a minimum of -3.5 dB for the growth geared engine takeoff in the international aircraft. Gearbox noise was not included in this evaluation since it was assumed to be much lower than other sources of noise and, therefore, not a problem.

#### h. Mission Evaluation

Geared fan mission performance was compared with direct drive, with results as shown in Table 36. Although the geared fan has a 3.9% uninstalled sfc advantage, the improvement in fuel usage is only 0.9% because of the weight and drag penalties. For  $\$92.46/\text{m}^3$  (35¢/gallon) fuel in the domestic trijet, the geared fan is estimated to have a 1.3% higher DOC than the direct-drive advanced engine. In the international aircraft (Table 37) with

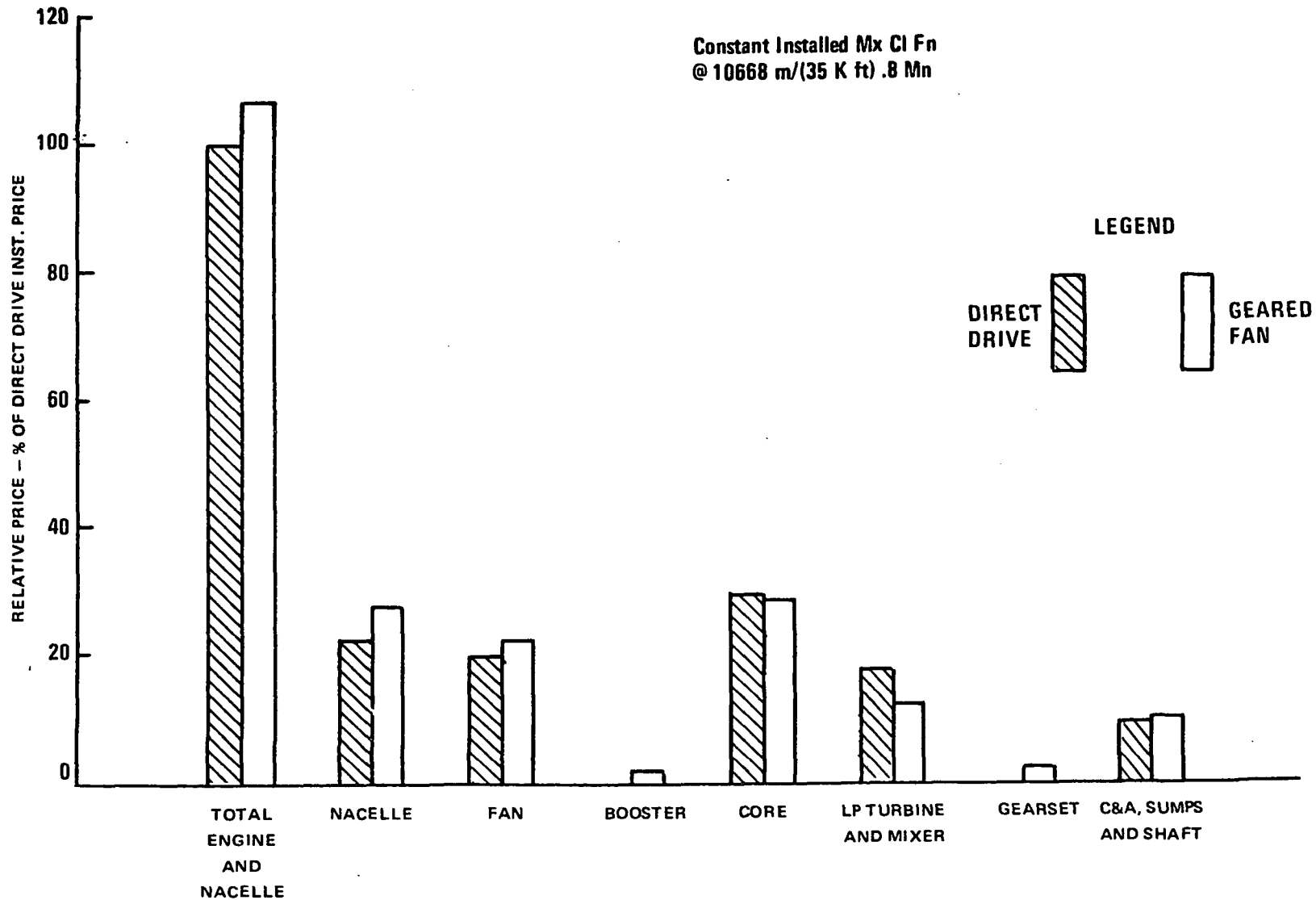


Figure 31. Geared Engine Price Comparison with Direct-Drive Engine..

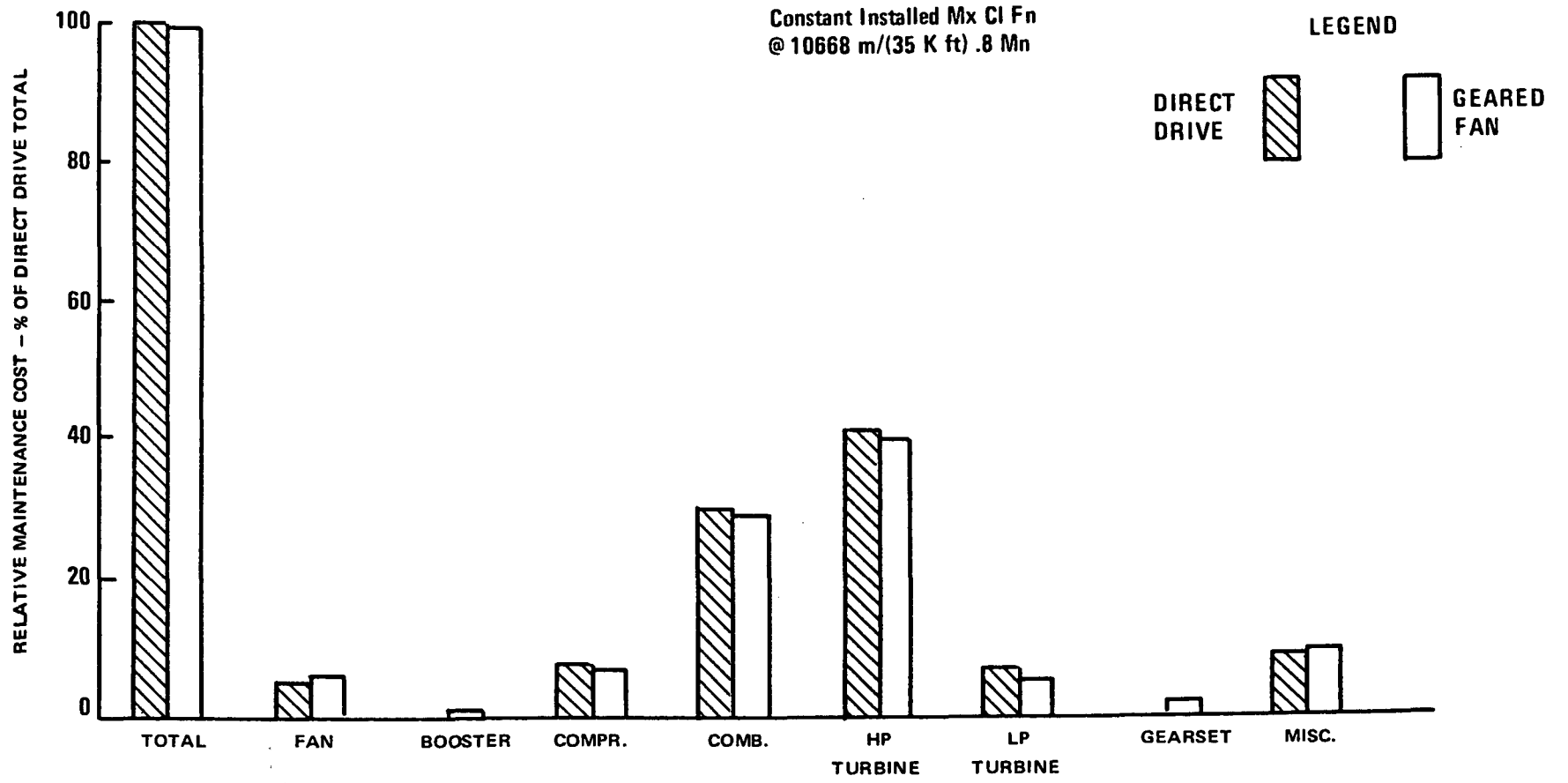


Figure 32. Geared Engine Maintenance Cost Comparison with Direct-Drive Engine.



TABLE 33

GEARED FAN GROWTH PATTERN - CONSTANT FAN DIAMETER

Growth Step	Initial Rating	Design Level	E <sup>3</sup>	
			Growth Step 1	Growth Step 2
No. of Booster Stages	1	1	2	2
LPT Flow Function	Base	Base	+5%	+3.7/+3.9%
Δ % RPM Fan/Core	-3/-1.3%	Base	+3/+2.7%	+3.7/+3.9%
<u>10668m (35K Ft.)/.80 Mach - Max. Climb</u>				
Δ F <sub>n</sub>	-10%	Base	+9%	+22%
Bypass Ratio	8.4	8.2	7.1	6.7
Cycle Pressure Ratio	35	38	43	48
Fan Pressure Ratio	1.5	1.55	1.58	1.65 (Redesign)
Fan Specific Flow, $W/\theta/\delta/A, \text{kg/m}^2$ (lb/ft <sup>2</sup> )	205.5 (42.1)	209.9 (43.0)	213.8 (43.8)	219.2 (44.9)
Boost Pressure Ratio (Incl. Fan Hub)	1.63	1.67	2.12	2.22
<u>10668m (35K Ft.)/.80 Mach - Max. Cruise</u>				
Δ % sfc	-0.7%	Base	+0.8%	+1.8%
<u>Sea Level/.25 Mach Takeoff</u>				
Δ F <sub>n</sub>	-10%	Base	+10%	+19%
Δ T <sub>41</sub>	-50°C (-90°F)	"	+14°C (+25°F)	+61°C (+110°F)
Δ T <sub>3</sub>	-19°C (-35°F)	"	+42°C (+75°F)	+64°C (+115°F)
Δ P <sub>3</sub>	-7.5%	"	+16%	+26%
Δ % Exhaust Velocity	-8.5%	"	+5%	+8%

TABLE 34

GEARED FAN EMISSIONS SUMMARY

	Geared Fan		Study Goals
	Design Level	Growth (+20% FN)	
	EPA Parameter (No Margin) kg (lbs)/1000 kg-hr (lbs-hr)		
CO	1.6	1.1	3.0
HC	.09	.04	0.4
NO <sub>x</sub>	2.7	4.0	3.0

TABLE 35

GEARED FAN NOISE ESTIMATES  
INCLUDING A/C NOISE - NO MARGIN

<u>Domestic A/C - Design Mission</u>		Design Level $F_n$ dB	Growth (+20% $F_n$ ) dB
Takeoff	- 6.48 Km (3.5 N.M.), 530/495 m (1740/1625 ft) Alt. EPNL	92.9	94.8
	Δ Rel. to FAR36 (1969)	- 9.5	- 9.1
	Δ Rel. to NPRM75-37C	- 4.7	- 4.0
Sideline	- .46 Km (.25 N.M.) EPNL	90.6	91.9
	Δ Rel. to FAR 36 (1969)	-15.4	-14.8
	Δ Rel. to NPRM75-37C	- 8.6	- 8.1
Approach	- 113 m (370 ft) Alt., 36% FN EPNL	95.7	96.5
	Δ Rel. to FAR36 (1969)	-10.4	-10.3
	Δ Rel. to NPRM75-37C	- 7.1	- 7.0
<u>International A/C - Design Mission</u>			
Takeoff	- 6.48 Km (3.5 N.M.), 424/389 m (1390/1275 ft) Alt. EPNL	96.0	97.8
	Δ Rel. to FAR36 (1969)	- 9.6	- 9.3
	Δ Rel. to NPRM75-37C	- 4.1	- 3.5
Sideline	- .46 Km (.25 N.M.) EPNL	91.9	93.1
	Δ Rel. to FAR36 (1969)	-15.6	-15.0
	Δ Rel. to NPRM75-37C	- 9.0	- 8.5
Approach	- 113 m (370 ft) Alt., 36% FN EPNL	97.4	98.3
	Δ Rel. to FAR36 (1969)	-10.1	- 9.8
	Δ Rel. to NPRM75-37C	- 6.9	- 6.7

TABLE 36

GEARED FAN MISSION EVALUATIONDOMESTIC AIRCRAFT, AVERAGE MISSION, 10668m (35K FT.)/.80/+10°C (+18°F,) MAX. CRUISE225 PAX, 55% LOAD FACTOR, FUEL PRICE \$92.46/m<sup>3</sup> (35¢/GAL.)

	$\Delta$ Relative to Direct-Drive Engine	$\Delta$ DOC %	$\Delta$ ROI PTS	$\Delta$ W <sub>f</sub> %
$\Delta$ % sfc Bare	-3.9*	-2.1	.6	-5.1
$\Delta$ Engine Weight, Kg (Lbs.)	254 (560)	1.1	-.4	1.5
$\Delta$ Engine Price, %	+2	.2	-.1	-
$\Delta$ Engine Maintenance, %	-.4	0	0	-
$\Delta$ Installation Weight, Kg, (Lbs.)	213 (470)	.5	-.4	1.2
$\Delta$ Installation Price, %	+24	.9	-.4	-
$\Delta$ Drag/Fn, %	1.0	.5	-.2	1.3
$\Delta$ Pylon Penalty		<u>+ .2</u>	<u>-.1</u>	<u>+ .2</u>
	Totals	1.3	-1.0	- .9

\*Max. cruise sfc and mission trade factors used.

Consideration of low speed performance will increase  $\Delta$ sfc somewhat.

TABLE 37

GEARED FAN MISSION EVALUATION

INTERCONTINENTAL AIRCRAFT, AVERAGE MISSION, 10668m (35K/.80/10°C (+18°F), MAX. CRUISE

225 PAX, 55% LOAD FACTOR, FUEL PRICE \$118.88/m<sup>3</sup> (45¢/GAL.)

	$\Delta$ Relative to Direct-Drive Engine	$\Delta$ DOC %	$\Delta$ ROI PTS	$\Delta W_f$ %
$\Delta$ % sfc Bare	-3.9*	-3.6	1.3	-6.6
$\Delta$ Engine Weight, Lbs	910	1.7	-0.8	2.4
$\Delta$ Engine Price, %	+2	0.1	-0.1	--
$\Delta$ Engine Maintenance, %	-0.7	0	0	--
$\Delta$ Installation Weight, Lbs	720	1.4	-0.6	1.9
$\Delta$ Installation Price, %	+24	0.4	-0.4	--
$\Delta$ Drag/ $F_n$ , %	1.0	0.9	-0.4	1.7
$\Delta$ Pylon Penalty		<u>+0.2</u>	<u>-0.1</u>	<u>+0.2</u>
Totals		1.1	-1.1	-0.4

\*Max. Cruise sfc and mission trade factors used. Consideration of low speed performance will increase  $\Delta$ sfc somewhat.

\$118.88/m<sup>3</sup> (45¢/gallon) fuel, nearly the same result, +1.1% DOC, was estimated for the geared engine compared to the direct-drive engine.

Since the geared engine has lower fuel consumption, it was of interest to established sensitivity of DOC and ROI to fuel price. Figure 33 shows relatively flat response to fuel price in the range currently of interest.

Gearset cost factors for new technology involves more uncertainty than for other engine components. Figure 34 shows the economic sensitivity to gearset price and maintenance costs.

### 1. Overall Comparison of Direct-Drive and Geared Engine

An overall summary comparing the Task II geared and direct-drive engines in the domestic aircraft is presented in Table 38. Also included is a summary of the emission, noise and growth aspects of the two systems. Whereas the geared engine is shown to have a 2.5% sfc advantage, fuel usage is reduced by only 0.9%. This is accompanied by a relatively large DOC increase of 1.3%. In addition to these study results summarized on Table 38, some question also exists as to airline acceptance of a geared engine.

### 3. Alternate Engine Configuration/Cycles for Reduced Noise

Two general noise suppressing methods were applied for this aspect of the study. The first was to investigate the noise reduction possible by maintaining fan tip speed, but reducing fan pressure ratio to reduce jet noise for a direct drive engine. This design was also coupled to extensions in the inlet duct length and increased blade number in the low pressure turbine.

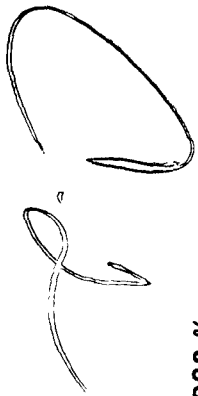
The second method involved progressive reduction of fan pressure ratio and fan tip speed for a series of geared and direct drive engines. Two different inlet lengths were utilized for this study also.

For both methods of suppressing noise, an economic analysis was made to ascertain the benefits or penalties of additional engine noise suppression. The following paragraphs summarize the procedure as it was applied to each of the design modifications under study. In all cases, noise levels are presented without an engineering margin. In practice, a 3 to 5 PNdB margin would be required to ensure noise certification compliance.

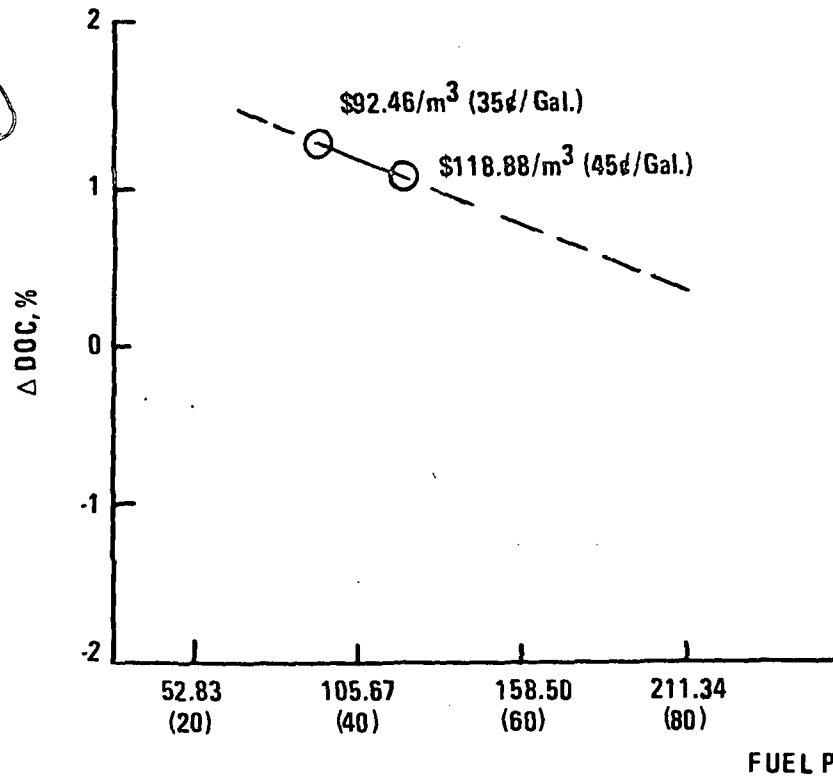
#### a. Lower Fan Pressure Ratio

A lower fan P/P engine will tend to have lower fan and jet noise. However, to retain the required engine cruise thrust level, a larger fan tip diameter would be required to deliver the necessary increase in airflow. Figure 35 shows the change in engine overall size when the design characteristics listed on Table 39 were applied to a direct drive design.

Table 40 shows the overall engine performance levels for the reduced P/P fan as compared to the baseline engine. The fan tip diameter has increased approximately 9% to deliver the 18% greater fan flow required to meet the original installed engine maximum cruise thrust level. The lower fan P/P version does realize a 1% gain in sfc at this cruise condition and a significant thrust increase at SL static but is more expensive in initial and continuing costs. As shown in Table 41, the direct drive engine version with the lower fan P/P results in a penalty in DOC and no improvement in fuel usage.



**DOMESTIC A/C**  
225 PAX Trijet  
1296 Km (700 NM) Mission, 55% Load Factor  
 $\Delta WF = -0.9\%$



**INTERCONTINENTAL A/C**  
225 PAX Trijet  
3704 Km (2000 NM) Mission, 55% Load Factor  
 $\Delta WF = -0.4\%$

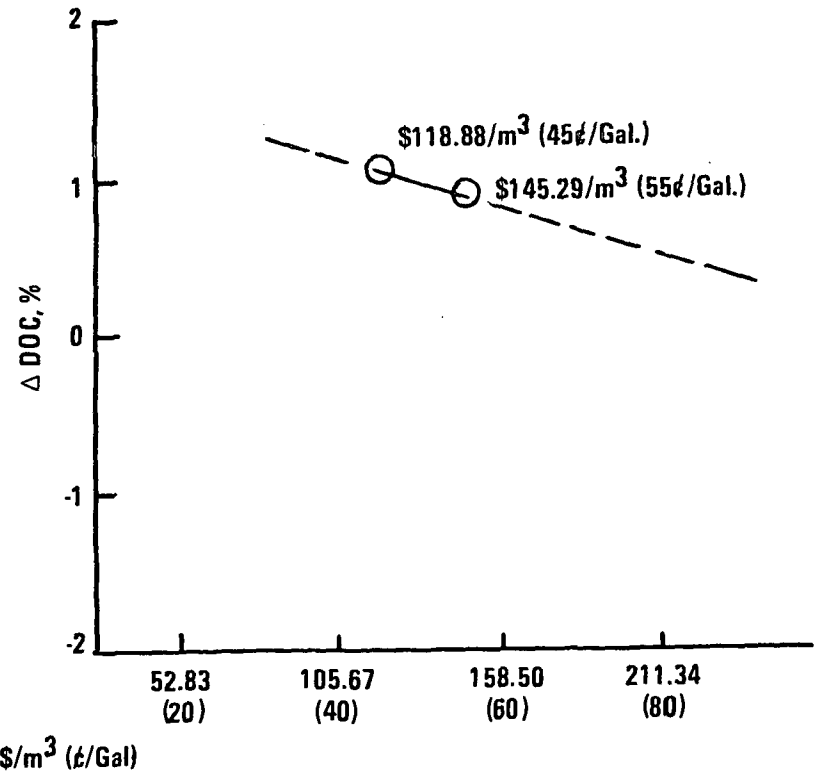


Figure 33. Geared Fan Evaluation, Sensitivity to Fuel Price, Relative to Direct-Drive Engine

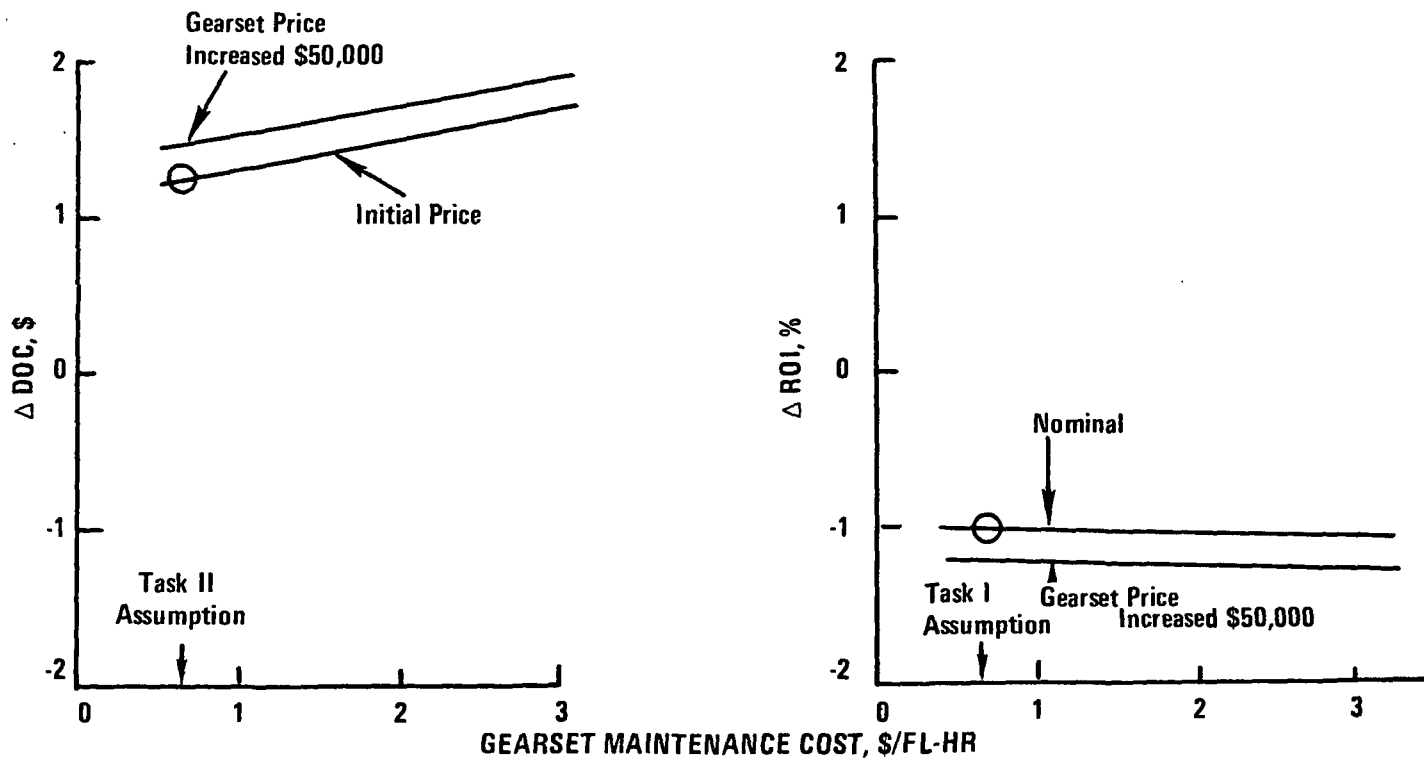


Figure 34. Sensitivity to Gearset Price and Maintenance Cost, Domestic A/C, Average Mission

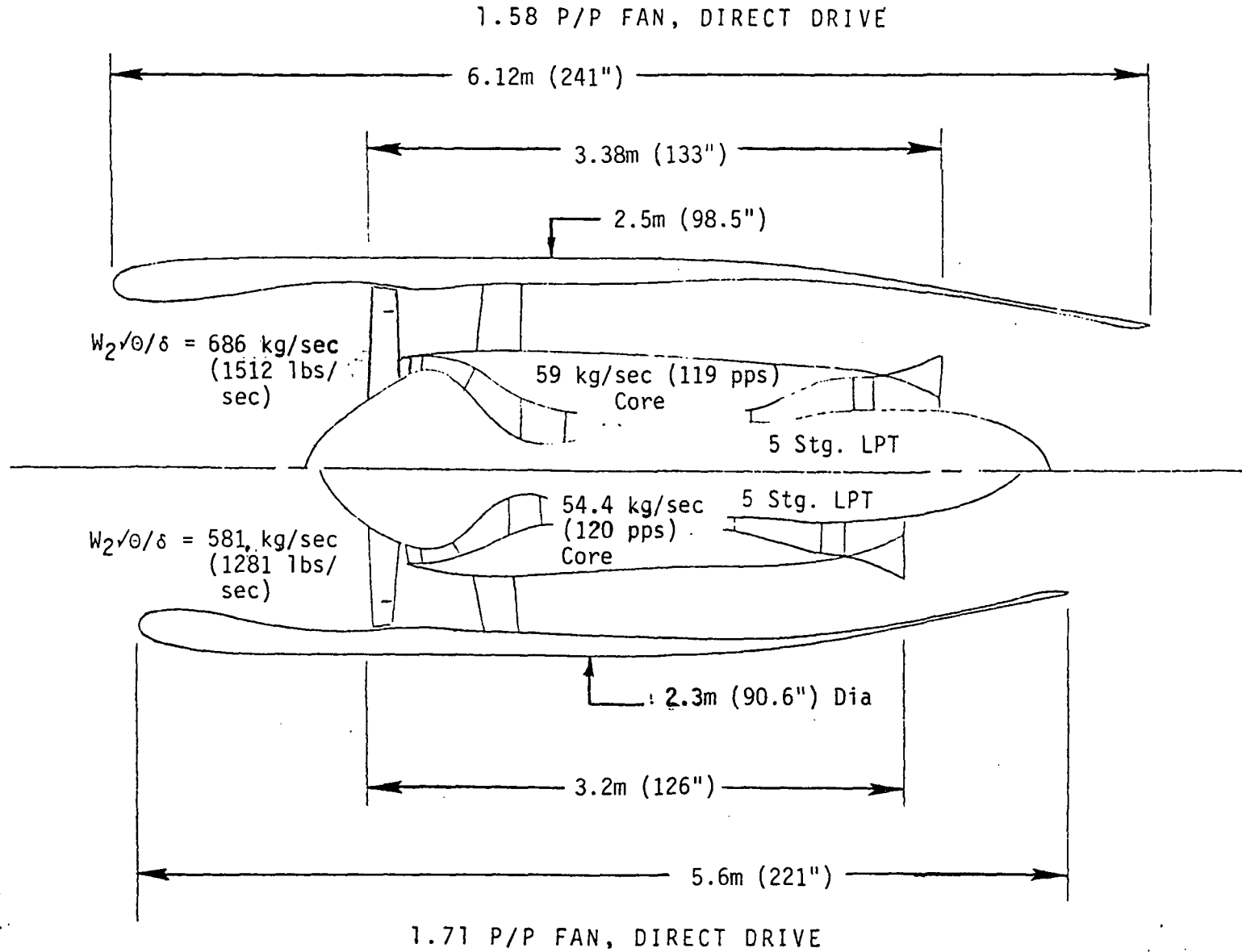


TABLE 38

SUMMARY OF COMPARISON BETWEEN  
ADVANCED GEARED AND DIRECT-DRIVE ENGINE AND CF6-50C  
INSTALLED ON DOMESTIC TRANSPORT

	<u>CF6-50</u>	<u>Direct-Drive</u>	<u>Geared Fan</u>
$\Delta sfc - \%$	Base	-12.1	-14.6
$\Delta W_f - \%$	Base	-17.8	-18.7
$\Delta DOC - \%*$	Base	- 8.2	- 6.9
Emissions	--	Meets 1981 std. except $NO_x$	Meets 1981 stds.
Noise	--	Meets FAR 36 (1977)	Meets FAR 36 (1977)
Growth Potential	--	Meets reqmts.	Meets reqmts.

\*No price or maintenance effects



ORIGINAL PAGE IS OF GOOD QUALITY

Figure 35. Low Fan Pressure Ratio Comparison with Baseline

TABLE 39

LOW FAN PRESSURE RATIO VS. DIRECT-DRIVE ENGINE COMPONENTS

		<u>Baseline Direct Drive</u>	<u>Lower Fan P/P</u>
Fan	Pressure Ratio (Mx. Climb)	1.71	1.58
	Tip Speed, $U_T/\sqrt{\theta}$ m/sec (ft/sec)	457 (1500)	457 (1500)
Boosters	No. Stages	0	0
	Fan Hub Pressure Ratio	1.67	1.67
Core	Configuration	Same	Same
LP Turbine	No. Stages	5	5
	Pitch Loading	1.25	1.5
Mixer Effectiveness, %		65	65

TABLE 40

LOWER FAN PRESSURE RATIO PERFORMANCE VS. BASELINE DIRECT-DRIVE ENGINECRUISE SIZED -  $F_{NI} = 37050$  N (8330 LBS) @ 10668m (35K FT)/.80 MAX. CLIMB

	<u>Baseline</u>	<u>Low P/P Fan</u>	<u><math>\Delta</math></u>
Fan Tip Diameter, m (in.)	2.024 (79.7)	2.2 (86.6)	+9%
<u>10668 m (35K Ft)/.80 Mach</u>			
$F_n - N$ (Lbs), Std. + 10°C (+ 18°F)	38830 (8730)	39100 (8790)	
$W_2 \sqrt{\theta}/\delta$ , kg/sec (Lb/sec), Std. + 10°C (+ 18°F)	581 (1281)	686 (1512)	+18
$T_{41}$ (°F), Std. + 10°C (+ 18°F)	1310 (2390)	1310 (2390)	
Cycle Pressure Ratio	38	38	
Core Corrected Flow, kg/sec (pps) Std.+10°C (+18°F)	54.4 (120)	53.8 (118.5)	-1%
$F_n - N$ (Lbs), Std + 10°C (+ 18°F)	36120 (8120)	36300 (8160)	
Bypass Ratio, Std. Day	6.2	7.6	
sfc Bare Engine, kg/N-hr (lb/lb.hr) Std. Day	.0566 (.555)	.0556 (.545)	-1.8%
Drag/ $F_n$	.050	.057	+ .8%
sfc Installed, kg/N-hr (lb/lb.hr) Std. Day	.0596 (.584)	.0589 (.578)	-1%
<u>Sea Level</u>			
$F_n - N$ (Lbs), Std. + 15°C (+ 27°F)	152570 (34300)	160580 (36100)	+5%
$T_{41}$ °C (°F), Std. + 15°C (+ 27°F)	1366 (2490)	1366 (2490)	

TABLE 41

LOWER FAN PRESSURE RATIO EVALUATION

DOMESTIC AIRCRAFT, AVERAGE MISSION, 10668m (35K Ft.)/.80/+10°C (+18°F) MAX. CRUISE

FUEL PRICE = \$92.46/m<sup>3</sup> (35¢/Gal), 1296 Km (700 NM) 55% LOAD FACTOR

	$\Delta$ Rel. to Dir. Drive 1.71 P/P Engine	$\Delta$ DOC	$\Delta$ ROI	$\Delta$ W <sub>F</sub>
$\Delta$ sfc Bare Engine	-1.8%	-.9	.3	-2.3
$\Delta$ Engine Weight	+163 kg (+360 lbs)	.7	-.3	+ .9
$\Delta$ Engine Price	+2.6%	.2	-.2	-
$\Delta$ Maintenance Cost	+ .5%	0	0	-
$\Delta$ Nacelle Weight	+ 79 kg (+175 lbs)	.4	-.1	+ .5
$\Delta$ Nacelle Price	+11.4%	.2	-.2	-
$\Delta$ Drag/ F <sub>n</sub>	+ .8	<u>+.4</u>	<u>-.1</u>	<u>+1.0</u>
Totals		+1.0	-.6	+ .1

To show the potential reduction in noise level estimated for the lower fan P/P version of this engine, Table 42 was prepared. As can be seen from Table 42 engine noise with the lower fan P/P falls well below the FAR36 (1969) requirement for both the domestic and international trijets and also satisfies the NRPM 75-37C proposed requirement. However, when compared to the direct drive baseline engine, a zero change in the total noise level is predicted for the lower fan P/P engine at T/O and a 0.5-0.7 EPNL increase is estimated for the sideline and approach conditions. This trend plus the above penalties in the economic factors preclude further consideration of this design change.

#### b. Increased Duct Length and Blade and Vane Solidity

The two other design approaches considered to suppress the engine noise level were an extended inlet duct length and increased blade number for the low pressure turbine blades and vanes as shown in Table 43.

An evaluation was made for each of these designs. With the results shown on Table 43, the economic factors for these designs are unfavorable thus negating their application to the baseline engine. A review of this chart shows the following:

- LPT blade and vane number reduces approach noise with little effect on A/C economics.
- Noise reductions for both approach and takeoff are achievable when using the long duct, but with a penalty in aircraft economics.

Figures 36 and 37 illustrate the trades between noise at full power takeoff and at approach with aircraft economics.

#### c. FAR36 (1969) -10 to -15 EPNdB Suppression Study

##### 1. Penalties

Three levels of suppression approximating FAR 36 (1969) -10, -12.5 and -15 were achieved using a combination of fan pressure ratio, fan tip speed and inlet duct length in addition to increased solidity LPT blading.

For approximating the FAR 36 (1969) -10 case, the Task II baseline geared and direct drive engines were used as a base. Then, two new direct and geared engine configurations and cycles were employed to attain the increased suppression desired. The change in weight, engine cost, sfc, drag and maintenance were assessed for each of the new engines and  $\Delta$ DOC and  $\Delta W_f$  were developed for each engine relative to the Task II baseline direct and geared engine.

A physical description of the highly suppressed engines is given in Table 44. Table 45 presents a summary of the aerodynamic and cycle design of each of the engines. Table 45 also provides an assessment of the installed  $\Delta$ SFC relative to the Task II direct drive engine and to the CF6-50C reference engine. It is interesting to note that although the installed SFC continued to decrease for the geared engines studied, the direct drive engines studied bottomed for the -12.5 EPNdB suppression case and got worse for the -15.0 EPNdB case. This was due to the fact that for the fan tip speed used for this case, effects of the increased LP turbine

TABLE 42

LOWER FAN PRESSURE RATIO DIRECT-DRIVE ENGINE NOISE ESTIMATES

GENERAL ELECTRIC STUDY AIRCRAFT

INCLUDES A/C NOISE, NO MARGINS

	TAKEOFF 6.5 Km (3.5 N. MI.)				SIDELINE .46 Km (.25 N. MI.)				APPROACH 36% F <sub>n</sub>				
	Altitude m (Ft)	Engine Noise EPNL	Δ EPNL Rel. to FAR36 (1969)	Δ EPNL Rel. to NPRM 75-37C	Δ EPNL Rel. to Direct- Drive Baseline Engine	Engine Noise EPNL	Δ EPNL Rel. to FAR36 (1969)	Δ EPNL Rel. to NPRM 75-37C	Δ EPNL Rel. to Direct- Drive Baseline Engine	Engine Noise EPNL	Δ EPNL Rel. to FAR36 (1969)	Δ EPNL Rel. to NPRM 75-37C	Δ EPNL Rel. to Direct- Drive Baseline Engine
Domestic Trijet	512 (1680)	93.1	-9.3	-4.5	0	90.5	-15.5	-8.3	+0.5	98.1	-8.1	-4.7	+0.7
International Trijet	405 (1330)	96.4	-9.2	-3.7	0	92.0	-15.5	-8.4	+0.5	99.9	-7.6	-4.4	+0.6

TABLE 43

## LOWER FAN PRESSURE RATIO NOISE SUPPRESSION STUDY SUMMARY

	DOMESTIC A/C				INTERCONTINENTAL A/C			
	0.54	1.0	0.54	1.0	0.54	1.0	0.54	1.0
Inlet $L_T/D$	0.54	1.0	0.54	1.0	0.54	1.0	0.54	1.0
LPT Turbine Blade Number in Stages 4 and 5	NOMINAL	NOMINAL	+16%	+16%	NOMINAL	NOMINAL	+16%	+16%
$\Delta$ DOC, %	Base	+1.46%	+0.07	+1.5	Base	+2.3%	+0.08	+1.3
$\Delta$ WF, %	Base	+1.9%	+0.04	+1.9	Base	+3.0%	+0.06	+1.5
Takeoff EPNL (No Margin) 6.5 km (3.5 NM)	93.1	90.3	93.1	90.3	96.4	95.3	96.4	95.3
$\Delta$ EPNL Rel. to FAR36 (1969)	-9.4	-12.2	-9.4	-12.2	-9.3	-10.4	-9.3	-10.4
Approach EPNL <sup>(1)</sup> (No Margin) .46 km (.25 NM)	97.4	96.2	97.0	95.1	99.3	98.4	98.9	96.9
$\Delta$ EPNL Rel. to FAR36 (1969)	-8.8	-10.0	-9.2	-11.1	-6.9	-7.8	-7.3	-9.3

(1) A/C Noise Included



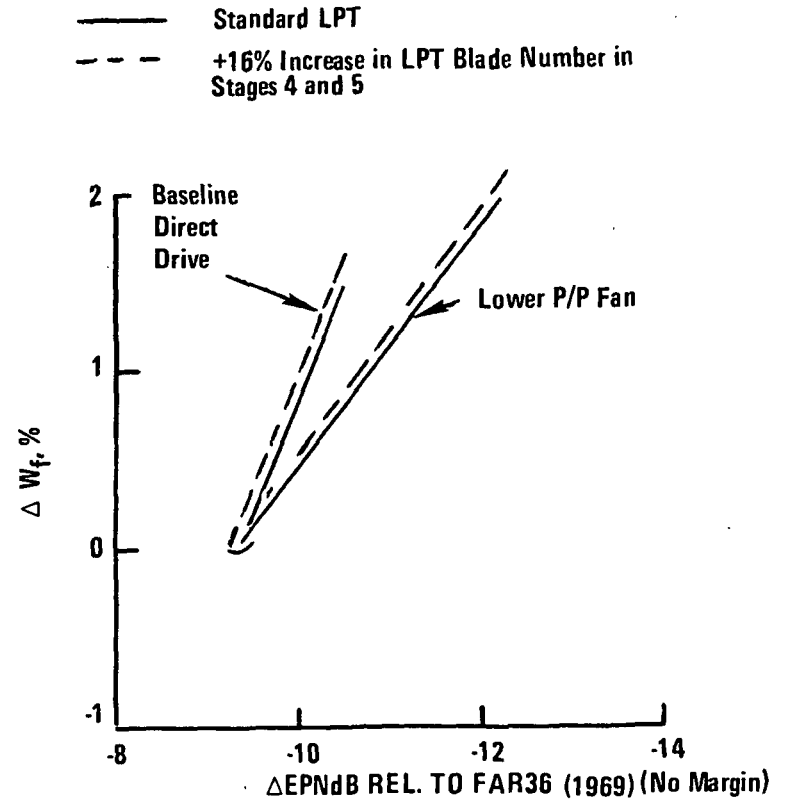
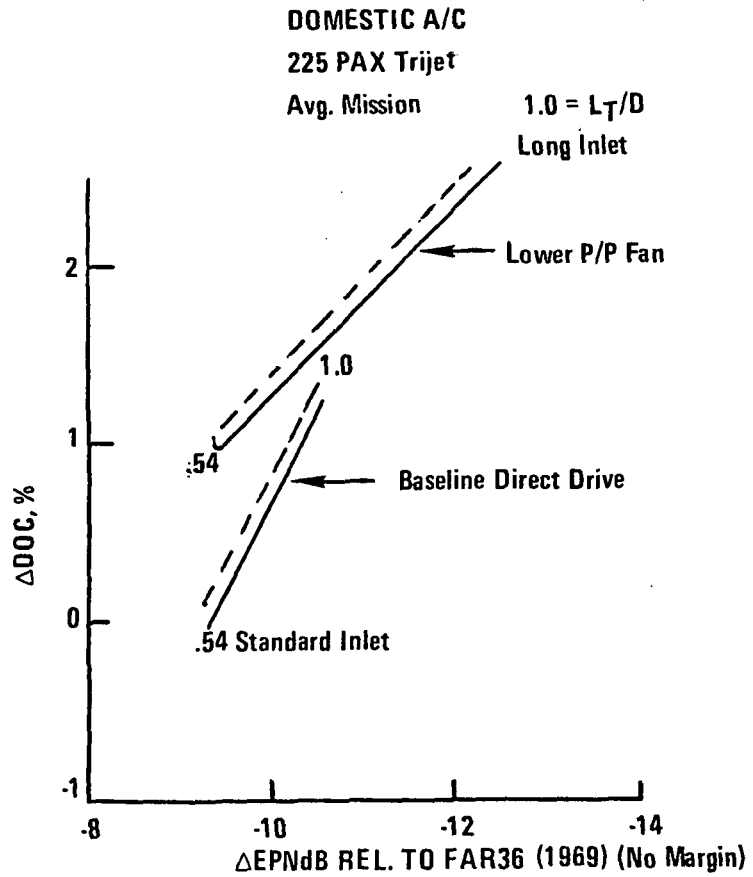


Figure 36. Economic Penalties of Additional Noise Suppression, Full Power Takeoff

GE DOMESTIC A/C  
 225 PAX Trijet  
 Avg. Mission

———— Standard LPT  
 - - - - +16% Increase in LPT  
 Blade Number in Stgs. 4 & 5

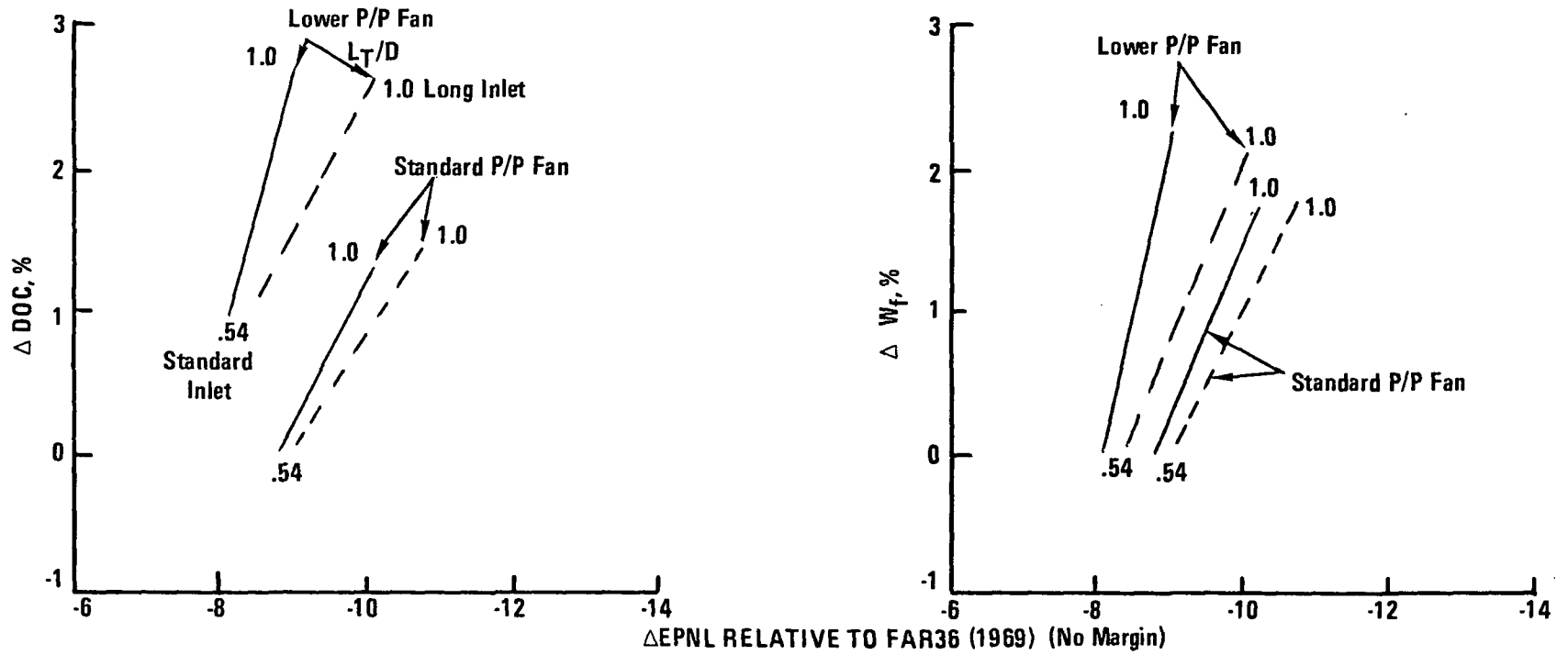


Figure 37. Economic Penalties of Additional Noise Suppression,  
 36% Approach Power

TABLE 44

SUPPRESSED ENGINE DIMENSIONS

	Task II Engines		Suppressed Engines		Highly Suppressed Engines	
	Direct Drive	Gear Drive	Direct Drive	Gear Drive	Direct Drive	Gear Drive
FAR 36 (1969) - $\Delta$ EPNdB (No Margin)	~10		~12.5		~15.0	
Fan Tip Diameter* m (Inches)	2.02 (79.7)	2.26 (89.0)	2.31 (91.1)	2.30 (90.5)	2.67 (105)	2.69 (105.8)
Inlet L/D Ratio	.54	.54	1.0	1.0	1.0	1.0
No. Boosters	0	1	1	1	2	2
Transition Duct (HPT/LPT)	No	No	Yes	No	Yes	No
LPT Stages	5	3	5	3	5	3
Nacelle Length - m (Inches)	5.66 (223)	5.92 (233)	7.16 (282)	7.11 (280)	8.28 (326)	8.31 (327)

\*For equivalent max. climb thrust.

TABLE 45

SUPPRESSED ENGINE PERFORMANCE

	<u>Baseline Task II</u> <u>Engines</u>		<u>Suppressed</u> <u>Engines</u>		<u>Highly Suppressed</u> <u>Engines</u>	
	Direct Drive	Gear Drive	Direct Drive	Gear Drive	Direct Drive	Gear Drive
FAR36 (1969) - $\Delta$ EPNdB (No Margin)	~10		~12.5		~15.0	
Fan Tip Diameter - m (Inches)	2.02 (79.7)	2.26 (89.0)	2.31 (91.1)	2.30 (90.5)	2.67 (105)	2.69 (105.8)
Installed $F_{NI}$ @ - Lbs. M = .8, 35K, MxCl.	8330 $\longrightarrow$					
Core Corr. Flow - Kg/Sec (Lbs/Sec) (MxCl.)	54.4 (120)	52.5 (115.8)	54.1 (119.2)	52.3 (115.4)	55.6 (122.6)	51.6 (113.7)
Fan Pressure Ratio (MxCl.)	1.71	1.55	1.53	1.53	1.38	1.38
Bypass Ratio (MxCl)	6.3	8.5	8.2	8.5	11.1	12.2
Fan Tip Speed (Corr.) m/sec (Ft/Sec)	457 (1500)	396 (1300)	402 (1320)	402 (1320)	352 (1155)	352 (1155)
Overall Pressure Ratio - (MxCl.)	38 $\longrightarrow$					
Fan Pressure Ratio - SLTO	1.53	1.4	1.4	1.4	1.3	1.3
Turbine Temperature °C (°F) Hot Day SLTO	1366 (2490) $\longrightarrow$					
Installed $\Delta$ sfc - %	Base	-2.9	-2.6	-3.4	-1.7	-4.8
Installed $\Delta$ sfc - % (CF6-50C Base)	-12.1	-14.6	-14.3	-15.1	-13.6	-16.3

loading and LP turbine transition duct cooling and losses exceeded the benefits of the increased propulsive efficiency of the larger fan. As in the previous geared engine studies, gearbox noise was not included.

Figure 38 indicates the effects upon fuel burned and DOC of the larger fan needed for high suppression. Fuel burned decreases slightly for the direct drive engines for an approximate -10.5 EPNdB suppression and then begins to increase rapidly as the inlet duct treatment L/D goes from .54 to 1.0. For the geared engines, fuel burned holds relatively constant and then begins to increase but at a much slower rate than the direct-drive engine.

A  $\Delta$ DOC breakdown of the highly suppressed engines is given in Table 46 for each of the major DOC contributors. Note that the largest single contributor to the increasing DOC penalty of the more highly suppressed engines is the increasing installed weight factor. Figure 38 shows the cumulative effect of all the factors for both the direct and geared engines. Take-off noise was used as a basis for comparison since it was more limiting than sideline or approach noise. Unlike the  $W_f$  trends, the DOC trends are upward for all the more highly suppressed engines. The  $\pm 1\%$  sfc band indicates the effect of not being exactly optimum in cycle or configuration.

From the preceding, it can be seen that additional suppression, over and above the Task II baseline direct drive and geared turbofans leads to increased fuel consumption for all but the most minor changes and to higher DOC for all engines studied.

## 2. Cycle and Performance Evaluation

The four engines that were matched out for this study consist of a matrix of two levels of design fan pressure ratio for both a direct-drive and a geared type of low pressure rotor system. The fan pressure ratios of 1.38 and 1.53 (at MxCl) were chosen for this study, in order to show a parametric excursion in noise reduction from the Task II direct-drive and geared engines. An installed performance analysis of the four engines was completed in order to evaluate the economic trade factors of DOC and fuel burned versus noise reduction. A summary of the cycle performance and component characteristics that changed from the respective Task II engines is given in Table 47.

The performance evaluation considered design changes in the fan, LP turbine and exhaust system. The same two fan designs were used for both types of rotor systems in order to evaluate a direct-drive versus a geared engine for the same fan design. The corrected tip speeds for the 1.38 and 1.53 fan pressure ratios were selected so as to produce the maximum fan efficiency. The bypass ratio for each of the four engines was determined by maintaining the same ratio of total pressures in the mixing plane as the respective Task II baseline engines.

The LP turbine designs for the direct-drive engines were based on increasing the pitchline LPT diameter of the Task II five-stage design, to minimize the effect of higher loading on LPT efficiency. A transition duct was included in the engine designs to account for the difference in flow-path diameters between the HPT exit and LPT diaphragm. In the case of the 1.53 P/P engine, a transition duct was used based on GE experience with the TF34 and its associated cooling and pressure drop performance. A reasonable work coefficient of 1.40 resulted from the cycle balance. In the case of the 1.38 P/P engine, however, the use of the same transition duct produced

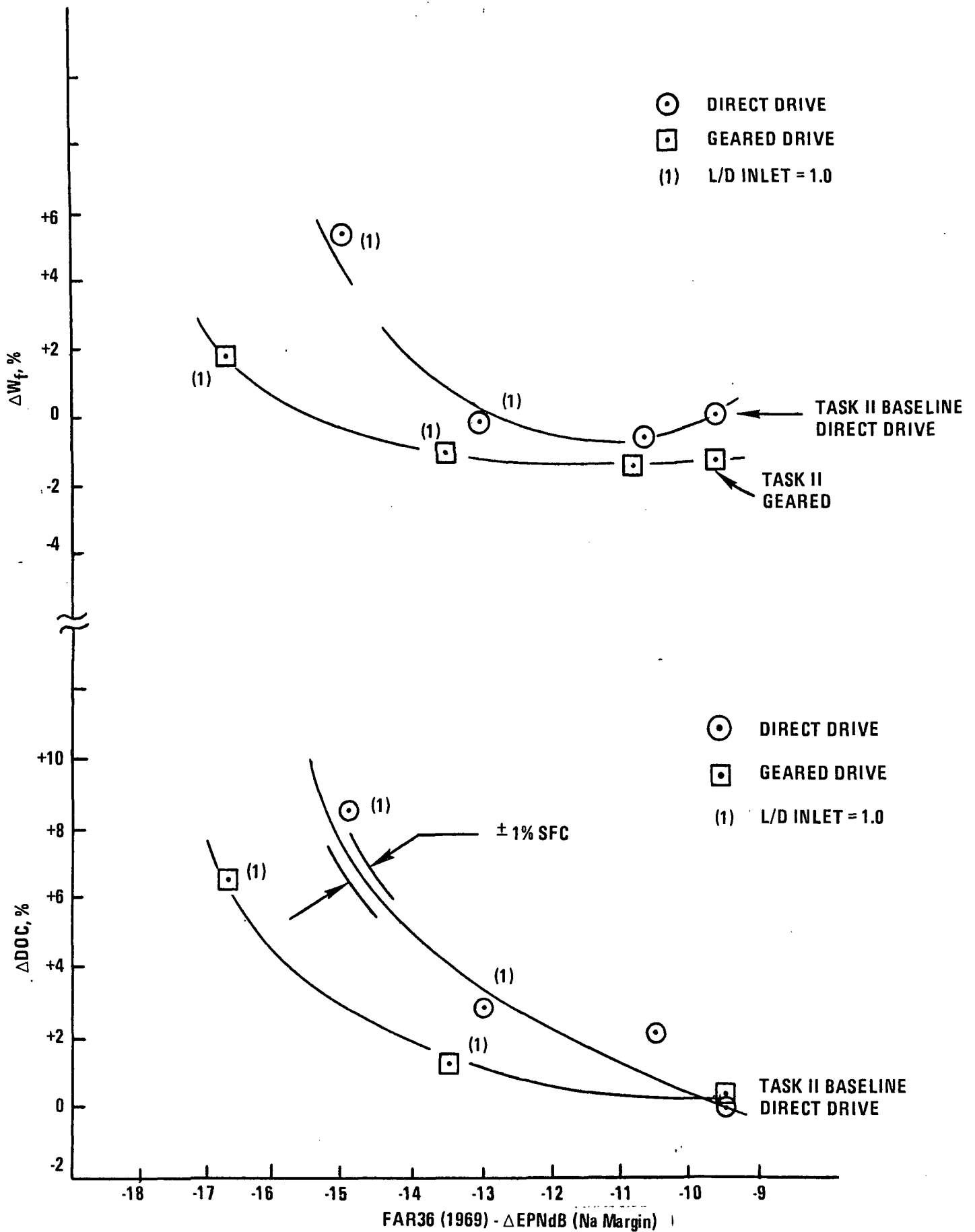


Figure 38. Max. Cruise  $\Delta W_f$  and  $\Delta DOC$  vs. Takeoff Noise - Domestic Aircraft

TABLE 46

Δ DOC BREAKDOWN FOR SUPPRESSED ENGINES

DOMESTIC MISSION

	Reference Task II Engines		Suppressed Engines		Highly Suppressed Engines	
	Direct Drive	Gear Drive	Direct Drive	Gear Drive	Direct Drive	Gear Drive
FAR36 (1969)- ΔEPNdB (No Margin)	~10		~12.5		~15.0	
Fan Tip Diameter - m (Inches)	2.02 (79.7)	2.26 (89.0)	2.31 (91.1)	2.30 (90.5)	2.67 (105)	2.69 (105.8)
ΔEngine Maintenance %	Base	-.03	+.67	+.06	+1.60	+1.01
Δsfc (Installed) %	Base	-1.71	-1.53	-2.00	-1.00	-2.83
ΔWt (Installed) %	Base	+1.71	+2.45	+2.50	+5.80	+6.27
ΔSelling Price %	Base	+.36	+1.16	+.76	+2.39	+2.06
ΔDOC - %	Base	+.33	+2.75	+1.32	+8.79	+6.51

TABLE 47

CYCLE AND LOW SPOOL COMPONENT PERFORMANCE SUMMARY.8  $M_n$ /10668 m (35K Ft.)/Std. + 10°C (+ 18°F) DayCYCLE

<u>Type of Drive</u>	<u>Direct</u>	<u>Direct</u>	<u>Geared</u>	<u>Geared</u>
% $\Delta$ sfc Inst MxC1	-13.6	-14.3	-16.3	-15.1
$\beta$ MxC1	11.1	8.2	12.2	8.5

COMPONENTSFan MxC1

Fan P/P	1.38	1.53	1.38	1.53
$U_T/\sqrt{\theta}$ - m/sec (ft/sec)	352 (1155)	402 (1320)	352 (1155)	402 (1320)
$\eta_{adb}$ .	.887	.882	.887	.887
r/r	.37	.37	.37	.37

LPT (MXCL)

$\frac{gJ\Delta h}{2U_p^2}$	1.85	1.40	.63	.73
No. Stages	5	5	3	3
Transition Duct	Yes	Yes	No	No
$\eta_{adb}$	.894	.914	.923	.923
Gear Loss	0	0	1.3%	1.3%



an unreasonable loading on the LP turbine. As a result, a maximum loading was established based on a work coefficient of 1.85 and a larger, less efficient transition duct was used.

The performance characteristics of the LP turbine designs for the geared engines are the same as the baseline Task II geared engine. The evaluation of these characteristics was conducted as follows:

- The LPT RPM was calculated from the criteria of maintaining the same value of "effective LPT discharge area times LPT RPM<sup>2</sup>" as the Task II geared engine.
- A work coefficient was calculated from the RPM as established above, the same pitchline diameter as the Task II geared engine, and the enthalpy requirement of the fan.

The work coefficients of the LPTs for both of the new geared engines were not enough different from the baseline engines to change the efficiency assumptions. As was the case for the baseline geared engine, the LPT efficiency was derated by 1.2 points to account for a 1.3% gear loss.

Exhaust system and external nacelle performance have been incorporated into the overall cycle performance evaluation for this study.

### 3. Installation Evaluation

Preliminary flowpath designs were conducted for four E<sup>3</sup> engine configurations. The engine configurations were defined on the basis of the noise requirements for the parametric noise study and included two design fan pressure ratios, 1.38 and 1.53, for both a direct-drive and a gear-driven engine system. The flowpaths, which included the inlet, nacelle, and exhaust system, were defined so that exhaust system internal performance and nacelle external drags could be determined for each engine for the installed performance cycle evaluation. Additionally, the flowpath definition allowed the determination of required engine weight estimates.

Flowpath designs were performed for each engine on a consistent basis using several ground rules. The engine flange-to-flange turbomachinery geometry was determined largely by noise considerations on the engine cycle. Flow areas were based on cycle data at a M.8/10668m (35K) maximum climb design point. Several geometric relationships were held essentially constant for all designs. These included:

$$\text{Inlet diameter ratio, } D_{H.L.}/D_{MAX} = .88$$

$$\text{Inlet length ratio, } L_I/D_{FAN} = .70$$

$$\text{Nozzle terminal boattail angle} = 10^\circ$$

The exhaust system mixers had 24 lobes and were designed to achieve 65% mixing effectiveness. The exhaust nozzles had a converging-diverging section with an area ratio,  $A_{exit}/A_{throat}$ , of 1.025 in order to provide desirable effective areas for the engine cycle at takeoff and cruise. Additionally, the nacelle flowpath was made compatible with a fan reverser system.

Major dimensions of the resulting nacelle configurations are shown in Table 48. The nacelle overall fineness ratio,  $L/D_M$ , and nacelle-to-fan diameter ratio,  $D_M/D_F$ , were nearly the same for all configurations. This is expected because of the consistency in the flowpath designs.

Following the definition of each nacelle, the aerodynamic performance was calculated. The performance evaluation included an estimate of the nacelle external drag and the exhaust system internal pressure losses. Calculation of the external drag was performed at  $M.8/10668m$  (35K) and included both the friction and pressure drag. Friction drag was calculated using equivalent flat plate, turbulent boundary layer equations with corrections for compressibility and supersonic velocity. Pressure drag was determined using a correlation of isolated nacelle wind tunnel test data. Results of the external drag estimates are presented in Figure 39. As can be expected, the drag increases with increasing fan diameter. The consistency of the nacelle designs resulted in a linear relationship between drag and fan diameter. In terms of percent net thrust (or sfc), the low pressure ratio fans cost nearly 2% in additional external drag.

Internal pressure losses were calculated for the fan duct, core duct, and nozzle tailpipe as shown schematically in Figure 40. Results of the internal performance estimates are presented in Table 49 which includes a breakdown of the loss elements. These pressure losses were based on a combination of analytical calculations using standard calculation procedures, and estimates using CF6-50 experience. Overall, the direct drive system has slightly better performance, about .2% sfc, largely due to the oil cooler required for the geared fan systems.

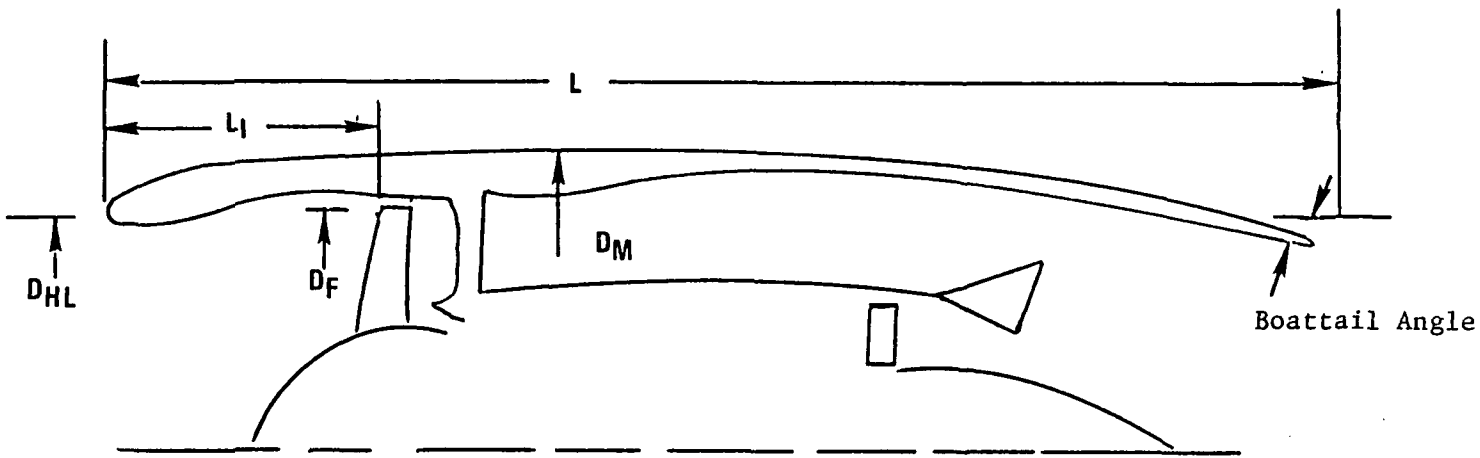
In summary, the exhaust system internal performance for all four flowpaths are nearly identical, within .2% cruise sfc, with no clear or significant advantage for any system. The external drags, however, show a clear advantage for the higher pressure ratio fans, nearly 2% sfc at cruise.

#### 4. Acoustic Evaluation

The cycle changes required to attain FAR36 (1969)-15 were evaluated for both a direct-drive and geared fan. Cycle data were obtained for both engines at 1.3 and 1.4 takeoff fan pressure ratio using a core size of 54.5 Kg/sec (120 lb/sec). Noise predictions were made for this size and then scaled to a maximum climb thrust equal to that of the baseline Task II engine on a 126645 Kg (279,000 lb) gross weight domestic trijet. Due to the larger lapse rate at cruise, the SLS thrust of the lower pressure ratio fans was increased relative to the Task II engine. This larger takeoff thrust in turn allowed the aircraft to attain a higher altitude at the 6.5 Km (3.5 nm) monitoring point which was factored into the noise calculations. For approach, the noise was estimated at a power setting of 35%. A summary of the engine/aircraft assumptions is given in Table 50.

TABLE 48

PARAMETRIC ENGINE NOISE EVALUATION NACELLE GEOMETRIES



	<u>Geared Fan</u>		<u>Direct Drive</u>	
	<u>1.53 P/P</u>	<u>1.38 P/P</u>	<u>1.53 P/P</u>	<u>1.38 P/P</u>
$D_F$ (ref) m (in.)	2.34 (92.3)	2.76 (108.7)	2.32 (91.42)	2.64 (103.85)
$D_{HL}$ m (in.)	2.42 (95.2)	2.83 (111.6)	2.37 (93.4)	2.73 (107.3)
$D_M$ m (in.)	2.73 (107.6)	3.22 (126.8)	2.70 (106.2)	3.09 (121.7)
$L_I$ m (in.)	1.65 (64.9)	1.94 (76.4)	1.63 (64.2)	1.88 (74.0)
$L$ m (in.)	6.75 (265.7)	7.82 (308.0)	6.82 (268.6)	7.52 (296.0)
Boattail Angle	10°	10°	10°	10°
$L/D_M$	2.47	2.43	2.53	2.43

	GEARED FAN		DIRECT DRIVE	
	1.53 FPR	1.38 FPR	1.53 FPR	1.38 FPR
FRICTION DRAG, N (lbs)	150 (339)	204 (458)	151 (340)	189 (425)
PRESSURE DRAG, N (lbs)	76 (171)	106 (238)	73 (164)	98 (220)
TOTAL	226 (510)	310 (696)	224 (504)	287 (645)
	□	△	○	◇
D/F <sub>n</sub> (MixCr)	.060	.079	.061	.079

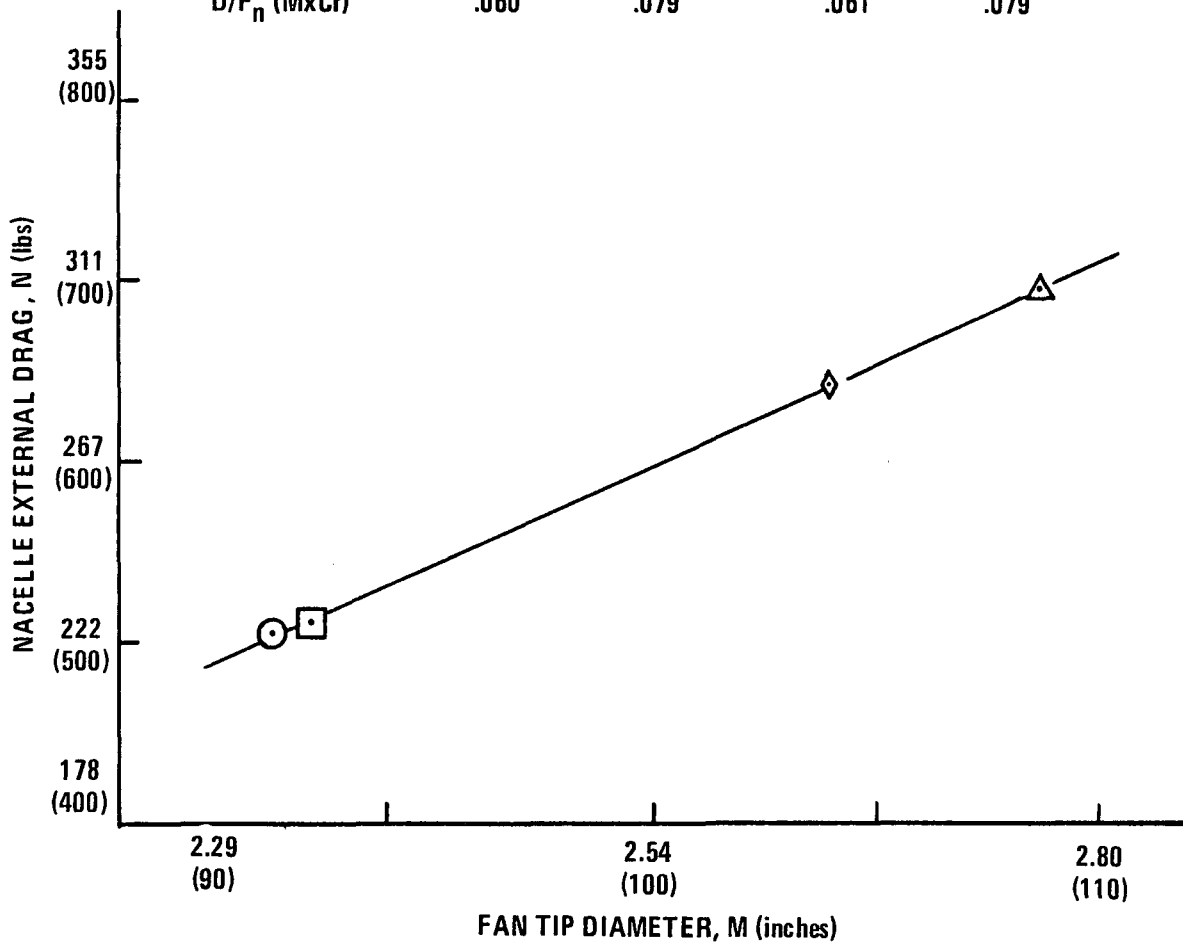


Figure 39, Highly Suppressed Engine, Nacelle Drag, M .8/35K.

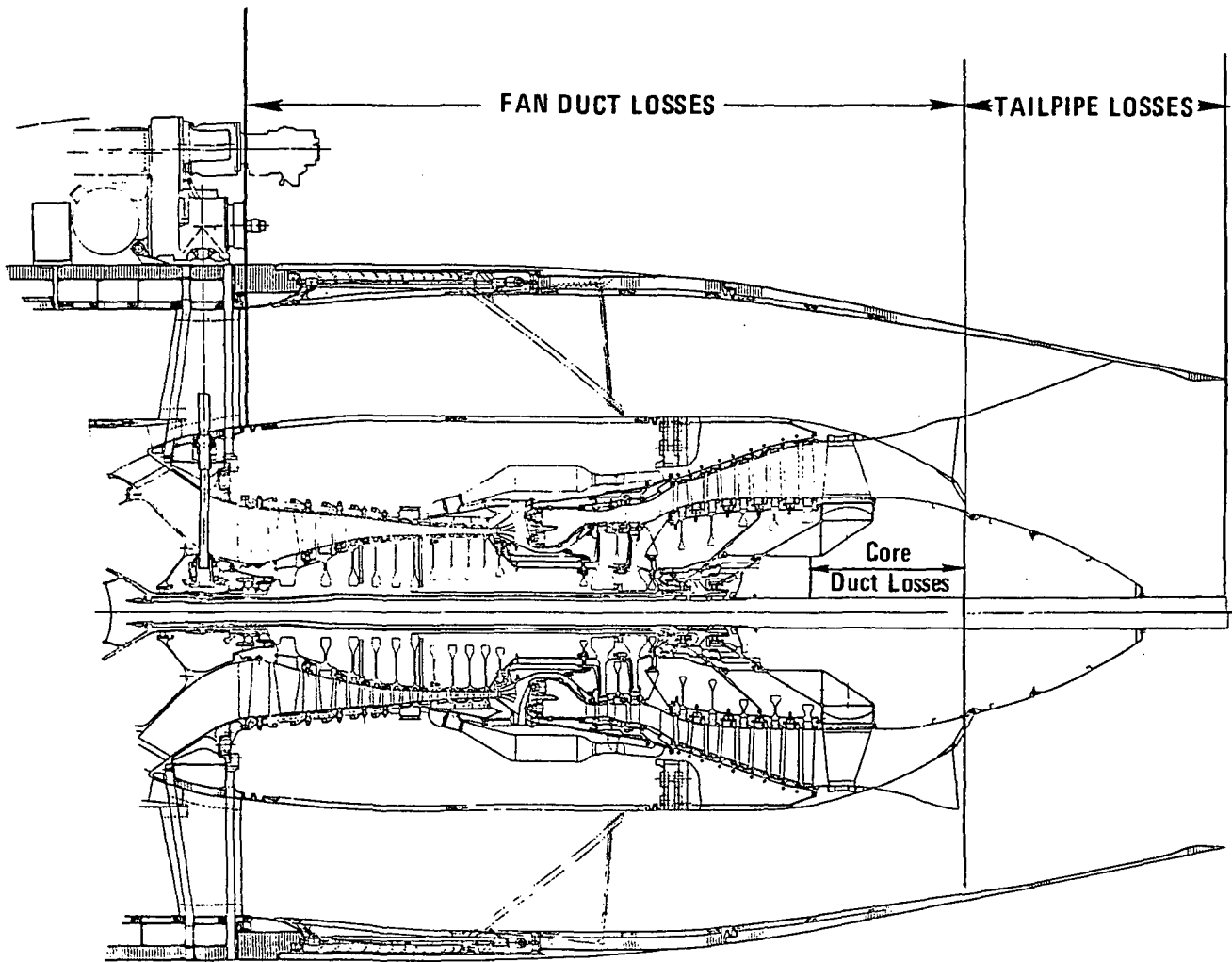


Figure 40. E<sup>3</sup> Exhaust System Schematic

TABLE 49

EXHAUST SYSTEM INTERNAL PRESSURE LOSS SUMMARY

.8 Mn/10668 m (35K Ft.)/Std. + 10°C (+ 18°F) Day

Loss Item	<u>Total Pressure Loss, % <math>\Delta P_t/P_t</math></u>			
	1.53 Direct Drive	1.38 Direct Drive	1.53 Geared Fan	1.38 Geared Fan
Fan P/P	1.53	1.38	1.53	1.38
Fan Drive	Direct Drive	Direct Drive	Geared Fan	Geared Fan
<u>Fan Duct</u>				
Friction	.39	.38	.33	.30
Acoustic Treatment (80%)	.12	.11	.10	.09
Mixer	.11	.11	.12	.11
Steps, Gaps, Pylon, Int.	.2	.2	.2	.2
Thrust Reverser	.07	.07	.07	.07
Scoops	.14	.14	.14	.14
Oil Cooler	-	-	.35	.35
Total	1.03	1.01	1.31	1.26
<u>Core Duct</u>				
Turbine Rear Frame	.11	.11	.11	.11
Friction	.20	.24	.14	.18
Mixer	.44	.65	.46	.68
Steps and Gaps	.05	.05	.05	.05
Total	.80	1.05	.76	1.02
<u>Tailpipe</u>				
Friction	.37	.32	.35	.33
Steps and Gaps	.05	.05	.05	.05
Total	.42	.37	.40	.38

TABLE 50

SCALED THRUST AND NOISE CHECKPOINT ALTITUDE

- DOMESTIC TRIJET (GENERAL ELECTRIC STUDY)
- 126645 Kg (279,000 LBS) GROSS WEIGHT

<u>Engine Type</u>	<u>Fan P/P @ Takeoff</u>	<u>SLS Thrust, N (Lbs)</u>	<u>Altitude @ 6.5 Km (3.5 nm), m (ft)</u>
Task II Baseline (Direct Drive)	1.53	11.3K (25.3K)	482 (1580)
Direct Drive	1.40	12.4K (27.6K)	536 (1760)
Direct Drive	1.30	13.7K (30.5K)	611 (2005)
Geared	1.40	12.4K (27.7K)	539 (1770)
Geared	1.30	13.9K (31K)	624 (2046)

Three levels of suppression were evaluated to attain FAR36 (1969)-15. These were:

1. Treated inlet length of .54 fan diameters plus inner and outer wall treatment in the fan exhaust duct.
2. Treated inlet length of 1.0 fan diameters plus inner and outer wall treatment in the fan exhaust duct.
3. Same as configuration 2 plus turbine treatment in the core exhaust duct. This configuration was evaluated only at approach for the 1.38 fan P/P case.

Results of the analysis are presented on Figures 41, 42, and 43. Figure 41 shows takeoff for the various configurations plus the Task II brochure levels. To meet FAR36 (1969)-15 with the long inlet treatment, the fan pressure ratio must be reduced to 1.3. The short inlet would require a fan pressure ratio below 1.3. With the geared drive fan, pressure ratio can increase to approximately 1.35. This is the benefit attained from lower turbine noise with the geared fan. To attain a comparable level, the direct drive turbine noise would have to be reduced 10 PNdB. Figure 42 shows approach levels with the aircraft noise added to the engine levels. As the fan pressure ratio drops and correspondingly fan rpm decreases, the turbine noise becomes more significant because it falls into the higher weighted PNL frequencies. Below a fan pressure ratio of 1.4 this causes an increase in noise as indicated on Figure 42. Aircraft noise, which is shown on Figure 42, is creating a noise floor which prevents any of the configurations from attaining FAR36 (1969)-15. Figure 43 shows the approach noise without the aircraft noise floor. The geared fan can attain FAR36 (1969)-15 at a fan pressure ratio of 1.35 with the short inlet treatment length. With the long inlet a fan pressure ratio of 1.45 to 1.50 could be utilized. The direct drive fan is prevented from reaching FAR36 (1969)-15 by turbine noise. Additional turbine suppression would be required at a fan pressure ratio of 1.4 to meet the goal. Comparison of Figure 43 with Figure 41 shows that takeoff noise is the more limiting factor in attaining FAR36 (1969)-15 if aircraft noise at approach is not considered. With aircraft noise, the approach case is limiting.

### C. Summary of Aircraft Subcontractor Studies

Commercial transport studies were conducted by three airplane subcontractors and by General Electric to define host aircraft and missions for the Advanced Turbofan Evaluation.

Each of the subcontractors, and General Electric, surveyed the future market potential for a domestic and for an intercontinental transport. The range, passenger load and aircraft configurations were chosen by Boeing, McDonnell-Douglas, Lockheed and General Electric and presented to NASA for approval. This choice was in each case influenced by the current market position and perception of the airframe subcontractors. Table 51 shows all of the host aircraft designs which were selected, and the TOGW and engine size required.



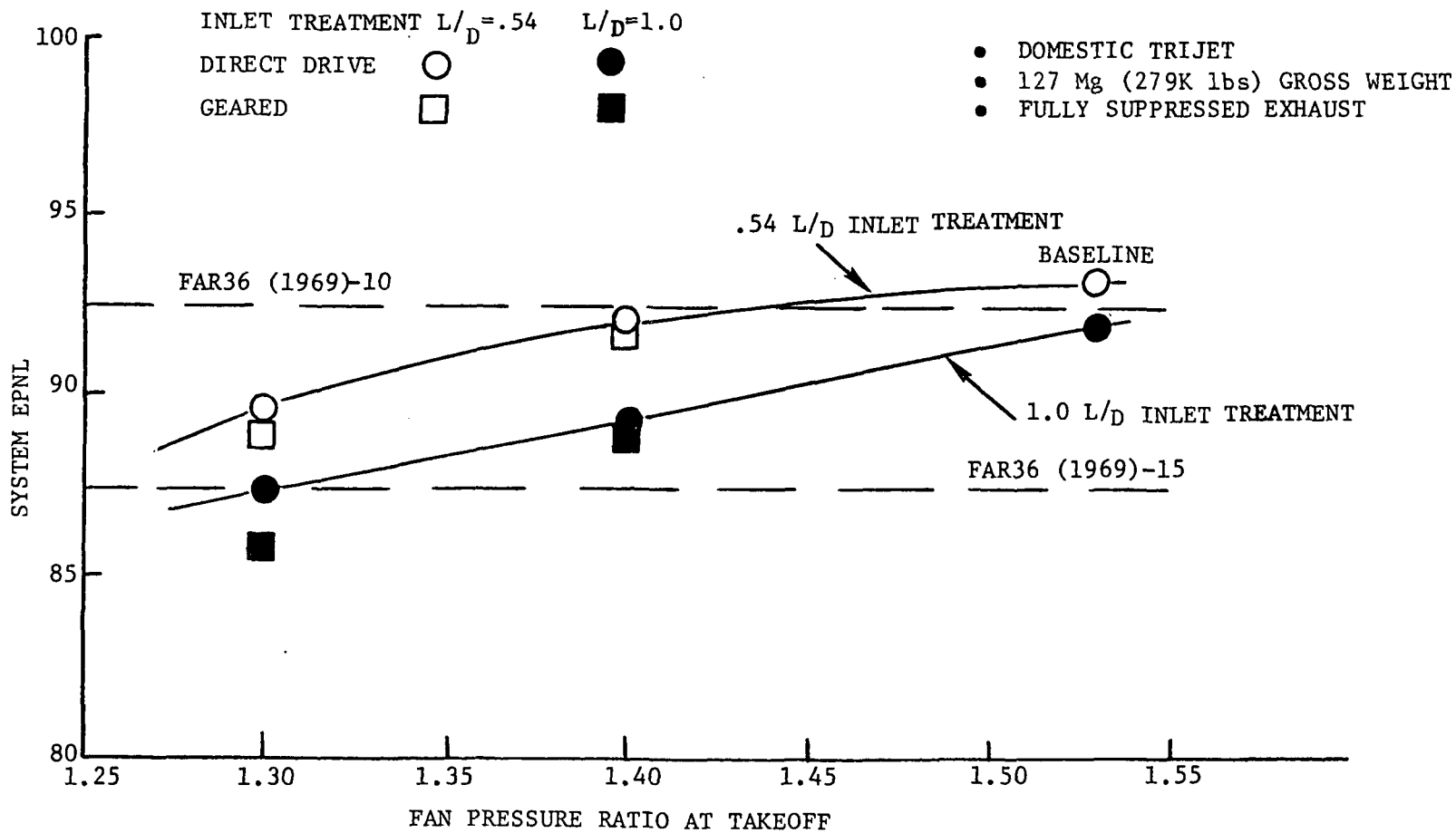


Figure 41. Cycle Effect on Takeoff Noise

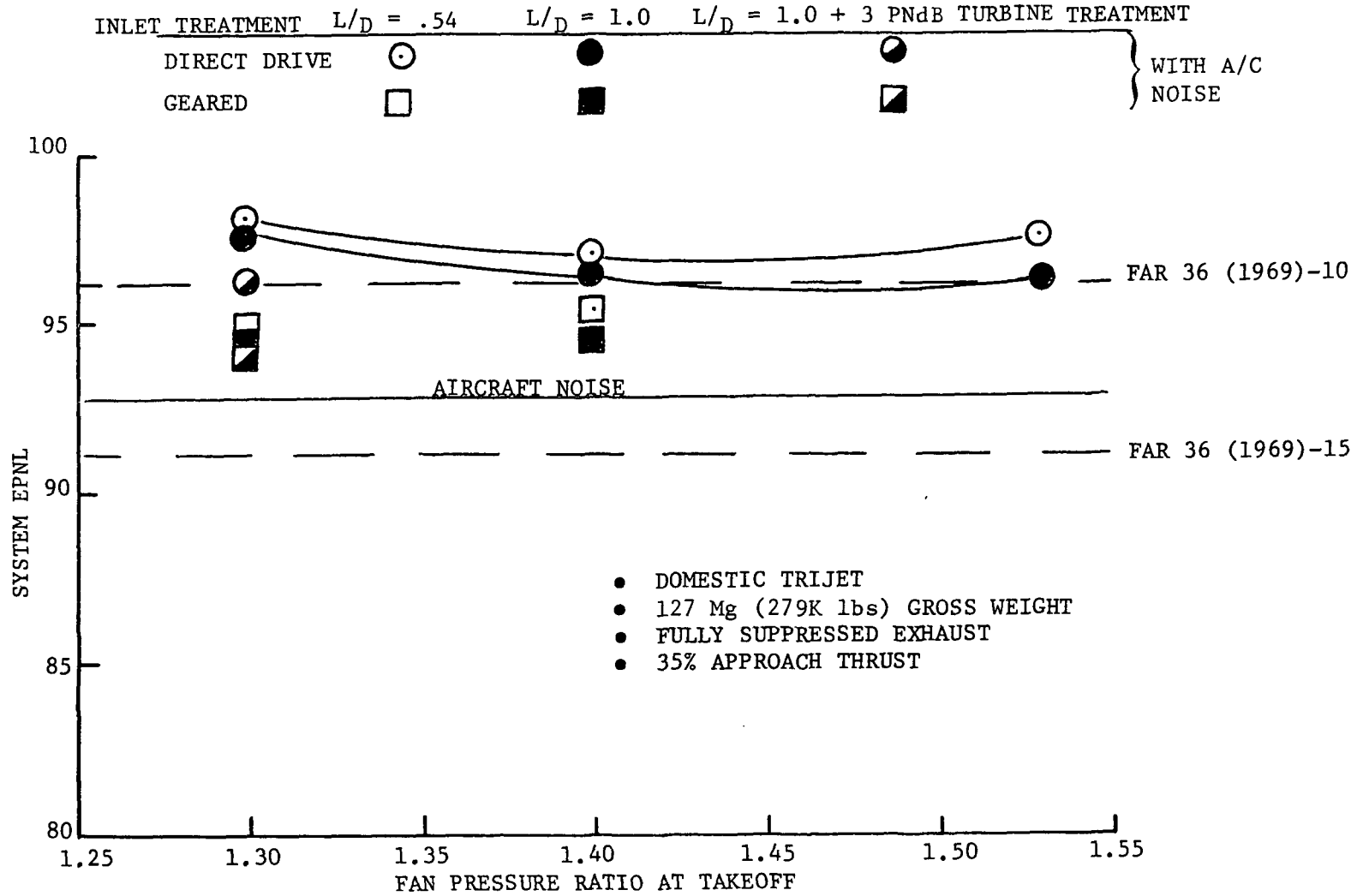


Figure 42. Cycle Effect on Approach Noise with Aircraft Noise Included.

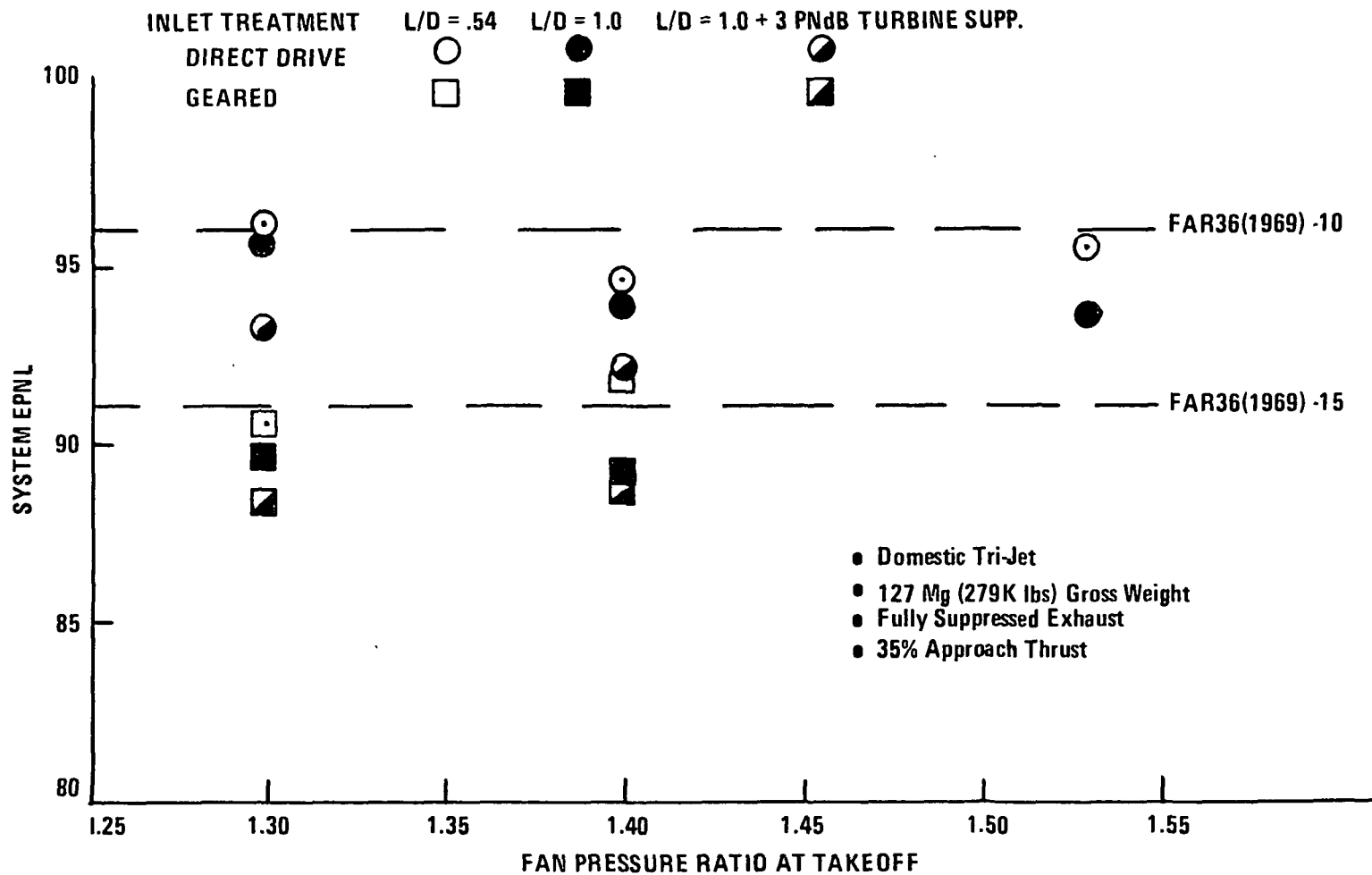


Figure 43. Cycle Effect on Approach Noise without Aircraft Noise

TABLE 51

AIRCRAFT DESIGNS BASED ON ADVANCED DIRECT-DRIVE ENGINE

	TBC		MCD		LCC		GE	
	DOM.	INT.	DOM.	INT.	DOM.	INT.	DOM.	INT.
Design Range - Km (N.MI.)	3704 (2000)	10186 (5500)	5556 (3000)	10186 (5500)	5556 (3000)	12038 (6500)	5556 (3000)	10186 (5500)
Design Pass, Load	196	196	458	438	400	400	225	225
No. of Engines	2	4	3	3	3	4	3	3
Des. TOGW - 1000 kg (1000 lbs)	113 (248)	170 (375)	225 (497)	288 (636)	184 (406)	262 (578)	126 (279)	195 (430)
Rated Engine Thrust - N (Lbs)	152,130 (34,200)	100,080 (22,500)	188,600 (42,400)	224,640 (50,500)	157,910 (35,500)	147,240 (33,100)	112,540 (25,300)	165,030 (37,100)
Total Installed Thrust/ TOGW	.275	.24	.256	.238	.262	.229	.272	.259

Each of the subcontractors conducted preliminary aircraft design studies using engine data supplied by General Electric for the advanced direct- and geared-drive baseline engine and the CF6-50 reference engine. Scaling data was supplied so that the proper engine size could be picked up for each mission-aircraft combination. The engine sizes required to propel these aircraft vary from 100,080 N (22,500 lb) to 224,640 N (50,500 lbs) T/O thrust.

Figure 44 indicates a reasonable consistency between the aircraft designs in terms of a domestic and an intercontinental family when design gross weight is plotted against number of passengers. Thrust trends vs. TOGW on Figure 45 show that Quadjets, Trijets, and Twins require successively larger engines for a given TOGW size.

The mission performance of the aircraft powered by scaled CF6-50's vs. the advance direct drive turbofan is summarized in Table 52 and Figure 46. The block fuel reductions of 11.7% to 17.8% for the domestic aircraft and 14.1% to 22.1% for the international aircraft, are for an average mission. Direct operating cost reductions (DOC), not including engine price and maintenance effects, were provided by Lockheed and General Electric. Estimates of DOC reductions for the McDonnell-Douglas aircraft were made using their engine sensitivity factors. There was no economic data available from the Boeing study.

Brief studies were made by Lockheed and Boeing using the Task II geared mixed-flow engine. The results of these studies indicated the fuel savings to be from 1.5 to 2.5% more for the geared engine than for the direct-drive engine. This additional fuel savings, however, was accompanied by an increase in DOC of approximately 0.5% based on Lockheed's study (no economic data was available from Boeing).

The aircraft characteristics necessary for noise estimates were also defined for each of the designs. The flight conditions, power settings, and aircraft-only noise were supplied by the aircraft companies. General Electric conducted the overall noise analyses. Table 53 shows the calculated noise at the measurement points along with the aircraft-only noise, altitude at the take-off checkpoint and approach power settings for each of the eight aircraft. The aircraft-only noise estimates for the three subcontractors and General Electric differ. Takeoff altitude at the checkpoint also varies considerably among the aircraft. The McDonnell-Douglas intercontinental aircraft takeoff altitude is only 302 M (990 feet), which is a strong factor in its high T/O noise, FAR 36 (1969)-8.6. The noise results alone are shown in bargraph form on Figure 47.

The initial cruise altitude, takeoff field length and altitude over the 6.5 Km (3.5 N.Mi.) checkpoint are summarized on Table 54 for all the study aircraft. These are generally consistent, except for the lower initial cruise altitude of the McDonnell-Douglas aircraft. The thrust relationship between takeoff and cruise selected for the direct drive advanced engine appears to be reasonably consistent for the aircraft considered.

For more details on the Task II studies performed by the subcontractors, refer to Appendix A.

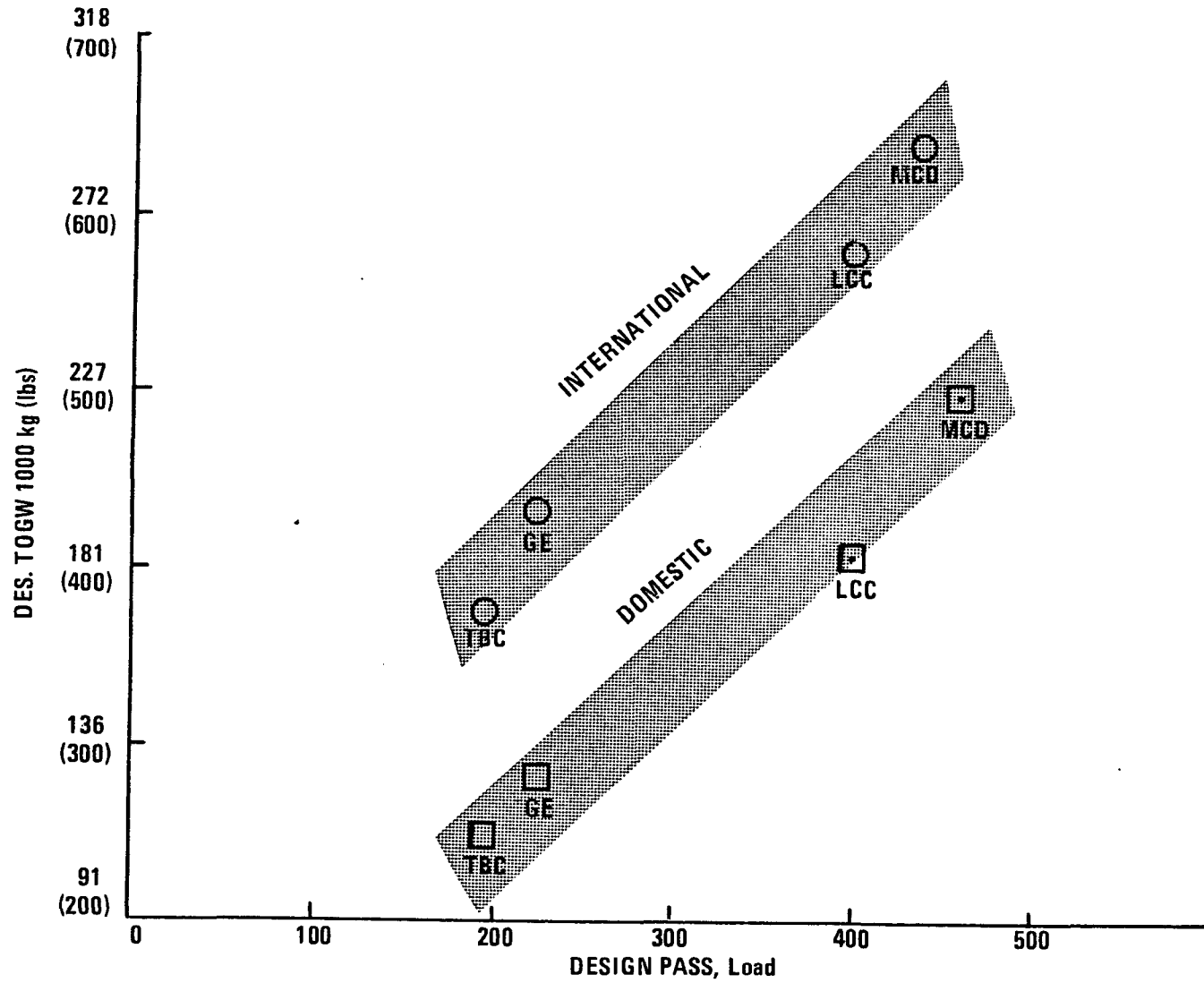


Figure 44, Aircraft Gross Weights, Advanced Direct-Drive Engine

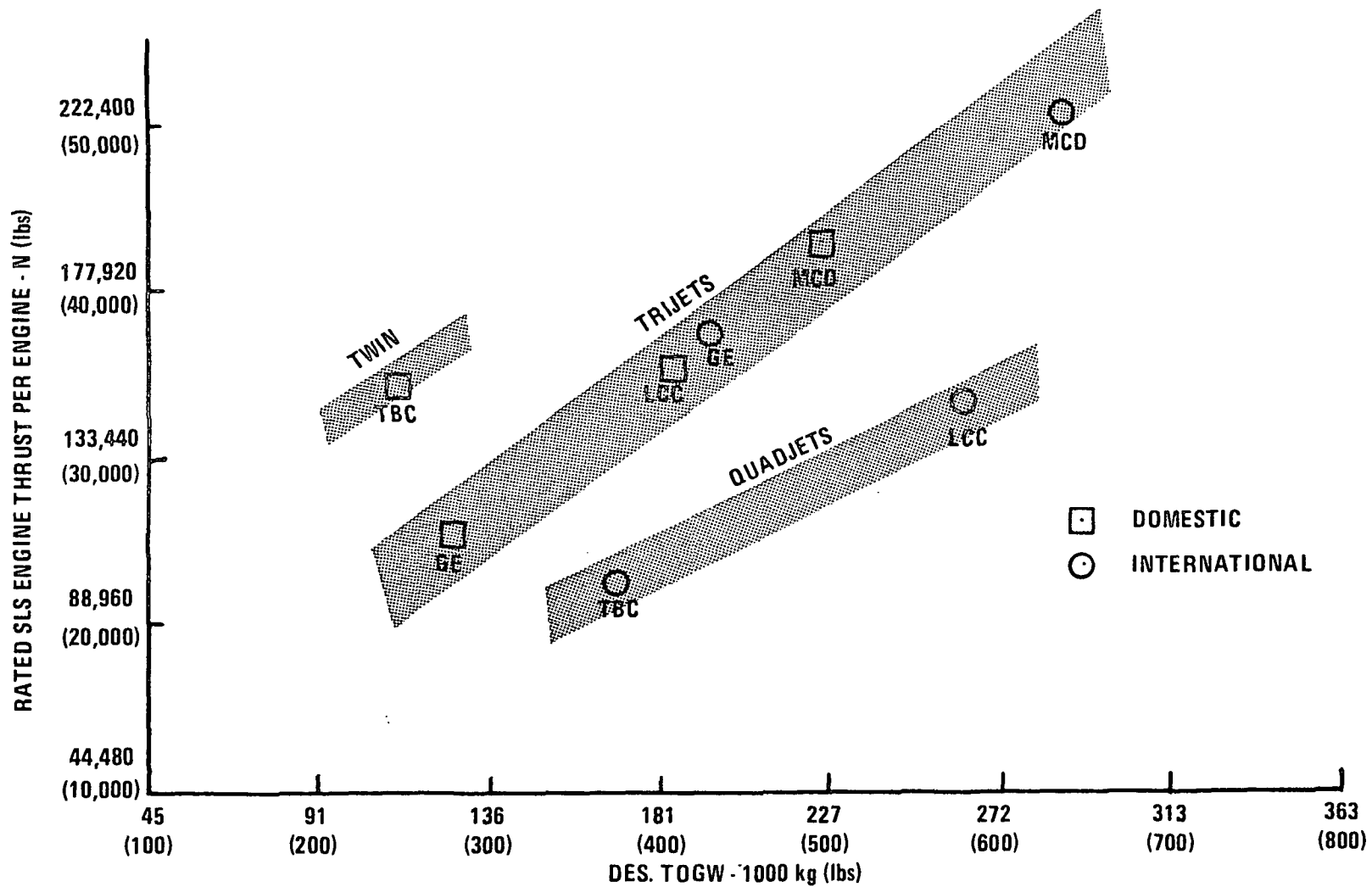


Figure 45. Engine Thrust Sizes, Advanced Direct-Drive Engine

TABLE 52

MISSION PERFORMANCEADVANCED DIRECT-DRIVE VS. SCALED CF6-50C - AVERAGE MISSION

	<u>TBC</u>		<u>MCD</u>		<u>LCC</u>		<u>GE</u>	
	<u>Dom.</u>	<u>Int.</u>	<u>Dom.</u>	<u>Int.</u>	<u>Dom.</u>	<u>Int.</u>	<u>Dom.</u>	<u>Int.</u>
$\Delta$ TOGW - %	-6.7	-11.2			-4.3	-11.1	-9.0	-11.6
$\Delta$ Block Fuel (Ave. Mission)	-11.7	-14.1	-14.6	-14.7	-14.6	-19.9	-17.8	-22.1
$\Delta$ DOC* (Ave. Mission)	**	**	- 7.0	- 6.2	-4.6	-9.1	-8.2	-13.2

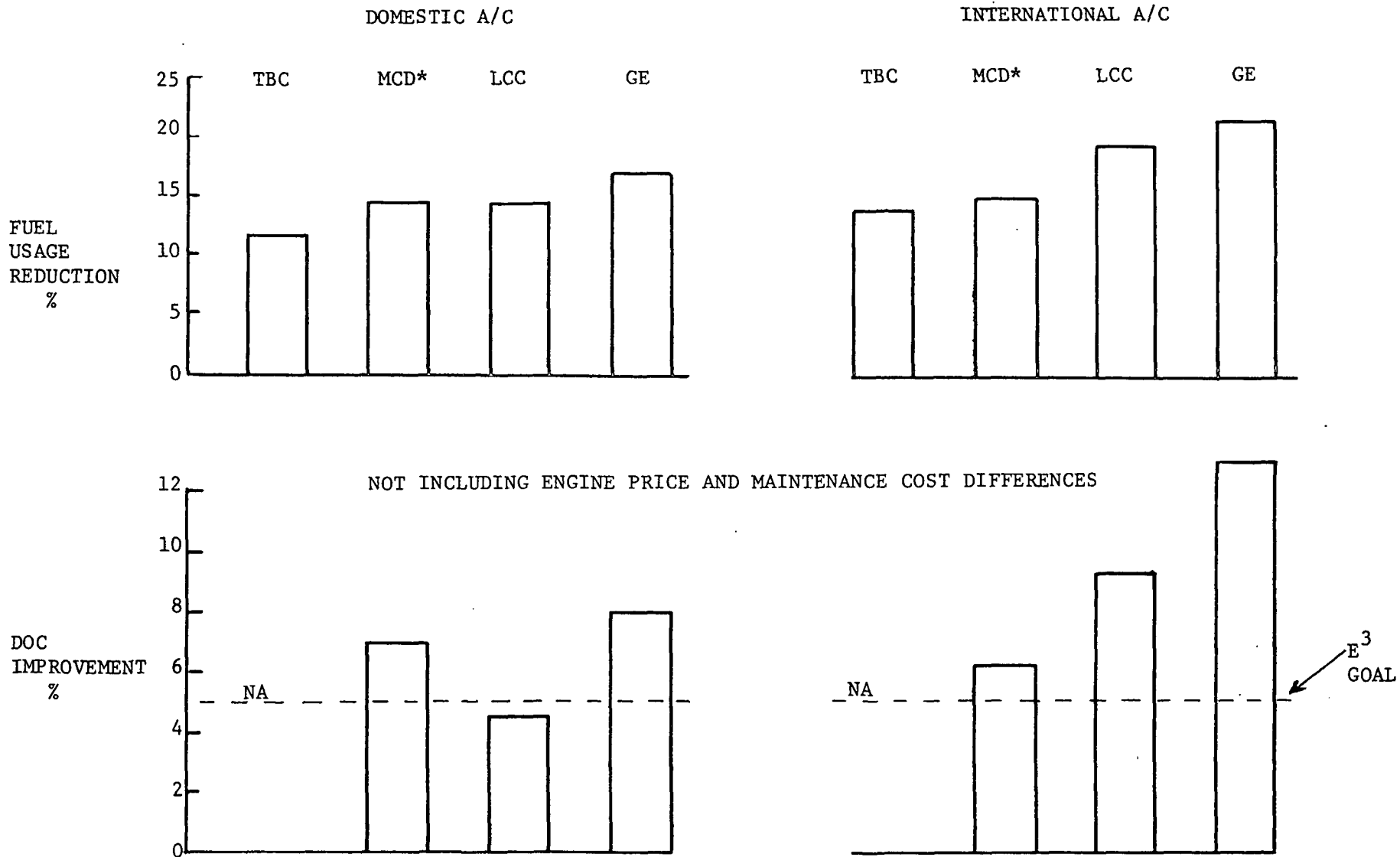
\*Based on same engine price and maintenance costs for both advanced and reference engine.

Fuel costs were as follows:

Domestic - \$92.46/m<sup>3</sup> (35¢/Gal.)  
 Intercontinental -\$118.88/m<sup>3</sup> (45¢/Gal.)

\*\*Economic calculations not made by TBC.





\*ESTIMATED BY GENERAL ELECTRIC USING SENSITIVITY FACTORS

NA - Data not Available.

Figure 46. Estimated Economic Improvements of Advanced Direct-Drive Engine Vs. Reference Engine (Scaled CF6-50C) - Average Mission

TABLE 53  
NOISE SUMMARY  
DIRECT-DRIVE MIXED - BASELINE SUPPRESSION, A/C NOISE INCLUDED  
NO MARGINS APPLIED

	Domestic				Intercontinental			
	TBC	MCD	LCC	GE	TBC	MCD	LCC	GE
<u>RE FAR36 (1969)</u>								
T/O*	-10.4	-11.1	-10.6	-9.3	-8.7	-8.6	-9.1	-9.1
Sideline	-16.5	-16	-15.8	-16	-17.8	-16.1	-17.1	-16
Approach	-8.5	-11.1	-11.1	-8.8	-8.8	-10.6	-10.8	-8.2
<u>RE NPRM 75-37</u>								
T/O*	-2.7	-5.4	-5.2	-4.5	-5.4	-3.1	-5.2	-3.6
Sideline	-9.1	-9.0	-8.6	-8.8	-10.6	-9.5	-10.1	-8.9
Approach	-5.1	-8.0	-7.9	-5.4	-5.5	-7.6	-7.7	-5.0
A/C Noise Only, EPNL	94.0	94.0	91.2	92.8	95.0	95.0	90.1	94.9
T/O Altitude, m (ft.)	544 (1800)	445 (1460)	485 (1590)	482 (1580)	347 (1140)	302 (990)	363 (1190)	375 (1230)
Approach % Fn	31	19	29	36	32	18	28	36
*No Cutback								

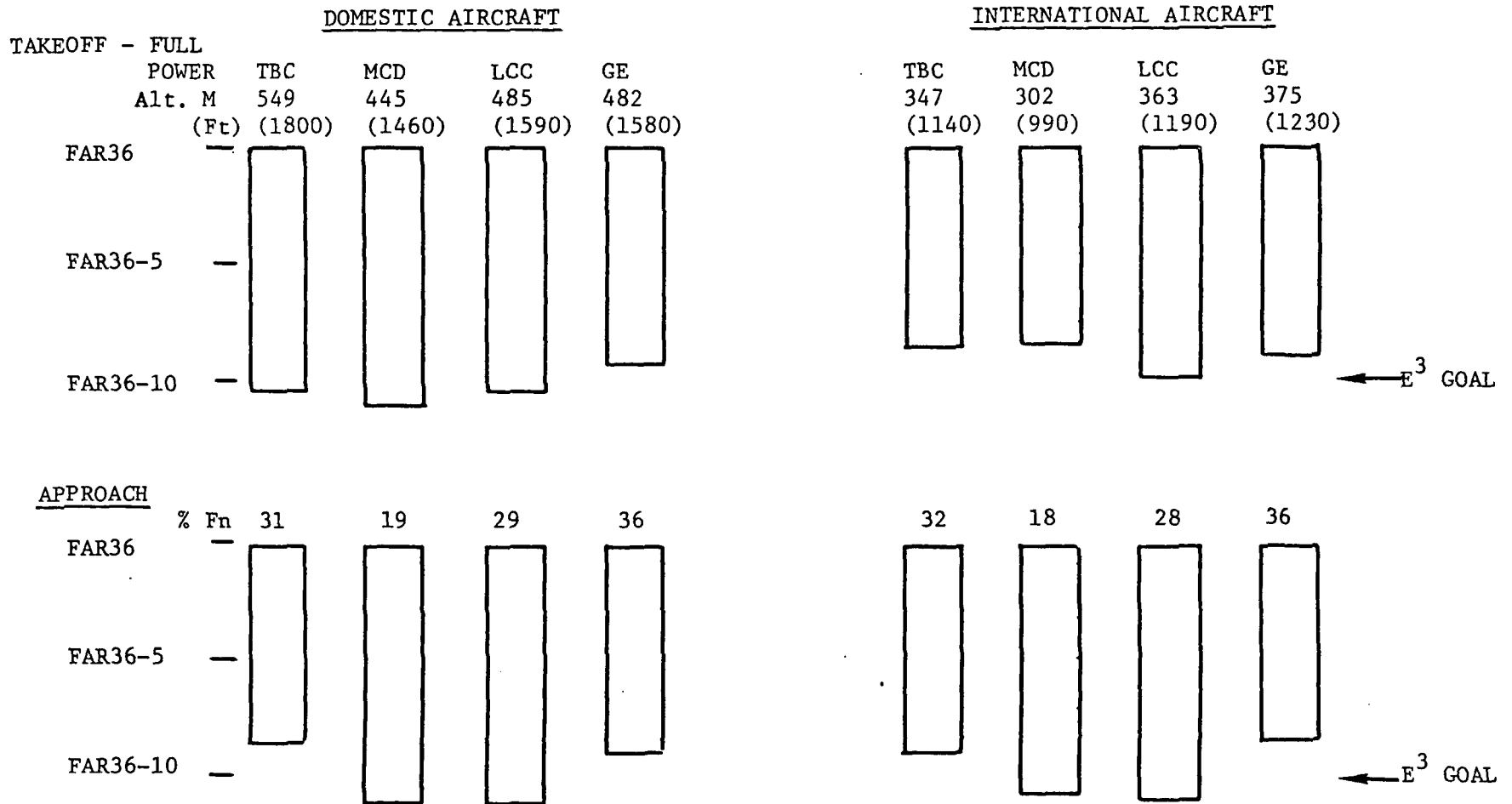


Figure 47 Noise Summary - Direct-Drive Adv. Engine Including A/C Noise, No Margins

TABLE 54

ENGINE THRUST MATCHING - ADVANCED DIRECT-DRIVE ENGINE

	TBC		MCD		LCC		GE	
	DOM.	INT.	DOM.	INT.	DOM.	INT.	DOM.	INT.
Initial Cruise Alt., m (ft.)	10,670 (35,000)	10,060 (33,000)	10,060 (33,000)	9,450 (31,000)	10,970 (36,000)	10,670 (35,000)	10,670 (35,000)	10,670 (35,000)
Takeoff Field Length, m Sea Level (ft.)	2290 (7500)	2830 (9300)	2090 (6870)	2940 (9650)	2130 (7000)	2900 (9500)	2290 (7500)	2800 (9200)
Altitude @ 6.5 Km (3.5 nm) Pt., m Full Power (ft.)	548 (1800)	347 (1140)	445 (1460)	302 (990)	485 (1590)	363 (1190)	482 (1580)	375 (1230)
Total Installed N/Kg Thrust/TOGW (lb/lb)	2.70 (.275)	2.35 (.24)	2.51 (.256)	2.33 (.238)	2.57 (.262)	2.55 (.229)	2.67 (.272)	2.52 (.257)

D. Conclusions/Recommendations

Based upon the results of this task, it was recommended that more refined preliminary design and analysis be applied to the Task II direct-drive mixed-flow baseline engine. This recommendation resulted from the apparent DOC advantage of the direct-drive engine over the geared engine and the lack of any significant fuel consumption or environmental advantage of the geared engine. In addition, the airframe subcontract results from Boeing and Lockheed appeared to verify these trends.

By mutual agreement with NASA, more configuration and cycle optimization effort was applied to the Task II direct-drive engine to provide a more efficient engine. The results of this effort are presented in Task III.

In order to verify more fully the results of the Task II geared engine study, it was also agreed that during Task III additional preliminary design work would be conducted on the geared engine's main transmission gearbox.

TABLE OF CONTENTS

	<u>PAGE NO.</u>
SECTION V . . . . .	147
TASK III - INITIAL PRELIMINARY DESIGN . . . . .	147
A. Introduction/Approach . . . . .	147
B. Significant Results . . . . .	148
1. Cycle/Performance/Configuration Optimization Study . . . . .	148
a. Study Background . . . . .	148
b. Low Pressure Rotor Component Design . . . . .	148
c. Discussion of Results . . . . .	152
2. Component Design Description . . . . .	153
a. Fan Rotor and Quarter Stage . . . . .	153
b. Fan Stator/Frame, Containment and Integrated Nacelle . . . . .	161
1. Structural Description . . . . .	161
2. Weight and Sizing . . . . .	168
c. Compressor Rotor . . . . .	169
1. Design and Analysis . . . . .	169
d. HPC Stator . . . . .	173
1. Description . . . . .	173
e. Combustor/Casing . . . . .	179
1. Description . . . . .	179
f. HPT Rotor/Stator . . . . .	183
1. Description . . . . .	183
g. LPT Rotor/Stator . . . . .	198
1. Description . . . . .	198
h. Rear Exhaust Frame and Mixer . . . . .	209
1. Description . . . . .	209
2. Preliminary Design Procedures . . . . .	214
i. Bearings, Seals and Drives . . . . .	217
j. Control System . . . . .	223
1. General Description . . . . .	223
2. Components . . . . .	223
k. Installation Structure . . . . .	230

PRECEDING PAGE BLANK NOT FILMED

TABLE OF CONTENTS  
SECTION V CONTINUED

	<u>PAGE NO.</u>
3. Component Performance Description . . . . .	232
a. Fan and Quarter Stage . . . . .	232
b. High Pressure Compressor . . . . .	234
c. Combustor . . . . .	235
1. Aerodynamic Design . . . . .	235
2. Aerodynamic Design Requirements . . . . .	237
3. Overall Aerodynamic Design Approach . . . . .	237
d. High Pressure Turbine . . . . .	241
1. Design Point Selection . . . . .	241
2. Aerodynamic Design . . . . .	242
3. Performance Prediction . . . . .	242
e. Low Pressure Turbine . . . . .	245
1. Aerodynamic Design Requirements . . . . .	245
2. Preliminary Design . . . . .	245
f. Mixer Design . . . . .	246
g. Pressure Losses . . . . .	248
h. Installation External Drag . . . . .	248
4. System Evaluation . . . . .	250
a. Secondary Flow . . . . .	250
1. Stage 1 Stator . . . . .	253
2. Stage 1 Rotor Blade . . . . .	253
3. Stage 2 Stator . . . . .	253
4. Stage 2 Rotor Blade . . . . .	254
b. Performance/Cycle . . . . .	254
1. Task III - Growth Engine Design . . . . .	263
c. Acoustics . . . . .	263
d. Emissions . . . . .	265
e. Engine/Installation . . . . .	272
1. Weight and Price Estimate . . . . .	272
2. Maintenance Cost Estimates . . . . .	272
f. Benefits . . . . .	274
5. Geared Turbofan Transmission Preliminary Design . . . . .	282
a. Summary . . . . .	282
b. Study Content and Requirements . . . . .	284
c. Study Results . . . . .	284
1. Gear Configuration Selection . . . . .	284
2. Bearing Selection . . . . .	289
3. Material Selection . . . . .	289

TABLE OF CONTENTS  
SECTION V CONTINUED

	<u>PAGE NO.</u>
4. Lubrication System and Efficiency Estimate . . . .	289
5. Cost/Weight Estimates and Maintenance . . . . .	296
6. Maintenance Factor Evaluation . . . . .	296
d. Conclusions . . . . .	301
C. Summary of Aircraft Subcontractor Studies . . . . .	301
D. Conclusions/Recommendations . . . . .	305



LIST OF FIGURES  
SECTION V  
TASK III - INITIAL PRELIMINARY DESIGN

<u>FIGURE NO.</u>	<u>TITLE</u>	<u>PAGE NO.</u>
48	Effect of Fan Tip Pressure Ratio on Fan Tip Speed and Bypass Ratio	149
49	Effect of Fan Tip Pressure Ratio on $\Delta$ Installed sfc Relative to Task II Baseline	150
50	Effect of Fan Tip Pressure Ratio on Efficiency Parameters	151
51	Task III, Advanced Study Engine	155
52	Advanced Technology Features of the Task III Engine	158
53	Performance Retention Features of the Task III Engine	159
54	Advanced Materials Incorporated in the Task III Engine	160
55	Fan Module Cross Section, Materials	162
56	Shrouded Fan Blade Campbell Diagram	164
57	Quarter Stage Fan Blade Campbell Diagram	165
58	Fan Module Cross Section, Blade Count	166
59	E <sup>3</sup> Fan Bypass Stators Campbell Diagram	170
60	E <sup>3</sup> Compressor Rotor Component Materials	171
61	E <sup>3</sup> Compressor Rotor Stress Distribution	174
62	E <sup>3</sup> Compressor Rotor	175
63	E <sup>3</sup> HPC Stator Configuration	176
64	Proposed E <sup>3</sup> Combustion System	180
65	Double-Annular Dome Assembly	181
66	E <sup>3</sup> High Pressure Turbine	184
67	E <sup>3</sup> HP Turbine Stage 1 Vane Manufacturing	187
68	E <sup>3</sup> HP Turbine Stage 1 Vane Cooling Design	188
69	E <sup>3</sup> HP Turbine Stage 2 Nozzle Diaphragm Configuration	190
70	E <sup>3</sup> HP Turbine Stage 2 Vane Design	191
71	E <sup>3</sup> HP Turbine Stage 1 Blade Cooling	193
72	E <sup>3</sup> HP Turbine Stage 1 Blade and Disk Dovetail Stresses	195
73	E <sup>3</sup> HP Turbine Stage 2 Blade Cooling	196
74	E <sup>3</sup> HP Turbine Steady State Temperatures and Stress Ratio	199
75	E <sup>3</sup> HP Turbine, Material Selection Static System	200
76	E <sup>3</sup> HP Turbine Material Selection Rotating System	201
77	Low Pressure Turbine Flowpath and Airfoil Count	202
78	LPT Blade Nomenclature	203
79	LPT Casing Cooling Manifold System	205
80	Temperature and Stresses - E <sup>3</sup> Stage 1 LPT Disk at 4057 RPM (104% Growth Speed)	210
81	LPT Containment Capability - Wall Thickness and Energy Comparison	212
82	Turbine Frame, Mixer, and Centerbody	213
83	Turbine Frame and Mixer	215
84	Turbine Frame Preliminary Temperature and Spring Rate; Takeoff, Hot Day	216

LIST OF FIGURES  
SECTION V CONTINUED

<u>FIGURE NO.</u>	<u>TITLE</u>	<u>PAGE NO.</u>
85	Lube System Schematic	219
86	Scavenge Pump Drive Gearbox	220
87	Schematic of Accessory Drive System	221
88	PTO Gearbox	222
89	Accessory Gearbox Cross Section	224
90	Control and Fuel System	225
91	Digital Control Functions	226
92	Flow Divider Functional Schematic	229
93	Fan Reverser Schematic	231
94	E <sup>3</sup> Combustion System Design	236
95	High Pressure Turbine Aerodynamic Flowpath	243
96	Turbine Cooling System - Cooling and Leakage Flows, Pressures and Temperatures	251
97	CF6-50C vs Task III Study Engine - Cruise Perfor- mance Comparison 10668m (35K)/0.80M/Standard Day	256
98	Task III Reverse Thrust Study % Fan Speed vs % Core Speed	262
99	Domestic Trijet - 90 EPNL Contours	268
100	International Trijet - 90 EPNL Contours	269
101	EPNL vs Slant Range for a High Bypass Ratio Turbofan Engine	270
102	Baseline Gear Configuration	285
103	Gear System Configurations	288
104	Star Gear Bearing Configuration	293
105	Lubrication System Schematic	295
106	Integrated Mission Fuel Burn/Direct Operating Cost - Design Mission	303

LIST OF TABLES  
SECTION V  
TASK III - INITIAL PRELIMINARY DESIGN

<u>TABLE NO.</u>	<u>TITLE</u>	<u>PAGE NO.</u>
55	Task III Engine Cycle Comparison	154
56	Growth Engine Characteristics	157
57	E <sup>3</sup> Fan Blade Geometry Summary	163
58	E <sup>3</sup> HP Turbine Life Requirements	186
59	High Pressure Turbine Stage 1 Blade Data	194
60	High Pressure Turbine Stage 2 Blade Data	197
61	CFX/E <sup>3</sup> LP Turbine Blades Stress/Life	207
62	Dovetail Stress and Life	208
63	LPT Disk Steady State Stress at Growth Engine Speeds	211
64	E <sup>3</sup> Combustion System Emissions Goals and Aero- dynamic Performance Requirements	238
65	Combustor Aerodynamic Design Parameter	239
66	Aerodynamic Status Comparisons of the HPT	244
67	E <sup>3</sup> - LP Turbine Preliminary Vector Diagram Parameter	247
68	System Pressure Loss Summary	249
69	Engine Cycle Definition	257
70	Engine Component Definition	258
71	Task III Component and Cycle Performance Summary	259
72	Flight Propulsion System and Max. Growth Engines E <sup>3</sup> Engine Performance for a Typical A/C Mission Profile	261
73	Engine/Aircraft Systems for Acoustic Evaluation	264
74	Estimated Engine Noise, Domestic Trijet, Suppressed Noise Levels - No Margin	266
75	Estimated Engine Noise, International Trijet, Suppressed Noise Levels - No Margin	267
76	Predicted Emissions Characteristics of E <sup>3</sup> Combustion System	271
77	Weight and Price Estimate Installed Flight Propul- sion System	273
78	GE Aircraft Analysis - A/C Technology Assumptions	275
79	GE Study Aircraft Description by Mission	276
80	GE Aircraft Analysis - Economic Study Rules	277
81	General Electric Study Aircraft and Fuel Savings	278
82	Benefit Analysis Derivatives	279
83	Task III Engine $\Delta$ DOC Breakdown vs CF6-50C Reference (Scaled)	280
84	Task III Engine $\Delta$ ROI Breakdown vs CF6-50C Reference (Scaled)	281
85	Task III Geared Engine $\Delta$ W <sub>f</sub> Breakdown vs CF6-50C Reference (Scaled)	283
86	Mission Profile for Fan Power Requirement	287
87	Bearing/Gear Data for Boxes Studied	290
88	Gear Set Selection Trade-off	291
89	Material Selection	292
90	Reduction Gear Design Features	294

LIST OF TABLES  
SECTION V CONTINUED

<u>TABLE NO.</u>	<u>TITLE</u>	<u>PAGE NO.</u>
91	Efficiency Estimate	297
92	Gearbox Cost/Weight Estimate	298
93	Reliability/Maintenance Cost Estimate	299
94	Gear Set Comparative Merit Factor Evaluation 700 N. Mile Domestic Mission - 92.4 \$/m <sup>3</sup> (35¢/ Gal) Fuel	300
95	Improved Advanced Engine Study Results	302
96	Task III E <sup>3</sup> Price and Maintenance vs Scaled CF6-50C DOC Effects	304

SECTION V

TASK III - INITIAL PRELIMINARY DESIGN

A. Introduction/Approach

Task III of the E<sup>3</sup> study consisted primarily of an initial preliminary design of the recommended direct drive energy efficient engine that evolved during Task II and in the early portion of Task III.

The preliminary design covered additional effort on the aerodynamic, mechanical and installation design of the advanced Flight Propulsion System (FPS). As in Task II, a mission benefit analysis was performed using a scaled CF6-50C system as the reference. Both the internal GE benefit analysis and the subcontractors' analyses were updated to reflect the design, configuration and performance characteristics of the Task III engine.

For the benefit comparison, both the FPS and CF6-50C were scaled to the mission size using the maximum climb power, 10668 m (35,000 feet), .8M condition as the sizing point for equivalent thrust. In addition to the performance and weight effect comparison of Task II, estimates of initial engine cost and maintenance effects were included in making the DOC comparisons for the General Electric study aircraft.

There were four major technical efforts performed in Task III. The first consisted of additional cycle/engine configuration optimization effort that was carried out at the beginning of Task III. The purpose of this was to identify any cycle/configuration alterations to the Task II direct-drive engine to increase the  $\Delta$  sfc margin over the reference engine to at least 14% to permit a margin over the 12% goal for the study.

The second technical effort was the preliminary engine design (and engine-aircraft integration) to further refine the estimates of engine characteristics such as performance, weight, cost, maintenance and overall configuration of the integrated FPS. The design reflects the mechanical and structural requirements of the growth cycle and thrust.

The third technical effort was devoted to evaluating and comparing the resulting FPS to the scaled CF6-50C to ascertain the fuel efficiency, economics, and environmental aspect (noise and emissions) benefits. Both internal General Electric and subcontractor updates of the system benefits of this refined Task III FPS system were carried out.

The fourth technical effort was a refinement of the Task II geared engine main transmission design. This effort was carried on separately from the main Task III effort. An economic evaluation of the differences between the Task II geared engine and the gearbox designed in Task III was then performed to see if fuel efficiency and economics had changed appreciably from the Task II results.

B. Significant Results

1. Cycle/Performance/Configuration Optimization Study

a. Study Background

As part of a Task III study contract supplement, a design study was conducted to investigate the effects of design fan tip pressure ratio and corrected tip speed on installed maximum cruise sfc. The intent of the study was to optimize the combination of low pressure rotor component performance and propulsive efficiency as a function of pressure ratio, rotor speed and bypass ratio. The study consisted of matching out three engines with different combinations of these parameters at the 10668 m (35K/.8M/MxC1) operating condition and comparing the maximum cruise installed sfc to the Task II baseline engine performance. All the engines that were used in the study are characterized as follows:

<u>Engine</u>	<u>Task II Baseline</u>	<u>Task II Revised</u>	<u>Task III A</u>	<u>Task III B</u>
Thrust Rating	MxC1	—————→		
Fan P/P	1.71	1.71	1.65	1.62
Fan $U_T/\sqrt{\theta}$ m/sec (ft/sec)	457 (1500)	427 (1400)	411 (1350)	404 (1325)
Engine $\beta$	6.1	6.1	6.8	7.1

Resulting Performance:

<u>Engine</u>	<u>Task II Baseline</u>	<u>Task II Revised</u>	<u>Task III A</u>	<u>Task III B</u>
Thrust Rating	MxC1	—————		
$\eta_{Propul.}$	0.476	0.479	0.484	0.469
$\eta_{Fan Tip}$	0.877	0.881	0.882	0.886
$\eta_{Fan Hub}$	0.838	0.851	0.892	0.890
$\eta_{LPT}$	0.917	0.919	0.916	0.914
$\Delta sfc_{install.}$	Base	-0.4%	-1.9%	-2.1%

The resulting performance is also presented in graphic form in Figures 48 through 50, plotted as a function of design fan tip pressure ratio.

b. Low Pressure Rotor Component Design

All three of the new engines that were matched out for this study included the same core engine design as the one for the Task II baseline engine. They all had the same LP turbine design. This LP turbine design was based on the largest average diameter that met constraints of: 1) a reasonable exhaust system flowpath and 2) using an interturbine flowpath (duct) that did not need to be cooled.

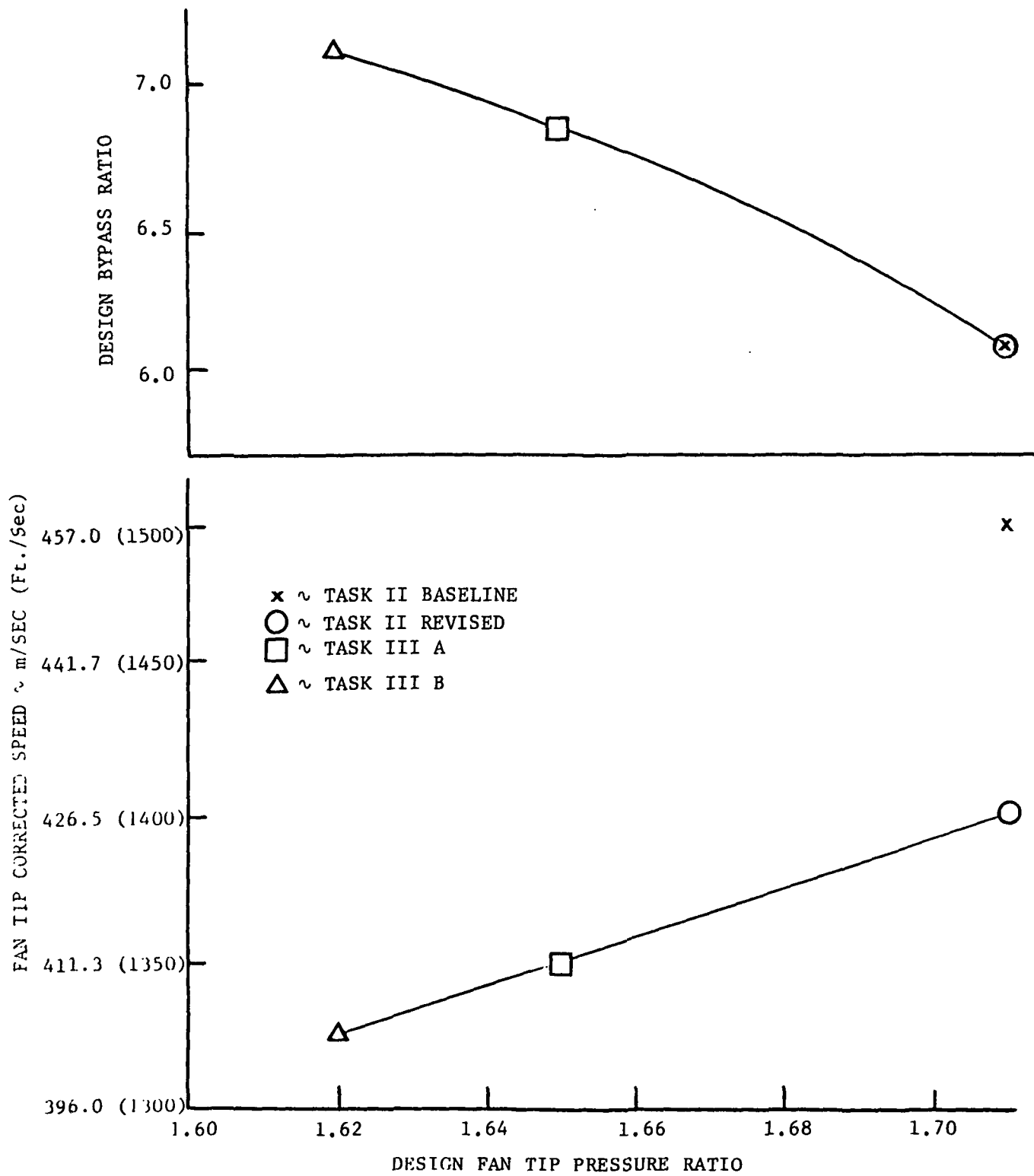


Figure 48. Effect of Fan Tip Pressure Ratio on Fan Tip Speed and Bypass Ratio

- x ~ TASK II BASELINE
- ~ TASK II REVISED
- ~ TASK III A
- △ ~ TASK III B

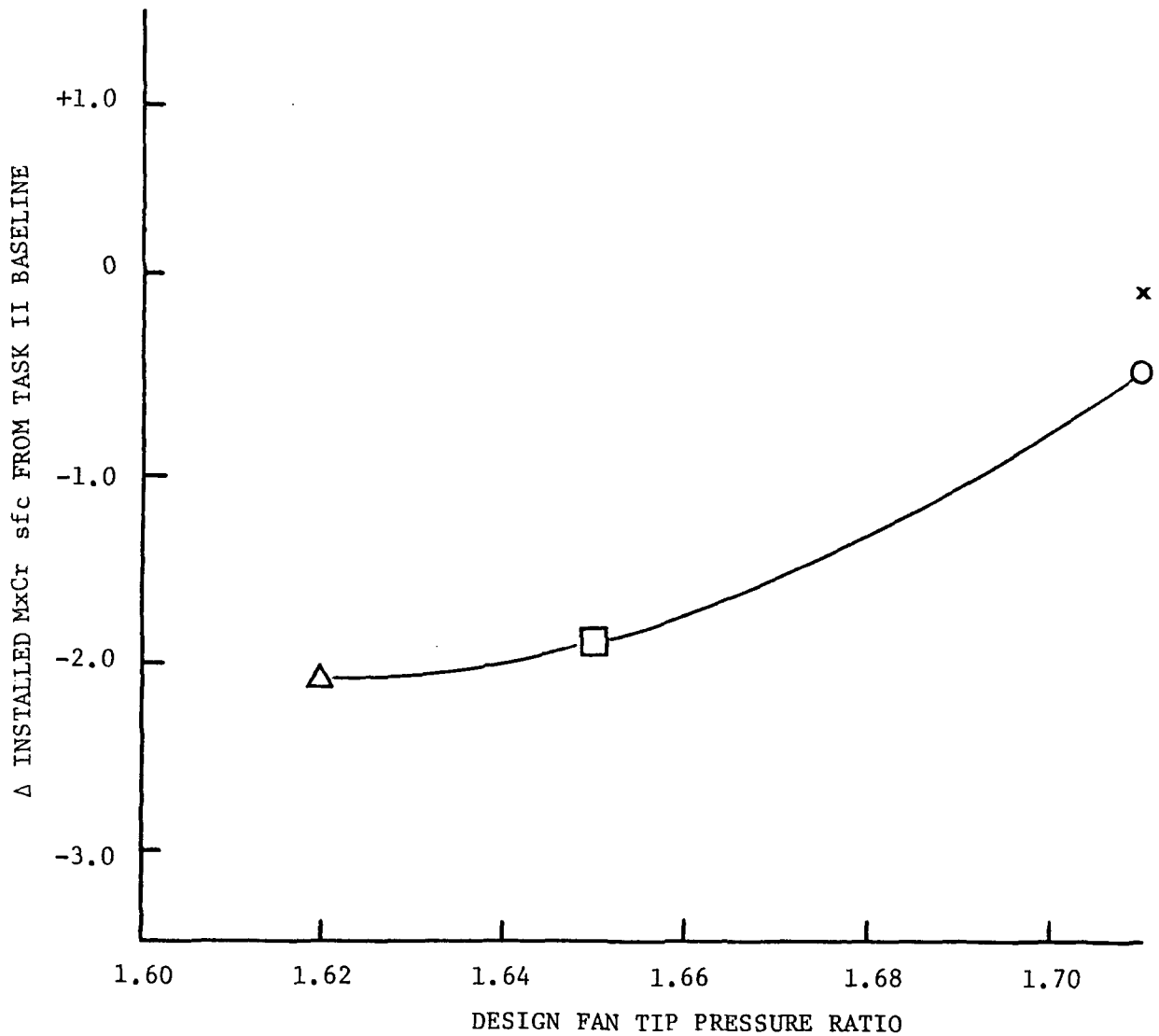


Figure 49. Effect of Fan Tip Pressure Ratio on  $\Delta$  Installed SFC Relative to Task II Baseline



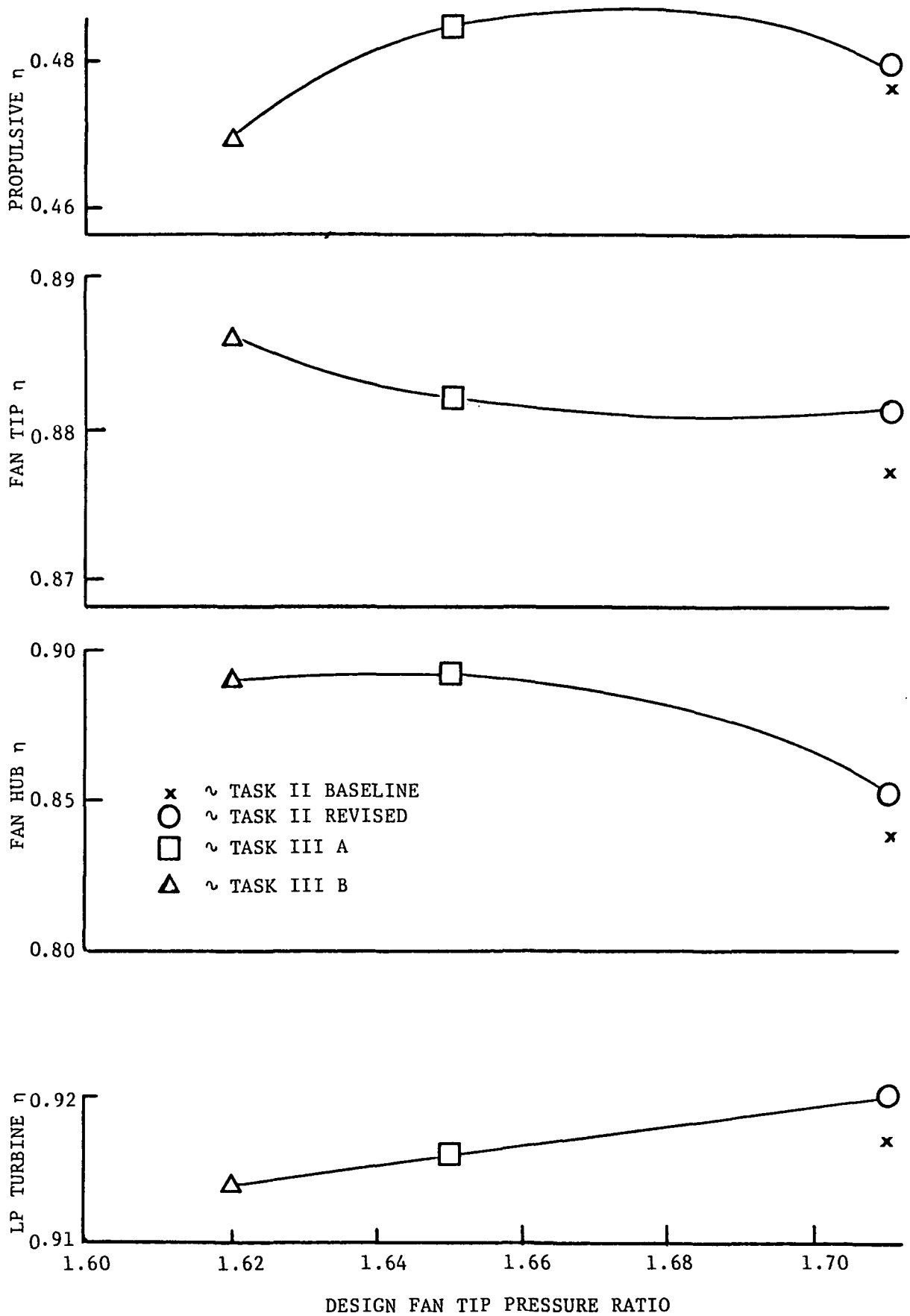


Figure 50. Effect of Fan Tip Pressure Ratio on Efficiency Parameters

The fan design for the Task II revised engine was designed to the same pressure ratio and bypass ratio as the Task II baseline engine, but the corrected tip speed was decreased from 457 m/sec (1500 fps) to 427 m/sec (1400 fps). The hub radius was increased from 0.374 to 0.42 to maintain enough wheel speed on the hub portion of the fan to produce the same core supercharging pressure ratio as the Task II baseline engine.

The fan design for the Task III/A engine was based on a reduction in fan tip pressure ratio from 1.71 to 1.65. A corrected tip speed was selected that would produce the maximum efficiency for climb and cruise operation. This tip speed of 411 m/sec (1350 fps) required a redesign of the fan hub and an addition of a booster stage to get the same design core supercharging pressure ratio as the Task II baseline engine.

The Task III/B engine design fan tip pressure ratio of 1.62 was selected for an additional reduction in this parameter. The corrected tip speed of 404 m/sec (1325 fps) was required to optimize fan tip efficiency. This engine also required a booster stage behind the fan hub.

The bypass ratio for each engine was selected by maximizing it for the various fan pressure ratios within the constraint of maintaining reasonable Mach numbers in the mixing plane of the exhaust duct for mixing performance considerations. Figure 48 shows the relationship of bypass ratio as a function of design fan tip pressure ratio that was used for this study.

### c. Discussion of Results

The performance results of the study are plotted in Figure 49, which shows  $\Delta$  installed MxCr sfc from the Task II baseline engine versus design fan tip pressure ratio. The rate of change of sfc improvement with pressure ratio is much lower below 1.65 than above this value. The improvement below 1.6 becomes negligible when other economic factors such as direct operating cost and fuel burned are considered.

Figure 49 also shows the effect of slowing the fan speed down by 30.5 m/sec (100 ft/sec) in design tip speed by comparing the Task II baseline versus the Task II revised engine. This comparison shows a 0.4% improvement in sfc. Note that approximately half of this improvement is due to the more efficient LP turbine that was used for this study. So the change in tip speed is worth about 0.2% in sfc as an individual design change.

Figure 50 illustrates the low pressure rotor component efficiencies and propulsive efficiency plotted versus design fan tip pressure ratio. Note that the improvement in fan hub efficiency for the 1.62 and 1.65 pressure ratios is due to the two-stage compression process.

To evaluate the economic benefits of the study engines, installed engine weight, cost, and maintenance were estimated. All the engines were scaled to produce an equivalent installed maximum climb thrust (Std. + 10°C (+18°F) Day) for the General Electric internal study aircraft on a domestic mission. The following results were obtained.

Engine (Installed)	Task II Baseline	Task II Revised	Task III A	Task III B
Wt. - Kg (Lbs)	Base	-41 (-90)	-32 (-70)	+11 (+25)
Eng. Price-\$K	Base	+12	+50	+70
Maintenance-\$/Flt. Hr.	Base	Same	+0.97	+1.22
DOC - %	Base	-0.26	-0.78	-0.61
W <sub>f</sub> - %	Base	-0.6	-2.8	-2.9

Based on the significant improvement in fuel burned and direct operating cost, Engine A was recommended over the Revised Task II and Engine B. Although Engine B had a slight (.1%) fuel burned advantage, it was much heavier, more costly, and had a significant DOC penalty. Engine A was approved as the Task III baseline engine. A summary of the changes from the Task II baseline engine follows:

- A more efficient fan design that results from a lower pressure ratio and lower tip speed.
- Addition of a quarter-stage behind the fan hub for more efficient core engine supercharging.
- A higher bypass ratio.
- An LP turbine design with a larger average diameter, which maintains nearly the same efficiency level at the slower rotational speed due to the addition of a short transition duct.
- Lower design  $T_{41}$  by 50°F.
- Revised secondary airflows.
- Addition of a cooling air/fuel heat exchanger.

Figure 51 is a cross section of the engine that was subsequently studied as the Task III baseline engine design. A description of the preliminary design is given in Table 55 while Table 56 is a comparison of the Task III baseline engine performance and a possible growth version.

Figure 52 illustrates many of the advanced technology features incorporated into the Task III study engine while Figure 53 shows some of the design features intended to prevent performance deterioration during service. Major advanced material technologies incorporated into the Task III study engine are illustrated in Figure 54.

## 2. Component Design Description

### a. Fan Rotor and Quarter Stage

The E<sup>3</sup> fan is a mid-span shrouded single stage configuration with 644 Kg/sec (1419 lb/sec) airflow at 1.65 pressure ratio, 6.8 bypass ratio for the .8M/10668m (35K) max climb design point. A quarter stage, which delivers a pressure ratio of 1.67 is provided for supercharging the core. It also minimizes foreign object ingestion into the high pressure compressor

TABLE 55

TASK III ENGINE CYCLE COMPARISON

	<u>REF. CF6-50C</u> <u>(Scaled)</u>	<u>Task III</u> <u>Baseline</u> <u>Engine</u>
Fan Tip Dia. m (Inches)	1.98 (77.9)	2.11 (83.0)
Installed Fn @ M=.8	38300 (8610)	38300 (8610)
10668 m (35K), MxC1 Hot Day - N (Lbs)		
Core Corr Flow - MxC1 Kg/sec (lb/sec)	53.8 (118.7)	54.4 (120.0)
Bypass Ratio - MxC1	4.2	6.8
Fan Pressure Ratio - MxC1	1.76	1.65
Overall Pressure Ratio - MxC1	32	38
$\Delta$ sfc -Uninstalled MxCr (STD) %	Base	-13.7
$\Delta$ sfc -Installed MxCr (STD) %	Base	-14.4

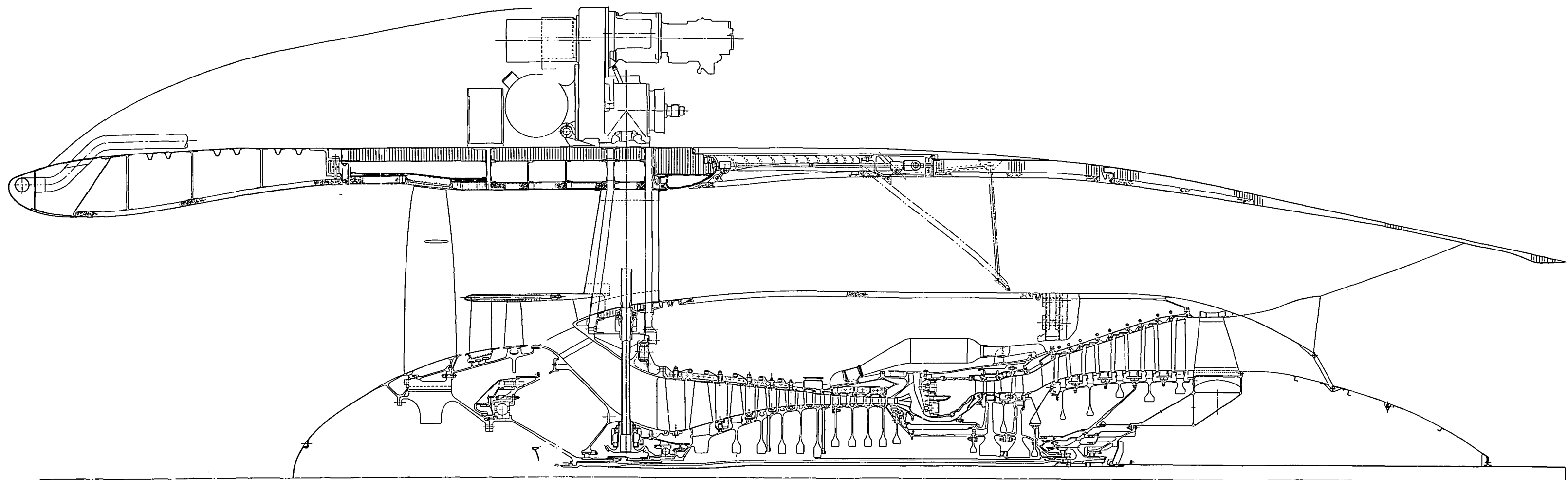


Figure 51. Task III, Advanced Study Engine

FOLDOUT FRAME

ORIGINAL PAGE IS  
OF POOR QUALITY  
ORIGINAL PAGE IS  
OF POOR QUALITY

155

ORIGINAL PAGE IS  
OF POOR QUALITY

2 FOLDOUT FRAME

TABLE 56

GROWTH ENGINE CHARACTERISTICS

(SAME FAN TIP DIAMETER AND NO CONFIGURATION CHANGES)

Power Setting	<u>Task III Engine</u>			<u>Task III Growth Engine</u>		
	SLTO	MxC1	MxCr	SLTO	MxC1	MxCr
Std. Day, + $\Delta C^{\circ}/(\Delta^{\circ}F)$	30/86	10/18	10/18	30/86	10/18	10/18
Fn - N (lbs) (Uninstalled)	162360 (36500)	40203 (9038)	37480 (8426)	187879 (42237)	48268 (10851)	45140 (10148)
$\Delta\%$	Base	Base	Base	+16	+20	+20
Bypass Ratio	7.4	6.8	7.0	6.2	5.6	5.7
Fan Pressure Ratio	1.49	1.65	1.61	1.57	1.75	1.71
Corr. Fan Tip Speed - m/sec (Ft/Sec.)	370 (1215)	411 (1350)	402 (1320)	400 (1315)	457 (1500)	446 (1465)
Core Flow Corr. - Kg/sec (Lb/Sec.)	48.4 (106.6)	54.4 (120)	53.1 (116.9)	51.1 (112.5)	56.7 (125*)	55.4 (122.1)
HPC Exit Temp. - $^{\circ}C$ ( $^{\circ}F$ )	578 (1072)	523 (974)	509 (948)	626 (1159)	567 (1053)	552 (1025)
HPT Blade Inlet Temp. $^{\circ}C$ ( $^{\circ}F$ )	1338 (2440)	1282 (2340)	1243 (2270)	1399 (2550)	1332 (2430)	1293 (2360)
$\Delta sfc$ Installed (Ref. CF6-50C)-%			-14.4			-11.6

\*Hi-Flowed Core Only.

PRECEDING PAGE BLANK NOT FILMED

**Fan**

- High Eff.—Low Tip Speed
- Structural EGV
- Integral Composite Frame

**¼ Stage Island Booster**

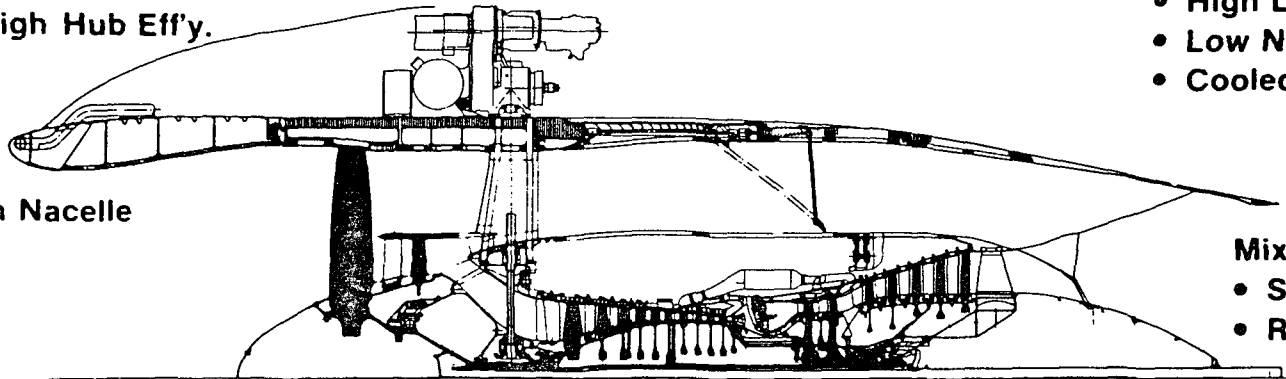
- Automatic Core Matching
- Reduced Core FOD
- High Hub Eff'y.

**HP Turbine**

- 2 Stage, High Eff.
- Improved Cooling Air Management
- Active Clearance Control
- Fuel/Air Hx

**LP Turbine**

- High Loading
- Low Noise Configuration
- Cooled Casing

**Thin Nacelle****Mixer**

- Short Mixing Length
- Reverse Thrust Spoiler

**Mechanical System**

- Stiff, Straddle Mounted Core
- Two Cold Support Struts
- Reduced Bearings
- Integrated Fan Frame/Nacelle
- Pylon Mounted Accessories

**HP Compressor**

- 10 Stage, 23:1 PR
- Low Aspect Ratio, Rugged Blades
- Digital Control Stators
- Active Clearance Control

**Combustor**

- Short, Double Annular
- Low Emissions
- Digital Control Staging
- Improved ECCP Design

Figure 52. Advanced Technology Features of the Task III Engine

#### Fan

- Low Tip Speed — Reduced Erosion
- Stiff Integrated Nacelle/Frame Casing

#### 1/4-Stage Island Booster

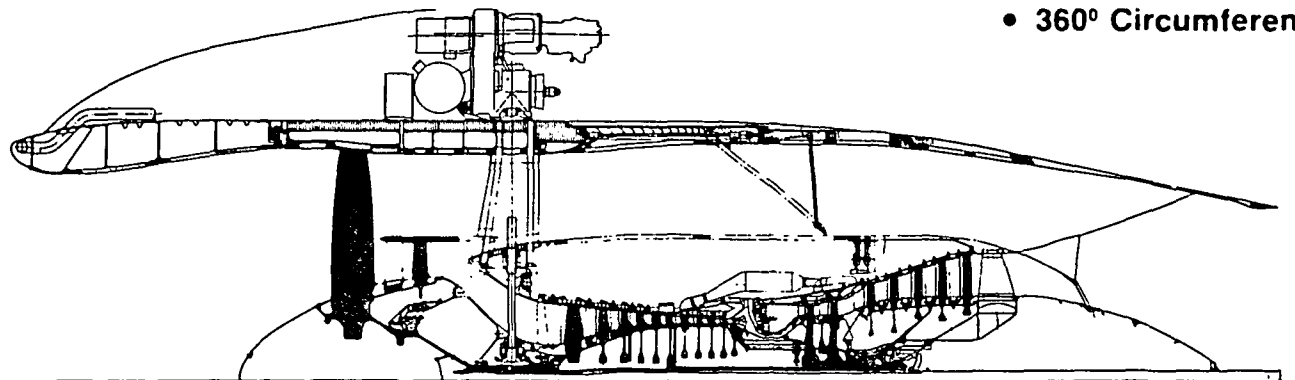
- Separates Debris From Core Air

#### HP Turbine

- Abradable Erosion Resistant Ceramic Shrouds
- Active Clearance Control
- Increased Cooling Air Levels

#### LP Turbine

- Casing Cooling
- 360° Circumferential Casing



#### Mechanical System

- Short, Rigid, Two-Bearing Core Engine
- Two-Bearing Core Support
- Two Cold Frame Bearing Supports
- Designed for Heavy Unbalance
- Load Isolating Aft Mount
- Thrust Links Reduce Engine Bending

#### HP Compressor

- Wide-Chord Erosion-Resistant Blading
- Abradable Casing Liners
- Aft Casing Isolation Mount
- Active Clearance Control
- Cooled Rotor

#### Combustor

- Short, Rugged Design
- Film/Impingement Cooling

Figure 53. Performance Retention Features of the Task III Engine



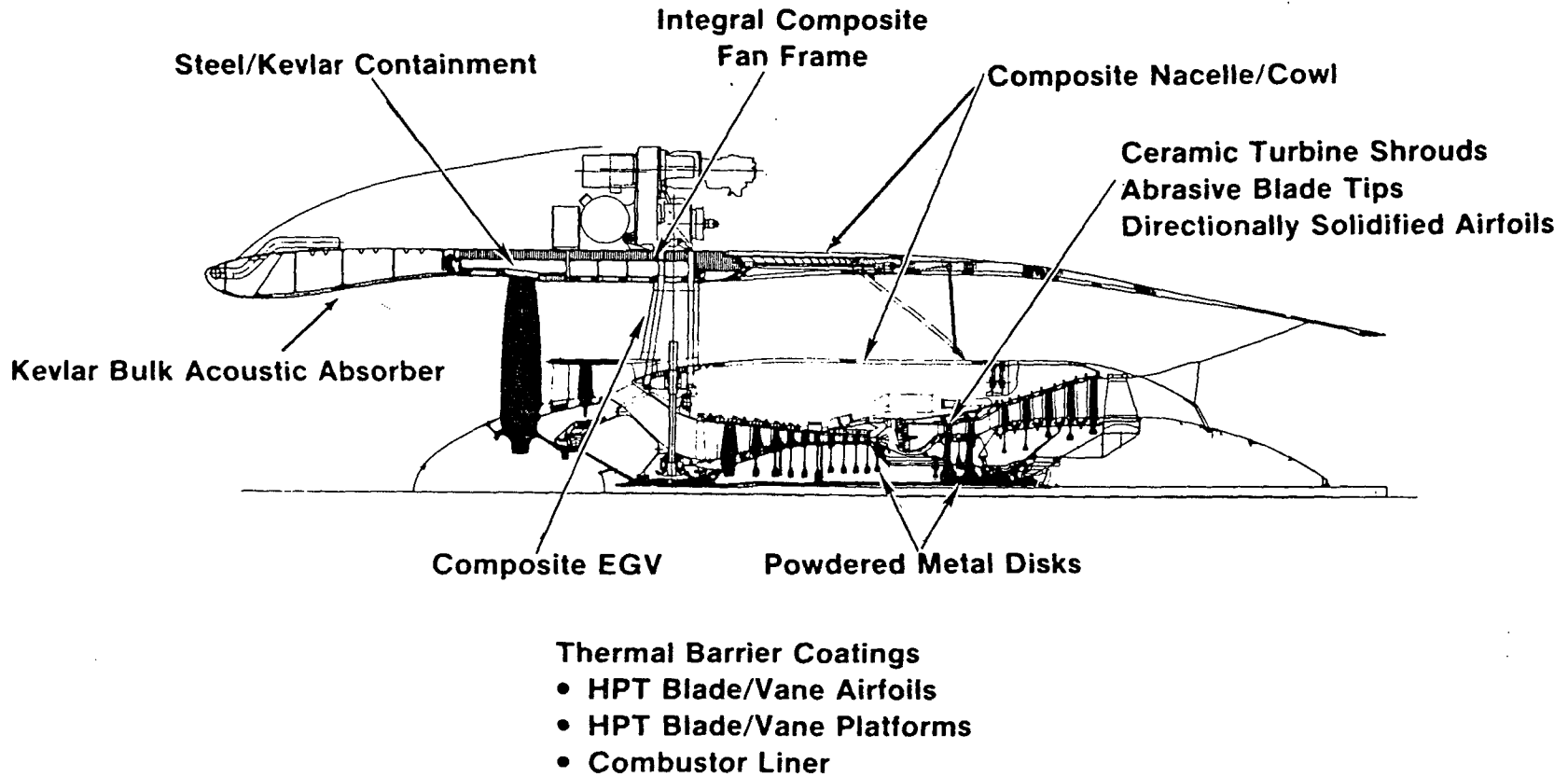


Figure 54. Advanced Materials Incorporated in the Task III Engine

due to its centrifuging action which discharges the foreign material out through the quarter stage bypass. A cross-section of the fan rotor and stator module is shown in Figure 55 along with material choices.

The fan and quarter stage rotor configuration shown utilizes material selections for low cost/high strength based on commercial cost reduction experience. The fan and quarter stage blade geometry characteristics are given in Table 57.

Many of the design features incorporated in the E<sup>3</sup> fan are similar to those in commercial use in the CF6 family of engines. Use of the technology provided by this commercial experience in high bypass turbofan engines, results in the fan design achieving advanced levels of mechanical durability, reliability and cost effectiveness.

The E<sup>3</sup> fan blade design will be very similar to the current advanced shrouded blade design being tested in the CF6 engine. A representative Campbell Diagram for the E<sup>3</sup> is shown in Figure 56. The quarter stage blade Campbell Diagram is shown in Figure 57.

Figure 58 illustrates the preliminary temperature conditions and effective stresses at points of interest for the fan rotor structure operating at the Max Climb Design Point (growth version at 4091 rpm). Characteristics of the Task III fan and quarter stage design determined during the initial preliminary design study are well within General Electric commercial experience.

## b. Fan Stator/Frame, Containment, and Integrated Nacelle

### 1. Structural Description

The overall fan module static structure of the E<sup>3</sup> (Figure 55) consists of: the fan frame, which integrally includes the fan casing and 40 fan bypass stator vanes; 60 Stage 1 vanes with their associated support structure; and 64 quarter-stage inner OGV's. The only primary engine support incorporated in this structure is a uniball located at the top rear of the core portion of the fan frame which provides vertical and side support.

The integrated E<sup>3</sup> fan frame itself consists of a metal core frame, advanced composite bypass stator vanes and fan casing, acoustic treatment in the fan casing, and an advanced fan blade containment system. The overall structural concept is based on the results of the QCSEE program (Reference 8) which produced the first General Electric all-composite integrated fan frame. That frame demonstrated the advantages of a unitized design concept and indicated that lightweight, advanced composite frames could be designed, fabricated and maintained and yet be both stiff and strong enough for engine operation. Insufficient running time, however, has been accumulated to verify the anticipated life characteristics of such a frame.

The metal core frame consists of the basic core flowpath, eight core struts, 64 spars that will form the backbone of the quarter-stage inner OGV's, 40 standoffs to attach the primary fan flow splitter, the secondary splitter for the quarter-stage discharge, core bearing supports, support structure for the composite bypass vane/fan casing assembly, the forward engine support uniball, and the forward support for the compressor case.

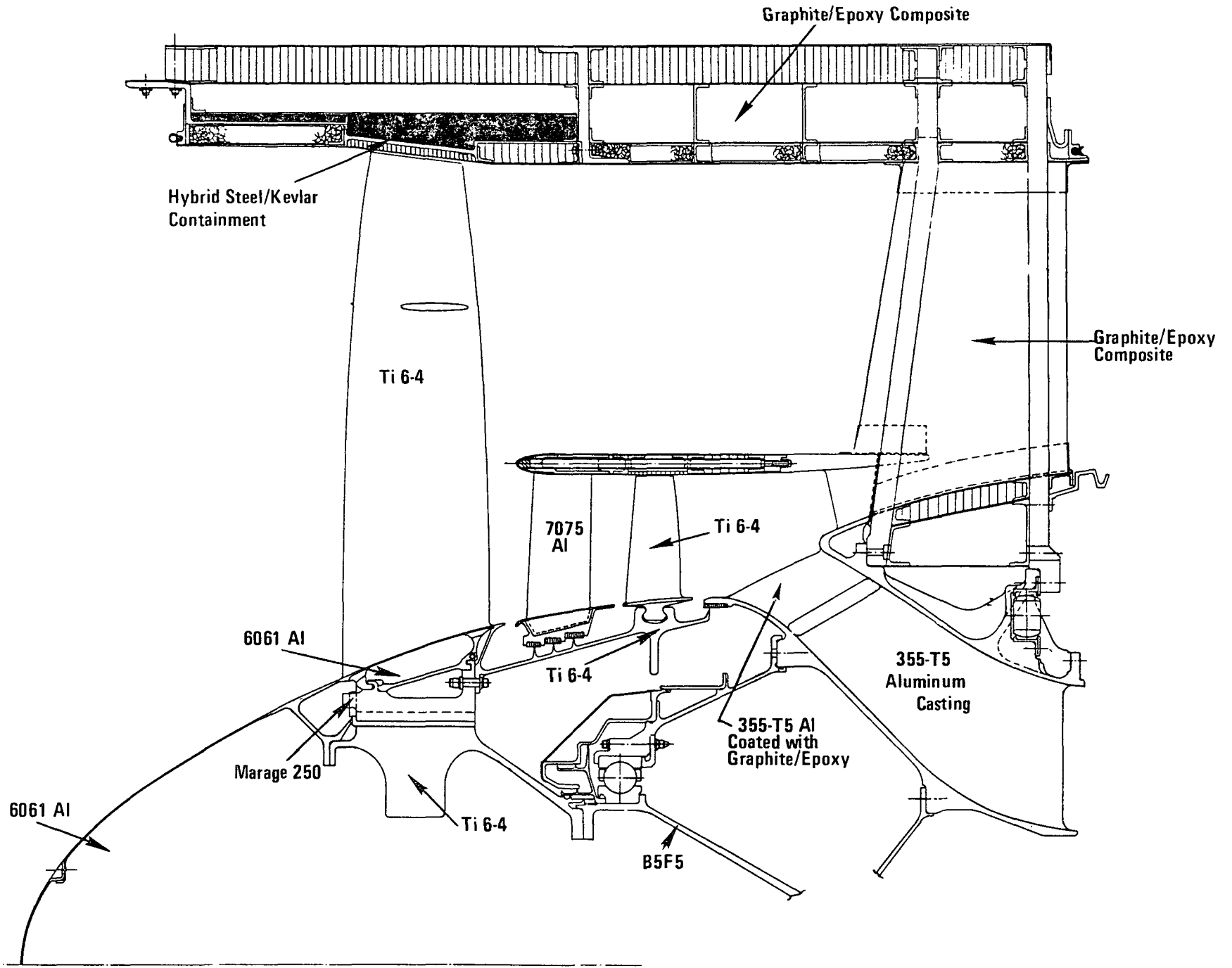


Figure 55. Fan Module Cross Section, Materials.

TABLE 57

E<sup>3</sup> FAN BLADE GEOMETRY SUMMARY

Stage	No. of Blades	Material	Airfoil Type	Length	Chord (in)	cm Tm/c*	Aspect Ratio	Stagger-°	Camber-°	Solidity
Fan	38	Ti 6-4	Arbitrary	25.2	24.4 OD (9.61)	0.025	3.3	58.2	16.2	1.400
					15.1 ID (5.95)	0.08				
Quarter Stage	57	Ti 6-4	Arbitrary	6.4	4.90 OD (1.93)	0.03	2.5	36.5	13.4	.701
					7.31 ID (2.88)	0.09				

\*Maximum Thickness/Chord

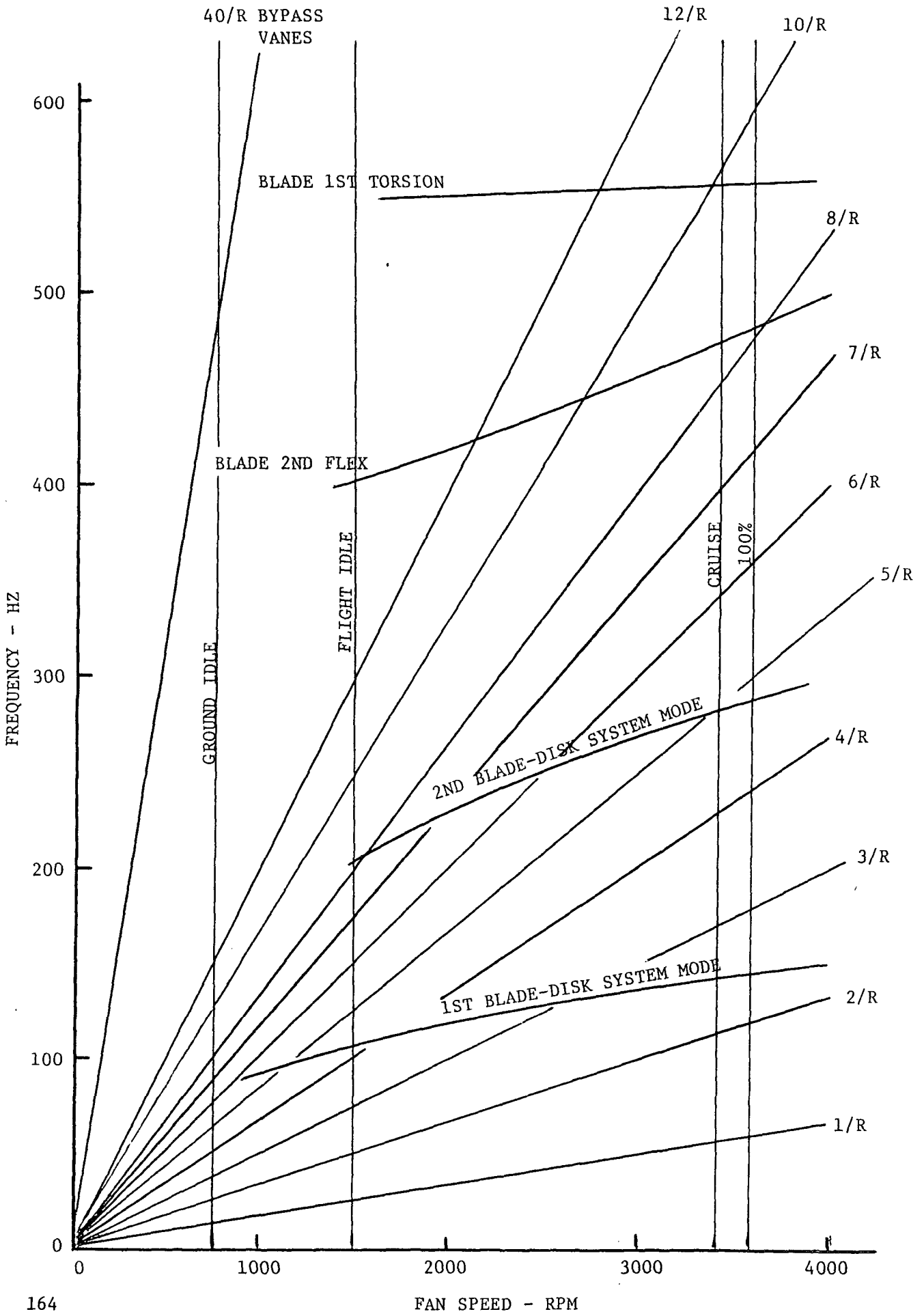


Figure 56. Shrouded Fan Blade Campbell Diagram

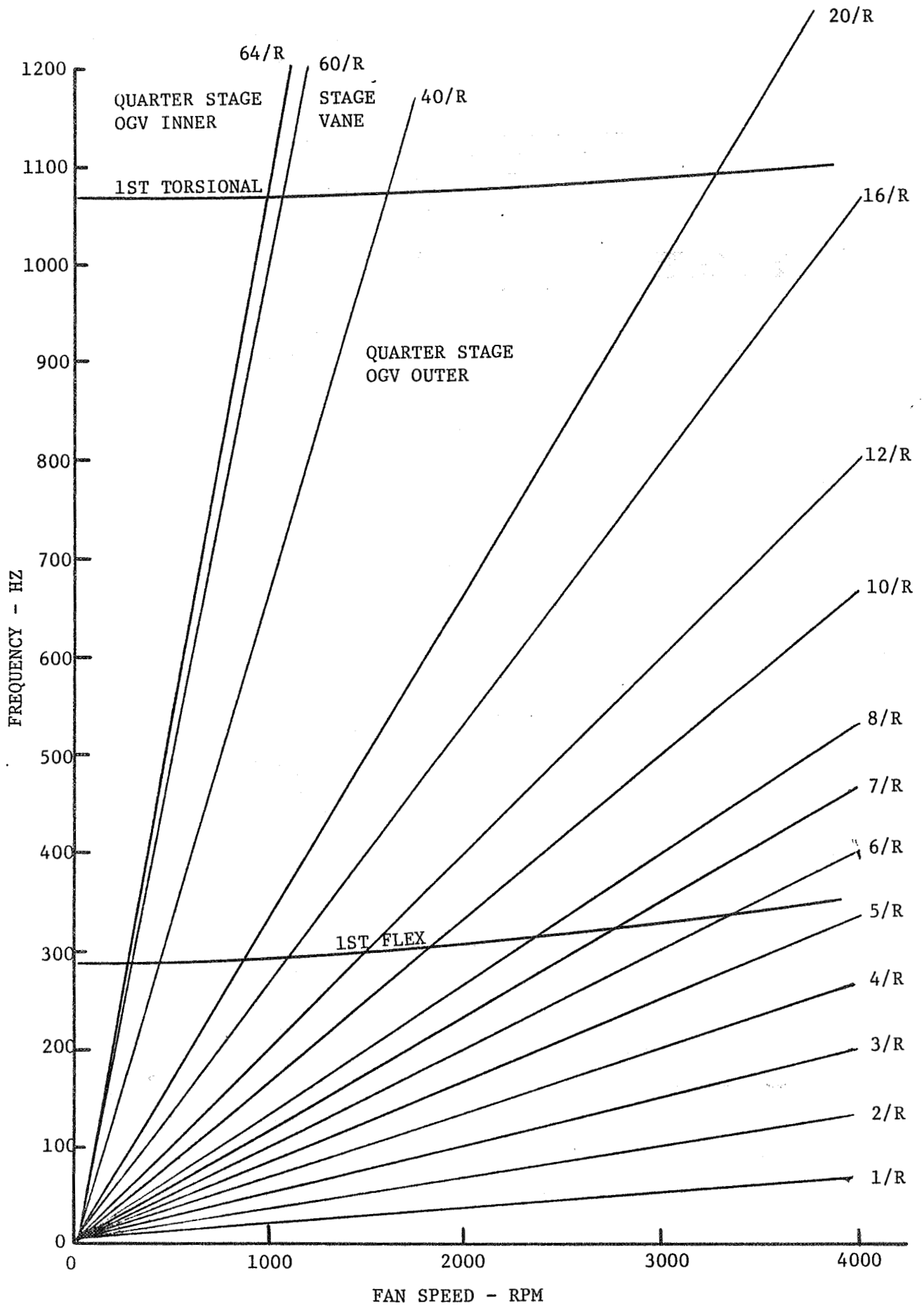


Figure 57. Quarter Stage Fan Blade Campbell Diagram

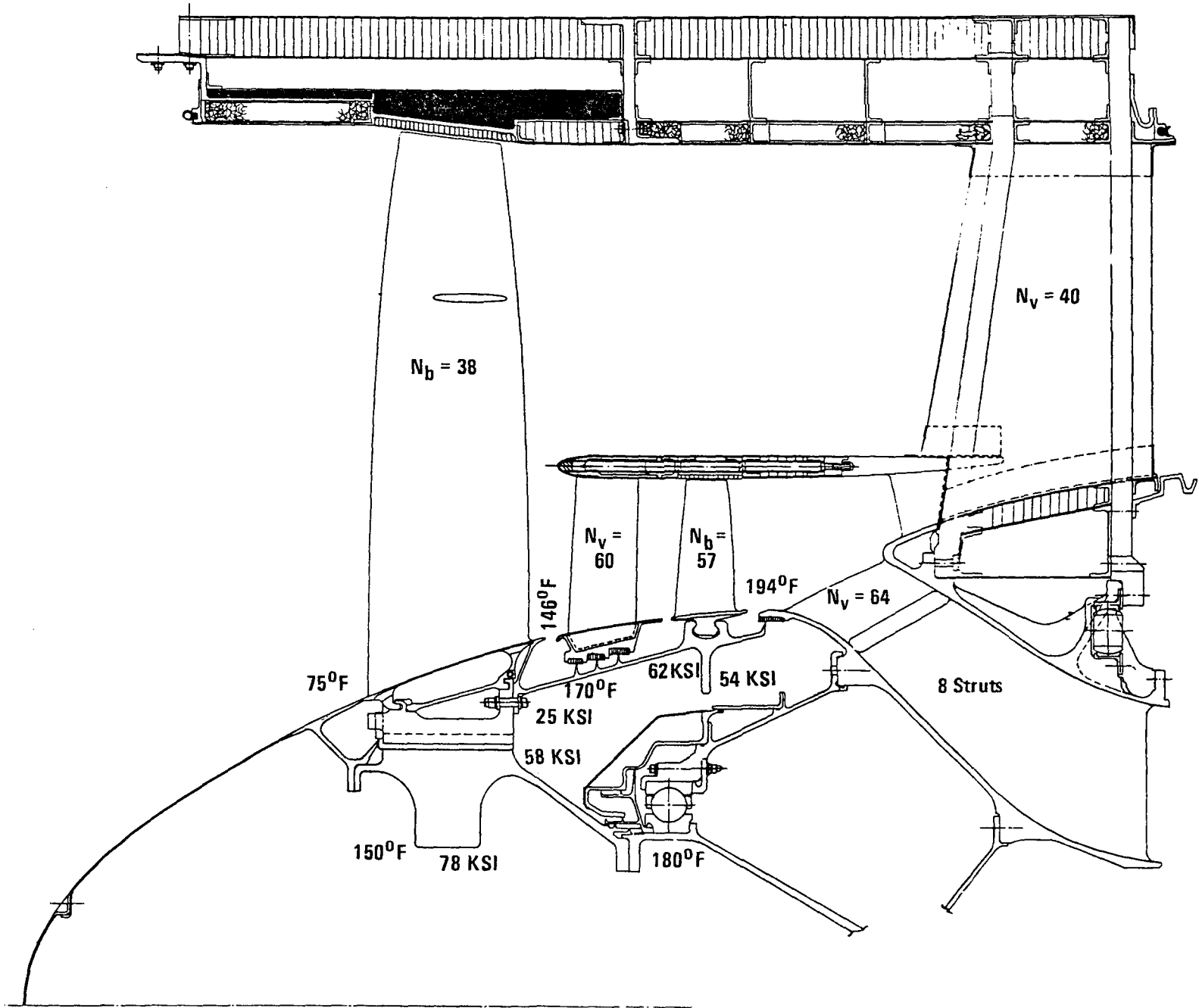


Figure 58. Fan Module Cross Section, Blade Count

The core struts are internally stiffened to provide support for the bypass vane/outer casing assembly and bearing cone loads. This core frame is a one-piece aluminum sand casting utilizing 355-T5 aluminum with the final casting being machined for mating hardware.

The integrated bypass vane/fan casing assembly is an all-composite structure except for portions of the containment structure and the acoustic facing for the bulk absorber acoustic treatment. The design concept for this portion of the frame is based primarily on the composite technology developed and demonstrated during the QCSEE program (reference 8). The bypass vanes consist of two graphite/epoxy wheels whose spokes provide the radial load carrying capability and whose rims provide the required circumferential stiffness for load transfer. The bypass vanes themselves are formed by airfoil shaped graphite/epoxy skins which are bonded to either side of the wheel spokes, thus, providing a shear tie between the two wheels as well as forming the shape and flow surface of the vanes.

The fan casing, which is integral with and supported by the bypass vane support structure, extends from the rear of the fan frame forward beyond the fan blade plane of rotation to the inlet attachment flange. This casing contains, as an integrated structure, the acoustic treatment and the fan blade containment system.

The main structure of the casing is a two inch thick sandwich structure, with graphite/epoxy facings, which forms the outer flowpath of the nacelle in this area. The inner flowpath of the casing is formed by the acoustic treatment and its supporting structure.

The containment structure consists of a steel ring facing the fan blade tips backed up by dry Kevlar cloth and closed out by a fiberglass/epoxy belt to hold the Kevlar in place during normal operation. This complete containment structure can be removed from the rest of the fan casing by removing two rows of bolts and sliding the containment subassembly forward out of the casing. If damaged, a new containment subassembly may readily be installed in this manner.

The 64 quarter-stage inner OGV's are located behind the quarter stage in the throat of the fan frame core flow path. As mentioned in the discussion of the fan frame, the core of these vanes is an integral part of the aluminum casting. The vane skins are graphite/epoxy bonded to the aluminum core, thus providing the vane aerodynamic shape. The vanes are divided into eight groups of evenly spaced vanes in order to match the struts.

The 60 Stage 1 vanes are located just aft of the fan hub and are supported by the primary fan discharge flow splitter which is cantilevered from the core casting of the fan frame. The vanes are heat-treated 7075 aluminum.

The inner shrouds for these vanes are glass/epoxy molding compound bonded to the lower portion of the vane which extends radially inward from the inner flow path. The outer portion of the shroud surface forms the inner flow path. The outer portion of the vane is bonded into, and supported from, the glass/epoxy splitter. The splitter is fabricated in



two axial sections with the forward portion supporting the Stage 1 vanes and containing the rub material for the quarter-stage rotor and the aft portion containing acoustical treatment. This splitter is attached to the core casting by axial bolts inserted through tubes extending the length of the splitter.

## 2. Weight and Sizing

The composite portion of the frame/casing was sized based on the QCSEE fan frame dimensions. That frame was designed to three times the operating load requirements of MIL-L-5007C and to the unbalance due to 5 composite blades (equivalent to 2-1/2 metal blades) out. The QCSEE frame was analyzed using General Electric's MASS structural modeling computer program and the resultant sizing checked by static testing. The E<sup>3</sup> frame sizing was based on this data. This resulted in the following weight breakdown of the composite portion of the E<sup>3</sup> frame/casing structure:

Structural Wheels	108 Kg (238 lbs)
Vane Panels	13 Kg ( 28 lbs)
Flanges & Supports	95 Kg (210 lbs)
Shells	54 Kg (120 lbs)
Adhesive	21 Kg ( 47 lbs)
Honeycomb	21 Kg ( 46 lbs)
	<hr/>
	312 Kg (689 lbs)

In addition, there is 7 Kg (16 lbs) of bulk absorber acoustic material in the fan casing.

The containment structure dimensions were selected based on a design goal to save one-third of the normal all-steel containment weight. This goal was then applied to the analysis of the present configuration. Based on current General Electric design practices derived from empirical data, an all-steel containment ring (including that protection necessary forward and aft of the fan plane of rotation) would weigh 162 Kg (357 pounds) and have a thickness over the blade of 7 mm (0.285) inch. Using one-third of this thickness, 2.4 mm (0.095 inch) of steel it was then computed, using small bore ballistic data, that an additional 5mm (0.20 inch) of dry Kevlar cloth would be required to provide adequate containment of an E<sup>3</sup> stage 1 fan air-foil. This resulted in a total containment weight of 74 Kg (163 lbs), which more than met the goal of saving one-third of the weight of an all-steel ring. Anticipated future development programs will provide the basis for evaluating the suitability of this design. However, until this is verified, the original decision to save one-third of the all-steel containment weight will be used in the E<sup>3</sup> design which results in a containment weight of 108 Kg (238 lbs).

The inlet attachment flange which ties the containment, the outer fan case, and the inlet together is an integral part of the containment ring, but not a part of the containment function or weight.

The other major portion of the E<sup>3</sup> fan frame is the cast aluminum core. The concept shown and the weight were derived from the existing TF34 frame casting which is very similar. The E<sup>3</sup> core frame weight, scaled from the TF34 core frame weight, is therefore 124 Kg (273 lbs).

The total frame weight, including containment, acoustic material, and the inlet attachment ring, is 597 Kg (1316 lbs). A potential 34 Kg (75 lbs) may be removed from this status weight pending verification of the containment configuration. This would result in a total weight of 563 Kg (1241 lbs.).

The natural frequency of the nominal configuration of the fan bypass stator vanes was determined by ratioing the first flexural frequency of the QCSEE vane test results by the vane length since the average cross section of the QCSEE vanes and the E<sup>3</sup> vanes are very nearly identical. This resulted in a first flexural frequency of the E<sup>3</sup> fan stator vanes of 527 Hertz. The Campbell diagram for these vanes is shown in Figure 59. Second flex crosses the 38/rev line at 63% fan speed.

The fan frame is designed for a maximum temperature of 149°C (300°F) and a minimum temperature of -51°C (-60°F). All interfaces are designed to accommodate the differing thermal coefficients over appropriate sections of this temperature range. The maximum delta T (plus or minus from 19°C (67°F) that occurs between composite and metal components is 111°C (200°F).

Since the E<sup>3</sup> fan frame sizing was primarily based on the QCSEE frame, the margins of safety for all normal operating conditions are based on 2.5 times limit load. The static portions of the E<sup>3</sup> fan module are designed to last two engine life times under normal operating conditions.

### c. Compressor Rotor

The E<sup>3</sup> compressor rotor is a 10 stage, high-stage-loading (HSL) configuration designed to produce a pressure ratio of 23 at 54.4 Kg/sec (120 lbm/sec) corrected airflow with the inlet flow pattern produced by the fan. This compressor rotor configuration evolved from that configuration established as having the best combination of high efficiency, low operating cost, low fuel usage, and acceptable development risk during the Preliminary Design Study of Advanced Multistage Axial Flow Core Compressors conducted in 1975 under Contract NAS3-19444 (reference 6). A cross section of the rotor and corresponding materials are shown in Figure 60.

#### 1. Design and Analysis

The compressor configuration was established based on the allocation of the overall engine requirements and on mechanical and performance interfaces with other engine components.

The E<sup>3</sup> compressor rotor structure consists of only two major components: an integral Stage 1 through 7 spool with forward stub shaft and an integral stage 7 through 10 spool with rear stub shaft. These two components are connected by a rabbeted bolt joint at the Stage 7 disk. This minimum bolt joint design concept has demonstrated excellent balance stability and has resulted in a reduction in the number of parts for both the CF6 and F101 engine families.

Titanium is employed to take advantage of high strength and low weight characteristics in the low operating-temperature environment of the forward spool. The higher temperature requirements of the aft spool are met by the exceptional strength, weldability, and temperature capabilities of Rene' 95. Utilization of these high tensile strength materials allows a large bore, thin web, lightweight spool design for the E<sup>3</sup> compressor rotor.

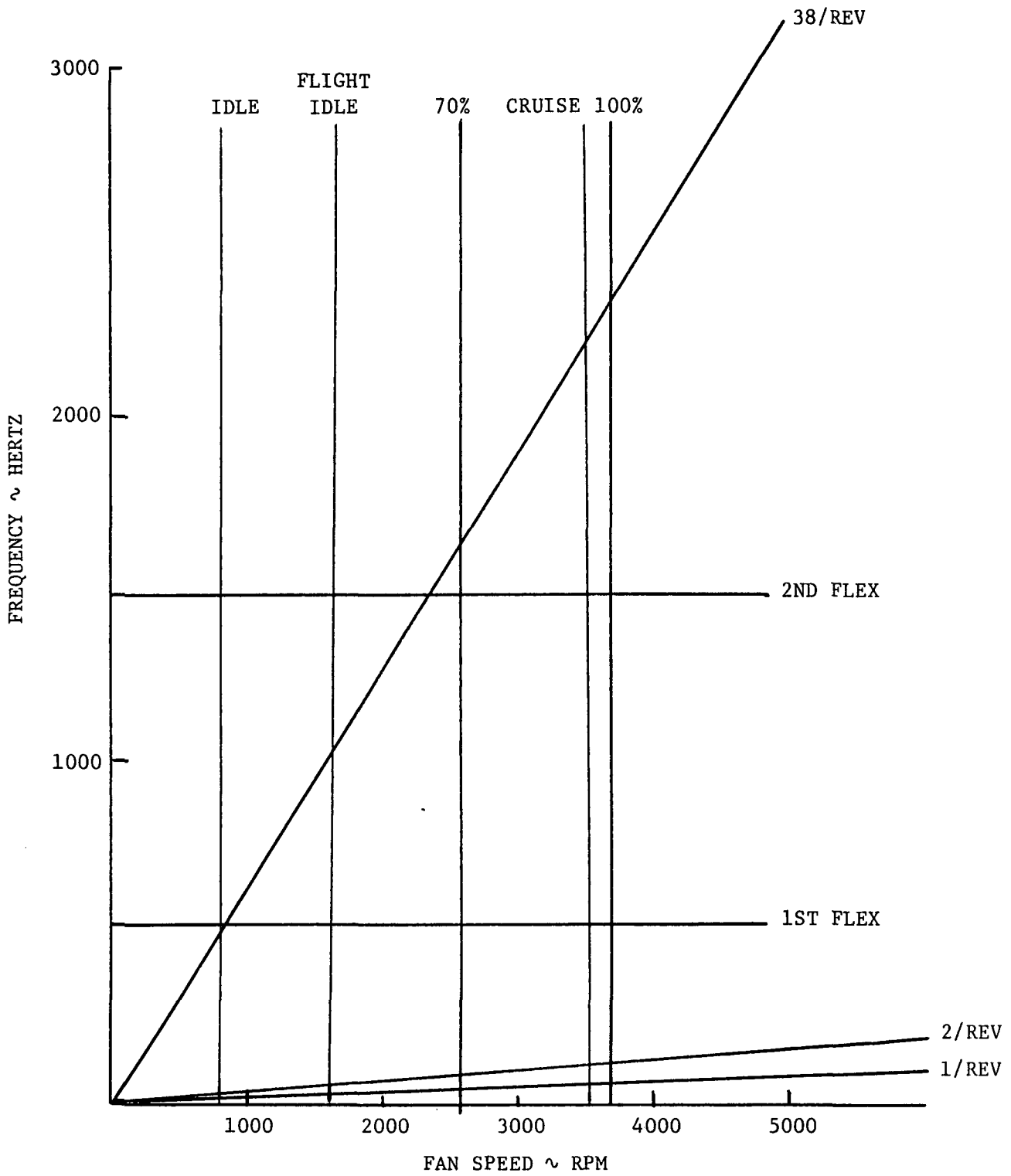


Figure 59. E<sup>3</sup> Fan Bypass Stators Campbell Diagram

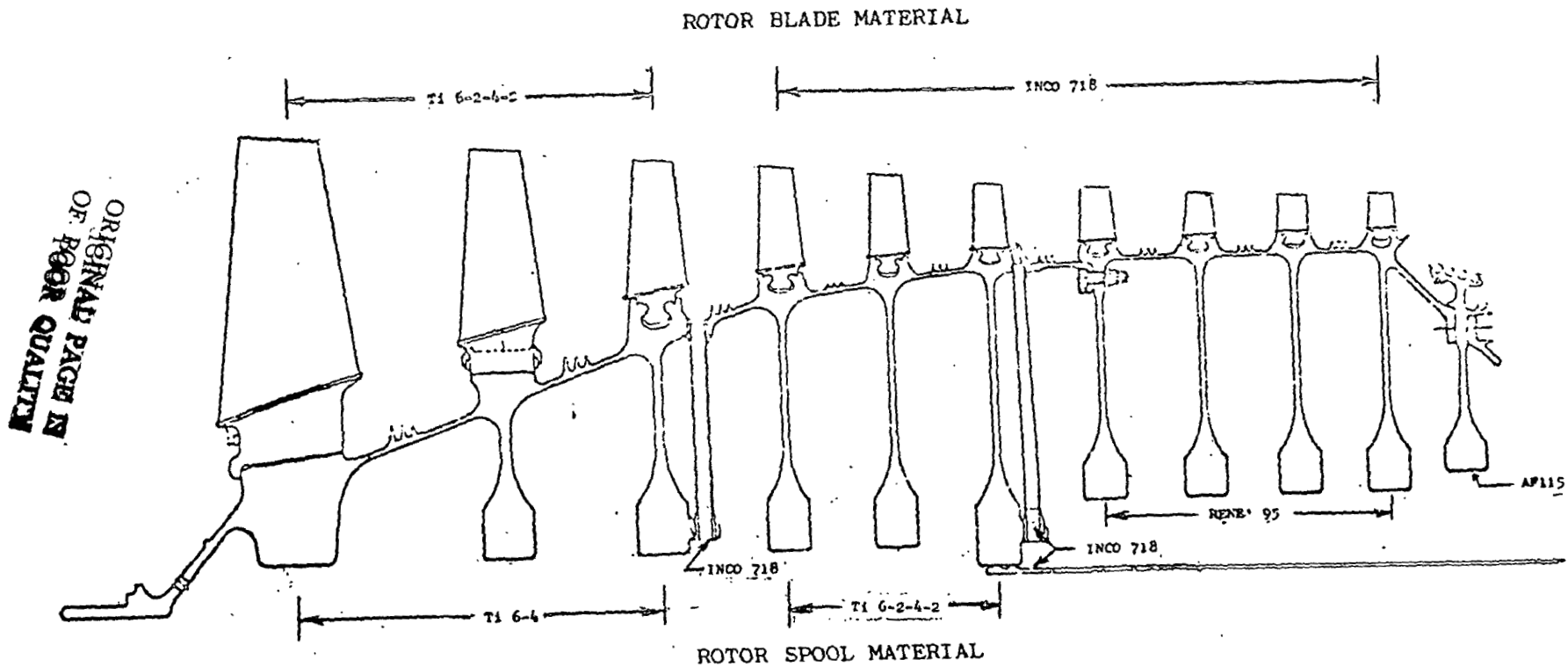


Figure 60. E<sup>3</sup> Compressor Rotor Component Materials

The one-piece, inertia-welded spool configuration offers the following advantages:

- Excellent joint material properties resulting from the material grain refinement inherent in the inertia-weld process
- Similar forgings for most stages of the spool
- Common tooling for most stages for fabrication and welding
- Elimination of internal bolted flanges which in turn:
  - Reduces rotor weight
  - Reduces quantity of component parts
  - Eliminates component shifting during operation (which could cause compressor unbalance)
  - Increases rotor stiffness

Both spools feature integral labyrinth seal teeth for interstage sealing. An abrasive coating (aluminum oxide) is applied to the teeth to eliminate metal-to-metal contact during a rub with the stationary seal.

The compressor discharge pressure (CDP) seal is located at the bolted joint between the aft stub shaft of the compressor rotor structure and the high pressure turbine (HPT) forward shaft. The operating clearances at the labyrinth seal teeth are minimized to reduce compressor discharge leakage, thus, improving compressor performance. The seal material is AF115 to take advantage of its high strength and high temperature capabilities. As with the interstage labyrinth seal teeth, the CDP seal teeth are coated with aluminum oxide to prevent metal-to-metal contact with the stationary seal during engine operation.

The rotor has two individual, radial-inflow-bleed systems, one aft of the Stage 3 disk and the other aft of the Stage 6 disk. The forward bleed system functions to pressure the seals of the forward and aft sumps. The aft system provides cooling air for the second-stage HPT blades.

Both inflow systems consist of lightweight, thin-wall tubes open at one end to the flowpath interstage-spool cavity and at the other to the spool inner cavity at a minimum radius established by the center shafting. This arrangement improves system performance by removing angular momentum from the bleed air as it flows inward.

The cooling airflow also provides several benefits for the compressor rotor structure. The cooling increases the thermal-response rate of the rotor and permits airfoil clearances to be reduced for all operating conditions. Use of the low pressure cooling air also results in an inward-acting pressure differential on the rotor spacers, which partially offsets the centrifugal loads, reducing stresses. Furthermore, the internal cooling air helps to eliminate the possibility of disk buckling.

The design criteria applied to the rotor structure, including the CDP seal, is based on General Electric's past experience in designing structurally efficient, safe, rotating structures for both military and commercial engines.

The design of each component is determined from the operating conditions and life requirements, cycles and hours, at particular locations of the component. Various design criteria are applied to each location, and the limiting criteria establish the component size.

The rotor stress distribution is presented in Figure 61 with the radial stress distribution of a typical disk (stage 4) shown in Figure 62.

The E<sup>3</sup> High Stage Loading (HSL) compressor design approach requires long blade chords to meet aerodynamic-loading and stall-margin requirements. This design approach benefited the mechanical design as follows:

- High blade stiffness reduced bending stresses
- High blade frequencies
- High tolerance to foreign object damage
- Low vibratory stresses
- Low susceptibility to blade flutter
- Low radial blade clearances due to high axial stiffness.

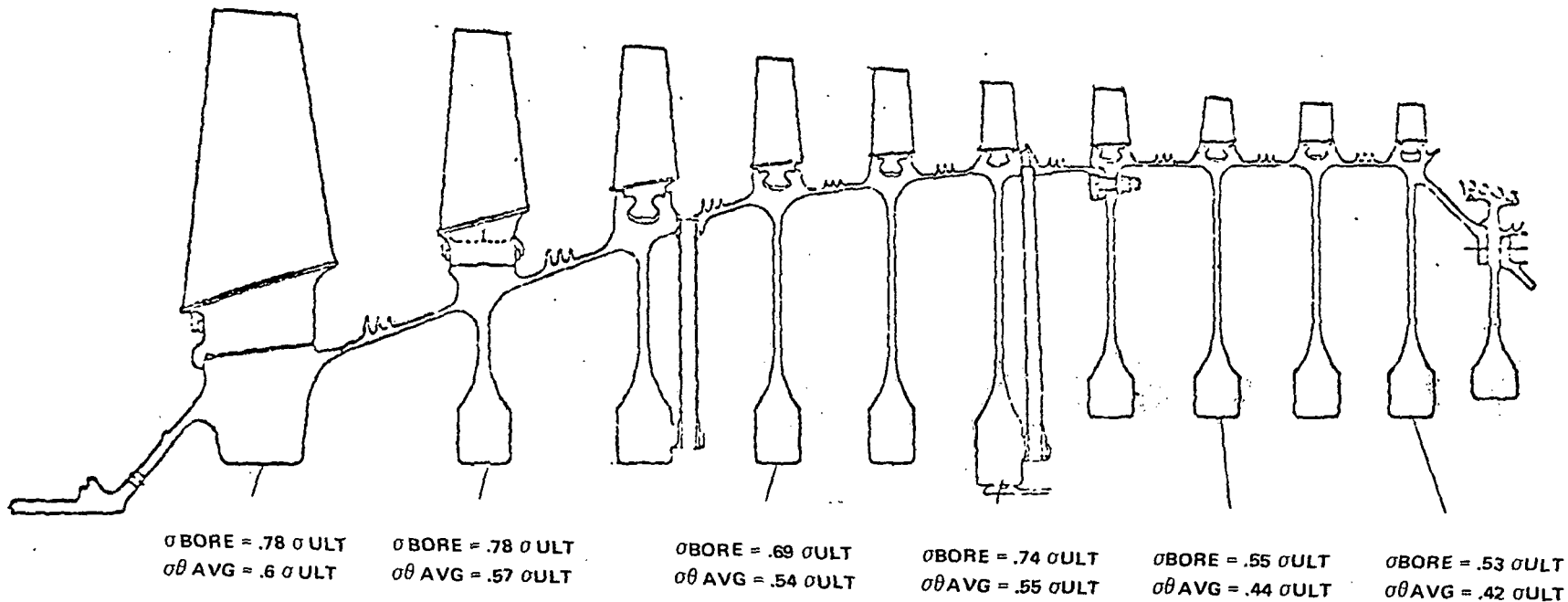
A particularly significant characteristic of HSL compressor designs is the low blade stress (due to blade geometry) measured during compressor stall. The low blade stress results in increased tolerance to stall damage and increased blade life. The low stall stresses also show that the blades are insensitive to flutter. The HSL design produces stable blades, in that compressor stall occurs before blade flutter.

The blade materials chosen (Ti 6Al-2Sn-4Zr-2Mo and Inco 718) exhibit high strength and ductility and have demonstrated good corrosion resistance to prevent performance and strength loss with extended operation.

#### d. HPC Stator

##### 1. Description

The compressor stator design shown in Figure 63 utilizes a front outer casing material of titanium 6Al-2Sn-4Zr-2Mo, and a rear inner casing of Inconel 718. The rear portion of the front casing is enlarged to circumferentially enclose the rear casing, thus creating a manifold for Stage 7 bleed in the space between the two casings. The front casing is the load-carrying, structural shell of the core engine and incorporates a manifold over the Stage 5 stator row for customer bleed requirements. Figure 63 designates the materials used throughout the stator design.



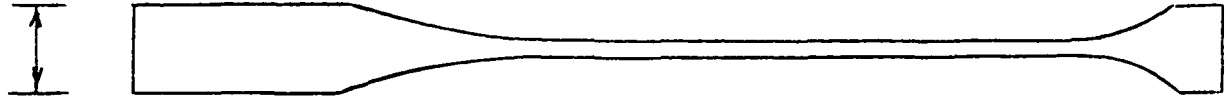
$\sigma_{ULT} \text{ STRESS} = \sigma_{ULT} \cdot 30$

Figure 61.  $E^3$  Compressor Rotor Stress Distribution

ORIGINAL PAGE IS  
OF POOR QUALITY

Typical Rotor Disk Stress Distribution  
(Stage 4 Disk)

2.54 cm (1.0")



ORIGINAL PAGE IS  
OF POOR QUALITY

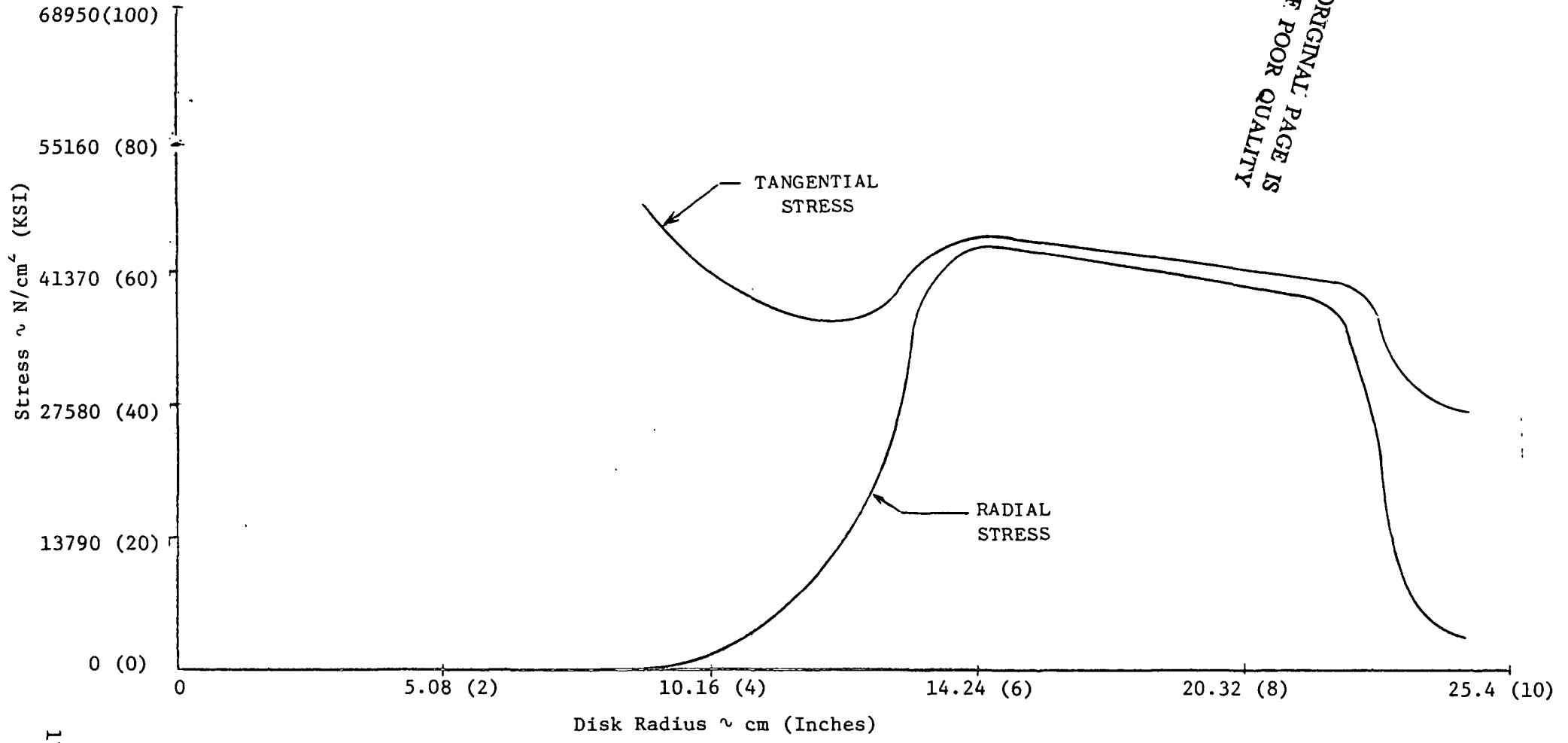


Figure 62. E<sup>3</sup> Compressor Rotor



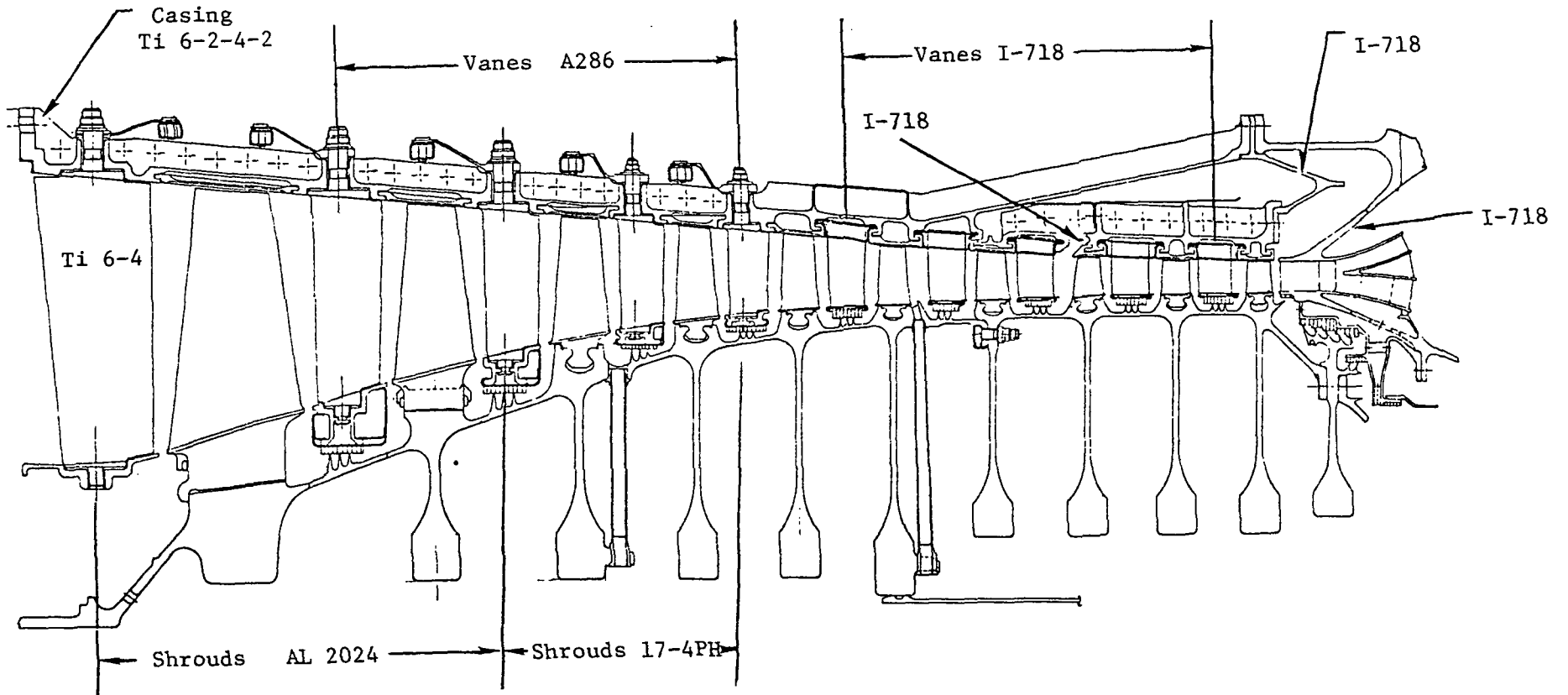


Figure 63. E<sup>3</sup> HPC Stator Configuration-Task III  
Rub Strip Material, Stage 1-10 Ni-Gr

Holes and counterbores are provided for the variable-vane, trunnion mountings. "T" slots are provided on the inside of the casings to mount the fixed-vane segments and blade-tip, rub-liner segments. In addition, the cavities formed by the "T" slots retard heat transmission. The flowpath contour is formed by the vane platforms and the rub liners. The liners are circumferentially segmented. In the event of a rotor rub or FOD, only those segments damaged beyond serviceable limits need be replaced. The rub-liner materials are as follows:

- Stages 1 through 3 - 17-4PH stainless steel
- Stages 4 through 10 - Inconel 718

The casings are split axially in halves. Removal of a stator half from an assembled engine allows easy access to the compressor blades and vanes for inspection, repair or replacement.

The casing has been designed such that unfavorable thermal gradients will not affect its ability to function satisfactorily.

Clearance Control - The E<sup>3</sup> compressor requires small, airfoil tip clearances for high efficiency and stall margin. Conversely, transient conditions require larger clearances to accommodate different thermal response rates between rotor and stator. Therefore, special design features are necessary to minimize the effect of thermal transients. For the E3, these features are:

- Insulate the casing from the compressor flowpath to reduce thermal growth of the casing.
- Flow cooling air over the outer wall of the casing (fan discharge for the front casing and seventh-stage bleed for the rear casing) to reduce thermal growth of the casing. The seventh-stage bleed is capable (through a valve in the bleed piping) of being diverted to flow over the entire rear case or being isolated to the Stage 7 area only to control rear-case thermal response.

Compressor Stator Bleed Summary - Stage 5 customer bleed is taken from bleed slots located between the vanes and connected to a common, circumferential manifold.

Stage 7 bleed air is extracted through the casing aft of Stator 7 for cooling the second-stage high pressure turbine (HPT) nozzle. Additional bleed capability is provided for engine starting.

CDP air is extracted at the middle of the flowpath on the back side of the OGV diffuser frame splitter. It is routed inward through hollow struts into the radial inducer located immediately aft of the CDP seal. This air is used to cool the Stage 1 HPT rotor.

Vanes and Shrouds - Material for the variable vanes is titanium 6Al-2Sn-4Zr-2Mo in the IGV and A286 for the remaining variable stages. Shroud material is aluminum 2024 for the IGV, Stage 1, and Stage 2, while the remaining variable shrouds are made from 17-4PH stainless steel.

All variable-vane outer trunnions are of "high boss" design in which the vane bearing reactions are perpendicular to the vane axis of rotation. This approach has been used successfully on other General Electric compressors including the GE4 and F101 and is a means of providing stiff vane mounting in the relatively thin, machined titanium casing.

Vanes in the fixed stages are fabricated into segmented sections. Airfoils (Inconel 718) are stabbed and brazed into two outer bands (forming a rigid box structure) and an inner shroud band. Honeycomb is brazed to the inner shroud band to form the interstage seals. The band material is Inconel 600, and the honeycomb is Hastelloy X.

Stator vane shrouds add significant resistance to impact failure from FOD because they permit impact loads to be shared by adjacent vanes. Vane shrouds help reduce bending stresses in the vanes, reduce vibratory stresses, raise the vane natural frequencies, and provide a relatively well-damped structure.

The Stage 10 vanes are the outlet guide vanes and are integrally cast into the Inconel 718 combustor-diffuser section. This section serves as the main structural element in the diffuser casing assembly and includes the combustor diffuser. The short inner casing and the outer casing which provide the connecting structure between the compressor casings and turbine case are butt-welded to the casting.

The stator vanes are stable and have satisfactory vibratory allowable limits throughout the entire engine operating range. They are designed such that the primary torsional, flexural, and plate modes do not coincide with blade-passing stimuli from two rotating stages in front and one rotating stage aft of each vane row within the 60 to 110% engine-speed range.

Vane Actuation - Movement of the variable vanes is coordinated by a bellcrank actuation system.

The bellcrank assembly on each side of the compressor consists of bellcranks mounted inside of the bellcrank support and connected together by a master rod. The fluid actuator is mounted on a bracket bolted to the bellcrank support. Turnbuckle links attach the bellcranks to the actuation-ring connector bridges to complete the system.

## e. Combustor/Casing

### 1. Description

The combustion system chosen for the E<sup>3</sup> engine is shown in cross-section in Figure 64. The combustor features a double-annular dome with a centerbody dividing the dome into two independent combustor zones and impingement-plus-film-cooled liners. The combustor/turbine stator interface features a machined, low-volume, fishmouth seal.

In this design, fuel is introduced into each of the fuel cups through an integral fuel body. Each dome annulus is fed independently. The combustion case is designed to support the fuel nozzles, the ignitors, the fuel manifolds, the combustor support pins, and borescope ports. The casing is an integral assembly with the diffuser. The diffuser is a cast structure with a splitter and support struts cast into the assembly.

The combustor life goals are a total of 18,000 cycles and 18,000 hours with one repair after 9,000 cycles and 9,000 hours. The maximum combustor inlet air conditions the combustor must be designed to accept are:

Combustor Inlet Temperature	662°C (1224°F)
Combustor Inlet Pressure	3764 KN/m <sup>2</sup> (546 psia)

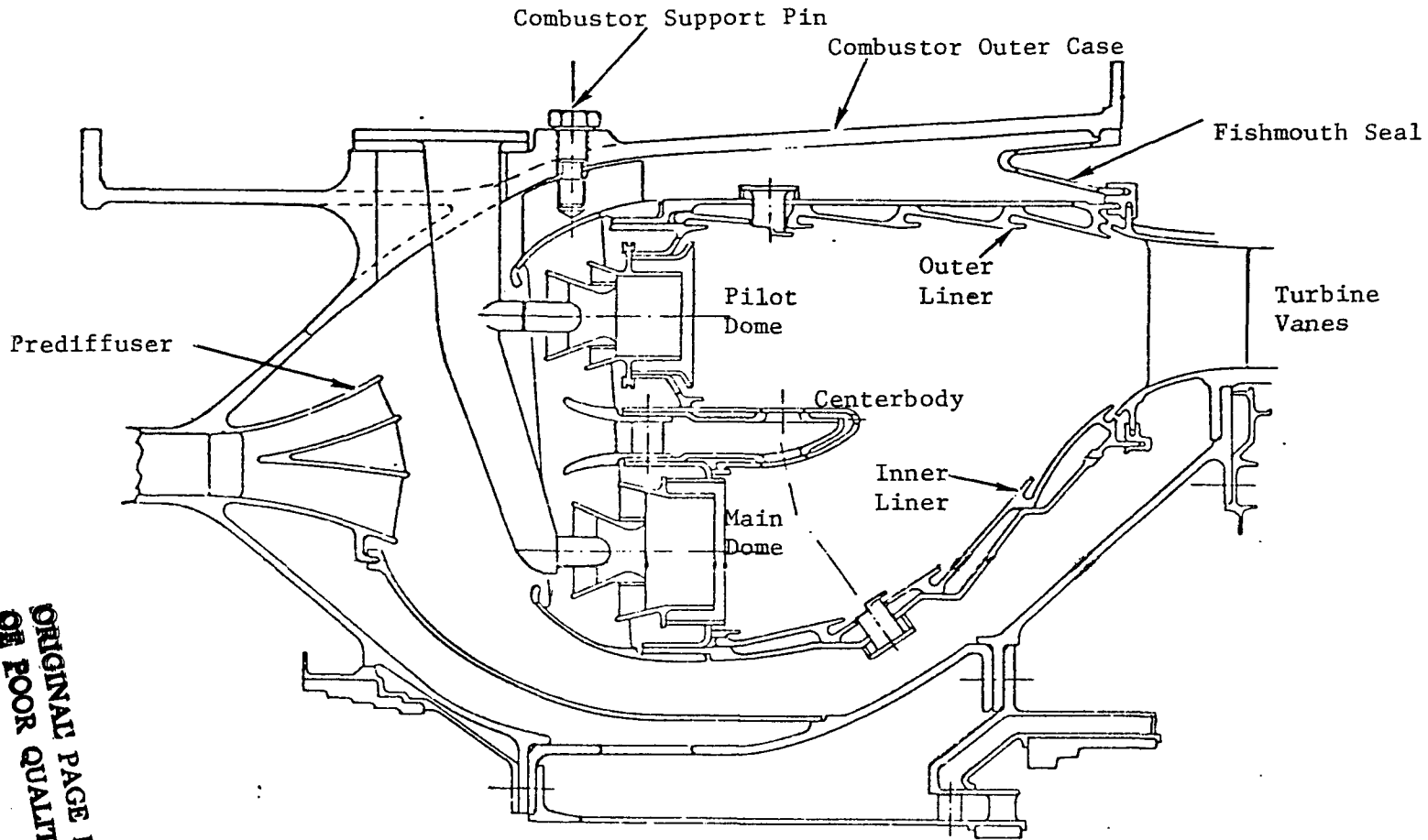
Following is a description of the various combustor components for the initial engine configuration.

Dome - The dome assembly consists of two rows of central-fuel injection swirl cups, a pilot-stage outer annulus, and a main-stage inner annulus. A cross section of this dome design identifying the various components is given in Figure 65. Each annulus of the E<sup>3</sup> combustor houses 28 swirl cups consisting of primary swirlers mounted concentrically to counterrotating secondary swirlers.

Mechanical stackup and thermal radial growth between the fuel tubes and the dome/liner assembly are absorbed with a radial flange slip joint mounting. Individual splash plates are attached to the dome spectacle plate for each fuel source to shield the dome structure. Holes are provided in the spectacle plate to impinge cooling air on the splash plates. Both the inner and outer domes are designed in a similar fashion on the E<sup>3</sup> combustor design.

The dome cowling is a one-piece assembly with airfoil-shaped struts located between swirl-cup/fuel-nozzle locations to provide structural rigidity. The cowl is designed to contain the dome/centerbody assembly and to pass the aerodynamic loads from the inner liner, across the dome, into the combustor casing.

The selected material for the dome, cowls, and swirler assemblies is Hastelloy-X, a nickel-based alloy. Hastelloy-X was chosen for its high-temperature operating capability, its good oxidation and corrosion resistance, and its weldability and formability features.



ORIGINAL PAGE IS  
OF POOR QUALITY.

Figure 64. Proposed E<sup>3</sup> Combustion System.

ORIGINAL PAGE IS  
OF POOR QUALITY

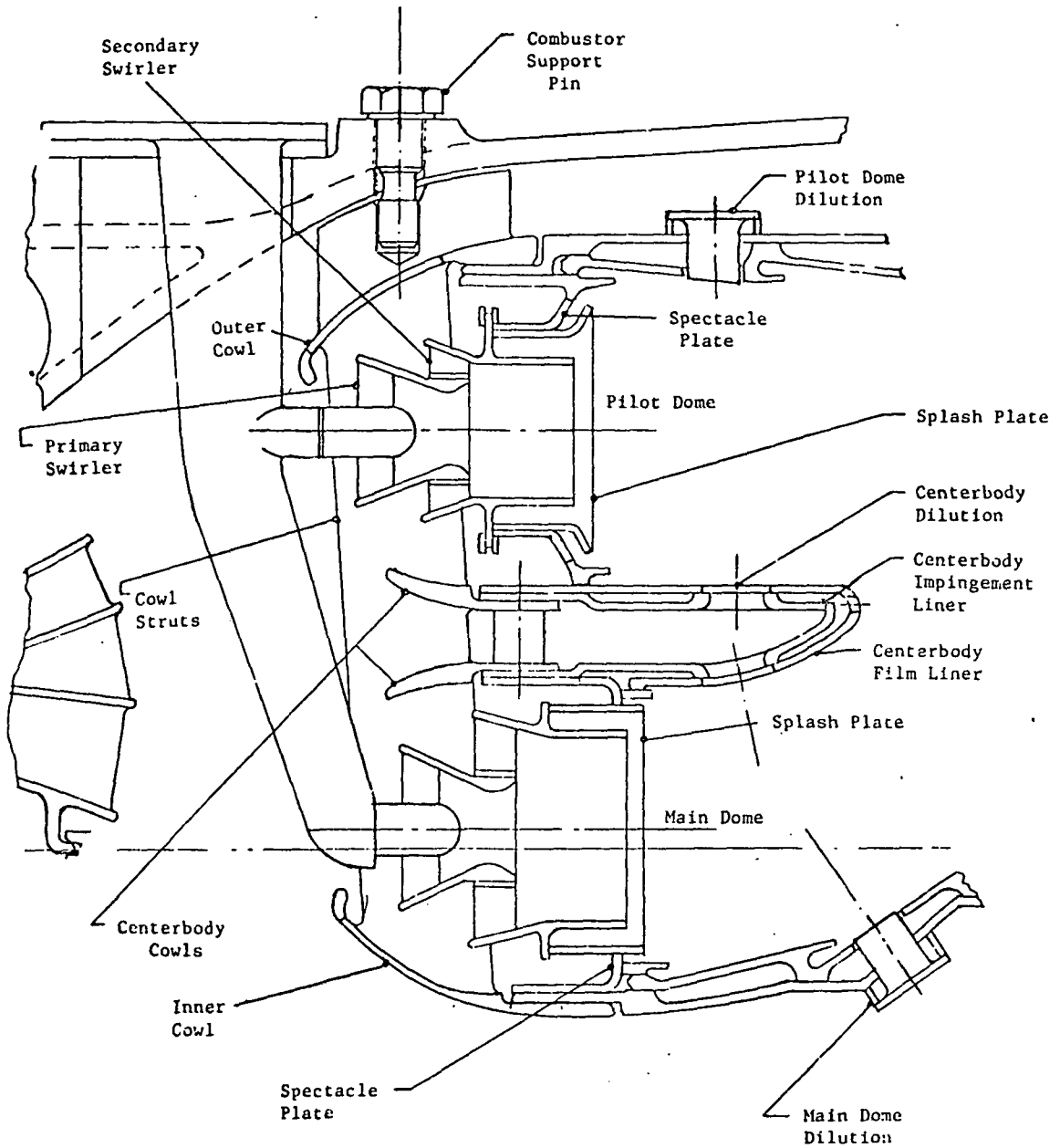


Figure 65. Double-Annular Dome Assembly.

A centerbody is used to divide the two concentric domes into separate burning chambers. This centerbody design features a double-wall impingement plus film-cooled structure similar to the cooling-liner design. Crossfire provisions are located at two cup centerline to provide minimal main-stage-ignition delays. The centerbody is equipped with entrance cowls, supported by the cowl struts, to minimize pressure losses into the dilution and cooling feed hole slots. Located around the impingement liner is a segmented film-cooled liner. The main structure of the centerbody is to be made from Inco 625. The film liner is to be made from Hastelloy-X or HS188 while the impingement liner will be A286.

Cooling Liners - The combustor design features an impingement-plus-film-cooled liner design consisting of a double-wall construction, with a sheet metal impingement liner and a machined-ring film liner.

Each liner carries a share of the external pressure load while the axial loads are transmitted to the dome through the impingement liner. In this manner, the cooler impingement liner is more highly stressed but, because it is operated at a lower temperature, can withstand the higher loading.

The film-cooled liner is a 360° piece supported by the impingement liner. The liners are attached at the aft end. Relative axial growth due to the temperature mismatch of the hot, film-cooled liner and the cold, impingement liner is absorbed at the forward attachment of the film-cooled liner. A slot between the dome/liner interface provides radial support to the film-cooled liner, but no axial restraints are imposed.

Two design approaches have been considered for the impingement cavity between the film-cooled and impingement liners. One approach is to design the liner system with a separate impingement cavity for each panel, as shown in Figure 64. An alternative approach is to use one continuous cavity between liners. The former approach allows specific tailoring of liner flow distribution while the latter eliminates thermal growth mismatch problems between the liner components.

The combustor liners use thimble ports to introduce dilution air. A portion of the spent impingement air that enters the combustor through the dilution annulus is used to reenergize the dilution-stripped, liner-cooling film aft of the dilution ports.

Thermal barrier coatings will be applied to the combustor film liner inner surfaces and dome splashplate surfaces to shield and insulate these areas from the combustion gases. These coatings should significantly improve the life capability of the combustor component.

Fuel Delivery System - In the E<sup>3</sup> combustor design, the fuel is delivered to both dome annuli by a single fuel nozzle body, as shown in Figure 65. Each body has independent passages to feed two fuel nozzle tips. These passages are insulated to prevent fuel coking.

The fuel nozzles are fed by individual manifolds for each dome stage. Flow splitting and scheduling to the two domes are accomplished by a fuel splitter.

Ignition System - The E<sup>3</sup> combustor design embodies a dual-igniter system. Both igniters will be designed to be externally removable from the engine assembly, with the engine installed in the airframe. The igniters will be mounted on the combustor outer casing at locations to provide the best ignition potential. The ignitor tip will protrude through a clearance hole in the liner into the combustor dome region. No loads will be transmitted from the igniter to the combustor liner. All loads will be absorbed by the combustor case. Attachment of the igniters to the case will be achieved with coarse screw threads on the igniter body which mate to a casing boss. A Vespel seal will be used at the outer fan-case-penetration region to prevent leakage.

Screens - The combustor will employ filtering screens to remove 0.015-in. diameter and larger particles from the turbine cooling air supply. The screens will be mounted on the combustor liner aft flange of the combustor casing. At one end, the screens will be hard mounted while the opposite end will have a slip joint. A tight-fitting, fishmouth-type seal will be used. The screens will only carry the pressure-drop load across the screen. The screen will be fabricated from Hastelloy-X.

Attachment/Loads - In the E<sup>3</sup> combustor design, the combustor inner and outer domes, the cowl, the centerbody, and the cooling liners are bolted into a one-piece assembly. The outer cowl fairing provides the interface for mounting the entire assembly to the outer casing. The combustor is mounted at the forward end with 28 support pins to permit radial, thermal expansion between the combustor and the support casing while restraining the combustor from axial movement induced by the pressure forces on the combustor dome and liners. The support pins position the combustor assembly in relationship to the engine centerline. The liner is supported at the aft end by fishmouth seals located at the turbine stator. The seals permit axial and radial-differential growth while separating and sealing the cooling-air passages between the liner and casing from the hot flow path.

Combustor Outer Case - The combustor outer casing will be designed to transmit the engine loads to the forward mounting system, support the combustor and the numerous combustor services, and form a major portion of the engine structural back-bone. The casing will be integrally fabricated with the diffuser and inner combustor case to form the main structure of the high pressure combustor/turbine stator assembly. The material chosen for the casing assembly is Inconel 718 (nickel base alloy).

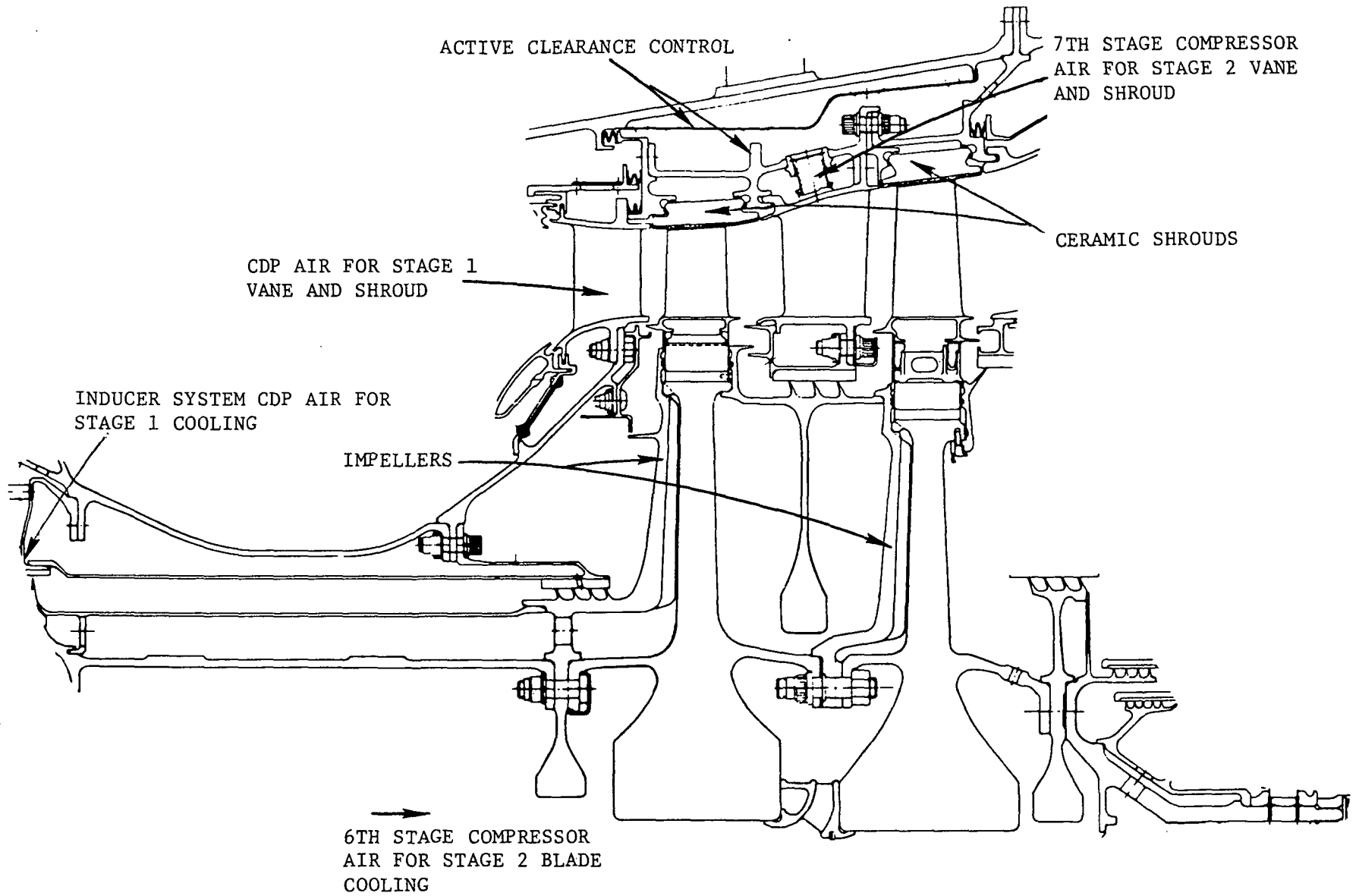
The casing will provide accessibility to the combustor for the 28 fuel tubes, igniters, and 28 mounting pins. In addition, ports will be provided in the casing for compressor discharge bleed, combustor borescope inspection, instrumentation pads, and fuel drainage.

#### f. HPT Rotor/Stator

##### 1. Description

The two-stage turbine is an air-cooled design using compressor discharge and interstage air as the coolant source for the nozzles and the blades. The general configuration and design features are illustrated in Figure 66.





ORIGINAL PAGE IS  
OF POOR QUALITY

Figure 66. E<sup>3</sup> High Pressure Turbine.

Table 58 illustrates the design life goals for major turbine parts to permit lowered maintenance costs. Cooling has been increased in order to achieve these life goals which exceed current commercial practice. In addition, borescope portholes are strategically located in both turbine stages to allow unobstructed viewing of blades and the interstage heat shield. The borescopes will be mounted between the vane airfoils in the outer band segments and will permit routine inspection without engine case disassembly to cut inspection costs.

Part Description - Stage 1 Vane - The nozzle is an assembly consisting of 46 airfoils, paired in 23 segments. The airfoil is machined from ODS alloy MA754, and is brazed in pairs to integral inner and outer bands. The bands are cast from MAR-M-509 alloy. The brazed assembly permits the flexibility of incorporating band changes for altering the vane throat area during development and also for growth. This can be achieved by rotating the airfoil orientation relative to the bands prior to brazing, and is an important feature allowing prompt fine tuning of the throat areas for optimum performance. Figure 67 shows a typical manufacturing vane to band assembly.

MA754 is an ODS alloy capable of withstanding higher surface metal temperatures and is stronger relative to Cobalt base X-40. This alloy is particularly suited for stage 1 vane application, especially for its higher burnout margin.

The vane cooling design circuit allows the spent impingement air in the forward vane cavity to exit through an array of 20° to the radial angled film holes at the vane leading edge. These holes form an excellent shower-head barrier resulting in a more uniform air film protection for the surface as shown in Figure 68. In addition to impingement cooling, film cooling is used on the pressure and suction side.

The mechanical and maintenance cost analysis is based on meeting the design requirements. To achieve this result, the following failure modes would be analyzed in a more detailed design evaluation.

- Low cycle fatigue resulting from transient and steady state thermal gradients in the airfoil, and combined with the mechanical load.
- Suction side ballooning.
- Trailing edge thermal distortion and buckling and creep.
- Oxidation.
- Hot corrosion.
- Rupture.

The inner and outer bands are cast MAR-M-509 material. The inner band design includes the bolted flange system to absorb the aerodynamic airfoil loads, but is free to expand thermally in all directions as shown in Figure 66.

Stage 2 Nozzle Diaphragm - The stage 2 nozzle diaphragm consists of 60 airfoils which are cast from Rene' 150 material. The casting consists of 2 airfoils, paired as an integral part of an inner and outer band segment. Thirty segments form and comprise the nozzle stage assembly.

TABLE 58E<sup>3</sup> HP TURBINE LIFE REQUIREMENTS

<u>Component</u>	<u>Service Life/Installed</u>		<u>Total Service Life w/Repair</u>	
	<u>Hrs.</u>	<u>Flt. Cycles</u>	<u>Hrs.</u>	<u>Flt. Cycles</u>
Blades/Vanes	9,000	4,500	18,000	9,000
Disks, Shafts	18,000	9,000	36,000	18,000
Heat Shield	9,000	4,500	18,000	9,000
Retainers	18,000	9,000	36,000	18,000
Combustor/Turbine Casing	18,000	9,000	36,000	18,000

Typical Flight Time = 117.5 Minutes.

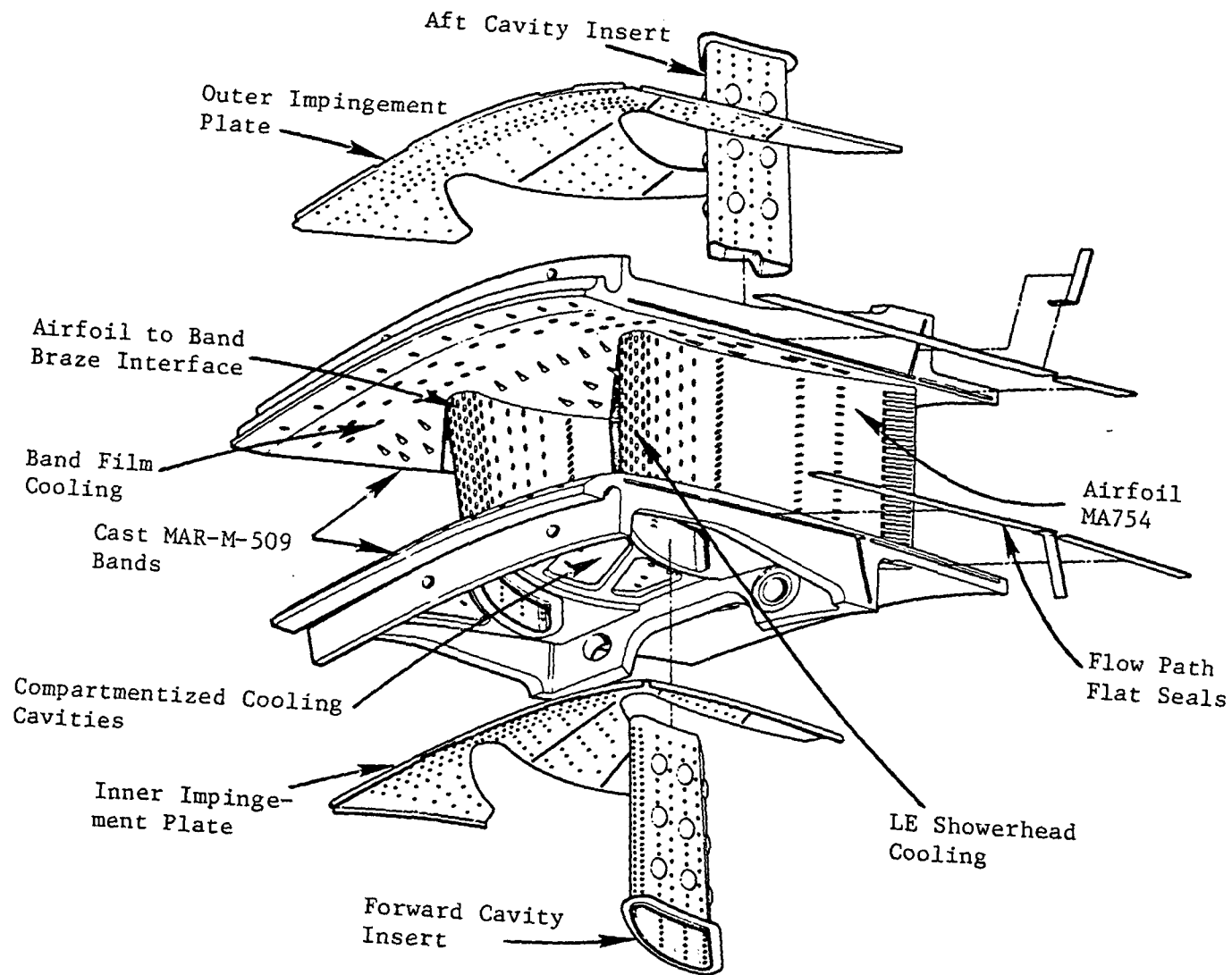
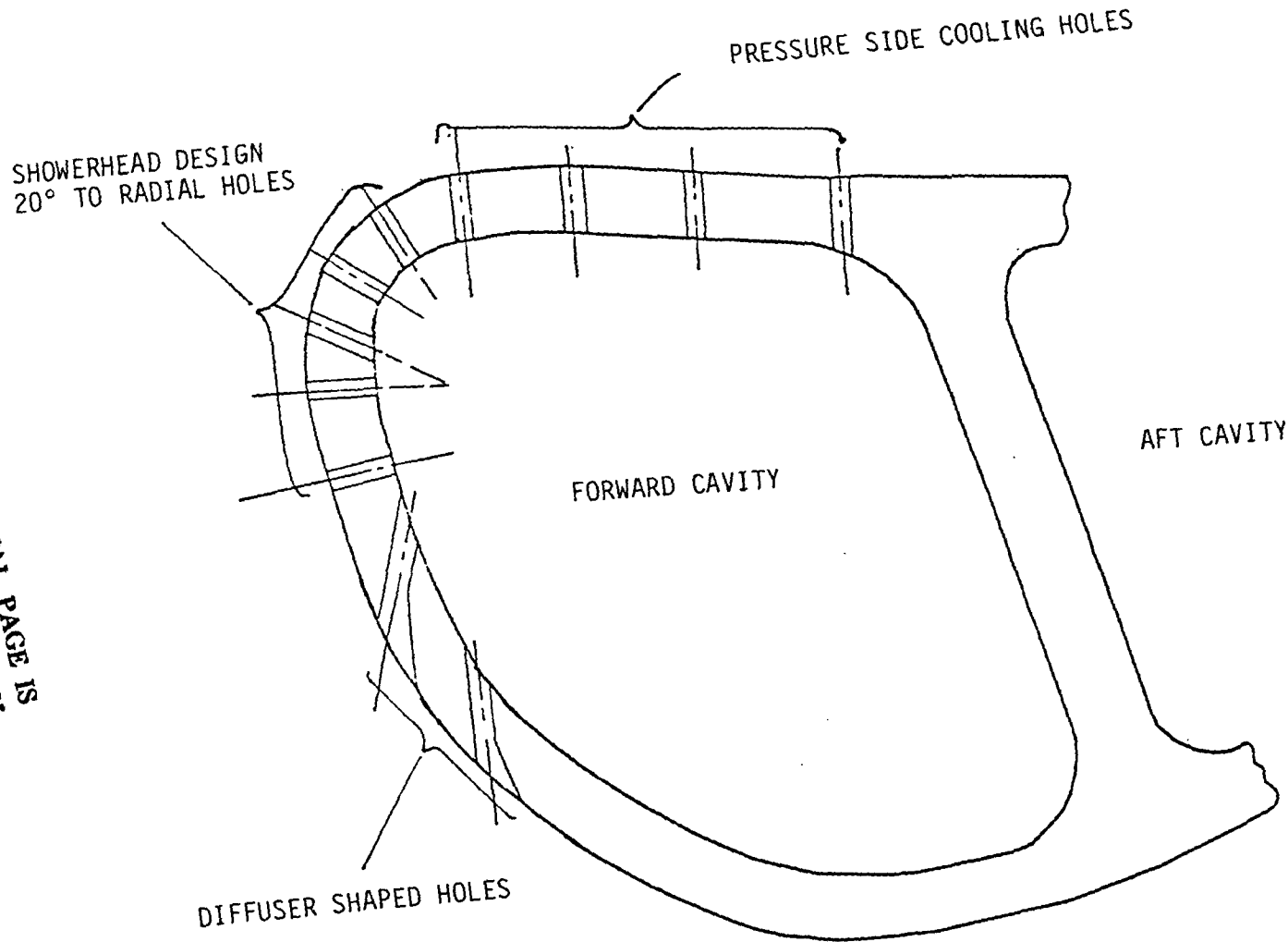


Figure 67. E<sup>3</sup> HP Turbine Stage 1 Vane Manufacturing

ORIGINAL PAGE IS  
OF POOR QUALITY.



$T_{GAS}$  (MAX PEAK) = 1799°C (3270°F)  
 $T_3$  = 597°C (1107°F)  
 $T_{COOL}$  = 619°C (1147°F)  
 $\% W_{2C}$  = 6.5  
 $T_{BULK}$  = 954°C (1750°F)

Figure 68. E<sup>3</sup> HP Turbine Stage 1 Vane Cooling Design.

As shown in Figure 69, the nozzle is supported at the outer band through a bolted flange arrangement to the nozzle and shroud support. The flange is structurally designed to absorb the aerodynamic gas loads and axial plug loads resulting from the differential pressure of the inner band/interstage cavity honeycomb seal.

The airfoil is cooled using 1.65%  $W_{2c}$  of 7th stage compressor bleed which passes through the fuel heat exchanger where the air temperature is reduced by 84°C (150°F). The airfoil cooling system, shown in Figure 70, consists of a hollow cast cavity allowing the impingement baffle to be inserted. Integrally cast chordwise ribs along the vane wall serve to maintain insert-to-wall distance for assuring optimum impingement cooling and to increase structural stiffness for minimizing suction side ballooning. After all the air impinges on the inner surfaces of the airfoil wall, 1%  $W_{2c}$  flows through axial TE slots for TE cooling before exit into the gas flow path. The remaining 0.65%  $W_{2c}$  flows into the inner band cavity of the inner honeycomb seal where it mixes and purges the hot flowpath gases through the interstage seal arrangement.

Ceramic Shrouds - The stages one and two shrouds, which form the outer diameter flowpath above the turbine blades as shown in Figure 69, are manufactured from advanced ceramic designs. They incorporate the advantages of ceramics relative to metallic shrouds in resisting oxidation and high velocity gas erosion.

The ceramic shroud configurations incorporate experience gained from previous General Electric ceramic work sponsored by NASA, AFAPL, and by General Electric corporate IR&D developments. The ceramic shroud consists of a strong structure backing material with a softer rub tolerant surface layer at the gas flowpath. The radial growth matching of the shroud support to the disk/blade growth is obtained by the HP turbine clearance control system.

The ceramic shrouds require no cooling, but the metallic structural hook attachments and support must be purged along the surfaces to ensure a firm clamping of the shroud. CDP air (0.40%  $W_{2c}$ ) is used to cool the stage 1 structural shroud support hooks and 7th stage compressor air (0.15%  $W_{2c}$ ) is used for the stage 2 support hooks.

Tip Clearance Control - The E<sup>3</sup> HP turbine design incorporates tip shroud control features to maintain the high turbine efficiency requirements. Present commercial turbine practices generally set the tip clearance for the power reburst operation without a rub. This practice results in excess clearance for other power settings, thereby reducing turbine efficiency.

In the E<sup>3</sup> HP turbine, seventh stage compressor air is used for the tip clearance control cooling system. At takeoff, the cooling air is bypassed, allowing slower outward tip shroud movement, thereby more closely matching and reducing the tip clearance. During the cruise condition, the air enters the casing above the turbine through flanged openings. After entering the casing, the air is enclosed within a 360° sheet metal plenum, where it impinges on the properly sized shroud support rings through an array of impingement holes in the sheet metal controlling shroud support temperature and diameter for proper clearance. After impingement, the air is routed for further cooling of the stage 2 shroud, the stage 2 HP nozzle, and the LP stage 1 nozzle.

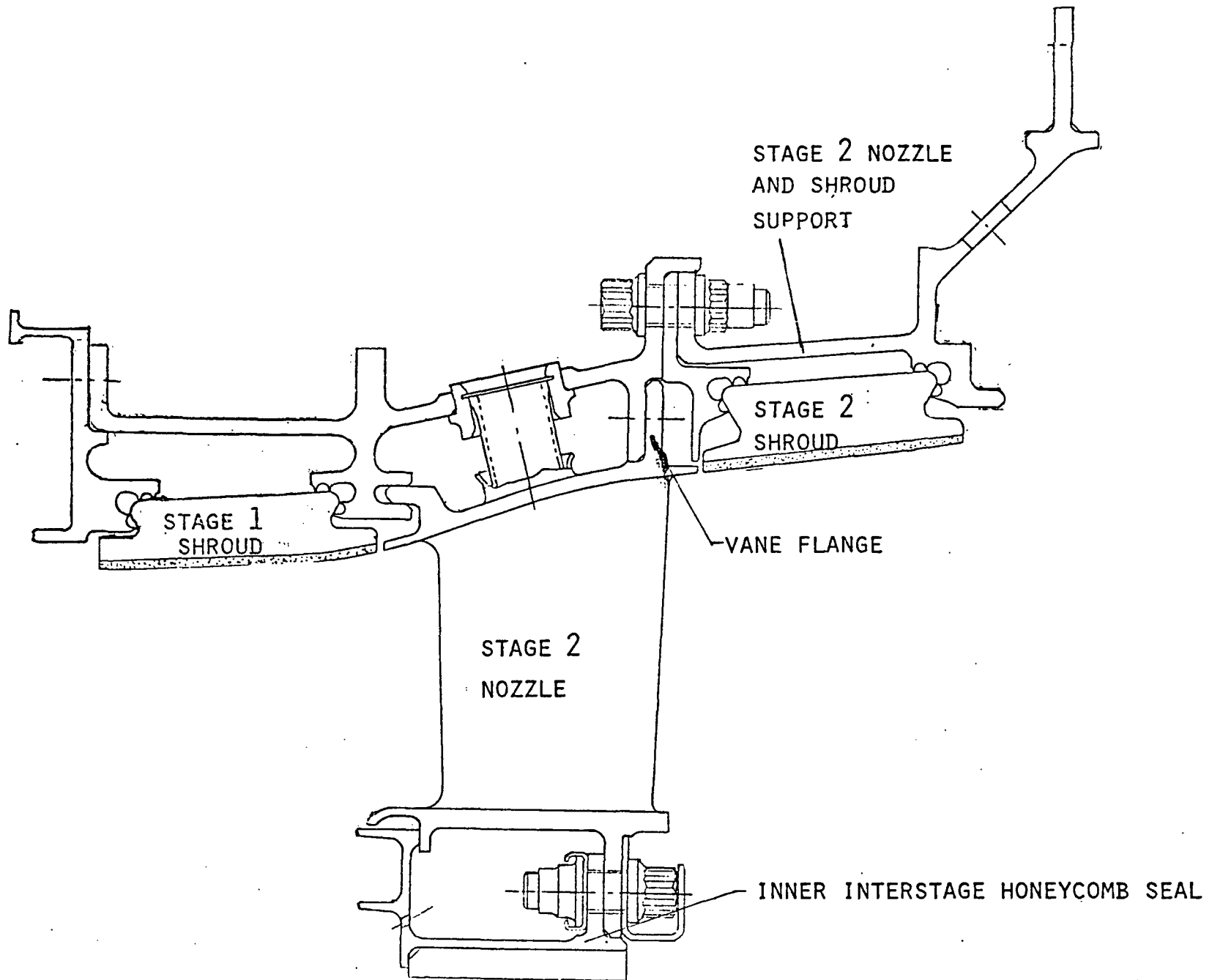
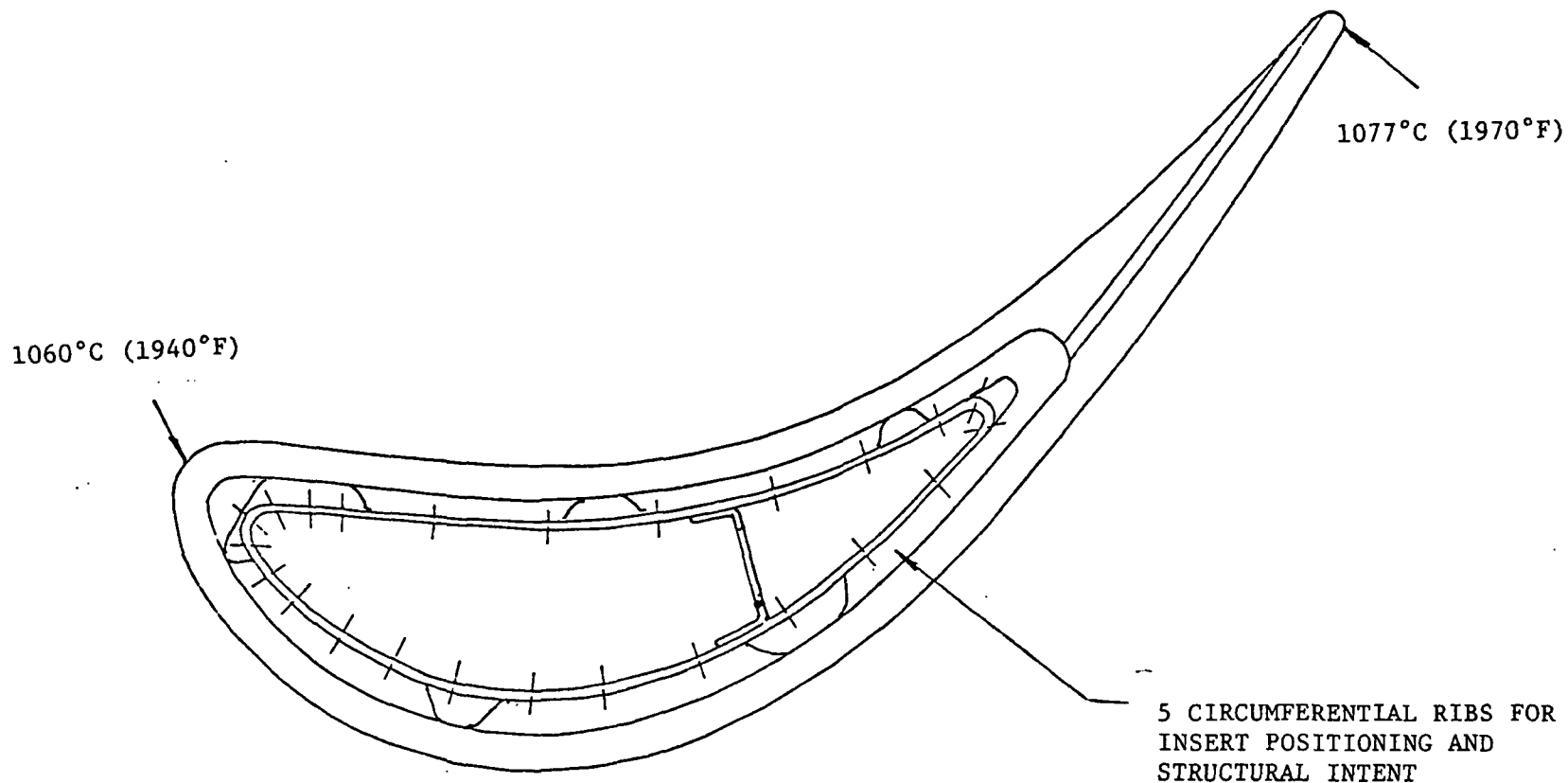


Figure 69. E<sup>3</sup> HP Turbine Stage 2 Nozzle Diaphragm Configuration.



$T_{\text{GAS}}$ (MAX PEAK)	- 1332°C (2429°F)	$N_v$	- 60
$T_3$	- 597°C (1107°F)	COOLING SOURCE	- 7th STAGE
$T_{\text{COOL}}$ (7th STAGE)	- 371°C (700°F)	(COOLED 84°C (150°F) BY FUEL-AIR HEAT EXCHANGER)	
% $W_{2C}$	- 1.65%		
$T_{\text{BULK}}$	- 927°C (1700°F)		

Figure 70. E<sup>3</sup> HP Turbine Stage 2 Vane Design.



During the critical clearance situation in which a hot rotor reburst could occur, the clearance control cooling air bypasses the high cooling mode impingement circuit, as soon as the throttle is chopped. This reduces the rate of shroud support cool down and inward shroud growth so that the turbine tip clearance grows enough to eliminate shroud to blade rubbing during a reburst.

Stage 1 Blade - Stage 1 consists of 86 blades utilizing a two tang design case from Rene' 150 material. The blade shank transition between the airfoil platform and the dovetail neck is contoured to allow the use of a vibration damper. These dampers are similar in the method of support arrangement to those in the present CF6-50 high pressure blades. The airfoil cooling concepts are based on experience gained from the commercial General Electric engines and advanced technology blade designs. The blade cooling system consists of cold bridge LE cooling, and serpentine radial passages. Two-dimensional turbulence promoters are included on the suction and pressure side surface of the serpentine passages to increase heat transfer. Total blade cooling is 3.4%  $W_{2C}$ , using CDP as the coolant source. Figure 71 shows the cooling concept and temperature data used for the blade design.

An analysis of the stage 1 blade to achieve 18,000 hours of mission-mix life requires an area ratio of root-to-tip of 1.5. The 25% span resulting bulk stress and temperature effects of mission-mix hours translate to a 615-hour life under takeoff conditions. The blade design exceeds this requirement. Pertinent blade data are listed in Table 59.

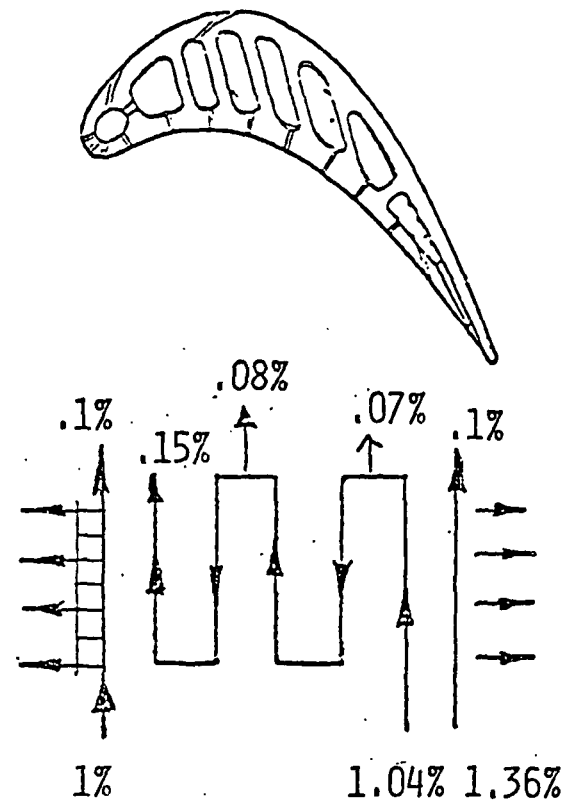
The blade loadings transmitted through the blade dovetail and to the disk post are supported by the disk structure. The dovetail stress is basically the result of the centrifugal loading and bending occurring at the 2 flank faces. The calculated dovetail stresses shown in Figure 72 are well within the design life of .2% yield material strength established as a design criteria.

Stage 2 Blade - Stage 2 consists of 90 airfoils case from Rene' 150 material. The blade design includes a two-tang dovetail similar in form to the stage 1 blade dovetail. A vibration damper is also included as in the stage 1 design.

The airfoil cooling concepts are based on experience learned from the General Electric commercial engines and also from the advanced cooling technologies in use in advanced General Electric engine programs. The blade cooling design is of a radial serpentine flow using a 2-circuit design as shown in Figure 73. Each circuit consists of a three-pass arrangement with the air entering at the bottom of the dovetail inlet and leaving at the blade tip. There are no film holes in the airfoil. Two-dimensional turbulence promoters are incorporated in the serpentine passages as in the stage 1 design.

In order to meet the 18,000 hours of mission-mix profile, the stage 2 blade area ratio is 1.75 at a bulk temperature of 889°C (1632°F) at 25% span. Table 60 shows the mechanical data in assessing and meeting the requirements. The aggregate of used-up life for the total mission hours is equivalent to 600 takeoff hours.

$T_{4.1}$ DESIGN	1467°C (2673°F)
$T_{COOL}$ D/T	577°C (1070°F)
$T_{BULK}$ PITCH/25% SPAN	954/919°C (1750/1687°F)
$T_{TB}$ DESIGN	1414°C (2577°F)
$T_3$	597°C (1107°F)
% COOLING $w_{2c}$ (CDP)	3.4
$T_{LE}$ } PITCH	1029°C (1885°F)
$T_{TE}$ }	1053°C (1928°F)



COLD BRIDGE  
 3 CIRCUIT DESIGN  
 3 ROWS OF L.E. HOLES  
 PRESSURE SIDE BLEED HOLE IN EVERY CAVITY

Figure 71. E<sup>3</sup> HP Turbine Stage 1 Blade Cooling.

TABLE 59

HIGH PRESSURE TURBINE STAGE 1 BLADE DATA

Number of Blades	86
Tip Speed, m/sec (ft/sec)	499 (1638)
Blade Weight, Kg (lbs)	0.1360 (0.30)
Centrifugal Stress (Pitch), MPa (KSi)	103.4 (15.0)
$A_R/A_T$	1.5
Equivalent Rupture hrs/Temp., °C (°F) (25% Span)	615/919 (1687)
Mission Hours (with Repair)	18,000
Material	Rene' 150
$\%W_{2C}/\text{Source}$	3.4/CDP

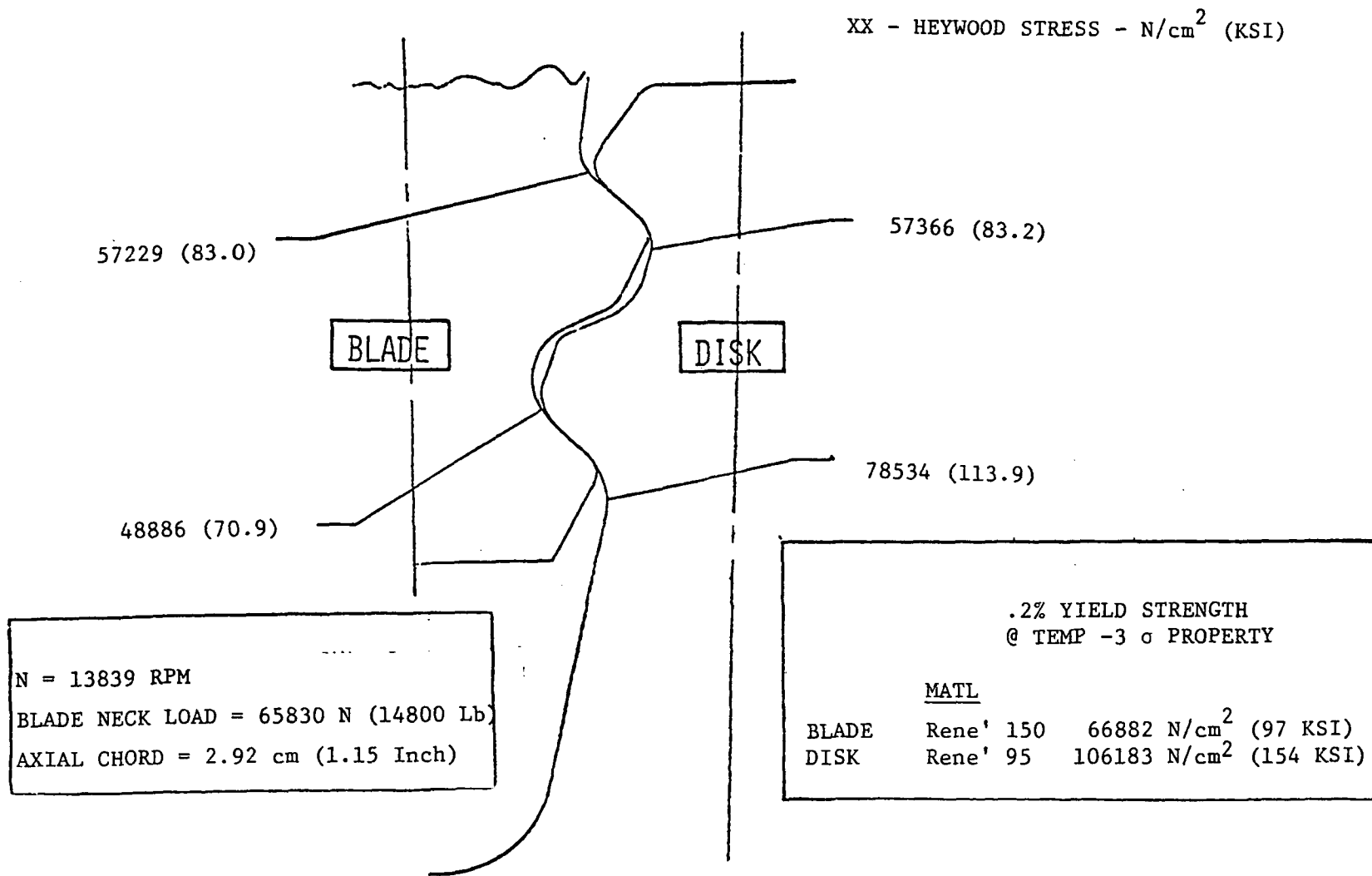
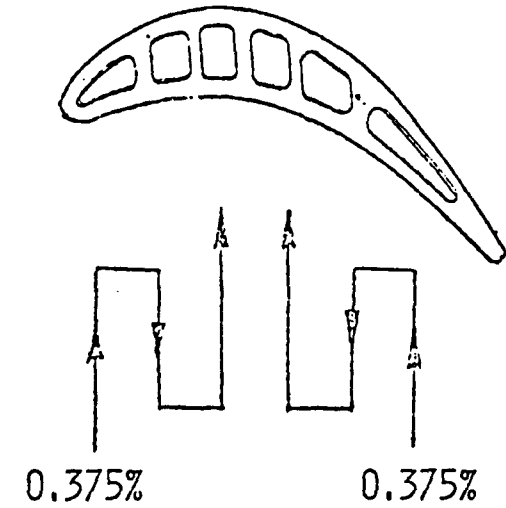


Figure 72. E<sup>3</sup> HP Turbine Stage 1 Blade and Disk Dovetail Stresses.

$T_{4.1}$ DESIGN	1467°C (2673°F)
$T_{COOL}$ @ D/T 6th STAGE	454°C (850°F)
$T_{BULK}$ PITCH/25% SPAN	927/889°C (1700/1632°F)
$T_{TB}$ DESIGN (PITCH)	1082°C (1980°F)
$T_3$	597°C (1107°F)
% COOLING $W_{2c}$ (6th STAGE)	0.75%
$T_{LE}$ } PITCH	1010°C (1850°F)
$T_{TE}$ }	1010°C (1850°F)



2 CIRCUIT DESIGN  
RADIAL PASSAGE WITH TIP EXIT

Figure 73.  $E^3$  HP Turbine Stage 2 Blade Cooling.

TABLE 60

HIGH PRESSURE TURBINE STAGE 2 BLADE DATA

Number of Blades	90
Tip Speed, m/sec (ft/sec)	520 (1705)
Blade Weight, Kg (lbs)	0.205 (0.452)
Centrifugal Stress (Pitch), MPa (KSi)	179.2 (26.0)
$A_R/A_T$	1.75
Equivalent Rupture Life hrs/Temp. °C (°F) (25% Span)	600/889 (1632)
Mission Hours (with Repair)	18,000
Material	Rene' 150
% $W_{2C}$ /Source	0.75/6th Stage

HP Rotor - The high pressure rotor is a two-stage design, rotating at a design speed of 13,500 rpm. The disks are manufactured from As HIP Rene' 95 material, and the interstage heat shield is manufactured from As HIP AF115 alloy. The impeller wheels, which are side mounted on the forward faces of each disk, are manufactured from Rene' 95 material. The power torque shaft, connecting the compressor rotor spool to the turbine, is machined from IN718. This alloy with its superior strength characteristics to 649°C (1200°F) is ideally suited for the shaft running at 482°C (900°F).

The rotor steady state stress analysis for the HP turbine is shown in Figure 74. The results are based on the steady state effects of temperatures, disk rim dead loads, and speed. A critical requirement for the disk design is its overspeed capabilities. This aspect of the disk design was investigated in the early analytical stages and complies with the requirements.

Material Selection - The selection of high temperature/high strength alloys is an important part of the HP turbine component design. The specific alloys defined in the turbine reflect an overall balanced system involving cost, weight, and life requirements/criteria.

This part of the design material selection and evaluation resulted in choosing the materials shown in Figures 75 and 76 for the stator and rotor structures.

g. LPT Rotor/Stator

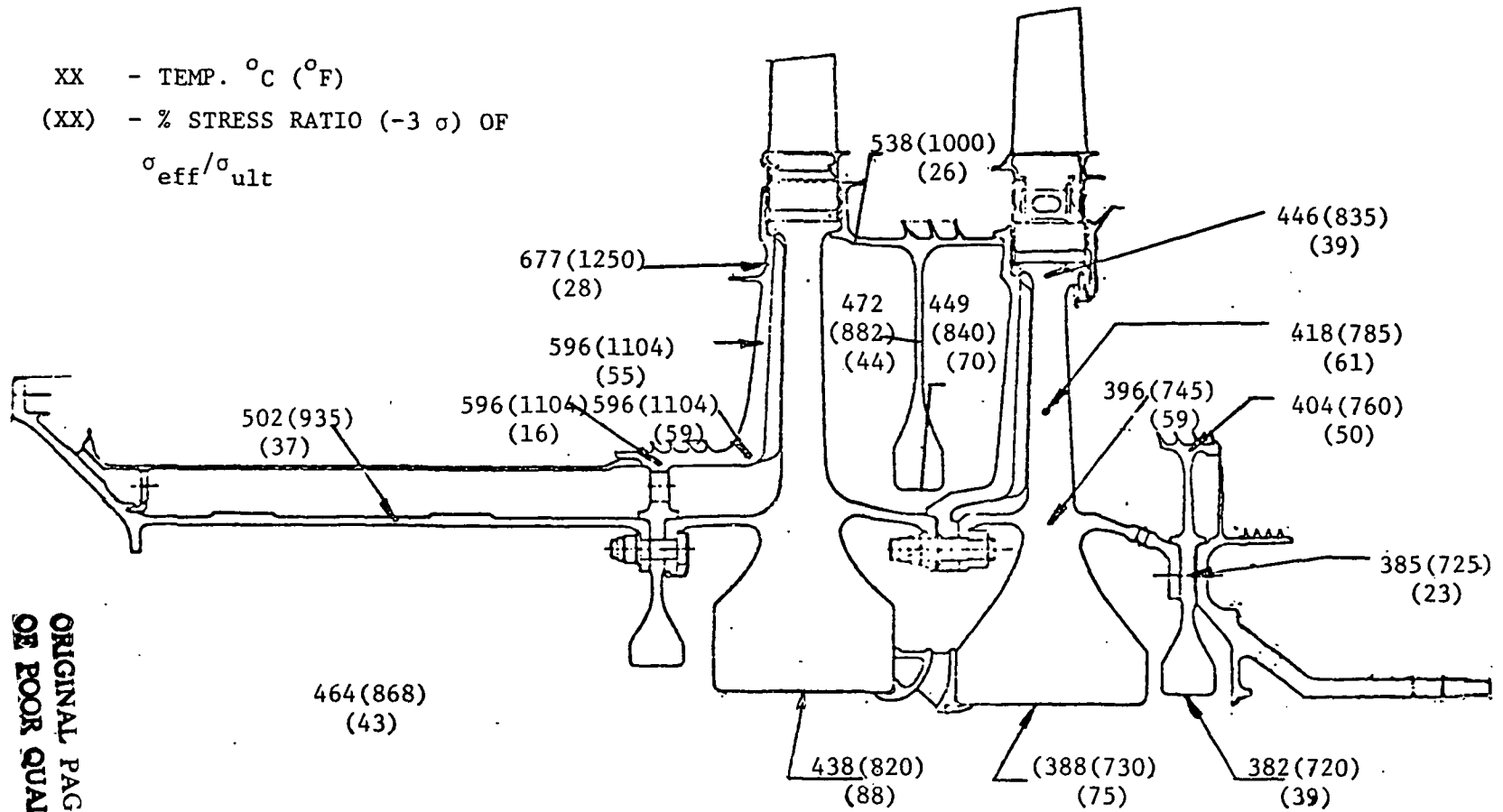
1. Description

The LPT is a highly loaded, close coupled 5-stage turbine with a short transition duct, as shown in Figure 77, and with all airfoils uncooled. The LPT casing is a continuous 360 degree design with local impingement cooling for improved clearance control. The stage 1 nozzle is a 2-vane segment attached by a hook tang and bolted design at the outer flowpath. The bands are brazed to the cast vanes and extend forward forming the transition duct. Stages 2-5 nozzles vanes are cast multi-vane segments attached by hook tang attachments to the outer case supports. Outer honeycomb seals (open cell) are brazed to sheet metal backing strips that hook into the outer casing and help retain the stage 2-5 nozzles. The inner honeycomb seals (also open cell) are bolted to the vane segments. Material selections for the LPT static parts are as follows:

Vane 1	Rene' 150 (MAR-M-509 Bands)
Vane 2	Rene' 80
Vane 3	Rene' 80
Vanes 4, 5	Rene' 77
Casing	Inconel 718
Seals	Hastelloy X
Bolts	Waspalloy
Nuts	Waspalloy

The LPT rotor is an uncooled design comprised of disks with integral spacer arms and bolted joints between each stage. Blading is a typical LPT cast design with tip shrouds and multi-tang dovetails as shown in Figure 78.

XX - TEMP. °C (°F)  
 (XX) - % STRESS RATIO (-3 σ) OF  
 $\sigma_{eff}/\sigma_{ult}$



ORIGINAL PAGE IS  
 OF POOR QUALITY

Figure 74. E<sup>3</sup> HP Turbine Steady State Temperatures and Stress Ratio.



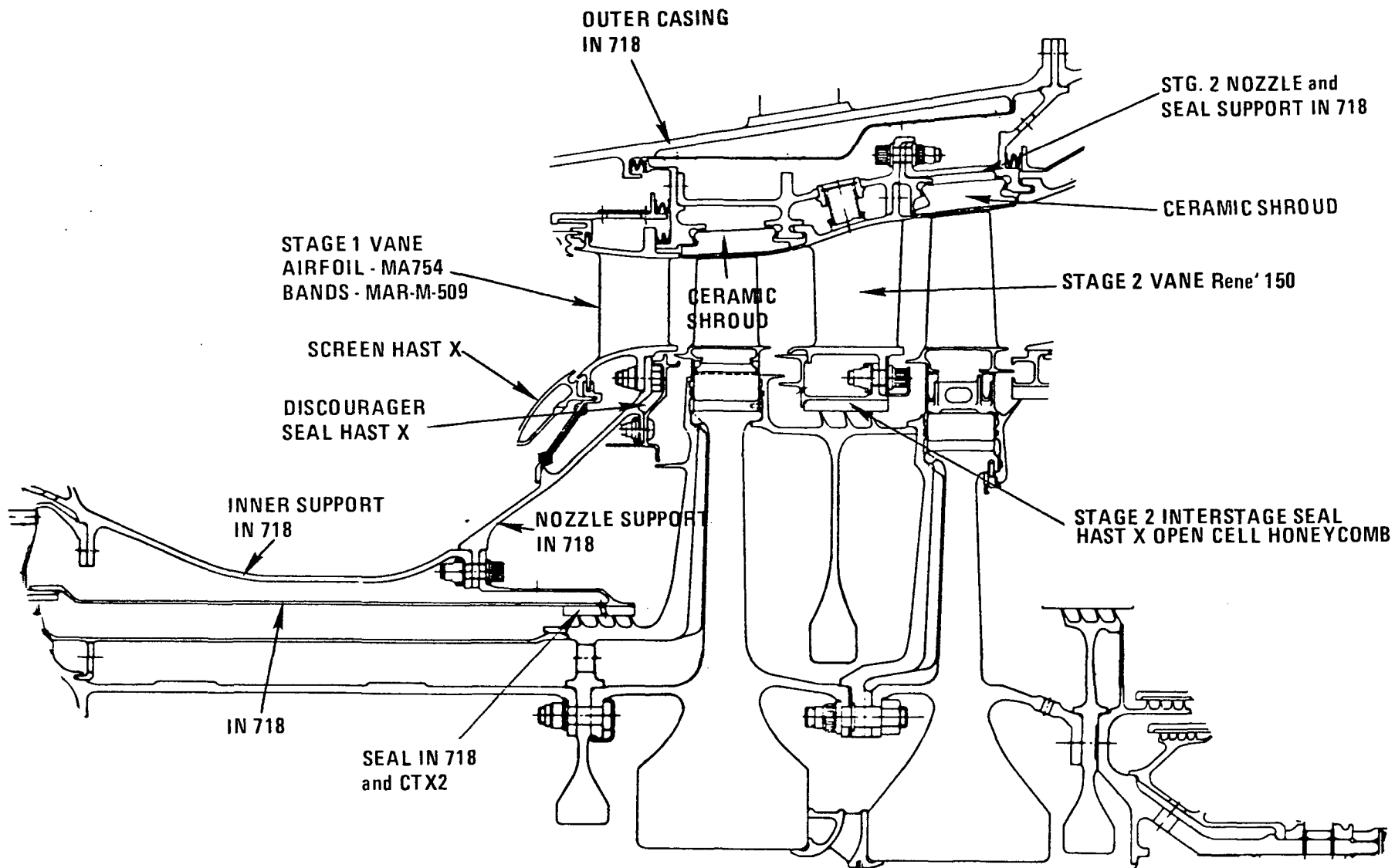
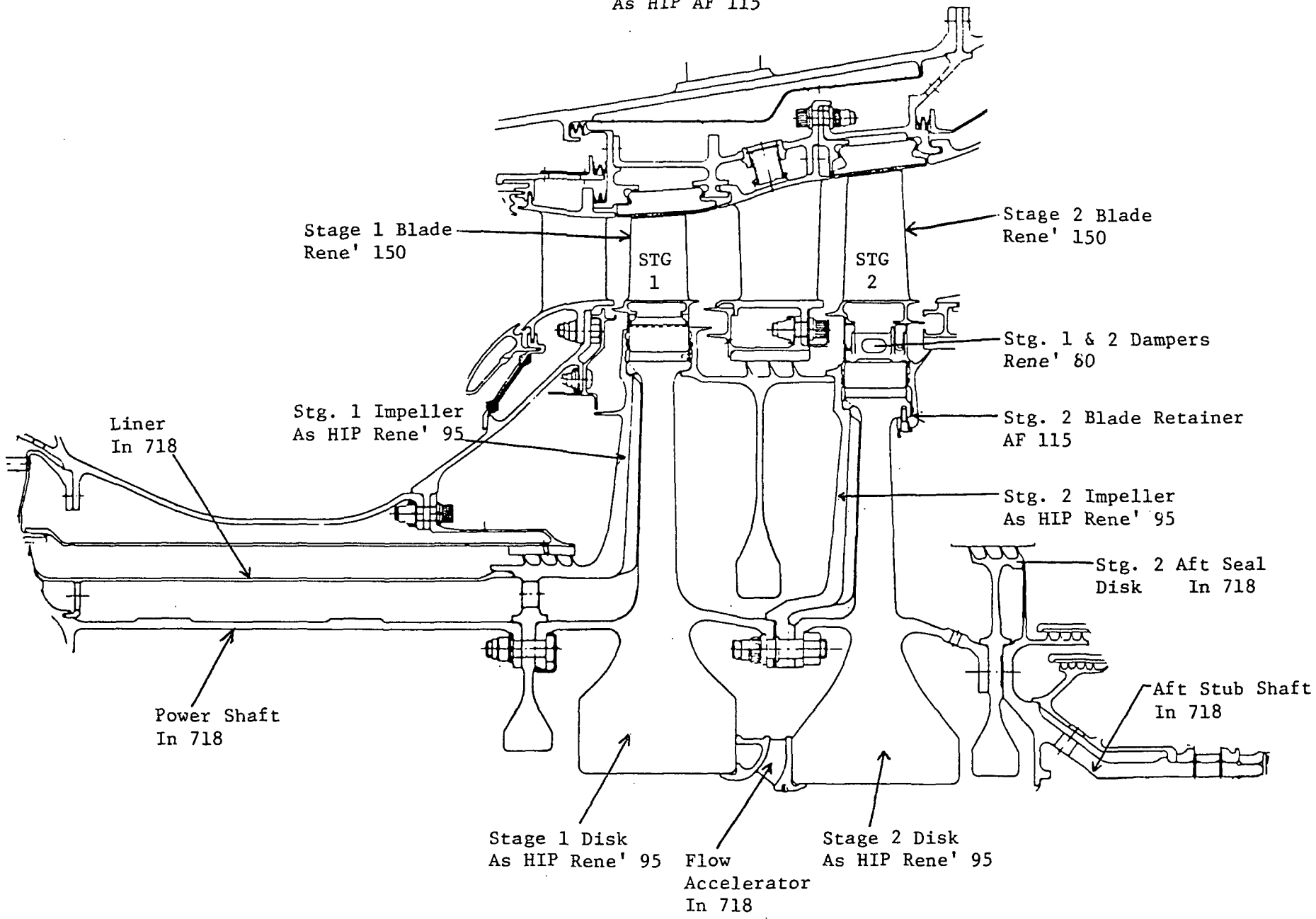


Figure 75. E<sup>3</sup> HP Turbine, Material Selection Static System

INTERSTAGE  
HEAT SHIELD  
As HIP AF 115



201

Figure 76. E<sup>3</sup> HP Turbine Material Selection Rotating System

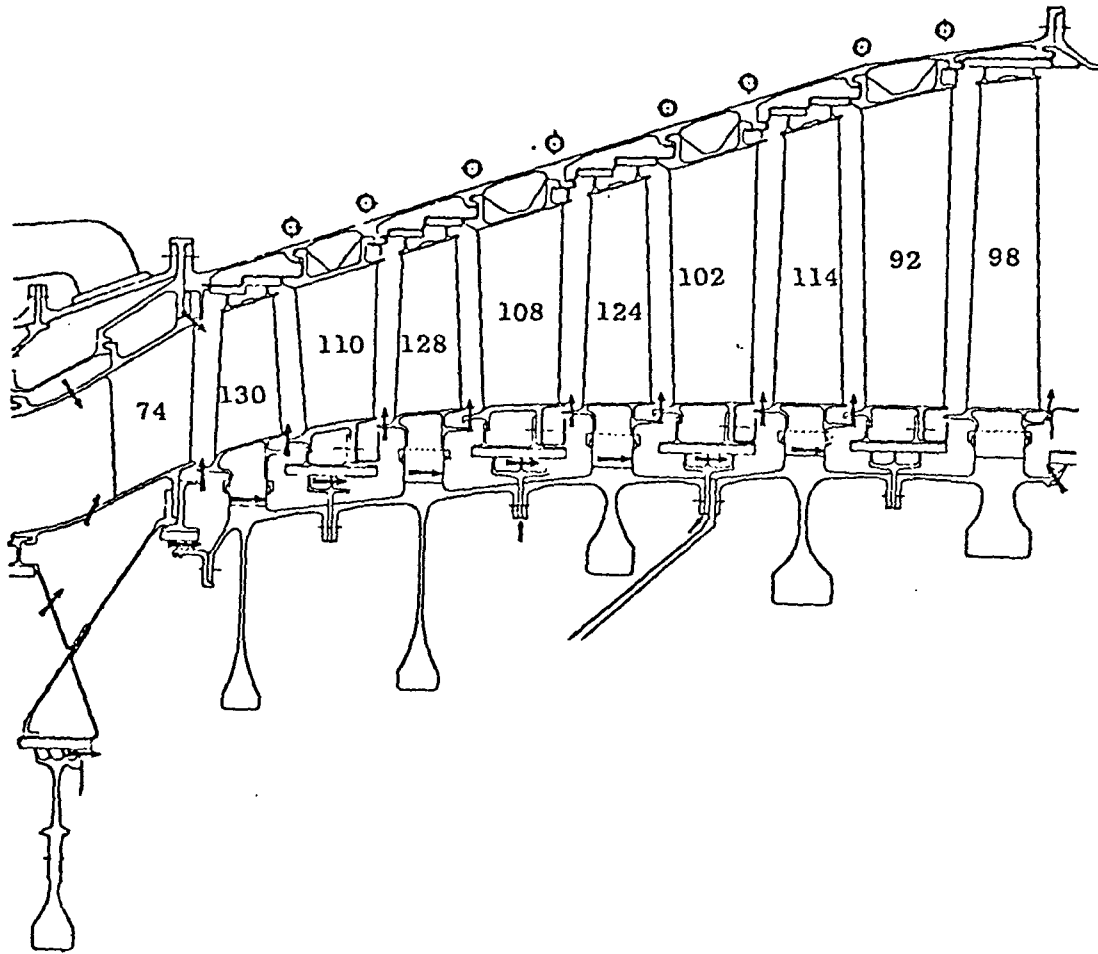


Figure 77. Low Pressure Turbine Flowpath and Airfoil Count.

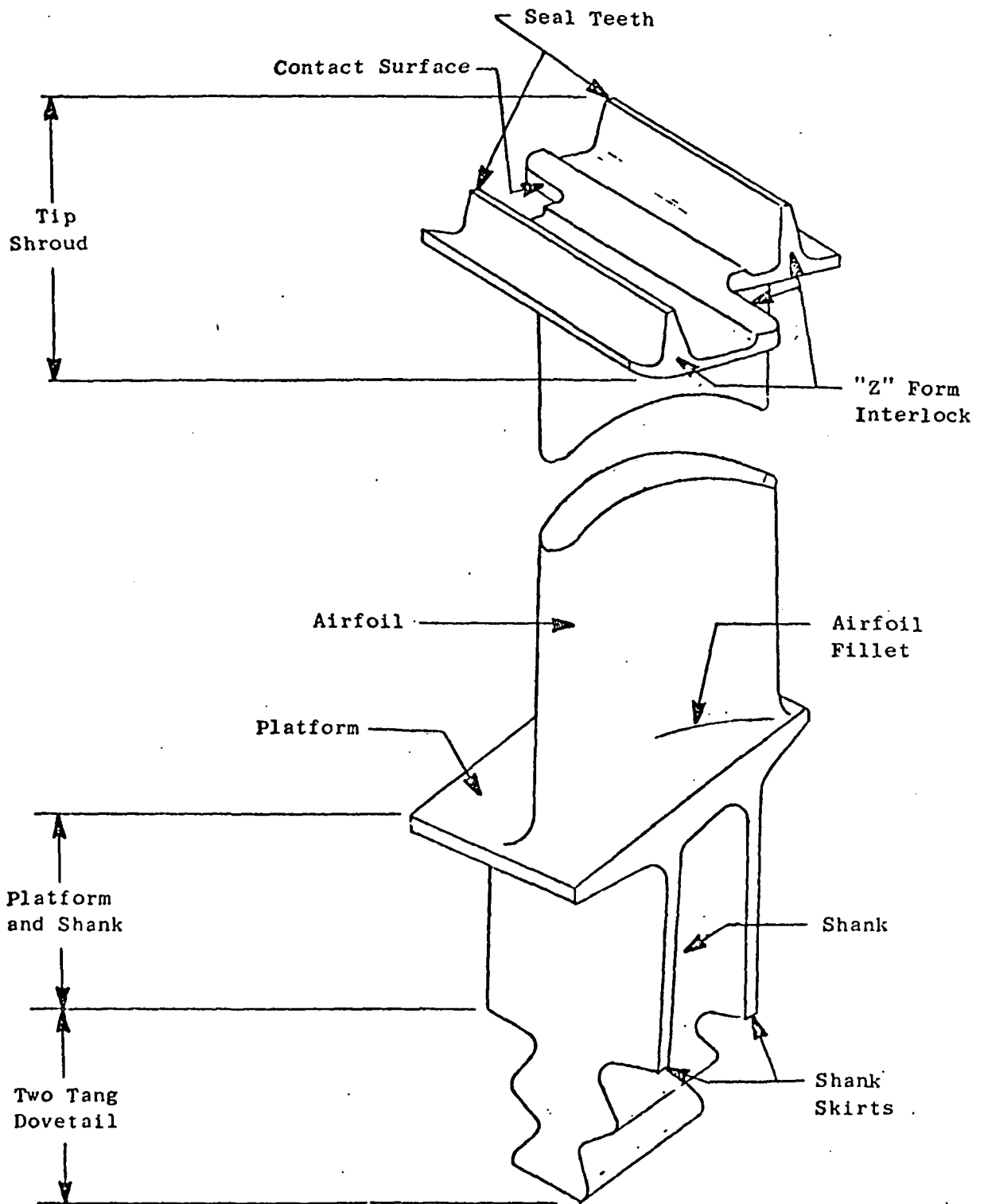


Figure 78. LPT Blade Nomenclature.

Inner stage seals of the LPT spool are a 3-tooth replacement design and are attached at the bolted flange joints between the disk spacer connection.

The rotor materials selected are as follows:

Blade 1	Rene' 150
Blade 2	Rene' 125
Blades 3, 4, and 5	Rene' 77
Disks 1-5	Inconel 718
Blade Retainers	Inconel 718
Nuts and Bolts	Inconel 718

Overall, the LPT configuration selected is a balanced design with strong emphasis on high efficiency and performance.

The LP turbine has incorporated features that provide maximum performance while retaining good maintainability and low cost. All airfoils have incorporated extended platform overlaps at the inner flowpath to give smoother gas flow, and thus improved turbine efficiency. These overlaps can be maximized since the turbine is a stacked rotor design utilizing a full 360° casing. This casing design eliminated the bolted flange of a horizontally split casing allowing: 1) reduced out-of-roundness from flange discontinuities, 2) ease of manufacture and lower cost, and 3) comparable ease of assembly and overhaul compared to a horizontally split casing.

The LPT blades all have tip shrouds and two-tang dovetails. In addition, all stages have shank "skirts" to prevent leakage across the stage and to provide a smooth wheel face for low windage losses.

The tip shroud is essential to high aspect ratio (length over chord) blading to prevent high vibratory stress. There are two labyrinth seal teeth on each tip shroud for leakage control across the tip of the stage. The pitch between these teeth is such that the wear tracks in the opposing stator shroud will not overlap to cause excessive leakage.

The LPT disks feature integral spacer arms for increased disk reliability, by placing the bolted flanges at the extremities of the spacer arms, the stress concentration effects of holes are removed from the disk. All the LPT disks are made of IN'718.

The LPT casing is not only the main structural member of the turbine stator but also is a prime engine structure since the main engine mount is aft of the turbine on the turbine rear frame. Casing cooling is provided by radiation to the external cowl and by an external impingement cooling manifold system. This manifold is also utilized to control the radial clearance of shrouds and inner seals. This system consists of 9.5 mm (0.375 in) diameter tubing formed in rings above each vane hanger support. The tubing is connected to a header which is fed by cool fan air. This manifold system is shown schematically in Figure 79.

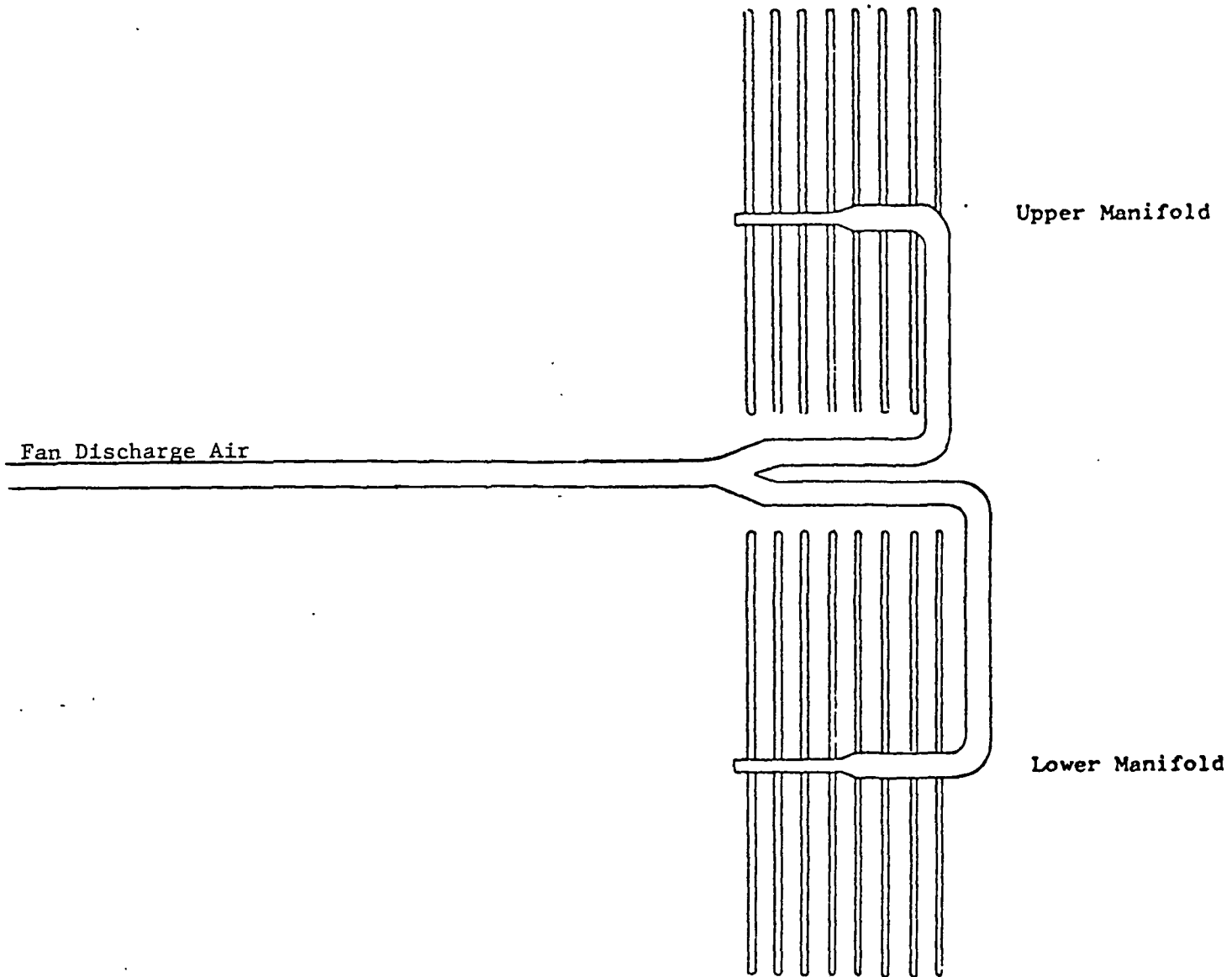


Figure 79. LPT Casing Cooling Manifold System.

The vanes are fabricated by manufacturing techniques matched to the materials required. The stage 1 nozzle segments consist of 2 Rene'150 airfoils brazed to inner and outer bands of MAR-M-509. All other stages are cast with band and vanes integral in segments, with the number of vanes per segment depending on the particular stage area design. At the present time there will be 5 vanes per segment in stage 2, 6 vanes per segment in stages 3 and 4, 4 vanes per segment in stage 5.

Cooling flows in the LPT are primarily purge type cooling. A schematic of these cooling flows is shown in Figure 77.

This figure shows 7th stage air utilized for vane 1 cooling and then being fed into the flowpath. Fan air is used to impinge on the casing and then is bled aft into the fan stream exhaust. Additional purge air is obtained from the 6th stage source as it is fed to the stage two HPT rotor cavity. This purge air is allowed to pass through local reliefs in the aft HPT stub shaft. One portion of this air proceeds radially outward purging the aft HPT stage 2 rotor cavity. Leakage of the purge air through the lower LPT seal is used to provide rim cooling for disk stages 1, 2, 3, and 4 as shown.

The LP turbine design utilizes many of the maintenance features proven through extensive CF6 experience. Also incorporated are new features that offer improved maintenance.

Since seals are so critical to the LPT performance, they have been designed to be easily replaced at periodic maintenance intervals during which the LP turbine is disassembled. All other rotor interstage seals are also separate parts which are bolted between adjacent disks.

Rubbing elements of the seals are all fabricated open cell honeycomb in order to keep seal tooth areas low while still maintaining low leakage. These honeycomb elements are segmented and easily replaced without rework of the adjacent supporting members (casing on the outside, vanes on the inside).

The casing attachment points for the vanes tend to become worn after extended engine operation. To avoid permanent casing damage and scrapping of the part, additional material is designed into these attachment areas which can be reworked during overhaul to provide fully acceptable geometry for vane attachment at low repair cost.

Blade Stresses/Life - All blades are solid uncooled designs but operate at relatively low tip speeds <229 m/sec (<750 fps) and moderate temperatures <900°F (<1650°F). Because of these conditions, large airfoil taper ratios are not required to keep blade stresses within allowables, and a tip to hub area ratio of 0.9 is used on all stages. Calculations of airfoil stress at the critical 25% span is shown in Table 61 along with calculated life capabilities. As seen, each blade exceeds the life requirements in all areas of concern (rupture, LCF, and HCF).

Dovetails - Dovetail forms have been selected from present engine designs that have operated successfully. Preliminary dovetail stresses and life calculations (LCF and rupture) have been made for all stages. These are shown in Table 62 and show that all dovetails satisfy the design life goals.

TABLE 61

CFX/E<sup>3</sup> LP TURBINE BLADES STRESS/LIFE

Stage	Blade Material	T <sub>Bulk</sub> (°F) (25% Span)	°C (25% Span)	MPa σ (KSI) (25% Span) σ Centrifugal	Design Capability Rupture Life (Hrs.)*	LCF (Cycles)* (Initiation)	HCF* (σ <sub>Vib</sub> , Mpa(KSI))
1	R'150	877(1611)		53.8 (7.8)	46,000	> 30,000	> 276 (40)
2	R'125	800(1472)		71.0(10.3)	> 30,000	> 30,000	> 276 (40)
3	R'80	732(1349)		87.6(12.7)	> 30,000	> 30,000	> 276 (40)
4	R'80	673(1243)		114.(16.6)	> 30,000	> 30,000	> 276 (40)
5	R'80	622(1152)		140.(20.3)	> 30,000	> 30,000	> 276 (40)

\* [ 27,000  
Hrs. Req'd.  
(with repair) ]

\* [ 27,000  
Cycles Req'd.  
(with repair) ]

\* [ 138 MPa  
(20 KSI)  
Req'd. ]



TABLE 62

DOVETAIL STRESS AND LIFE

Stage	Centrifugal Load N (lbs)	Gas Load		Max. Combined Stress		Blade DT Life		Disk DT Life	
		Tangential N (lbs)	Axial N (lbs)	Blade MPa(ksi)	Disk MPa(ksi)	LCF (Cycles)	Rupture (Hours)	LCF (Cycles)	Rupture (Hours)
1	7112 (1599)	598 (134.4)	215 (48.4)	400 (58.0)	321 (46.6)	> 10 <sup>5</sup>	> 10 <sup>5</sup>	> 10 <sup>5</sup>	15,000
2	8136 (1939)	699 (157.2)	236 (53.1)	298 (43.3)	312 (45.3)	> 10 <sup>5</sup>	> 10 <sup>5</sup>	> 10 <sup>5</sup>	18,000
3	10973 (2467)	738 (165.9)	210 (47.4)	353 (51.2)	304 (44.1)	> 10 <sup>5</sup>	> 10 <sup>5</sup>	> 10 <sup>5</sup>	20,000
4	13825 (3108)	705 (158.5)	280 (63.0)	363 (52.6)	301 (43.7)	> 10 <sup>5</sup>	> 10 <sup>5</sup>	> 10 <sup>5</sup>	20,000
5	18287 (4111)	647 (145.5)	264 (59.4)	348 (50.5)	258 (37.4)	> 10 <sup>5</sup>	> 10 <sup>5</sup>	> 10 <sup>5</sup>	40,000

Disks - Preliminary disk stress analyses have been conducted on all 5 stages of disks. The design point operating condition considered is the worst hot day takeoff case where centrifugal stress is at a maximum and material allowable strength is at a minimum. The complete design description for the stage 1 disk (stress, temperature distributions as well as disk thickness variation) at the design point is shown in Figure 80. Critical stress points for each disk are presented in Table 63 which shows that all disks are acceptable. A verification of disk overspeed acceptability was made by calculating stress distribution at 122% of maximum operating speed. The resulting average tangential stress values are acceptably low in comparison with the material ultimate strength as shown in Table 63.

Vanes - The stage 1 vane and seal support system is the most highly loaded LPT static component. Two areas are of prime interest; the airfoil and the attachments. Both areas are loaded due to aerodynamic forces acting on the airfoil and acting across the lower seal support. Design goals for the vane are to achieve temperatures no hotter than 907°C (1665°F) at a maximum local stress of 138 MPa (20 KSI) with a structure of Rene'150 in order to assure a full rupture resistant life of 9,000 hours and 9,000 cycles before repair. Design calculations indicate that this life can be achieved.

Vanes for stages 2-5 are loaded much less and operate in cooler gas stream temperatures than stage 1. As a result, they will be stressed below 69 MPa (10 KSI), operate below 900°C (1650°F), and have greater than required life.

Casing - The casing thickness is compatible with blade containment requirements and other less severe requirements, such as axial loading. As shown in Figure 81, the minimum casing wall thickness is adequate to contain the energy available on the basis of a single blade airfoil failed above the platform.

Material Selection - Stator and rotor materials are listed on page 214. The high confidence in the LPT materials is based largely on the wealth of excellent operating experience from the nickel alloys of the CF6 and other successful General Electric turbines. The Rene' series of advanced nickel alloys for blades and vanes has been developed by General Electric specifically to meet the needs of advanced aircraft turbines operating in the extreme environment of high temperatures for long times. Shroud materials of nickel alloy honeycomb (open cell) were chosen for their long life, low wear and good sealing characteristics.

The rotor structure is based extensively on Inconel 718 which has proven to serve well in other General Electric engines as the most economical high strength forged alloy in the moderate temperature range.

#### h. Rear Exhaust Frame and Mixer

##### 1. Description

The turbine frame assembly consists of an outer structural ring connected to an inner ring or hub by eight semitangential struts as shown in Figure 82. Rigid support of the rear-bearing sump is provided by a sump-support structure which is integral with the hub. The turbine frame is made of Inconel 718 for its high strength and easy formability.

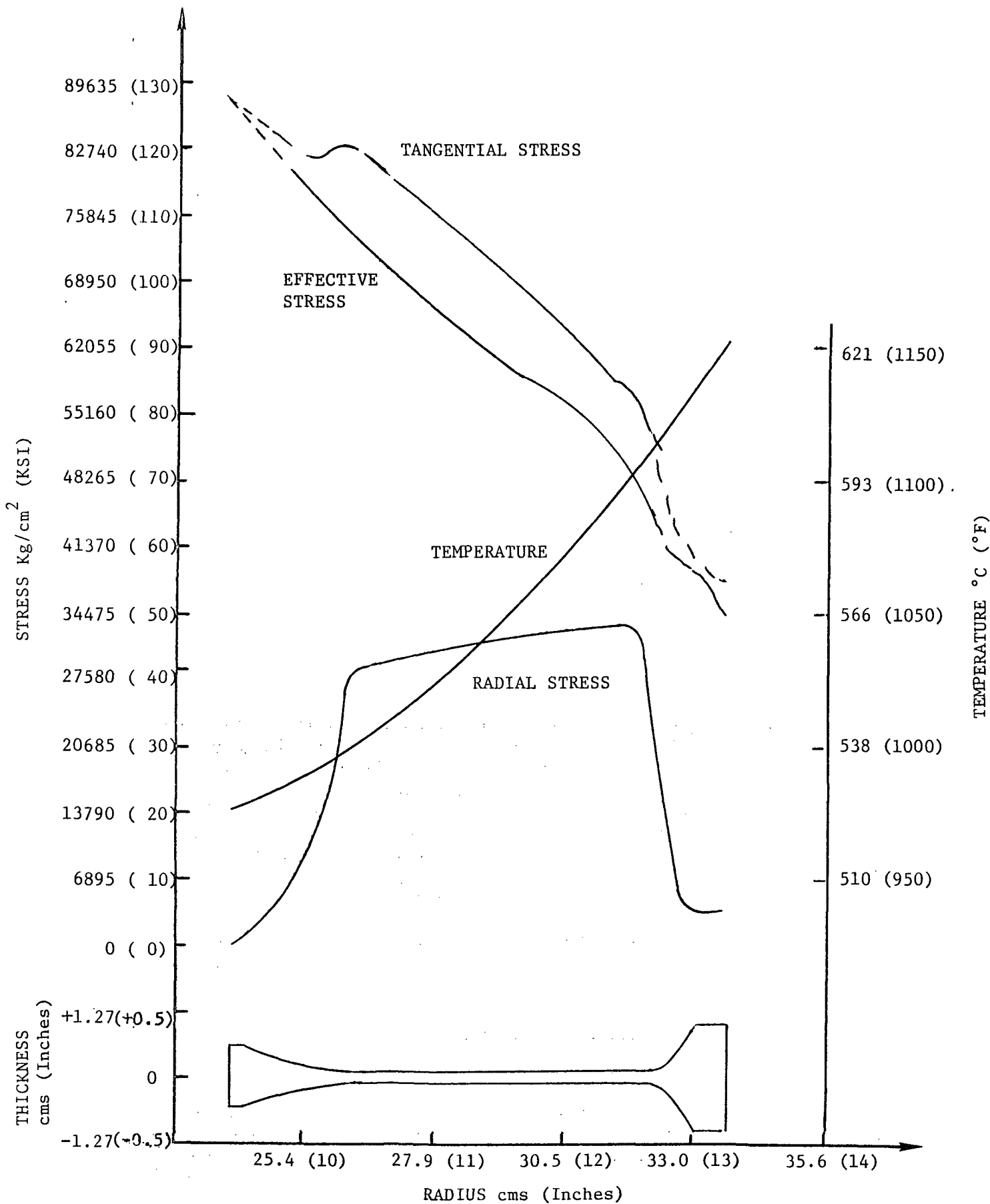


Figure 80. Temperature and Stresses -  $E^3$  Stage 1 LPT Disk at 4057 RPM (104% Growth Speed)

TABLE 63

LPT DISK STEADY STATE STRESS AT GROWTH ENGINE SPEEDS

<u>Criteria</u>	<u>Stages</u>	<u>MPa</u>				
		<u>Stress (PSI)</u>				
		<u>1</u>	<u>2</u>	<u>3</u>	<u>4</u>	<u>5</u>
<u>Bore Stress @ 104% N<sub>GR</sub></u>						
Calculated		879.1 (127,500)	889.4 (129,000)	775.7 (112,500)	882.5 (128,000)	861.8 (125,000)
0.2% Yield		410.1 (132,000)	910.1 (132,000)	896.3 (130,000)	923.9 (134,000)	910.1 (132,000)
<u>Maximum Rim - Effective</u>						
<u>Stress @ 104% N<sub>GA</sub></u>						
Calculated		365.4 (53,000)	417.1 (60,500)	448.2 (65,000)	193.1 (28,000)	444.7 (64,500)
0.02% Yield		737.7 (107,000)	744.6 (108,000)	737.7 (107,000)	723.9 (105,000)	744.6 (108,000)
<u>Average Tangential</u>						
<u>Stress @ 122% N<sub>GR</sub></u>						
Calculated		896.3 (130,000)	841.2 (122,000)	868.7 (126,000)	820.5 (119,000)	875.6 (127,000)
90% UTS		903.2 (131,000)	910.1 (132,000)	903.2 (131,000)	896.3 (130,000)	910.1 (132,000)

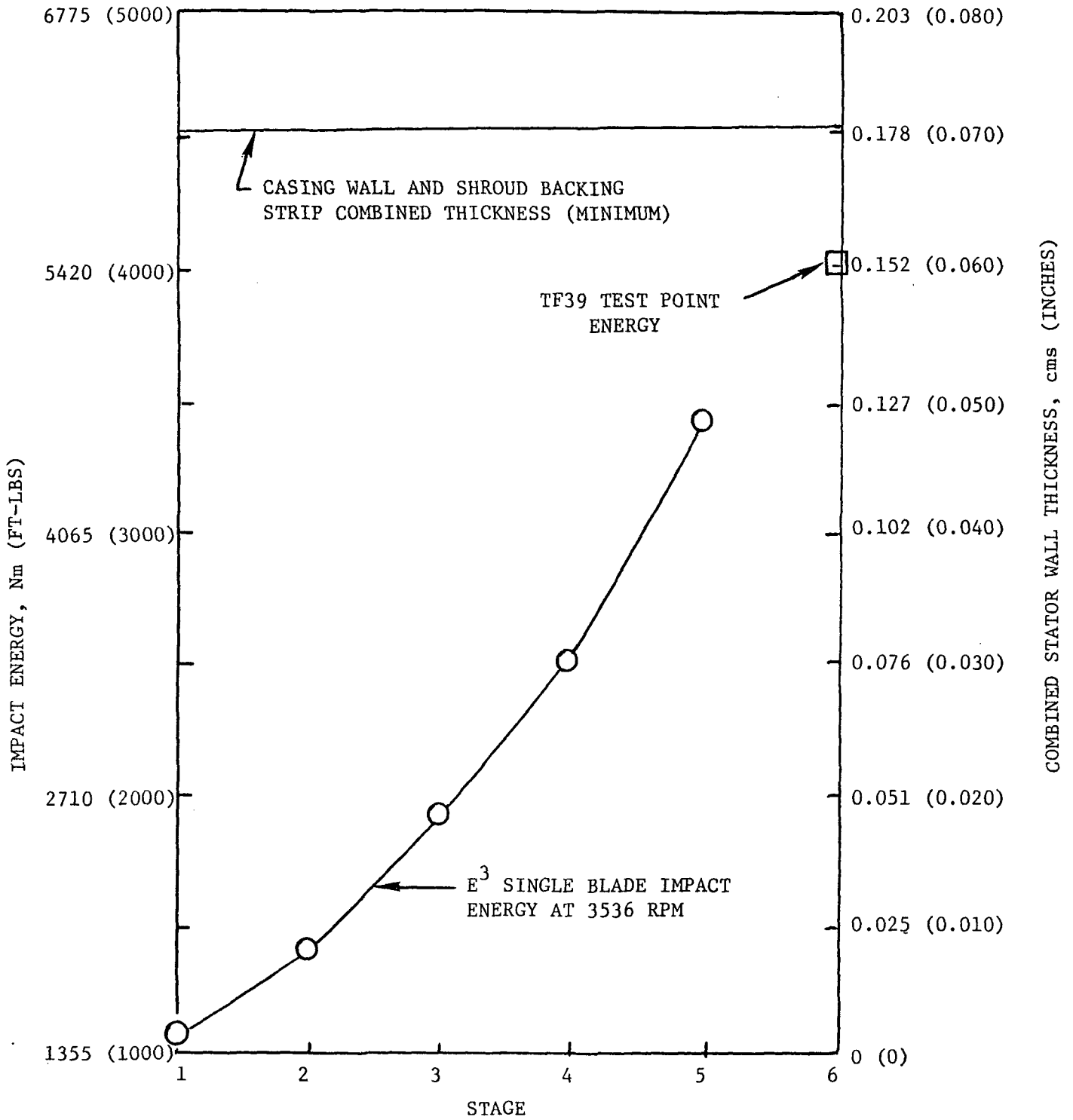


Figure 81. LPT Containment Capability - Wall Thickness and Energy Comparison

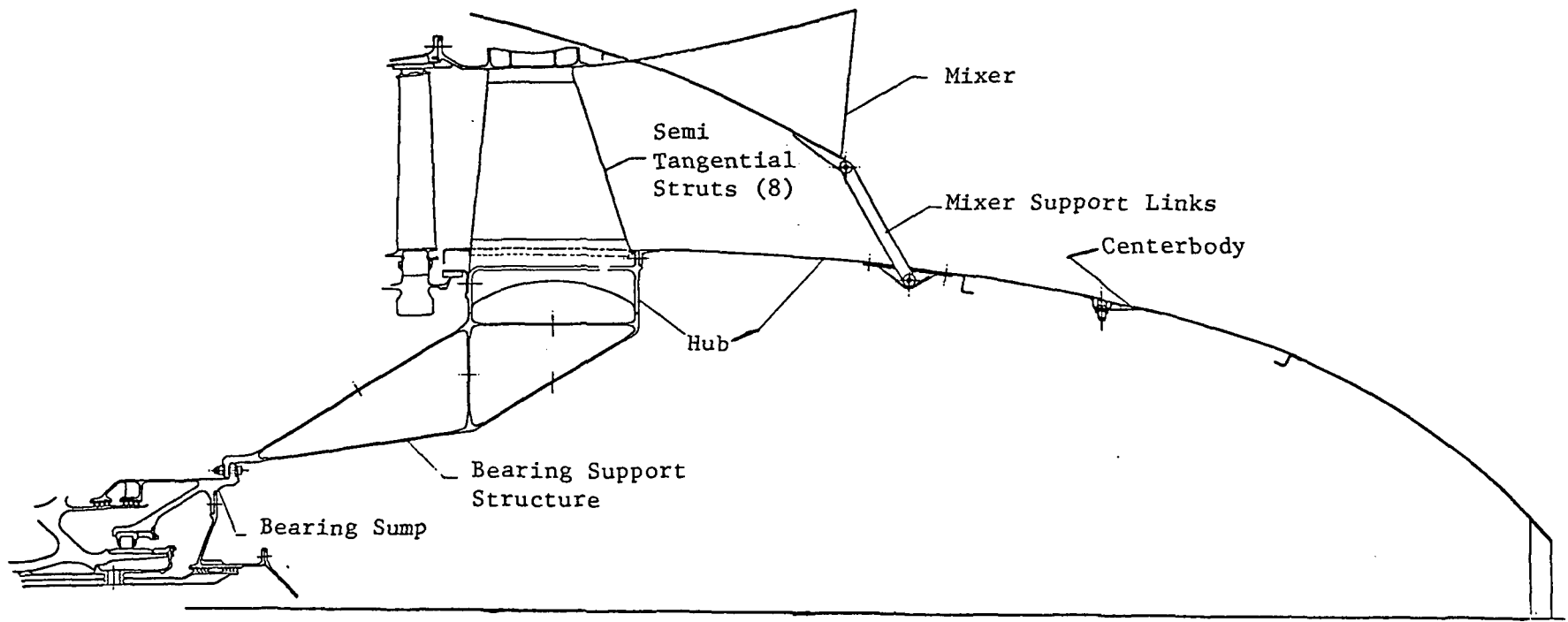


Figure 82. Turbine Frame, Mixer, and Centerbody.

The mixer consists of 24 die-formed chutes butt-welded together and then welded to the turbine frame as shown in Figure 82 and 83. The mixer is supported at the aft end by links which attach the inner lobe of each chute to the ring stiffened centerbody. The mixer and centerbody are made of Inco 625 material.

## 2. Preliminary Design Procedure

Preliminary frame stiffness values were obtained with the use of a time-sharing computer program for stress analysis of planar structures, ASIST. The outer ring, struts and hub were modeled for the frame. Two cases were run for the frame: 1) in-plane case (radial load imposed in plane of struts), and 2) out of plane case (overturning moment imposed at hub). For an assumed nominal radial load at the hub of 22.2 KN (5000 lbs) elastic deflections were determined. These deflections provided the contribution of the outer ring, struts, and hub to the overall frame spring constant. Three other items considered which contribute to the overall stiffness are: the support cone stiffness, support cone inner flange flexibility, and hub ring deformation. Since the ASIST program is limited to planar structures, the deflections of the aforementioned items were hand calculated using classical elastic theory. The contribution to the radial deflection at the bearing due to each item considered is shown in the table below. Also shown are the radial and overturning moment stiffness values for the frame.

<u>Item Considered</u>	<u>Radial Bearing Deflection mm (In)</u>	
Outer Ring Struts, Hub (Radial)	0.25	(0.00985)
Outer Ring, Struts, Hub (Overturning Moment)	0.15	(0.00594)
Support Cone Stiffness	0.015	(0.00058)
Hub Ring Deformation	0.085	(0.00337)
Sump Flange Flexibility	0.080	(0.00317)
<u>Spring Constants</u>		
Radial	38.1 MN/m	(2.18 x 10 <sup>5</sup> lb/in)
Overturning Moment	7.16 $\frac{\text{MNm}}{\text{rad}}$	(6.34 x 10 <sup>7</sup> $\frac{\text{in lb}}{\text{rad}}$ )

Of major concern in this design is the large axial offset between the rear-bearing and the frame. A large overturning moment spring constant is required in order to minimize the bearing deflection relative to the turbine frame.

Figure 84 shows the resulting preliminary design of the turbine frame. Major sources of structural deflection are given in percentage of the total radial deflection at the bearing. The temperatures used for this preliminary design study are also shown. The hot day, takeoff cycle point was used for the gas temperature. The metal temperatures were estimated based on previous experience in CF6 engines.

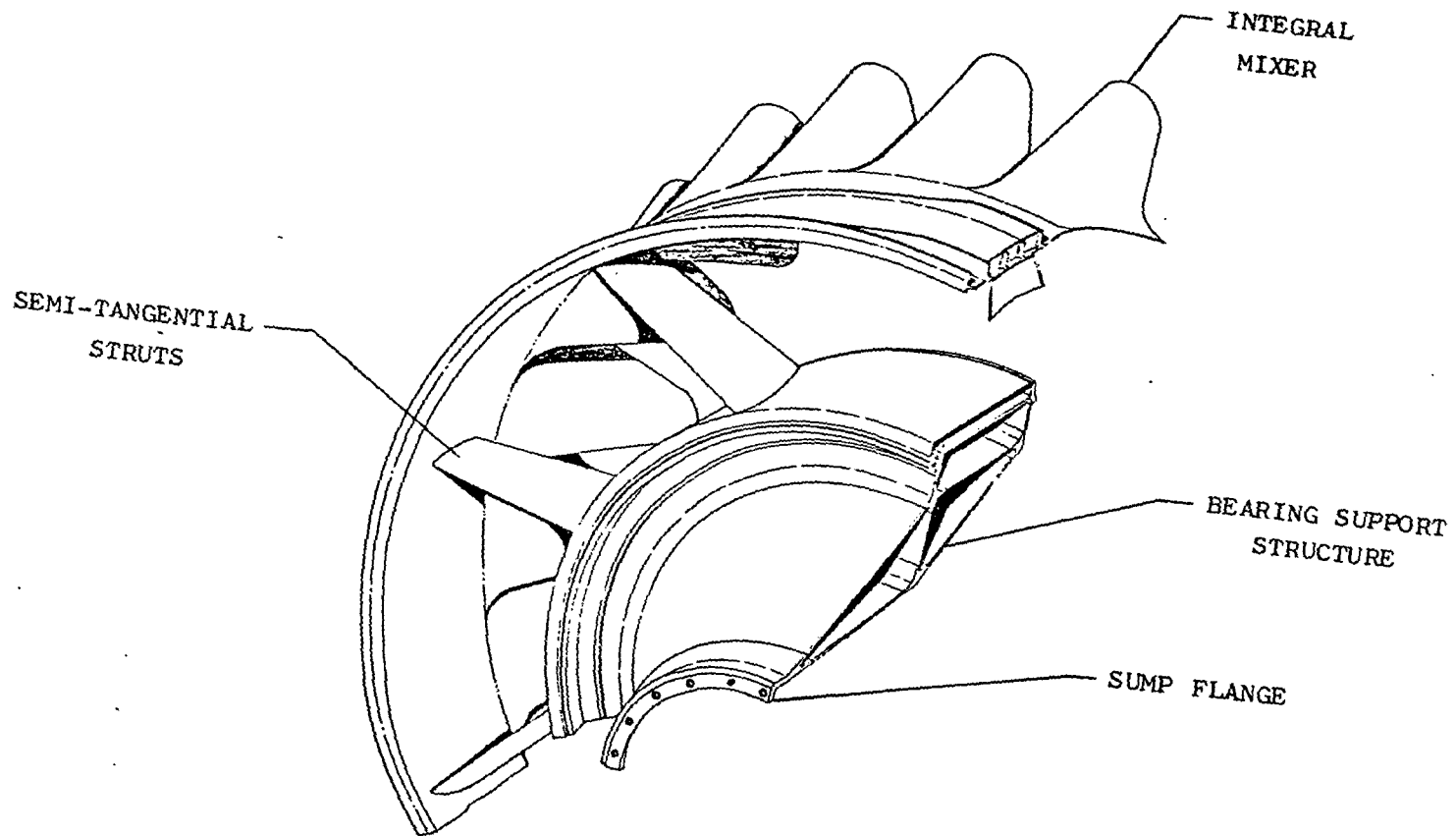


Figure 83. Turbine Frame and Mixer.



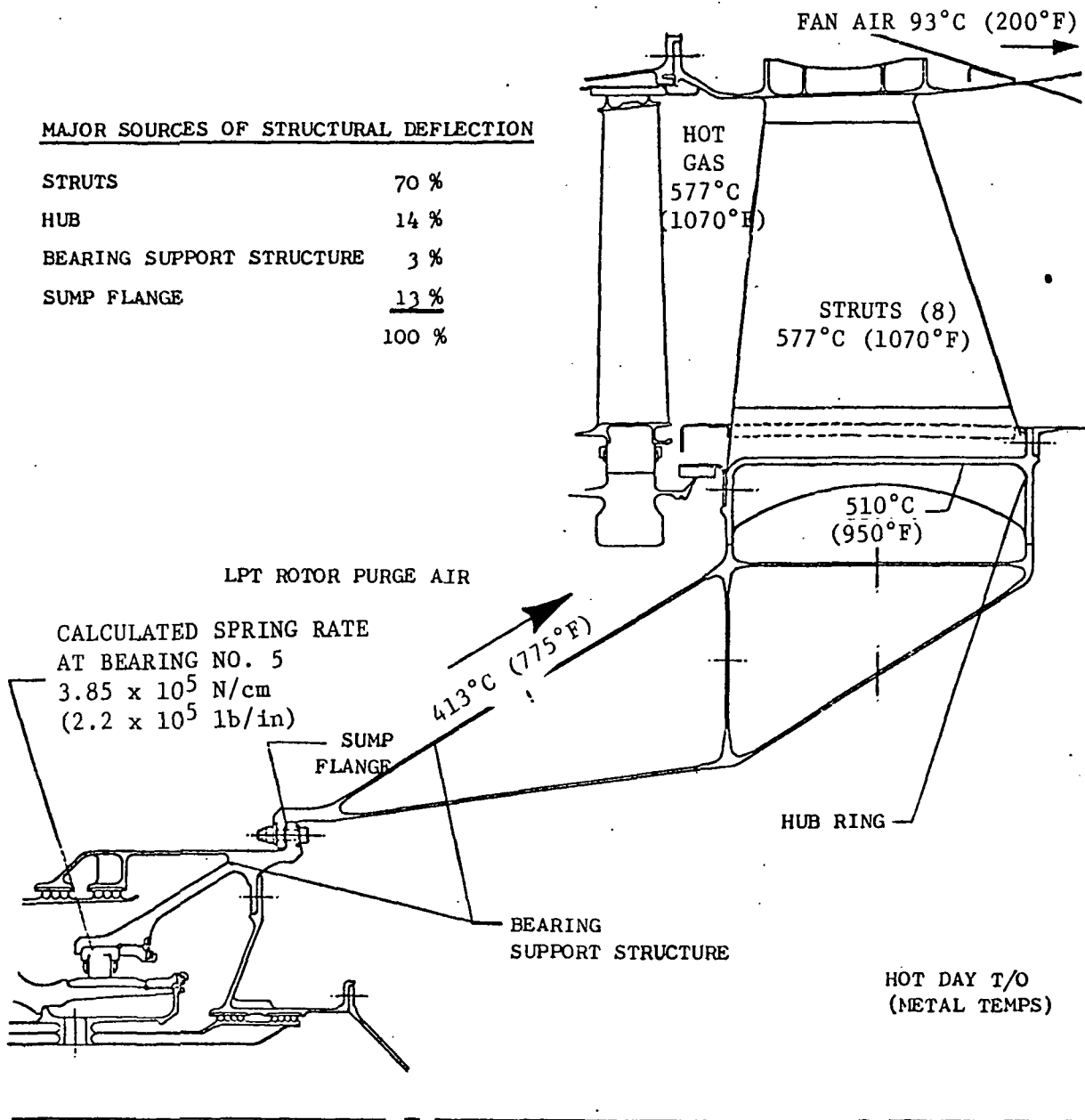


Figure 84. Turbine Frame Preliminary Temperature and Spring Rate; Takeoff, Hot Day.

The E<sup>3</sup> mixer and centerbody preliminary design was based on previous mixer and centerbody production design. The mixer makes the maximum possible use of double curved surfaces consistent with aeroacoustic design limitations. Double curved surfaces are advantageous because flat chute walls and straight-line chute elements in general are undesirable from the standpoint of stiffness and acoustic fatigue life. Neither of these parts are highly loaded and are, therefore, a problem of rigidity more than strength.

#### 1. Bearings, Seals and Drives

The engine rotor system is supported by five main-shaft bearings. Supporting the high-pressure rotor is a thrust bearing (No. 3) in the front sump and an intershaft roller bearing (No. 4) in the aft sump. The low-pressure rotor support system includes a thrust bearing (No. 1) and roller bearing (No. 2) mounted in the front sump and a roller bearing (No. 5) located in the aft sump.

The forward sump is enclosed within the fan frame. The No. 1 thrust bearing support is bolted to the frame structure just forward of the core strut leading edges. The bearing support housing is machined from Ti6Al-4V. Just forward of the No. 1 bearing, is the forward seal. A labyrinth seal is used, pressurized by internal piping from the No. 3 bearing housing. A seal drain is provided from the labyrinth seal housing to drain any incipient oil leakage that may occur during a transient or shutdown condition.

The No. 2 bearing supporting the aft end of the fan shaft coupled to the forward end of the low pressure turbine (LPT) shaft is also located in the forward sump. This bearing position is selected to minimize the bearing span length in LPT shaft. Between the No. 2 and No. 3 bearing is situated the PTO gearbox described separately in this report. The No. 3 thrust bearing is mounted in a 17-4PH housing bolted to the aft end of the fan frame housing. Just aft of the bearing is arranged the labyrinth seal. This seal and the No. 1 bearing seal are pressurized from an interstage bleed of the compressor. Pressurizing air is directed to the hub cavity of the compressor and pressurizes the cavity aft of the No. 3 bearing through holes in the compressor front stub shaft. A seal drain is provided from the No. 3 bearing seal cavity.

The aft sump is supported from the LPT frame. The No. 5 bearing support housing and the majority of sump associated hardware are manufactured from Inco 718 material. The intershaft No. 4 bearing outer race is mounted to the lower speed LPT shaft and the inner race to the high pressure turbine (HPT) shaft. Special attention is given to determining the proper operating clearance for all bearings. This is especially true for the intershaft bearing (No. 4) where both the outer and inner races rotate.

A labyrinth sealing system is also used in the aft sump. Special care is taken in arranging the rotating hardware in the aft sump so oil leakage cannot find its way into hot turbine cavities, but rather into a seal drain cavity to be directed overboard. Seals are pressurized by the same source as the forward sump. Cooling air is also directed around the sump to prevent oil coking and reduce heat rejection to the aft sump oil.

All main engine bearings are M-50 material with cages of AMS 6414, silver plated. Design loads are determined from the rotor thrust and VAST (Vibration Analysis System) computer programs.

The latest approaches to improve life during oil interruption and normal operation are being used in the design of the lubrication/cooling methods for the main shaft bearing. For higher DN values, bearing testing has shown that under-race cooled bearings with inner-land riding cages are superior to jet lubricated outer-land riding cages. The NO. 3 (with a DN of  $2 \times 10^6$ ) and No. 4 high-pressure rotor support (DN of  $2.4 \times 10^6$ ) bearings are under-race cooled based on this test experience. Since the DN values of the No. 1, No. 2 and No. 5 bearings are low ( $< 1.5 \times 10^6$ ), conventional jet lubrication with outer-land riding cages is used.

The overall lube system is shown schematically in Figure 85. A dry-sump system typical of aircraft engines is used. A lube tank supplies oil to the inlet of the supply pump. This pump will have a capacity of 12 to 14 gpm. Supply oil is filtered before it enters the sumps and gearboxes. The system pressure level is established by the flow network; pressure-regulating valves are not utilized in the pump. Oil is scavenged from sumps and gearboxes by individual scavenge elements enclosed in a common pump housing. It is proposed to drive this pump by a small gear train, shown in Figure 86, mounted in the core cowl area. Four elements are used to scavenge the E<sup>3</sup>. These elements are sized to provide at least a 2-to-1 scavenge ratio.

Scavenged oil is pumped through a filter and heat exchanger and then back to the tank.

A typical drive system is shown schematically in Figure 87 and is representative of a flight-type design.

Engine accessory power is extracted from the core shafting through right-angle bevel gearing and is transmitted through radial drive shafting to a top mounted accessory gearbox and to a scavenge pump gearbox mounted in the core cavity area on the bottom vertical. In a flight configuration, to minimize the frontal area projection of the engine, the width of the accessory gearbox will be limited to be compatible with the width of the pylon strut.

The right-angle gearing assembly shown in Figure 88 that extracts accessory power from the core engine shaft constitutes the power takeoff gearbox (PTO).

Gear sizing is based on current pitch-line velocity experience 152 m/sec ( $< 30,000$  fpm) and gear design practices established by General Electric and the AGMA (American Gear Manufacturers Association). Bending stress, compressive stress, and scoring indexes are all within current design limits of AISI 9310 case-carburized gear material lubricated with MIL-L-7808 or MIL-L-23699 lubricants. The driver and driven bevel gears are mounted in the same assembly to limit the path of thermal growth and to allow shimming the bevel gears for proper backlash and load-bearing patterns as a module before assembling into the engine.

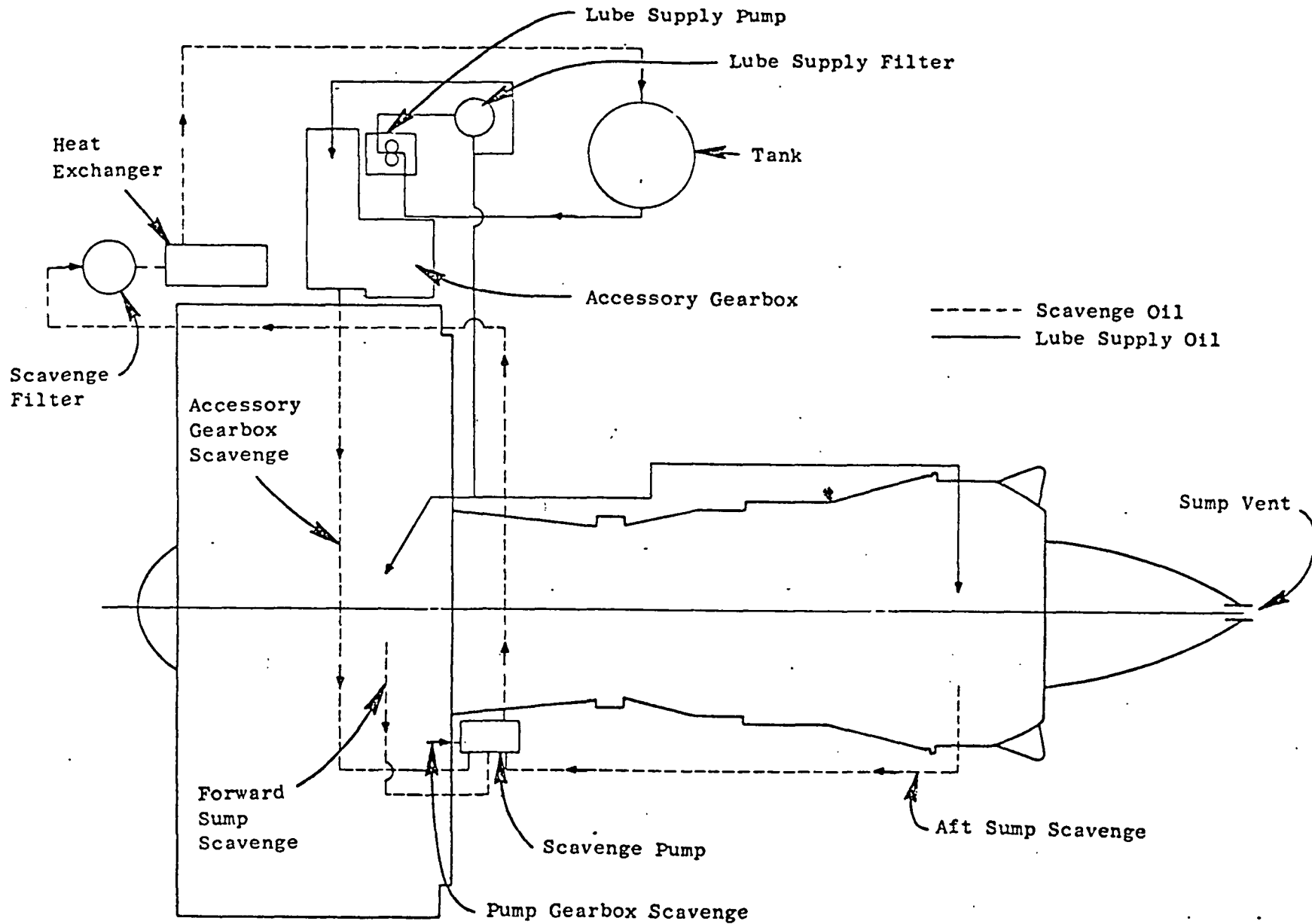


Figure 85. Lube System Schematic.

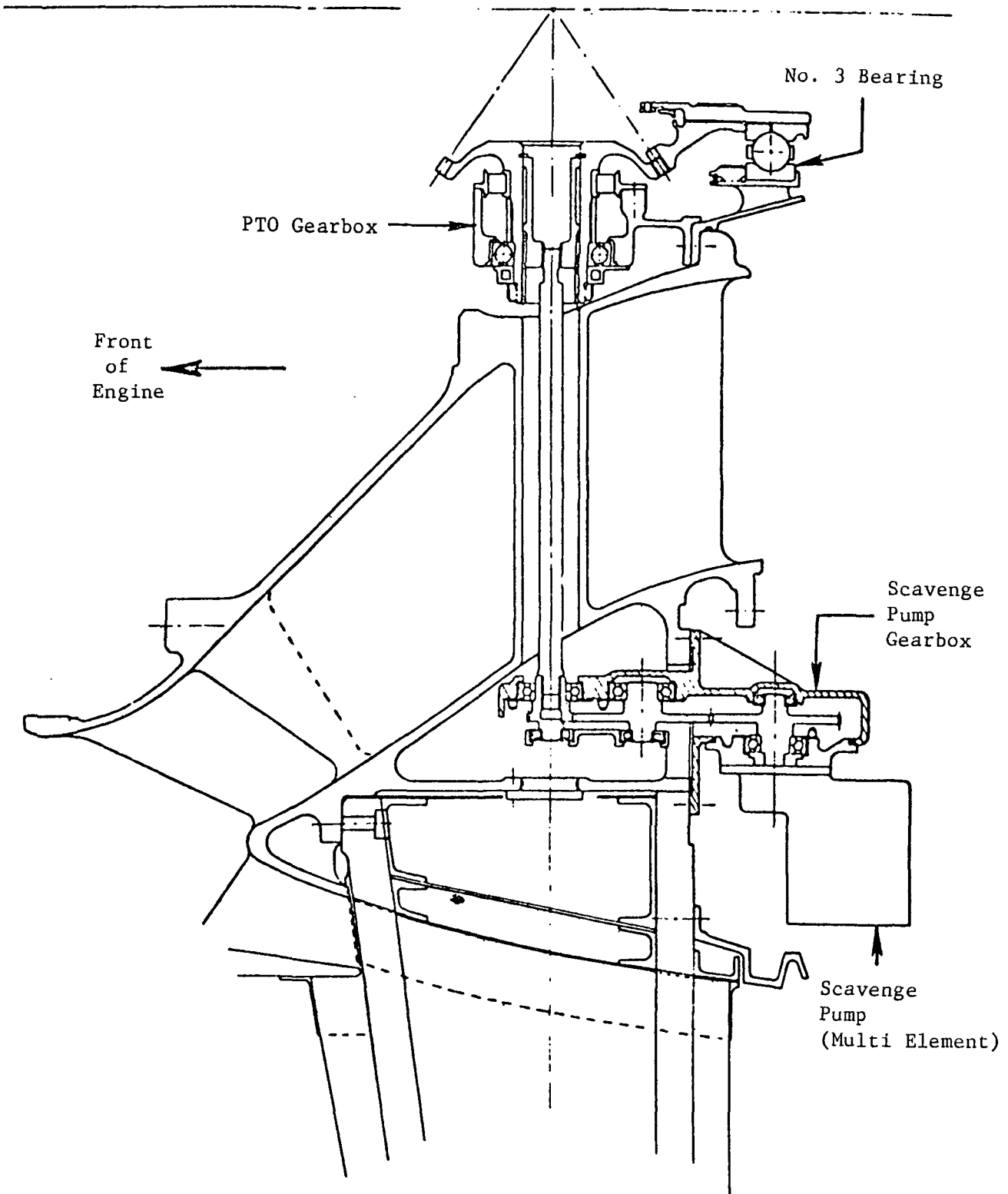


Figure 86. Scavenge Pump Drive Gearbox

ORIGINAL PAGE IS  
OF POOR QUALITY

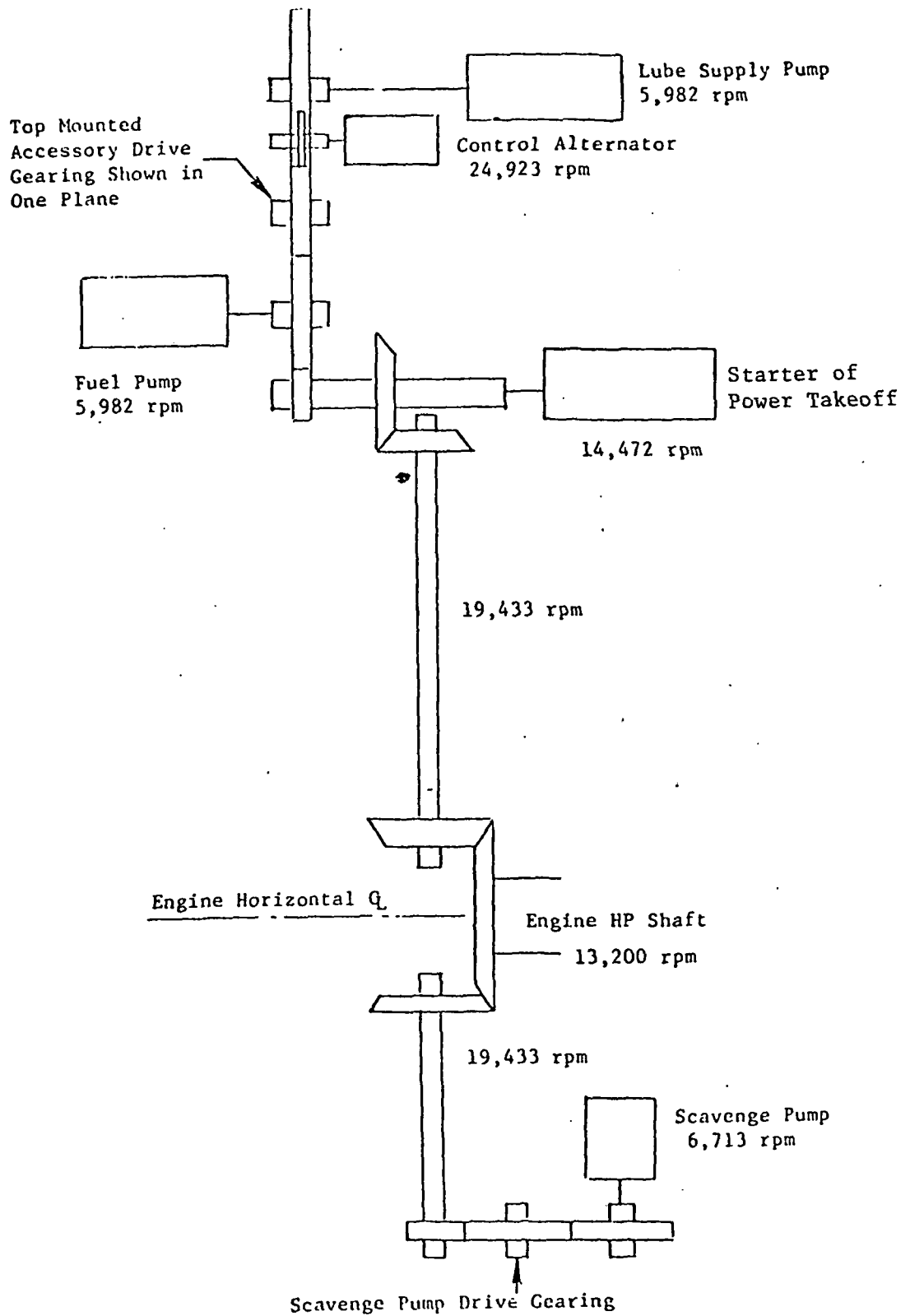


Figure 87. Schematic of Accessory Drive System.

ORIGINAL PAGE IS  
OF POOR QUALITY

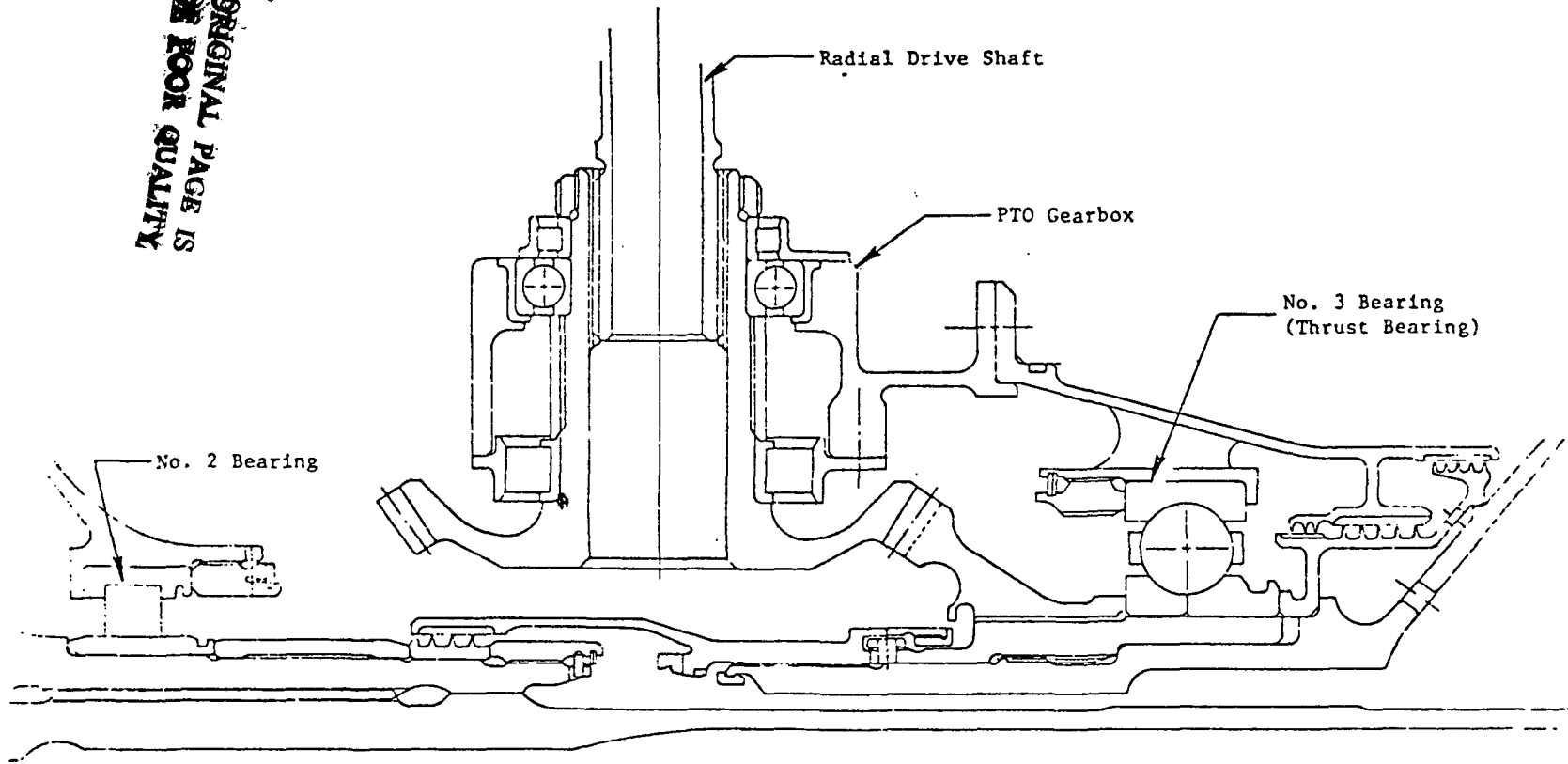


Figure 88. PTO Gearbox.

The bevel gear mounted on the core engine shaft is supported by the engine main shaft bearings. The thrust bearing mounted in proximity to the bevel gear eliminates the majority of the thermal stackup of the support system.

All bearings supporting the PTO gears will be M-50 with steel cages of AMS 6414, silver plated.

A cross-section of a typical accessory gearbox is shown in Figure 89. The gearbox shown is a "semi-plug-in" design where gear clusters are built up and as subassemblies are assembled into a one-piece housing. Spiral bevel gearing is utilized and spur gears are used to drive the accessories. Bending stress, compressive stress and scoring indexes are all within current design limits of AISI 9310 case carburized gear material. A ball and roller bearing is used at each gear position. All bearings are M-50 with steel cages of AMS 6419, silver plated. All housings and adapters are cast aluminum.

## j. Control System

### 1. General Description

The control system which has evolved from the E<sup>3</sup> preliminary design effort is shown schematically on Figure 90. The system has as its foundation many of the proven concepts and component designs used on the CF6. A major difference is the addition of digital electronic computation which provides significant improvements in control flexibility, accuracy, and aircraft/engine integration capability.

The primary function of the system is to control thrust by controlling fuel flow. In addition, the system controls the fuel flow split to the double-annular combustor, positions core compressor variable stators, starting bleed valves, and active clearance control valves, controls thrust reverser actuation, provides active clearance control air-to-fuel heat transfer, and furnishes ignition logic. The system also utilizes the data-handling capabilities of the digital control to gather engine and control condition monitoring data and transmit it over a multiplexed data link to the aircraft data system.

### 2. Components

Control system components are listed and described below.

Digital Control - The digital control is a solid-state electronic component utilizing Large Scale Integrated (LSI) micro-processor technology. As shown on the functional schematic in Figure 91, the control accepts aircraft thrust and mode commands, engine system inputs, and engine condition monitoring data and provides outputs to engine control elements and to the aircraft data system. The outputs are controlled on a time-sharing basis by the digital computational elements which include a micro-processor, micro-program, program memory, program counter, and clocks. The computer will have a maximum addressable memory capacity of 64,000 16-bit words, a random access memory



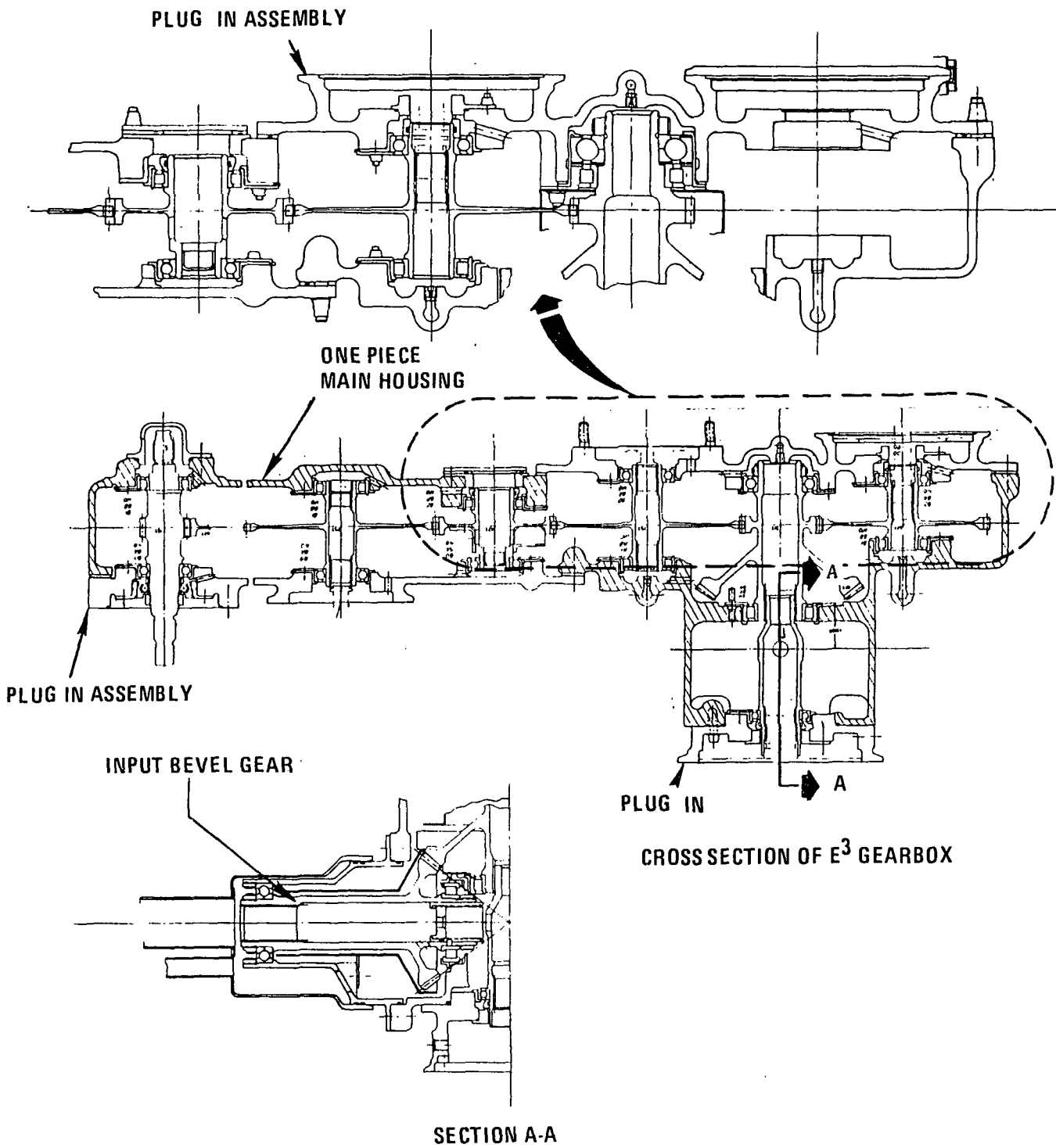


Figure 89. Accessory Gearbox Cross Section.

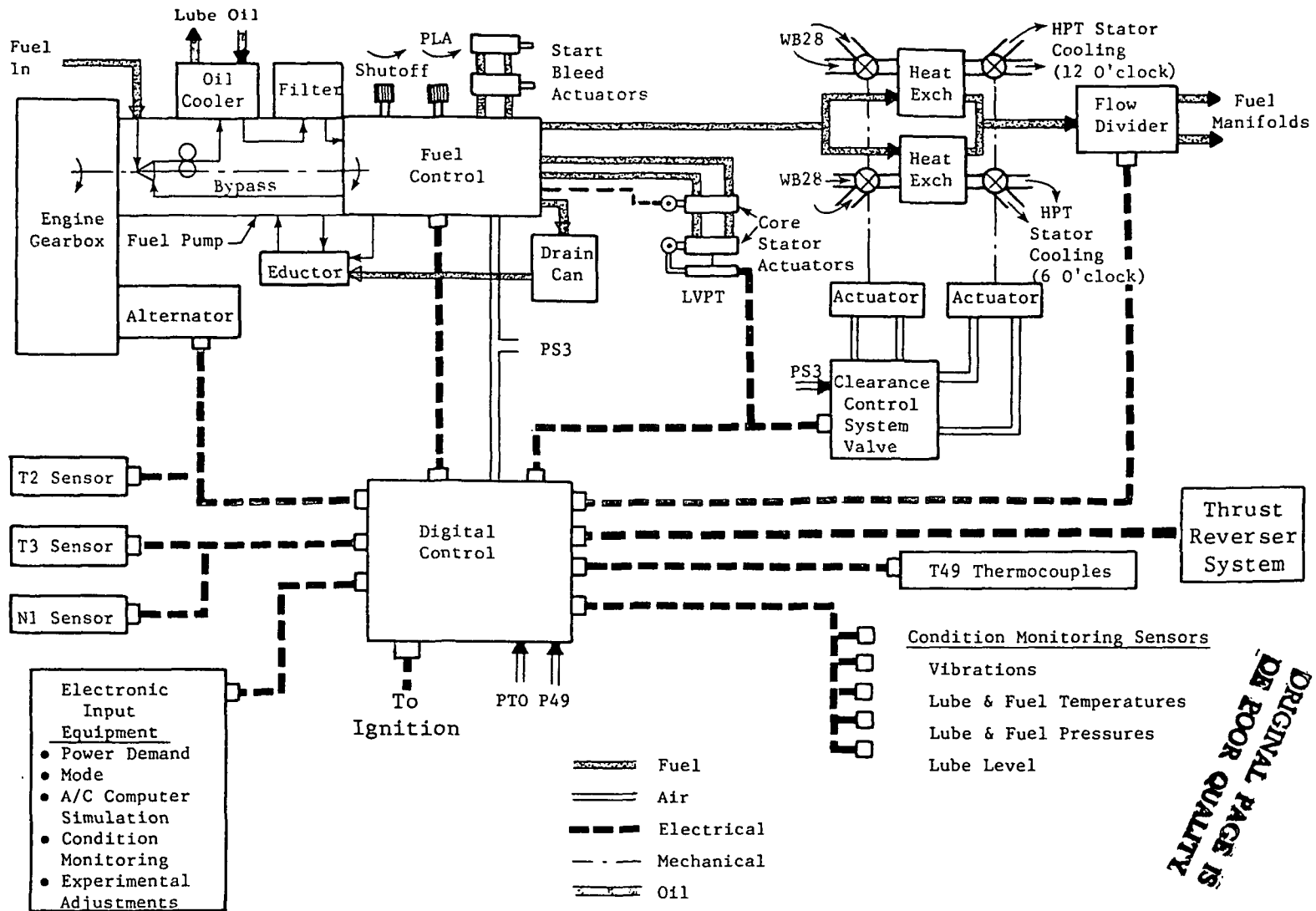


Figure 90. Control and Fuel System.

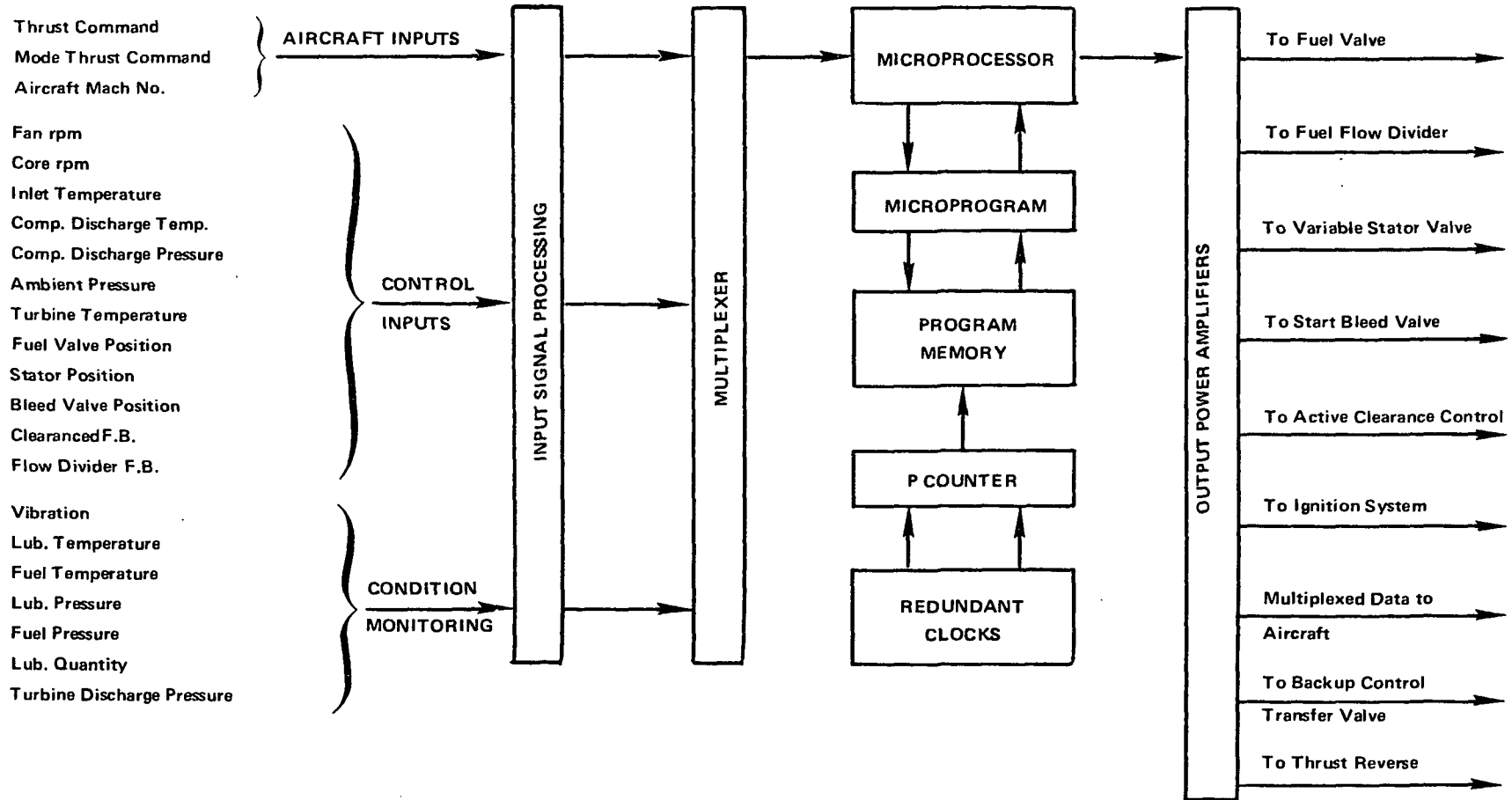


Figure 91. Digital Control Functions

capacity of 512 16-bit words, and a constants memory capacity of 512 16-bit words. It will have a clock rate of 3.5 megahertz which will result in an estimated running time for an E<sup>3</sup> control program of 4 milliseconds. The integrated circuit elements in the computer will be of the low power Schottky TTL type. Estimated size of the digital control in a production configuration is 8 x 8 x 4.7 inches and estimated weight is 5.9 Kg (13 lbs).

Fuel Control - The fuel control is an electro-hydraulic component which controls engine fuel flow and variable core stators in response to electrical signals from the digital control, provides simplified hydro-mechanical backup control of these two variables if electrical control elements malfunction, and provides fuel for actuation of the starting bleed valves. The control will be mounted on the fuel pump and passages through the mounting pad will supply pump flow into the control and return control bypass flow to the pump. Fuel flow to the engine will be controlled by the combined operation of a variable-area metering valve and a bypass valve which maintains a fixed pressure differential across the metering valve. Fuel for operation of the core stator actuators will be controlled by a four-way valve in the control. Electrohydraulic servovalves within the control which respond to signals from the digital control are the primary means of positioning the fuel metering valve and core stator valve but a 2-position valve in the control is provided to allow transfer of metering valve and stator valve control to the backup hydro-mechanical control elements which are also included in the fuel control package.

Fuel Pump - An engine-gearbox-driven, positive displacement, gear pump with integral centrifugal boost element.

Fuel/Oil Heat Exchanger - A fuel-pump-mounted unit which transfers heat to fuel, which flows through a group of small tubes within the unit. Engine scavenge oil flows over the tubes.

Fuel Filter - A pump-mounted, metal element, 46 micron filter between the fuel/oil heat exchanger and the fuel control.

Core Stator Actuators - Fuel operated, cylindrical ram actuators similar to those used on the CF6.

Drain Can - A container which is used to collect fuel manifold drainage fuel and store it for return to the fuel pump by the eductor pump. The can includes a float-operated shutoff valve.

Eductor - A fuel-operated jet pump which uses a high velocity stream of fuel, bled from the main fuel pump discharge, to draw fuel from the drain can and return it to the fuel pump inlet. Valves within the eductor allow it to be shut off during normal engine operation to prevent introduction of air into the fuel pump and to operate only during engine coastdown.

T2 Sensor - A platinum resistance temperature detector housed within a structural airfoil in such a manner that it can be inserted in the engine inlet and sense inlet air temperature accurately without damage due to inlet air contamination (birds, iceballs, etc.).

N<sub>1</sub> Sensor - A dual-coil, electromagnetic sensing element mounted in a tubular housing which, in turn, will be inserted in the engine fan frame so that the sensing element is near a serrated, ferromagnetic disk rotating with the fan shaft. A number of electrical pulses proportional to fan rpm will be generated as the disk passes the sensor.

T<sub>3</sub> Sensor - A chromel-alumel thermocouple mounted in a probe which will be mounted in the core compressor discharge flow path.

T<sub>49</sub> Sensors - Dual-element, chromel-alumel thermocouples mounted in 11 separate probes which will be inserted in the gas stream between the high pressure and low pressure turbines. The elements will be connected in parallel to give an average T<sub>49</sub> reading.

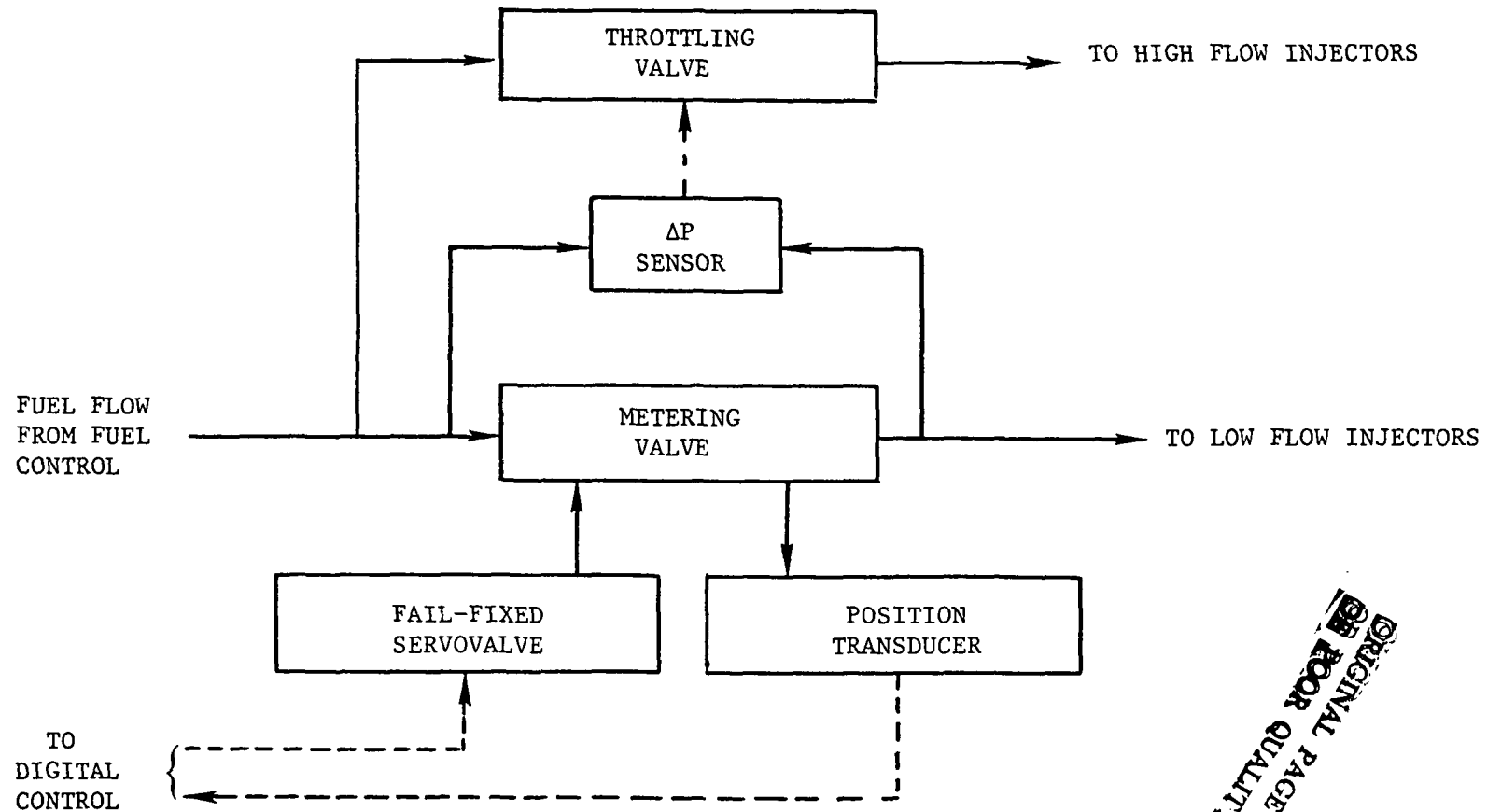
Starter - An air turbine with output reduction gearing and overrunning clutch which delivers the torque-speed characteristic required to start the engine. The starter will drive the core engine through a pad on the engine gearbox.

Flow Divider - A fuel valve which divides fuel flow as required by the double annular combustor, providing flow to only one group of fuel nozzles when total fuel flow is low and providing fuel to all fuel nozzles when total flow is high. Figure 92 shows schematically the probable mechanization of this valve.

Fuel/Air Heat Exchanger - A component which transmits heat between the engine fuel and the compressor bleed air used for active clearance control. This heat exchanger provides a dual benefit to the engine cycle by reducing the amount of cooling air required and by reducing the energy required to vaporize fuel in the combustor. The component does, however, present two major considerations: (1) positive means to avoid leakage of fuel into the air in the event of a heat exchanger failure, and (2) control means to assure that fuel is not overheated. Pertinent to this is the fact that the clearance control system is designed so that lack of heat exchanger performance (higher temperature air) can only result in an increase in turbine blade clearance and not in a tip rub.

Control Alternator - An electrical alternator which supplies power and core engine speed intelligence to the digital control and power to the ignition exciter. The alternator consists of a permanent magnet rotor mounted on one of the engine accessory gearbox output drive shafts and a multi-coil stator mounted to the gearbox housing so that it encases the rotor. The alternator generates three-phase power which, compared to the single phase power used on current engines, has less output ripple and thus allows a significant reduction in filter networks. Saturable reactors will be included in the stator to provide some voltage regulation capability within the alternator, thereby eliminating some voltage regulating elements and their associated heat load from the digital control.

Core Stator LVPT (Linear Variable Phase Transformer) - An electrical position transducer mounted in the core stator actuation system to provide stator position feedback to the digital control. The LVPT is an electro-mechanical device that senses mechanical motion and outputs an electrical signal that is directly convertible to digital form. Its construction is very similar to a linear-variable differential transformer (LVDT) having



ORIGINAL PAGE IS  
OF POOR QUALITY

Figure 92. Flow Divider Functional Schematic

three coils (two primary and one secondary) arranged in line on a bobbin through which an iron core is moved. The two primary coils are excited by a constant-amplitude alternating current with specific phase separation that is also kept constant. The primary currents induce an alternating magnetic flux in the core which is the vector sum of the fluxes that would be induced separately in the core by the primary windings. The secondary coil is used to detect the magnitude and/or phase of the core flux. The phase of the secondary current is a function of the core position. This phase angle can be detected by the digital control and converted to a binary word that can be used directly in a digital closed-loop system.

Physically, the LVPT is similar to the LVDT in size, shape, and materials. Therefore, it has similar reliability and mounting requirements.

Active Clearance Control Valve Actuators - Pneumatically operated cylindrical ram actuators are proposed for actuation of the clearance control valves.

Active Clearance Control Actuator Control Valve - A component which will contain two electropneumatic four-way valves for controlling the position of the active clearance control valves. Compressor discharge air will be used as the high pressure supply for the valves.

Start Bleed Valve Actuators - Fuel-operated cylindrical rams are proposed for actuation of the starting bleed valves. These will be similar in design to the core stator actuators but should be somewhat smaller.

Electrical Cables - Electrical interconnections in the E<sup>3</sup> control system will be accomplished with connector and cable designs equivalent to those used on current G.E. engines. Stainless steel connectors will be used throughout the system. Interconnecting cables are made up of wires combined in shielded, twisted pairs to minimize electromagnetic radiation effects.

#### k. Installation Structure

The structures package of the engine nacelle covers the design of the inlet, fan reverser, exhaust nozzle and core cowl. The nacelle is of the integrated engine/nacelle type as previously pioneered by General Electric on the NASA Quiet, Clean, Short-Haul Experimental Engine program (QCSEE). The E<sup>3</sup> nacelle is a symmetric, long-ducted, mixed flow design that makes extensive use of lightweight composites to reduce cost and weight. Sound suppression is integrated into the inner walls (engine flowpath) of the nacelle components.

The inlet consists of two main composite subsections (inner and outer barrels) joined together at the forward ends by a metal nose which contains anti-icing provisions. At the aft ends they are joined by the fan frame attachment rings and in between by composite rings or bulkheads. The resulting assembly is structurally integrated for maximum strength and minimum weight.

The fan reverser is located in the outer fan duct immediately aft of the fan frame. It incorporates a fixed cascade, articulating fan duct blocker door, and translating outer sleeve (see Figure 93) similar to the General Electric designed TF39 and CF6 fan reversers. This design was chosen on the basis of its compatibility with the long duct, integrated engine/nacelle and for its adaptability to efflux pattern tailoring for various

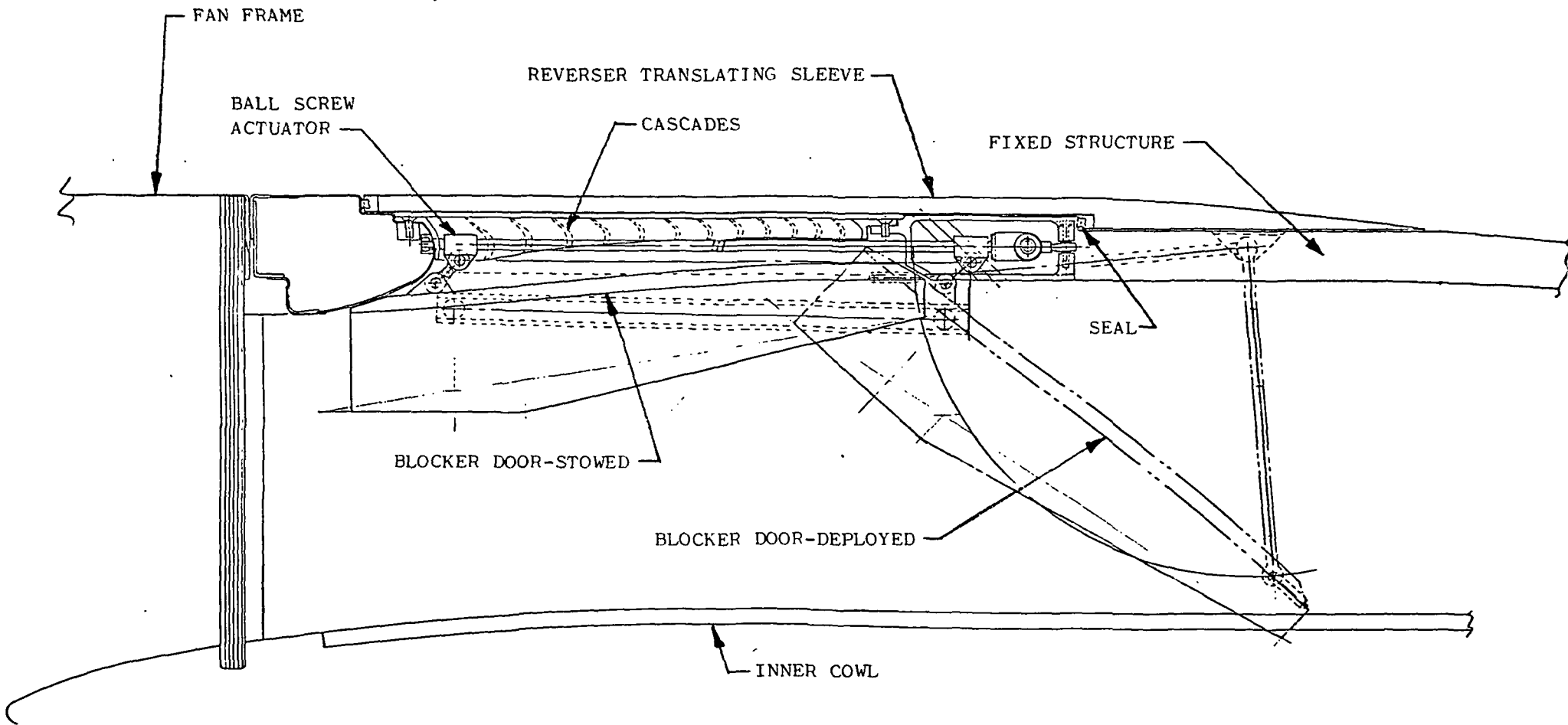


Figure 93. Fan Reverser Schematic.



aircraft installations. Another factor in its selection was the long time experience with this type of reverser, the CF6 having nearly four million commercial flight operation hours at this time. Again, composites will be used extensively to reduce the component weight. The fan nozzle is two full depth honeycomb, semicircular sections, or doors, hinged to the pylon and latched together at the bottom along the axial split line. The attachment between the reverser and the nozzle components is of the circumferential tongue and groove design capable of transmitting axial loads. This joint will be provided with a pressure and acoustic seal. Due to the probable recirculation of some of the core engine exhaust gases into the fan duct during reverse thrust operation, the materials used in the nozzle will have to withstand higher temperatures than those in the rest of the outer nacelle components. Sound Suppression treatment will be included in the inner wall back to the mixer area. The inner cowl is similar in concept and materials to the fan nozzle, being two full depth honeycomb, semicircular bondment sections, hinged to the inner pylon and latched together along the bottom split line. These sections, or doors will be attached to the fan frame by means of a circumferential tongue and groove sealed against pressure and acoustic transmission. Cooling air from the fan duct will be introduced to the cavity between the engine and cowl during operation. The normal operating temperatures of the nacelle components, with the exception of the fan nozzle and inner cowl are relatively low, less than 93°C (200°F). Fire safety requirements for all the components have been taken into account.

The design criteria included the following:

- a) Aircraft Flight and Maneuver Envelopes
- b) Crash, Gust and Handling Conditions
- c) Life and Duty Cycle for a 1990 aircraft
- d) Acoustic Suppression
- e) Weight
- f) Cost
- g) Fire Safety
- h) Emergency Landing
- i) Aborted Takeoff
- j) Inadvertent Deployment of Reverser
- k) Maintainability

These criteria have been supplemented by the design experience gained in the operation of the General Electric designed commercial and military thrust reversers and in the testing of the QCSEE integrated engine/nacelle. The final structures design is believed to best balance E<sup>3</sup> program objectives.

### 3. Component Performance Description

#### a. Fan and Quarter Stage

Bypass stream pressure ratio of the E<sup>3</sup> fan at the maximum cruise thrust operating condition is 1.61 at a corrected tip speed of 402 m/sec (1321 ft/sec). The E<sup>3</sup> fan's estimated bypass performance was established by taking the demonstrated efficiencies of recent advanced fan components as a base, and making adjustments for differences in configuration and technology advancements.

Negative adjustments for use of a low aspect ratio vane frame, thicker leading edges for ruggedness and increased flow/annulus area were estimated using the General Electric efficiency prediction model. A negative adjustment was also made for quarter stage tip loss to reflect the casing wall boundary layer and rotor tip leakage losses that are present in the 40% of the quarter stage flow that is returned to the bypass stream. A positive efficiency adjustment for reduced fan tip clearance was estimated from test data on fans running at several different clearance levels. Finally, a positive adjustment of about 0.002 was allowed for improved airfoil design to reflect the use of advanced analytical techniques during the aerodynamic design for closer control of shock structures and surface velocity distributions. The resulting E<sup>3</sup> fan bypass efficiency at max. cruise was estimated as 0.882.

Fan stall margin is expected to be somewhat higher than in current production fans. Since tip speed, solidity, rotor aspect ratio and bypass stream pressure ratio at cruise conditions are nearly the same, comparable stall margins would be expected. However, the higher specific flow and smaller tip clearance of the E<sup>3</sup> fan should permit an increased stall margin over current fans. Current General Electric production fans have about 15% stall margin relative to the cruise operating line, and their in-service record of freedom from fan stalls has been excellent.

Fan core stream efficiency was also estimated by using demonstrated efficiencies as a base, and making adjustments for differences in configuration. After adjustments for differences in speed, flow/annulus area, use of a booster stage and expected technology advances, the estimated E<sup>3</sup> fan core flow efficiency at max. cruise was 0.892. Advanced aerodynamic design technology was estimated to be capable of improving efficiency in the hub region by about one-half point by the 1985-1990 time period when the production E<sup>3</sup> engine is expected to enter service; the efficiency of 0.872 thus includes an adjustment of +0.005 for advanced technology.

Fan hub plus quarter stage stall margin was estimated to be quite adequate. Preliminary axisymmetric flow analysis of fan operation at a bypass ratio of 10.5, typical of values encountered at flight idle or during a throttle-chop transient, indicated that quarter stage rotor incidence angles increased by 4 to 5° and the D-Factor reached a maximum value of 0.57 at the hub. This was judged to be well within the capability of this type of lightly-loaded, subsonic blading. The similarity of the E<sup>3</sup> fan hub configuration to that of current fans also gave assurance that the same characteristic of stall free fan operation in normal commercial service could be achieved in the E<sup>3</sup> engine.

The transition duct, or "gooseneck", was designed to minimize losses into the HP compressor. The axial length was selected to be consistent with a correlation of normalized length versus radius change based on past General Electric experience with similar transition duct designs having low losses.

## b. High Pressure Compressor

It is recognized that developing the compressor to the point where its performance objectives are achieved will be a major challenge. The peak efficiency goal for this compressor configuration is about 91% polytropic, and stall margin requirements are equally challenging. The methods employed to estimate the efficiency and stall margin capabilities of the compressor are described as follows.

The peak efficiency goal was set to be consistent with the General Electric preliminary design procedure used during the AMAC compressor studies (reference 6). The efficiency prediction model is intended to forecast the potential peak efficiency of a well-designed, fully-developed compressor. It thus attempts to account for all sources of loss present at the minimum-loss operating condition: blade surface profile drag; shocks in the blading; part-span shroud losses; and endwall region losses due to wall boundary layers, secondary flows and leakage. The influence of all important design parameters is accounted for. Blade profile losses, for example, are related to suction surface diffusion, blade maximum and trailing edge thicknesses, Reynolds number, surface roughness, Mach number and steam tube contraction. Passage shock losses are dependent upon both inlet and exit Mach number, and leading edge bow shock losses depend on inlet Mach number, leading edge thickness, solidity and stagger. The model for part span shroud loss, although not a factor in the proposed compressor configuration, is based on both analytical formulations for drag coefficient and experimental data. Finally, measured endwall boundary layer thicknesses have been correlated versus aspect ratio, solidity, stagger, tip clearance, blade row axial spacing and aerodynamic loading level to determine endwall losses. The model's predicted peak efficiency has been compared to test data from numerous high speed and low speed multistage compressors. These comparisons indicate that in most cases the model agrees with the experimental data within one point in efficiency at the speed for which the compressor stages are best matched.

For the E<sup>3</sup> core compressor, certain advancements in aerodynamic and mechanical technology were assumed. Aerodynamic technology advancements were assumed to consist primarily of reductions in endwall losses. It was assumed that a 15% reduction in these losses below that predicted by the model would result from research efforts now in progress or anticipated in the near future. This advanced aerodynamic technology assumption raised the predicted adiabatic efficiency level by about one point. Achievement of in-service tip clearance levels equal to those in recent demonstrator engines was also assumed. Finally, it was assumed that the fan for the E<sup>3</sup> engine would be designed to minimize the ingestion into the core engine of foreign objects such as sand and bird fragments. This allows retention of the very smooth blade surface finishes that are possible using advanced manufacturing methods, and allows the use of relatively sharp leading edges. These mechanical technology assumptions contributed an additional one point to the predicted efficiency compared to that given by the model for clearances and surface finishes found in current production engines.

An item of uncertainty that could affect the achievable efficiency of the core compressor, is the extent to which airfoil shapes might have to be compromised to allow adequate off-design performance for this 23:1 pressure ratio spool. Through the employment of variable stators and starting bleed, it is expected that any penalty in peak efficiency due to the high pressure ratio will be minimal, but this is an item of concern.

The design speed stall margin potential was continuously monitored throughout the definition and refinement of the E<sup>3</sup> core compressor. The General Electric Compressor Unification Study stall pressure rise correlation was used for this purpose. This is a computerized procedure which contains a correlation of stall pressure rise data measured in a large number of tests of low speed, repeating stage groups covering a wide range of stage geometries. These data, expressed as peak pressure rise coefficients, are related to stage solidity, aspect ratio, reaction, tip clearance and Reynolds number. Virtually all the low speed data have been correlated to within +5%. For high speed multistage compressors at design speed stall, experimental data are expressed as a ratio of each stage's pressure rise coefficient to that predicted by the low speed correlation. The average values of this ratio for multistage compressors lie generally in the range from 0.88 to 0.96. The value of this figure of merit usually depends on whether some block of stages is unloaded at design speed; this is sometimes done purposely to favor part-speed performance, or occasionally happens because the stages are not matched in a way that allows all of them to load up at design speed. However, in nearly all cases, a group of stages having ratios very close to 1.0 can be identified, and these are believed to be the stall-limiting stages. There is little evidence that there is any penalty in average stall loading ratio associated with a high pressure ratio per spool at least up to design pressure ratios of 16 or 17 to one.

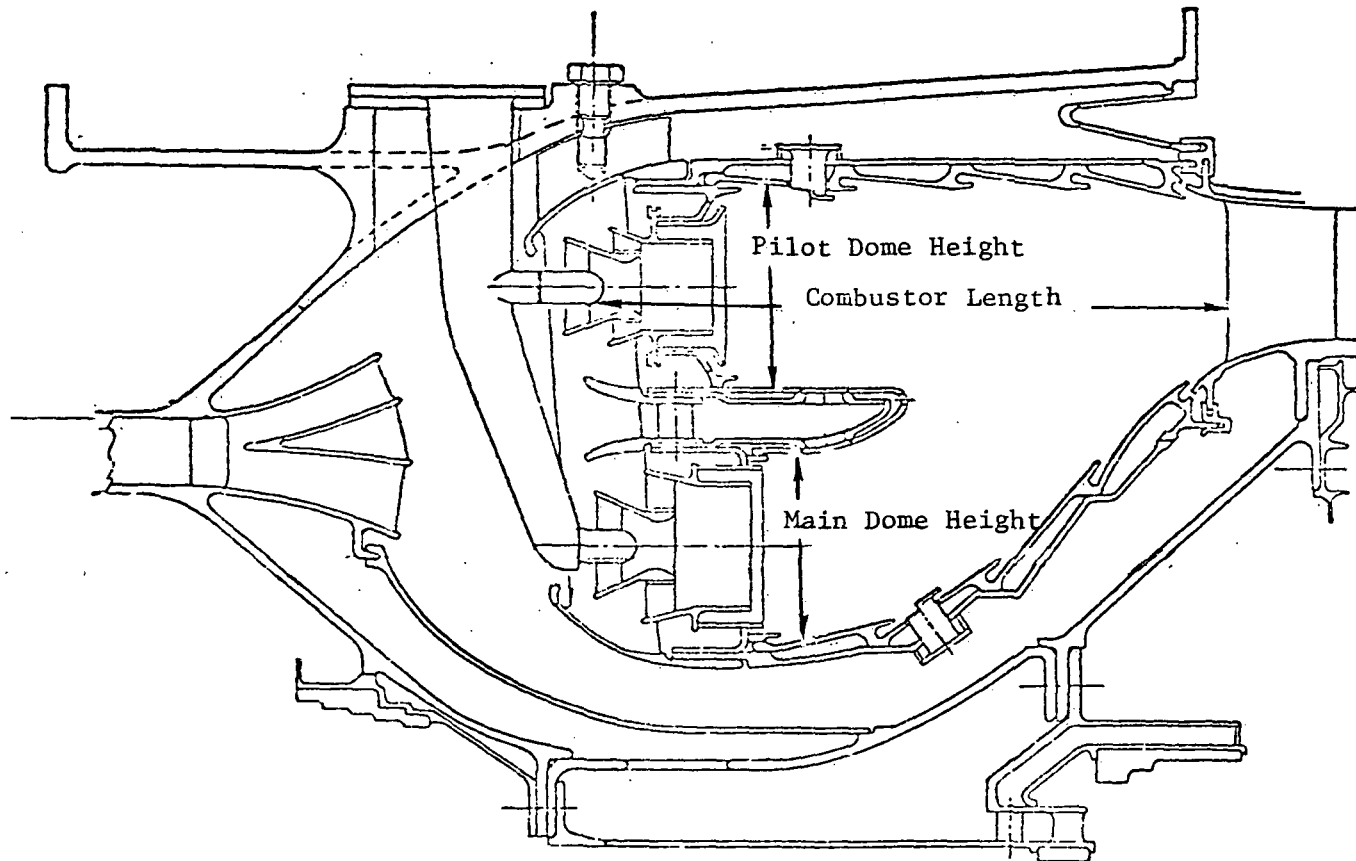
Design speed stall margin estimates for the 10 stage E<sup>3</sup> core compressor were made assuming that the average loading ratio at stall would be 0.95. This is consistent with stall loadings demonstrated by current high speed, highly-loaded compressors of somewhat lower overall pressure ratio. Realization of the compressor's full potential of 25% stall margin would require airfoils of rather high camber that could adversely affect operating line efficiency somewhat. Also, it is dependent upon the achievement of good tip clearances. However, it is estimated that 20% stall margin could still be available with clearances typical of engines currently entering service and with little compromise in efficiency.

Estimates of part-speed performance were conducted under Task 5 of the E<sup>3</sup> Preliminary Design Study contract using a stage characteristic and stage stacking procedure. These are described in a later section of this report.

### c. Combustor

#### 1. Aerodynamic Design

The combustion system designed for the Task III E<sup>3</sup> study program is illustrated in Figure 94. This design is an advanced, short, light-weight, double-annular combustor based on the low emissions combustor design technology developed in the NASA Experimental Clean Combustor Program (ECCP) and in the NASA QCSEE double-annular, low-emissions combustor development program. The technology evolved in other ongoing General Electric low emissions combustor development programs has also been factored into this E<sup>3</sup> combustion system design.



Cm (Inch)

Combustor Length 17.8 (7.0)

Pilot Dome Height 6.1 (2.4)

Main Dome Height 5.6 (2.2)

ORIGINAL PAGE IS  
OF POOR QUALITY

Figure 4 . E<sup>3</sup> Combustion System Design.

As illustrated in Figure 94, the E<sup>3</sup> combustion system design is a short-length, scaled-down adaptation of the CF6-50 NASA ECCP double-annular combustor configuration together with a short, double passage diffuser design. In this design, the outer annulus of the combustor is used for light-off and idle power operating conditions. As the engine throttle is advanced to higher power operating conditions, fuel is admitted to the inner annulus of the combustor, and at full power conditions, about 80 to 85 percent of the total fuel flow is burned in the inner annulus.

## 2. Aerodynamic Design Requirements

The E<sup>3</sup> combustion system is designed to provide the specified temperature-rise capabilities and to meet all of the other engine system requirements throughout the entire operating range of the engine. The combustor inlet pressure and temperature at the sea level takeoff conditions are quite severe from a mechanical design standpoint. Hence, the combustor design technology evolved at GE for use in the CF6-50 and other high cycle pressure ratio engines has been factored into the design of the E<sup>3</sup> combustion system.

The emissions goals, along with some of the key aerodynamic/thermodynamic performance requirements, of the E<sup>3</sup> combustion system are summarized in Table 64. In addition to these goals and requirements, the E<sup>3</sup> combustion system must operate with a carefully specified, circumferentially averaged radial temperature profile at the exit plane. Also, the E<sup>3</sup> combustion system must be capable of providing consistent ground starts with cold fuel, as well as consistent air starts at altitudes up to 9,144 m (30,000 ft).

## 3. Overall Aerodynamic Design Approach

The double-annular combustion system design selected for the E<sup>3</sup> is a compact design with a very short overall length. The combustor inlet diffuser, with an annular splitter vane, is a very short-length design and the combustor liner has a short length with relatively large dome heights. A list of the important aerodynamic design parameters of this combustion system is presented in Table 65, along with those for the CF6-50 double-annular combustor as developed in the NASA ECCP. (CF6-50C core flow at takeoff is 119 Kg/sec (262 lb/sec) versus 63 Kg/sec (139 lb/sec) for the E<sup>3</sup>).

In general, the length-to-dome-height ratios of the E<sup>3</sup> combustor are smaller than those for the CF6-50 design, but the E<sup>3</sup> reference velocity and dome velocities are lower than those of the CF6-50 design. Together, the short lengths and low velocities of the E<sup>3</sup> combustor result in bulk-residence times that are almost the same as for the CF6-50 design. These low velocities are expected to provide better flame stability and better ignition performance.

In the double-annular combustor design concept, fuel is supplied to only the outer annulus at idle and other low-power operating conditions. At higher power operating conditions, fuel is supplied to both annuli. In the NASA ECCP, the lowest CO, HC and NO<sub>x</sub> levels were obtained by highly biasing the combustor airflow distribution in favor of the inner annulus. In this manner near-stoichiometric fuel-air ratios are provided in the low-velocity and long-residence-time, outer-dome region and, as a result, high combustion efficiencies and low CO and HC emissions levels are obtained at low-power operating conditions. At the high-power engine operating conditions, increasing percentages of fuel flow are supplied to the inner annulus. At

TABLE 64

E<sup>3</sup> COMBUSTION SYSTEM EMISSIONS GOALS AND  
AERODYNAMIC PERFORMANCE REQUIREMENTS

Emissions

CO (Max)	}	(Pounds per	Kg per	3.0
HC (Max)	}	1000 pound	1000 Kg	0.4
NO <sub>x</sub> (Max)	}	thrust-hours	thrust-hours	3.0
		per cycle)	per cycle	
Smoke (SAE-SN)				20.0

Performance

Combustion Efficiency - at High Power (min), %	99.5
Total Pressure Drop (Max), %	5.0
Exit Temperature Pattern Factor (Max)*	0.25
Carboning of Swirl Cups Parts	None
Resonance/Rumble	None

\*Pattern Factor (max) = 
$$\frac{T_{\text{max local}} - T_{\text{avg}}}{T_{\text{avg}} - T_3}$$

T max local - maximum localized gas temperature in combustor discharge annulus

T avg - average gas temperature in combustor discharge annulus

T<sub>3</sub> - average compressor discharge temperature

TABLE 65

COMBUSTOR AERODYNAMIC DESIGN PARAMETER

Combustion System	E <sup>3</sup> Double Annular	CF5-60 Double Annular
Combustor Length - m (in.)	0.1778 (7.0)	0.328 (12.9)
Outer Dome Height - m (in.)	0.061 (2.4)	0.069 (2.7)
Inner Dome Height - m (in.)	0.0567 (2.2)	0.061 (2.4)
Length/Dome Height.- Outer	3.0	4.8
Length/Dome Height - Inner	3.3	5.4
Number of Fuel Injectors	56	60
Reference Velocity - m/sec (ft/sec)	16.76 (55)	22.86 (75)
Space Rate - $\frac{W}{m^3 \text{ atm}} \times 10^{-6}$ (Btu/hr-ft <sup>3</sup> -atm x10 <sup>-6</sup> )	82.7 (8.0)	63.1 (6.1)
Outer Dome Velocity m/sec (ft/sec)	5.49 (18)	9.75 (32)
Inner Dome Velocity m/sec (ft/sec)	19.51 (64)	26.52 (87)
Outer Passage Velocity m/sec (ft/sec)	42.67 (140)	36.58 (120)
Inner Passage Velocity m/sec (ft/sec)	42.67 (140)	46.03 (151)



climbout and takeoff operating conditions, about 80 to 85 percent of the total fuel flow is supplied to the inner annulus. Consequently, lean combustion is maintained in both annuli at these conditions, along with very short residence times in the high-velocity inner dome annulus. As a result, low NO<sub>x</sub> and smoke emissions levels are obtained.

The E<sup>3</sup> combustor is designed to operate in a similar manner. This operating procedure, based on test results obtained with the CF6-50 engine using the NASA ECCP double-annular combustor, is expected to result in high combustion efficiencies and low emission levels throughout the operating range of the E<sup>3</sup>.

Diffuser Design - As illustrated in Figure 94, the E<sup>3</sup> combustor inlet diffuser accepts core engine airflow from the compressor outlet guide vanes and divides this flow into two parallel passages. The outer passage curves outward and directs about 40 percent of the flow toward the outer dome annulus of the combustor. The inner passage directs the remaining 60 percent of the flow toward the inner dome annulus of the combustor. Each of these two passages has a diffusion area ratio of 1.6 and is designed to fall below the line of no stall on the Stanford diffuser flow regime correlation (reference 9).

Flow leaving this short prediffuser is dumped into the combustor liner passages and into the plenum region upstream of the combustor domes. The dumping area ratio in the liner passages is 2.0, and the resulting dumping pressure loss is small because the compressor exit velocity head, which is 5.5 percent of the total pressure at takeoff conditions, is reduced to 2.1 percent by the prediffuser. Nearly all of this prediffuser exit velocity head is recovered in a "free stream" diffusion region entering the plenum region ahead of the combustor domes. With this configuration, total pressure losses from the compressor OGV's to the combustor domes are very small.

Total pressure losses into the liner passages are estimated to be about 2.1 percent and the loss into the dome plenum region is estimated to be about 0.85 percent of the compressor exit total pressure. Trade-off studies relating prediffuser area ratio and length to engine weight and sfc show that this diffuser design represents the best combination of these parameters.

Dome Design - The double-annular combustion system selected for the E<sup>3</sup>, as illustrated in Figure 94 is actually two parallel combustors. The outer combustor-dome assembly is designed to operate with low CO and HC emissions levels and good performance at idle and other low power flight conditions. The inner dome assembly is designed to operate with low NO<sub>x</sub> and smoke emissions levels at the high power flight conditions.

Twenty-eight swirl cups are equally spaced around the outer dome annulus. These cups pass about 10.3 percent of the total combustor airflow into the outer annulus combustion zone. When all of the fuel flow is supplied to the outer, this amount of airflow results in relatively rich fuel-air mixtures in the outer zone and, thus, good performance at light-off and idle operating conditions. Twenty-eight swirl cups are also equally spaced around the inner dome annulus. The inner annulus cups pass about 33.3 percent of the combustor airflow into the inner annulus combustion zone. This high flow results in lean fuel-air mixtures and high velocities in the inner annulus and, thus, low NO<sub>x</sub> emission levels at high power conditions.

Cooling Liners - The combustor liner cooling arrangement for the E<sup>3</sup> combustion system is a double-wall, impingement-plus-film-cooled configuration. This advanced liner-cooling design approach required less cooling flow than conventional film-cooling designs and increases the life capability of the combustion system.

With this cooling arrangement, an impingement baffle is used to meter small jets of cooling air that impinge on the outer surface of the combustor liner, providing very efficient cooling of this liner. This cooling air then flows upstream between the two walls and through film-slot-metering holes to the hot side of the combustor liner where the cooling flow becomes a protective film covering the entire inside surface of the liner.

Dilution Air Design - A single stage of liner dilution airflow is used for the outer and the inner annulus of the E<sup>3</sup> combustor, with dilution air introduced from the outer and inner liner walls and also from the outer and inner centerbody walls. In the outer combustor annulus, the dilution air is used to provide rapid dilution of the overstoichiometric-combustion gases leaving the swirl cups at idle operating conditions to provide an average primary-combustion zone equivalence ratio of about 0.6. If these conditions are maintained in the primary zone for a sufficient length of time, most of the CO that is generated will be consumed. In the inner annulus, dilution air is added to reduce NO<sub>x</sub> emission levels at high-power operating conditions by providing small jets of air that mix rapidly with the swirling fuel-air mixture leaving the dome swirl cups.

Although secondary dilution holes are not shown in the E<sup>3</sup> combustor design presented in Figure 94, a band of small dilution holes may be required near the aft end of the combustor to modify or trim the exit temperature profile characteristics. These dilution holes may be required in the outer liner or the inner liner, or in both. The need for these dilution holes will be determined by combustor development test experience.

#### d. High Pressure Turbine

##### 1. Design Point Selection

Turbine requirements at the primary operating points are summarized in the following table.

<u>Point</u>	<u>SLTO</u>	<u>Mx Cl</u>	<u>Mx Cr</u>
Energy Function, $\Delta h/T$	0.0832	0.0833	0.0833
Corrected Speed, $N/\sqrt{T}$	243.7	238.7	239.4
Flow Function, $W\sqrt{T}/P$	17.51	17.54	17.53
Stage Loading, $\Psi\Delta h/2u^2$	0.631	0.659	0.655
Efficiency, $\eta_T$	0.922	0.925	0.925

Since maximum values of temperature and stress are encountered at SLTO conditions, HP turbine mechanical design is usually performed at this point. In view of E<sup>3</sup> program goals and the small differences in aerodynamic parameters (between SLTO and max cruise) however, max. cruise conditions were selected for the aerodesign operating point.

## 2. Aerodynamic Design

Previous studies identified a two-stage HP turbine as the most appropriate configuration for E<sup>3</sup>. Cycle and fan improvements during Task III led to a substantial reduction in LP shaft speed and a consequent increase in LP turbine aerodynamic loading. In order to avoid an attendant reduction in LP turbine efficiency, the LP turbine flowpath was redesigned to accommodate an inter-turbine transition duct. In order to avoid excessive duct length and endwall curvature, the HP turbine flowpath was also redesigned. Primary aerodynamic features of this flowpath are:

- Constant hub diameter
- Conical rotor tip shroud permitting a more gentle contouring of the outer wall
- Improved stator band/rotor platform axial gap geometry
- Recent developments indicate potential for reduction of secondary flow losses through stator annulus convergence. In order to exploit this and also to provide a smoother combustor/turbine flowpath transition, stage one stator endwalls were contoured as shown in Figure 95.

The flowpath geometry is shown compared to CF6-50 in Figure 95.

Vector diagram calculations were made for a stage energy distribution of 0.55/0.45 for stages 1 and 2 respectively. Resultant internal aerodynamic parameters are summarized in Table 66. Blading geometry selections were made generally consistent with CF6 engine experience except where recent aerodynamic development indicated beneficial deviations.

## 3. Performance Prediction

Due to substantial similarity to the CF6-50 HP turbine, the E<sup>3</sup> HP turbine efficiency prediction for a fully developed turbine was accomplished by employing the status efficiency of the -50 turbine as a base and applying adjustments for identifiable differences relative to the E<sup>3</sup> turbine. The final Task III prediction is summarized as follows.

### High Pressure Turbine Efficiency

	<u>E<sup>3</sup></u>
Base Uncooled Efficiency (zero tip clearance)	0.943
- Adjusted to $\Psi = 0.655$	0.001
- Reduced aspect ratio	-0.001
- Rotor tip clearance loss (clearance)	-0.015 (0.016 in.)
- Improved band/platform overlap	0.001
- Rotor 1 pressure side bleed	0.001
- Improved airfoils and flowpath	0.003
- Cooling effects	-0.008
Installed Efficiency	0.925

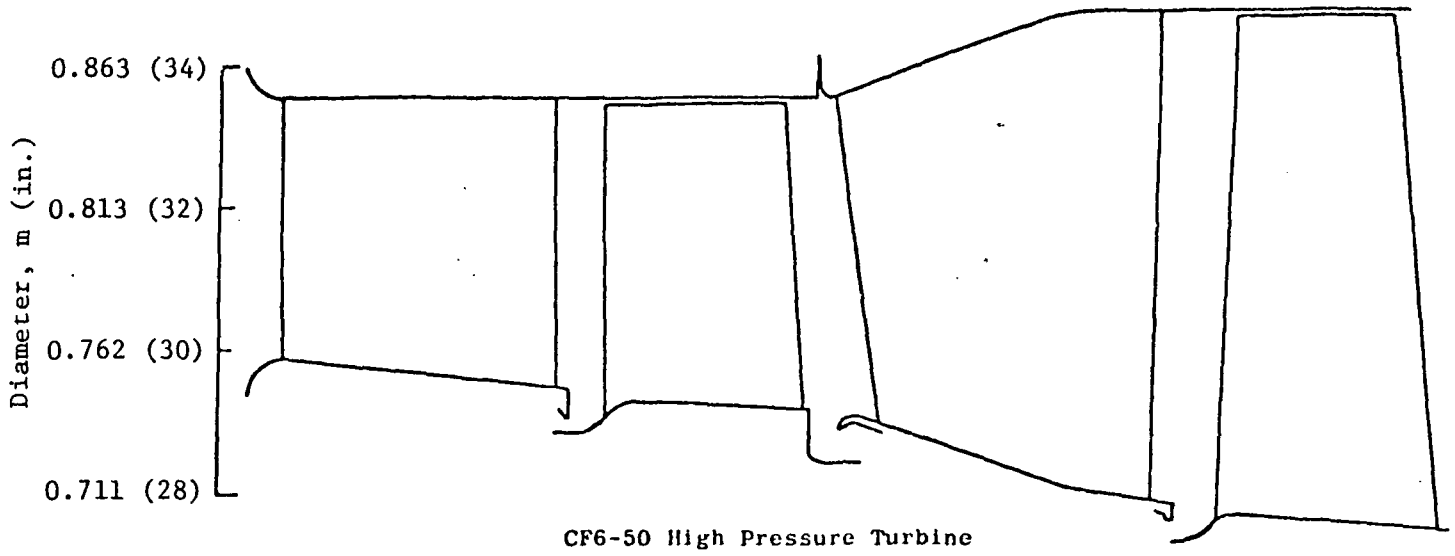
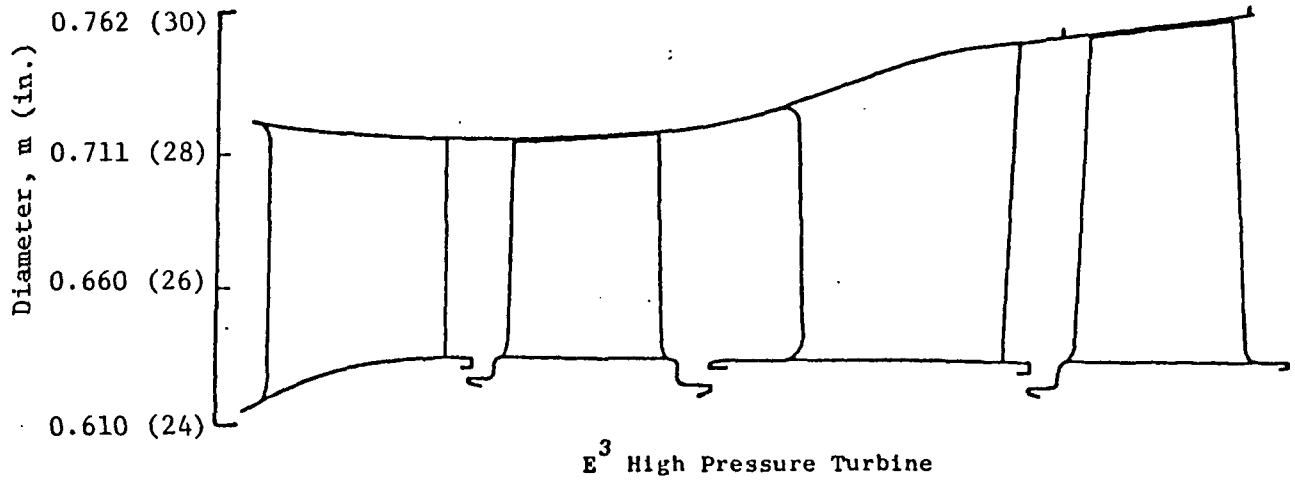


Figure 95. High Pressure Turbine Aerodynamic Flowpath.

TABLE 66

AERODYNAMIC STATUS COMPARISONS OF THE HPT

Engine	<u>E<sup>3</sup> - Task III</u>		<u>CF6-6</u>		<u>CF6-50</u>	
	1	2	1	2	1	2
Stage						
$\Delta h/T$	0.046	0.044	0.041	0.041	0.047	0.038
P/P	2.25	2.17	2.06	2.07	2.29	1.91
$\psi \sim \Delta h/2u^2$	0.74	0.57	0.84	0.72	0.82	0.55
$\alpha_1$ pitch	73.9°	66.9°	73.2°	69.0°	71.7°	64.7°
$\beta_2$ pitch	65.2°	57.4°	63.1°	60.4°	62.9°	56.7°
$M_2$ abs	0.34	0.46	0.36	0.44	0.43	0.46
Swirl	11.5°	0	15.0°	16.5°	20.1°	2.7°
$M_1$ hub	1.01	0.99				
$M_1$ rel hub	0.47	0.45				
$\beta_1$ hub	55.3°	38.7°				
$M_2$ rel pitch	0.79	0.86				
Reaction	0.26	0.31				
Radius Ratio	0.883	0.833				
No. of Vanes	46	60				
Ax Width, AW	1.3	1.50				
Zweifel No., $\psi_z$	0.73	0.91				
Edge Blockage	0.065	0.063				
Aspect Ratio, $h/d_o$	2.96	3.76				
Aspect Ratio, $h/AW$	1.06	1.61				
No. of Blades	86	90				
Ax Width, AW	1.04	1.13				
Zweifel No., $\psi_z$	1.11	1.02				
Edge Blockage	0.067	0.071				
Aspect Ratio, $h/d_o$	3.95	4.76				
Aspect Ratio, $h/AW$	1.59	2.19				

h = radial height

 $d_o$  = throat opening

### e. Low Pressure Turbine

Based on study, the E<sup>3</sup> low pressure turbine is a five-stage, close-coupled design requiring no airfoil cooling. The loading of this turbine is moderate with an overall loading factor of 1.24 (first two stages more highly loaded), an energy function ( $\Delta h/T$ ) of 0.0775, and a fully developed efficiency of 91.7% which includes an allowance for a small (.4%  $\Delta P/P$ ) transition loss.

The selection of the moderately loaded, five-stage turbine was based on results obtained during IR&D and NASA-funded programs aimed at fundamental research and development of highly loaded, low-pressure turbines. Extensive system studies were also made in conjunction with the fan design so as to obtain the best impact on sfc and DOC. In addition, the design selected for the E<sup>3</sup> application derives maximum benefit from the outstanding efficiency of the TF39, CF6, and TF34 high-bypass-ratio turbofans.

#### 1. Aerodynamic Design Requirements

The aerodynamic design requirements for the low pressure (LP) turbine at the  $0.8 M_n / 10668 \text{ m}$  (35K) max cruise operating point are:

Inlet Pressure  $P_T = 251.4 \text{ KPA}$  (36.46 psia)

Inlet Temperature  $T_T = 1011^\circ\text{K}$  (1901°F)

Rotational Speed  $N = 3457 \text{ rpm}$

Energy Function  $\Delta h/T = 0.0775$

Corrected Speed  $N/\sqrt{T} = 79.3$

Flow Function  $W\sqrt{T}/P_T = 79.64$

Pressure Ratio  $P_{T_2}/P_T = 4.50$

Efficiency  $\eta_{TT} = 0.917$

#### 2. Preliminary Design

The objective of the preliminary aerodynamic design task was to evaluate candidate turbine systems that meet overall objectives with particular attention given to features that will reduce losses without incurring undue risk.

A preliminary design for the E<sup>3</sup> LP turbine was conducted in Task III of the E<sup>3</sup> study contract. The flowpath design, stage loading distribution, and airfoil-solidity selection were based on proven designs from the NASA Three Stage Highly Loaded Fan Turbine Program, the General Electric IR&D-funded Highly Loaded Fan Turbine Program, and General Electric CF6-50 fan turbine experience.

It was concluded from these experimental programs that the items causing most concern to the aerodynamic design of highly loaded LP turbines are:

- Large annulus flare between blade rows with potential diffusion losses.

- Increased end-wall, secondary-flow losses generated within the blade rows which continue to interact with the mainstream and generate additional losses in downstream blade rows.
- Rotor blade tip leakage losses.
- Aerodynamic coupling of the main gas stream and wheel space cavities. Experimental results indicate significant radial pumping of main gas stream fluid into and out of wheel space cavities behind highly loaded blade rows due to nonuniform circumferential static pressure gradients.

In view of the above items, a preliminary configuration was selected for the E<sup>3</sup> LP turbine (Figure 77). The associated vector diagram information is presented in Table 67. Salient aerodynamic features of this preliminary turbine design, which address these aerodynamic problem areas, are given below:

- The aerodynamic loading level, which is higher than those found in current-production LP turbines, was selected based on two factors: (1) recent experimental results of advanced LP turbine aerodynamic designs show that through the utilization of advanced design concepts the number of stages and/or diameters can be reduced (increased loading) and still maintain or improve turbine performance levels relative to existing production turbines, and (2) trade-off studies involving the impact of turbine loading on performance, weight, and cost indicate a net gain in DOC for the loading level selected for this design.
- The aerodynamic loading on the first two stages was maintained at a reasonable level by including a short transition duct ahead of the stage-one stator to transport the main gas stream radially outward while minimizing engine length.
- Through-flow Mach numbers, the stage energy extraction distribution, and the transition duct design were selected to maintain moderate slopes and curvatures on the flowpath walls, except in the stage-one nozzle, where a relatively large slope is employed.
- The rotor airfoils are shrouded and include a tip clearance control system to reduce tip leakage losses at design and off-design operating conditions.
- The preliminary stator and rotor airfoil solidity selection was based on existing General Electric solidity criteria. Pure tone blade passing frequencies were considered in selecting the number of blades in the last two stages.

#### f. Mixer Design

The Mixer Design was based on the data obtained at General Electric on scale model and full scale engine tests as well as the data of T.H. Frost (Reference 10).

TABLE 67

E<sup>3</sup> - LP TURBINE PRELIMINARY VECTOR DIAGRAM PARAMETER

Parameter	Stage				
	1	2	3	4	5
Stator					
Inlet Angle-°	0.0	39.18	36.24	30.00	20.38
Exit Angle-°	57.22	54.32	52.98	51.17	46.98
Total Turning-°	57.22	93.50	89.22	81.17	67.36
Exit Mach Number	0.720	0.761	0.716	0.648	0.566
Rotor					
Inlet Angle-°	50.28	46.57	44.50	40.95	32.17
Exit Angle-°	54.44	53.05	51.22	47.61	38.70
Total Turning-°	104.72	99.62	95.72	88.56	70.87
Inlet Mach Number	0.581	0.614	0.571	0.513	0.450
Exit Mach Number	0.739	0.754	0.700	0.641	0.600
Wheel Speed m/sec(ft/sec)	(543.0)	(585.0)	(628.1)	(671.5)	(700.8)
	165.5	178.3	191.5	204.7	213.6
Stage					
Efficiency	0.888	0.894	0.907	0.916	0.920
Energy Function	0.0186	0.0203	0.0193	0.0168	0.0128
Pressure Ratio	1.380	1.422	1.390	1.329	1.240
Loading	1.85	1.65	1.32	0.99	0.67
Exit Swirl-°	39.2	36.2	30.0	20.4	6.2



The resultant design for a 65% mixing effectiveness using the current design practice curve, calls for a  $\frac{PL}{D_h^2}$  of 7.3. This was accomplished with

a 24 lobe mixer having a perimeter at the mixing plane of 16.26 m (640 inches) with a mixing length of .889 m (35 inches) and an integrated average hydraulic diameter of 1.404 m (55.5) inches.

g. Pressure Losses

The inlet pressure recovery ( $P_{T2}/P_{T0}$ ) at cruise was evaluated using data obtained from the CF6/DC10. The design cruise inlet throat Mach number was 0.72 which results in an inlet recovery of 0.9957 while the growth engine inlet Mach number was 0.761 which results in an inlet recovery 0.9954.

The fan duct was designed starting with the initial (fan exit) Mach number of 0.5 and then transitioning to approximately 0.46 (to minimize friction losses) and then again transitioning to M - 0.56 at the mixing plane. The mixing plane Mach number was an optimization of the external boattail angle and internal losses. The design criteria for mixing plane Mach number is Mach 0.5 to 0.6, thus the Mach 0.56 was acceptable. The skin friction drag pressure losses were determined using the DUCTLS computer program which uses a one-dimensional analysis to establish wall Mach numbers and pressure distributions to calculate the friction pressure losses. For those portions (80% was assumed) of the duct which have acoustic treatment, the friction pressure loss is increased by 37.5% to account for the additional loss due to the increased surface roughness of the acoustic treatment. The remainder of the losses were evaluated in previous studies and were used directly for this duct loss evaluation. A summary of these losses is given in Table 68.

The pressure losses due to the mixer and ducting are discussed above. However, the pressure loss due to the thermodynamic mixing of the two flows is calculated in the cycle deck based on momentum, energy and continuity equations.

h. Installation External Drag

The design of the nacelle began with the inlet sizing which considered both the baseline engine and the potential growth engine. The inlet corrected airflows used were:

	<u>Nominal</u>	<u>Growth Engine</u>
Cruise	633 Kg/sec (1396 lb/sec)	648 Kg/sec (1428 lbs/sec)
Max Climb	644 Kg/sec (1419 lb/sec)	659 Kg/sec (1453 lbs/sec)
Takeoff	578 Kg/sec (1274 lb/sec)	604 Kg/sec (1331 lbs/sec)

Also it was assumed that this inlet would be subjected to take-off crosswind requirements of 12.86 m/s (25 knots) similar to the CF6 family of engines. This resulted in a throat which was elliptical. The throat minor axis (horizontal) is 1.885 m (74.2 in) and the throat major axis (vertical) is 1.916 m (75.4 in) while the hilit diameter is 2.153 m (84.7 in). This design gives a  $\frac{D_{HL}}{D_{TH}}$  = 1.142 along the horizontal axis (sides) and 1.124 for

the vertical axis (top and bottom) which is similar to the CF6-DC10.

TABLE 68

SYSTEM PRESSURE LOSS SUMMARY

E<sup>3</sup> - TASK III ENGINE

Conditions: Standard Day, M = 0.8, 35K Ft. Altitude (Cruise)

<u>FAN DUCT PRESSURE LOSS</u>	$\Delta P_T / P_{T13}$ in Percent
- Friction	0.58
- Acoustic Treatment (80% duct treated)	0.17
- Mixer Chutes (friction and Pressure)	0.11
- Steps, Gaps, Pylon Interference	0.20
- Thrust Reverser	0.07
- Scoops (similar to CF6 engine)	0.14
- Oil Cooler (none in fan duct)	-----
Fan Duct Total	<u>1.27</u>

<u>CORE DUCT PRESSURE LOSSES</u>	$\Delta P_T / P_{T57}$ in Percent
- Turbine Rear Frame	0.11
- Friction	0.20
- Mixer Chutes (friction and pressure)	0.47
- Steps and Gaps	<u>0.05</u>
Core Duct Total	<u>0.83</u>

<u>TAIL PIPE PRESSURE LOSSES</u>	$\Delta P_T / P_{T7}$ in Percent
- Friction	0.27
- Steps and Gaps	<u>0.05</u>
Tail Pipe Total	<u>0.32</u>

The  $D_{HL}/D_{MAX}$  was chosen as 0.88 to minimize the nacelle maximum diameter (the CF6/DC10 has a  $D_{HL}/D_{MAX} = 0.83$ ) and thus minimize the maximum cross sectional area and the resultant nacelle pressure drag. This resulted in a maximum nacelle diameter of 2.446 m (96.3 in) which is reached at a distance of .978 m (38.5 in) (X) aft of the hilite, for a  $X/D_{MAX} = 0.4$ . This value of  $X/D_{MAX}$  was chosen to avoid inlet drag rise for the  $A_0/A_{MAX} = 0.58$  at cruise. (Inlet drag rise design Mach number was 0.87.)

The afterbody was designed with a  $R/D_{MAX} = 4.0$  and maintained a terminal boattail angle of  $11^\circ$ . This was an optimization of the external drag at cruise and Mach number (losses) in the mixing region. The afterbody length was set to obtain the 65% mixing effectiveness noted in the previous mixer design section.

The external friction drag was calculated using flat plate skin friction with a supersonic velocity correction factor and a 1.05 multiplier (roughness factor) to account for steps and gaps and other protuberances which have not yet been defined in sufficient detail to evaluate accurately. This 1.05 roughness factor is consistent with other experience at General Electric. Both friction and pressure drag are calculated using the EXT Drag computer program. The isolated nacelle pressure drag was calculated utilizing the correlation curve of  $L/D_{eq}$  versus  $C_{D\pi}$ . It should be noted that the isolated nacelle pressure drag does not account for any interference drag which might occur by the interaction of the wing and nacelle/engine flow fields. This is booked separately and is highly dependent upon the installation. However, consideration was given to the installation of the E<sup>3</sup> nacelle on the supercritical wing in the nacelle design. The results of this isolated (interference free) nacelle drag analysis is as follows.

#### External Drag

Inlet, Fan Cowl and Afterbody Friction Drag	126.10Kg	(278 lbs)
Nacelle Pressure Drag (Isolated)	<u>65.7 Kg</u>	<u>(145 lbs)</u>
External Drag Total	191.8 Kg	(423 lbs)

#### 4. System Evaluation

##### a. Secondary Flow

A partial engine cross section which includes the high pressure turbine, combustor, and a portion of the compressor is presented in Figure 96 to show an overall view of the turbine cooling system. The turbine cooling and leakage flow rates and flowpaths are noted along with local pressures and temperatures for the nominal "heat transfer design" SLTO  $F_n$  point.

The cooling supply systems which route the coolant from the compressor extraction point to the cooled components have been designed for low pressure drop to maintain the high level of thermodynamic efficiency. The coolant pressure required at the component must be sufficient to achieve the required convection pressure drop, with margin for adequate hot gas backflow protection at the limits of operating conditions including allowance for manufacturing tolerances. With the component supply pressure levels established to meet the backflow criteria, low pressure drop supply systems and compressor source locations were selected based on the compressor interstage pressure distribution.

SUMMARY

<u>Description</u>	<u>Source</u>	<u>Flow - %W<sub>2</sub></u>
HP Turbine Non-Chargeable	CDP	9.83
HP Turbine Chargeable	CDP	5.31
	6th Bore Entry	1.10
	7th Fuel Heater	2.10
LP Turbine Non-Chargeable	6th Bore Entry	0.15
	7th Fuel Heater	0.20
LP Turbine Chargeable	6th Bore Entry	0.75

Total Cooling and Leakage Flows (%W<sub>2</sub>)

- CDP - 15.14%
- 6th Bore Entry - 2.0%
- 7th Fuel Heater - 2.30%

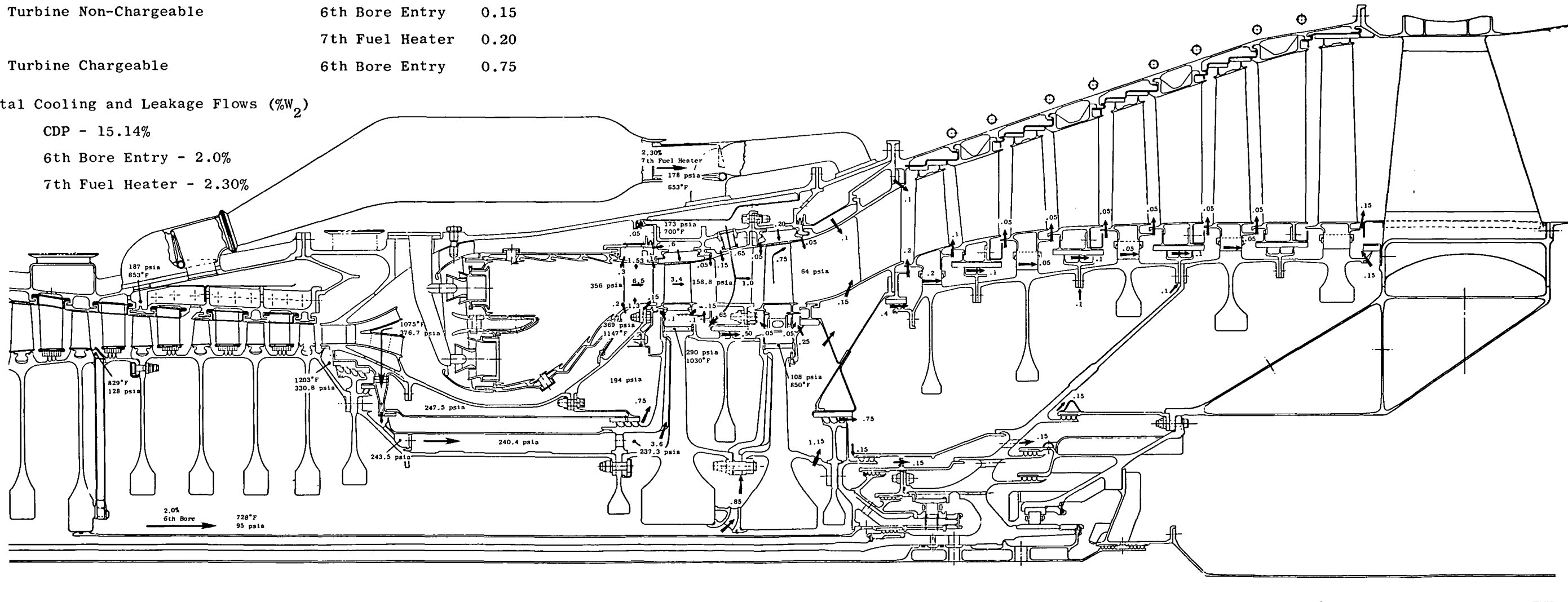


Figure 96. Turbine Cooling System -- Cooling and Leakage Flows, Pressures and Temperatures.

ORIGINAL PAGE IS  
OF POOR QUALITY

FOLDOUT FRAME

ORIGINAL PAGE IS  
OF POOR QUALITY

FOLDOUT FRAME

Low pressure drop piping and supply systems were selected to minimize the coolant throttling losses which could reduce thermodynamic efficiency. In addition, the design intent was to provide most of the coolant throttling at coolant discharge orifices (film holes, trailing edge holes, tip discharge holes, etc.) in order to assure better coolant flow control and minimize coolant mixing losses.

Upstream compressor bleed locations were chosen to supply cooling air to the Stage 2 turbine stator and rotor while satisfying backflow criteria. Use of the lower pressure air for coolant improves thermodynamic efficiency because less shaft work has been utilized in compression and a smaller quantity of coolant is required due to its reduced temperature.

### 1. Stage 1 Stator

The first-stage stator is cooled by air extracted from the inner and outer combustor liners. Low pressure drop screens are installed to trap contaminants, thereby preventing plugging of cooling holes. The vane leading edge cavity is fed from the inner flowpath and the aft cavity is fed from the outer flowpath. The rib separating the two cavities is slanted aft from tip to hub to provide maximum entrance areas for the two cavities.

### 2. Stage 1 Rotor Blade

The first-stage rotor blade is cooled by air extracted from the diffuser mean line to pick up cooler pitch line compressor discharge air. The expander which is used to accelerate the coolant in the direction of rotation and the coolant supply system seals are combined with the compressor discharge seal into one balanced sealing system which is located radially to provide adequate rotor thrust balance. The diffuser mean line bleed flow is also used to backpressure the compressor discharge seal, which results in a cooler operating seal temperature because the mean line bleed is 55°C (100°F) cooler than the endwall flow upstream of the compressor outlet guide vane. The compressor discharge seal leakage bypasses the expander discharge cavity to prevent heating of the rotor blade coolant. The bypass system routes the leakage to a cavity between teeth of the aft expander seal. The expander seal leakage then is used to purge the forward wheel space.

The cooling air expander is utilized to accelerate the Stage 1 rotor blade coolant in the direction of rotation at the location where the coolant enters the rotor, thereby reducing the power required to pump the coolant to the blades and reducing the associated temperature rise. The result is lower blade coolant temperature and thus lower coolant flow rate. The cooling air expander pressure ratio is chosen consistent with the blade coolant pressure required to satisfy the backflow criteria utilizing air at compressor discharge pressure. The reduced power required to pump the coolant corresponds to the shaft work which would be saved if the coolant were extracted from an upstream compressor stage sufficient to supply the required coolant pressure.

### 3. Stage 2 Stator

The Stage 2 stator coolant is extracted from the compressor at the Stage 7 stator. This flow is collected in manifolds and routed by pipes through a heat exchanger and to the turbine with a temperature drop. The

air is first used to cool the turbine casing and support structure to aid in clearance control. A valved bypass system is included in the turbine manifold to either route the coolant through or around the stator structure impingement plate for active clearance control.

A regenerative heat exchanger has been selected to reduce the temperature of the Stage 2 stator coolant thus reducing the quantity of air required. This regenerative system is a fuel-air heat exchanger, thus the heat removed from the coolant is rejected to the fuel and re-enters the cycle at the maximum pressure location giving maximum benefit to the cycle.

The heat exchanger improves the thermodynamic efficiency by reduced Stage 2 stator coolant flow and by reduced fuel flow.

#### 4. Stage 2 Rotor Blade

The Stage 2 blade is cooled with compressor Stage 6 bleed air which is extracted at the flowpath hub, behind the rotor. The coolant is routed through a radial inflow turbine, aft through the compressor drum, under the Stage 1 turbine disk and is pumped to the Stage 2 blades through a radial flow compressor. This design is similar to systems which have been demonstrated for Stage 1 rotor coolant supply on GE14 and GE23 advanced technology demonstrator engines.

##### b. Performance/Cycle

Task III included a more detailed review of the Task II baseline direct-drive, mixed-flow engine design. The major areas of study were directed at the low pressure spool components (i.e., fan/booster/LPT), design bypass ratio and HPT rotor inlet temperature (T41). As a result of these studies, the following changes were made to the Task II baseline engine to achieve the Task III FPS engine design:

- A more efficient fan design that results from a lower pressure ratio and lower tip speed.
- Addition of a quarter-stage behind the fan hub for more efficient core engine supercharging.
- A higher bypass ratio.
- An LP turbine design with a larger average diameter, which maintains nearly the same efficiency level at the slower rotational speed due to the addition of a short transition duct.
- Lower design T41 by 50°F.
- Revised secondary airflows.
- Addition of a cooling air/fuel heat exchanger.

The result of these design changes on performance was to improve the installed  $MxCr$  sfc advantage over the CF6-50, from the 12.1% of the Task II baseline engine to 14.4% for the Task III FPS. Figure 97 illustrates the installed sfc advantage (including nacelle drag) of the Task III FPS engine (scaled to the CF6-50C thrust size) over the CF6-50C across a cruise thrust operating range at 35K/0.80M/Std. day.

An overall definition of the Task III FPS engine cycle is given in Table 69. Airflow and thrust information are presented in the "design size" that resulted from the engine/airframe integration studies that are discussed in another section. A summary of engine component characteristics is presented in Table 70. Table 71 contains a detailed summary of component and cycle performance of the Task III FPS engine at the three rating points of 10668 m (35K)/0.80M/Std + 10°F (+18°F)/ $MxCl$ , 10668 m (35K)/0.80M/Std Day/ $MxCr$  and SLS Std -2.7°C (-27°F). Thrust and sfc for a typical flight profile are presented in Table 72.

Discussion of the parametric cycle design work that led to the changes involving the fan booster, LP turbine and bypass ratio is presented in an earlier section. The addition of the cooling air/fuel heat exchanger produced two benefits to the cycle performance:

- 1) it reduced the amount of cooling air required from the compressor 7th stage due to heat in this air stream being transferred to the fuel, and
- 2) the fuel has a higher average entering temperature which is represented in the cycle deck by an increase in Fuel Heating Value of 135 KJ/kg (58 BTU/lbm). Besides the effect of the heat exchanger, the revision of the secondary airflow system was due to the lower T41, a materials change to the HPT rotor, and a more detailed analysis than had been previously applied to this area of the engine design.

As part of the decision to use a quarter stage behind the fan hub, an investigation was conducted of the effect that a fan speed/core speed mismatch during reverse thrust operation might have on the operating line of the booster. During reverse thrust operation, all the fan bypass flow is diverted through the reverser with the core flow dumped into the large exhaust system. This will increase the extraction across the LP turbine and increase fan speed at a given core speed. Since the fan operating line also affects LP turbine energy requirements, two operating lines (i.e., reverser effective areas) were investigated. One matched the nominal operating line for the forward flight mode and the other was a 5% lower operating line. Figure 98 shows the shifts in fan speed versus core speed for these operating lines as compared to the nominal forward thrust mode configuration. The worst case indicates a 2.5% increase in fan speed at a given core speed. This would result in about a 3.5% reduction in booster stall margin. Even with this reduction, the booster will have adequate stall margin during reverse thrust operation.

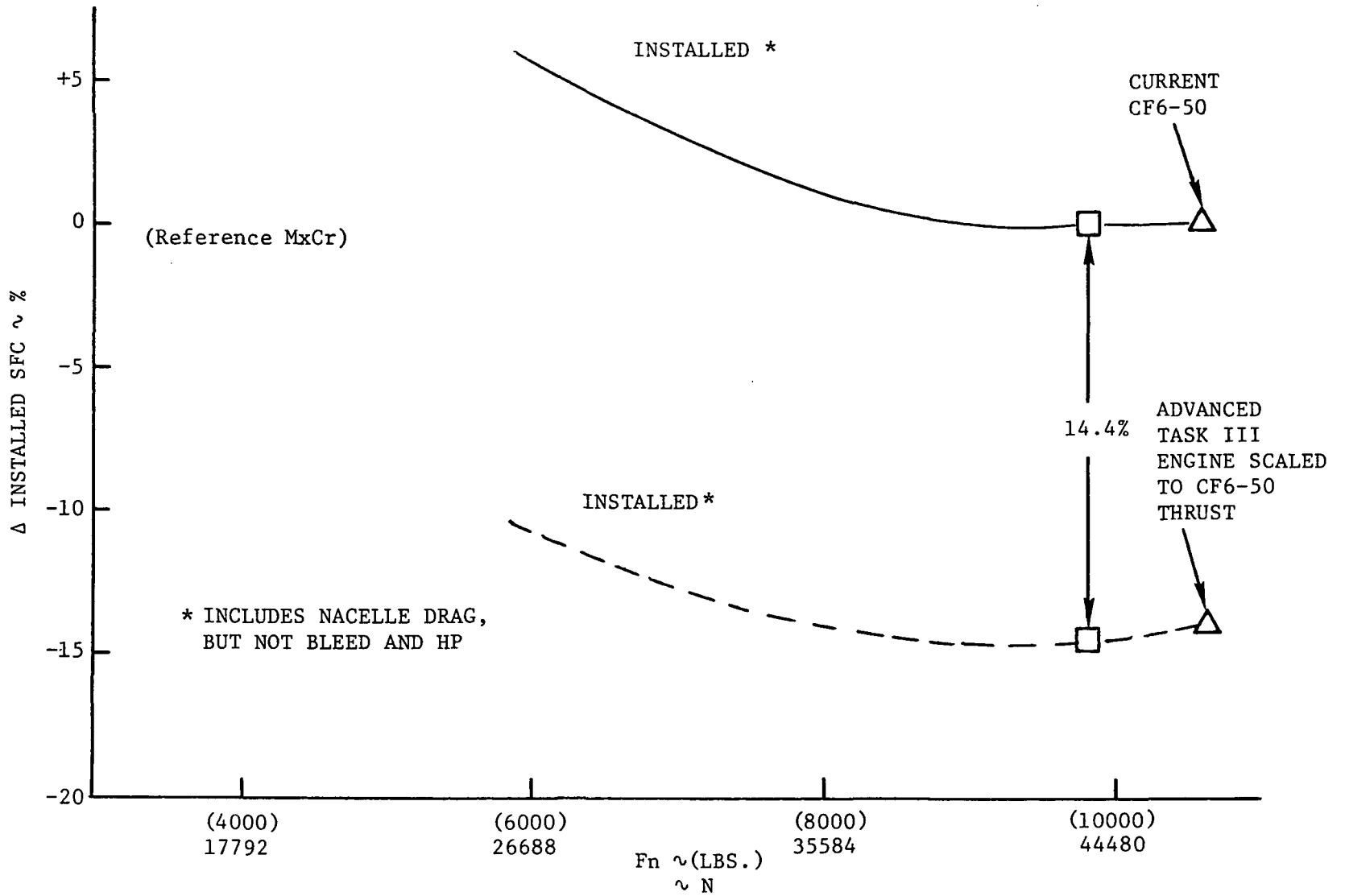


Figure 97. CF6-50C vs. Task III Study Engine - Cruise Performance Comparison  
10668m (35K)/.80M/Standard Day



TABLE 69

ENGINE CYCLE DEFINITION

Design Point at MxCl Mn = 0.8, 10,670 m (35K ft)

	<u>Task III - FPS</u>	
<u>Takeoff Std. Day +15°C (+27°F)</u>		
- $F_n$ , N (lb)	162,350	(36,500)
- $T_{41}$ , Turb. Rotor Inlet (Average Cycle)	1338°C	(2440°F)
- Fan Pressure Ratio (P/P)	1.50	
- Bypass Ratio	7.4	
<u>Mn = 0.80, 10,668 m (35K ft) Std. Day +10°C (+18°F)</u>		
- MxCl $F_n$ , N (lb)	40,200	(9040)
- $W\sqrt{\theta}/\delta$ at MxCl, kg/sec (lb/sec)	643	(1419)
- Fan $U_T/\sqrt{\theta}$ at MxCl, m/sec (ft/sec)	412	(1350)
- Bypass Ratio at MxCl	6.8	
- MxCr $F_n$ N (lb)	37,500	(8425)
- Booster P/P at MxCr	1.64	
- Core Comp. P/P/ $W\sqrt{\theta}/\delta$ kg/sec (lb/sec) at MxCr	22.3/53.2	(22.3/117.4)
- Overall P/P at MxCr	36.1	(37.7 at Design Point)
- $T_{41}$ at MxCr	1240°C	(2265°F)
- $T_{41}$ at MxCl	1282°C	(2340°F)

TABLE 70

ENGINE COMPONENT DEFINITION

	Task III - FPS
Fan Tip Diameter, m (in.)	2.11 (83.0)
Fan r/r	0.35
Fan Design	Part-span Shrouded Titanium
No. of Boosters	1 (quarter stage)
No. of Core Compressor Stages	10
Core Compressor r/r	0.50
Combustor Type	Double Dome, Low Emissions
No. HPT Stages	2
Cooling	Film Impingement; Bore-Entry Supply
No. LPT Stages	5
Average LPT Work Coefficient $\frac{gJ\Delta h}{2 U_p^2}$	1.24
Nozzle	Fixed Convergent/Divergent
Mixed-Flow Exhaust System	65% Effectiveness

TABLE 71

TASK III COMPONENT AND CYCLE PERFORMANCE SUMMARY  
FLIGHT PROPULSION SYSTEM AND MAX. GROWTH ENGINES

- Zero Bleed and HP Extraction, 100% RAM, Avg. New Engine

Rating	Flight Propulsion System			20% Growth Engine		
	Des. Point Max. Climb	Max. Cruise	Takeoff	Max. Climb	Max. Cruise	Takeoff
Altitude	10668m (35,000)	10668m (35,000)	0	10668m (35,000)	10668m (35,000)	0
Mach No.	0.80	0.80	0	0.80	0.80	0
Std. + T <sub>amb</sub> , °C (°F)	10 (+18)	0	15 (+27)	10 (+18)	0	15 (+27)
F <sub>n</sub> (W/O Drag), N (lbs)	40210 (9040)	37474 (8425)	162,352 (36,500)	48261 (10,850)	45103 (10,140)	194,822 (43,800)
sfc (W/O Drag)	0.599	0.540	0.301	0.580	0.588	0.334
Bypass Ratio	6.83	6.96	7.41	5.52	5.63	6.01
Overall Pressure Ratio	37.7	36.1	29.7	45.0	43.2	37.0
T41, °C (°F)	1283(2342)	1183(2161)	1338(2440)	1338(2440)	1236(2256)	1427(2600)
Fan Tip						
Corrected Airflow, kg/sec (lb/sec)	644 (1419)	635 (1399)	578 (1274)	659 (1453)	549 (1431)	613 (1351)
Pressure Ratio	1.65	1.61	1.50	1.75	1.71	1.60
Efficiency	0.874	0.882	0.897	0.864	0.872	0.886
RPM	3539	3387	3445	3926	3757	3916
Fan Hub & Booster						
Corrected Airflow, kg/sec (lb/sec)	82.2 (181.2)	79.65 (175.6)	68.7 (151.5)	101.1 (222.9)	97.9 (215.9)	87.4 (192.6)
Pressure Ratio	1.67	1.64	1.54	2.04	2.01	1.90
Efficiency	0.885	0.891	0.901	0.876	0.882	0.889
HP Compressor						
Corrected Airflow, kg/sec (lb/sec)	54.4 (120.0)	53.25 (117.4)	48.4 (106.6)	56.7 (125.0)	55.6 (122.5)	51.8 (114.2)

TABLE 71 (Con'td.)

Rating	Flight Propulsion System			20% Growth Engine		
	Des. Point Max. Climb	Max. Cruise	Takeoff	Max. Climb	Max. Cruise	Takeoff
Pressure Ratio	23.0	22.3	19.5	22.5	21.9	19.8
Efficiency	0.857	0.862	0.871	0.857	0.862	0.869
RPM	12,645	12,255	13,137	13,068	12,664	13,675
Combustor						
Efficiency	0.995	0.995	0.995	0.995	0.995	0.995
HP Turbine						
Pressure Ratio	4.89	4.91	4.89	5.19	5.22	5.20
Efficiency	0.925	0.925	0.921	0.924	0.924	0.921
LP Turbine						
Flow Function	78.8	78.8	79.0	87.9	87.1	88.2
Pressure Ratio	4.43	4.37	3.96	4.19	4.15	3.92
Efficiency*	0.917	0.917	0.921	0.914	0.915	0.920
Pressure Losses						
Intercompressor, %	1.80	1.71	1.39	1.97	1.89	1.61
Combustor, %	4.91	4.94	5.00	5.49	5.52	5.56
Core Exhaust Duct, %	0.55	0.53	0.44	0.62	0.61	0.56
Bypass Exhaust Duct, %	1.05	1.07	1.01	0.92	0.94	0.95
Tailpipe, %	0.34	0.34	0.34	0.34	0.34	0.34
Cooling & Parasitic Flows						
Non-Chargeable, %	9.83	9.83	9.83	11.90	11.90	11.90
Total Chargeable, %	10.11	10.11	10.11	11.34	11.34	11.34

\*Includes Transition Duct  $\Delta P$  loss.

TABLE 72

E<sup>3</sup> ENGINE PERFORMANCE FOR A TYPICAL A/C MISSION PROFILE

(Zero A/C Bleed and Horsepower Ext., 100% RAM)

Altitude Km	Altitude (FT <sub>1</sub> )	Mach No.	Std. + $\Delta T_0$ °C (°F)	Rating	Uninstalled Thrust		Performance sfc				
					(lbs)	(N)	lb/lb-hr	Kg/N-hr			
0	(0)	0.0	+15 (+27)	Takeoff	(36500)	162360	(0.302)	0.0308			
0	(0)	0.250	+15 (+27)	Takeoff	(27770)	123527	(0.401)	0.0409			
1524	(5000)	0.413	+10 (+18)	Max. Climb	(20560)	91455	(0.463)	0.0472			
3048	(10000)	0.452	↓	↓	(18280)	81313	(0.473)	0.0482			
3048	(10000)	0.576			(16725)	74396	(0.529)	0.0539			
6096	(20000)	0.692			(13290)	59117	(0.551)	0.0562			
9144	(30000)	0.800			(10370)	46128	(0.567)	0.0578			
10668	(35000)	0.800			(9040)	40212	(0.559)	0.0570			
10668	(35000)	0.800			Max. Cruise	(8425)	37476	(0.555)	0.0566		
10668	(35000)	0.740			Flt. Idle	(-1290)	-5738	(-0.283)	-0.0288		
9144	(30000)	0.667			↓	↓	(-1295)	-5760	(-0.339)	-0.0346	
6096	(20000)	0.547					(-1225)	-5449	(-0.519)	-0.0529	
4572	(15000)	0.497					(-1130)	-5026	(-0.676)	-0.0689	
3048	(10000)	0.452					(-980)	-4359	(-0.925)	-0.0943	
1524	(5000)	0.413					(-790)	-3514	(-1.37)	-0.1392	
113	(370)	0.200					Approach	(10440)	46439	(0.389)	-0.0397

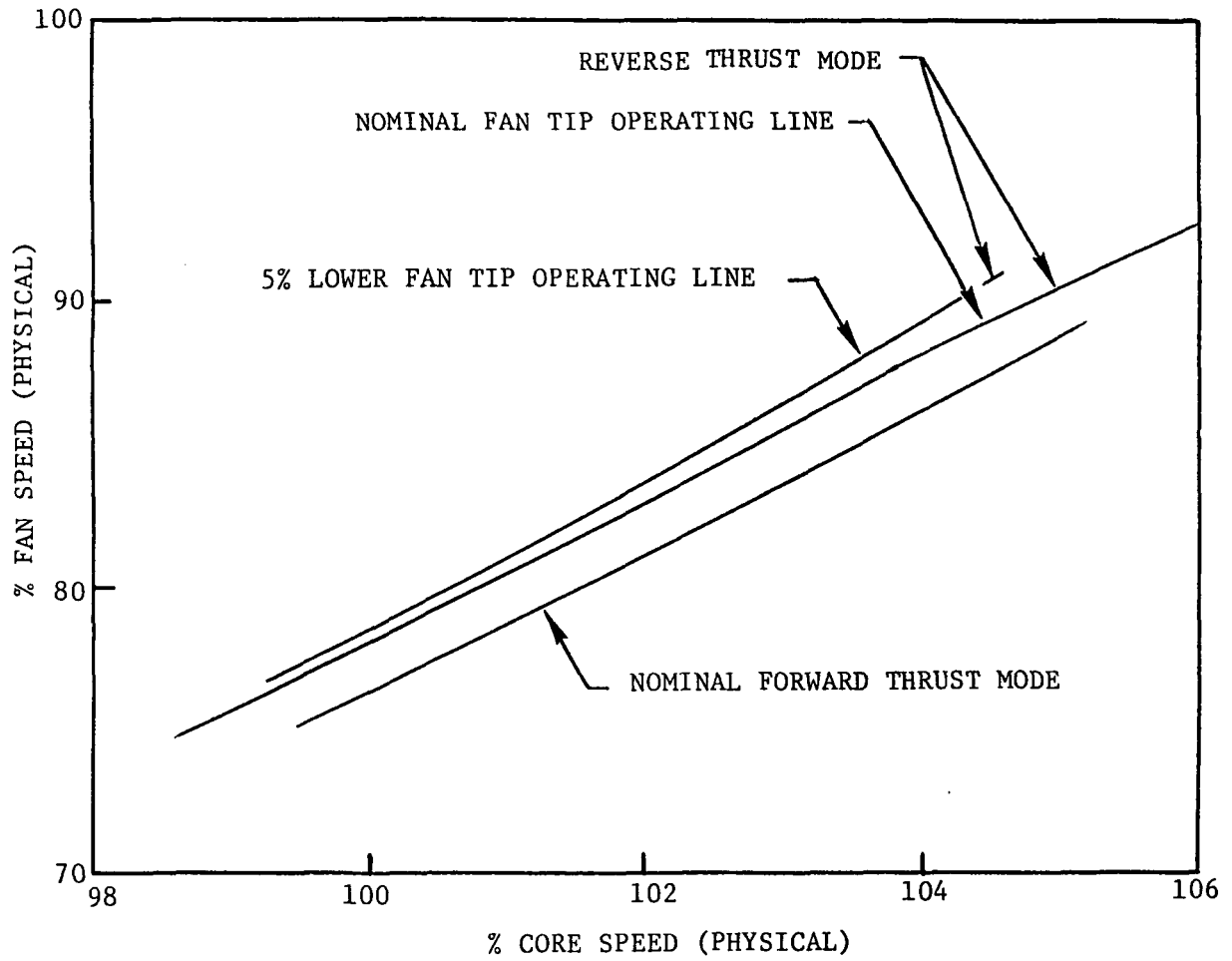


Figure 98. Task III Reverse Thrust Study % Fan Speed vs. % Core Speed

## 1. Task III - Growth Engine Design

The major goal in developing a growth engine design was to achieve a 20% balanced growth in thrust capability with a minimum of new engine hardware and material development. The growth engine design, whose component and cycle performance is summarized in Table 71, is based on the following changes from the Task III

<u>Design Change</u>	<u>Cycle</u>
Re-blade the fan at the same diameter	1.75 P/P at MxC1 457 m/sec (1500 ft/sec) Corr. Tip Speed
Increase the supercharging P/P	2.04 Boost P/P at MxC1 (45.0 Overall P/P at MxC1)
Readjust compressor stator schedule	4% more airflow at core speed
Higher design T41	+10°C (+18°F) / MxC1 T41=1338°C (2440°F) +15°C (+27°F) / TO R41=1427°C (2600°F)
Increased cooling flow	+2.1% non-chargeable +1.2% chargeable
Larger HPT diaphragm	$\Delta W_{41R} = + 3.9\%$
Larger LPT diaphragm (required to maintain the fan/core speed match)	$\Delta W_{49R} = + 12.0\%$
New mixer design (without changing the total mixed area)	$\Delta A_{E17} = -\Delta A_{E57} = 60 \text{ in}^2$
Smaller exhaust nozzle	$\Delta A_8 = -2.5\%$

The estimated installed MxCr sfc advantage of the growth engine over the CF6-50C in the same thrust size is 11.6%.

### c. Acoustics

System noise predictions were made for both a domestic and inter-continental trijet. Cycle data for the baseline and growth engines with a 54.4 Kg/sec (120 lb/sec) core were used to predict the engine component noise levels. These levels were then scaled to the appropriate thrust size to match the various engine/aircraft systems given by Table 73.

The inlet was assumed to have wall treatment equal to 0.54 fan diameter and the fan exhaust duct to have treatment on both the inner and outer walls. The aircraft altitude and Mach number at the takeoff monitoring point 6.486 Km (3.5 nm) from brake release and the thrust requirement at approach were defined by the aircraft systems studies. These are also shown on Table 73. The component noise levels were corrected to these flight conditions and a total system EPNL determined at each of the FAR36 certification points.

TABLE 73

ENGINE/AIRCRAFT SYSTEMS FOR ACOUSTIC EVALUATION

## Trijets

Type	Engine	Thrust SLS, kN (lbs)	Gross Weight, Kg (lbs)	Takeoff		Approach Thrust, %
				6.48 Km (3,5, nm) Altitude, m (ft)	Mach No.	
Domestic	Baseline	116.09 (26.1K)	126.64K (279.2K)	472.47 (1550)	0.22	35
Domestic	Growth	134.3 (30.2K)	152K (335K)	451.1 (1480)	0.22	35
Domestic	Reference (CF6-50)	134.3 (30.2K)	139.3K (307K)	612.6 (2010)	0.22	33
Intercontinental	Baseline	170.35 (38.3K)	196.4K (433K)	374.9 (1230)	0.24	35
Intercontinental	Growth	197.1 (44.3K)	235.7K (519.6K)	344.4 (1130)	0.24	35
Intercontinental	Reference (CF6-50)	203.3 (45.7K)	222.2K (489.9K)	502.9 (1650)	0.24	33



The noise estimation procedure used in these studies has been developed by General Electric for preliminary design efforts in which specific component and suppression spectra are not defined. Component and suppression estimates are made on the basis of PNL. The PNdB levels are summed logarithmically to obtain a total system PNL which is then corrected to EPNL using an empirical relationship. For the PNL to EPNL correction, the total in-flight spectrum is assumed to be primarily broadband in nature and requires no significant tone correction.

Tables 74 and 75 give the estimated noise levels for the respective aircraft. Also shown on the Table are the levels relative to both the 1969 and 1977 FAR36 requirements. With the domestic trijet (Table 74), all three engines, baseline, growth and reference, will meet the 1969 certification requirements with ample margin.

The 1977 requirements are more stringent and the reference engine would be marginal in meeting these levels. Both the baseline and growth engines will meet the 1977 requirements with margin. The growth engine has only 1.9 EPNL margin at takeoff but with trading of excess margin at approach and sideline conditions, would be acceptable.

With the international trijet (Table 75), essentially the same results are obtained. The higher takeoff noise levels relative to the goals are primarily related to the lower altitude attained at the 6.486 Km (3.5 nm) monitoring point. With this lower altitude the growth version has only 1 EPNdB margin but with trading would still be potentially acceptable.

Figures 99 and 100 give the resulting noise footprints for the domestic and international trijets using the baseline engine and reference engine. These footprints were generated using the slant range curves shown in Figure 101. These curves were generated by extrapolating available measured flight data to various distances using the standard procedure outlined in FAR36 (1969). The higher bypass ratio E<sup>3</sup> engine is significantly better at both approach and takeoff. The 90 EPNL exposure is reduced by approximately a factor of 3 for both systems.

#### d. Emissions

The predicted emissions levels of the E<sup>3</sup> double-annular combustion system are presented in Table 76. These predictions are based on correlations developed to predict the effects of cycle changes on emissions levels of the NASA ECCP double-annular combustion system. As shown in Table 76, the E<sup>3</sup> combustion system, with the standard engine cycle, is expected to meet all of the prescribed emissions requirements. With the growth-cycle version of this engine, the predicted CO and HC emissions levels are further reduced below the standards. The NO<sub>x</sub> emissions levels are increased because of the higher combustor inlet temperature and pressures at the growth cycle conditions.

These emissions predictions are based on test data obtained with the NASA ECCP double-annular combustion system. The engine cycle parameters for the E<sup>3</sup> are very similar to the parameters for the CF6-50C engine at equivalent cycle points. As mentioned previously, the somewhat lower combustor velocities and shorter system lengths of the E<sup>3</sup> combustion system result in bulk-residence times for the E<sup>3</sup> combustor that are almost the same as those for the CF6-50 double-annular combustor. Therefore, the

TABLE 74

ESTIMATED ENGINE NOISE  
DOMESTIC TRIJET  
SUPPRESSED NOISE LEVELS - NO MARGIN

	<u>Baseline</u>			<u>Growth</u>			<u>Reference</u>		
	<u>Task III Engine</u>			<u>Task III Engine</u>			<u>CF6-50</u>		
	T/O	APP	SL	T/O	APP	SL	T/O	APP	SL
Engine Noise, EPNdB	93.1	96.0	90.9	96.7	97.6	93.5	99.4	99.7	98.2
$\Delta$ Relative To:									
FAR36 (1969)	-9.4	-9.8	-14.9	-7.1	-8.7	-12.8	-3.8	-6.3	-7.8
FAR36 (1977)	-4.5	-5.8	-8.0	-1.9	-4.7	-6.1	+1.3	-2.4	-1.0

TABLE 75

ESTIMATED ENGINE NOISE  
INTERNATIONAL TRIJET  
SUPPRESSED NOISE LEVELS - NO MARGIN

	<u>Baseline</u>			<u>Growth</u>			<u>Reference</u>		
	<u>Task III Engine</u>			<u>Task III Engine</u>			<u>CF6-50</u>		
	T/O	APP	SL	T/O	APP	SL	T/O	APP	SL
Engine Noise, EPNdB	96.5	98.2	91.3	100.2	99.3	97.0	101.3	101.2	98.5
$\Delta$ Relative To:									
FAR36 (1969)	-9.2	-8.8	-15.7	-6.8	-8.3	-10.6	-5.2	-6.2	-8.9
FAR36 (1977)	-3.6	-4.9	-9.2	-1.0	-4.3	-4.2	+0.5	-2.2	-2.5

TOTAL AREA OF CONTOUR,  $\text{KM}^2$  (ACRES)

CF6-50 22.4 (5547)

$E^3$  7.54(1865)

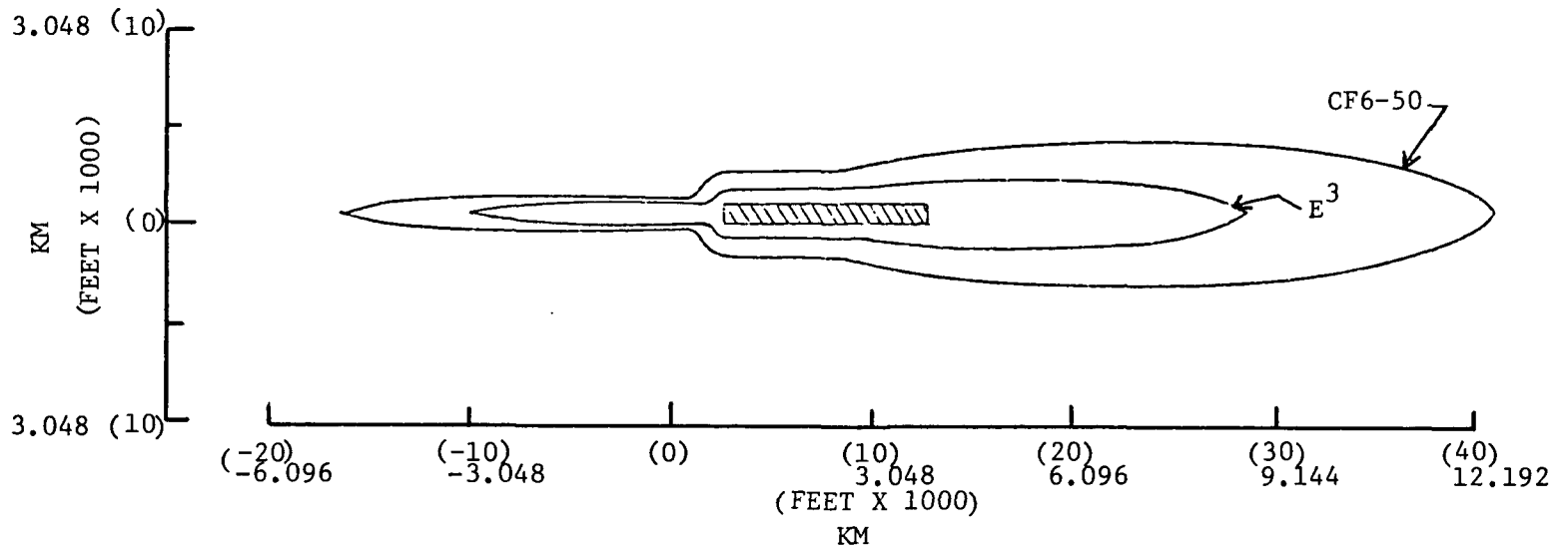


Figure 99. Domestic Trijet - 90 EPNL Contours

TOTAL AREA OF CONTOUR,  $\text{KM}^2$  (ACRES)

CF6-50 25.66 (6341)

$E^3$  9.92 (2452)

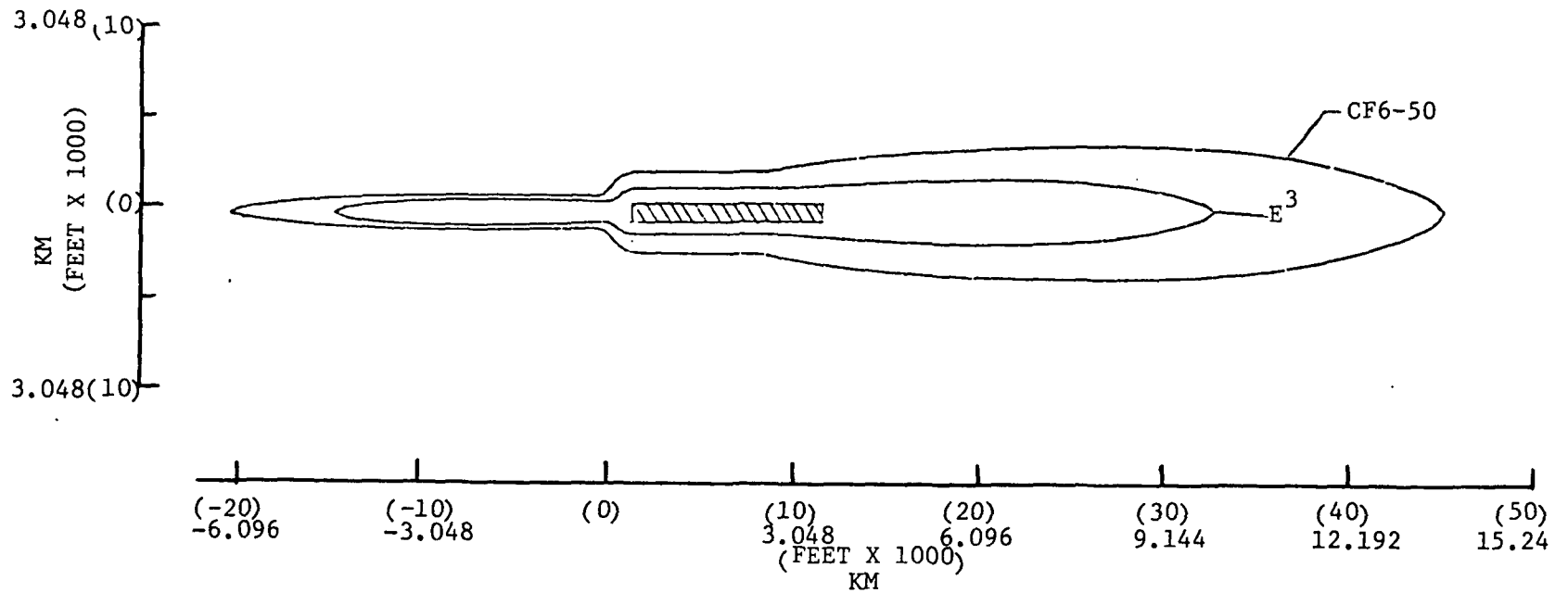


Figure 100. International Trijet - 90 EPNL Contours

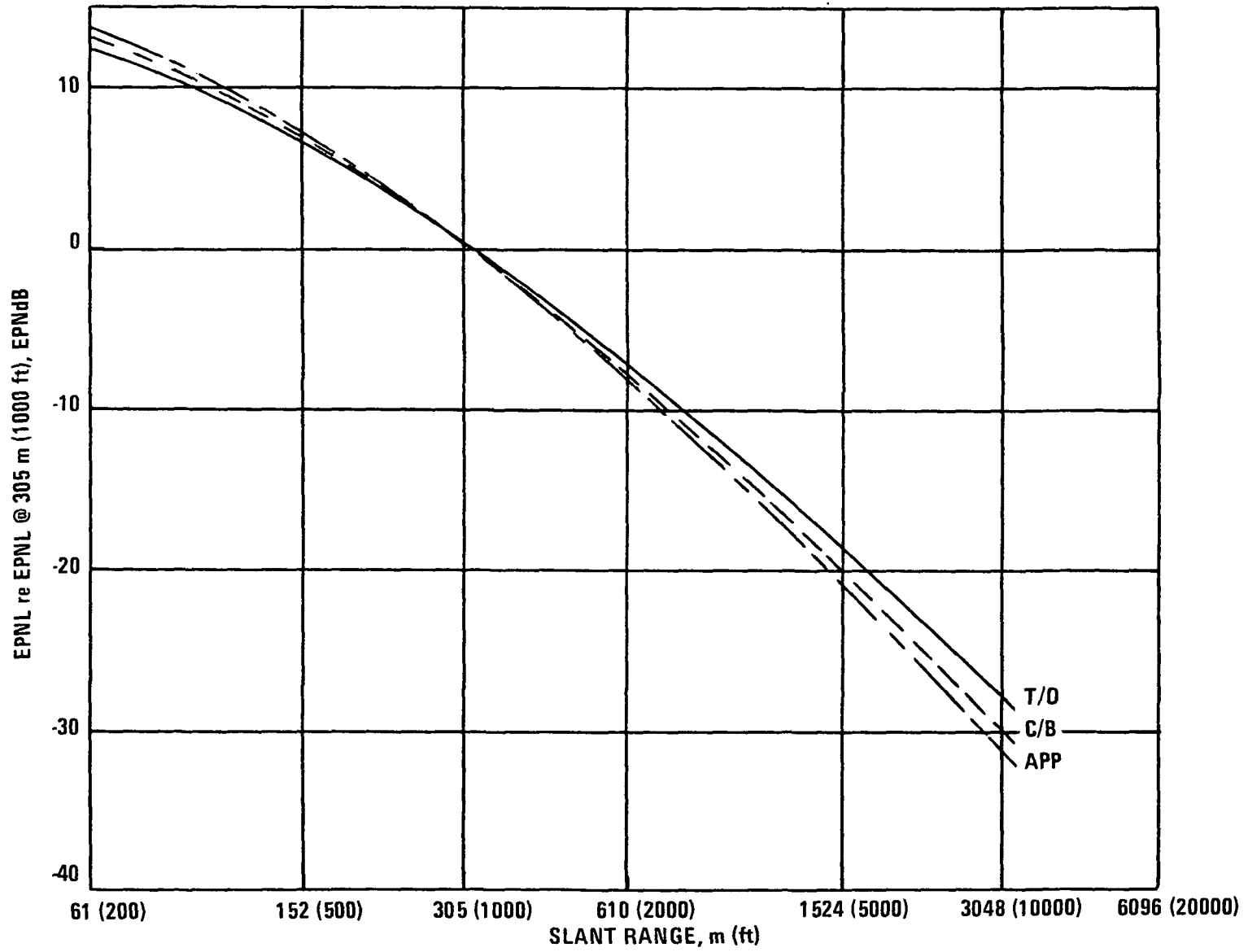


Figure 101. EPNL vs Slant Range for a High Bypass Ratio Turbofan Engine

TABLE 76

PREDICTED EMISSIONS CHARACTERISTICS OF E<sup>3</sup> COMBUSTION SYSTEM

Emission Category	E <sup>3</sup> Standard Cycle		E <sup>3</sup> Growth Cycle 6% Idle	Study Goals
	4% Idle	6% Idle		
CO	} Kg (lb) per 1000 lb Thrust hr-Cycle	2.4	1.5	3.0
HC		2.0	0.1	0.4
HO <sub>x</sub>		3.0	4.0	3.0
Smoke (SAE Smoke Number)		15.0	15.0	20.0

corrections applied to the NASA ECCP emissions data to predict the E<sup>3</sup> combustion system emissions are small. Thus, the predicted emissions values for the E<sup>3</sup> combustor are expected to be realized with an adequate amount of development effort.

e. Engine/Installation

The Task III preliminary design resulted in the definition of an installed engine configuration that followed the installation of the Task II engine. A long duct mixed flow installation with pylon mounted accessories was retained through Task III.

Characteristics of the Task III engine were estimated in the areas of weight, price and maintenance cost for use in the benefit analysis. These values are given in the Task III design size (54.4 Kg/sec (120 lb/sec) corrected core flow) and were subsequently converted to mission size in the next section.

1. Weight and Price Estimate

The weight and cost of a production flight propulsion system was estimated in the Task III engine design size ( $F_n = 162 \text{ KN (36500 lbs)}$ ) @ SLTO). Price was estimated based on a production cost of the 250th engine in 1977 dollars with a mark up to a selling price based on a factor used throughout the E<sup>3</sup> study.

Results are given in Table 77 for weight and selling price estimates for the bare engine, the installation and the installed engine.

2. Maintenance Cost Estimates

Maintenance cost estimates were taken from CF6-50C experience and CFM56 projections for a mature engine. Differences in part design lives, part costs and operating environments were factored into the estimate. Based on this, a parts cost per flight hour for a mature engine was estimated.

A total maintenance cost per hour was developed by taking 42.8% of the parts cost and using this as the direct labor cost component. This was patterned after typical airline experience as reflected in CAB reports. In addition to the parts cost, and direct labor cost, a burden of 200% of the direct labor cost was added to produce a total maintenance cost per flight hour per engine.

The results for the design size Task III engine are as follows:

Parts cost per flight hour	\$26.10
Direct labor cost per flight hour	11.19
Labor burden @ 200% D.L.	<u>22.37</u>
Total maintenance cost per flight hour	\$59.66



TABLE 77

WEIGHT AND PRICE ESTIMATE  
INSTALLED FLIGHT PROPULSION SYSTEM

Component	162353 N F <sub>n</sub> SLTO -(36500 Lbs.)	
	Weight (lbs)	Price (K\$)
Fan Module	(2405) 1091	519.7
LPT Module	(1315) 596.5	482.7
Core Module	(1920) 871.	715.7
Miscellaneous	( 750) 340.	237.2
Bare Engine Totals	(6390) 2899	1955.3
<u>Installation Item</u>		
Inlet	( 385) 174.6	94.7
Fan Reverser & Duct	( 915) 415.	240.2
Core Cowl	( 150) 68.04	37.2
Tailpipe	( 145) 65.8	34.2
Engine Build-Up	( 540) 245.	171.4
Installation Totals	(2135) 968.	577.7
Installed Engine Totals	(8525) 3867.	2533.

#### f. Benefits

The benefits analysis was performed in the same manner that the Task II benefits analysis was performed. Basically, a completely rubberized aircraft and engines were evaluated against a properly scaled CF6-50C powered aircraft with the same advanced aircraft technology applied. Only the mission and payload were fixed. An optimum aircraft was selected that satisfied all mission requirements from carpet plots covering a range of wing loading and thrust to weight ratio at the sea level take-off condition.

The expected benefit from a given advanced engine installed on an advanced aircraft can vary somewhat with the assumed aircraft technology level. These differences in technology can reflect themselves in TOGW differences and somewhat different lift/drag ratios at some of the more critical flight conditions such as take-off or climb. The characteristics of the General Electric advanced aircraft are given in Table 78 and go with the derivatives and benefit results obtained.

The same aircraft design used to evaluate the Task II engine was utilized for Task III. A partial description of the aircraft/mission/payload is given in Table 79. A set of rules used for the General Electric aircraft analysis economic study is given in Table 80. Table 81 is a more complete description of the General Electric study aircraft along with fuel burned savings for both a design and average mission relative to a scaled CF6-50C powered advanced aircraft.

Derivatives were developed for the General Electric study aircraft from making an analysis of a bare aircraft and engine and then perturbing the assumed engine characteristics slightly to determine the effect on mission merit factors such as DOC, Wf and TOGW. A set of derivatives for both aircraft flying an average mission with two levels of fuel pricing for each mission is given in Table 82. These were used to develop the benefits of the advanced engine when compared to the reference CF6-50C engine.

Table 83 presents a breakdown of the differences in  $\Delta$ DOC for the four major design/performance areas associated with the advanced engines. Two fuel cost levels were used for each average mission. All design values are in the mission sized engine thrusts. For the average domestic mission, there is an estimated 11-12% DOC reduction while the advanced engine produced an approximate 18.5% DOC reduction on the average intercontinental mission.

For the above results, the sfc effect at the maximum cruise condition was used for the  $\Delta$ DOC due to fuel savings.

Table 84 shows an estimated  $\Delta$ ROI result for two levels of fuel pricing for the domestic and international mission. Again, the maximum cruise level of  $\Delta$ sfc was used to determine the  $\Delta$ ROI impact of reduced fuel usage.

In terms of fuel burned, the estimated reduction at maximum cruise for an average domestic mission would be approximately 21% while the intercontinental mission produces nearly a 28% fuel reduction. The breakdown of

TABLE 78

GENERAL ELECTRIC STUDY AIRCRAFT ANALYSIS - A/C TECHNOLOGY ASSUMPTIONS

Wing Sweep 1/4C	30°
Wing Aspect Ratio	10
Wing T/C Average	12.5%
Wing Design	Supercritical
Fuselage Design	Wide Body - Twin Aisle
Aircraft Structural Weight	
Partial Composites	Tail, Surface Controls, Fuselage Floor, Pylon
Advanced Materials	Wing, Landing Gear
5% Lighter Wing, Fuselage, Landing Gear and Engine Pylons than 1976 Designs	
10% Lighter Tail	
15% Lighter Surface Controls	
Active Controls	
Partial	
0.95 Factor Applied to Tail Area	
0.95 Factor Applied to Wing Weight	
Engine Location	Two Engines on Wing, One in Tail
Payload	Pass Only. No Cargo in Design Payload
Aircraft Aerodynamics	1% Reduction in Interference Drag vs 1976 Design Level

TABLE 79

GENERAL ELECTRIC STUDY AIRCRAFT DESCRIPTION BY MISSION

	<u>Domestic</u>	<u>International</u>
Design Range -(N Mi)* Km	(3000) 5559	(5500) 10186
Design Payload - No. Passengers	225	225
Cruise Mach No.	0.8	0.8
Initial Cruise Altitude - Design Mission **	(35000')10668m)	(35000') 10668m
Takeoff Field Length - Design Mission	(8000') 2438m)	(10000') 3048m
No. of Engines	3	3
Timing	Mid 80's	Mid to Late 80's

\* Plus Standard ATA Reserves.

\*\* Step Cruise Used Where Possible and Efficient.

TABLE 80

GENERAL ELECTRIC STUDY AIRCRAFT ANALYSIS - ECONOMIC STUDY RULES

- TBC 1977 Update of Std. ATA DOC
- STD IOC Method Normally Used by Industry Updated to 1977 \$.
- ROI Calculated to Reflect the Discounted Return on Investment - "Present Value" of Money Considered.
- Interest Added as a Separate Expense (50% of Investment Borrowed)
- Revenue Yield Estimated Based on Data Available.
- Mature Engines and Airframe Used as Base.

TABLE 81

GENERAL ELECTRIC STUDY AIRCRAFT AND FUEL SAVINGS

	<u>Domestic Trijet</u>			<u>Intercontinental Trijet</u>		
Payload - Kg (Lbs.)	21126 (46575)	-	225 PAX	24392 (53775)	-	225 PAX
Design Range - Km (N. Mi.)		5556 (3000)			10186 (5500)	
Engine	Advanced E <sup>3</sup>		Scaled CF6-50C	Advanced E <sup>3</sup>	Scaled CF6-50C	
Wing Loading - Pa (lb/ft <sup>2</sup> )		5746 (120)			6703 (140)	
TOGW - Kg (Lbs.)	124740 (275000)		139255 (307000)	193687 (427000)		232697 (513000)
Fn/Engine - N (Lbs)	116093 (26100)		134330 (30200)	170358 (38300)		211280 (47500)
TOBFL @ 84°F - m (ft)	2256 (7400)		2133 (7000)	2743 (9000)		2560 (8400)
Approach Vel - m/sec (V <sub>K</sub> )	66.88 (130)		66.36 (129)	69.96 (136)		(135)
Fuel Burned - Kg (Lbs.)	26209 (57780)	<u>Δ's</u> -20%	32727 (72150)	63103 (139115)	<u>Δ's</u> -25%	83803 (184750)
Reserve Fuel - Kg (Lbs.)	5699.9 (12566)		6872 (15150)	10872 (23969)		13254 (29220)
Total Fuel - Kg (Lbs.)	31909 (70346)		39599 (87300)	73975 (163084)		97057 (213970)
BTU/Passenger Mile	1575			2068		
KWH/Passenger Km	0.249			0.327		
		1296 Km (700 N.Mi. Avg.) 55% LF			3704 Km (2000 N.Mi. Avg.) 55% LF	
Fuel Burned - Kg (Lbs.)	6235 (13745)	-20%	7811 (17220)	20446 (45076)	-24%	26939 (59390)
BTU/Passenger Mile	2920			3352		
KWH/Passenger Km	0.462			0.530		

TABLE 82

BENEFIT ANALYSIS DERIVATIVES

	<u>Domestic Trijet</u>				<u>International Trijet</u>			
Design Range (N. Mile) Km	(3000) 5556				(5500) 10186			
Avg. Mission Range (N. Mile) Km	(700) 1296				(2000) 3704			
Load Factor - %	55				55			
Fuel Costs (¢/Gal) \$/m <sup>3</sup>	(35/45) 92.46/118.88				(45/55) 118.88/145.30			
	Δ's - %				Δ's - %			
	DOC	ROI	TOGW	W <sub>f</sub>	DOC	ROI	TOGW	W <sub>f</sub>
1% sfc	.53/.59	-.17/-.18	.51/.57	1.31/1.31	.93/.98	-.36/-.38	1.12/1.12	1.69/1.69
(100 Lb.)45.36 Kg Engine/Nacelle	.19/.20	-.08/-.08	.31/.31	.26/.26	.19/.19	-.09/-.09	.28/.28	.26/.26
\$1/Flt. Hr. - Maint. Cost <sup>Wt.</sup>	.16/.15	-.03/-.03	---	---	.14/.13	-.03/-.03	---	---
\$1000 Engine/Nacelle Price	.005/.004	-.004/-.004	---	---	.003/.003	-.003/-.003	---	---

Note: Benefits Arise When:

- ΔDOC = -
- ΔROI = +
- ΔTOGW = -
- ΔW<sub>f</sub> = -

TABLE 83

TASK III ENGINE  $\Delta$  DOC BREAKDOWN  
 VS.  
CF6-50C REFERENCE (SCALED)

	Mission Sized			
	Domestic (Average)		International (Average)	
	<u>Design Value</u>	<u><math>\Delta</math> DOC-%</u>	<u>Design Value</u>	<u><math>\Delta</math> DOC-%</u>
Fuel Cost -( $\text{c}/\text{Gal}$ ) $\$/\text{m}^3$	$\Delta$	(35/45) 92.46/118.88	$\Delta$	(45/55) 118.88/145.30
Installed Wt. -(Lbs) Kg	(-909)-412	-1.7/-1/8	(-1398)-634	-2.7/-2.7
Installed Cost - K\$	+107.3	+0.5/+0.4	+124.5	+0.4/+0.4
*Maint. Cost - $\$/\text{Flt-Hr.}$	-14.51	-2.3/-2.2	-17.90	-2.5/-2.3
Installed $\Delta$ sfc-%	-14.4	-7.6/-8.5	-14.4	-13.4/-14.1
(Mx Cr. Std Day)				
		<u>-11.1/-12.1</u>		<u>-18.2/-18.7</u>

\* Includes a 200% Direct Labor Burden



TABLE 84

TASK III ENGINE Δ ROI BREAKDOWN  
 VS.  
CF6-50C REFERENCE (SCALED)

	<u>Domestic (Average)</u>		<u>International (Average)</u>	
	<u>Design Value</u>	<u>Δ ROI-%</u>	<u>Design Value</u>	<u>Δ ROI-%</u>
Fuel Costs -(¢/Gal) \$/m <sup>3</sup>	Δ	(34/45) 92.46/118.88	Δ	(45/55) 118.88/145.3
Installed Wt. -(Lbs) Kg	(-909) -412	+0.7/+0.7	(-1398) -634	+1.3/+1.3
Installed Cost - K\$	+107.3	-0.4/-0.4	+124.5	-0.4/-0.4
*Maint. Cost - \$/Flt-Hr.	-14.51	+0.4/+0.4	-17.90	+0.5/+0.5
Installed Δ sfc-%	-14.4	+2.4/+2.6	-14.4	+5.2/+5.5
(MxCr - Std Day)				
		+3.1/+3.3		+6.6/+6.9

\*Includes 200% Direct Labor Burden.

fuel saved as a function of installed  $\Delta sfc$  and installed weight difference is given in Table 85 to illustrate the relative contribution of engine weight and  $sfc$  to the total fuel burned savings.

## 5. Geared Turbofan Transmission Preliminary Design

### a. Summary

A preliminary design of an advanced main transmission gear for the geared turbofan of Task II was carried out. The major features of the design were higher 232°C (450°F) vs 165°C (300°F) operating temperatures to reduce gearbox accessory weight and permit lower windage losses than state-of-the-art designs.

Estimated weight savings over a conventional gearbox designed for the same life and mission are as follows:

● Lube Transfer Components	4.536 Kg	(10 lbs)
● Lube Oil Cooler	45.36	(100 lbs)
● Oil Storage Weight	<u>9.072 Kg</u>	<u>(20 lbs)</u>
	Total	58.97 Kg (130 lbs)

To permit operation at elevated temperatures, a synthetic ether base lubricant, MIL-L-27502 was assumed to be used. In addition, the gear and bearing material assumed was Timken CBS-600. This high temperature material has had some preliminary screening tests performed at General Electric under NASA Contract NAS3-14302. Although property evaluation of CBS-600 is incomplete, for the purposes of this study, CBS-600 at 232.2°C (450°F) was assumed equivalent to AISI 9310 at 148.9°C (300°F).

The baseline configuration selected as a result of trade-off studies was a 6 branch star type epicyclic gear train located in the forward sump of the geared turbofan as shown in Figure 102. Other results of the study are as follows:

● Total Weight (Gearbox and Accessories)	(542 lbs)	246 Kg
● Estimated Manufacturing Cost (250th Unit - 1977 Dollars)	\$47.2K	
● Estimated Efficiency		
Rating Point	T/O	Cruise
Fan(H.P.)KW	(32700) 24384	(12877) 9602.4
Fan RPM	3024	2960
Overall Efficiency - %	99.12	98.75
Heat Rejection -(Btu/Min) KW	(12126) 213.05	(6800 ) 119.5

With the above cost/weight and efficiency estimates, the system benefits for the Task II geared turbofan were slightly reduced from those obtained with a more preliminary gear design and evaluation. The more refined gear box design suggests that going from the Task II to these Task III results would mean a DOC increase of .15% over the Task II value and a 0.07% increase in mission fuel usage. Although small, the real significance is that the more refined gearbox study performed in Task III did not uncover any potential for expected improvements in the advanced geared turbofan.

TABLE 85

TASK III GEARED ENGINE  $\Delta W_f$  BREAKDOWN  
 VS.  
CF6-50C REFERENCE (SCALED)

	<u>Mission Sized (Mx.Cr. Condition Only)</u>			
	<u>Domestic (Average)</u>		<u>International (Average)</u>	
	<u>Design Value</u>	<u><math>W_f</math> - %</u>	<u>Design Value</u>	<u><math>W_f</math> - %</u>
	$\Delta$		$\Delta$	
Installed Wt. -(Lbs.) Kg	(-909) 412.32	-2.4	(-1398) 634.1	-3.6
Installed $\Delta$ sfc-%	-14.4	-18.9	-14.4	-24.3
(Mx.Cr. - Std Day)		<u>-21.3</u>		<u>-27.9</u>

## b. Study Content and Requirements

The following areas were covered by the study of an advanced technology main transmission gear for the Task II geared turbofan.

- Selection of gear box type.
- Bearing selection.
- Material selection.
- Lubrication System.
- Efficiency Estimate.
- Cost/Weight Estimates.
- Reliability/Maintenance Cost Estimates.
- Comparative Maintenance Factor Evaluation.

Design requirements laid out for the advanced gear box study were as follows:

- Minimum efficiency, 99.1% at T/O - 98.7% at cruise
- High reliability and safety
- 232 °C (450°F) gearbox and bearing capability
- Infinite gear life
- Individual B-1 bearing life of 8000 hours
- System B-10 life of 18000 hours
- Modular design concept
- Minimum system weight through high allowable oil temperatures.

The mission profile used for the gear box design is given in Table 86. A total mission time of just under two hours was used as an average. Bearing and gear lives were calculated based on the power spectrum given in Table 86.

## c. Study Results

### 1. Gear Configuration Selection

Three basic gear configurations were considered for this study. They were as follows:

- Planetary
- Star Drive
- Jack Shaft

A schematic of each of the above gear types is given in Figure 103. Although considered, the planetary gear was quickly eliminated since it did not seem well suited for the high speed operation or the gear ratio required (approximately 2.5:1). The high rpm requirements resulted in a very heavy planet gear carrier and the resulting centrifugal loads reduced the ability of the planet bearings to handle the high gear loads.

The major effort in the gear selection process was therefore devoted to evaluating the advantages (and disadvantages) of the star gear and jack shaft arrangements.

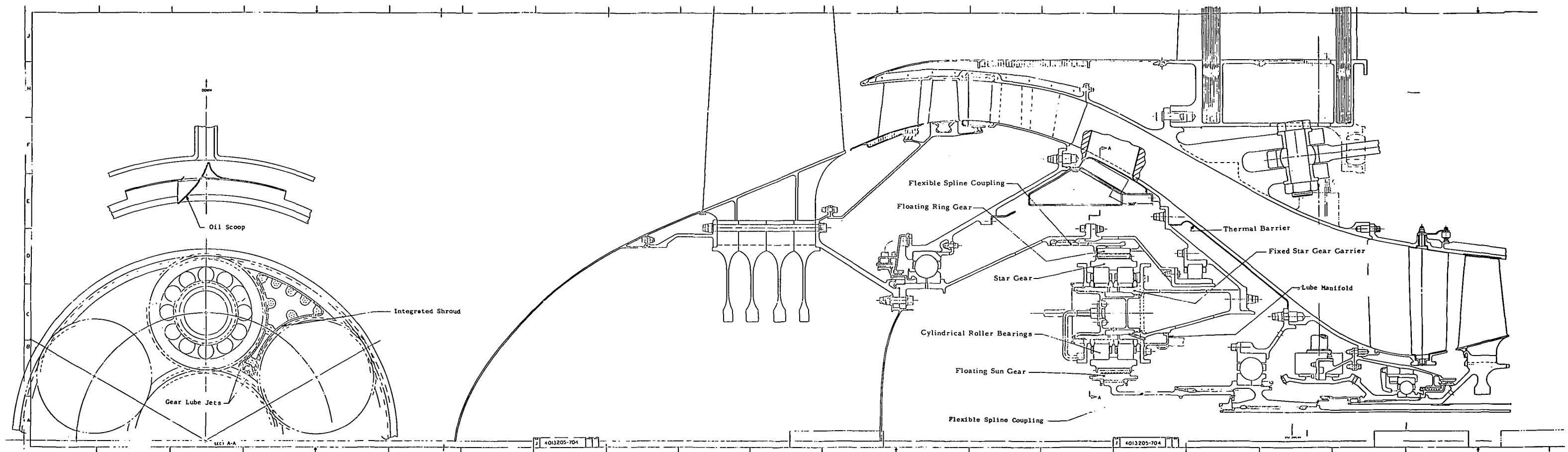


Figure 102. Baseline Gear Configuration

ORIGINAL PAGE IS  
OF POOR QUALITY

**FOLDOUT FRAME**

ORIGINAL PAGE IS  
OF POOR QUALITY  
2 **FOLDOUT FRAME**

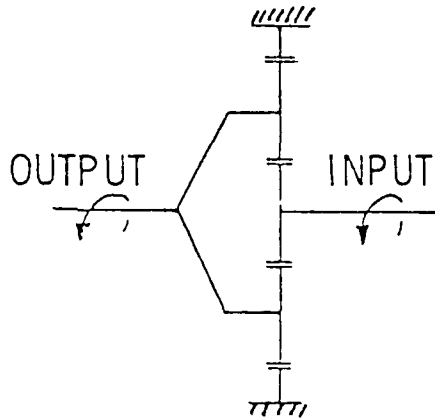
TABLE 86

MISSION PROFILE FOR FAN POWER REQUIREMENT

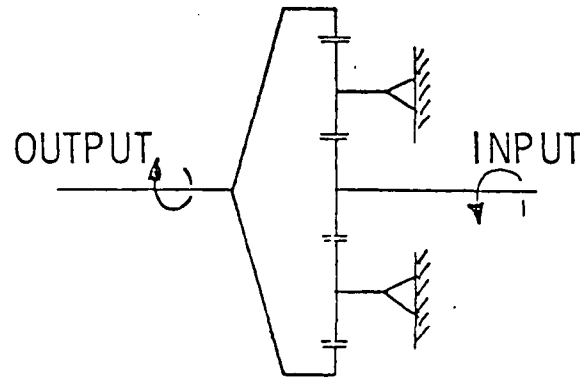
Rating	Fan Power		Fan Speed		Time	
	MW (HP)	%	RPM	%	Min.	%
Ground Idle	0.402 (540)	1.6	821	27.0	18	15.3
Take-Off	24.38 (32,700)	100	3024	100	2	1.7
Climb	24.40 (24,365)	74.5	3024	100	22	18.7
Cruise	96.02 (12,877)	39.4	2959	97.8	48	40.8
Descent	1.087 (1,458)	4.4	1570	51.9	17	14.5
Loiter	5.3 (7,108)	21.7	2037			
Approach	7.18 (9,640)	29.5	2148	71.0	5	4.3
Reverse	24.38 (32,700)	100	3024	100	5	0.4
					117.5	100%

PRECEDING PAGE BLANK NOT FILMED

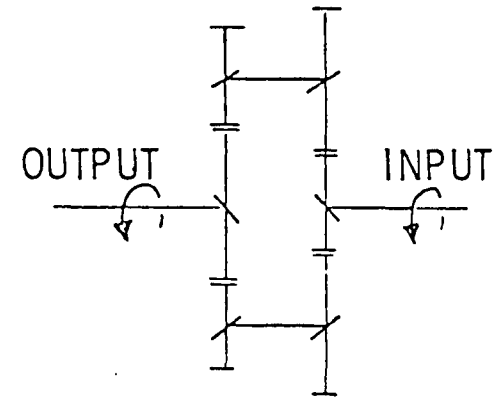
### PLANETARY GEAR SYSTEM



### STAR DRIVE SYSTEM



### JACK SHAFT ARRANGEMENT



- BEST SUITED FOR OVERALL SPEED RATIO OF 3.5 TO 4.1
- ADDITIONAL CF BRG. LOADS

- PRIME CANDIDATE
- SPUR OR DOUBLE HELICAL

- LARGE NO. OF GEARS
- HELICAL GEARS

Figure 103. Gear System Configurations

Two gear types, spur and helical, were used for the star gears while only helical gears were used for the jack shaft system. As a first step, some of the more pertinent characteristics of each candidate system were determined for an equivalent gear box design. The results of this study are shown in Table 87. Gear face widths, stresses and operating angles were determined. In addition, bearing and system bearing lives were calculated to help compare the gear arrangements.

A gear selection trade-off was then made incorporating as many characteristic choices as possible. Table 88 illustrates what major characteristics were considered and how each was weighted. Some of the values were based on calculations, but some were based on subjective judgements and experience such as the development risk evaluation. After applying the weighting factors, the star gear system with spur gear teeth was chosen as showing the most potential for this particular application. The jack shaft system, however, was a very close second and can be considered to be very appropriate for this type of application also.

Figure 102 (shown earlier) illustrates the integration of the star gear into the Task II geared turbofan engine. The gear does not appear to introduce any mechanical or structural compromises into the front sump area of the geared turbofan.

## 2. Bearing Selection

The next choice made was the type of bearing to use to support the individual star gears. A roller type was compared with a spherical roller type and the roller was chosen due to:

- High load capacity
- Lower cost
- Higher efficiency
- A potential oil flooding problem with the spherical roller design
- Spherical roller bearing self-alignment capability not required due to carrier design features.

## 3. Material Selection

Table 89 illustrates the material selections that were made and incorporated into the preliminary design of the advanced technology gearbox. CBS-600 is used extensively for the gearing material. To save weight, the star gear carrier is fabricated from cast Titanium 6-4. As noted before, the 232°C (450°F) properties of CBS-600 were assumed to be equivalent to those of AISI 9310 at 165°C (300°F). Figure 104 shows a more detailed cross section of the star gear arrangement and shows the location of the major M50 and CBS-600 components.

## 4. Lubrication System and Efficiency Estimate

The lubrication system schematic including the cooling circuit is shown in Figure 105. Many of the components needed are similar to those used in the engine's oil system. However, the cooling requirements are more severe and as a result, an air-oil heat exchanger cooled by fan air is required.



TABLE 87

BEARING/GEAR DATA FOR BOXES STUDIED

<u>Gear Set</u>	<u>Star Gear/Spur</u>	<u>Star Gear/D. Helical</u>	<u>Jack Shaft/D. Helical</u>
Ratio/Branches	2.56/6	2.56/6	2.56/4
Pressure Angle	20°	20°	20°
Face Widths (Pitch Dia)-in.			
Sun/1	2.6 (10.93)	1.5 (10.82)	/3 (8.34)
Star/2	2.8 ( 8.52)	1.7 ( 8.32)	/2.8 (10.77)
Ring/3	2.6 (27.96)	1.5 (27.74)	/4.1 (12.63)
/4			
Tooth Stresses @			
T/O $-\sigma_B$ (KSI) - MPA			
Sun/1	(40.5) 279	(36.4) 250	(/58.0)/400
Star/2	(39.5) 272	(37.3) 257	(/55.5)/382
Ring/3	(36.6) 252	(34.7) 239	(/45.5)/313
/4			
No. of Bearings	12	12	5 + 5
Indiv. $B_{10}$ Lives - Hrs.	110400	102950	60630F/357630A
System $B_{10}$ Life - Hrs.	21000	19400	19780

TABLE 88

GEAR SET SELECTION TRADE-OFF

Weighting Factors

Reliability - 10 (Highest)  
 Efficiency - 9  
 Dev. Risk - 6  
 Weight - 7  
 Cost - 7

Rating Factors

1 → 5 (Best)

	<u>Star/Spur</u>		<u>Star/Helical</u>		<u>Jack Shaft/Helical</u>	
	Rating	Score	Rating	Score	Rating	Score
Reliability	5	50	3	30	5	50
Efficiency	3	27	4	36	5	45
Dev. Risk	4	24	3	18	4	24
Weight	4	28	3	21	2	14
Cost	5	35	3	21	3	21
Total		<u>164</u>		<u>126</u>		<u>154</u>

Selected

TABLE 89

MATERIAL SELECTION

Input Quill Shaft	AMS 6414
Sun Gear	CBS-600* Rc 60 Min.
Star Gear	CBS-600 Rc 60 Min.
Ring Gear	CBS-600 Rc 60 Min.
Carrier	Cast TI 6-4
Bearings (Star)	
O.R.	CBS-600 Rc 60 Min.
Cage	AMS 6414 Steel - Silverplated
Rollers	AMS 6491 Vim Var M50 Rc 61 Min.
I.R.	AMS 6491 Vim Var M50 Rc 61 Min.

\* Min. Mech. Properties and Hardness Assumed Equal or Better than(300°F) 148.9°C  
AISI 9310.

ORIGINAL PAGE IS  
OF POOR QUALITY

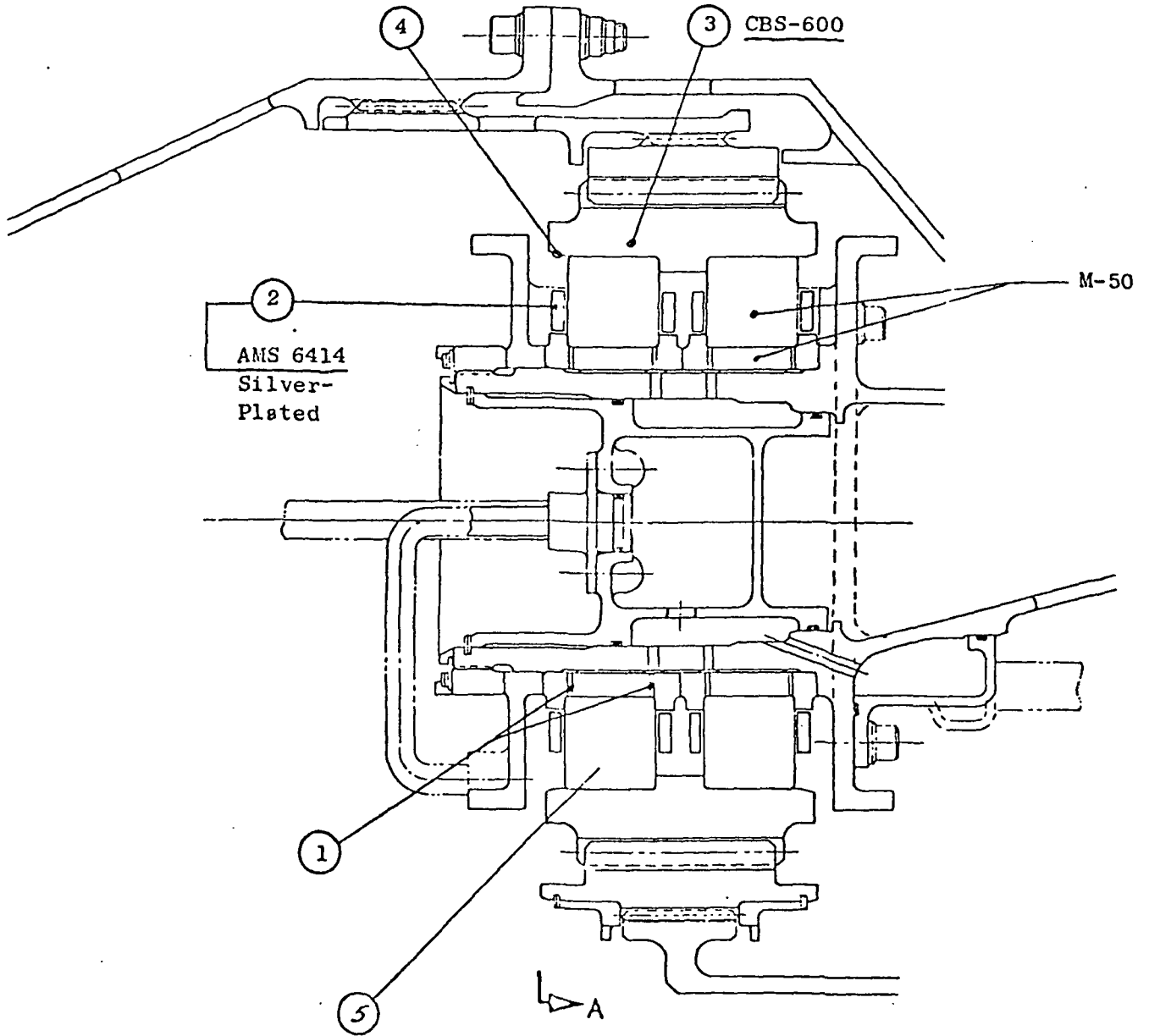


Figure 104. Star Gear Bearing Configuration.

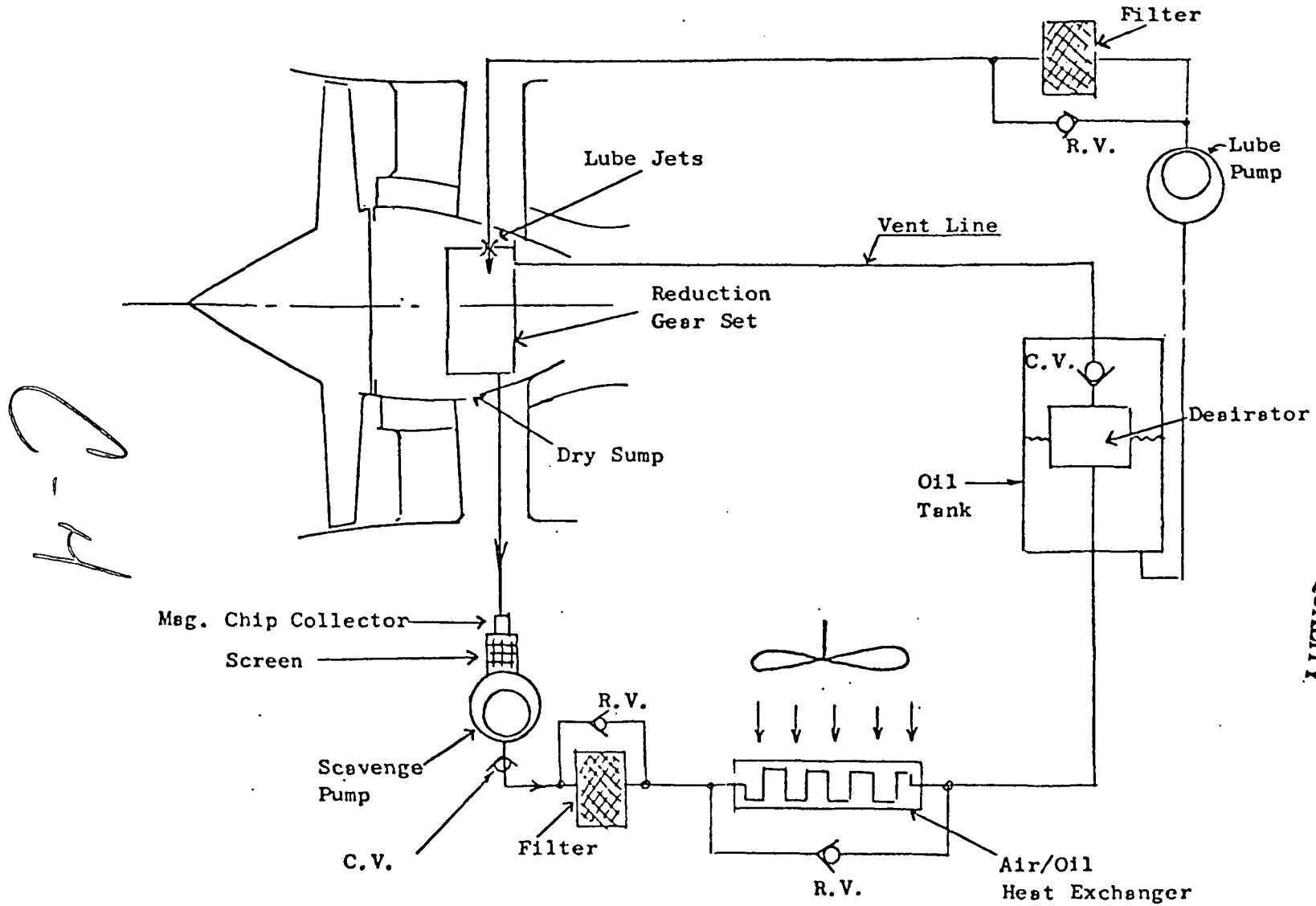
Refer to Table 90 for Design Features 1 through 5.

TABLE 90

REDUCTION GEAR DESIGN FEATURES

(Refer to Figure 104)

1. The bearings are lubricated by direct pressure feed through the inner race to insure a flushing action through the bearing and to maintain inner race shoulder lubrication, thus providing adequate lubrication and cooling.
2. The cages (retainers) are machined and inner race guiding, for design simplicity.
3. Outer races are integral with the star gear to obtain: light-weight compact design, eliminate fretting/wear problems, maintain good control of internal clearances due to minimized tolerance stackup and thermal transients.
4. Outer races are open to the outside for easy oil escape (prevents flooding).
5. Rollers have a partially crowned profile to reduce edge loading due to misalignment and deflections.



ORIGINAL PAGE IS  
OF POOR QUALITY

Figure 105. Lubrication System Schematic.

An aluminum plate-fin type of air-to-oil heat exchanger was used in the study. It is located in the circumference of the nacelle and fan air is passed through the exchanger. The flow of the air is controlled to maintain the desired oil out temperature required for efficient gear operation.

Estimates of the amount of rejected heat from the gearbox (and efficiency) were made based on experience with other large gearboxes and correlation equations developed through gearbox testing. Table 91 shows the estimates for various operating points of interest. For comparison, the Task II and Task III values are shown at the bottom of the table.

#### 5. Cost/Weight Estimates and Maintenance

When the preliminary design of the advanced gearbox was defined, manufacturing cost estimates were made. The costs were for an assumed 250th unit and were done in 1977 dollars. Likewise, weight estimates of the various components of the complete gearbox system were developed. Table 91 presents an itemized listing of the major components and their respective weight and manufacturing cost.

From Table 92 it can be seen that the heat exchanger system total cost and weight were ~~\$3200~~ and 29.03 Kg (64 lbs) respectively. The gear set itself was estimated to cost \$44,000 and weigh 216.8 Kg (478 lbs). The total system cost and weight was \$47,200 and 245.5 Kg (542 lbs).

Maintenance cost estimates were also made based on scheduled and unscheduled maintenance. Table 93 shows the estimated time to remove and install a complete gear box module. This was used to develop the maintenance cost summary shown at the bottom of Table 93. A total gear box maintenance cost per flight hour of 96¢ was estimated based on scheduled and unscheduled maintenance projections.

#### 6. Maintenance Factor Evaluation

All of the information developed in the preliminary study regarding weight, cost, efficiency and maintenance cost were incorporated into a merit factor analysis. For comparative purposes the General Electric domestic mission aircraft was used as a basis with the Task II geared turbofan results for a base.

Table 94 presents the results of the analysis for 92.47  $\$/m^3$  (35¢/gallon) fuel and a 1296 KM (700 N. mile) domestic mission. From Table 93 it can be seen that the gear set weight estimate increased from Task II and the selling price increased while the maintenance cost estimate decreased slightly and there was a small gain in efficiency. Totalling up the various effects in terms of  $\Delta$ DOC showed that the Task III estimates produced a 0.15% increase in DOC over Task II, a 0.07% increase in fuel burned and a 0.11% increase in TOGW of the aircraft. The preceding merit factor results were obtained by the use of sensitivity factors for the small changes in the engine-aircraft system.

TABLE 91

EFFICIENCY ESTIMATE

Power Condition	T/O			Cruise			Descent		
Input MW (H.P.)	24.38 (32700)			9.6 (12880)			1.09 (1460)		
	KW	(H.P.)	(Btu/Min)	KW	(H.P.)	(Btu/Min)	KW	(H.P.)	(Btu/Min)
Gear Mesh Loss	146	(196)	(8310)	57.4	(77)	(3265)	4.0	(5.3)	(225)
Bearing Loss	17.2	(23)	(975)	15.7	(21)	(890)	6.5	(8.7)	(370)
Churning Loss	50.0	(67)	(2841)	46.6	(62.5)	(2646)	6.8	(9.2)	(390)
Totals	2.3.2	(286)	(12126)	119.7	(160.5)	(6800)	17.3	(23.2)	(985)
Gearbox Efficiency - %	99.13			98.75			98.4		
Task II Values	99.0			98.7					



TABLE 92

GEARBOX COST/WEIGHT ESTIMATE

	<u>Cost Est. - \$(250th)</u>	<u>Weight Est. - Kg (Lbs.)</u>
Heat Exchanger System		
Exchanger	1500	13.61 (30)
Oil Lines/Pumps	375	9.07 (20)
Air System	1325	6.35 (14)
Sub Total	<u>3200</u>	<u>29.03 (64)</u>
 Gear Set		
Sun Gear	2500	7.62 (16.8)
Star Gears	12000	58.20 (128.3)
Ring Gear	5000	20.05 (44.2)
Carrier	13500	62.28 (137.3)
Star Bearings	6000	47.36 (104.4)
Input/Output Quills	4000	15.92 (35.1)
Miscellaneous	2500	5.03 (11.1)
Sub Total	<u>44000</u>	<u>216.46 (478)</u>
Gear Box System Total	47200	245.49 (542)

TABLE 93

RELIABILITY/MAINTENANCE COST ESTIMATE

Reduction Gear Module Removal/Installation Man-Hours

	<u>Removal</u>	<u>Installation</u>
Fan Rotor	16.0	32.0
Support Thrust Bearing	0.4	0.5
Drive Gear Shaft	1.0	3.0
Reduction Gear	0.5	1.6
Total	17.9	37.1

Scheduled and Unscheduled Maintenance Cost Estimate

Unscheduled MMH/Flt.-Hr.	0.0018
Scheduled MMH/Flt.-Hr.	0.0188 (Assumes 6000 TBO)
Parts Cost Est. \$/Flt.-Hr.	0.60
Total Maintenance Cost/Flt.-Hr.	0.96/Flt. Hr.

TABLE 94

GEAR SET COMPARATIVE MERIT FACTOR EVALUATION  
700 N. MILE DOMESTIC MISSION - 92.4 \$/m<sup>3</sup> (35c/GAL) FUEL

Component	Task II	Task III Δ	Δ DOC %	Δ W <sub>f</sub> %	Δ TOGW %
Gear Set System Wt. -(Lbs.) Kg	Base	(+39) 17.69	+0.07	+0.10	+0.12
Selling Price - \$	Base	+18000	+0.09	-	-
Maintenance Cost - \$/Flt. Hr.	Base	-0.01	~ 0	-	-
Gear Set η (Cruise) - %	Base	+0.05(-0.02% sfc)	<u>-0.01</u>	<u>-0.03</u>	<u>-0.01</u>
		Totals	+0.15	+0.07	+0.11

#### d. Conclusions

A refined preliminary design confirmed the results of the Task II geared turbofan systems with a slight deterioration in system performance projected over the Task II results. The design effort defined in much more detail the characteristics of the gearbox and accessory system and lent credibility to the potential use of such systems in future aircraft systems. However, previous Task II and Task III studies indicate that a direct drive turbofan engine can out perform a geared turbofan in terms of system merit factors for the mission definition used for this study. An illustration of a back to back comparison of the final Task III direct drive and final Task II geared drive turbofan is shown in Table 95. Although the geared engine has a 0.7% sfc advantage over the direct-drive engine, weight, cost, and installation effects create a 2.1% DOC penalty and a 1.9% fuel burned penalty relative to the direct drive engine.

#### C. Summary of Aircraft Subcontractor Studies

Three subcontractors, Boeing, McDonnell-Douglas and Lockheed, were engaged for this study to perform an independent evaluation of the E<sup>3</sup> engine for both Task II and Task III. The aircraft and missions described earlier in Task II were retained with only the new Task III engine characteristics altered. This resulted in a further improvement in the estimated benefits of the Task III E<sup>3</sup> engine over the previously described Task II results.

The improvements in  $\Delta W_f$  and  $\Delta \text{DOC}$  over the Task II results are shown in Figure 106. These results still did not have engine price or maintenance effects incorporated but did account for weight, size and sfc differences. For the contractors that supplied  $\Delta \text{DOC}$  values, the DOC improvement relative to current technology ranged from 5.5% for a Lockheed domestic mission aircraft to 10.2% for a Lockheed intercontinental mission aircraft. The Douglas values fell between these two extremes. Therefore, the 5% DOC improvement goal of NASA would appear to have been met.

To indicate what additional DOC advantage may be available if maintenance and cost effects are added, Table 96 shows results for just these two components of DOC as calculated for a domestic and intercontinental General Electric study aircraft used in this study. The DOC penalty for the estimated higher first cost of the E<sup>3</sup> engine is overwhelmed by the estimated maintenance cost savings such that there is a net DOC advantage of 1.8% and 2.1% for the domestic and intercontinental mission study aircraft respectively.

The estimated  $\Delta W_f$  savings ranged from approximately 14.8% for the Boeing domestic mission aircraft to 22.2% for the Lockheed intercontinental mission aircraft. All the other estimated fuel savings ranged in between these two extremes.

Details of the Task III studies performed by the subcontractors are included in Appendix B.

TABLE 95

IMPROVED ADVANCED ENGINE STUDY  
RESULTS  
(EQUIVALENT INSTALLED MAX. CLIMB THRUST)

	<u>Final Geared Drive</u>	<u>Final Direct Drive</u>
Bypass Ratio - Mx.Cr.	8.6	6.98
Fan Pressure Ratio Mx.Cl.	1.55	1.65
Installed Weight - kg. - (lbs.)	+482 (+1065)	Base
$\Delta$ sfc Installed - % (Rel. Baseline)	-0.7	Base
$\Delta$ DOC - % (Domestic Mission)	+2.1	Base
$\Delta W_f$ (Fuel Burned) - %	+1.9	Base

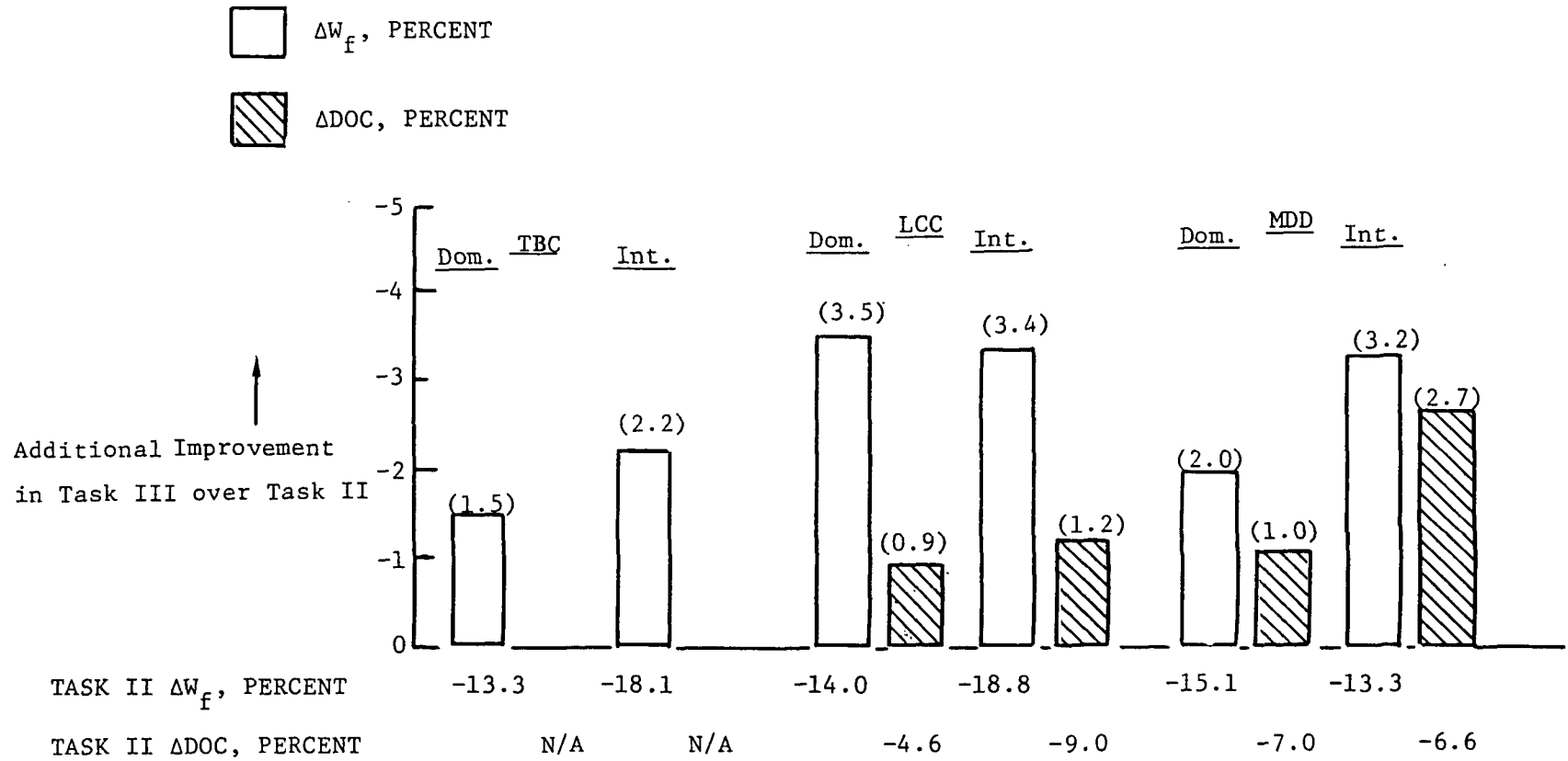


Figure 106. Integrated Mission Fuel Burn/Direct Operating Cost - Design Mission

TABLE 96

TASK III E<sup>3</sup> PRICE AND MAINTENANCE  
 VS.  
 SCALED CF6-50C  
 DOC EFFECTS

---

	Mission Sized			
	Domestic		International	
	<u>Design Value</u>	<u>Δ DOC - %</u>	<u>Design Value</u>	<u>Δ DOC - %</u>
Installed Cost - K\$	+107.3	+0.5	+124.5	+0.4
Maint. Cost - \$/Flt-Hr. (Parts + Labor + O.H.)	- 14.51	-2.3	- 17.90	-2.5
		<u>-1.8</u>		<u>-2.1</u>
Fuel Cost(35¢/Gal.) 92.4 \$/m <sup>3</sup> Domestic (45¢/Gal.) 118.88 \$/m <sup>3</sup> International				

D. Conclusions/Recommendations

Based on the design and economic evaluations performed in Task III, it is believed that the Task III E<sup>3</sup> engine meets all NASA goals and requirements with adequate margin in all areas except emissions where the EPA 1981 Standards are estimated to be just met for NO<sub>x</sub>.

In addition, it is believed that the design configuration will satisfy all current and anticipated commercial requirements. Based on this, it is recommended that the Task III E<sup>3</sup> engine be further refined and component technology development work begun. Successful conversion of the advanced technology of the Task III E<sup>3</sup> engine into a future commercial engine would result in large fuel savings and economic benefits that would preserve the leadership of the United States in the area of commercial transport aircraft and engines.



TABLE OF CONTENTS

	<u>PAGE NO.</u>
SECTION VI . . . . .	309
TASK IV - RISK/COST/BENEFITS SENSITIVITY EVALUATION . . . . .	309
A. Introduction/Approach . . . . .	309
B. Significant Results . . . . .	309
1. Performance Derivatives . . . . .	309
2. Performance Risk Analysis . . . . .	310
a. Method . . . . .	310
b. Component Levels . . . . .	318
c. Engine Level . . . . .	318
3. Benefits . . . . .	321

PRECEDING PAGE BLANK NOT FILMED

LIST OF FIGURES  
SECTION VI  
TASK IV - RISK/COST/BENEFITS SENSITIVITY EVALUATION

<u>FIGURE NO.</u>	<u>TITLE</u>	<u>PAGE NO.</u>
107	Fan Tip, Hub and Booster Performance Probabilities	312
108	High Pressure Compressor and Turbine Performance Probabilities	313
109	Combustor and Low Pressure Turbine Performance Probabilities	314
110	Mixer and Leakage System Performance Probabilities	315
111	Fan and Core Duct Mixer Loss Probabilities	316
112	Clearance Control and Combustor Loss Probabilities	317
113	Probability of Achieving % $\Delta$ sfc Reduction vs CF6-50C (Rubber Engine)	319
114	Probability of Achieving % $\Delta$ sfc Reduction vs CF6-50C (Variable- Fixed Engine)	320
115	Cash Flow Evaluation Procedure	322

LIST OF TABLES

<u>TABLE NO.</u>	<u>TITLE</u>	<u>PAGE NO.</u>
97	E <sup>3</sup> Derivatives for Performance Risk Analysis	311
98	Potential Program Benefits (GE Study Aircraft Avg. Mission)	323

## SECTION VI

### TASK IV - RISK/COST/BENEFITS SENSITIVITY EVALUATION

#### A. Introduction/Approach

In this task, the sensitivity of the benefits to be derived from a Flight Propulsion System (FPS) consisting of an E<sup>3</sup> type engine installed on an advanced aircraft are determined subject to shortfalls in component technology.

The process was begun by evaluating the performance derivatives of major component and engine systems as they affect ultimate sfc levels.

In turn, these derivatives, when coupled to an estimate of expected performance shortfall of an experimental component development program, were utilized to provide estimates of expected levels of performance.

The expected levels were derived through a modified "Delphi" method where multiple estimates of the probability of meeting a continuum of component performance were supplied by Aircraft Engine Group designers. By averaging these estimates together, a "master curve" of expected performance and related probabilities was developed for each component and system considered.

These "master curves" were then statistically combined to provide an estimate of the performance levels of an initial build engine in an experimental program as related to various probability levels.

The benefits of a program to develop an E<sup>3</sup> type engine to commercial service were then estimated based on fully developed performance goal levels and on an expected level after an initial experimental development program.

#### B. Significant Results

##### 1. Performance Derivatives

Derivatives were developed through use of the Task III E<sup>3</sup> cycle deck representation. Each of the component performance levels were changed to obtain the sfc effect of a 1% increase in each of the items of interest. Twelve items were evaluated in this way for two types of engines. The first type was a "rubber" engine where the ability to change and rematch any component to compensate for the effect of any other component's performance level is allowed.

A second type of derivative system was evaluated for a "Variable-Fixed" engine. For this case, a limited ability to rematch components through changes in nozzle areas, for instance, is assumed. This would be very nearly the case for an experimental engine program where some changes can still be made in the experimental hardware.

The derivatives for the "rubber" engine and the "Var-Fixed" engine are shown in Table 97.

## 2. Performance Risk Analysis

### a. Method

A statistical method of combining and evaluating the statistical distribution of expected performance in an experimental development program was developed. It is described as follows.

Because twelve factors of engine operation were considered to affect specific fuel consumption (sfc), a procedure for assessing their combined effect on sfc was utilized. With a performance probability distribution estimated for each engine factor and appropriate derivatives to relate delta changes in the performance parameters to delta changes in sfc, the general mathematical procedure of convolution was used to combine the factors. In convoluting statistical distributions each distribution is integrally combined with every possible combination of all the other distributions; the result (the summation of the probabilities for all the combinations) is then the distribution of combinations possible from the set of distributions being convoluted.

Since the combinations obtainable from convoluting continuous distributions are essentially infinite, a simple, but highly accurate, piecewise approximation procedure was used to convolute the distributions. Figures 107 through 112 show the approximated performance distributions used for the 12 engine factors. The midpoint values and the probability intervals for the straight line segments are used to represent the distributions. Utilizing these approximations, a simple (time-share) computer program was used to calculate and sum the probabilities of the distributions' combinations.\* The computational procedure used is as follows. With the deviation of each factor from its technology demonstration goal correctly adjusted (with derivative) to obtain its impact on sfc, the sfc deviations are summed for each combination of engine factors. The probability of each combination occurring is obtained by multiplying the interval probabilities together. Thus, for each possible combination, the sfc deviation is determined and its chance (probability) of occurring is calculated. Then by summing all the combinations' probabilities as a function of sfc deviation, the resulting distribution of sfc deviations is obtained for the convolution of the 12 factors.

---

\*Even with the simple approximations used for the 12 factors being considered, the number of possible combinations is 1,209,323,520,000. Since this is a formidable number even for a modern, high-speed computer, the actual convolution was made by first combining three sets of four factors each and then combining these three distributions to obtain the final results. This procedure still required 164,488 combinations, but represents a 7,350,000 to 1 reduction in the number of combinations required if the direct approach were used. The properties of convolution permit combining distributions in any order.

TABLE 97

E<sup>3</sup> DERIVATIVES\* FOR PERFORMANCE RISK ANALYSIS

Engine Factor	Engine Configuration	
	"Rubber"	"Var-Fixed"
Fan Tip $\eta$	-0.44	-0.500
Fan Hub $\eta$	-0.07	-0.13
Compressor $\eta$	-0.36	-0.482
HP Turbine $\eta$	-0.53	-0.667
LP Turbine $\eta$	-0.52	-0.593
Combustor $\eta$	-1.0	-1.0
Mixer $\eta$	-0.046	-0.044
Leakage $W_{cool}$ Kg/s (#/sec)	.072 (+0.16)	0.181 (+0.398)
Fan Duct $\Delta P/P$	+0.94	+1.056
Core Duct $\Delta P/P$	+ .25	+0.315
Clearance Control $\Delta sfc$	+1.0	+1.0
Combustor $\Delta P/P$	+0.27	+0.167

\*% change in SFC for a +1.0% change in engine factor.

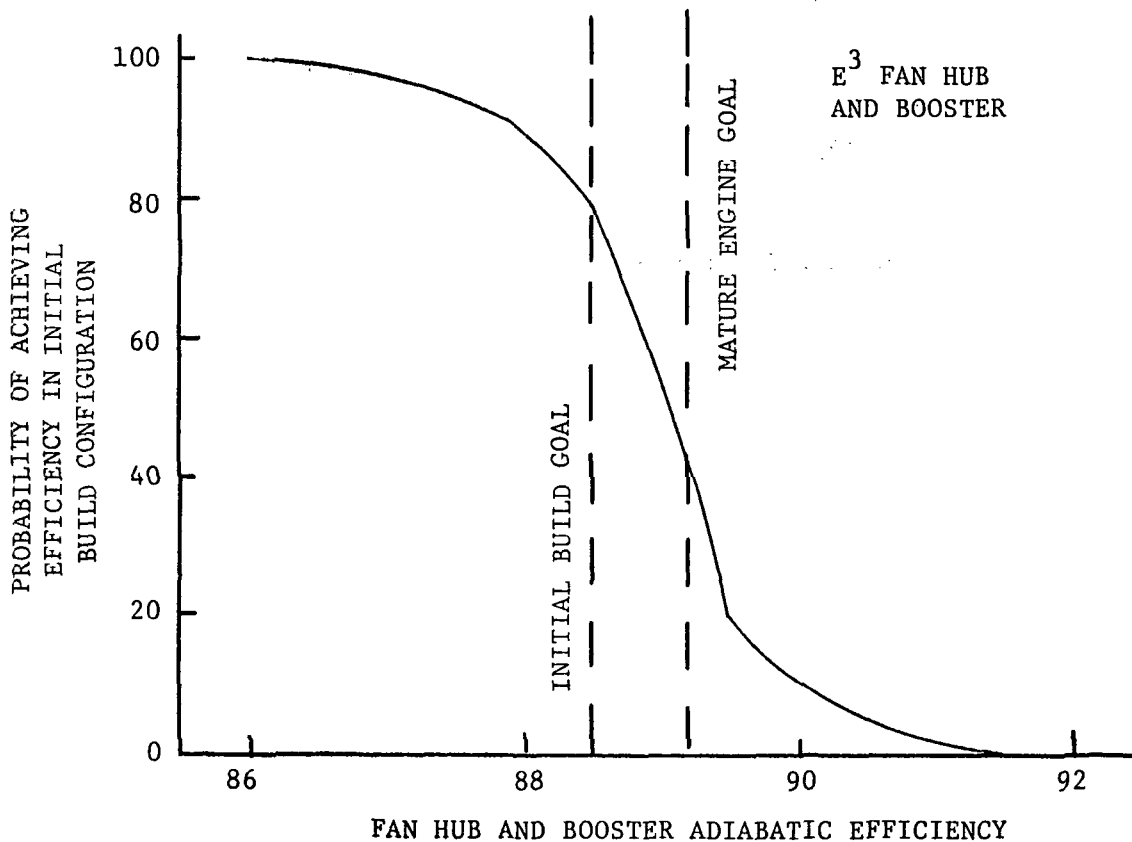
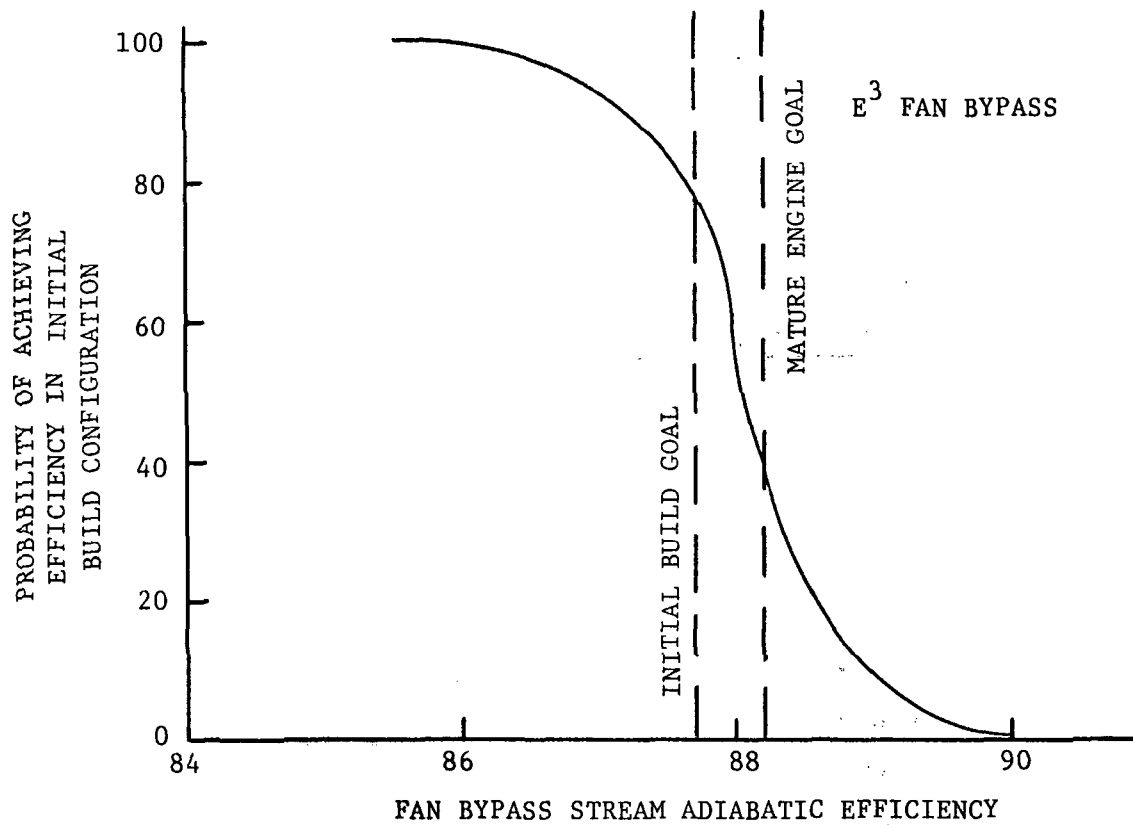


Figure 107. Fan Tip, Hub and Booster Performance Probabilities

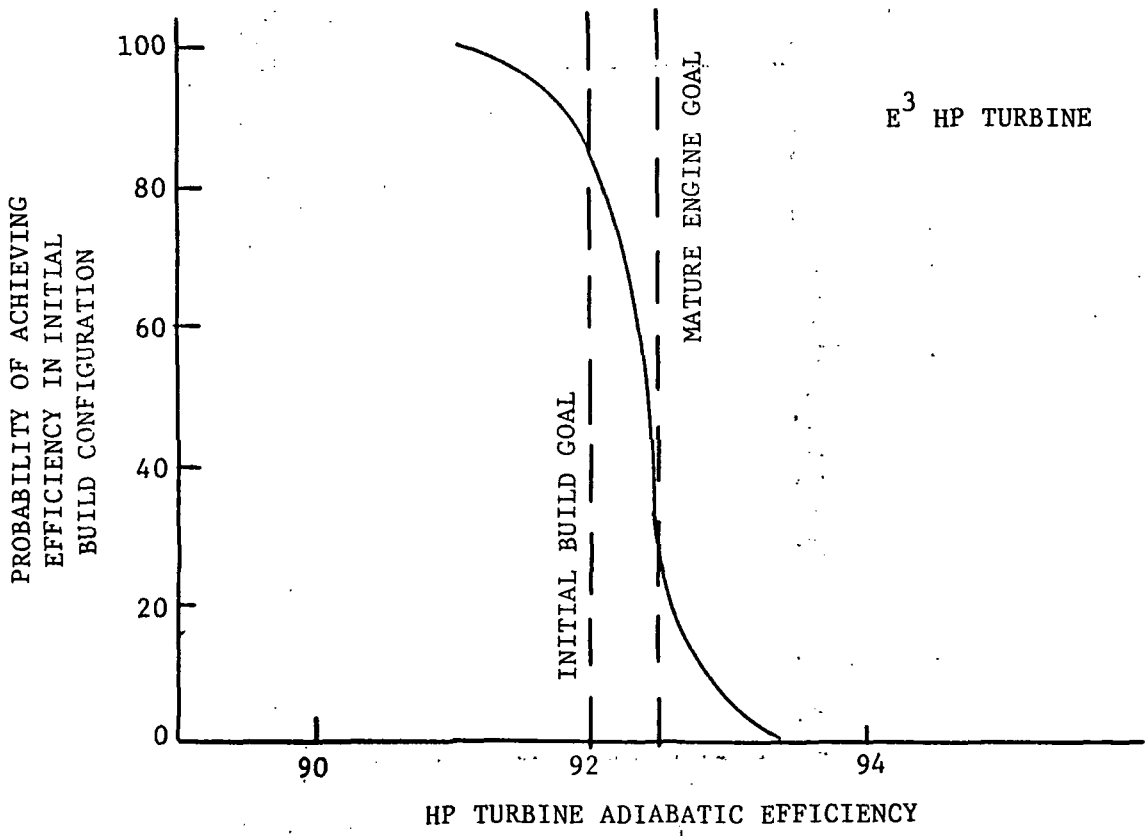
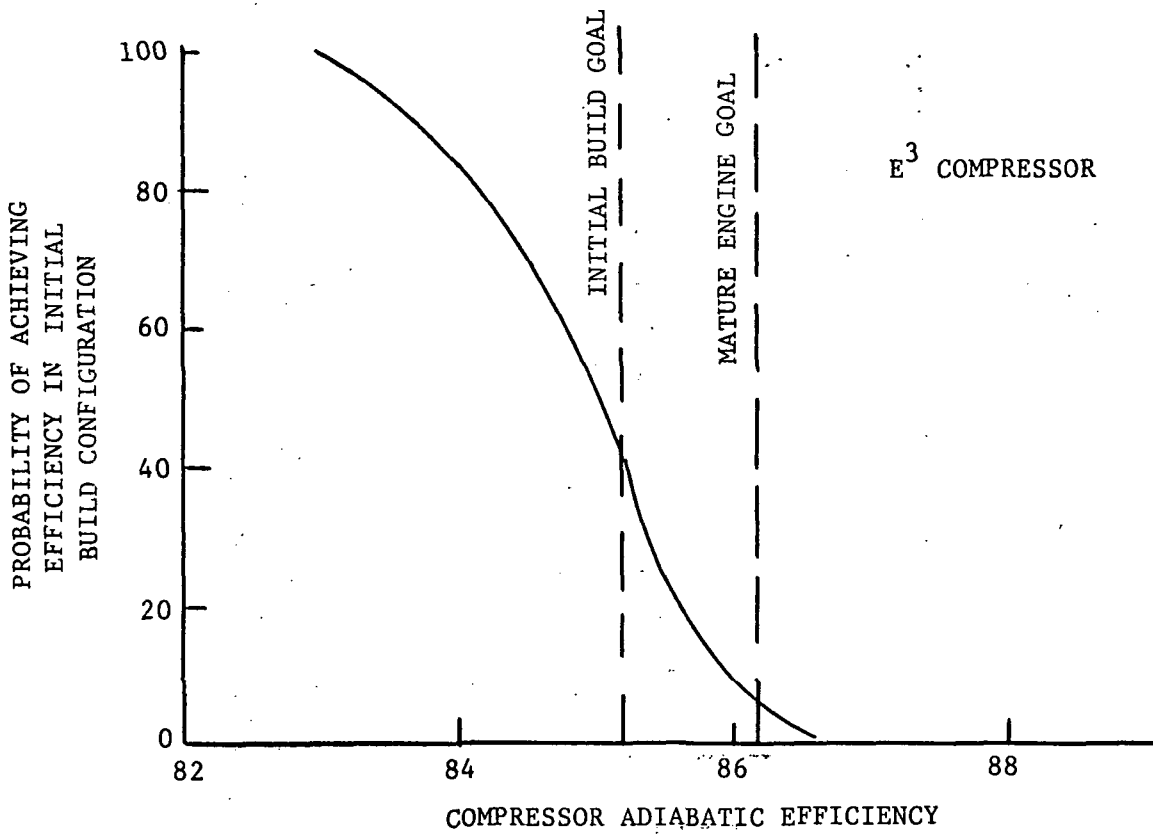


Figure 108. High Pressure Compressor and Turbine Performance Probabilities

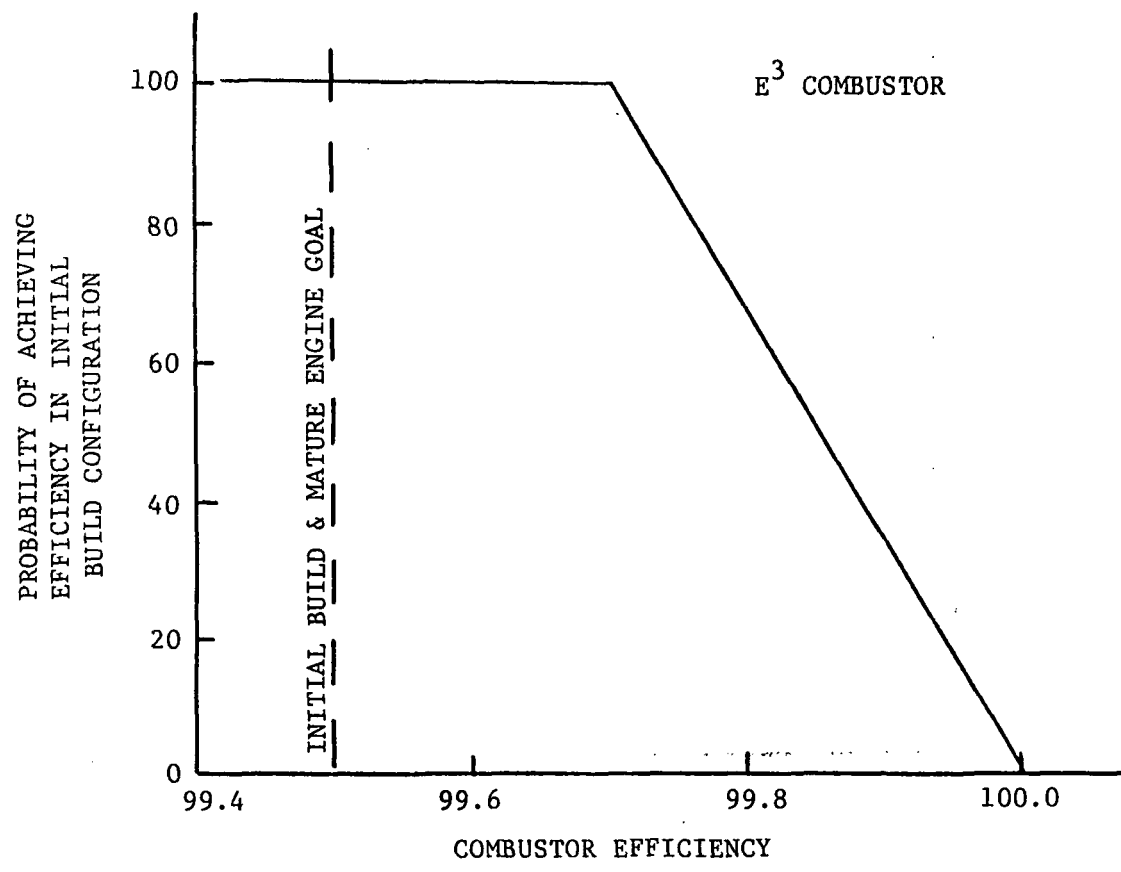
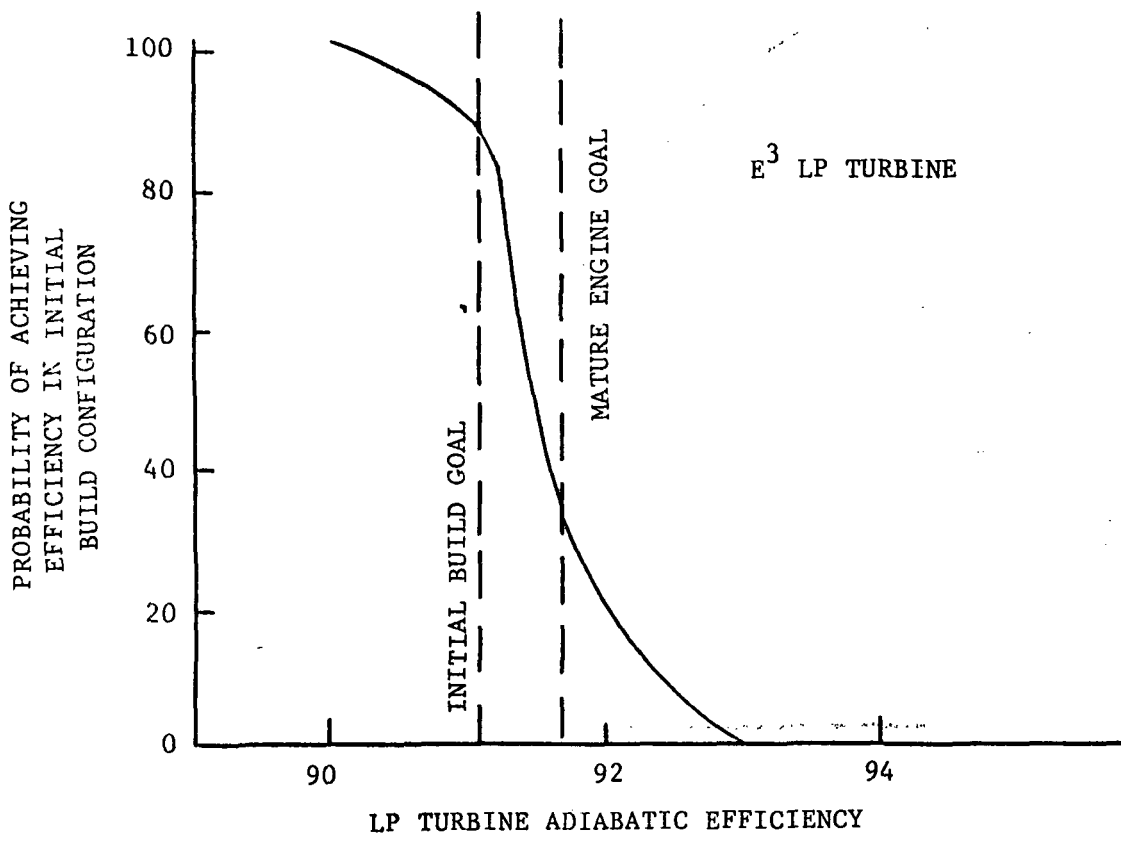


Figure 109. Combustor and Low Pressure Turbine Performance Probabilities



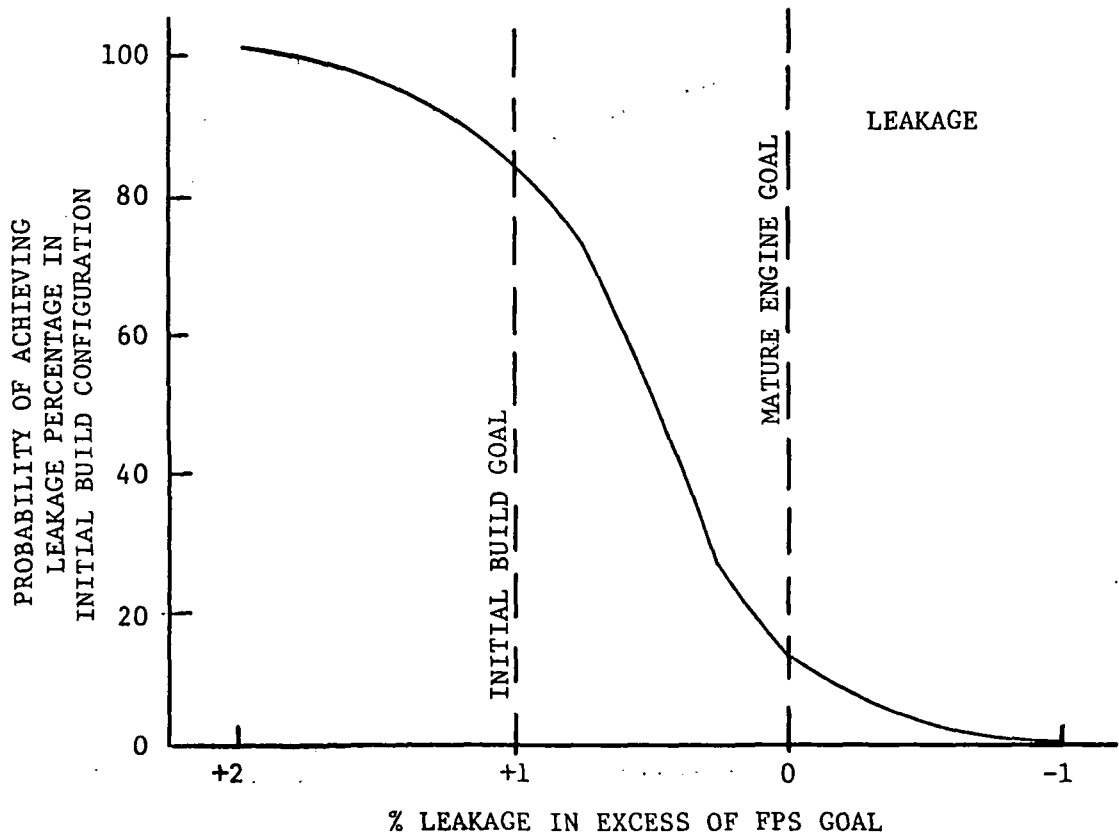
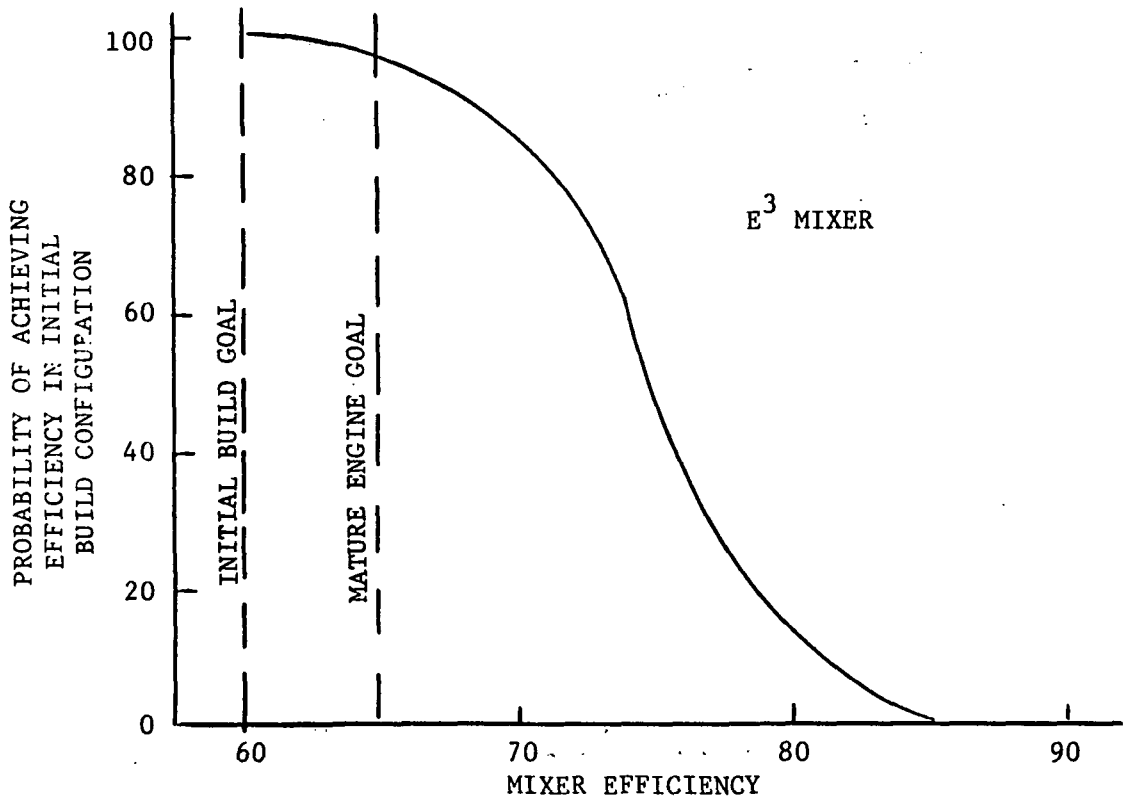


Figure 110. Mixer and Leakage System Performance Probabilities



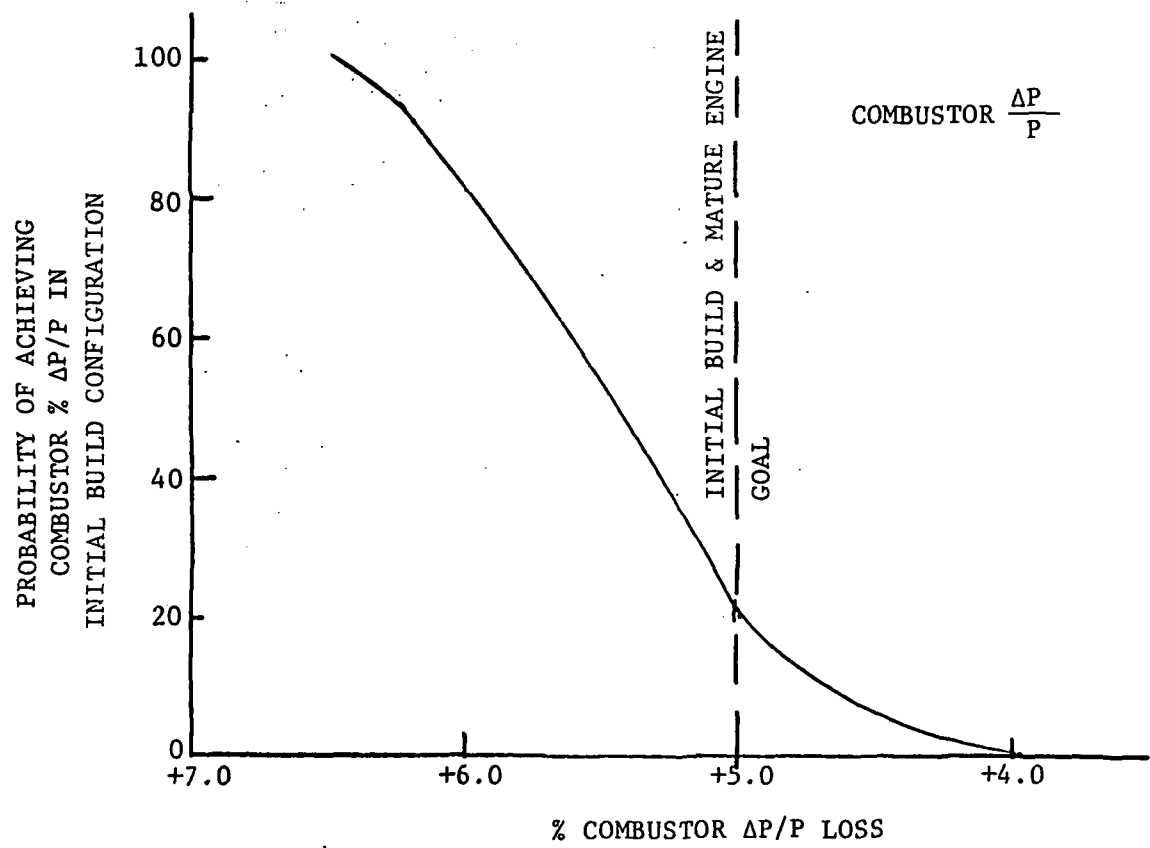
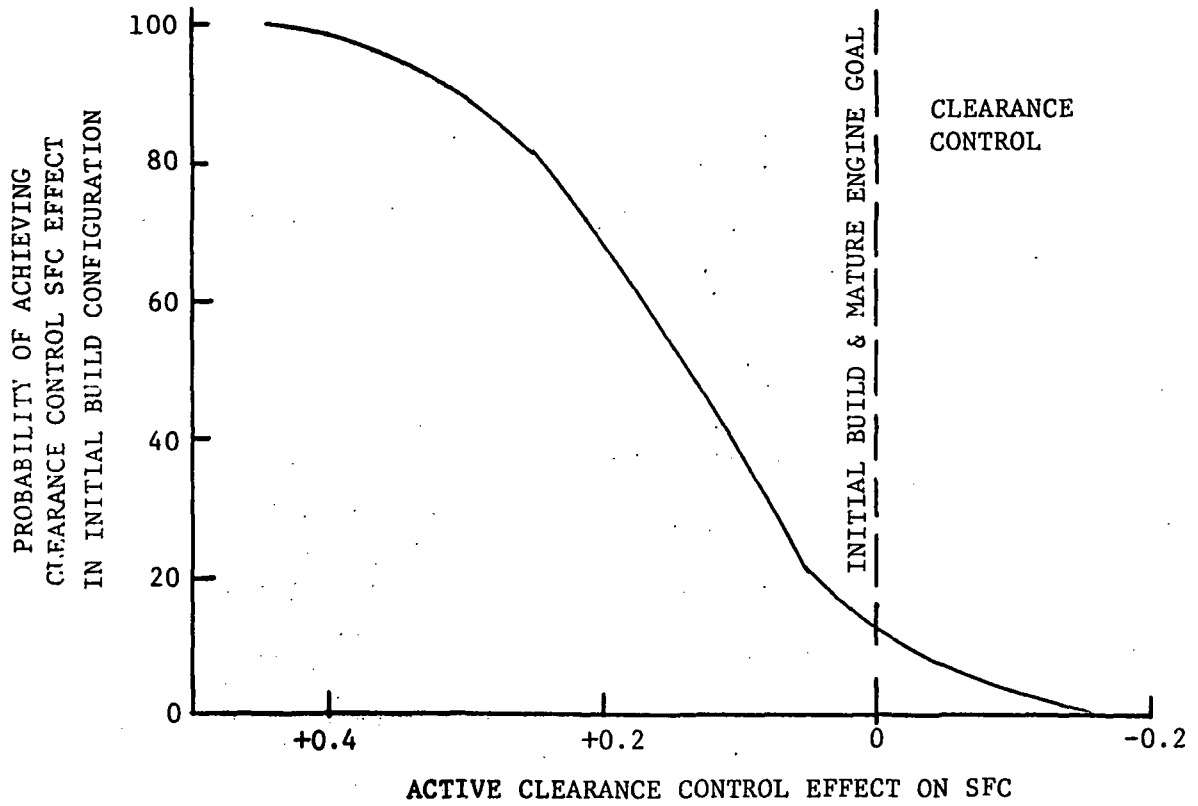


Figure 112. Clearance Control and Combustor Loss Probabilities

## b. Component Levels

An average curve of all the expert estimates of probable performance level for each of the twelve performance qualities are developed. These are shown in Figures 107 through 112. These curves of performance level versus the probability of attaining those levels are what was then statistically combined to provide an estimate of combined engine performance level versus the probability of obtaining those levels.

Each averaged component or system performance is a combination of the best estimate of various Aircraft Engine Group aerodynamic designers and reflects their experience and judgement in extrapolation of probable performance levels. Each designer was asked to make essentially four estimates of performance. Two extremes were asked for. The first was to estimate the lowest level of performance that the designer would judge to be essentially 100% probable of being achieved in a development program. The second point was the maximum level of performance that the designer would consider to have a 0% probability of achievement. The third and fourth levels of performance and probability of achieving those levels were those associated with the E<sup>3</sup> mature engine goal and a somewhat lower goal that was set as a goal in a development program. These four "hard" points were then combined into a continuous smooth curve of a 100% to 0% probability of achieving the minimum to maximum expected level of component performance.

## c. Engine Level

The twelve curves of performance versus probability of achieving that performance were then combined statistically as described in the previous Method section.

Two statistical combinations were generated. The first was for a completely "Rubber" engine and is shown in Figure 113. A technology demonstration target of -12.4% and a Task III -14.4% sfc reduction (relative to the CF6-50C) are shown on the curve. The respective estimated probabilities for achieving these levels with a rubber engine would be 95% and 9%.

The second estimate reflects a "Variable - Fixed" engine that would most nearly reflect an actual experimental program where some engine adjustments could be made to compensate for component off-design migration. This probability curve is shown in Figure 114. For the initial configuration target and Task III goal, respective achievement probabilities of 95% and 20% were estimated.

Both of the estimates indicate that the probability of achieving a full Task III level of sfc reduction over the base CF6-50C is relatively low. However, the probability of achieving a reduced level performance equivalent to a 12.4% reduction in sfc is relatively high for a technology demonstration program.

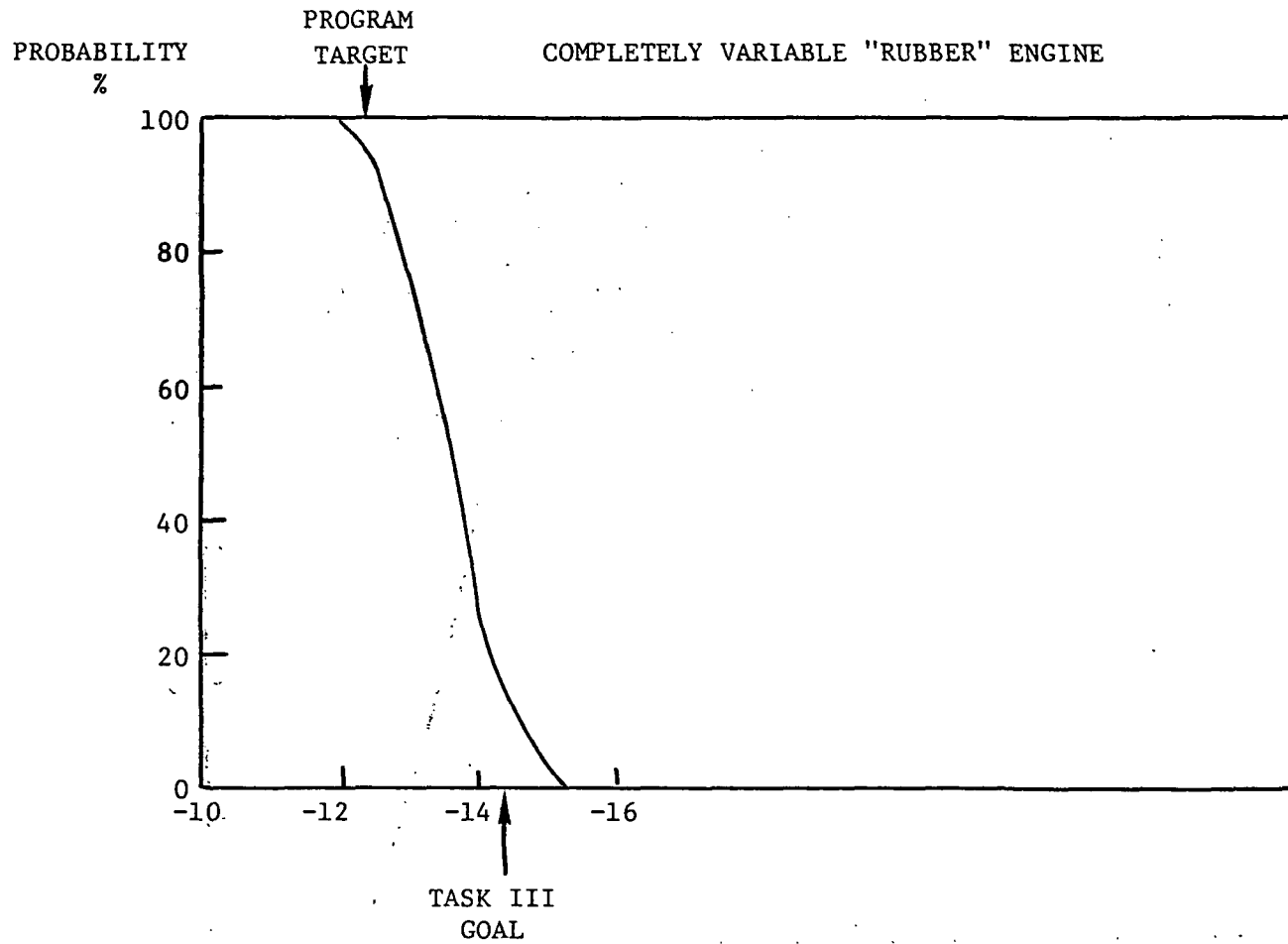


Figure 113. Probability of Achieving % Δ SFC Reduction vs. CF6-50C (Rubber Engine)

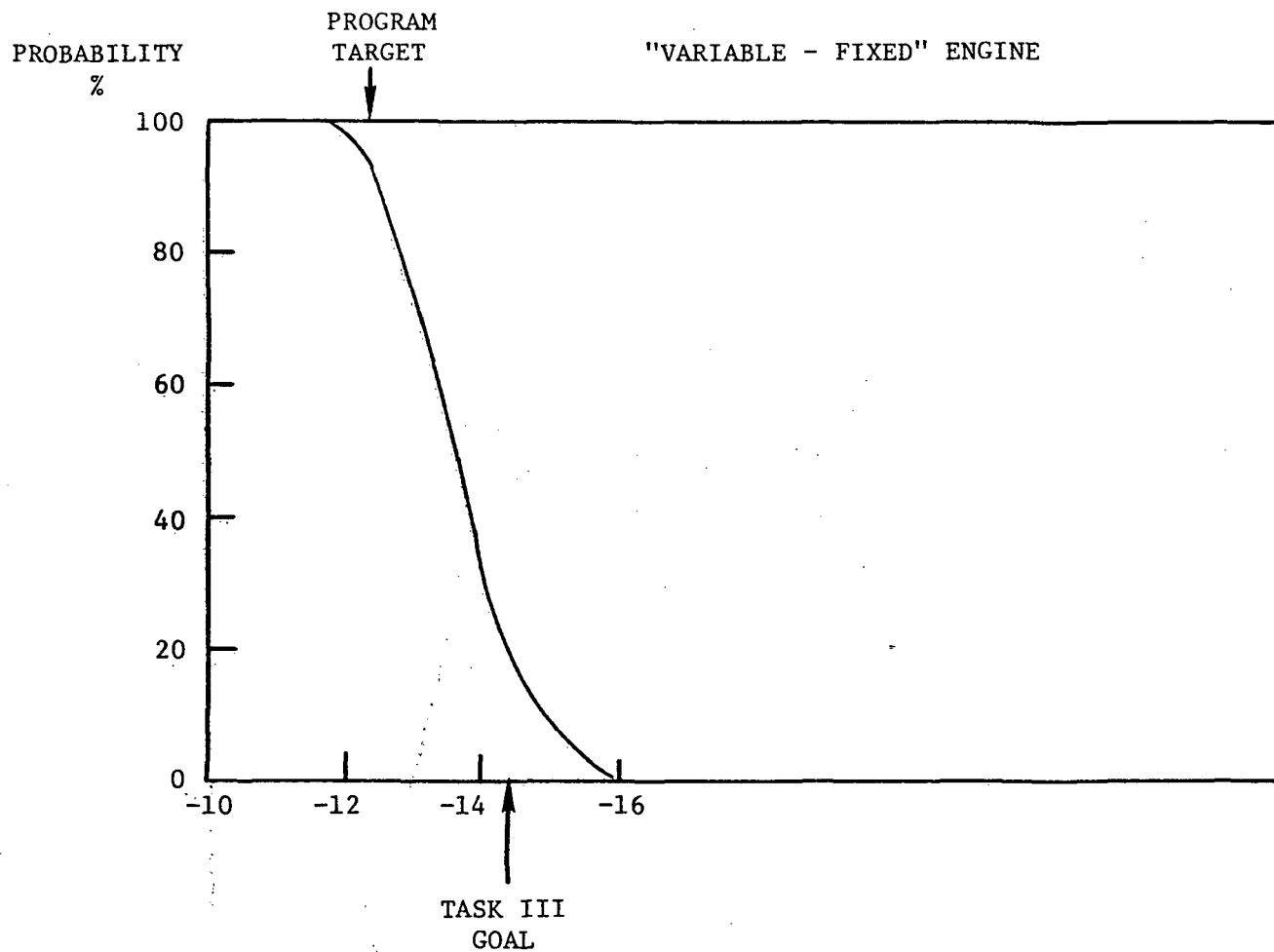


Figure 114. Probability of Achieving % Δ SFC Reduction vs. CF6-50C (Variable-Fixed Engine)

### 3. Benefits

Benefits of achieving both the full Task III level of performance and the reduced levels of performance expected after a technology demonstration program were estimated.

Basically, full and reduced DOC reductions were converted into future cash flow benefit for two hypothetical fleets of domestic and intercontinental mission aircraft. The operating costs and DOC conversions were based on the General Electric study aircraft. The economic assumptions and the fleet build-up and decline and fleet size assumptions are given in Figure 115. For the economic assumptions made, a 1% DOC change was worth 272.6 and 421.9 million dollars in future cash flow for a domestic and intercontinental fleet respectively.

Assuming that only the sfc effect of not achieving the full Task III goals impacts the DOC reduction,  $\Delta$ DOC estimates scaled from advanced aircraft operated with properly scaled CF6-50C engines were made. These are reflected in Table 98 for both the assumed domestic and intercontinental aircraft fleet for an average mission. The value of the E<sup>3</sup> program could be quite large since the total savings of both fleets would result in an improved cash flow of over eleven billion dollars to the airline operations. Even the reduced engine goals would project out to over ten billion in savings during the fleet life of 21 years.

	TRANSCONTINENTAL	INTERCONTINENTAL
DOC - \$/FLT. HR.	\$ 1755	\$ 2351
UTILIZATION - HRS/YR-AIRCRAFT	3452	3988
1% DOC - M\$ (THEN YEAR SAVINGS)	272.62	421.91

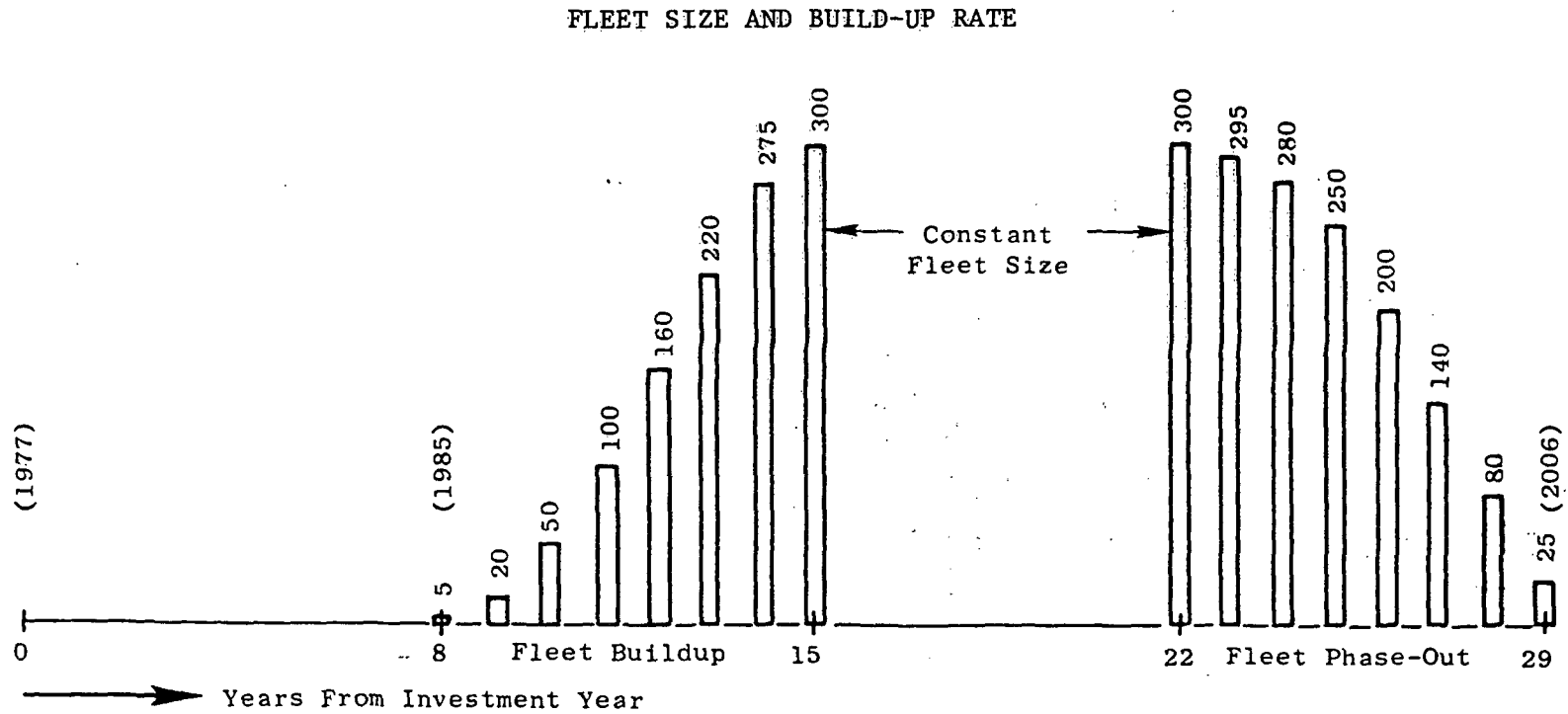


Figure 115. Cash Flow Evaluation Procedure



TABLE 98.

POTENTIAL PROGRAM BENEFITS (GE STUDY AIRCRAFT, AVG. MISSION)

	<u>Potential Development</u>		<u>Full Task III Goals</u>	
	<u>Program Result (95% Probability)</u>		<u>Dom.</u>	<u>Inter.</u>
$\Delta$ sfc (Rel CF6-50C) - %	-12.4		-14.4	
Mission	Dom.	Inter.	Dom.	Inter.
$\Delta$ DOC (Rel CF6-50C) - %	-10.9*	-16.7*	-12.1	-18.7
Cash Savings - $\$10^6$	2971.	7046.	3299.5	7890.5

\*sfc Shortfall Effects Only.

TABLE OF CONTENTS

	<u>PAGE NO.</u>
SECTION VII . . . . .	327
TASK V - AERODYNAMIC DESIGN OF CORE COMPRESSOR . . . . .	327
A. Introduction/Approach . . . . .	327
1. Preliminary Design Studies . . . . .	327
B. Significant Results . . . . .	328
1. Detailed Aerodynamic Design . . . . .	328
2. Preliminary Blade Shapes . . . . .	332
3. Off-Design Performance Predictions . . . . .	339
C. Conclusion/Recommendations . . . . .	344

PRECEDING PAGE BLANK NOT FILMED

LIST OF FIGURES  
SECTION VII  
TASK V - AERODYNAMIC DESIGN OF CORE COMPRESSOR

<u>FIGURE NO.</u>	<u>TITLE</u>	<u>PAGE NO.</u>
116	E <sup>3</sup> Compressor Cross Section	330
117	Stagewise Distributions of Core Compressor Solidity and Aspect Ratio	331
118	Core Compressor Aerodynamic Design Flowpath and Calculated Stream Surfaces	333
119	Radial Distributions of Stage Inlet Absolute Air Angle	334
120	Radial Distributions of Rotor Loss Coefficient	335
121	Stagewise Distribution of Rotor Inlet Pitchline Meridional Mach Number	337
122	Stagewise Distributions of E <sup>3</sup> Compressor Rotor and Stator Diffusion Factor	338
123	Estimated State 2 Characteristics	341
124	E <sup>3</sup> Stage 7 Characteristic Compared to Stage A Data	342
125	Core Compressor Performance Map Estimated from Stage Characteristics, without Starting Bleed	343

LIST OF TABLES

<u>TABLE NO.</u>	<u>TITLE</u>	<u>PAGE NO.</u>
99	Comparison of E <sup>3</sup> Task V and Recommended AMAC Core Compressor Design Parameters	329
100	Summary of Compressor Vector Diagram Data	336
101	Summary of Task V Blade Geometry	340

## SECTION VII

### TASK V - AERODYNAMIC DESIGN OF CORE COMPRESSOR

#### A. Introduction/Approach

The core compressor configuration for the E<sup>3</sup> engine has been studied and refined throughout the various tasks of this study. Efficiency and stall margin potential estimates were under continuous review, using the Compressor Unification Study procedure outlined in Reference 7, as the preliminary studies led to selection of a flowpath shape and a set of blade geometry specifications that were suitable for detailed aerodynamic design studies. Detailed aerodynamic design calculations were performed under Task V using axisymmetric flow computational methods. Stagewise and radial distributions of rotor and stator losses, stage work input and stator exit swirl angle were refined to produce well-balanced loading and Mach number distributions. Preliminary blade shapes were then specified consistent with the detailed vector diagrams. A parallel effort to predict the expected off-design performance of the core compressor was also carried out in Task V. An estimated performance map and preliminary stator schedule were generated during this phase of the work.

#### 1. Preliminary Design Studies

The E<sup>3</sup> core compressor configuration has evolved from the 10-stage, 23:1 pressure ratio design defined during the Advanced Multistage Axial-Flow Compressor (AMAC) preliminary design studies conducted by General Electric under NASA Contract NAS3-19444 (Reference 6). The object of this earlier study was to identify an advanced core compressor for use in new high-bypass ratio turbofan engines to be introduced into commercial service in the 1980's. A parametric screening study was conducted based upon a forecast of anticipated 1985 compressor and engine system technology levels to determine the influence of the major compressor design features upon efficiency, weight, cost, aircraft direct operating cost and fuel usage. Design parameters examined were aspect ratio, solidity, inlet specific flow, exit Mach number, reaction, inlet radius ratio, exit radius ratio and number of stages. Compressor speed was set to allow each particular configuration to meet an objective level of stall margin. The study is described in detail in Reference 6 but the major conclusions can be summarized as follows:

- 1) Best core compressor efficiency is obtained using:
  - a) medium average aspect ratio (1.3 - 2.0)
  - b) medium average solidity (1.2 - 1.5)
  - c) medium-to-high reaction (0.5 - 0.7)
  - d) low exit Mach number ( $\sim 0.28$ )
  - e) low inlet specific flow ( $\sim 35 \text{ lbm/sec-ft}^2$ ) 170.9 Kg/sec-m<sup>2</sup>
  - f) low inlet radius ratio ( $\sim .5$ )
  
- 2) Higher blade speeds do not severely penalize performance if front rotor tip relative Mach number is held below about 1.4.

- 3) Reducing the number of stages by using higher speeds reduces compressor length and cost, but not necessarily core engine weight. Efficiency need not be greatly reduced provided that blading Mach numbers do not become excessive.
- 4) Medium-to-high rear radius ratios can be beneficial, provided that it helps hold the front stage tip Mach number below the level at which high shock losses are present. The optimum rear radius ratio is likely to increase as the number of stages is reduced.

At the conclusion of the reference 6 study, a 10-stage 23:1 pressure ratio compressor was recommended for further development. This recommended design incorporated those features listed above as contributing to high efficiency. The recommendation to use 10-stages was made in the belief that this would offer a design having the best combination of desirable features such as compactness, low cost, high efficiency, low engine operating cost and low fuel usage.

#### B. Significant Results

The recommended AMAC core compressor served as the basis of the E<sup>3</sup> core compressor, and various design refinements were made through Tasks I - V of the E<sup>3</sup> study program. The most significant refinements that were incorporated into the core compressor design were an increase in the specific flow and reductions in aspect ratio, solidity and speed. These changes were made mainly to reduce costs through the use of fewer, longer chord airfoils and to increase blade life and general ruggedness. An increase in stall margin potential was estimated as a result of these refinements, and only a small efficiency penalty was calculated. Table 99 compares the principal design parameters of the recommended AMAC compressor, from contract NAS3-19444, (reference 6), to those of the final Task V E<sup>3</sup> core compressor which evolved from it during the course of the current E<sup>3</sup> Preliminary Design Study. The tabulated data for the AMAC design have been scaled to the same flow size as the E<sup>3</sup> compressor to make these comparisons easier.

A layout of the E<sup>3</sup> core compressor is shown in Figure 116. Low aspect ratio, unshrouded rotors are used throughout and all stators are shrouded at their inner ends. Stagewise distributions of aspect ratio and solidity are plotted in Figure 117. Bleed flows are extracted in stages 3, 6 and 7 and in the discharge diffuser. The inlet guide vanes and the first four stator vanes are variable for off-design matching, and extra stage 7 air (over and above turbine cooling requirements) can be extracted to aid stage matching in the engine start region.

#### 1. Detailed Aerodynamic Design

Work on the initial phase of the detailed aerodynamic design of the core compressor was conducted under Task V of the current E<sup>3</sup> Preliminary Design Study. This effort involved establishment of flowpath contours, calculation of vector diagrams using an axisymmetric flow calculation procedure and a preliminary definition of blading shapes.

TABLE 99

COMPARISON OF E<sup>3</sup> TASK V AND RECOMMENDED AMAC  
CORE COMPRESSOR DESIGN PARAMETERS

	<u>AMAC</u>	<u>E<sup>3</sup></u>
Number of Stages	10	10
Total-Pressure Ratio	23	23
Corrected Airflow, Kg/sec(lbm/sec)	54.43 (120)	54.43 (120)
Corrected Tip Speed, m/sec(ft/sec)	469.4 (1540)	455.7 (1495)
Inlet Radius Ratio	.476	.503
Flow/Annulus Area, Kg/sec-m <sup>2</sup> (lbm/sec-ft <sup>2</sup> )	178.2 (36.5)	185.5 (38)
Inlet Tip Diameter, m (in.)	0.718 (28.26)	0.707 (27.85)
Exit Hub Speed, m/sec (ft/sec)	358.1 (1175)	352.3 (1156)
Exit Radius Ratio	0.93	0.93
Exit Mach Number	0.26	0.29
Number of Rotors and Stators	1959	1602
Average Aspect Ratio	1.72	1.47
Average Pitchline Solidity	1.40	1.38
Average Reaction Ratio	0.67	0.71
Adiabatic Efficiency	0.860	0.857
Stall Margin Potential, %	18	25

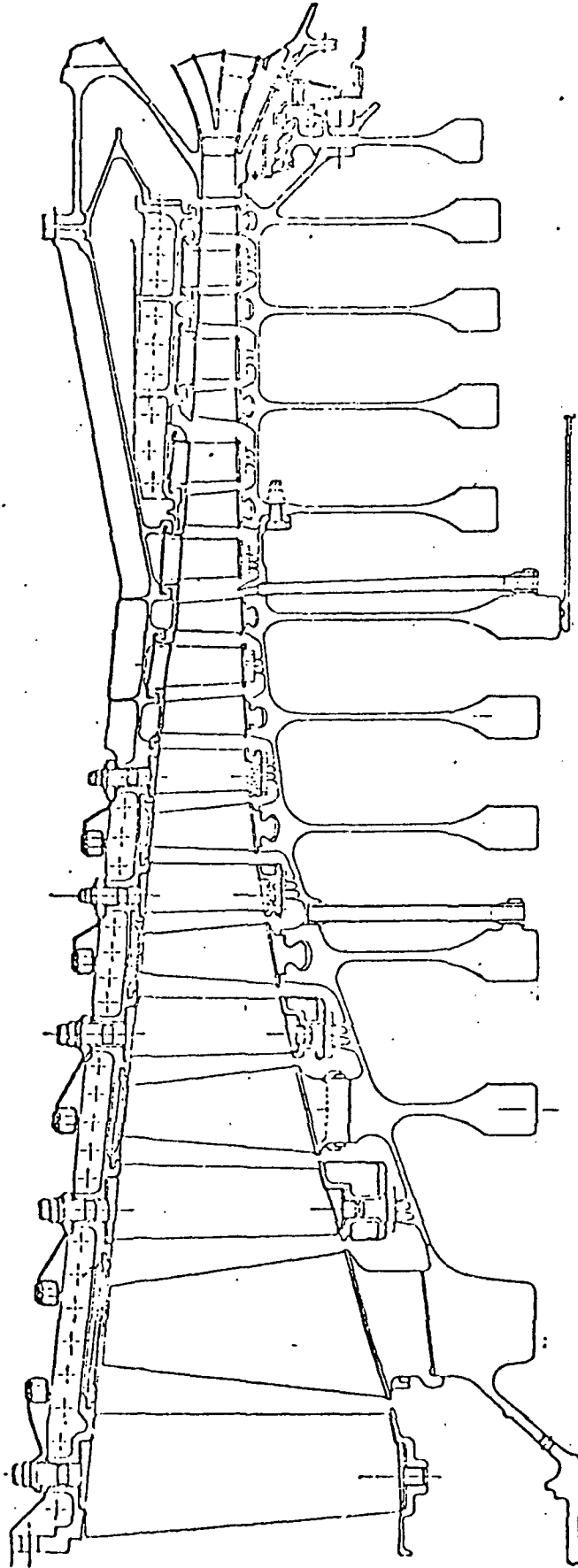


Figure 116. E<sup>3</sup> Compressor Cross Section.

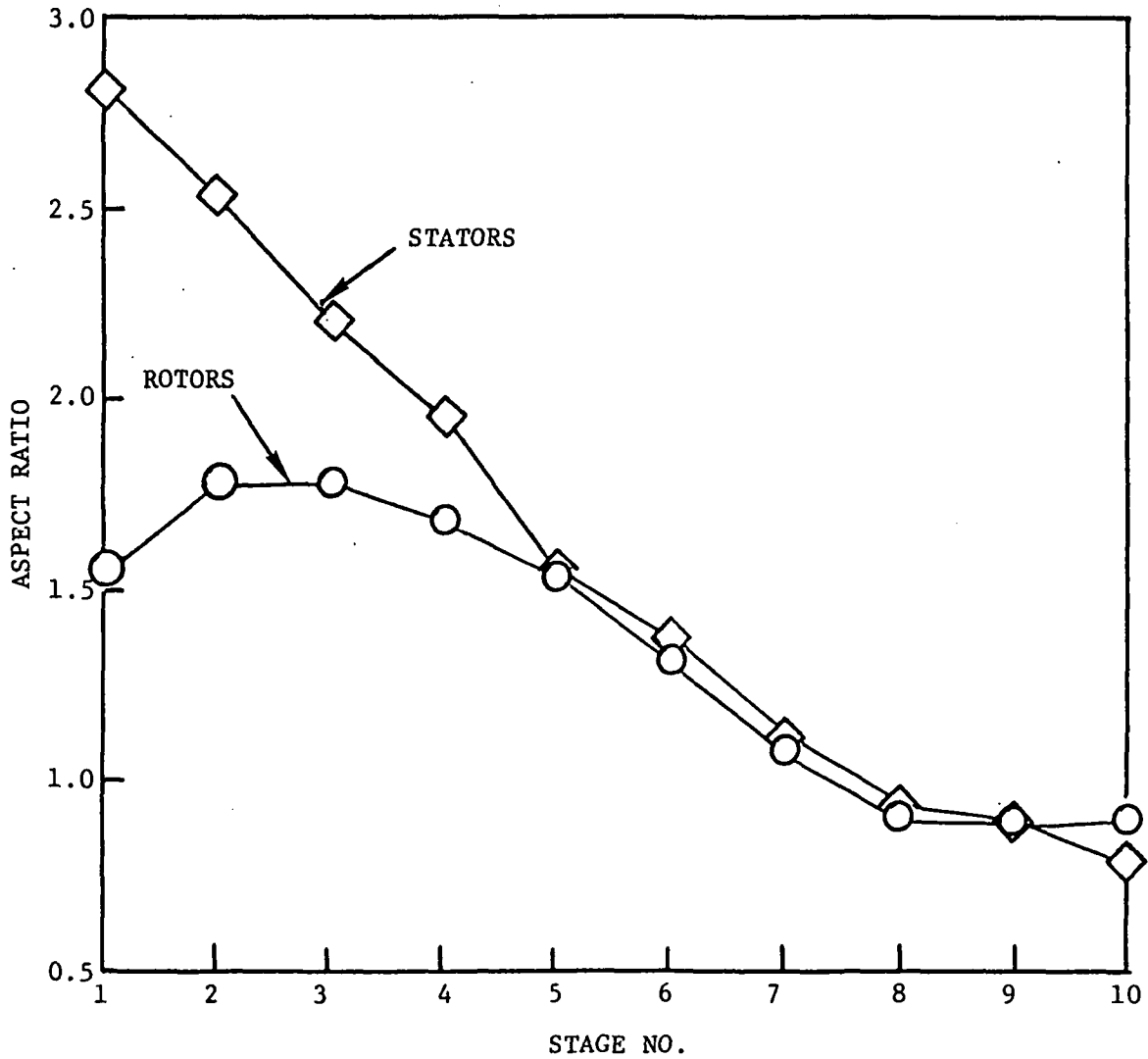
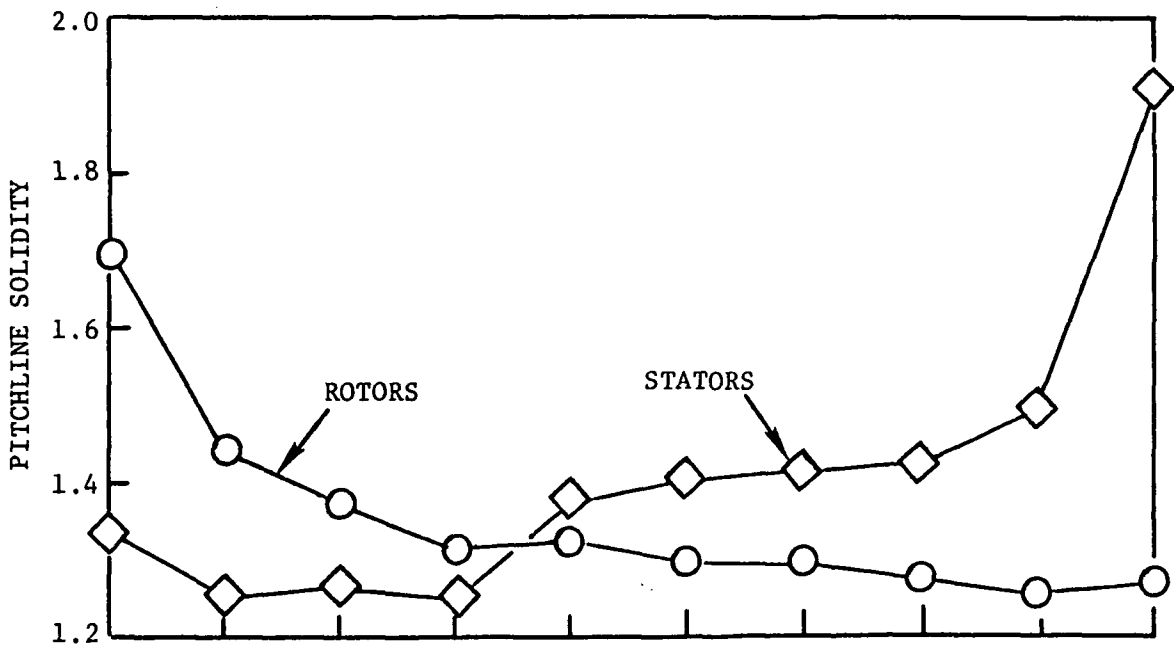


Figure 117. Stagewise Distributions of Core Compressor Solidity and Aspect Ratio



The primary calculation tool used in these design studies was the General Electric Circumferential Average Flow Determination (CAFD) computer program. This program calculates average vector diagram parameters and fluid properties along numerous stream surfaces. For Task V, calculations were made at leading and trailing edges of each blade row. The calculations included the inlet gooseneck region and the combustor diffuser section in order to properly model the radial distributions of static pressure set up by stream-tube convergence and curvature at the core compressor inlet and exit. Bleed extractions at stages 3, 5, 6 and 7 were also accounted for by the calculation procedure. The design flowpath and calculated stream surfaces are shown in Figure 118.

Aerodynamic design calculations were performed at the 100% corrected speed, (120 lbm/sec) 54.43 Kg/s corrected flow, 23:1 total-pressure ratio operating line point. Sea-level standard-day inlet conditions were specified. A blockage factor, or effective area coefficient, was specified at each calculation station to represent the influence of end wall boundary layers and free stream wakes. A blockage of 0.975 was specified at the first rotor inlet station, decreasing to 0.920 at the exit of the last stator. Radial distributions of stator exit total pressure and absolute air angle plus loss coefficients for both rotor and stator were input to perform the calculations of the flow field. These radial distributions were specified consistent with correlations predicting the radial extent of end wall effects so that the calculated vector diagram parameters and loading levels would resemble those measured in high speed compressors. Typical radial distributions of swirl angle and loss coefficient are shown in Figures 119 and 120 for stage 2 and stage 7. The magnitudes of the loss coefficients were specified to be approximately consistent with the efficiency goal of engines of this type during early stages of development. The stagewise trend of loss coefficients was taken from the Compressor Unification Study efficiency prediction model.

A summary of calculated vector diagram parameters is given in Table 100 for the final Task V flowpath. Relatively low through-flow meridional Mach numbers were specified throughout this compressor, as shown in Figure 121. This resulted in acceptable blade row inlet Mach numbers despite the high blade speed, and led to somewhat increased blade heights (and smaller clearance to blade height ratios) in the middle and rear stages. Relative inlet tip Mach numbers for the rotors were about 1.4 for rotor 1, 1.0 for rotor 4 and 0.7 for rotor 10. Absolute stator inlet hub Mach numbers were also moderate, equalling about 0.8 for stator 1 and 0.5 for stator 10. Stagewise distributions of rotor and stator pitchline diffusion factor are plotted in Figure 122. These are near the upper end of General Electric's core compressor experience, but are appropriate considering the relatively low level of aspect ratio that was employed and the high level of loading that this type of blading can sustain.

## 2. Preliminary Blade Shapes

Upon calculation of suitable vector diagrams for the final Task V flowpath, a blade-setting procedure was employed to calculate preliminary blade shapes for initiation of mechanical design and analysis. The blade setting procedure uses Carter's Rule, plus an input empirical adjustment, to determine the deviation angle of a cascade of equivalent two-dimensional, circular-arc meanline blades having the same circulation as the particular streamline

ORIGINAL PAGE IS  
OF POOR QUALITY

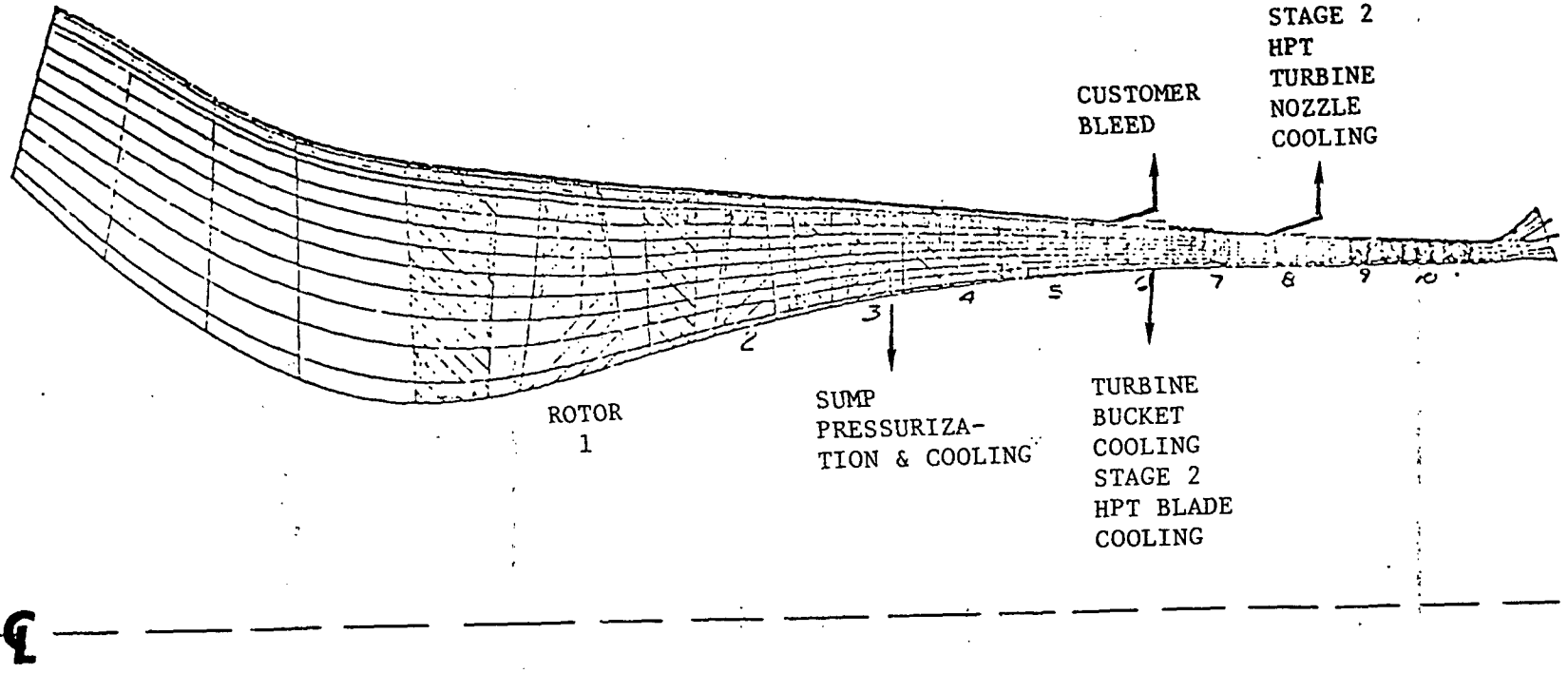


Figure 118. Core Compressor Aerodynamic Design Flowpath and Calculated Stream Surfaces

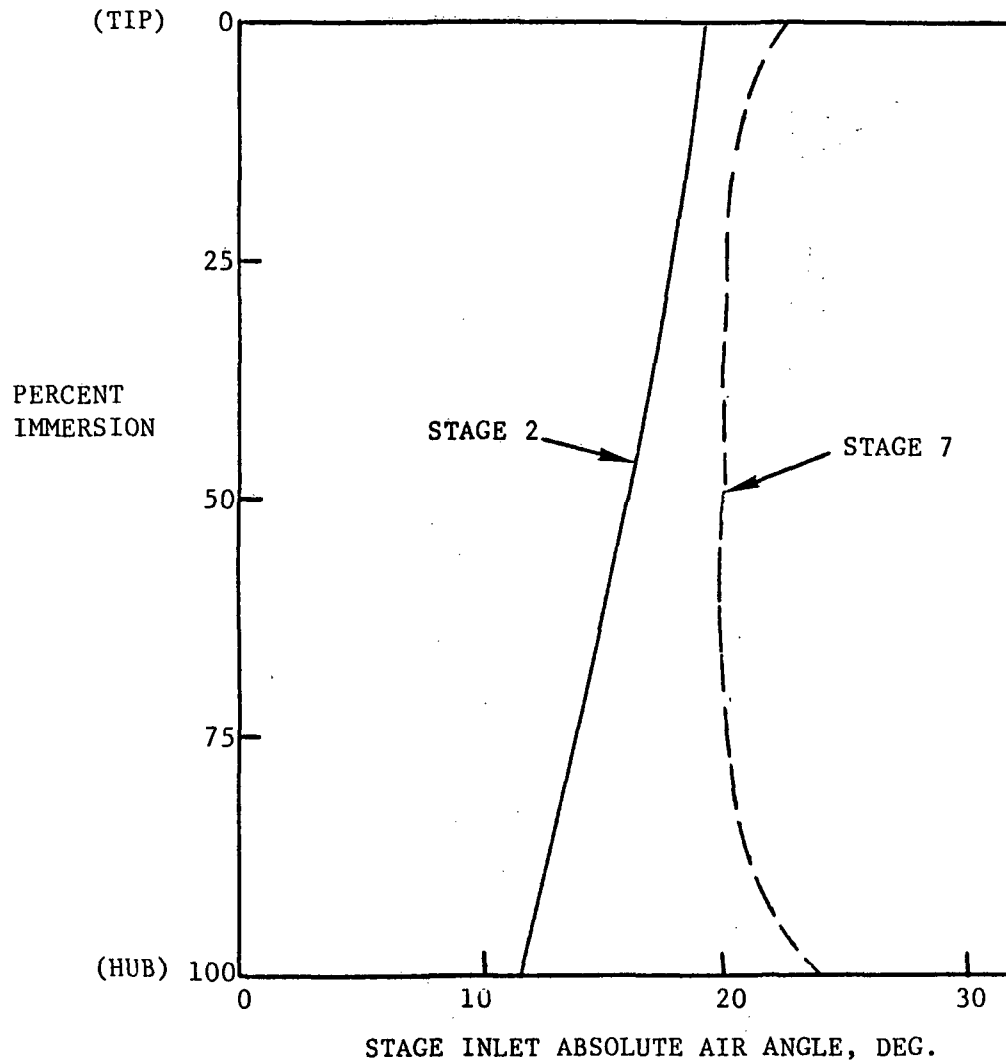


Figure 119. Radial Distributions of Stage Inlet Absolute Air Angle

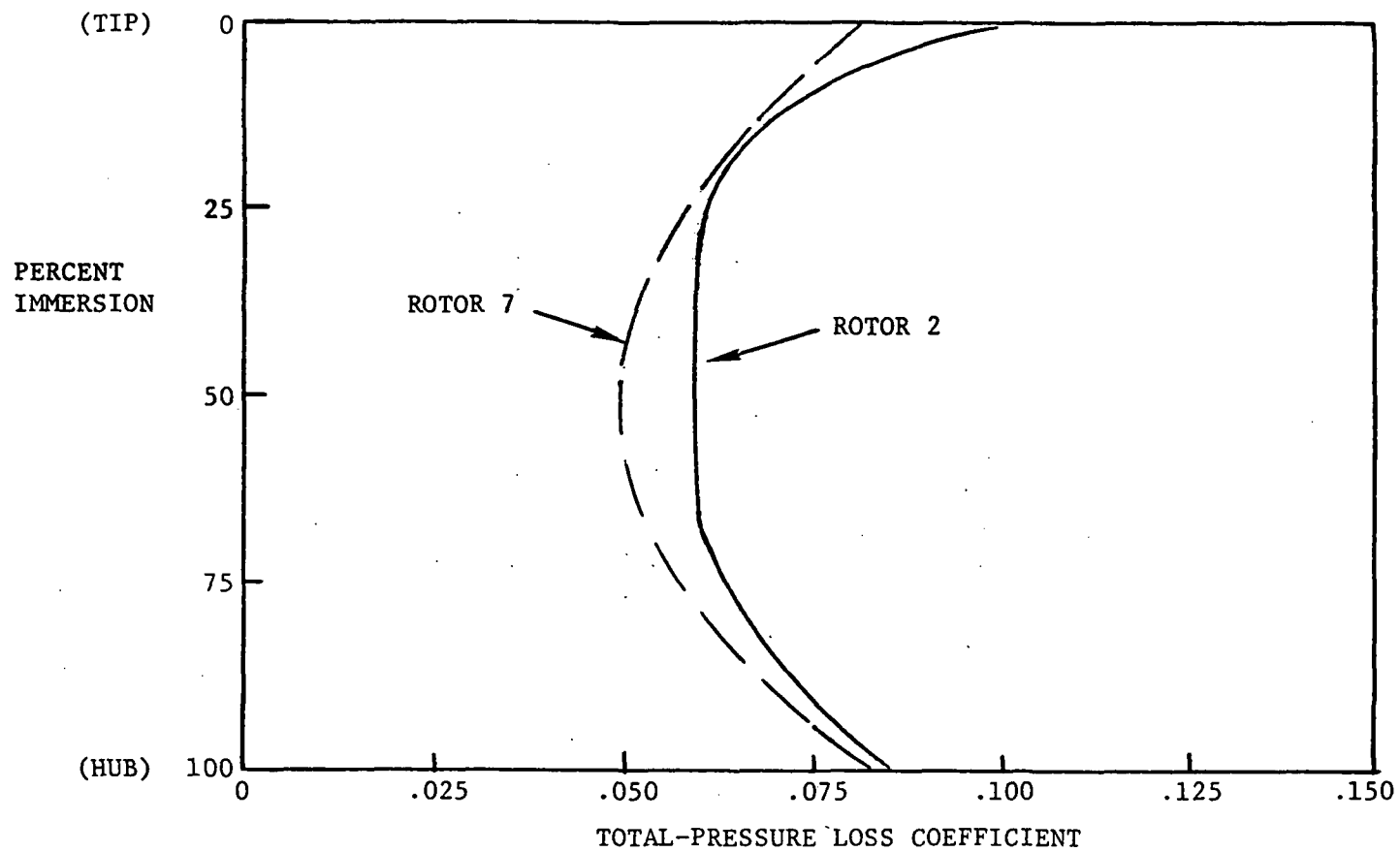


Figure 120. Radial Distributions of Rotor Loss Coefficient

TABLE 100

## SUMMARY OF COMPRESSOR VECTOR DIAGRAM DATA

		Stage Number									
		1	2	3	4	5	6	7	8	9	10
Tip Speed @ Rotor Inlet (fps)m/sec		455.7 (1495)	635.9 (1430)	426.1 (1398)	417. (1368)	408.7 (1341)	398.7 (1308)	392.6 (1288)	385.6 (1265)	381.9 (1253)	379.2 (1244)
Radius Ratio @ Rotor Inlet		.503	.655	.746	.804	.841	.873	.894	.913	.923	.930
Meridional Mach Number @ Rotor Inlet Pitch		.57	.53	.49	.46	.43	.41	.39	.36	.34	.30
Relative Mach Number @ Rotor Inlet	Tip	1.35	1.13	1.02	.93	.85	.80	.74	.72	.67	.64
	Pitch	1.14	1.00	.92	.87	.83	.79	.75	.72	.69	.66
	Hub	.85	.88	.81	.78	.74	.71	.68	.65	.63	.60
Absolute Mach Number @ Stator Inlet	Tip	.65	.63	.62	.59	.57	.55	.53	.50	.48	.45
	Pitch	.70	.69	.67	.63	.61	.58	.55	.52	.49	.46
	Hub	.79	.76	.73	.68	.64	.60	.58	.54	.51	.47
Absolute Air Angle @ Rotor Inlet Pitch		7.9	15.7	20.2	20.3	20.4	20.3	20.7	20.7	20.6	20.8
Rotor Diffusion Factor	Tip	.451	.434	.439	.468	.493	.503	.530	.526	.549	.543
	Pitch	.452	.447	.440	.447	.451	.459	.456	.474	.473	.468
	Hub	.452	.482	.493	.523	.534	.560	.546	.571	.573	.570
Stator Diffusion Factor	Tip	.477	.483	.479	.483	.479	.479	.520	.521	.547	.574
	Pitch	.407	.434	.469	.471	.471	.462	.488	.505	.509	.559
	Hub	.456	.452	.513	.511	.510	.500	.534	.550	.552	.582
Pressure Ratio @ Stage Exit		1.65	2.54	3.70	5.19	7.07	9.34	12.05	15.30	18.95	23.00
Temperature Ratio @ Stage Exit		1.181	1.353	1.522	1.689	1.857	2.020	2.185	2.345	2.505	2.660

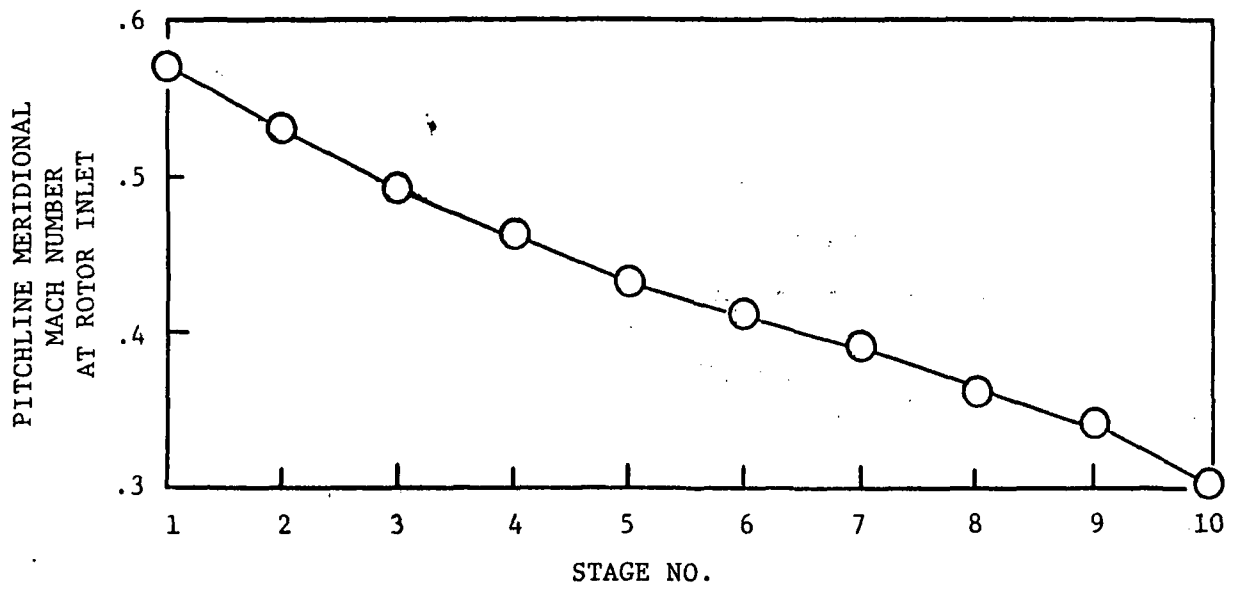


Figure 121. Stagewise Distribution of Rotor Inlet Pitchline Meridional Mach Number

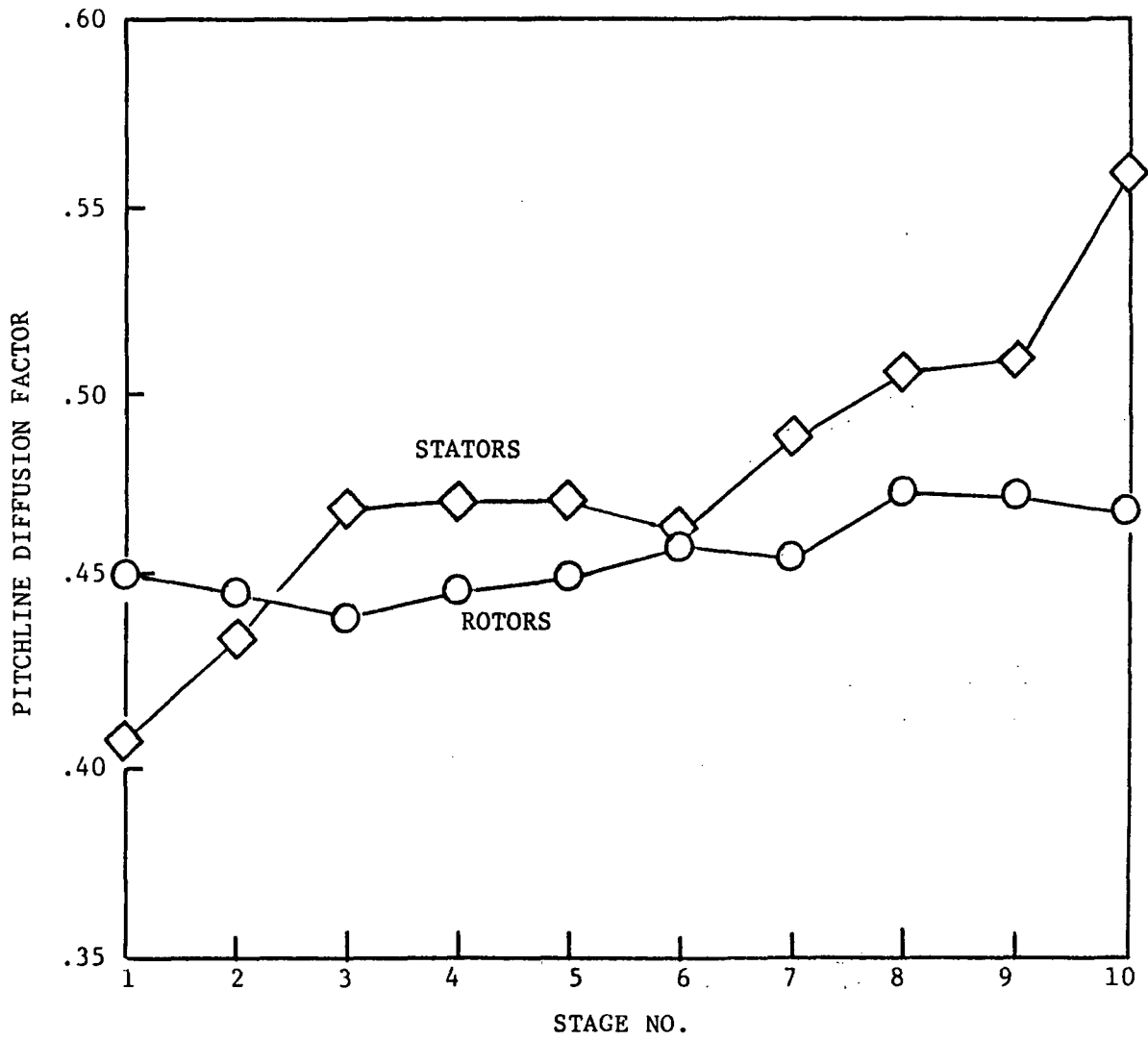


Figure 122. Stagewise Distributions of E<sup>3</sup> Compressor Rotor and Stator Diffusion Factor

section in the actual vector diagrams. Incidence angles for the higher Mach number front stages were input consistent with established practices for this type of airfoil. For the lower Mach number rear stage blades, a correlation (based on potential-flow cascade calculations) was used to determine the incidence angle that places the inlet stagnation point exactly at the leading edge of the blade. All blades were assumed to have circular-arc meanlines, with double-circular-arc thickness distributions for the rotors and NACA 65-series distributions for the stators. It is expected that most, if not all, of the later blades will ultimately employ special airfoil shapes tailored to local flow conditions, and that some of the stator vane rows will also employ special airfoils. A summary of preliminary rotor and stator blade geometry, including the calculated stagger and camber values from the blade setting procedure, is given in Table 101.

### 3. Off-Design Performance Predictions

Estimates of part-speed performance were conducted under Task V of the E<sup>3</sup> Preliminary Design Study contract using a stage characteristic and stage stacking procedure. Stage design speed characteristics were constructed consistent with each stage's design point and its stalling static pressure rise coefficient given by the General Electric stall prediction model. The stagewise distribution of design work input was taken from a preliminary Task V design axisymmetric flow calculation. Efficiency levels for each stage were consistent with the losses input to the Task V axisymmetric flow vector diagram calculations. Semi-empirical methods were used to estimate the variation of losses and turning above and below the design point. The characteristics were expressed as normalized flow and pressure rise coefficients, formulated to include corrections for stage inlet swirl variations produced by the front variable stators, and for variations in axial velocity ratio. Despite the use of normalized characteristics, it was necessary to generate a different characteristic at each speed for the variable-geometry front stages in order to represent the reduced rotor turning and high stator losses encountered when the stators are closed more than about 20°. The characteristics for stage 2 are shown in Figure 123 as an example. The fixed-geometry rear stages were represented by a single characteristic for all corrected speeds. A typical example of a rear stage characteristic is shown in Figure 124 for stage 7. Also shown in this figure is test data from a low speed model of a typical E<sup>3</sup>/AMAC core compressor rear stage. This low-speed Stage A was designed and tested under NASA contract NAS3-20070 to help develop the advanced-technology blading required for the E<sup>3</sup> core compressor. The test results from Stage A provide verification that the flow range, pressure rise and efficiency levels assumed for the high speed E<sup>3</sup> core compressor off-design performance estimates should be achievable.

Results of this analysis are summarized in the performance map shown in Figure 125. Calculations were made for speeds of 75% through 100% of design speed, encompassing the entire engine operating range from ground idle to maximum climb thrust at altitude. A practical stator schedule was identified that produced part-speed stall margins of 25% or more in the flight operating range with good overall efficiencies. A key finding was that it did not appear to be necessary to use any stage 7 starting bleed in the flight operating range of the engine to achieve acceptable low speed stall margin. To achieve this level of stall margin and efficiency did require substantial stator closures, amounting to 66° and 50° at 75% speed for the IGV and first



TABLE 101

SUMMARY OF TASK V BLADE GEOMETRY

		Stage Number									
		1	2	3	4	5	6	7	8	9	10
No. Rotor Blades		28	42	56	66	76	80	80	80	88	98
Rotor Aspect Ratio		1.55	1.78	1.78	1.68	1.53	1.31	1.07	.89	.88	.89
Rotor Solidity	Tip	1.32	1.21	1.20	1.18	1.22	1.21	1.22	1.22	1.20	1.21
	Pitch	1.70	1.44	1.37	1.31	1.32	1.29	1.29	1.27	1.25	1.26
	Hub	2.42	1.79	1.58	1.46	1.44	1.38	1.36	1.33	1.30	1.30
Rotor Stagger	Tip	61.7	58.4	56.3	54.6	53.2	52.1	51.2	51.2	52.4	54.1
	Pitch	48.7	48.3	48.1	48.9	48.9	49.1	48.8	49.7	50.8	52.7
	Hub	28.9	34.1	35.7	40.2	41.5	42.8	43.8	45.3	47.0	49.5
Rotor Camber	Tip	3.1	10.8	14.5	18.0	19.9	20.7	21.9	23.0	22.3	21.7
	Pitch	13.2	16.2	17.8	18.7	20.4	20.4	21.4	21.8	21.0	20.1
	Hub	40.2	32.7	31.4	29.4	29.2	28.0	28.0	28.3	26.3	24.6
No. Stator Vanes		50	62	74	82	90	100	100	100	110	140
Stator Aspect Ratio		2.80	2.53	2.20	1.94	1.54	1.37	1.11	.94	.89	.79
Stator Solidity	Tip	1.25	1.25	1.26	1.25	1.38	1.40	1.41	1.42	1.49	1.90
	Pitch	1.34	1.25	1.26	1.25	1.38	1.40	1.41	1.42	1.49	1.90
	Hub	1.75	1.48	1.43	1.38	1.49	1.49	1.48	1.48	1.54	1.96
Stator Stagger	Tip	32.0	31.8	32.2	33.9	34.6	34.4	35.5	34.7	36.0	25.8
	Pitch	27.9	31.8	32.2	32.4	32.6	32.5	32.7	33.2	33.2	23.2
	Hub	25.3	30.9	33.0	34.2	35.2	35.2	35.8	36.5	36.6	26.9
Stator Camber	Tip	49.0	46.4	44.2	47.0	46.8	45.5	49.6	47.2	50.9	68.8
	Pitch	37.6	36.5	38.6	39.5	37.8	37.2	38.1	39.9	39.3	58.7
	Hub	46.4	39.4	44.4	46.1	44.7	44.8	47.3	49.7	49.3	69.0

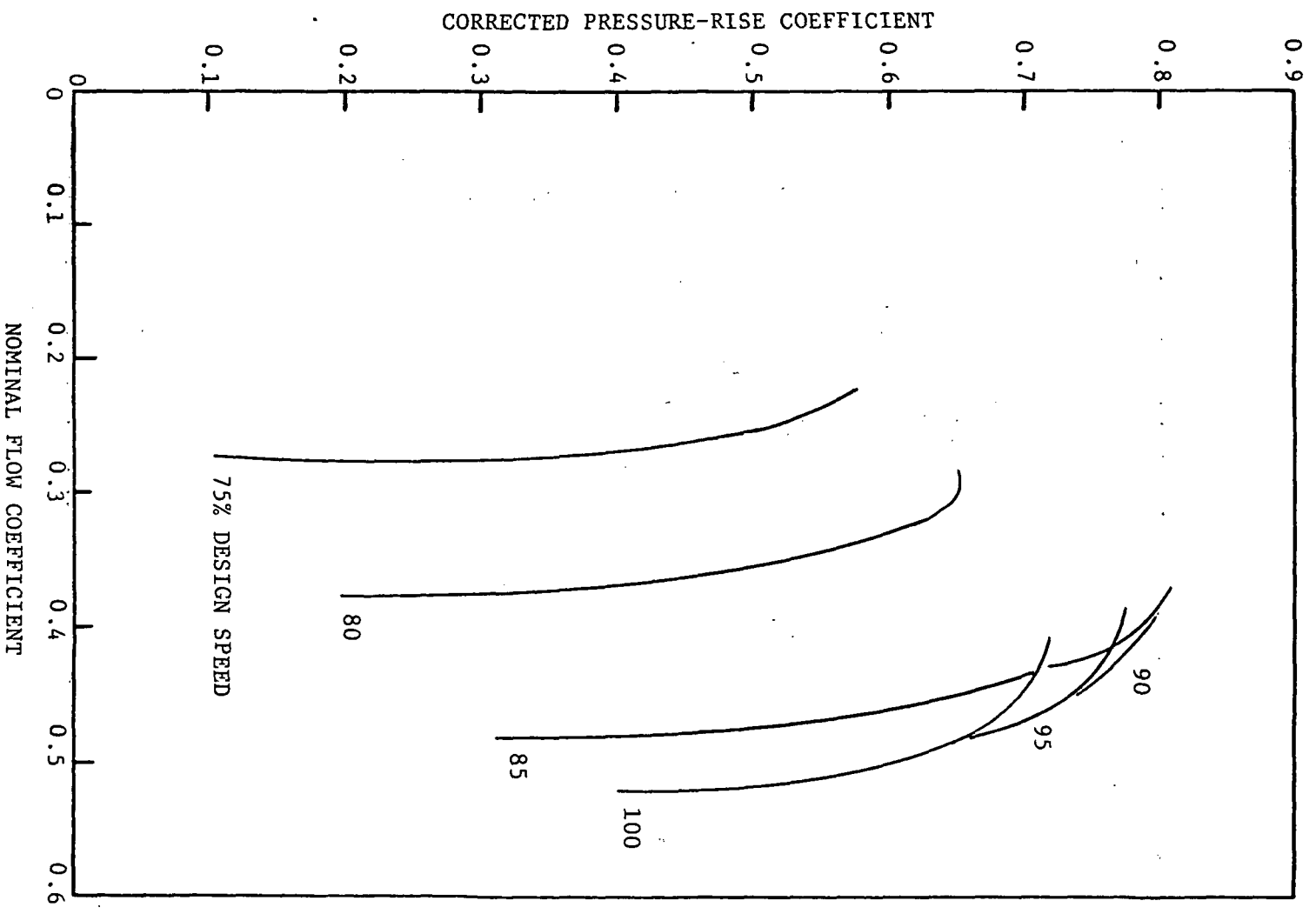


Figure 123. Estimated Stage 2 Characteristics

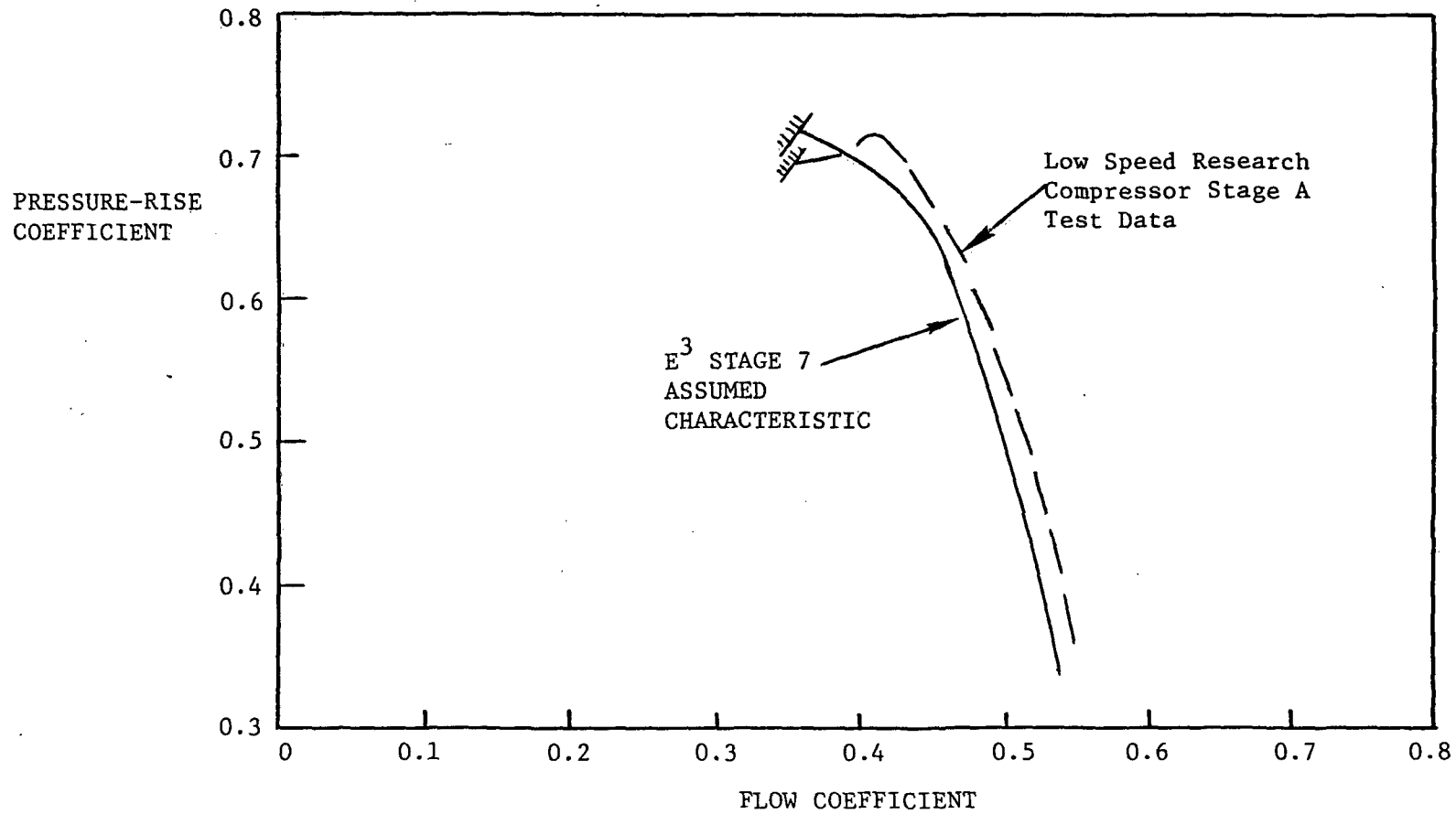
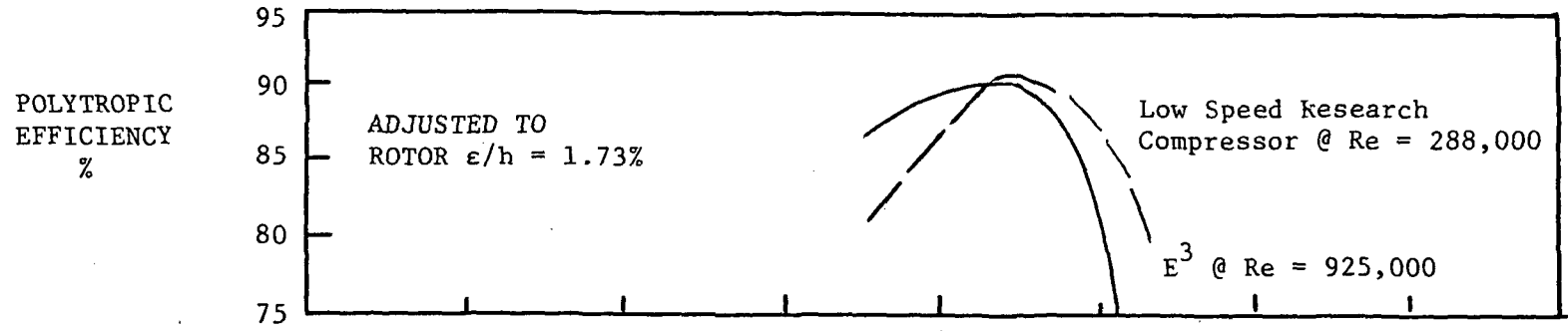


Figure 124.  $E^3$  Stage 7 Characteristic Compared to Stage A Data

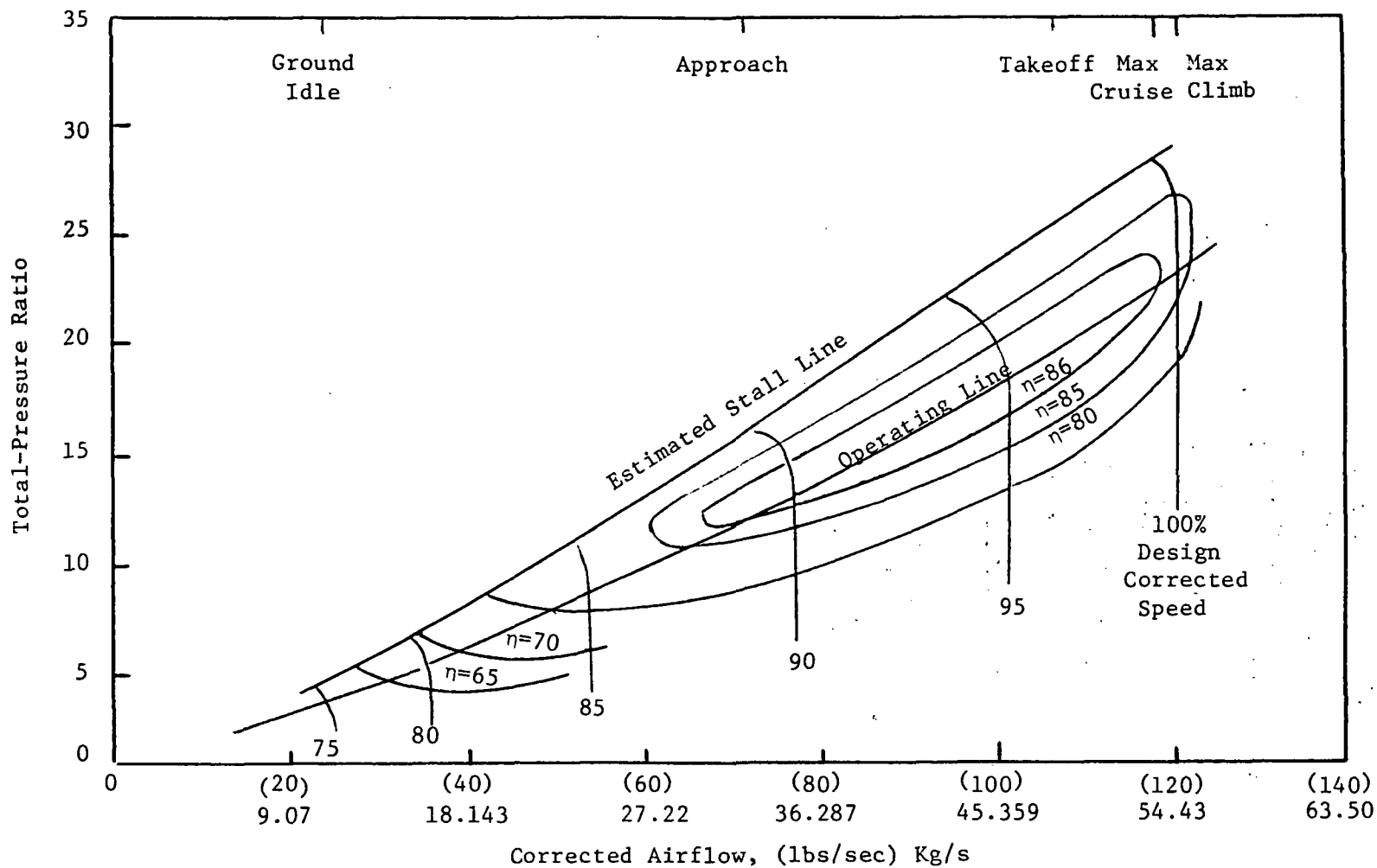


Figure 125. Core Compressor Performance Map Estimated from Stage Characteristics, without Starting Bleed.

stator, respectively. This stator schedule produces a flow versus speed relationship in which the flow is only about 20% of the design value at 75% speed. This is a desirable characteristic for the core compressor of a subsonic turbofan engine, however, since it reduces the core engine speed change required for a given thrust change which tends to reduce the time needed for accelerations. Another key finding was that, for the stagewise distribution of work input assumed when constructing the estimated characteristics, the middle stages of the compressor were the stall-limiting stages at high speed. It is generally desirable for the rear stages to be stall-limiting at high speed, so the work distribution used in the Task V axisymmetric flow design calculations was adjusted slightly to unload the middle stages and to load the rear stages.

### C. Conclusion/Recommendations

Based on the results of this Task and the previous AMAC Study (reference 6), it is believed that the identified 10 stage highly loaded compressor would be a good balance of the performance, economics and ruggedness required for a commercial advanced turbofan engine. The more detailed design efforts of this Task have not identified any previously unknown problems that would prevent a successful technology demonstration of the advanced aerodynamic performance potential embodied in this design.

## SECTION VIII

### CONCLUSIONS

The results of this study indicate that a more fuel efficient engine cycle and configuration is achievable and could be certified for use in the late 1980's. All NASA study goals for the more fuel efficient engine are projected to be met or surpassed except the acoustic goal. The final direct-drive energy efficient engine is predicted to not meet the FAR 36 (1969) - 10 EPNdB NASA study goal, but could meet the FAR 36 (1978) requirements.

The exhaust configuration comparisons showed that a mixed-flow exhaust system was clearly better than a separate flow system for the mission studied. It is necessary for lightweight composite fan duct and nozzle technology to be available, however, to achieve the full projected fuel savings from mixing.

Although the studies consistently showed the geared turbofans to have an uninstalled sfc advantage over the direct-drive turbofans, the Task III direct-drive turbofan was recommended for continued design and development. This was for the following reason:

Installed drag, first cost and weight penalties of the final geared engine resulted in the direct-drive engine having better mission fuel consumption and direct operating cost.

Mission evaluation of the direct and geared engines by the airframe subcontractors tended to verify these results.

An assessment of the risk involved in achieving the target engine performance, in a technology program, was completed. Achievement of fully developed component performance goals was estimated to have a probability of only 20%. A target achievement of 12.4% sfc improvement over the CF6-50C reference was thought to be 95% probable, however.

More detailed preliminary aerodynamic design of the very advanced 23:1 high pressure compressor did not uncover any severe performance problems. Starting the compressor still continues to be of most concern, but the starting bleed and variable geometry provisions should permit reliable operation.

PRECEDING PAGE BLANK NOT FILMED

TABLE OF CONTENTS

	<u>PAGE NO.</u>
APPENDIX A . . . . .	349
TASK II SUBCONTRACTOR STUDIES . . . . .	349
A. The Boeing Company . . . . .	349
1. Aircraft and Mission Definition . . . . .	349
a. Mission Selection and Design Constraints . . . . .	349
b. Advanced Technology Features . . . . .	350
c. Engine Placement . . . . .	350
2. Results of Airplane Sizing Studies . . . . .	355
a. Airplane Data . . . . .	355
b. Take-off Gross Weight and Fuel Burned Comparison . . . . .	355
B. Lockheed California Company . . . . .	355
1. Aircraft and Mission Definition . . . . .	355
a. Aircraft Design Characteristics . . . . .	355
b. Airframe Technology Levels . . . . .	355
c. Aircraft Mission and Payload Definition . . . . .	358
2. Airplane Sizing Studies . . . . .	362
a. Concept Design of Reference Aircraft . . . . .	362
b. Integration of Advanced Technology Engines . . . . .	362
c. Aircraft Performance Comparisons . . . . .	362
d. Airframe Noise Estimates . . . . .	362
C. McDonnell Douglas Corporation . . . . .	362
1. Airplane Definition and Performance . . . . .	362
2. Advanced Technology Concepts--Long Duct Mixed Flow Nacelle . . . . .	362
a. Improved Performance . . . . .	372
1. Improved Internal Performance . . . . .	372
2. Reduced Drag . . . . .	372
3. Reduced Engine Deterioration . . . . .	373
4. Weight Reduction . . . . .	373
b. Noise Reduction . . . . .	373
1. Forced Mixing . . . . .	376
2. Composite Long Duct . . . . .	376
3. Improved Inlet Acoustic Treatment . . . . .	376

LIST OF FIGURES  
APPENDIX A  
TASK II SUBCONTRACTOR STUDIES

<u>FIGURE NO.</u>	<u>TITLE</u>	<u>PAGE NO.</u>
126	Boeing Intercontinental Airplane Configurations	351
127	Boeing Domestic Airplane Configurations	352
128	Engine Placement Guidelines - Boeing	354
129	Aircraft Weight and Fuel Burned Comparison, Task II Boeing Study	357
130	Carpet Plot, Domestic Aircraft - CF6-50C Engine	363
131	Block Fuel - Lockheed Study	366
132	Operating Cost - Lockheed Study	367
133	Conventional Design of a "Stretched" DC-10 Type Airplane - McDonnell Douglas Study	368
134	Advanced INtegrated Nacelle - McDonnell Douglas Study	371
135	Reverse Flow Directivity Requirement - McDonnell Douglas Study	374

LIST OF TABLES

<u>TABLE NO.</u>	<u>TITLE</u>	<u>PAGE NO.</u>
102	Advanced Airframe Structure for E <sup>3</sup> Studies - Boeing	353
103	Boeing Airplane Characteristics and Performance - Task II	356
104	Advanced Composites Effects - Lockheed Study	359
105	World Traffic Forecast - Lockheed Study	360
106	Total Long Haul Aircraft Requirements - Lockheed Study	361
107	Reference Aircraft Characteristics - Lockheed Study	364
108	Aircraft Performance Characteristics - Lockheed Study	365
109	Aircraft Characteristics - McDonnell Douglas Study	369
110	Aircraft Weight Breakdowns - McDonnell Douglas Study	370
111	Estimated Noise Reduction ( $\Delta$ EPNdB) for Long Duct Nacelle with Mixer Nozzle and Bulk Treatment in the Inlet at Maximum Certified Gross Weight - McDonnell Douglas Study	375



## APPENDIX A

### TASK II SUBCONTRACTOR STUDIES

#### A. The Boeing Company

##### 1. Aircraft and Mission Definition

##### a. Mission Selection and Design Constraints

Examination of the possible 1990 market situation suggested that the future airline market place would be similar to the existing market place, i.e., familiar size airplanes flying familiar routes and schedules. This prediction was based on the supposition that the air traveling community in the 1990's will be approximately the same percentage of the total population as today's air travelers with a small (4% to 6%) annual incremental growth. The air cargo market should experience similar growth unless a large dedicated airfreighter is developed which might stimulate increased air cargo growth.

Many of the current narrow body aircraft will probably be retired from active service by the major airlines in the late 1980's. These include the intercontinental range 707-320B and C models plus the DC-8 Sixty series airplanes, and the 727-200 model domestic range airplanes. There are currently some 500 fan powered 707's and about 250 DC-8 Sixty series airplanes in service along with over 1000 727-200 models.

Hence, barring unforeseen developments, there should be a market in the late 1980's for a large number of replacement aircraft in the 180-220 passenger size range with intercontinental or domestic range capability. Accordingly, the design missions and sizing constraints selected for the EEE study are:

	<u>Domestic Airplane</u>	<u>Intercontinental Airplane</u>
Design Range, Km (n. mi.)	3704 (2000)	10186 (5500)
Nominal Payload, Pax (15/85 mix)	196	196
Cruise Mach No.	0.80	0.80
T.O.F.L., m (feet) (max)	2287 (7500)	3354 (11000)
Max V <sub>App</sub> , Km/hr (kts.)	232 (125)	250 (135)
ICAC, m <sup>3</sup> (ft.) (min)	10061 (33000)	10061 (33000)
Reserves	ATA Dom.	ATA Int'l.

For economic assessments, the following off-design missions were selected:

	<u>Domestic Airplane</u>	<u>Intercontinental Airplane</u>
Range Km (n. mi.)	1852 (1000)	3704 (2000)
Payload, pax (15/85 mix)	108	108
Cruise Mach No.	0.80	0.80

Both airplanes provide for a three-man flight crew.

The key factors in determining the configuration on any new airplane design are the choice of the number of engines, engine size, and the choice of body diameter/seating arrangement. For the intercontinental model, it was decided to use four wing mounted engines and a wide body with seven-abreast double aisle seating. The choice of four engines over three engines was not based on any intrinsic advantage, but was done to simplify the engine installation problems and avoid scaling of the center engine installation, plus providing wing bending relief and flutter suppression. The choice of a wide body over a conventional body with six-abreast seating was based on the preference shown by passengers for double aisle seating on very long (greater than 10 hours) flights. The choice of body diameter and the seven-abreast seating follows from the number of passengers and the comfort standards desired. The lower lobe can accommodate seventeen LD-3 containers side by side.

The configuration of the domestic airplane was selected for high commonality with the intercontinental airplane; hence it has the same body and seating arrangements with two wing mounted engines.

#### b. Advanced Technology Features

The advanced technology features are summarized on the airplane configuration drawings, Figures 126 and 127.

A discussion of the aerodynamic and structural advanced technology features is given below:

Aerodynamics - A baseline drag level was derived from representative wind tunnel model data. Improvements to this baseline drag data base were applied as follows:

- Cruise - 2% reduction in cruise drag due to improved wing-airfoil design and improved component integration. In addition, it was assumed that the advanced active control system would produce zero trim drag.
- Take-off and Landing - A five percent improvement in lift-drag ratio was assumed for the domestic 2-engine airplane. This reflected the following changes: Sealed leading edge flaps, seals between nacelle struts and lateral edges of the leading edge flaps, and aileron droop. No improvement in take-off and landing lift-drag ratio was made for the four-engine intercontinental airplane.

Weights & Structures - Application of advanced aluminum alloys and advanced composite structures on airframe components along with potential weight savings is shown in Table 102.

#### c. Engine Placement

Guidelines were established for the chordwise engine placement on the wing which provided minimum interference drag with no vortex shedding over the wing and no jet wake impingement. These guidelines are defined in Figure 128.



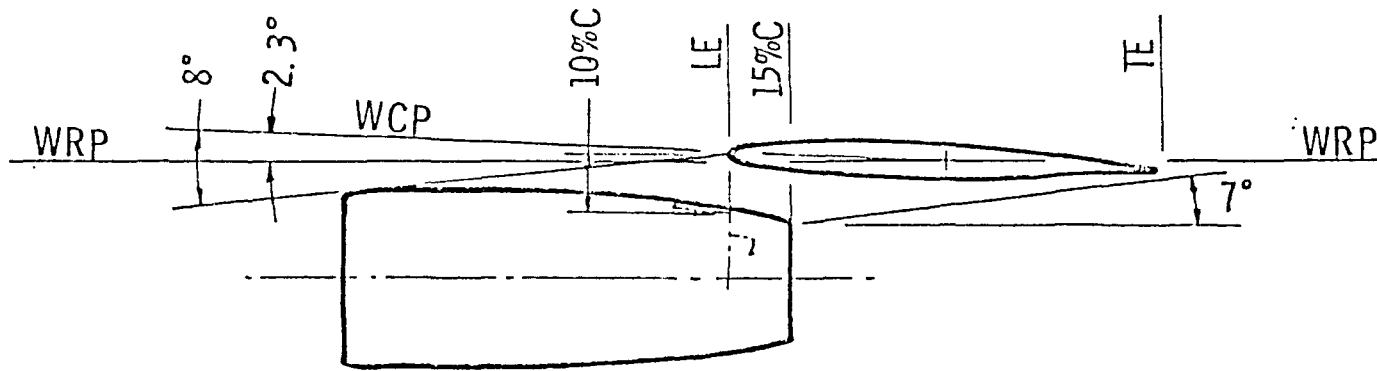


TABLE 102

ADVANCED AIRFRAME STRUCTURE FOR E<sup>3</sup> STUDIES - BOEING

CURRENT TECHNOLOGY	NEW TECHNOLOGY		
MATERIAL	MATERIAL	STRUCTURAL COMPONENT	WEIGHT SAVING % OF COMPONENT WEIGHT
STANDARD ALUMINUM ALLOYS (CURRENT 747)	ADVANCED ALUMINUM ALLOYS	WING BOX FUSELAGE EMPENNAGE BOX	6% 4% 6%
CONVENTIONAL ALUMINUM CONSTRUCTION	ADVANCED COMPOSITE STRUCTURE (GRAPHITE)	CONTROL SURFACES LANDING GEAR DOORS	25%
	CARBON	MAIN LANDING GEAR BRAKES	40%
	TITANIUM FITTINGS	LANDING GEAR SUPPORT SIDE OF BODY RIB EMPENNAGE BODY ATTACH ENGINE STRUT ATTACH FLAP SUPPORT	20%

ORIGINAL PAGE IS  
OF POOR QUALITY.



- \* Minimize Interference Drag
  - Nacelle primary nozzle forward of 15% of chord
  - Nacelle fan exit forward of leading edge
  - Fan exit upper edge vertical position below wing chord plane by 10% chord or greater
- \* No Vortex Shedding Over Wing
  - Forward lip of cowl must be below an 8 degree line measured with respect to local chord plane
- \* No Jet Wake Impingement
  - Jet wake based on equivalent diameter at the plane of primary nozzle and expanding 7 degrees must not contact lower wing surface

Figure 128. Engine Placement Guidelines - Boeing

The spanwise engine positions were selected from flutter considerations. The inboard engines were located at 34.8% and the outboard engines at 72.0% of the wing semi-span.

## 2. Results of Airplane Sizing Studies

### a. Airplane Data

Airplane characteristics and performance of the intercontinental and domestic airplanes powered by the CF6-50C and the Task II direct-drive mixed-flow baseline engine are shown in Table 103.

### b. Take-off Gross Weight and Fuel Burned Comparison

The take-off gross weight, OEW, and fuel burned for the airplanes powered with the Task II engines are compared to the CF6-50C on Figure 129. For the domestic airplane with direct drive engines, the fuel burned on an average mission is 11.7% less than required for the CF6-50. For the intercontinental airplane, the corresponding reduction in fuel burned is 14.1%.

## B. Lockheed California Company

### 1. Aircraft and Mission Definition

Definition of aircraft design characteristics, airframe technology levels, and mission requirements were established for both a domestic and intercontinental aircraft for introduction into service in the early 1990's. These definitions were as follows:

#### a. Aircraft Design Characteristics

- Provide passenger comfort comparable to current commercial aircraft.
- Utilization of same engine size for both domestic and intercontinental aircraft.
- Capability for operation from existing airport facilities.
- Compatibility with existing air traffic control systems.

#### b. Airframe Technology Levels

For the early 1990's time frame, the following technology features and levels were incorporated into the airframe design for all aircraft considered during this study.

- Supercritical wing
- Active controls
- Composite structure

The refined, supercritical airfoil features a more rounded leading edge and a cambered trailing edge. These revisions reduce shock wave strength (allowing higher cruise speeds), provide better chordwise loading, and permit use of reduced sweep and thicker airfoil sections. For this study, an aspect ratio of 10, sweep of 30°, and a thickness ratio of 12% was selected as the best geometry for fuel savings due to the decrease in wing structural weight requirements.

TABLE 103

BOEING AIRPLANE CHARACTERISTICS AND PERFORMANCE - TASK II

	(1)		(2)	
	Intercontinental Airplane		Domestic Airplane	
	CF6-50C	Task II Direct Drive Baseline Engine	CF6-50C	Task II Direct Drive Baseline Engine
TOGW Kg (lb)	191737 (422700)	170191 (375200)	119297 (263000)	112493 (248000)
OEW Kg (lb)	91278 (201230)	84311 (185870)	74645 (164560)	71497 (157620)
Wing Area, M <sup>2</sup> (Sq. ft.)	302 ( 3252)	268 ( 2886)	233 ( 2505)	219 ( 2362)
SLS F <sub>n</sub> N (lb)/Eng.	115075 ( 25870)	99951 ( 22470)	170988 ( 38440)	151950 ( 34160)
TOFL (S.L., 84°F) m (ft)	2323 ( 7619)	1005 ( 3296)	1530 ( 5018)	2287 ( 7500)
ICAC, m (ft)	10061 ( 33000)	10061 ( 33000)	10722 ( 35170)	10722 (35170)
VAPPR, Km/hr (Knots)	215 (116)	219 (118)	222 (120)	224 (121)
Block Fuel @ Des. Payload/Range Kg(lb)	70353 (155100)	57698 (127200)	19582 ( 43170)	16969 ( 37410)
@ Typ. Payload/Range	20571 ( 45350)	17663 ( 38940)	9086 ( 20030)	8024 ( 17690)
Block Time @ Des. Payload/Range (hr.)	12.32	12.32	4.69	4.69
@ Typ. Payload/Range	4.69	4.69	2.52	2.52

(1) Design Payload/Range = 196 Pax/(5500 N. Mi.) 10186 Km  
 Typical Payload/Range = 108 Pax/(2000 N. Mi.) 3704 Km

(2) Design Payload/Range = 196 Pax/(2000 N. Mi.) 3704 Km  
 Typical Payload/Range = 108 Pax/(1000 N. Mi.) 1852 Km



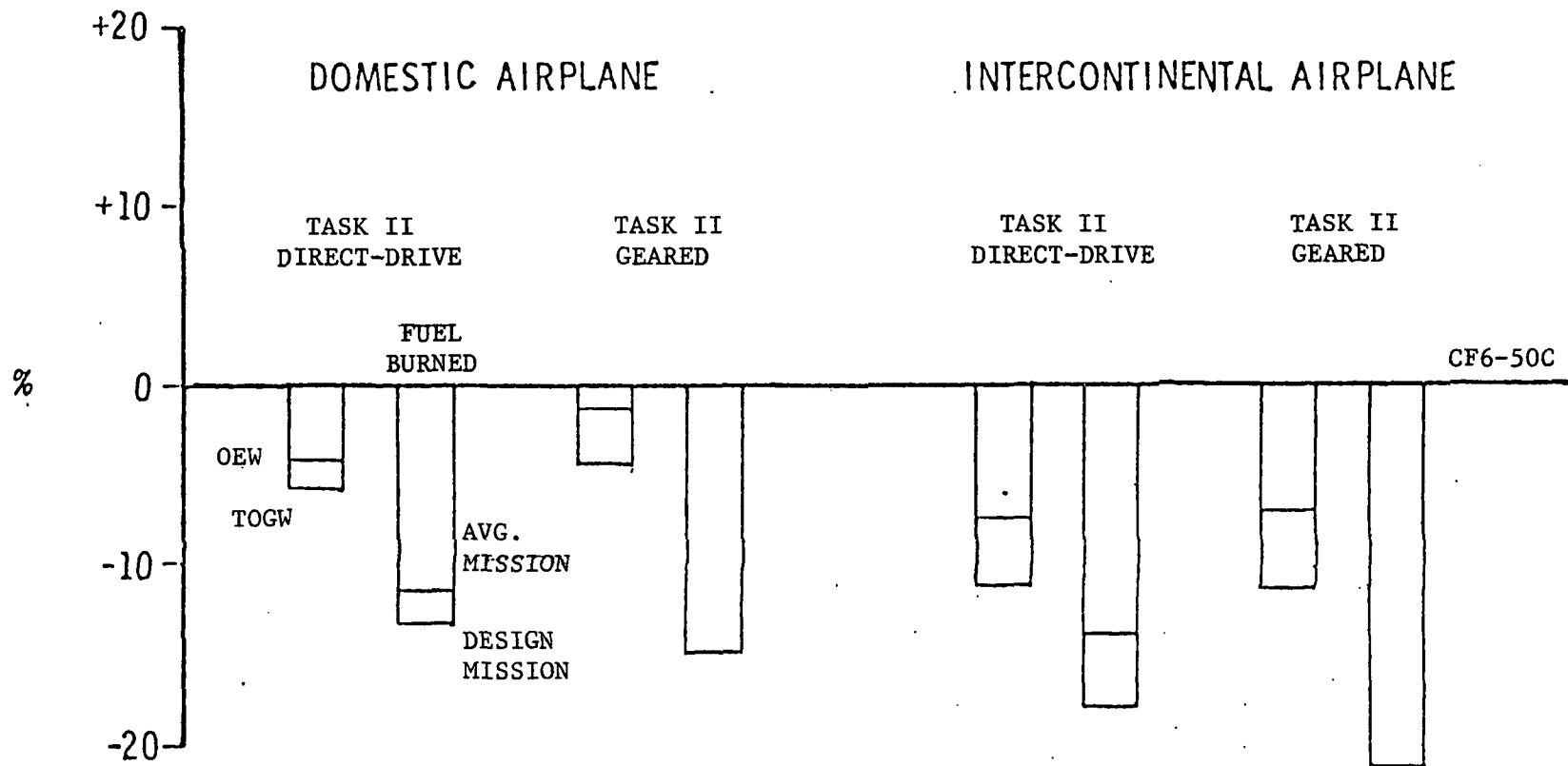


Figure 129. Aircraft Weight and Fuel Burned Comparison, Task II - Boeing Study

An active controls system is incorporated to provide additional fuel savings benefits by providing load relief and relaxed static stability. The active controls system is a computerized system where the airplane control surfaces are activated by computers using sensor inputs rather than pilot commands.

Load relief, by the use of active ailerons, provides redistribution of wing loading and results in reduced bending moments permitting reduction in wing and body structural weight. Relaxation of static stability, allowing a reduction in static margin, results in a smaller horizontal tail size. The effect of active controls on aircraft configurations for this study are:

- Load relief --- Reduction in wing weight of 5.5%  
Reduction in body weight of 1%
  
- Relaxed stability -- Reduction in tail size of 28%

Advanced composite structures incorporated include internal and external secondary structure as well as a significant portion of primary structure. Use of composite materials for aircraft structure results in empty weight savings of 5 to 10 percent (see Table 104) with attendant fuel savings of 2 to 4 percent. The benefits of composite structure is a reduction in parts count, simplified fabrication, improved structural efficiency, enhanced corrosion resistance, reduced material and labor costs, and reduced weight.

#### c. Aircraft Mission and Payload Definition

Lockheed market projections to the year 2000 were utilized to establish total world traffic demand. Traffic distribution patterns were utilized to establish design range requirements for both domestic and intercontinental aircraft designs. The world traffic forecast, shown in Table 105, combined with traffic distribution was utilized to provide an estimate of the number of aircraft, by seating capacity, which would be required to accommodate this market. The results of this projection are shown in Table 106. Aircraft design range was established as 5556 Km (3000 nautical miles) for the domestic mission and 12038 Km (6500 nautical miles) for the intercontinental mission. A 5556 Km (3000 nautical mile) range encompasses all domestic routes and a 12038 Km (6500 nautical mile) range would accommodate approximately 93% of the total long range traffic projected for the year 2000. Aircraft sizing considerations (number of passengers were based on considerations of reduction in seat mile costs and reduced airport congestion along with airline and passenger criteria such as less flexible operation and less frequent service. These considerations were combined with the projected number of aircraft required to provide an economically viable program. Aircraft sizing for 400 passengers was selected as the best size for both the domestic and intercontinental missions.

Selection of cruise speed was based on previous studies accomplished by Lockheed which showed that optimum fuel utilization and lowest operating costs are attained at a cruise speed of mach 0.80.

TABLE 104

ADVANCED COMPOSITES EFFECT - LOCKHEED STUDY

COMPONENT	$\Delta$ WT %	
Wing	23	
Tail	20	
Body	7	
Landing Gear	4	
Macelles	19	
Air Induction	19	
Surface Controls	5	
Furnishings	0	
	DOMESTIC	INTERCONTINENTAL
Total reduction in manufacturing empty weight	8.7%	9.2%

**ORIGINAL PAGE IS  
OF POOR QUALITY.**

TABLE 105

WORLD TRAFFIC FORECAST - LOCKHEED STUDY

MAJOR LONG-HAUL MARKETS (OVER 3000 S.M.)  
ONE-WAY DAILY AVERAGE PASSENGERS

<u>MARKET</u>	<u>1975*</u>	<u>1990</u>	<u>AVG. ANNUAL GROWTH RATE</u>	<u>2000</u>	<u>AVG. ANNUAL GROWTH RATE</u>
NO. AMERICA-EUROPE	16,986	34,979	4.9	51,777	4.0
EUROPE-ASIA/OCEANIA	4,071	15,864	9.5	28,410	6.0
NO. AMERICA-ASIA/OCEANIA	3,425	14,668	10.2	28,850	7.0
EUROPE-AFRICA	2,328	11,222	11.1	22,078	7.0
EUROPE-SO. AMERICA	1,644	8,025	11.1	15,787	7.0
NO. AMERICA-LATIN/SO. AMERICA	<u>1,506</u>	<u>6,303</u>	<u>10.0</u>	<u>12,298</u>	<u>7.0</u>
GROUP TOTAL	29,960	91,061	7.7	159,394	5.8

\*LOCKHEED ESTIMATE

TABLE 106

TOTAL LONG-HAUL AIRCRAFT REQUIREMENTS - LOCKHEED STUDY

<u>Km</u>	<u>(N. Mi.)</u>	<u>AIRCRAFT SEATING CAPACITY</u>				
		<u>200</u>	<u>300</u>	<u>400</u>	<u>500</u>	<u>600</u>
5556-7408	( 3,000- 4,000)	448	298	222	176	146
7408-9260	( 4,000- 5,000)	395	259	195	152	126
9260-11112	( 5,000- 6,000)	374	246	186	145	120
11112-12964	( 6,000- 7,000)	245	161	119	93	78
12964-14816	( 7,000- 8,000)	26	15	7	7	6
14816-16668	( 8,000- 9,000)	21	13	8	6	5
16668-18520	( 9,000-10,000)	27	17	13	10	8
18520-20372	(10,000-11,000)	<u>20</u>	<u>13</u>	<u>10</u>	<u>8</u>	<u>7</u>
	<b>Total</b>	<b>1,556</b>	<b>1,022</b>	<b>760</b>	<b>597</b>	<b>496</b>

## 2. Airplane Sizing Studies

### a. Concept Design of Reference Aircraft

Concept designs of a domestic and intercontinental reference aircraft were accomplished using a scaled CF6-50C turbofan engine. These designs were similar to the Task III configurations shown later in Figures 144 and 145. Parametric sizing studies were conducted to determine minimum fuel and DOC as shown in the carpet plot, Figure 130 for the domestic design. Point design parameters were selected from the carpet plots and are listed with the aircraft design and performance characteristics in Table 107.

### b. Integration of Advanced Technology Engines

Results of aircraft sizing studies with each advanced technology engine, along with the CF6-50C reference engine, are shown in Table 108.

### c. Aircraft Performance Comparisons

Incorporation of the advanced technology turbofan engines into the domestic and intercontinental aircraft result in significant savings in mission fuel and direct operating cost when compared to the reference configuration (CF6-50C engine). Comparison of block fuel and DOC for the advanced technology engines and CF6-50C are depicted in Figures 131 and 132. The direct drive data was compared with that of other airframe companies previously in Table 52 and Figure 46.

### d. Airframe Noise Estimates

Estimates of airframe noise levels (engines excluded) at landing approach were generated for the reference aircraft and the aircraft incorporating the direct drive advanced technology engine. These data were presented earlier in Table 53.

## C. McDonnell Douglas Corporation

### 1. Airplane Definition and Performance

A conceptual design of a "stretched" DC-10 type airplane (Figure 133) was used by McDonnell Douglas in studies conducted to assess the payoffs of the E<sup>3</sup> type engines. The aircraft characteristics for the domestic and intercontinental designs are shown in Table 109. A weight breakdown is shown in Table 110. The results of the fuel and DOC payoff studies compared to a CF6-50C powered airplane incorporating similar design features are shown in Table 52 and in Figure 46. Noise data are summarized in Table 53 and Figure 47.

### 2. Advanced Technology Concepts--Long Duct Mixed Flow Nacelle

The long duct mixed flow nacelle constitutes a major advance in technology from that used in current DC-10 applications. The major nacelle features, shown in Figure 134 include forced mixing, composite long duct, improved pylon, directed flow reverser, load sharing composite core cowl, improved acoustic treatment, composite inlet, aerodynamically improved inlet, inlet vortex control, and a recirculating fuel system.

DOMESTIC DESIGN ---- CF6-50C  
 400 PASSENGERS/5556 Km (3000 nmi) RANGE/MACH = 0.8  
 SWEEP (C/4) = 30 DEG/ T/C = 12./AR = 10

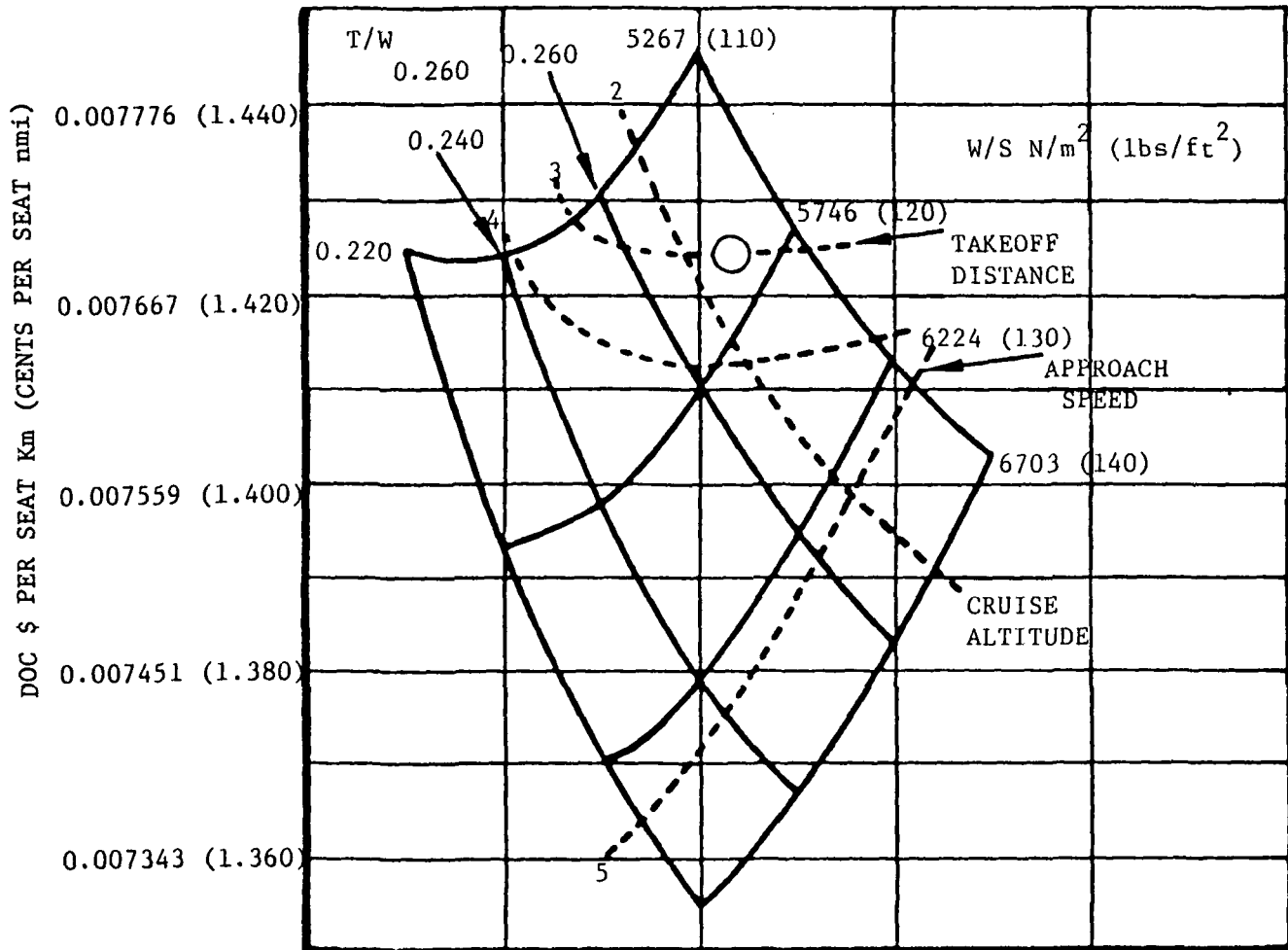


Figure 130. Carpet Plot, Domestic Aircraft Using CF6-50C Engine - Lockheed Study

TABLE 107

## REFERENCE AIRCRAFT CHARACTERISTICS - LOCKHEED STUDY

	DOMESTIC (CL 1333-1)	INTERCONTINENTAL (CL 1333-2)
Range Km (NM.)	5556 (3000)	12038 (6500)
Cruise Speed	0.8 M	0.8 M
No. Passengers	400	400
No. Engines	3	4
Sweep (0.25C)	30°	30°
W/S N/m <sup>2</sup> (lb/ft <sup>2</sup> )	5650 (118)	6895 (144)
T/W N/Kg (lb/lb)	2.69 (0.274)	2.42 (0.247)
AR	10	10
t/c	12	12
TOGW Kg (lb)	192503 (424389)	295431 (651127)
OEW Kg (lb)	106903 (235676)	127459 (280995)
Block Fuel Kg (lb)	41770 (92085)	114471 (252362)
Thrust/Eng. N (lb)	172417 (38761)	179209 (40288)
Wing Span m (ft)	57.8 (189.6)	64.8 (212.6)
Body Length m (ft)	69.6 (228.3)	69.9 (229.3)
Body Diameter m (ft)	5.97 (19.6)	5.97 (19.6)
DOC \$/SKm (¢/SM)	0.0076 (1.407)	0.0089 (1.650)
Init. Cruise Alt m (ft)	10973 (36000)	10668 (35000)
TOFL m (ft)	2124 (6968)	2878 (9442)
Approach Speed Km/hr (KTS)	249.8 (134.9)	244.1 (131.8)
Power Plant	CF6-50C	CF6-50C



TABLE 108

AIRCRAFT PERFORMANCE CHARACTERISTICS - LOCKHEED STUDY

	<u>CF6-50C Reference</u>		<u>Mixed Flow Direct</u>		<u>Mixed Flow Geared</u>	
	<u>Domestic</u>	<u>Intercontinental</u>	<u>Domestic</u>	<u>Intercontinental</u>	<u>Domestic</u>	<u>Intercontinental</u>
TOGW Kg (lb)	192503 (424389)	295431 (651300)	184151 (405976)	262769 (579294)	185307 (408525)	264388 (582865)
Thrust/Eng N (lb)	172417 (38761)	179624 (40381)	157712 (35455)	148166 (33309)	167182 (37584)	173756 (39062)
Block Fuel Kg (lb)	41771 (92087)	114546 (252525)	35929 (79209)	93004 (205035)	35231 (77669)	91246 (201160)
Cruise (Avg) SFC Kg/N-hr lbs/lbs-hr	0.0684 (0.671)	0.0694 (0.681)	0.060 (0.588)	0.0607 (0.595)	0.0568 (0.557)	0.0574 (0.563)
Propulsion Wt Kg(lb)	12501 (27559)	16695 (36806)	12682 (27959)	15298 (33725)	14062 (31000)	16874 (37200)
DOC \$/S Km (¢/SM)	0.0076 (1.407)	0.0089 (1.651)	0.0072 (1.342)	0.0081 (1.503)	0.0073 (1.351)	0.0082 (1.513)

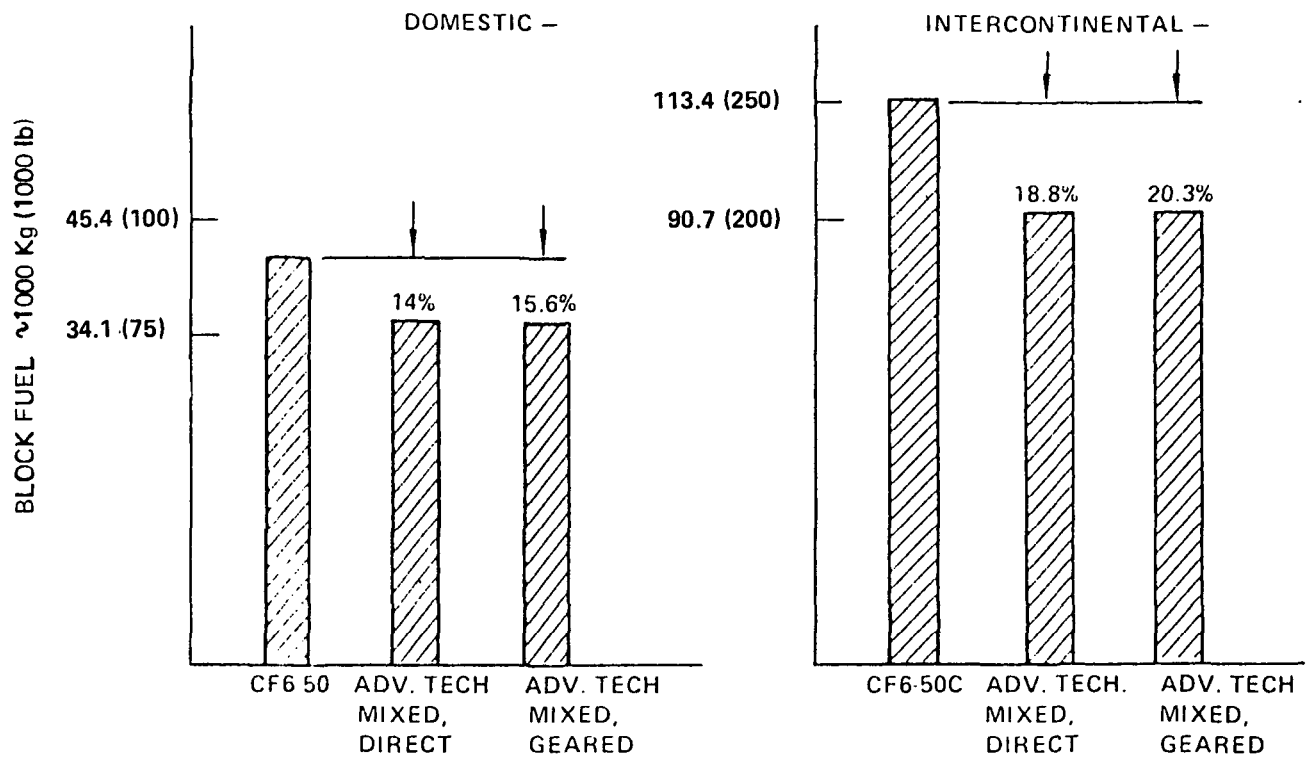


Figure 131. Block Fuel - Lockheed Study

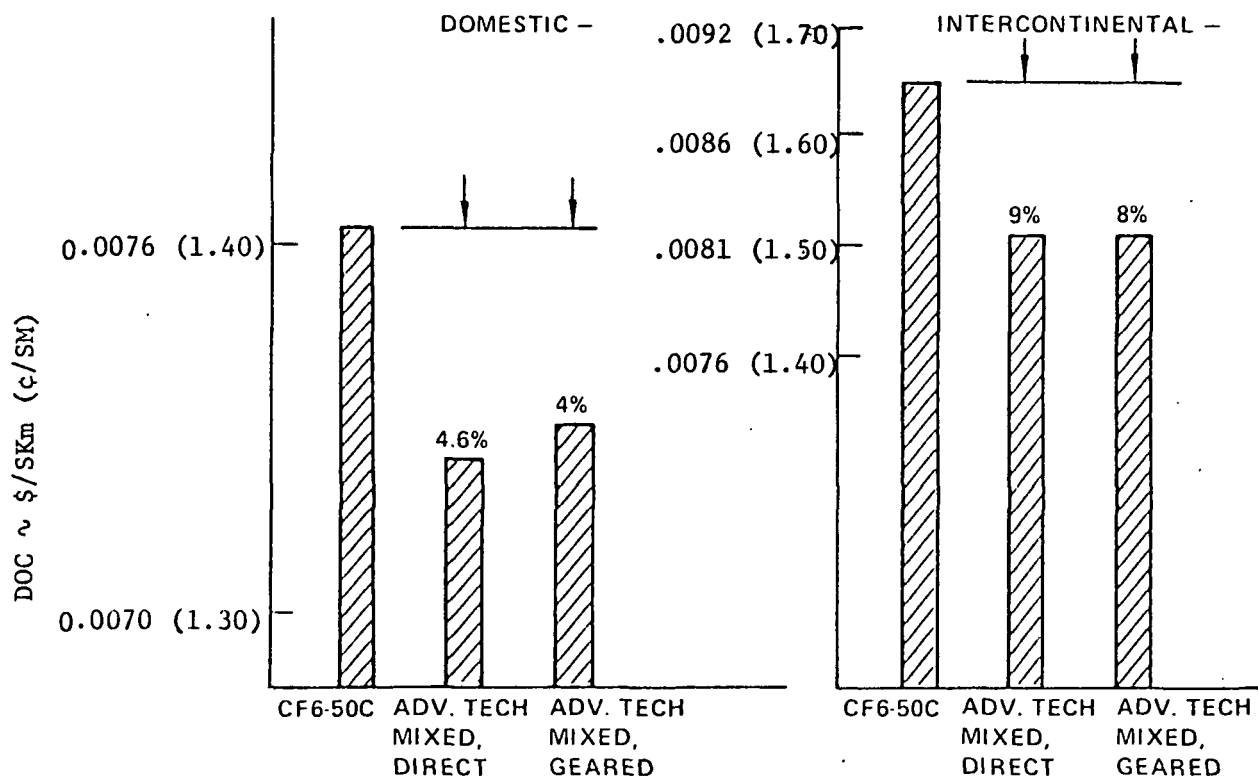


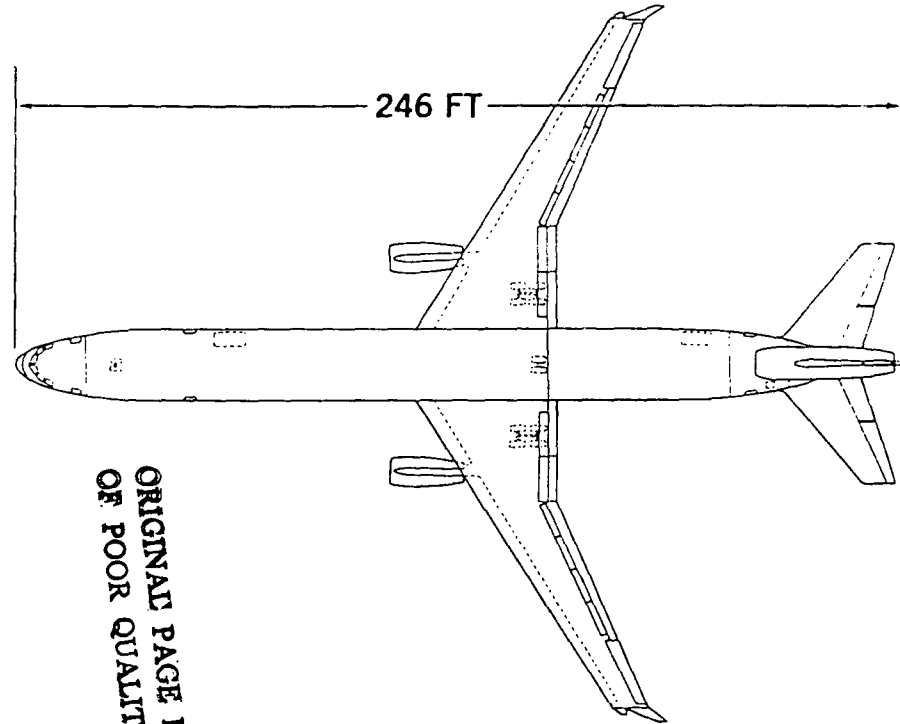
Figure 132. Operating Cost - Lockheed Study

# GENERAL ARRANGEMENT

ENGINE THRUST SIZE

DOMESTIC 42,370 LB

INTERNATIONAL 50,520 LB



ORIGINAL PAGE IS  
OF POOR QUALITY

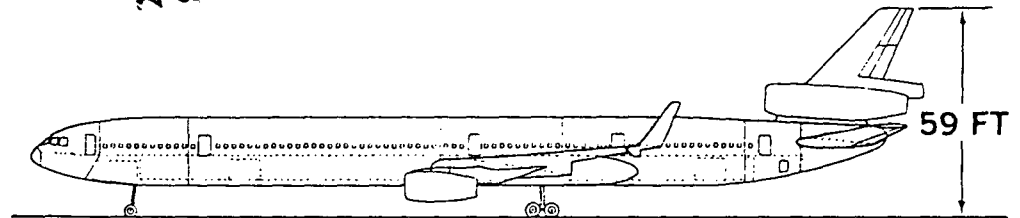
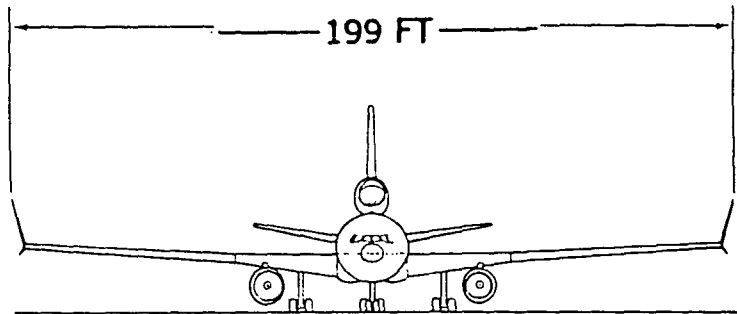


Figure 133... Conventional Design of a "Stretched" DC-10 Type Airplane - McDonnell Douglas Study 7-GEN-23154 A

TABLE 109

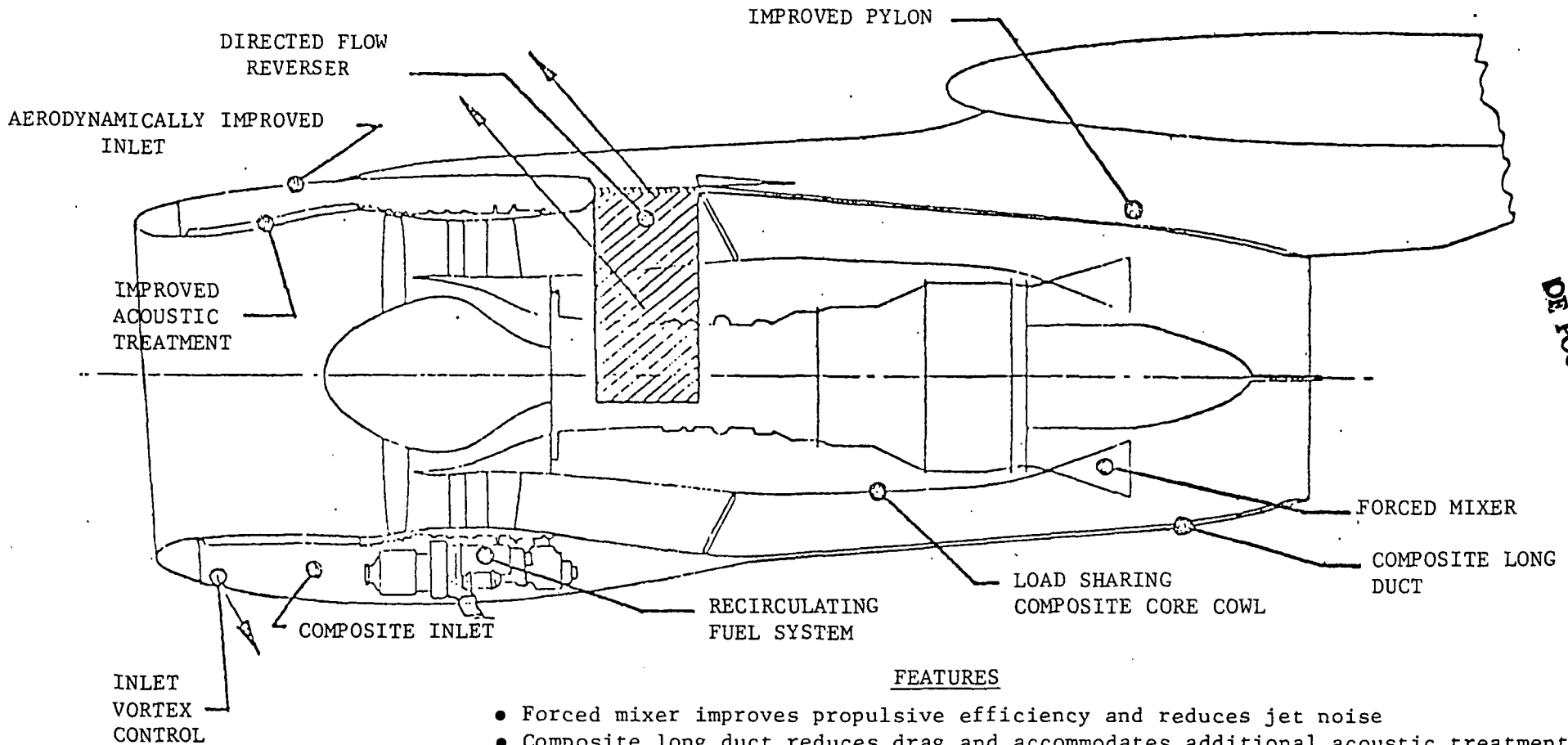
AIRCRAFT CHARACTERISTICS - McDONNELL DOUGLAS STUDY

	<u>DOMESTIC</u>		<u>INTERNATIONAL</u>	
Mixed Class Seating		458		438
Design Range (N MI) Km	5556	(3000)	10186	(5500)
Engine Thrust Size (Lb/Engine) N/Engine	188469	(42370)	224722	(50520)
Wing Area (Sq Ft) M <sup>2</sup>	374.4	(4030)	374.4	(4030)
Weights:-Maximum Takeoff (Lb) Kg	225530	(497200)	288626	(636300)
-Operators Empty (Lb) Kg	127616	(281340)	135300	(298280)
-Manufacturers Empty (Lb) Kg	117296	(258590)	125384	(276420)
Cruise Mach Number		0.80		0.80
Takeoff Field Length (Ft) M	2094	(6870)	2941	(9650)
Mtow, Sl, 84°F				
Approach Speed (Keas) Km/Hr	226	(122)	233	(126)
Psgs, Bags, Reserves				
Thrust Limited Initial Cruise	10058	(33000)	9449	(31000)
Altitude (Ft) M				
Buffet Limited Initial Cruise	11491	(37700)	9876	(32400)
Altitude (Ft) M				
Fuel Burned At Design Range (Lb) Kg	47483	(104680)	98359	(216840)
Typical Stage Length (N Mi) Km	1852	(1000)	2778	(1500)
Fuel Burned at Typical Range (Lb)	16461	(36290)	24794	(54660)

TABLE 110

AIRCRAFT WEIGHT BREAKDOWNS - McDONNELL DOUGLAS STUDY

	<u>Domestic</u>		<u>International</u>	
	Kg	(lbs)	Kg	(lbs)
Wing	24066	(53,055)	25805	(56,890)
Horizontal Tail	1896	(4,180)	2062	(4,545)
Vertical Tail	1887	(4,150)	2039	(4,495)
Fuselage	27270	(60,120)	27620	(60,890)
Landing Gear	8743	(19,275)	11410	(25,155)
Propulsion	16218	(35,755)	19822	(43,700)
APU	651	(1,435)	651	(1,435)
Fuel System	869	(1,915)	869	(1,915)
Flight Controls and Hydraulic System	3878	(8,550)	3878	(8,550)
Instruments	794	(1,750)	794	(1,750)
Air Conditioning and Pneumatics	2252	(4,965)	2252	(4,965)
Electrical	2930	(6,460)	2930	(6,460)
Avionics	1388	(3,060)	1388	(3,060)
Furnishings	24172	(53,290)	23578	(51,980)
Ice Protection	259	(570)	259	(570)
Handling Gear	27	(60)	27	(60)
Manufacturers Empty Weight	117296	(258,590)	125384	(276,420)
Operators Items	10319	(22,750)	9916	(21,860)
Operators Empty Weight	127616	(281,340)	135300	(298,280)



ORIGINAL PAGE IS  
OF POOR QUALITY

FEATURES

- Forced mixer improves propulsive efficiency and reduces jet noise
- Composite long duct reduces drag and accommodates additional acoustic treatment without weight increase
- Improved Pylon to minimize interference drag
- Directed flow reverser reduces engine erosion and reduces airplane stopping distance
- Load sharing composite core cowl reduces engine deterioration
- Improved acoustic treatment reduces noise
- Composite inlet reduces weight
- Aerodynamically improved inlet improves performance
- Inlet vortex control reduces engine erosion
- Recirculating fuel system reduces cooling losses

Figure 134. Advanced Integrated Nacelle - McDonnell Douglas Study

## a. Improved Performance

The improved performance discussion is divided into four subsections; improved internal performance, drag reduction, reduced engine deterioration and reduced weight.

### 1. Improved Internal Performance

Two features were incorporated in the advance design nacelle which improved the internal performance of the engine. These features are forced mixing and a recirculating fuel system.

#### a. Forced Mixing

The forced mixer is a mechanical device that promotes rapid mixing between the primary and fan flows. The particular design used in this study is a daisy nozzle. The propulsive efficiency of the aircraft is improved, resulting in reducing cruise fuel consumption by about two percent.

#### b. Recirculating Fuel System

Most aircraft drive the electrical alternators with a constant speed drive to maintain accurate electrical frequency control. The constant speed drive is driven by an engine gearbox which operates through a wide range of rpm's and is dependent on engine power setting. The constant speed drive's output speed is controlled by a self contained oil system which also serves as a self lubricating system. A considerable amount of heat is generated by the system and is dissipated through an air/oil cooler positioned in the fan stream. The air/oil cooler creates a performance loss which is due to the blockage and pressure drop through the cooler. It is the intention of this feature to eliminate the air/oil cooler and use the aircraft's airplane wing fuel tanks as a heat sink. By using this process there will not be any performance losses incurred in the fan stream. Further, by adding heat to the fuel tank a cruder grade of fuel could be used which has a higher freezing point.

### 2. Reduced Drag

Two features were added to the long duct mixed flow nacelle to reduce the overall drag of the pod and pylon. These features helped to improve the performance of the aircraft and are discussed below.

#### a. Composite Long Duct and Improved Pylon

The current DC-10 has a short fan duct nacelle. In this configuration the fan exhaust causes high mach number scrubbing drag along the pylon and core cowl. Due to the local pressure field under the wing, an adverse shock wave occurs which causes flow separation. The long duct nacelle encloses the entire fan stream and has sufficient area to maintain a low mach number until the flow reaches the exit nozzle. This nozzle is located aft of the pylon so that this external surface of the nacelle and the pylon are exposed only to the free stream velocity. The elimination of high mach number scrubbing drag and separation tendencies improves installed performance. When the long duct is installed some pylon fairings or surface camber may be required to minimize interference drag.



### b. Aerodynamically Improved Inlet

The upper loft line of the upper barrel will be modified by adding slightly more camber to the upper surface. This new line prevents high mach number shock waves from occurring during elevated cruise velocities and helps maintain laminar flow during climb.

## 3. Reduced Engine Deterioration

### a. Directed Flow Reverser

One of the design features to reduce debris ingestion is a directed flow reverser. The principle behind this scheme is to direct fan flow upward so the flow does not impinge the ground. This is accomplished by concentrating the reverser cascades in the upper two-thirds of the nacelle (lower 120° blanked off). Refer to Figure 135.

### b. Load Sharing Composite Core

Under high thrust and high "G" load conditions the cylindrical cases of the engine tend to ovalize. Because of these conditions larger than desired tip clearances must be maintained between rotating and fixed portions of the engine. This problem can be alleviated by taking advantage of the nacelle structure and allowing the loads induced by ovalization to be reacted into the nacelle and subsequently into the pylon. Preliminary designs show that a load sharing nacelle can be developed with very little weight penalty due to the excellent physical properties of composite structures.

### c. Inlet Vortex Control

Sand and debris are ingested by wing mounted engines during low speed operations on the ground. The inlet vortex is a contributor to this particular ingestion which results in engine erosion. Inlet vortex control is accomplished by directing high velocity jets down and aft from the lower surface of the inlet. This prevents formation of the inlet vortex by inducing an effective forward velocity on the lower surface of the inlet. Eliminating the inlet vortex will decrease erosion due to particle ingestion.

## 4. Weight Reduction

The feasibility of the long duct mixed flow nacelle was made possible by the use of advance composites. A weight savings of 15-20 percent was associated with the use of these materials over similar metallic materials. The basic reason for the weight saving is that composite materials have a higher strength to weight ratio.

### b. Noise Reduction

Noise is reduced by the long duct mixed flow nacelle, as shown in Table 111, which helps relieve some of the public pressure relating to this topic. There are three basic features which help reduce the decibel level around the nacelle. These features are stated below and amount to a reduction of three decibels.

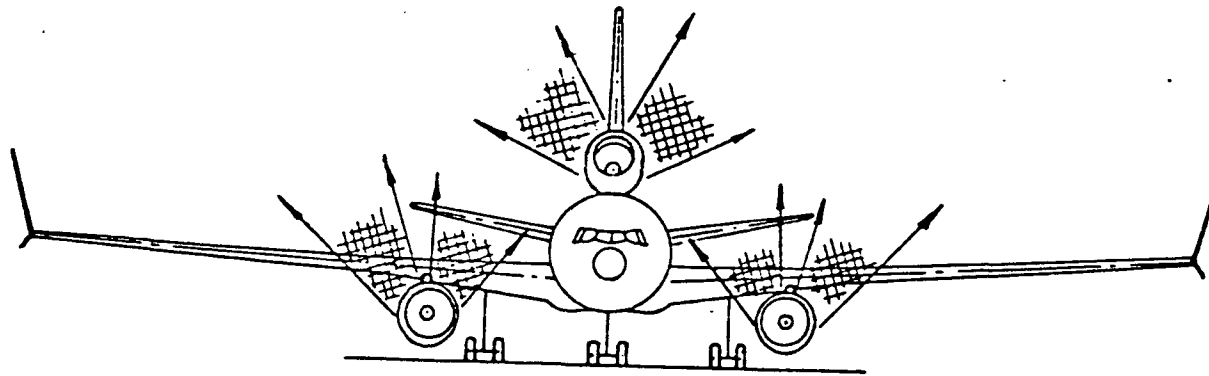


Figure 135. Reverse Flow Directivity Requirement - McDonnell Douglas Study

TABLE 111

ESTIMATED NOISE REDUCTION ( $\Delta$ EPNdB) \*

FOR

LONG DUCT NACELLE WITH MIXER NOZZLE AND BULK TREATMENT

IN THE INLET AT MAXIMUM CERTIFIED GROSS WEIGHT - McDONNELL DOUGLAS STUDY

TOGW 26T624 Kg (590,000 LB.)      LGW 197770 Kg (436,000 LB.)

---

AIRPLANE CONFIG.	TAKEOFF	SIDELINE	APPROACH @ MAX FLAP
DC-10-30/CF6-50C	3-4	3-4	2-3

---

\*Reduction is relative to the short duct, separated flow nacelle installation of the CF6-50C in the DC-10 airplane.

### 1. Forced Mixing

The mixer will lower jet noise by reducing the maximum velocities in the exhaust flow. It will also help reduce the turbine noise level in that some noise attenuation will result as the noise progresses through the turbulent flow behind the mixer.

### 2. Composite Long Duct

The long duct mixed flow nacelle has a larger area which is acoustically treated than the current short duct nacelle. The additional treatment absorbs some of the noise emitted by fan and turbine flows. This provides the long duct with a decrease in overall nacelle noise.

### 3. Improved Inlet Acoustic Treatment

The use of bulk absorber treatment, double layer honeycomb, and multi-degree of freedom construction are considered as candidate inlet noise absorption systems. Whichever construction is selected, it is expected to result in improved noise attenuation.

TABLE OF CONTENTS

	<u>PAGE NO.</u>
APPENDIX B . . . . .	379
TASK III SUBCONTRACTOR STUDIES . . . . .	379
A. The Boeing Company . . . . .	379
1. Airplane Sizing Studies - Updated Advanced Technology Engines . . . . .	379
a. Selection of Airplane Design Points . . . . .	379
b. Update of Airplane Sizing Studies . . . . .	379
c. Airframe Noise Estimates . . . . .	379
d. Airplane Drag Polars . . . . .	385
2. Thrust Reverser . . . . .	385
3. Control System Features . . . . .	385
B. Lockheed California Company . . . . .	389
1. Airplane Sizing Studies - Updated Advanced Technology Engines . . . . .	389
2. Nacelle Configuration . . . . .	389
a. Composite Structure . . . . .	389
b. Access Provisions . . . . .	389
c. Thrust Reverser . . . . .	389
d. Nacelle - Wing Interference . . . . .	389
C. McDonnell Douglas Corporation . . . . .	402
1. Material Selection . . . . .	402
2. Weights . . . . .	404

LIST OF FIGURES  
APPENDIX B  
TASK III SUBCONTRACTOR STUDIES

<u>FIGURE NO.</u>	<u>TITLE</u>	<u>PAGE NO.</u>
136	Design Selection Chart, Intercontinental Airplane ATE Update Engines	380
137	Design Selection Chart, Domestic Airplane, ATE Update Engines	381
138	Aircraft Weight and Fuel Burned Comparison - Boeing Study	384
139	Drag Polars CF6-50C - Boeing Study	386
140	Drag Polars ATE Update - Boeing Study	387
141	Thrust Reverser Flow Control Intercontinental Airplane - Boeing Study	388
142	Asset Carpet Plot - Domestic	390
143	Asset Carpet Plot - Intercontinental	391
144	General Arrangement - Domestic with Task III E <sup>3</sup> Engine - Lockheed Study	393
145	General Arrangement - Intercontinental with Task III E <sup>3</sup> Engine - Lockheed Study	394
146	Thrust Reverser Flow Directivity - Lockheed Study	401
147	Typical Nacelle Installation - Lockheed Study	403

LIST OF TABLES

<u>TABLE NO.</u>	<u>TITLE</u>	<u>PAGE NO.</u>
112	Airplane Characteristics and Performance Update - Boeing Study	382
113	Airplane Weight Statements - Boeing Study	383
114	Aircraft Point Design Characteristics - Lockheed Study	392
115	Weight Statement - Lockheed Study	395
116	Mission Summary - Lockheed Study	396
117	Drag Coefficients - No External Stores - Lockheed Study	397
118	Cost Summary - Lockheed Study	398
119	Operational Costs - Lockheed Study	399
120	Weight Statement - Lockheed Study	400
121	Nacelle Weight Comparison Kg (Lbs) - McDonnell Douglas Study	405

## APPENDIX B

### TASK III SUBCONTRACTOR STUDIES

#### A. The Boeing Company

##### 1. Airplane Sizing Studies - Updated Advanced Technology Engines

###### a. Selection of Airplane Design Points

Design selection charts for the intercontinental and domestic airplanes with the updated advanced technology engines are shown in Figures 136 and 137.

The wing loading of the intercontinental airplane was selected as a compromise between minimum block fuel, takeoff gross weight, fuel volume, and growth buffet. The thrust loading was selected by the 33,000 foot initial cruise altitude requirement (ICAC). This altitude choice was a compromise between Pan American's desire for a higher initial altitude capability (10668 Km or 35,000 feet) and the smaller takeoff gross weight, fuel burned, and engine size possible at 9144 Km (30,000 feet) ICAC. ICAC at 10058 Km (33,000 feet) results in a takeoff field length (sea level, 84<sup>0</sup> day) of 2317 - 2469 m (7600 - 8100 ft.).

For the domestic airplane, the wing loading was selected for minimum takeoff gross weight and block fuel but with a constraint of 7500 foot takeoff field length (instead of 10058 Km or 33,000 feet ICAC) determining the thrust loading.

###### b. Update of Airplane Sizing Studies

Airplane characteristics and performance with the Task III E<sup>3</sup> engine and the CF6-50C are shown in Table 112. These resized airplanes reflect changes in wing weight for flutter (both engines) and advanced technology engine performance. Drawings of the final domestic and intercontinental airplanes are shown in Figures 126 and 127.

Results of a weight analysis on both the domestic and intercontinental airplanes with the Task III E<sup>3</sup> engine and the CF6-50C are shown on Table 113. These weights reflect the advanced technology features discussion in Section IV.C.2a.

Figure 138 shows fuel burned and aircraft weights referred to the CF6-50C. For the domestic airplane on the average mission, the airplane with Task III E<sup>3</sup> engines uses 12.7% less fuel than the CF6-50C powered airplane. The corresponding fuel saving for the intercontinental airplane is 17.7%. Reductions in OEW are 4.2% and 7.8% respectively.

###### c. Airframe Noise Estimates

Estimates of airframe noise levels (engines excluded) at landing approach were generated for the reference aircraft and the aircraft incorporating the direct drive advanced technology engine. These data were printed earlier in Table 53.

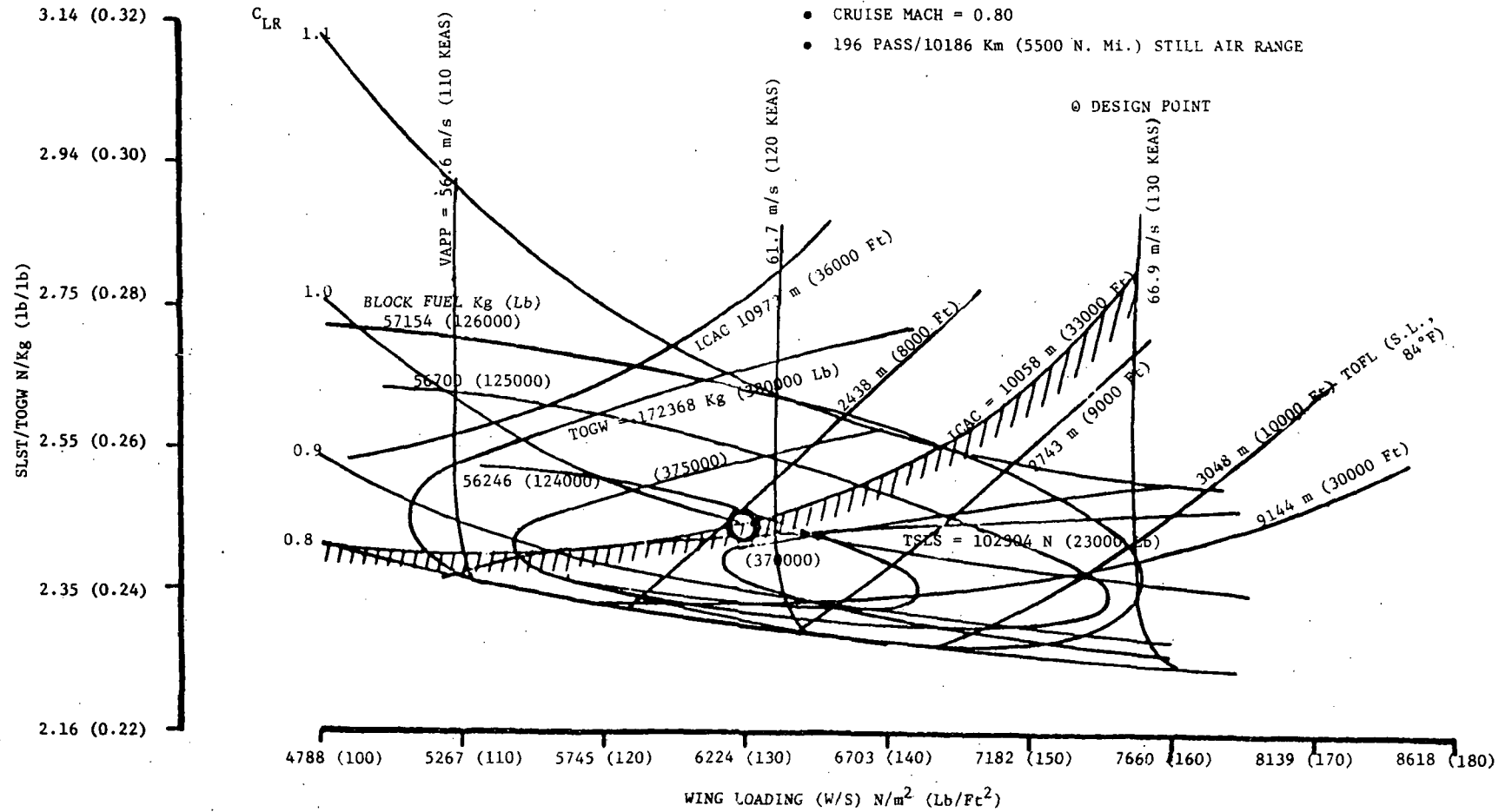


Figure 136. Design Selection Chart, Intercontinental Airplane, Task III  
 E<sub>3</sub> Engines - Boeing Study



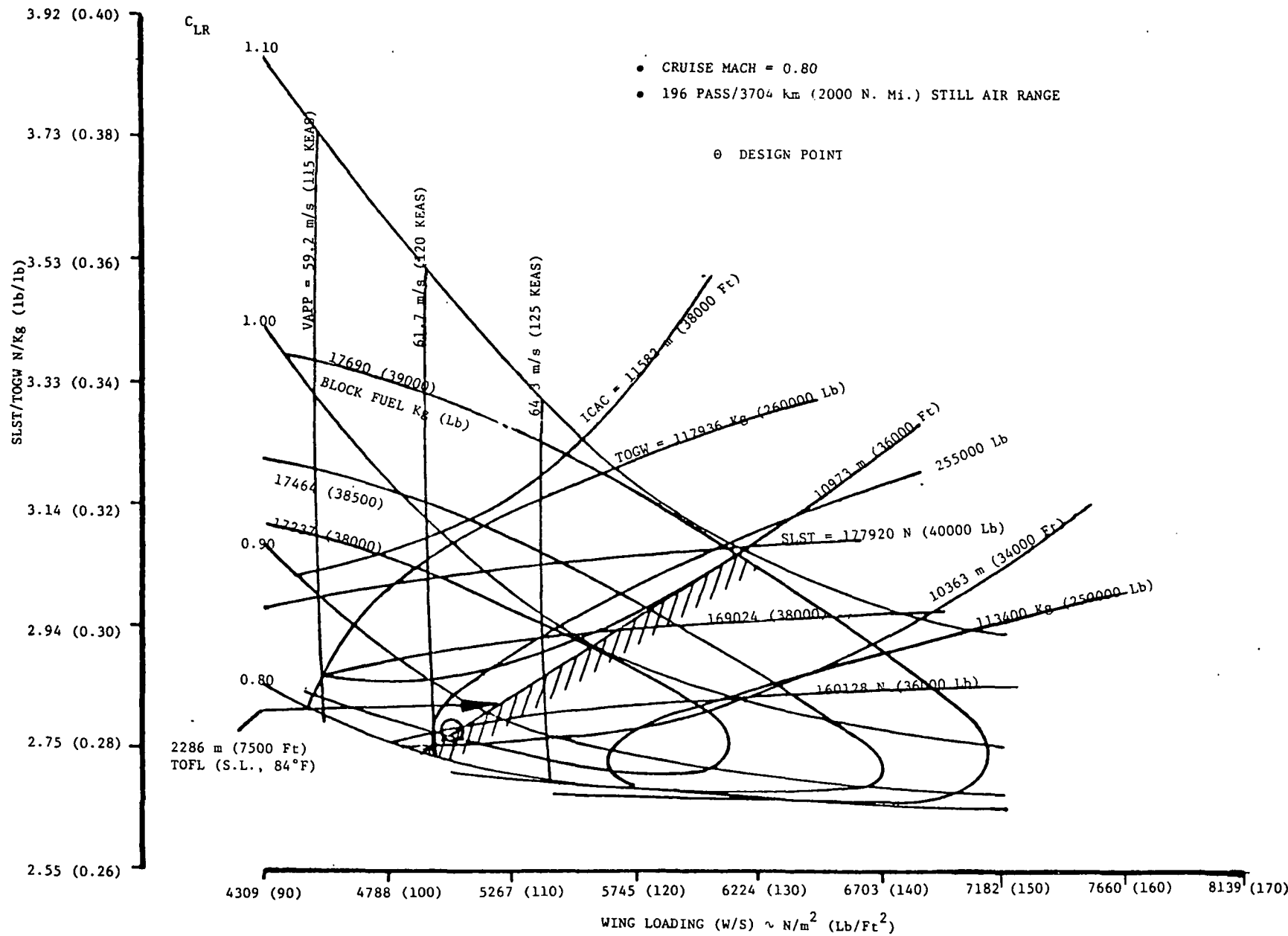


Figure 137. Design Selection Chart, Domestic Airplane, Task III E<sup>3</sup> Engines - Boeing Study

TABLE 112

## AIRPLANE CHARACTERISTICS AND PERFORMANCE UPDATE - BOEING STUDY

	(1)		(2)	
	INTERCONTINENTAL AIRPLANE CF6-50C	TASK III E <sup>3</sup> ENGINE	DOMESTIC AIRPLANE CF6-50C	TASK III E <sup>3</sup> ENGINE
TOGW Kg (LB)	192236 (423800)	168604 (371700)	122745 (270600)	115351 (254300)
OEW Kg (LB)	91614 (201970)	84497 (186280)	77466 (170780)	74196 (163570)
WING AREA, m <sup>2</sup> (SQ. FT.)	303 (3260)	266 (2860)	240 (2580)	225 (2420)
SLS F <sub>n</sub> N (LB)/ENG.	115297 (25920)	102931 (23140)	171611 (38580)	159646 (35890)
TOFL (S.L., 84°F) <sub>m</sub> (FT)	2317 (7600)	2469 (8100)	1646 (5400)	2287 (7500)
ICAC, m (FT.)	10061 (33000)	10061 (33000)	10549 (34600)	10549 (34600)
VAPPR, (Knots)Km/hr.	215 (116)	220 (119)	222 (120)	224 (121)
BLOCK FUEL @ DES. PAYLOAD/RANGE				
Kg (LB)	70535 (155500)	56201 (123900)	20109 (44330)	17123 (37750)
@ TYP. PAYLOAD RANGE	20625 (45470)	16974 (37420)	9317 (20540)	8133 (17930)
BLOCK TIME @ DES. PAYLOAD/RANGE (HR)	12.32	12.32	4.69	4.70
@ TYP. PAYLOAD/RANGE	4.69	4.68	2.52	2.51

(1) DESIGN PAYLOAD/RANGE = 196 PAX/(5500 N.MI.) 10186 Km  
TYPICAL PAYLOAD/RANGE = 108 PAX/(2000 N.MI.) 3704 Km

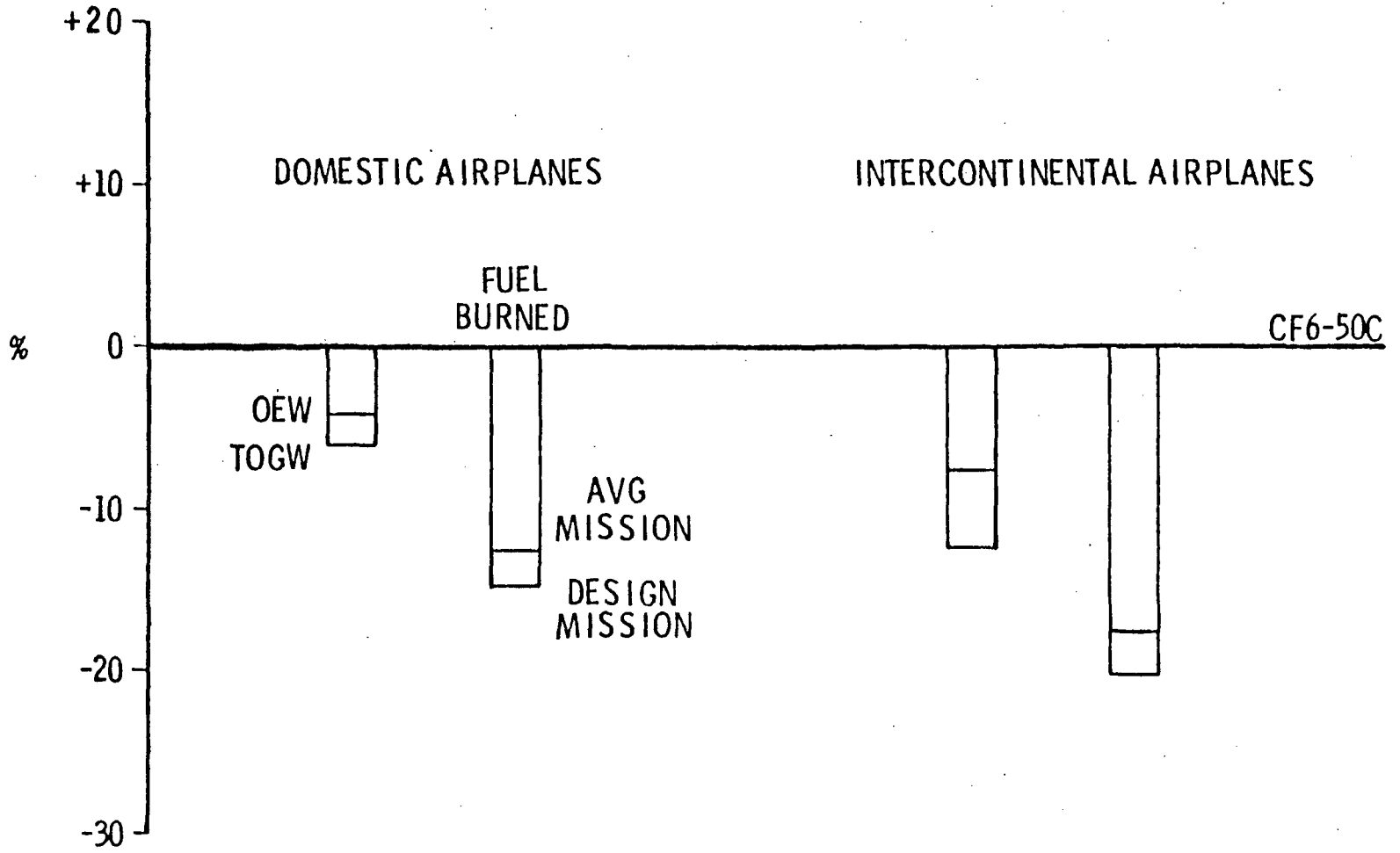
(2) DESIGN PAYLOAD/RANGE = 196 PAX/(2000 N.MI.) 3704 Km.  
TYPICAL PAYLOAD/RANGE = 108 PAX/(1000 N.MI.) 1852 Km.

TABLE 113

AIRPLANE WEIGHT STATEMENTS - BOEING STUDY

	WEIGHT - Kg (LB)			
	DOMESTIC		INTERCONTINENTAL	
	CF6-50C	TASK III E <sup>3</sup> ENGINE	CF6-50C	TASK III E <sup>3</sup> ENGINE
WING	17409 (38380)	15391 (33930)	21882 (48240)	18257 (40250)
EMPENNAGE	2844 (6270)	2703 (5960)	3325 (7330)	2921 (6440)
BODY	15427 (34010)	15259 (33640)	16552 (36490)	16035 (35350)
NACELLE	4173 (9200)	3720 (8200)	5507 (12140)	4717 (10400)
GEAR	5910 (13030)	5910 (13030)	6877 (15160)	6350 (14000)
TOTAL STRUCTURE	45764 (100890)	42983 (94760)	54142 (119360)	48281 (106440)
PROPULSION SYSTEM	7058 (15560)	6654 (14670)	8922 (19670)	7947 (17520)
FIXED EQUIPMENT	19473 (42930)	19387 (42740)	20294 (44740)	20013 (44120)
STD & OPER. ITEMS	5171 (11400)	5171 (11400)	8256 (18200)	8256 (18200)
OEW	77466 (170780)	74196 (163570)	91614 (201970)	84497 (186280)

Figure 138. Aircraft Weight and Fuel Burned Comparison - Boeing Study



#### d. Airplane Drag Polars

Airplane drag polars for the CF6-50C and the Task III E<sup>3</sup> engine are shown on Figures 139 and 140.

#### 2. Thrust Reverser

The thrust reverser in combination with all other retarding devices provide an operational landing field length which does not exceed the basic takeoff design runway length under the following conditions:

- Airplane at maximum landing gross weight
- Maximum landing flap
- Wheel braking coefficient = 0.05 above 185 Km/hr (100 kts) and 0.08 below 185 Km/hr (100 kts).
- All retarding devices (flaps, spoilers, brakes and thrust reverser) operated under the normal, certified operating procedure.
- Sea level, standard day ambient conditions assumed.

To provide interchangeability, one set of reverser parts must fit any engine position. The reversers must provide proper flow control to eliminate or minimize reingestion and to avoid excessive reduction in airplane drag during the landing roll. Consequently, it is usually desirable to divert a large portion of the fan flow over the wing. Suggested fan reverser flow patterns for 4-engine airplanes are shown in Figure 141 for the intercontinental airplane.


#### 3. Control System Features

Study of the control system indicated the following features to be necessary:

- All thrust command inputs should go through the throttle levers or their equivalent for both normal (presumably automated) and abnormal (presumably manual) engine control. This is the primary interface between the airplane and engine control systems and should be implemented in this fashion.
- Engine mounted digital electronic control of all engine control functions.
- Fibre-optic links between all components of the envisioned engine control system (i.e., cockpit displays and control input sensors; engine sensors, engine mounted controllers), with redundant channelling and isolated routing to meet safety and reliability standards.

Induced electromagnetic transients from lightning currents have been identified as a possible threat to be overcome by judicious engineering of the control and other data links. Optical data links, emerging for other reasons in many technology fields at this time, promise total protection from this threat and are compatible with the transmission of digital intelligence.

- Controls to be self-powered by dedicated engine driven alternator(s), doubling as rpm sensor.

$M = 0.8$   
  $C/4 = 30^\circ$   
 $(t/c) = 10.3\%$  (OUTBOARD)

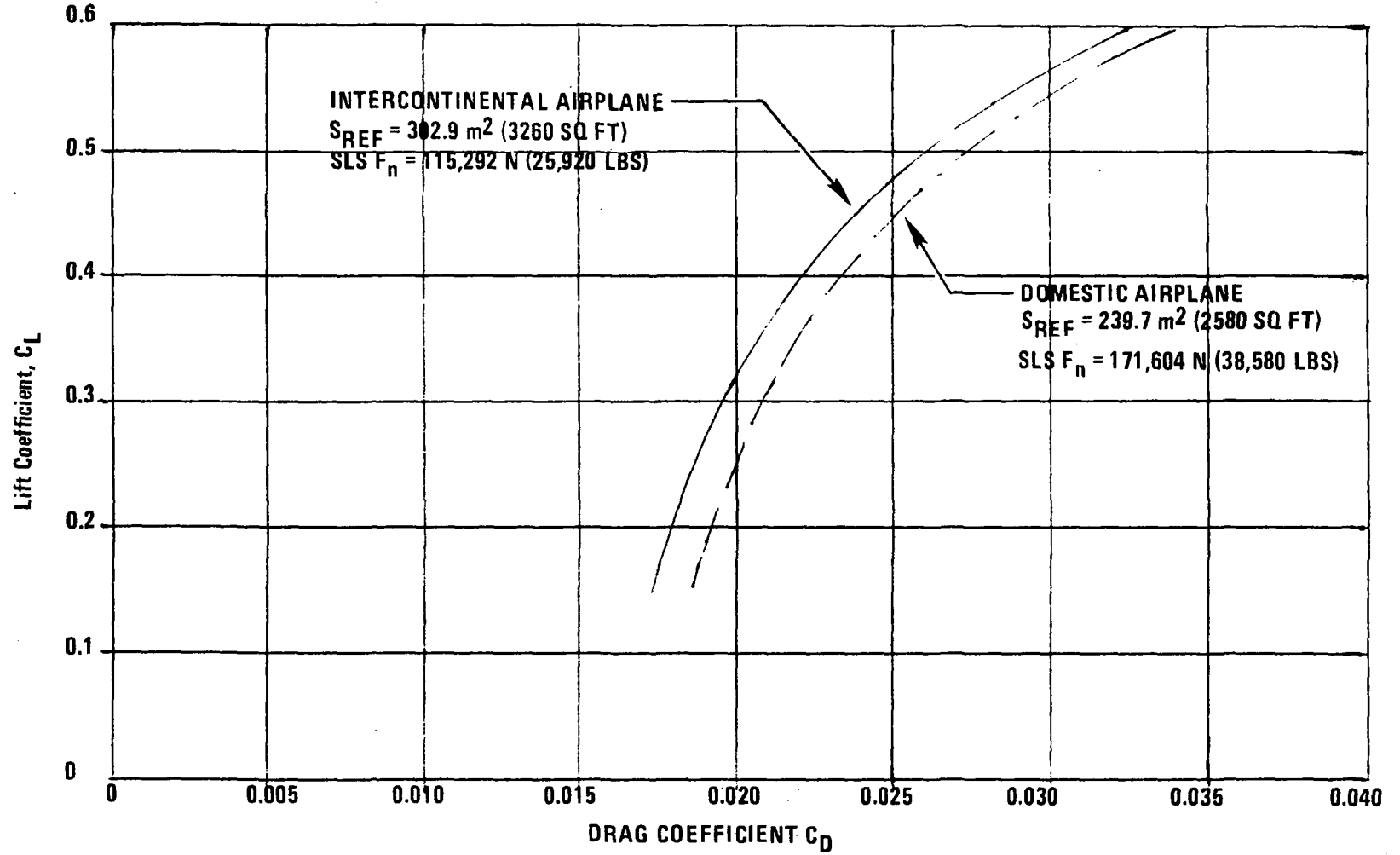



Figure 139. Drag Polars CF6-50C - Boeing Study

$M = 0.8$   
  $C/4 = 30^\circ$   
 $(t/c) = 10.3\% \text{ (OUTBOARD)}$

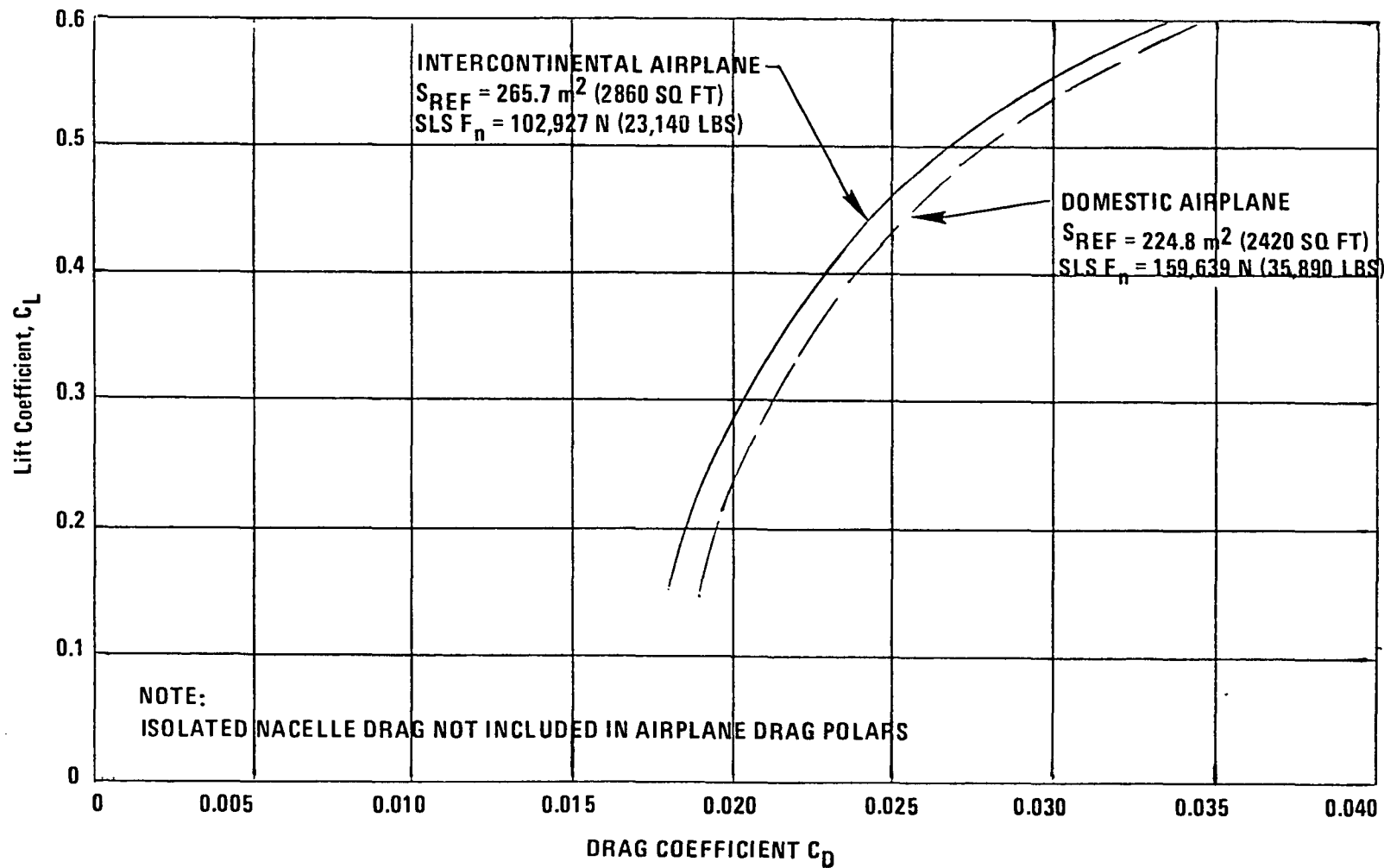


Figure 140. Drag Polars ATE Update - Boeing Study

ORIGINAL PAGE IS  
OF POOR QUALITY

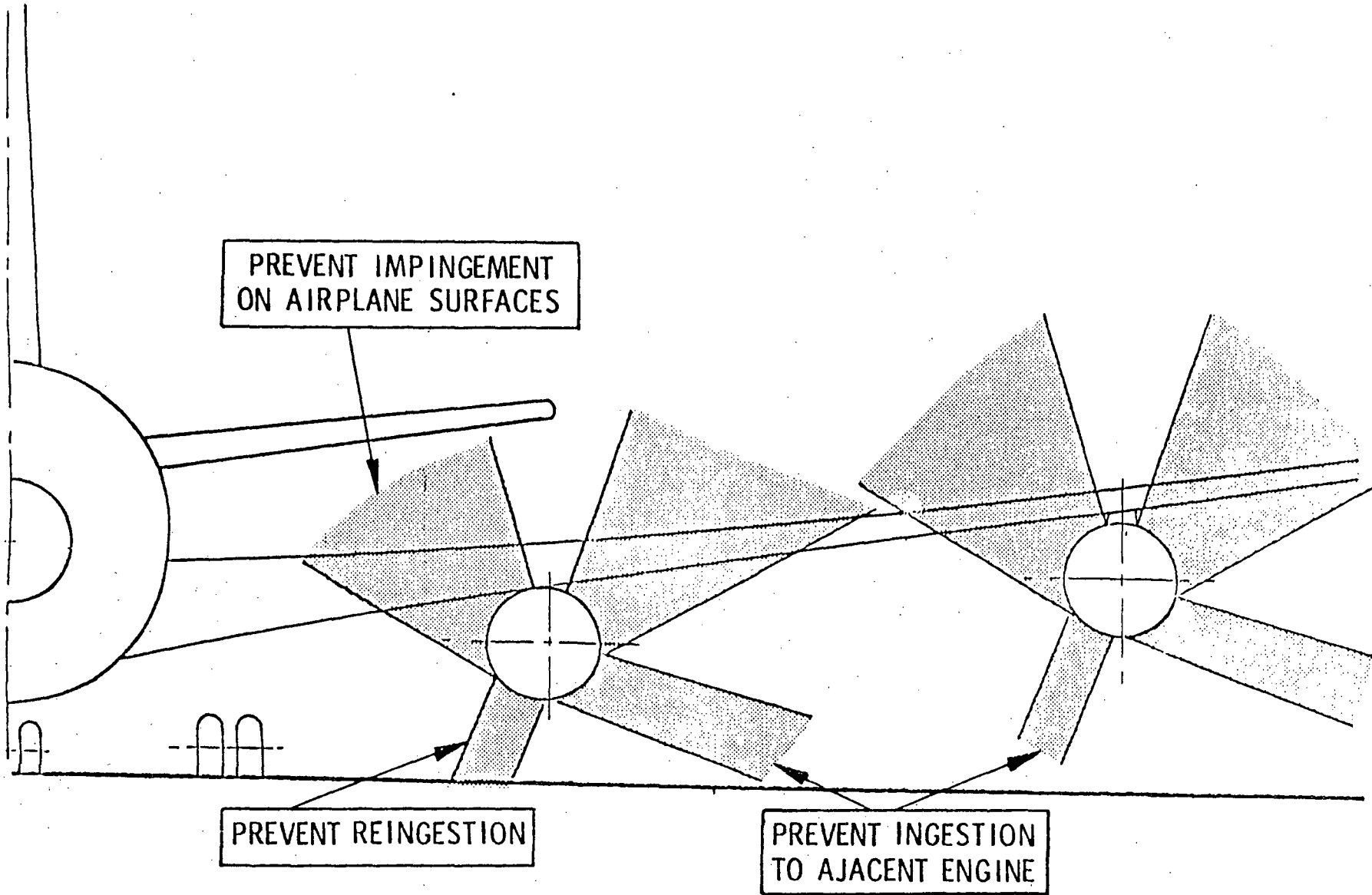


Figure 141. Thrust Reverser Flow Control Intercontinental Airplane - Boeing Studies



## B. Lockheed California Company

### 1. Airplane Sizing Studies - Updated Advanced Technology Engines

Both the domestic and intercontinental aircraft were re-sized to incorporate the refined mixed flow, direct-drive engine (Task III E<sup>3</sup> engine). Airframe technology levels were maintained and parametric analysis was accomplished with varying wing loading and thrust/weight ratios to obtain aircraft point designs optimized for minimum mission fuel and operating cost. Results of the parametric analysis are shown in the asset carpet plots, Figures 142 and 143. Aircraft point design characteristics with the refined engines are shown in Table 114 and general arrangement drawings are included in Figures 144 and 145.

The  $\Delta$ DOC and  $\Delta W_f$  data obtained in these studies have been discussed earlier on page 301 and compared with that of the other airframe companies in Figure 106.

Detailed data used in these studies, including weight breakdown, mission summaries (showing thrust, Mach number, and sfc versus altitude) and airplane drag polar information for the domestic aircraft are shown in Tables 115, 116, and 117. Production and operating cost data are presented in Table 118 and 119. A weight breakdown used in similar studies of the intercontinental aircraft is presented in Table 120.

### 2. Nacelle Configuration

#### a. Composite Structure

A detailed investigation was accomplished regarding the use of composites for a mixed-flow nacelle. A total weight savings of approximately 15% per nacelle appears to be feasible.

#### b. Access Provisions

Large cowl doors should be incorporated to provide access to engine and aircraft components and to the engine core.

#### c. Thrust Reverser

Reverse thrust should be provided by a set of cascades which are uncovered by a translating cowl during reverse thrust operating mode. Reverse thrust mechanism is confined to the fan stream only - no mechanism in the hot stream - to enhance system durability. Utilization of the translating cowl provides the capability of minimizing leakage and enhancing the structural arrangement. Flow directivity, as depicted in Figure 146, is required to minimize flow impingement on aircraft control surfaces and re-ingestion.

#### d. Nacelle - Wing Interference

Integration of the full length, mixed flow nacelle to the aircraft wing requires assessment of the interference effects which resulted in the following conclusions:

DOMESTIC DESIGN  
 400 PASSENGERS/5556 Km (3000 nmi) RANGE/MACH = 0.8  
 SWEEP (C/4) = 30. DEG/ T/C = 12./AR = 10

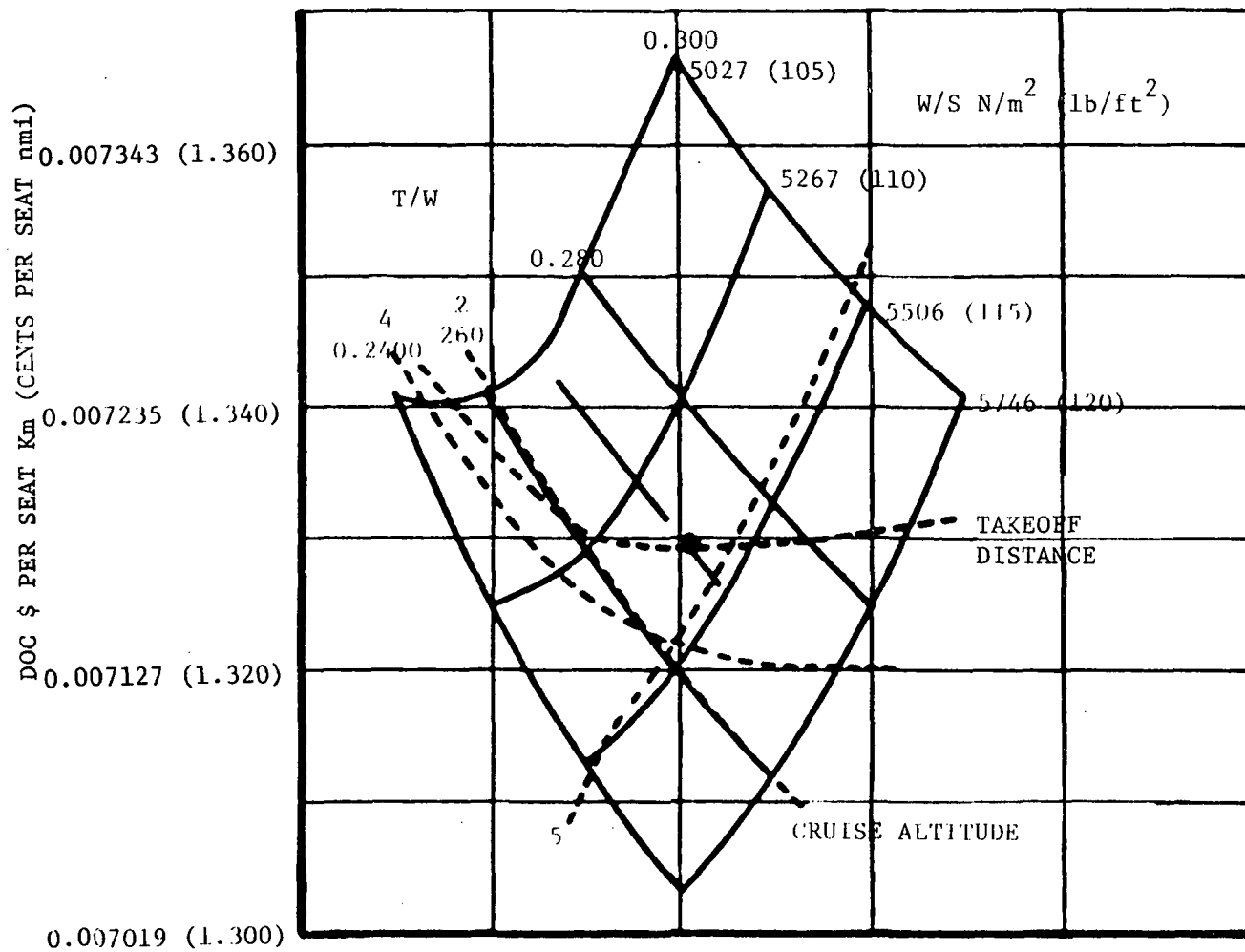


Figure 142. Asset Carpet Plot - Domestic - Lockheed Study

INTERNATIONAL DESIGN  
 400 PASSENGERS/6500 nmi RANGE/MACH = 0.8  
 SWEEP (C/4) = 30. DEG/ T/C = 12./AR = 10

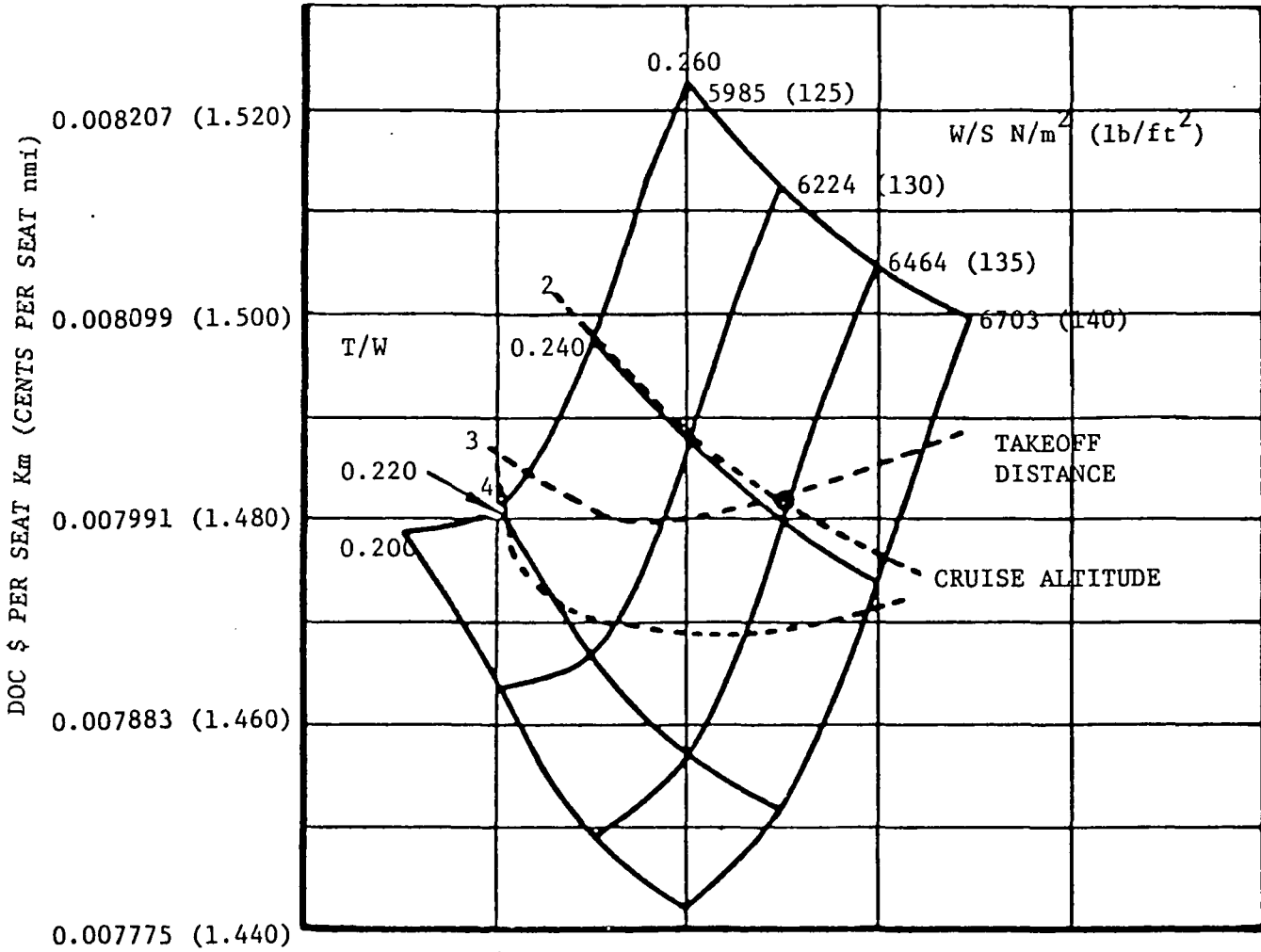


Figure 143. Asset Carpet Plot - Intercontinental - Lockheed Study

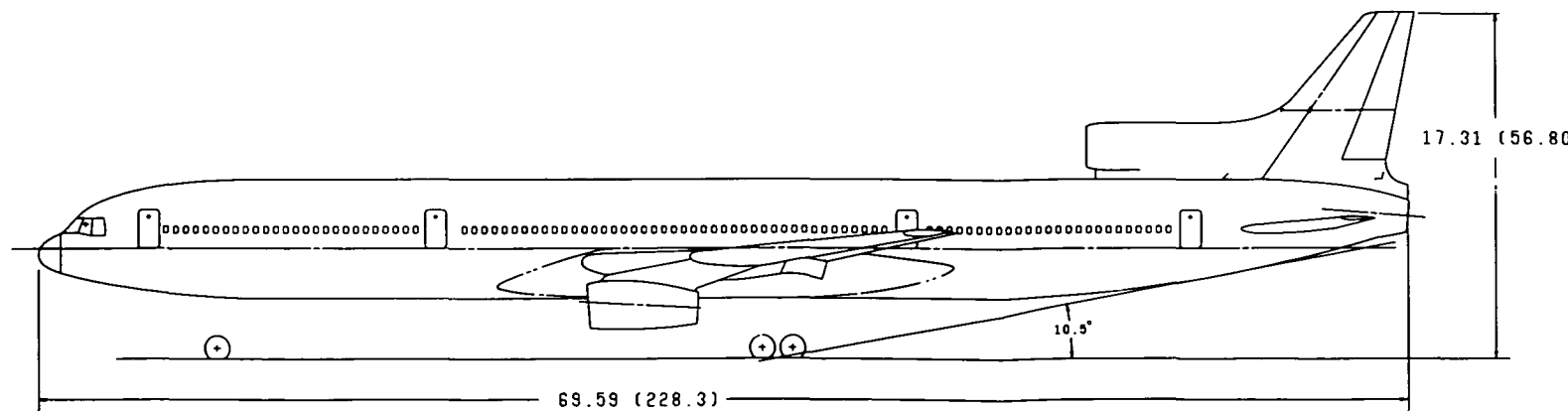
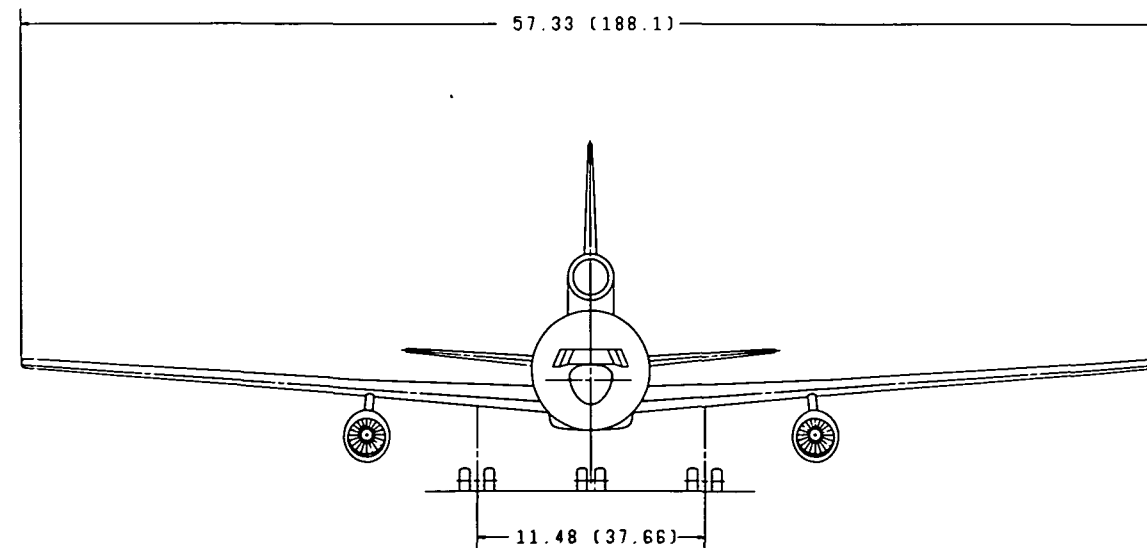
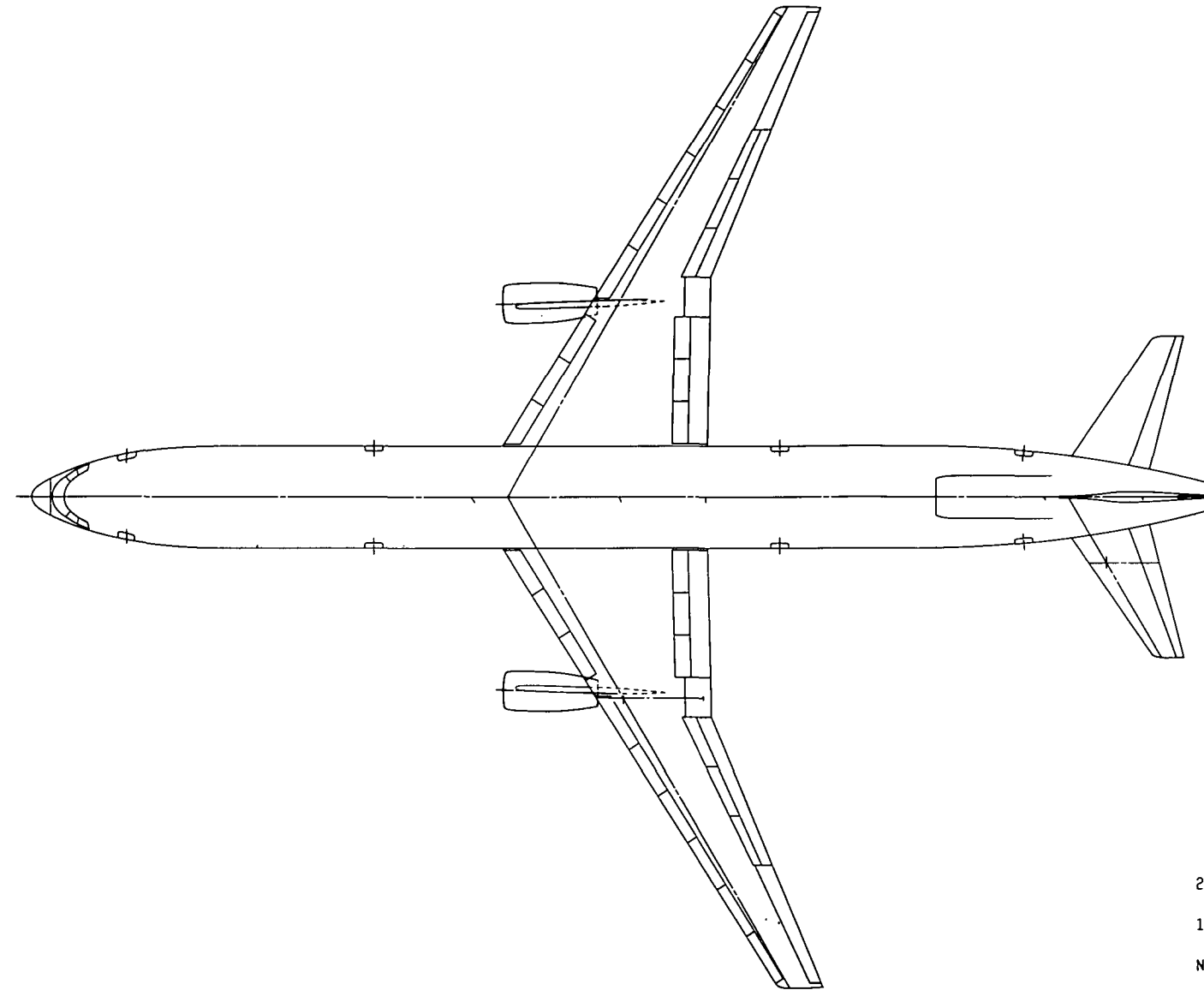
TABLE 114

AIRCRAFT POINT DESIGN CHARACTERISTICS -- LOCKHEED STUDY

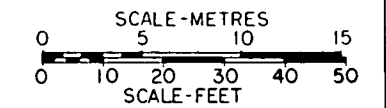
	<u>DOMESTIC</u>	<u>INTERCONTINENTAL</u>
Range Km (nmi)	5,556 ( 3,000)	12,038 ( 6,500)
Cruise Speed	0.8M	0.8M
Number of Passengers	400	400
Wing Sweep (.25c)	30°	30°
W/S N/m <sup>2</sup> (lb/ft <sup>2</sup> )	5,410 ( 113)	6,454 ( 134.8)
T/W N/kg (lb/lb)	2.65 ( 0.270)	2.36 ( 0.241)
AR	10	10
T/C	12	12
TOGW Kg (lb)	181,349 (399,800)	257,554 (567,800)
OEW Kg (lb)	104,343 (230,034)	118,125 (260,416)
Thrust/Eng. N (lb)	160,048 ( 35,982)	152,357 ( 34,253)
Wing Span m (ft)	57.33 ( 188.1)	62.54 ( 205.2)
Block Fuel Kg (lb)	34,468 ( 75,988)	89,083 (196,390)
DOC \$/SKm (¢/SM)	0.007176 ( 1.329)	0.008002 ( 1.482)
Init. Cruise Alt. m (ft)	10,973 ( 36,000)	10,668 ( 35,000)
TOFL m (ft)	2,138 ( 7,016)	2,901 ( 9,519)
Approach Speed Km/hr (knots)	248.7 ( 134.3)	244.1 ( 131.8)
Propulsion Wt. Kg (lb)	12,377 ( 27,287)	15,098 ( 33,284)

CHARACTERISTICS	WING	HORIZONTAL TAIL	VERTICAL TAIL
AREA SQ. M. (SQ. FT.)	328.70 (3538.1)	70.92 (763.4)	44.12 (474.9)
ASPECT RATIO	10	5	1.6
SPAN M. (FT.)	57.33 (188.1)	18.78 (61.6)	8.40 (27.57)
ROOT CHORD M. (IN.)	8.82 (347.27)	5.79 (227.96)	8.08 (318.14)
TIP CHORD M. (IN.)	2.65 (104.18)	1.74 (68.38)	2.42 (95.44)
TAPER RATIO	0.30	0.30	0.30
MAC M. (IN.)	6.29 (247.96)	4.13 (162.48)	5.69 (224.18)
SWEEP RAD. (DEG.)	0.524 (30)	0.524 (30)	0.611 (35)
T/C ROOT	12	10	10
T/C TIP	12	10	10

GROSS WEIGHT - 181349 KG. (399800 LB.)  
 POWER PLANT (3) G.E. TASK III E<sup>3</sup> TURBOFAN  
 INSTALLED THRUST - 160048 N (35982 LB.)  
 PASSENGERS - 400  
 RANGE - 3,000 N.M.



2. DIMENSIONS IN METRES (FEET), OR NOTED  
 1. CADAM REF DWG. CL1333-9-1,1,2,3  
 NOTES



<b>ADVANCED DESIGN</b>		CL1333-9
GEN. ARR. - E <sup>3</sup> 3000 N.M.		
G.E. TASK III E <sup>3</sup> TURBOFAN		
A. L. WILLIAMS		CL1333-9-1
10-28-77		1/100

**2** ~~BOLDOUT FRAME~~  
 ORIGINAL PAGE IS  
 OF POOR QUALITY

Figure 144. General Arrangement - Domestic with Task III E<sup>3</sup> Engine - Lockheed Study

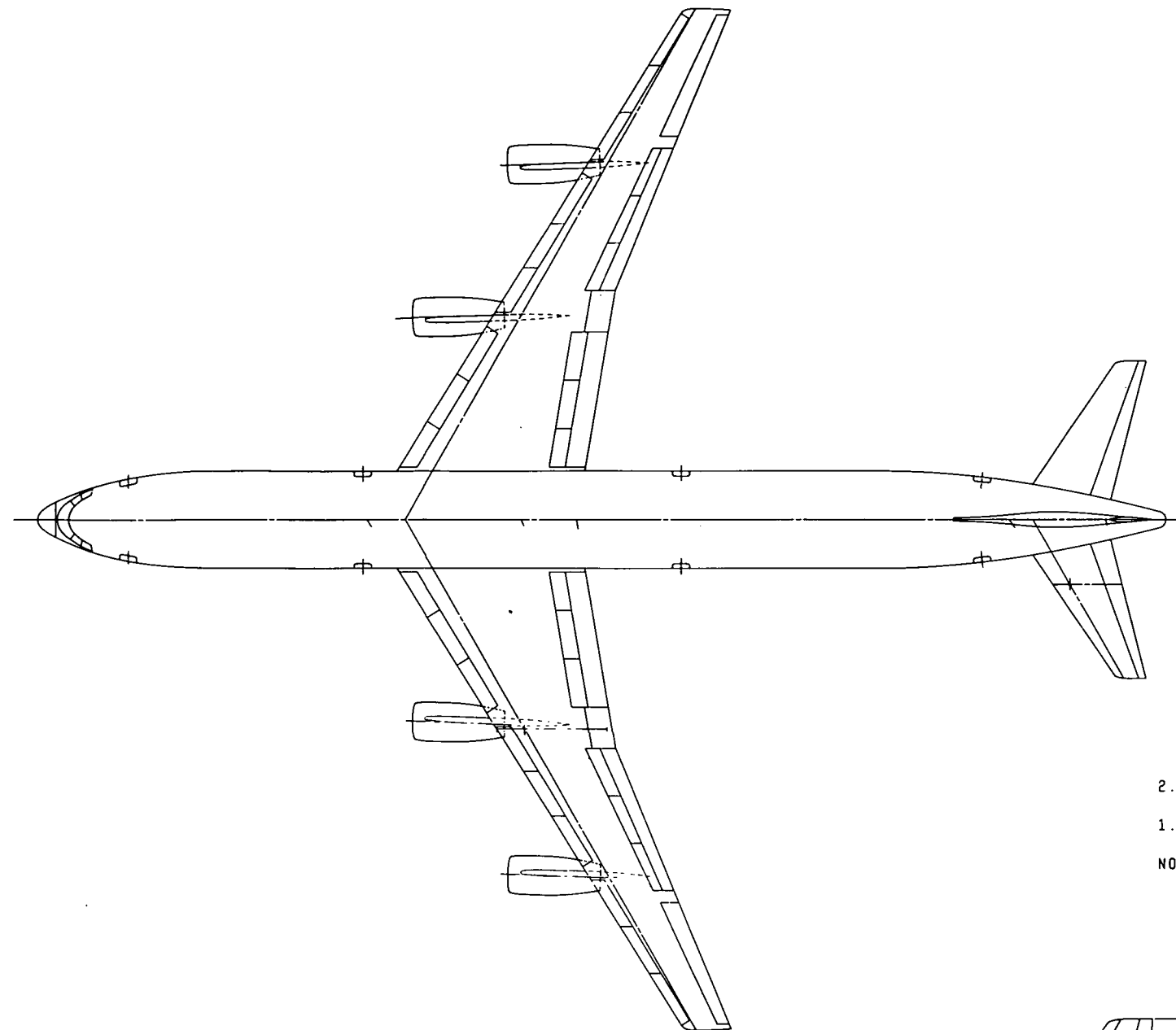
**2** ~~BOLDOUT FRAME~~

**3** ORIGINAL PAGE IS  
 OF POOR QUALITY

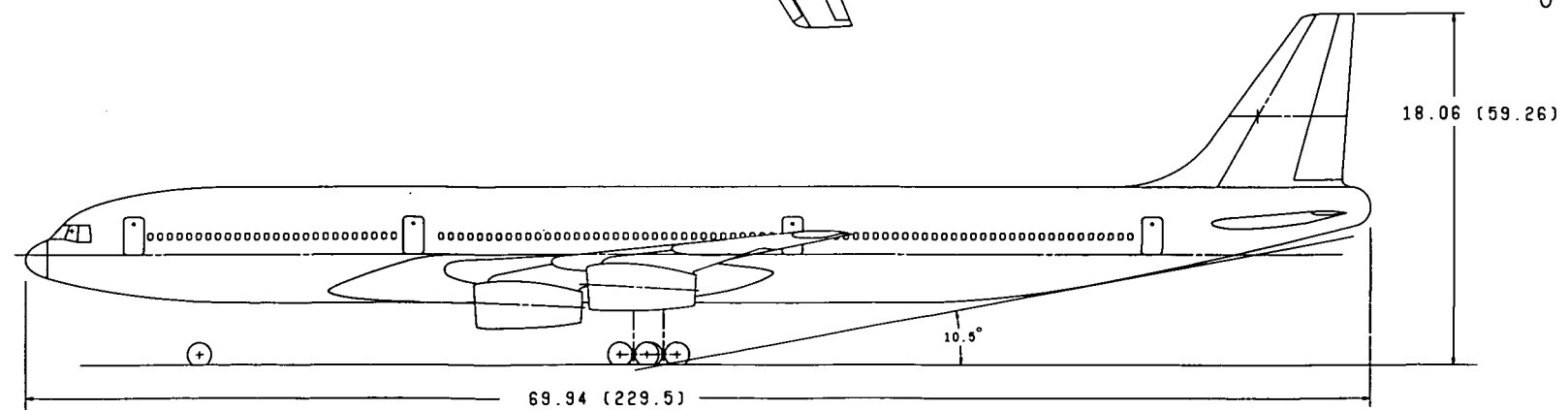
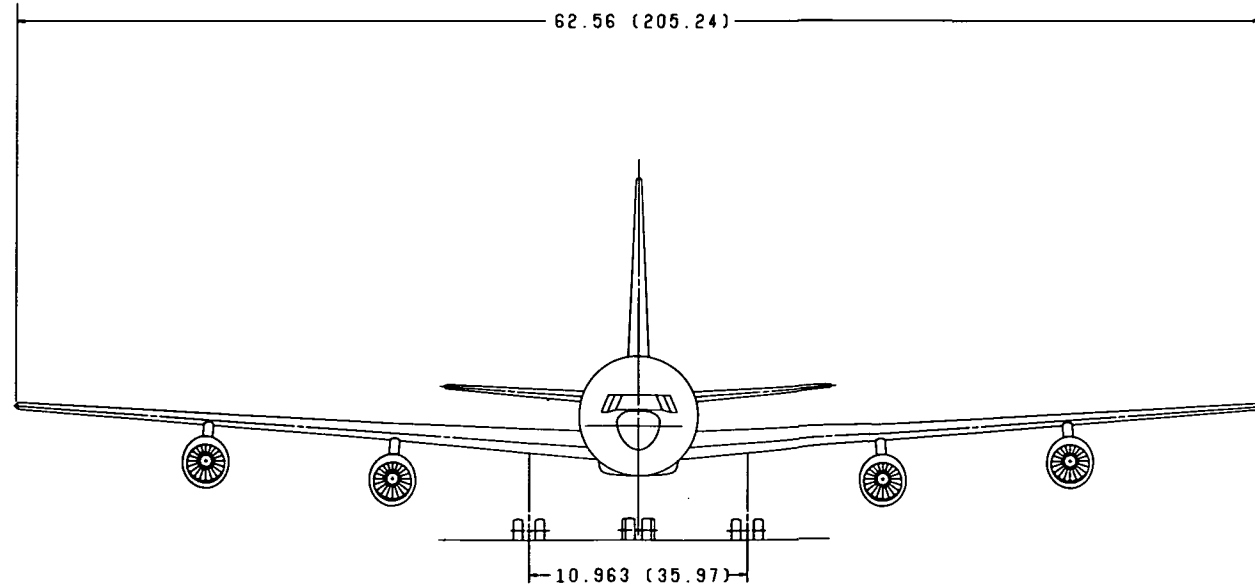
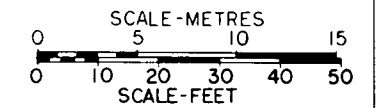
393  
**3** ~~BOLDOUT FRAME~~

CHARACTERISTICS	WING	HORIZONTAL TAIL	VERTICAL TAIL
AREA SQ. M. (SQ. FT.)	381.33 (4212.2)	75.62 (814)	49.53 (533.1)
ASPECT RATIO	10	5	1.6
SPAN M. (FT.)	62.56 (205.24)	19.46 (63.85)	8.90 (29.20)
ROOT CHORD M. (IN.)	9.62 (378.87)	5.98 (239.40)	8.96 (356.88)
TIP CHORD M. (IN.)	2.89 (113.65)	1.79 (70.61)	2.97 (101.1)
TAPER RATIO	0.30	0.30	0.30
MAC M. (IN.)	6.86 (270.14)	4.26 (167.87)	6.03 (237.52)
SHEEP RAD. (DEG.)	0.924 (30)	0.925 (30)	0.924 (30)
T/C ROOT °	12	10	10
T/C TIP °	12	10	10

GROSS WEIGHT - 257,599 KG. (567,800 LB.)  
POWER PLANT (4) G.E. TASK III E<sup>3</sup> TURBOFAN  
INSTALLED THRUST - 152,357 N (34,253 LB.)  
PASSENGERS - 400  
RANGE - 6,500 N.M.



2. DIMENSIONS IN METRES (FEET), OR NOTED  
1. CADAM REF. DWG. CL1333-10-1,1,2,3  
NOTES:



ADVANCED DESIGN		REVISED DESIGN NO.
GEN. ARR. - E <sup>3</sup> 6,500 N.M.		CL1333-10
G.E. TASK III E <sup>3</sup> TURBOFAN		
DESIGNED BY	LOCKHEED - CALIFORNIA DIV.	
CHECKED BY	1030-77	
DATE	1/100	
A.L. HILLIARS		CL1333-10-1

FOLDOUT FRAME

ORIGINAL PAGE IS  
OF POOR QUALITY

Figure 145. General Arrangement - Intercontinental with Task III E<sup>3</sup> Engine - Lockheed Study

2 FOLDOUT FRAME

ORIGINAL PAGE IS  
OF POOR QUALITY

TABLE 115

WEIGHT STATEMENT - LOCKHEED STUDYTASK III E<sup>3</sup> ENGINEE<sup>3</sup> AIRCRAFT /400 Pass/5556KM (3000 N MI)/M = 0.80

	<u>Kg.</u>	<u>Pounds</u>
Take-off Weight	181,350	399,800
Fuel Available	40,718	89,766
Zero Fuel Weight	140,632	310,034
Payload	36,288	80,000
Operating Weight	104,344	230,034
Operating Items	6,339	13,974
Standard Items	1,970	4,343
Empty Weight	96,036	211,718
Wing	19,375	42,714
Tail	2,192	4,833
Body	24,854	54,792
Landing Gear	7,711	16,999
Surface Controls	1,943	4,283
Nacelle and Engine Section	1,623	3,577
Propulsion	12,377	27,287
Engines	8,621	19,005
Thrust Reversal + Exhaust	1,962	4,328
Air Induction System	838	1,847
Fuel and Oil System	634	1,392
Engine Controls + Starter	324	715
Lift Engines	0	0
Vector Control System	0	0
Power Transmission	0	0
Auxiliary Power Unit	506	1,116
Instruments	390	860
Hydraulics	1,085	2,393
Electrical	3,102	5,839
Avionics	998	2,200
Furnishings and Equipment	16,672	36,754
Environmental Control System	3,485	7,682
Auxiliary Gear	0	0
Anti-Icing System	177	391
A.M.P.R.	81,682	180,074
Excess Full Capacity - Body	251,680	554,349
Excess Full Capacity - Wing	38,757	85,442

TABLE 116

## MISSION SUMMARY - LOCKHEED STUDY

TASK III E<sup>3</sup> ENGINE 400 PASS / 3000 N MI / M = 0.80

Segment	INIT Altitude (FT)	INIT Mach No.	INIT WEIGHT (LB)	SEGMENT FUEL (LB)	TOTAL FUEL (LB)	SEGMENT DIST (N MI)	TOTAL DIST (N MI)	SEGMENT TIME (MIN)	TOTAL TIME (MIN)	ENGINE THRUST TAB ID	AVG. L/D RATIO	AVG. SFC (FF/T)
Takeoff												
Power 1	0.	0.0	399800.	0.	0.	0.	0.	0.0	0.0	325501.	0.0	0.299
Power 2	0.	0.0	399800.	687.	687.	0.	0.	1.3	1.3	325501.	0.0	0.299
Climb	0.	0.378	399113.	6932.	7619.	114.	114.	20.3	21.7	325201.	19.72	0.503
Accel	40000.	0.692	302181.	815.	8504.	25.	139.	3.4	25.0	325201.	18.26	0.560
Climb	30700.	0.800	391296.	3153.	11667.	102.	240.	13.1	38.2	325201.	17.84	0.571
Cruise	36000.	0.800	388133.	60475.	72142.	2510.	2750.	328.1	366.3	-325101	18.34	0.568
Descent	34000.	0.800	327657.	40.	72183.	21.	2771.	2.7	369.0	203301	16.92	-0.389
Decel	30000.	0.800	327617.	14.	72197.	6.	2777.	0.8	369.9	203301.	16.93	-0.407
Decent	30000.	0.692	327603.	494.	72691.	92.	2869.	17.4	387.3	203301.	18.39	-1.117
Cruise	39000.	0.200	327109.	932.	75623.	131.	3000.	17.1	404.4	-325101.	18.05	0.570
Loiter	1500.	0.250	324177.	366.	75988.	0.	3000.	3.0	407.4	-325101.	18.64	0.422
RFSFT	0.	0.0	323811.	0.	75988.	-3000.	0.	0.0	407.4	0.	0.0	0.0
RESET	0.	0.0	323811.	0.	75988.	0.	0.	0.0	407.4	0.	0.0	0.0
Climb	0.	0.378	323811.	1483.	77471.	15.	15.	3.3	410.7	325201.	18.24	0.471
Accel	10000.	0.455	322328.	0.	77471.	0.	15.	0.0	410.7	325201.	18.23	0.481
Climb	10000.	0.450	322328.	3505.	89076.	65.	80.	11.1	421.9	32501.	18.20	0.511
Cruise	30000.	0.690	318823.	235.	81211.	10.	90.	1.4	423.3	-325101.	18.02	0.567
Descent	30000.	0.692	318588.	251.	81473.	63.	153.	11.1	434.4	203301.	18.16	-0.729
Decel	10000.	0.458	318327.	0.	81473.	0.	153.	0.0	434.4	203301.	18.12	-1.187
Descent	10000.	0.456	318327.	210.	81683.	26.	179.	5.7	440.1	203301.	18.15	-1.766
Cruise	30000.	0.690	318116.	512.	82195.	21.	200.	3.1	443.2	-325101.	18.00	0.567
Cruise	1500.	0.378	317604.	349.	82544.	0.	200.	2.0	445.2	-325101.	18.55	0.613
Cruise	30000.	0.690	317255.	7336.	89930.	0.	200.	45.0	490.2	-325101.	18.03	0.566



ORIGINAL PAGE IS  
 OF POOR QUALITY

TABLE 117

DRAG COEFFICIENTS -- NO EXTERNAL STORES - LOCKHEED STUDY

ALTITUDE = (0. FEET ) 0 Km  
 LIFT COEF. = 0.0

MACH NO.	0.10	0.20	0.30	0.40	0.50	0.60
0.200	0.01747	0.01782	0.01886	0.02058	0.02300	0.02611
0.400	0.01588	0.01623	0.01727	0.01900	0.02142	0.02453
0.750	0.01449	0.01484	0.01589	0.01765	0.02012	0.02333
0.800	0.01450	0.01486	0.01602	0.01793	0.02059	0.02405
0.820	0.01477	0.01513	0.01634	0.01828	0.02096	0.02444
0.850	0.01560	0.01595	0.01721	0.01920	0.02201	0.02624
0.900	0.01834	0.01894	0.02152	0.02668	0.03693	0.04916

ALTITUDE = (10000. FEET ) 3048 Km  
 LIFT COEF. = 0.0

MACH NO.	0.10	0.20	0.30	0.40	0.50	0.60
0.200	0.01815	0.01850	0.01953	0.02126	0.02368	0.02679
0.400	0.01647	0.01681	0.01785	0.01958	0.02200	0.02512
0.750	0.01499	0.01534	0.01639	0.01815	0.02062	0.02383
0.800	0.01500	0.01536	0.01652	0.01843	0.02109	0.02454
0.820	0.01527	0.01563	0.01683	0.01877	0.02146	0.02494
0.850	0.01609	0.01644	0.01770	0.01969	0.02250	0.02673
0.900	0.01882	0.01942	0.02260	0.02716	0.03741	0.04965

ALTITUDE = (20000. FEET ) 6096 Km  
 LIFT COEF. = 0.0

MACH NO.	0.10	0.20	0.30	0.40	0.50	0.60
0.200	0.01894	0.01928	0.02032	0.02205	0.02447	0.02758
0.400	0.01714	0.01749	0.01853	0.02026	0.02268	0.02580
0.750	0.01557	0.01592	0.01697	0.01873	0.02120	0.02441
0.800	0.01557	0.01593	0.01709	0.01900	0.02166	0.02512
0.820	0.01583	0.01620	0.01740	0.01934	0.02202	0.02551
0.850	0.01665	0.01700	0.01826	0.02025	0.02306	0.02729
0.900	0.01937	0.01997	0.02255	0.02772	0.03796	0.05020

ALTITUDE = (30000. FEET ) 9144 Km  
 LIFT COEF. = 0.0

MACH NO.	0.10	0.20	0.30	0.40	0.50	0.60
0.200	0.01983	0.02018	0.02121	0.02294	0.02536	0.02847
0.400	0.01791	0.01826	0.01929	0.02102	0.02345	0.02656
0.750	0.01622	0.01657	0.01762	0.01938	0.02185	0.02506
0.800	0.01622	0.01658	0.01774	0.01965	0.02231	0.02576
0.820	0.01648	0.01684	0.01804	0.01999	0.02267	0.02615
0.850	0.01729	0.01764	0.01890	0.02089	0.02370	0.02793
0.900	0.02000	0.02060	0.02318	0.02835	0.03859	0.05083

ALTITUDE = (40000. FEET ) 12192 Km  
 LIFT COEF. = 0.0

MACH NO.	0.10	0.20	0.30	0.40	0.50	0.60
0.200	0.02106	0.02140	0.02244	0.02417	0.02659	0.02970
0.400	0.01896	0.01931	0.02034	0.02207	0.02450	0.02761
0.750	0.01711	0.01746	0.01851	0.02027	0.02274	0.02595
0.800	0.01710	0.01747	0.01863	0.02053	0.02319	0.02665
0.820	0.01736	0.01772	0.01892	0.02087	0.02355	0.02703
0.850	0.01816	0.01851	0.01977	0.02176	0.02457	0.02880
0.900	0.02085	0.02146	0.02404	0.02920	0.03944	0.05168

TABLE J18

## COST SUMMARY - LOCKHEED STUDY

TASK III E<sup>3</sup> ENGINE

RDT And E	Production			Total Per Prod A/C **	Per Prod A/C **		
	Total *	Material	Labor				
Prototype A/C	450.93	Wing	1442.43	2233.61	3686.04	Production A/C	35238.39
Design Engineering	172.04	Tail	136.43	328.24	484.67	Prod. Engineering	152.58
DVLP Test Articles	117.44	Fuselage	1012.04	4575.39	5637.44	Maint. Trainers	0.0
Flight Test	85.83	Landing Gear	485.98	26.23	512.21	Operator Trainers	360.68
Eng.Dvlpmnt - Cruise	0.0	Nacelles	130.81	605.25	736.06	Prod. Tooling	9.98
Eng.Dvlpmnt - Lift	0.0	Surface Controls	439.83	417.29	657.12	Spcl. Supp. Equip.	690.67
Avionics Dvlpmnt	0.0	Engine Section	0.0	0.0	0.0	Prod. Spares	4469.13
Maint Trnr Dvlpmnt	0.0	Engine Controls	2.77	4.67	7.44	Technical Data	49.51
Upper Trnr Dvlpmnt	0.0	Engine Starter	46.77	9.26	56.03		
Dvlpmnt Foiling	477.08	Eng. Installation	0.0	22.87	22.87		
Spcl Supp Equip	6.49	Thrust Reverser	0.0	5.21	5.21		
Dvlpmnt Sparts	103.39	Air Induction	48.14	76.22	124.36		
Technical Data	35.45	Fuel System	50.11	62.35	112.46		
		Vector Control	0.0	0.0	0.0		
		Power Transmission	0.0	0.0	0.0		
		APU	169.85	21.01	130.86		
		Instruments	54.32	55.69	110.01		
		Hydraulics	104.36	297.39	401.75		
		Electrical	352.01	1054.02	1406.02		
		Avionic Install	25.85	304.02	329.85		
		ECS	353.07	494.39	847.46		
		Furn and Equip	776.77	3592.74	4369.51		
		Armament	0.0	0.0	0.0		
		Auxiliary Gear	0.0	0.0	0.0		
		Anti-Icing	17.97	25.17	43.14		
		Sys. Integration	400.91	491.45	892.36		
		Eng. Change Orders			441.07		
		Sustaining Eng. Cost			1052.62		
		Prod. Tooling Cost			1654.63		
		Quality Assurance Cost			1930.57		
		Miscellaneous Cost			588.10		
		Total Airframe Cost			26469.84		
		Total Engine Cost			4356.62		
		Total Manufacturing Cost			31070.89		
		Profit			4007.14		
		Taxes & Insurance			0.0		
		Warranty			180.29		
		TOTAL PRODUCTION			35238.30		
						TOTAL INVESTMENT	40970.80
						* - Millions of Dollars	
						** - 1000 of Dollars Per	
						Production Aircraft	

ORIGINAL PAGE IS  
OF POOR QUALITY

TABLE 119

OPERATIONAL COSTS - LOCKHEED STUDY

TASK III E<sup>3</sup> ENGINE

Direct Operational Cost (DOC)			Indirect Operational Cost (IOC)				
	C/SM**	Percent		C/SM**	Percent		
Flight Crew	0.21491	16.1723	System	0.14031	14.31551	Total Revenue Per Year *	1330.96
Fuel and Oil	0.25264	10.00993	Local	0.05407	5.51708	Total Expense Per Year *	658.59
Insurance	0.01979	1.4889	Aircraft Control	0.00174	0.17801	Total Investment * Incl. Facilities	1883.54
Depreciation	0.40678	10.61950	Cabin Attendant	0.17399	17.75174	ROI Before Taxes (0/0)	71.39
Maintenance	0.43479	32.71375	Food and Beverage	0.12259	12.50707	ROI After Taxes	35.70
			Passenger Handling	0.08690	8.86612		
Total DOC	1.32889	100.00	Cargo Handling	0.05119	5.22250		
			Other Passenger Expense	0.26226	26.75752		
			Other Cargo Expense	0.00516	0.52693		
			General Administration				
			Total IOC	0.98013	100.000		
			Misc. Data				
			Range (St. Miles)		3454.59		
			Block Speed ( PH)		481.59		
			Fare		272.22		
			Fleet Size		39.31		
			Rev, Passenger (Mil, per year)		4.81		
			Average Cargo Per Flight		14756.60		
			Flights Per A/C Per Year		525.14		

\* - Millions of Dollars  
\*\* - Cents per Seat Mile

ORIGINAL PAGE IS  
FOLDED TO  
FIT  
ORIGINAL PAGE IS

TABLE 120

## WEIGHT STATEMENT - LOCKHEED STUDY

TASK III E<sup>3</sup> ENGINEE<sup>3</sup> Aircraft /400 PASS/12038 Km (6500 N MI)/M = 0.80

	<u>Kg</u>	<u>Weight (Pounds)</u>
Take-off Weight	257555	567800.1
Fuel Available	103115	227384.
Zero Fuel Weight	154413	340416.1
Payload	36288	80000.
Operating Weight	178125	260416.1
Operating Items	6352	14003.
Standard Items	3317	7312.
Empty Weight	108457	239102.1
Wing	24536	54091.
Tail	2373	5231.
Body	24346	53673.
Landing Gear	10209	22507.
Surface Controls	2150	4739.
Nacelle and Engine Section	2579	5685
Propulsion	15098	33284.1
Engines	10872	23968.1
Thrust Reversal + Exhaust	2532	5581.
Air Induction System	529	1166.
Fuel and Oil System	738	1627.
Engine Controls + Starter	430	942.
Lift Engines	0	0.
Vector Control System	0	0.
Power Transmission	0	0.
Auxiliary Power Unit	506	1116.
Instruments	481	1061.
Hydraulics	1488	3280.
Electrical	3036	6693.
Avionics	1815	2900.
Furnishings and Equipment	16672	36754.
Environmental Control System	3485	7682.
Auxiliary Gear	0	0.
Anti-Icing System	185	407
A.M.P.R.	90496	199505.1
Excess Fuel Capacity - Body	259170	566950.
Excess Fuel Capacity - Wing	3196	7045.

ORIGINAL PAGE IS  
OF POOR QUALITY

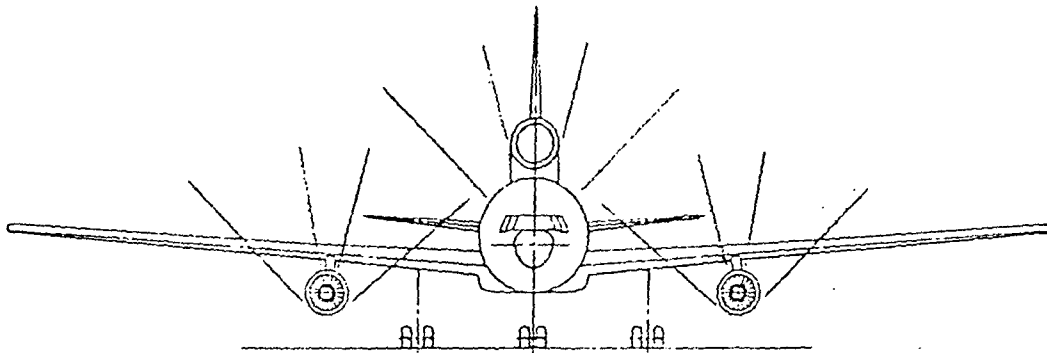


Figure 146. Thrust Reverser Flow Directivity - Lockheed Study

- At cruise angle of attack, the mixed flow nacelle does not appear to be significantly different from the L-1011 type nacelle.
- Installation of a mixed flow nacelle will probably require additional aerodynamic development, but shows no potential interference problems that could not be solved by proper configuration tailoring.

The mixed flow nacelle was positioned, with respect to the wing, using the same relative dimensions as the L-1011, as depicted in Figure 147. Zero interference drag was utilized which is compatible with L-1011 experience.

### C. McDonnell Douglas Corporation

In Task III, McDonnell Douglas conducted additional system payoff studies, the results of which are presented in Figure 106 for the domestic and intercontinental airplanes. In addition, detailed studies of the long duct nacelle construction were made. These resulted in a definition of materials and a revised weight estimate as discussed below.

#### 1. Material Selection

To be able to incorporate the long duct mixed flow nacelle with minimum effect on airframe support structures, composite materials are used to keep the weight of the long duct design to a minimum. The basic long duct nacelle construction is a thin walled design concept using composite face skins bonded to a honeycomb core.

The material chosen for a majority of the face skins is a Graphite/Kevlar 50/50 hybrid fabric. The Graphite in the face skins enables the conduction of current due to secondary lightning strikes. The Graphite has good tensile and compressive strength to weight ratios which reduces the number of plies. The Graphite alone has poor impact characteristics. This leads to the need for a second material, Kevlar, which is chosen for its impact characteristics. The Kevlar also has good tensile strength to weight ratio but has a poor compressive strength to weight ratio. This weakness is compensated by the characteristics of Graphite. The Kevlar and Graphite are used in a bi-woven hybrid and the weak characteristics of one material is compensated for by the strength of the other material.

The material is chosen in a fabric form over the conventional tape form due to the dimensions of the nacelle. With the large shapes of the nacelle components, the use of fabrics reduces lay-up time and labor costs. This cost savings outweighs the weight increase caused by using the heavier fabric.

A polyimide resin (matrix) system is used in the composite face skins. The polyimide resin has not had as an extensive testing program in industry as epoxy resin and will require development. Several advantages make this development worthwhile. An increase in impact resistance occurs

ORIGINAL PAGE IS  
OF POOR QUALITY

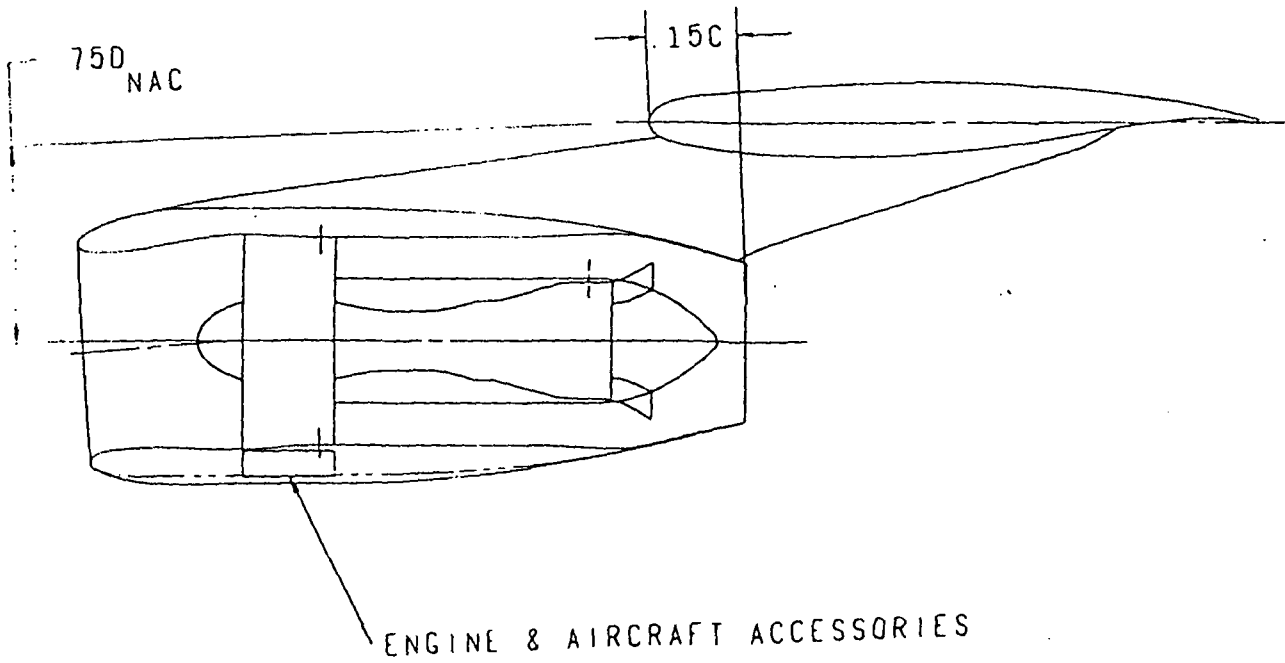


Figure 147. Typical Nacelle Installation - Lockheed Study

when a polyimide resin is substituted for an epoxy resin in the use of composite panels. Polyimide resin also has a higher service temperature 232° C (450° F) than that of an epoxy 177° C (350° F) and better fire resistance than epoxy resins.

The core material chosen is a nylon phenolic or Homex honeycomb. This material is used in all areas except in the inner barrel of the inlet.

## 2. Weights

After selecting the materials and construction of the long duct mixed flow nacelle, a weight estimation was made for the total nacelle. A separate weight estimate is made for the tail nacelle due to a slight variation in dimensions. These estimated weights along with the current pod weight are compared in Table 121. As shown in the Table, the long duct mixed flow nacelle with composites is approximately eight percent lighter than current pods with turbine reversers.



TABLE 121

NACELLE WEIGHT COMPARISON Kg (Lbs) - McDONNELL DOUGLAS STUDY

CF6-50C, EBU of 359 Kg (792 lb) and engine not included

	CURRENT PODS WITH TURBINE REVERSERS	LONG DUCT MIXED FLOW WITH COMPOSITES % CHANGE *
WING	1468 (3237)	1340 (2955)      -8.71
TAIL	1283 (2828)	1182 (2605)      -7.89
TOTAL A/C	4219 (9302)	3862 (8515)      -8.46

\* Percent change with respect to current pods with turbine reversers

**DRIFT**  
**OF**

**ORIGINAL PAGE IS  
OF POOR QUALITY**

APPENDIX C

NOMENCLATURE/SYMBOLS

C&A	Controls & Accessories
CDP	Compressor Discharge Pressure
CG	Center of Gravity
$C_L/L$	Clearance / Blade Height
D	Diameter, meters (feet)
DHL, $D_{HL}$	Inlet Highlight Diameter, meters (feet)
$D_{Max}$	Nacelle Maximum Diameter, meters (feet)
$D_T$	Fan Tip Diameter, meters (feet)
DOC	Direct Operating Cost
E.B.U.	Engine Build-up Items
EPA	Environmental Protection Agency
EPNL	Effective Perceived Noise Level, dB
F	Thrust, newtons (lbf)
$F_n$	Net Thrust, newtons (lbf)
$F_{NI}$	Installed Net Thrust, newtons (lbf)
$F_n/W_2$	Specific Thrust, newtons/kg (lbf/lbm)
FOD	Foreign Object Damage
HP	High Pressure
HPC	High Pressure Compressor
HPT	High Pressure Turbine
L	Inlet Length, meters (feet)
L.F.	Load Factor
LP	Low Pressure
LPC	Low Pressure Compressor

~~PRECEDING~~ PRECEDING PAGE BLANK NOT FILMED.

LPT	Low Pressure Turbine
M or $M_n$	Mach Number
Maint./M.H.	Maintenance in Man Hours
MxCl	Maximum Climb Rating
MxCr	Maximum Cruise Rating
$N_B$	Number of Blades
$NO_x$	Nitric Oxide and Nitrous Oxide
P	Pressure, newtons/meter <sup>2</sup> , absolute (lbf/in. <sup>2</sup> )
P/P	Pressure Ratio
PAX	Passenger
PNLT	Perceived Noise Level Total, dB
$P_3$	Compressor Discharge Pressure, newtons/meter <sup>2</sup> (lbf/in. <sup>2</sup> )
r	Radius, meters (feet)
$r_H$	Hub Radius, meters (feet)
$r_T$	Tip Radius, meters (feet)
r/r	Radius Ratio
ROI	Return on Investment
SDOF	Single Degree of Freedom
sfc	Specific Fuel Consumption, kg/newton-hr (lbm/lbf-hr)
$sfc_I$	Installed Specific Fuel Consumption, kg/newton-hr (lbm/lbf-hr)
SLS	Sea Level Standard
T	Temperature, °C (°F)
$T_{TB}$	Blade Relative Total Temperature
To or $T_o$	Ambient Temperature, °C (°F)
$T_{41}$ or $T_{4.1}$	Turbine Rotor Inlet Temperature, °C (°F)
TO or T/O	Takeoff (Take-off power)
TOGW	Takeoff Gross Weight

$U_H/\sqrt{\theta}_2$ B	Hub Speed Corrected to Booster-Rotor Inlet Conditions, m/sec (ft/sec)
$U_T$	Tip Speed, m/sec (ft/sec)
$U_{T_i}/\sqrt{\theta}_2$	Corrected Tip Speed, m/sec (ft/sec)
$V_9$	Primary-jet Velocity, m/sec (ft/sec)
$V_{29}$	Fan Jet Velocity, m/sec (ft/sec)
$W_{EI}$	Weight of Installed Engine, kg (lb)
$W_f$	Fuel Flow, kg/sec (lbm/hr)
$W\sqrt{\theta}/\delta, W_2\sqrt{\theta}/\delta$	Engine Inlet Airflow, kg/sec
$W\sqrt{\theta}/\delta - \Delta A$	Corrected Inlet Airflow per Annulus Area, kg/sec-m <sup>2</sup> (lbm/hr-ft <sup>2</sup> )
$W_2$	Engine Inlet Mass Flow, kg/sec (lbm/sec)
$W_{2C}$	High Pressure Compressor Inlet Flow, kg/sec (lbm/sec)
$W_{2C}\sqrt{\theta}/\delta$	Compressor Inlet Airflow, kg/sec (lbm/hr)
$W/W_{2C}$ HPT	HPT Cooling and Leakage Flow, % Compressor Flow
$W/W_{2C}$ LPT	LPT Cooling and Leakage Flow, % Compressor Flow
$W_{B1}$	Intermediate Compressor Bleed, % Compressor Flow
$\beta$	Bypass Ratio
$\Delta$	Delta, Difference
$\Delta H$	Enthalpy Change, joules/kg (BTU/lb)
$\Delta T_o$	Difference from Ambient Temperature, °C (°F)
$\delta$	P/14.696
$\epsilon$	Effectiveness
$\eta$	Efficiency
$\eta_{TT}$	Turbine Efficiency
$\theta$	T/518.7
$\sigma$	Stress
$\bar{\psi}$	Turbine Blade Loading Parameter
$\bar{\psi}_p$	Mean Loading of Turbine Stage

REFERENCES

1. Neitzel, R. E., Hirschcron, R., and Johnston, R.P., General Electric Company, "Study of Turbofan Engine Designed for Low Energy Consumption," NASA CR-135053, prepared for NASA under Contract No. NAS3-19201.
2. Neitzel, R.E., Hirschcron, R., and Johnston, R.P., General Electric Company, "Study of Unconventional Aircraft Engines Designed for Low Energy Consumption," NASA CR-135136, prepared for NASA under Contract No. NAS3-19519.
3. Steinberger, C.A., Stotler, C.L., and Neitzel, R.E., General Electric Company, "Study of the Cost and Benefits of Composite Material in Advanced Turbofan Engines," NASA CR-134696, prepared for NASA under Contract No. NAS3-17775.
4. Ross, E.W., Johnston, R.P., and Neitzel, R.E., General Electric Company, "Cost Benefit Study of Advanced Materials Technology for Aircraft Turbine Engines," NASA CR-134702, prepared for NASA under Contract No. NAS3-17805.
5. Hillery, R.V., and Johnston, R.E., General Electric Company, "Cost Benefit Study of Advanced Materials Technology for Aircraft Turbine Engines," NASA CR-135235, prepared for NASA under Contract No. NAS3-20074.
6. Wisler, D.C., Koch, C.C., and Smith, Jr., L.H., General Electric Company, "Preliminary Design Study of Advanced Multistate Axial Flow Core Compressor," NASA CR-135133, prepared for NASA under Contract No. NAS3-19444.
7. Koch, C.C., and Smith, Jr., L.H., "Loss Sources and Magnitudes in Axial-Flow Compressors," Transaction of ASME, Journal of Engineering for Power, Vol. 98, Series A, No. 3, July 1976, page 411.
8. Advanced Engineering and Technology Department, General Electric Company, "Quiet Clean Short-Haul Experimental Engine (QCSEE) - Composite Fan Frame Design Report," NASA CR-135278, September, 1978, Contract No. NAS3-18021.
9. Reneau, L.R., Johnston, J.P., and Kline, S.J., Department of Mechanical Engineering, Stanford University, "Diffuser Design Manual," Report PD-8, September, 1964.
10. Frost, T.D., "Practical Bypass Mixing Systems for Fanjet Aero Engines," Aeronautical Quarterly, May, 1966.

410  
PAGE 1 INTENTIONALLY BLANK